BACTERIOCINS AND OTHER RIBOSOMALLY SYNTHESISED AND POST-TRANSLATIONALLY MODIFIED PEPTIDES (RIPPS) AS ALTERNATIVES TO ANTIBIOTICS

EDITED BY: Harsh Mathur, Paul David Cotter, Des Field and Mathew Upton
PUBLISHED IN: Frontiers in Microbiology

frontiers Research Topics

frontiers

ISSN 1664-8714
ISBN 978-2-88971-111-6
DOI 10.3389/978-2-88971-111-6

About Frontiers

Frontiers is more than just an open-access publisher of scholarly articles: it is a pioneering approach to the world of academia, radically improving the way scholarly research is managed. The grand vision of Frontiers is a world where all people have an equal opportunity to seek, share and generate knowledge. Frontiers provides immediate and permanent online open access to all its publications, but this alone is not enough to realize our grand goals.

Frontiers Journal Series

The Frontiers Journal Series is a multi-tier and interdisciplinary set of open-access, online journals, promising a paradigm shift from the current review, selection and dissemination processes in academic publishing. All Frontiers journals are driven by researchers for researchers; therefore, they constitute a service to the scholarly community. At the same time, the Frontiers Journal Series operates on a revolutionary invention, the tiered publishing system, initially addressing specific communities of scholars, and gradually climbing up to broader public understanding, thus serving the interests of the lay society, too.

Dedication to Quality

Each Frontiers article is a landmark of the highest quality, thanks to genuinely collaborative interactions between authors and review editors, who include some of the world's best academicians. Research must be certified by peers before entering a stream of knowledge that may eventually reach the public - and shape society; therefore, Frontiers only applies the most rigorous and unbiased reviews.
Frontiers revolutionizes research publishing by freely delivering the most outstanding research, evaluated with no bias from both the academic and social point of view. By applying the most advanced information technologies, Frontiers is catapulting scholarly publishing into a new generation.

What are Frontiers Research Topics?

Frontiers Research Topics are very popular trademarks of the Frontiers Journals Series: they are collections of at least ten articles, all centered on a particular subject. With their unique mix of varied contributions from Original Research to Review Articles, Frontiers Research Topics unify the most influential researchers, the latest key findings and historical advances in a hot research area! Find out more on how to host your own Frontiers Research Topic or contribute to one as an author by contacting the Frontiers Editorial Office: frontiersin.org/about/contact

BACTERIOCINS AND OTHER RIBOSOMALLY SYNTHESISED AND POST-TRANSLATIONALLY MODIFIED PEPTIDES (RIPPS) AS ALTERNATIVES TO ANTIBIOTICS

Topic Editors:
Harsh Mathur, Teagasc Food Research Centre, Ireland
Paul David Cotter, Teagasc Food Research Centre, Ireland
Des Field, University College Cork, Ireland
Mathew Upton, University of Plymouth, United Kingdom

Prof Upton is the director of Amprologix, a company developing new bacteriocins; the other editors declare no competing interest in regard to editing this Research Topic.

Citation: Mathur, H., Cotter, P. D., Field, D., Upton, M., eds. (2021). Bacteriocins and Other Ribosomally Synthesised and Post-translationally Modified Peptides (RiPPs) as Alternatives to Antibiotics. Lausanne: Frontiers Media SA. doi: 10.3389/978-2-88971-111-6

Table of Contents

frontiers in Microbiology

EDITORIAL
published: 08 June 2021
doi: 10.3389/fmicb.2021.695081

Editorial: Bacteriocins and Other Ribosomally Synthesised and Post-translationally Modified Peptides (RiPPs) as Alternatives to Antibiotics

Harsh Mathur[1]*, *Des Field*[2], *Mathew Upton*[3] and *Paul D. Cotter*[1]

[1] Teagasc Food Research Centre, Co. Cork, Ireland, [2] School of Microbiology and APC Microbiome Ireland, University College Cork, Cork, Ireland, [3] School of Biomedical Sciences, University of Plymouth, Plymouth, England, United Kingdom

Keywords: bacteriocins, RiPPs, antimicrobials, antimicrobial resistance, genetic engineering

Editorial on the Research Topic

Bacteriocins and Other Ribosomally Synthesised and Post-translationally Modified Peptides (RiPPs) as Alternatives to Antibiotics

OPEN ACCESS

Edited by:
Rustam Aminov,
University of Aberdeen,
United Kingdom

Reviewed by:
Koshy Philip,
University of Malaya, Malaysia
Juan F. Martin,
Universidad de León, Spain

***Correspondence:**
Harsh Mathur
105022894@umail.ucc.ie

Specialty section:
This article was submitted to Antimicrobials, Resistance and Chemotherapy, a section of the journal Frontiers in Microbiology

Received: *14 April 2021*
Accepted: *10 May 2021*
Published: *08 June 2021*

Citation:
Mathur H, Field D, Upton M and Cotter PD (2021) Editorial: Bacteriocins and Other Ribosomally Synthesised and Post-translationally Modified Peptides (RiPPs) as Alternatives to Antibiotics. Front. Microbiol. 12:695081. doi: 10.3389/fmicb.2021.695081

This Research Topic concerns bacteriocins and others RiPPs (Ribosomally synthesized and Post-translationally modified Peptides) as alternatives to antibiotics. Due to the increasing problem of antibiotic resistance globally, there is a pressing need to source such alternative antimicrobials. Here, in this editorial, we summarize the key papers that were published as part of this Research Topic, which consisted of a diverse range of research as well as review articles, pertaining to several different bacteriocins and RiPPs.

A number of these studies report the discovery of novel bacteriocins or RiPPs, either through *in silico* genome mining approaches, laboratory experimental-based approaches or a combination thereof. In one such study, using a combination of lab-based and *in silico* approaches, Angelopoulou et al. reported the discovery of a range of bacteriocins synthesized by strains isolated from human milk. More specifically, the authors isolated bacteriocin producers from 37 human milk samples and found 73 putative bacteriocin gene clusters, which included 16 completely novel prepeptides. Amongst the key findings of the study were the discovery of 2 novel lantibiotics, 3 class IIa bacteriocins, 4 sactibiotics, 1 novel class IIb bacteriocin, 4 new class IIc, and 2 class IId bacteriocins, highlighting that the human milk microbiota is a potentially rich source of diverse antimicrobials. In a separate *in silico* study, Sabino et al. found that ruminal bacteria are a potentially rich source of lasso peptides. More specifically, a genome mining approach was employed by the authors, using tools such as BAGEL4 and antiSMASH5 to screen 425 bacterial genomes from the rumen ecosystem for lasso peptide production. Overall, Sabino et al. found 23 incomplete and 11 complete putative lasso peptide gene clusters amongst the genomes analyzed. Finally, a study by Zendo et al. reported the discovery of a novel nisin variant, kunkecin A, synthesized by *Apilactobacillus kunkeei* FF30-6, a lactic acid bacterium isolated from honey bees. The study describes its antimicrobial activity against *Melissococcus plutonius*, one of the major bacterial pathogens of honeybee broods. Furthermore, the genome sequence of *A. kunkeei* FF30-6 revealed that the biosynthetic machinery of the novel bacteriocin resides in the plasmid pKUNFF30-6. A more in-depth analysis of the kunkecin A gene cluster also revealed that it is quite distinct from the nisin A gene cluster, and is devoid of genes corresponding to *nisR*, *nisK*, and *nisI*. However, both nisin A and kunkecin A are likely to share similar post-translational modification processes. The structure of kunkecin A was

also proposed in the study, on the basis of observed and calculated molecular masses of the peptide. Together, these studies emphasize the growing importance of sequence mining approaches in the discovery of novel RiPPs.

A few studies as part of this Research Topic report the investigation of the activities of nisin variants and/or semi-synthetic hybrids of nisin. In one such interesting study, Reiners et al. provided insights into the antimicrobial activity of nisin H, a natural variant of nisin, in addition to the nisin H F_1I derivative. The authors expressed the peptide in a heterologous host and determined the yield, the cleavage efficiency using NisP as well as effects on the post-translational modification using mass spectrometry techniques. In addition, the authors determined the effects of nisin H and nisin H F_1I on the activity of NisI and NisFEG responsible for nisin immunity, as well as the resistance determinants SaNSR and SaNsrFP from *Streptococcus agalactiae*. Overall, the authors found that nisin H and nisin H F_1I were more potent than nisin A when tested against clinical isolates of *Enterococcus faecalis*, *Enterococcus faecium* and *Staphylococcus aureus*. In a separate study, Deng et al. reported that biologically active and stable forms of nisin are generated upon conjugation of synthetic hydrophobic polyproline moieties to the lipid II binding fragments of the nisin peptide. The authors used click chemistry technology to conjugate moieties of synthetic polyproline to either nisin AB (encompassing rings A and B of nisin) or to nisin ABC (encompassing rings A, B, and C of nisin). Importantly, the authors found that the conjugation of the synthetic polyproline O63K with nisin ABC resulted in a 16-fold increase in bioactivity, compared to nisin ABC, highlighting the potential of semi-synthetic nisin hybrids as novel antimicrobials. Furthermore, such nisin ABC hydrids are recalcitrant to degradation by nisinase and other proteolytic enzymes at the C-terminus of nisin. These semi-synthetic hybrids, which maintain potent or enhanced antimicrobial activity, could present viable means to circumvent certain nisin resistance mechanisms. Albeit resistance to bacteriocins has been described in several studies over the years, such instances have mainly related to resistance demonstrated in *in vitro* studies rather than in clinical settings/food systems. Thus, bacteriocins may present viable alternatives used in clinical settings, especially in light of the widespread reports of antibiotic resistance globally. In this regard, the use of semisynthetic derivatives of lantibiotics such as nisin and other such hybrid compounds and/or non-ribosomally synthesized peptides, such as those described above, may be a possible means to circumvent issues relating to antibiotic resistance in the clinic. By gaining insights into the precise mode of action of different bacteriocins against specific clinical pathogens, the use of such hydrid compounds could be particularly important as a means to tailor-make narrow spectrum antimicrobials with a view to targeting specific pathogens in the clinic, whilst minimizing the impact on the overall host microbiome.

In relation to class II bacteriocins, a very interesting study by Ross et al. reported the design of synthetic peptide libraries derived from a minimal alpha helical domain of enterocin AS-48 homologs and antimicrobial activities thereof. The alpha helical region of this circular bacteriocin enterocin AS-48 is chiefly responsible for its membrane-permeating and resultant antibacterial activity. The authors conducted homology-based searches of similar domains in several bacterial genomes, used these alpha helical domains as scaffolds to design minimal peptide libraries and assessed their antimicrobial activity. An impressive total of 384 synthetic peptides were evaluated for antimicrobial activity in the study and the authors found that MICs in the low nanomolar range were obtained for the most potent peptides, with no concomitant cytotoxic effects. Thus, studies like this present a blueprint or scaffold for the rational design of semi-synthetic bacteriocin peptide libraries for further evaluation. In a separate study, Vermeulen et al. described the expression of plantaricin 423 and mundticin ST4SA, both class IIa bacteriocins in *E. coli* as a heterologous host, using Green Fluorescent Protein as a fusion partner. Importantly, the authors reported that His-tagged GFP fusion proteins encompassing these bacteriocins, in addition to being autofluorescent, overcame the issue of inclusion body formation, and also decreased the toxicity of these bacteriocins during heterologous expression. The autofluorescence also facilitated real-time quantification of protein yields during heterologous expression.

With regards to studies focused on the potential for bacteriocin resistance development, an interesting study by Campelo et al. reported that a Bce-like bacitracin resistance module in *Lactococcus lactis* is activated upon exposure to the bacteriocin Lcn972. A further possible concern in this regard is that general MFS transporters may contribute to multidrug resistance in pathogenic bacteria, which may also include resistance to bacteriocins. These types of studies are extremely important as they highlight the potential downsides of utilizing bacteriocins, as in certain cases, resistance to other antimicrobials may inadvertently be enhanced as well. YsaDCB is a *L. lactis* ABC transporter that along with TCS-G, forms a detoxification module conferring protection against the cell wall biosynthesis inhibitors bacitracin and the bacteriocin Lcn972. By using a combination of heterologous expression and RT-qPCR, the authors elucidated the precise function of the *ysaDCB* operon. Overall, the authors found that *ysaB* encodes a putative Bce-like permease, whilst *ysaD* encodes a secreted peptide which is likely to be associated with signal relay between the YsaDCB ABC transporter and TCS-G and are together involved in largely similar but somewhat distinct mechanisms of resistance to bacitracin and Lcn972. Telhig et al. published an interesting review article relating to the use of bacteriocins to attenuate antimicrobial resistance in Gram negative bacteria. More specifically, the authors describe the potential use of unmodified and modified microcins, including lasso peptides, nucleotide peptide, siderophore peptides, and linear azole(in)e-containing peptides as a means to decrease the likelihood of antimicrobial resistance amongst Gram negative bacteria. In addition, the review described the potential of the development of cross-resistance and co-resistance in Gram negative bacteria, to various antibiotics and microcins.

Finally, a number of review articles covering a range of topics pertaining to bacteriocins and other RiPPs were published as part of this Research Topic. A very interesting review article by Karbalaei-Heidari and Budisa highlighted the potential of

utilizing genetic code expansion strategies in lanthipeptides with a view to attenuating the likelihood of the development of antimicrobial resistance to lanthipeptides. This is because the conventional genetic code and protein engineering strategies are limited to merely 20 canonical amino acids. However, the authors in this review highlight the prospective use of non-canonical amino acids during protein translation with a view to forming semi-synthetic lantibiotics with enhanced biological and chemical properties compared to their natural variants. Another interesting review by Lagedroste et al. summarized recent studies investigating the precise roles and mechanisms of action of enzymes involved in the post-translational modification processes of lanthipeptides. Finally, a review by Rooney et al. summarized the potential of bacteriocins as "plantibiotics of the future" by reporting the details of recent studies of the antimicrobial activity of bacteriocins against Gram-negative phytopathogenic bacteria. It must be noted however that much remains to be elucidated with regards to the impact that extraneous factors such as solar radiation, alterations in light intensity, humidity and temperature have on the stability and antimicrobial activity of bacteriocins and non-ribosomal peptides when potentially being used as antimicrobial agents to control plant infections.

In conclusion, this Research Topic has significantly added to the field of research relating to bacteriocins and RiPPs by highlighting the role of new approaches like *in silico* mining and RiPP engineering, but also addressing some of the potential issues faced by those wishing to commercialize RiPPs for clinical, agricultural, or industrial use.

AUTHOR CONTRIBUTIONS

HM wrote the initial draft of the manuscript. DF, MU, and PDC reviewed and revised the drafts. All authors have approved submission of the manuscript.

FUNDING

This work was supported by Science Foundation Ireland (SFI) Grant Number SFI/12/RC/2273_P2.

Conflict of Interest: The authors declare that the research was conducted in the absence of any commercial or financial relationships that could be construed as a potential conflict of interest.

frontiers in Microbiology

ORIGINAL RESEARCH
published: 19 May 2020
doi: 10.3389/fmicb.2020.00788

Diverse Bacteriocins Produced by Strains From the Human Milk Microbiota

*Angeliki Angelopoulou[1,2], Alicja K. Warda[2], Paula M. O'Connor[2,3], Stephen R. Stockdale[2], Andrey N. Shkoporov[2], Des Field[1,2], Lorraine A. Draper[2], Catherine Stanton[2,3], Colin Hill[1,2] and R. Paul Ross[1,2,3]**

[1] School of Microbiology, University College Cork, Cork, Ireland, [2] APC Microbiome Ireland, University College Cork, Cork, Ireland, [3] Teagasc Food Research Centre, Moorepark, Fermoy, Ireland

Microbial colonization of the infant gut is a convoluted process dependent on numerous contributing factors, including age, mode of delivery and diet among others that has lifelong implication for human health. Breast milk also contains a microbiome which acts as a source of colonizing bacteria for the infant. Here, we demonstrate that human milk harbors a wide diversity of bacteriocin-producing strains with the potential to compete among the developing gut microbiota of the infant. We screened 37 human milk samples and found isolates with antimicrobial activity and distinct cross-immunity profiles. From these isolates, we detected 73 putative gene clusters for bacteriocins of all known sub-classes, including 16 novel prepeptides. More specifically, we detected two novel lantibiotics, four sactibiotics and three class IIa bacteriocins with an unusual modification of the pediocin box that is composed of YDNGI instead of the highly conserved motif YGNGV. Moreover, we identified a novel class IIb bacteriocin, four novel class IIc and two class IId bacteriocins. In conclusion, human milk contains a variety of bacteriocin-producing strains which may provide them a competitive advantage in the colonization of the infant gut and suggests that the milk microbiota is a source of antimicrobial potential.

Keywords: human milk, bacteriocins, lantibiotics, sactibiotics, antimicrobials, genome mining, antibiotic resistance, human microbiota

OPEN ACCESS

Edited by:
Rustam Aminov, University of Aberdeen, United Kingdom

Reviewed by:
Takeshi Zendo, Kyushu University, Japan
Dzung B. Diep, Norwegian University of Life Sciences, Norway
Pablo E. Hernández, Complutense University of Madrid, Spain

***Correspondence:**
R. Paul Ross
p.ross@ucc.ie

Specialty section:
This article was submitted to Antimicrobials, Resistance and Chemotherapy, a section of the journal Frontiers in Microbiology

Received: *04 February 2020*
Accepted: *02 April 2020*
Published: *19 May 2020*

Citation:
Angelopoulou A, Warda AK, O'Connor PM, Stockdale SR, Shkoporov AN, Field D, Draper LA, Stanton C, Hill C and Ross RP (2020) Diverse Bacteriocins Produced by Strains From the Human Milk Microbiota. Front. Microbiol. 11:788. doi: 10.3389/fmicb.2020.00788

INTRODUCTION

Human breast milk supplies the newborn with all essential nutrients required for growth (Martin et al., 2016). It also furnishes immunological benefits to the infant and acts as a gut-colonizing bacterial 'inoculum' for the infant's gastro-intestinal (GI) microbiota (Fernández et al., 2013). Human milk is a dynamic milieu that can alter in composition along the stages of lactation (Cabrera-Rubio et al., 2012). Previously, human milk was considered to be sterile, yet many recent studies have provided evidence to the contrary (Heikkilä and Saris, 2003; Collado et al., 2009; Hunt et al., 2011; Mediano et al., 2017). The exact mechanisms of bacterial colonization of milk have yet to be fully elucidated. The skin, the infant oral cavity and even the partner's microbes are potential sources of bacteria for human milk (Hunt et al., 2011; Kort et al., 2014; Biagi et al., 2017; Ross et al., 2017). Moreover, bacteria of the maternal GI microbiota can spread to the mammary gland through the entero-mammary pathway (Perez et al., 2007).

While international and national health organizations promote exclusive breastfeeding for the first six months of life (WHO, 2000; Abou-Dakn et al., 2010), this may not always be feasible

for a variety of reasons (Li et al., 2008). Mastitis is an inflammation of breast tissue and is a common disease that can affect up to 33% of women, often culminating in the discontinuation of breastfeeding (Jiménez et al., 2008; Civardi et al., 2013). Moreover, we have recently found that the incidence of subclinical mastitis could be as high as 38% (Angelopoulou et al., 2020). Major etiological agents of mastitis include *Staphylococcus aureus*, *Staphylococcus epidermidis,* and members of Corynebacteriales. The main standard treatment for the infection is antibiotics (Angelopoulou et al., 2018) although scientists are endeavoring to search for alternative therapies such as bacteriocins (Fernández et al., 2008). These are ribosomally synthesized antimicrobial peptides produced by bacteria that have either broad or narrow range inhibition spectra (Cotter et al., 2013). Bacteriocin producing microbes can be identified via traditional plating methods (O'Sullivan et al., 2019), and more recently through metagenomic *in silico* predictions, using programs such as BAGEL and antiSMASH (Collins et al., 2017; Egan et al., 2018).

Bacteriocins produced by Gram positive bacteria are grouped in two classes, namely class I and class II (Kotelnikova and Gelfand, 2002). The class II bacteriocins may be further subdivided in the pediocin-like (class IIa) bacteriocins, the two-peptide (class IIb) bacteriocins, the cyclic (class IIc) bacteriocins, and the linear, non-pediocin-like (class IId) bacteriocins (Cotter et al., 2005, 2013). Additional bacteriocin subgroups have been also suggested. To date, two class I bacteriocins, lacticin 3147 (Crispie et al., 2005; Klostermann et al., 2009) and nisn (Angelopoulou et al., 2018) have been suggested as alternative treatments for bovine and human mastitis, respectively. They are believed to act as a first line of defense, protecting the host against pathogen invasion (Chikindas et al., 2018). Bacteriocin-producer organisms can impede pathogens from becoming established in a niche by preventing biofilm formation via inhibition of quorum sensing with low level production of bacteriocins (Algburi et al., 2017).

The present study aimed to screen 37 asymptomatic human milk samples for bacteria that produce bacteriocins that target mastitic pathogens with the ultimate aim to identify novel bacteriocin clusters that could provide alternative therapeutic options to counter antibiotic resistance. This study presents discovery and analysis of 16 novel bacteriocin gene clusters.

MATERIALS AND METHODS

Detection and Isolation of Antimicrobial-Producing Human Milk Isolates

Thirty-seven asymptomatic lactating mothers were recruited through Cork University Maternity Hospital to donate breast milk, which was approved by the Cork Clinical Research Ethics Committee and the participants provided written informed consent. Approximately 10 mL aliquots of milk were collected aseptically using sterile gloves in a sterile tube with the first few drops (∼500 μL) being discarded. The nipples and the mammary areola had been cleaned with sterile alcohol-free aqueous solution moist wipes (Ted Kelleher, First Aid & Hygiene Supplies Ltd, Macroom, Ireland) in order to avoid contaminating the milk with skin-colonizing bacteria. Samples were stored below 4°C overnight until they were further processed. Aliquots of 1 mL of milk were cultivated within 24 h of donation. Aliquots of milk sample, 1 mL, were mixed with 9 mL of maximum recovery diluent (MRD; Oxoid, Basingstoke, United Kingdom) to make an initial 10^{-1} dilution. Serial dilutions were enumerated by the spread plate method in duplicate onto: (a) Blood agar base (Oxoid, Basingstoke, United Kingdom) supplemented with 7% v/v defibrinated sheep blood (Cruinn Diagnostics, Dublin, Ireland) and incubated at 37°C for 48 h aerobically; which is a non-selective medium and (b) Baird Parker agar (Oxoid) supplemented with Egg Yolk Tellurite Emulsion (Oxoid) and incubated at 37°C for 48 h aerobically; which selects for staphylococci. Blood agar and Baird Parker plates with separate colonies were replicated in three clean Blood agar and Baird Parker plates, respectively using a replicator stamp (Karl Roth, Karsruhe, Germany). Replicated plates were incubated at 37°C, aerobically for 48 h. The day after the 48 h incubation, plates were exposed to UV light for 45 min and then overlaid with Brain Heart Infusion (BHI) sloppy (Oxoid) containing 0.75% agar seeded with: (a) 0.25% of an overnight culture of *S. aureus* APC 3759 and grown aerobically overnight at 37°C; (b) 0.25% of an overnight culture of *M. luteus* DSM 1790 and grown aerobically overnight at 37°C and (c) 0.25% of an overnight culture of *P. aeruginosa* PA01 and grown aerobically overnight at 30°C. In total, 174 colonies exhibited antimicrobial activity against the tested strains and were grown overnight in BHI, streaked for purity and stocked in 40% glycerol in two 96-well plates which were stored at −80°C for further characterization.

Cross-Immunity

To determine the relatedness of the bacteriocins produced by the strains, cross-immunity assays were performed during which the producing strains were tested against each other by conducting spot bioassays using each producing strain as a producer and also as a target strain. More precisely, the two 96-well plates were stamped using a replica platter (Sigma-Aldrich, Germany) onto clean Tryptic Soy Agar (TSA) plates or Mueller Hinton (MH; Oxoid) plates; the plates were incubated aerobically overnight at 37°C, before UV irradiation for 45 min. These were then overlaid with the same media (0.75% w/v agar seeded with 0.25% of an overnight culture of the producing strains) and grown aerobically overnight. Cross-immunity was performed for each of the two 96-well plates separately. Strains with a distinct profile from the two 96-well plates were merged into one and cross-immunity was repeated as described-above leading to 80 strains with a distinct profile (**Supplementary Table S1**). The 80 strains were stored individually.

16S rRNA Sequencing

Colony PCR was performed on antimicrobial-producing strains with a distinct cross-immunity profile. Cells were lysed in 10% Igepal 630 (Sigma-Aldrich, Germany) at 95°C for 10 min. PCR was performed in a total volume of 25 μL using 10 μL of Phusion

Green Hot Start II High Fidelity PCR master mix (Thermo Fisher Scientific), 10 μL of PCR-grade water, 1.5 μL of the non-specific primers 27F and 1495R (primer stocks at 0.1 ng μL^{-1}; Sigma-Aldrich) and 2 μL of DNA template from lysed cells. Amplification was carried out with reaction conditions as follows: initial denaturation at 98°C for 30 s, followed by 35 cycles of 98°C for 10 s, annealing at 55°C for 30 s and elongation at 72°C for 30 s with a final extension step at 72°C for 10 min.

To confirm species, degenerate primers targeting the *dnaJ* gene (Shah et al., 2007) forward primer, 5′-GCCAAAAGA GACTATTATGA-3′, and reverse primer, 5′-ATTGYTTACC YGTTTGTGTACC-3′, were used for the PCR reactions, following conditions described by Shah et al. (2007).

Five microliters of the resulting amplicons from each reaction were electrophoresed in a 1.5% (w/v) agarose gel. A GeneGenius Imaging System (Syngene, Cambridge, United Kingdom) was used for visualization. The PCR products were purified using the GeneJet Gel Extraction Kit (Thermo Fischer Scientific, Waltham, MA, United States). DNA sequencing of the forward strand was performed by Source BioScience (Tramore, Ireland). The resulting sequences were used for searching sequences deposited in the GenBank database using BLAST[1] and the identity of the isolates was determined on the basis of the highest scores (≥98%).

Spectrum of Inhibition

The spectrum of inhibition was completed on overnight cultures of 29 antimicrobial-producing isolates with a distinct immunity profile using 29 distinct indicator strains by a spot bioassay as described above with small modifications. More precisely, 5 μL of an overnight culture of the 29 antimicrobial-producing isolates were spotted on a clean TSA plate and incubated aerobically overnight at 37°C, before UV irradiation for 45 min. The rest of the procedure was performed as described above. The indicator strains employed to detect antimicrobial activity and their optimal growth conditions are listed in **Table 1**. Anaerocult A gas packs (Merck, Darmstadt, Germany) were used to generate anaerobic conditions where necessary for a selection of the indicator strains used in the study. Zone size was measured as follows: diameter of zone – diameter of spot in millimeters. The experiment was performed in three independent replicates.

DNA Extraction and Sequencing

Genomic DNA was extracted from the 79 strains (with the exception of *S. lugdunensis* APC 3758) using the DNeasy Blood and Tissue kit (Qiagen, Hilden, Germany) with slight modifications. For Gram positive bacteria, 2 mL of an overnight culture (TSB; 1% inoculum) were centrifuged at 18,078 *g* for 10 min and the supernatant was discarded. The cell pellet was resuspended in 180 μL of enzymatic lysis buffer and was incubated for 2 h at 37°C. The remaining steps were performed according to the original protocol. For the Gram-negative isolate *P. protegens* APC 3760, 2 mL of an overnight culture (TSB; 1% inoculum) were centrifuged at 18,078 *g* for 10 min and the supernatant was discarded. The cell pellet was resuspended in 180 μL buffer ATL with the remaining steps being performed according to the original protocol. Genomic DNA was quantified using a Qubit dsDNA HS Assay Kit (Invitrogen, Thermo Fisher Scientific, Waltham, MA, United States). Apart from *S. lugdunensis* APC 3758, the remaining 79 strains were subjected to library preparation using the Nextera XT DNA Library Preparation Kit (Illumina, San Diego, CA, United States) and bead-based normalization following the standard manufacturer's protocol. Ready-to-load libraries were sequenced using a proprietary modified protocol using 2 × 300 bp paired-end chemistry on an Illumina HiSeq 2500 platform (Illumina) at GATC Biotech AG, Germany.

Cells of *S. lugdunensis* APC 3758 were grown to mid-log phase in Tryptic Soy broth (TSB) and centrifuged at 2,400 *g* for 20 min. A 600 mg pellet of cells was then snap frozen by placing the centrifuge tube into ethanol which had been previously cooled for 24 h to −80°C. Chromosomal DNA was isolated by commercial sequence provider GATC Biotech, Ltd (Kostanz, Germany). Single-molecule real-time (SMRT) sequencing was performed on Pacific Biosciences RS II sequencing platform (executed by GATC Biotech, Ltd.).

The rapid sequencing kit (SQK-RAD004, Oxford Nanopore Technologies) was also used to prepare the *P. protegens* APC 3760 DNA library according to the manufacturer's instructions. *P. protegens* APC 3760 DNA was sequenced on a MinION device using R9.4 flow cell. The run duration was 24 h. Raw data was processed and basecalled using ONT Albacore Sequencing Pipeline Software (version 2.3.3).

Genome Assembly and Annotation

Following sequencing, Illumina adaptors were removed from fastq reads using CutAdapt (version 1.9.1; Martin, 2011). Paired-end adaptor-free reads were trimmed using Trimmomatic (version 0.32; Bolger et al., 2014) to a Phred score of 30 across a 4 bp sliding window. Surviving reads less than 70 bp were discarded. The final quality of reads was assessed using FastQC (version 0.11.5)[2]. Finally, both paired and unpaired Illumina reads were assembled using SPAdes (version 3.10.0; Nurk et al., 2017). Assembly of complete *S. lugdunensis* APC 3758 genome from raw Pacific Biosciences SMRT reads was done using Flye (version 2.4.1). Hybrid draft assembly of *P. protegens* APC 3760 genome from trimmed Illumina HiSeq and raw ONT MinION reads was performed using SPAdes in 'careful' mode. Annotation of the genomes was provided by the SEED viewer and the RAST annotation server (Overbeek et al., 2014).

Bacteriocin *in silico* Identification

The bacteriocin mining tool BAGEL3 (van Heel et al., 2013) was used to identify putative bacteriocin operons in combination with antiSMASH5 (Blin et al., 2019) which detects secondary metabolites. The genome visualization tool CLC Sequence viewer 8.0 (CLC Bio, Qiagen, Aarhus, Denmark) was subsequently used for manual analysis of the bacterial genomes. To determine the degree of novelty in the bacteriocins identified by BAGEL3 and antiSMASH5, BLASTP (Altschul et al., 1990) searches were performed for each putative bacteriocin peptide against

[1]http://www.ncbi.nlm.nih.gov/BLAST/

[2]http://www.bioinformatics.babraham.ac.uk/projects/fastqc/

TABLE 1 | Growth conditions for the indicator strains used in this study.

		Growth conditions		
Species	**Strain**	**Temperature (°C)**	**Atmosphere**	**Growth media**
Listeria monocytogenes	L028	37	Aerobic	BHI, TSB, MH
	ATCC 33007			
	EDG-e			
Bacillus cereus	DPC 6087	37	Aerobic	BHI, TSB, MH
B. subtilis	NCTC 10073	37	Aerobic	BHI, TSB, MH
Lactococcus lactis subsp. *cremoris*	HP	30	Aerobic	GM17
E. faecium	DPC 3675	37	Aerobic	BHI, TSB, MH
E. faecalis	ATCC 29200	37	Aerobic	BHI, TSB, MH
	DPC 5152			
	DSM 2570			
	VRE V583			
S. aureus	APC 3759	37	Aerobic	BHI, TSB, MH
	DPC 5243			
	Newman			
	DPC 7673			
	RF122			
M. luteus	DSM 1790	37	Anaerobic	BHI, TSB, MH
P. aeruginosa	PA01	30	Aerobic	BHI, TSB, MH
MRSA	BSAC ST528	37	Aerobic	BHI, TSB, MH
	BSAC ST530			
Escherichia coli	MG 1655	37	Aerobic	LB
	0157			
St. agalactiae	ATCC 13813	37	Aerobic	TSB, MH
St. uberis	DPC 5344	37	Aerobic	TSB, MH
C. kroppenstedtii	APC 3845	37	Anaerobic	TSB, MH
C. tuberculostearicum	APC 3844	37	Anaerobic	TSB, MH
Cutibacterium avidum	APC 3846	37	Aerobic	TSB, MH
St. salivarius	APC 3843	37	Anaerobic	TSB, MH
St. pyogenes	DPC 6992	37	Anaerobic	TSB, MH
Lactobacillus delbrueckii subsp. *bulgaricus*	LMG 6901	37	Anaerobic	MRS

ATCC, American Type Culture Collection; APC, APC Microbiome Ireland Culture Collection; DPC, Teagasc Culture Collection; LMG, Laboratorium voor Microbiologie, Universiteit Gent, Belgium; NCTC, National Collection of Type Cultures, Public Health England; BSAC, British Society for Antimicrobial Chemotherapy; DSM, Leibniz Institute DSMZ – German Collection of Microorganisms and Cells Cultures.

those identified in the BAGEL and antiSMASH screen. The levels of identity described in this study are derived from MUSCLE. Structural peptides were aligned using the Multiple Sequence Alignment (MSA) tool MUSCLE (Edgar, 2004) and then visualized using Jalview (Waterhouse et al., 2009). Novelty was defined when there was a difference of two or more amino acids between the predicted bacteriocin and the one which was previously discovered.

RESULTS

Isolation of Potential Antimicrobial-Producing Human Milk Isolates

Thirty-seven lactating mothers were recruited who agreed to donate milk samples. Approximately 5,100 colonies isolated from these samples were screened against three indicator organisms; *S. aureus* APC 3759, *Micrococcus luteus* DSM 1790 and *Pseudomonas aeruginosa* PA01. *S. aureus* APC 3759 was chosen as an indicator microorganism as it is not a bacteriocin producer and is just a representative strain. *P. aeruginosa* PA01 is a Gram-negative bacterial indicator whereas *M. luteus* DSM 1790 was selected based on its use to screen for antimicrobial activity (Janek et al., 2016; Wayah and Philip, 2018). No strain displayed inhibitory activity against *P. aeruginosa* PA01, but 174 potential antimicrobial-producing isolates were active against at least one of the other two indicators. Isolates with antimicrobial activity were identified in 25 out of 37 milk (67.6%) samples (data not shown).

One of the essential features of bacteriocin-producing bacteria is the requirement for immunity genes, which protect producers from the antimicrobial action of the bacteriocin they produce. Consequently, strains showing the same immunity pattern are likely to have the ability to produce the same bacteriocin(s). Based on the cross-immunity assay from 174 potential antimicrobial-producing isolates, 80 distinct

profiles were observed by eliminating strains that displayed cross-immunity and consequently suspected to produce the same or a very similar bacteriocin (**Supplementary Table S1**).

16S rRNA amplicon sequencing of the 80 antimicrobial-producing isolates revealed one Gram-negative bacterium namely *Pseudomonas protegens*, 47 *S. epidermidis isolates*, one *S. hominis*, one *S. lugdunensis*, 18 *S. aureus* isolates, one *Enterococcus faecalis*, and 11 *E. faecium* isolates. Subsequently, the genomes of the 80 identified isolates were sequenced to enable genome-mining to identify the antimicrobial encoding genes and their potential novelty.

Spectrum of Inhibition

We selected 29 of the 80 strains that exhibited the strongest inhibitory activity against the indicator organisms *S. aureus* APC 3759 and *M. luteus* DSM 1790 (data not shown) for examination of their inhibition spectra. **Table 2** shows the inhibition spectra of a panel of 29 antimicrobial producers against 29 indicators including known human mastitis pathogens such as *S. aureus* (Delgado et al., 2011), Methicillin Resistant *S. aureus* (MRSA) (Holmes and Zadoks, 2011), *Corynebacterium kroppenstedtii* (Wong et al., 2017) and *C. tuberculostearicum* (Paviour et al., 2002). The detected zones of inhibition could be attributed to any of the antimicrobial(s) produced by each of the tested strains. The antimicrobial produced by *E. faecalis* APC 3825 demonstrated the broadest spectrum of activity, inhibiting 19 of the indicator strains including vancomycin resistant *E. faecalis* V583, *S. aureus* APC 3759, *S. aureus* Newman, *S. aureus* DPC 5243, *St. pyogenes* DPC 6992, *C. tuberculostearicum* APC 3844 and the bovine mastitis pathogens *St. agalactiae* ATCC 13813 and *St. uberis* DPC 5344. *S. epidermidis* APC 3806, *S. epidermidis* APC 3804, and *S. epidermidis* APC 3782 inhibited 16, 15, and 14 of the indicators, respectively. All three of these *S. epidermidis* strains were isolated from the same donor (**Table 3**) yet their inhibition profile differed. *S. aureus* APC 3813 and *S. epidermidis* APC 3810 exhibited the narrowest inhibition spectra – inhibiting only three of the tested indicators. *S. lugdunensis* APC 3758 and *P. protegens* APC 3760 displayed inhibitory activity against the tested *S. aureus* strains, including the two MRSA strains, namely ST528 and ST530. Twenty-three of 29 strains inhibited the growth of *S. aureus* strains tested with only two impeding the specific MRSA strains tested. Representative zones of inhibition from a selection of the 29 potential bacteriocin producers are presented in **Figure 1**. None of the 29 potential bacteriocin producers inhibited *Corynebacterium kroppenstedtii* APC 3845, *Bacillus cereus* DPC 6087, *B. subtilis* NCTC 10073, *E. coli* MG1655 or *E. coli* O157.

Bacteriocin Identification

Bacteriocins are a divergent group of antimicrobials which utilize different systems for modification, transport, and immunity (Kotelnikova and Gelfand, 2002). We implemented an *in silico* approach to determine the diversity of the bacteriocins encoded by the 80 isolates which had a distinct immunity profile. The bacteriocin classification scheme suggested by Cotter et al. (2005, 2013) was used to distinguish between the different bacteriocin classes for Gram-positive bacteria with class I including lantibiotics and class II including the non-lantibiotics. This screen led to 49 isolates that contained 73 potential bacteriocin gene clusters (PBGCs) based on the predictions from BAGEL3 and antiSMASH5 (**Table 3** and **Figure 2**).

Additionally, BAGEL3 identified homologs of delta-lysins in 33 of the tested isolates and antiSMASH5 found genes associated with the production of terpenes, siderophores, polyketides (PKS), and Non-Ribosomal Peptide Synthetases (NRPSs) among a plethora of secondary metabolites (**Table 3**). Four potential bacteriocin gene clusters were excluded due to the absence of a detectable structural gene (*S. lugdunensis* APC 3758) or essential biosynthetic-associated genes (*P. protegens* APC 3760). Of the 69 bacteriocin gene clusters identified, one was identical to the previously characterized cytolysin from *E. faecalis* (Coburn and Gilmore, 2003), one to Enterocin 1071 (Balla et al., 2000) and three to the mature peptide of Enterocin P (Cintas et al., 1997) although in some cases the leader was atypical. The remaining 64 clusters represented potentially novel bacteriocin candidates belonging to class I (n = 11) and class II (n = 53) families. From the 64 potentially novel bacteriocin gene clusters (PBGCs) identified, 16 potentially novel bacteriocin prepeptides were potentially produced by a single strain while the rest were identified in more than one isolate. A flow chart of the procedures followed is presented in **Figure 2**.

Similar to Egan et al. (2018), the homology of the predicted bacteriocin gene clusters to existing genes and their genetic arrangement were examined. Below we grouped PBGCs by bacteriocin class.

Class I Bacteriocins

Class I bacteriocins are comprised of ribosomally produced, post-translationally modified bacteriocins (RIPPs). While initially lantibiotics were the sole occupant of class I bacteriocins, nowadays it includes more than 18 subclasses (Arnison et al., 2013).

Lantibiotics

The new lantibiotics predicted in this study (**Figure 3**) were grouped according to their amino acid similarity in order to facilitate comparison with previously characterized bacteriocins. Three lantibiotic gene clusters were detected in four genomes, including one classified as class IA and the remaining two as class IB (**Figure 3**). *S. epidermidis* APC 3775 and APC 3810 both potentially produce a class IA bacteriocin with a prepeptide displaying 81.8% similarity to epilancin 15X (Uniprot accession number: I6YXA9; Ekkelenkamp et al., 2005) and 24% to epidermin (P08136; Bierbaum et al., 1996) and contained the conserved domain PF08130 that corresponds to class IA lantibiotics.

In both of the strains encoding a class IA lantibiotic the bacteriocin modification, secretion, and immunity genes located within cluster type one (**Figure 3A**) exhibited strong similarities (>65%) to the bacteriocin-related genes of epilancin 15X (Elx, Velásquez et al., 2011). The cluster contained three putative immunity proteins, two modification enzymes (70.4% similarity with ElxC and 70.7% with ElxB), a protease (69.2% similarity with

TABLE 2 | Spectrum of inhibition of potential bacteriocin-producing human milk isolates against indicator strains by spot bioassays.

Isolates ↓/Indicator →	*L. monocytogenes* L028	*L. monocytogenes* ATCC 33007	*L. monocytogenes* EDGe	*L. lactis* HP	*M. luteus* DSM 1790	*E. faecium* DPC 3675	*E. faecalis* ATCC 29200	*E. faecalis* DPC 5152	*E. faecalis* DSM 2570	*E. faecalis* VRE V583	*S. aureus* APC 3759	*S. aureus* DPC 5243	*S. aureus* Newman	*S. aureus* MRSA ST528	*S. aureus* MRSA ST530	*S. aureus* DPC 7673	*S. aureus* RF122	*St. agalactiae* ATCC 13813	*St. uberis* ATCC 5344	*C. tuberculostearicum* APC 3844	*C. avidum* APC 3846	*St. salivarius* APC 3843	*St. pyogenes* DPC 6992	*L. bulgaricus* LMG 6901
***E.faecalis* APC 3825**	1.5± 0.3			11.5± 0.6	9.9± 0.2	10.6± 0.3	11.7± 0.5	2.5± 0.7	1.4± 0.4	7.6± 0.9	9.9± 0.2	5.3± 0.5	9.9± 0.2					7.4± 0.2	12.7± 0.4	1.4± 0.4	5.3± 0.5	7.6± 0.9	7.9± 0.3	
E.faecium																								
APC 3835	1.7± 0.2	5.1± 0.6	6.5± 0.6	4.9± 0.4			2.3± 0.3				2.1± 0.1							4.1± 0.4						
APC 3832	1.0± 0.2	4.7± 0.3	7.0± 0.5	5.3± 0.2		2.2± 0.3					2.5± 0.3													
APC 3836	1.5± 0.2	5.3± 0.5	7.0± 0.6	5.4± 0.2		2.1± 0.3	2.8± 0.2				2.7± 0.4							2.0± 0.6						
APC 3826	1.3± 0.2	5.8± 0.5	9.4± 0.5	5.2± 0.2		2.4± 0.2	2.0± 0.2				2.8± 0.6							2.0± 0.6						
APC 3830	1.0± 0.2	4.9± 0.5	7.2± 0.7	1.5± 0.4			2.8± 0.2				3.1± 0.2													
APC 3837	1.2± 0.2	5.0± 0.4	6.7± 0.4	6.3± 0.5							3.4± 0.1							1.9± 0.6						
APC 3831	1.1± 0.1	5.1± 0.4	6.2± 0.4	5.2± 0.6							4.5± 0.2							1.8± 0.6						
APC 3833		4.6± 0.4	6.5± 0.5	4.4± 0.3				4.4± 0.3			5.1± 0.3							4.2± 0.3						
APC 3829	2.2± 0.2		6.0± 0.4		4.2± 0.3						5.3± 0.2													
S.epidermidis																								
APC 3793					7.8± 0.3	9.7± 0.6	5.2± 0.2	6.0± 0.3		6.4± 0.4								5.8± 0.4						
APC 3803		3.0± 0.8		8.8± 0.5	4.0± 0.3	6.2± 0.3	4.1± 0.3	5.7± 0.4		5.3± 0.4								6.2± 0.4	5.9± 0.3					
APC 3801				13.6± 0.1	8.7± 0.4	8.7± 0.3	5.6± 0.4			6.4± 0.2		9.0± 0.5						6.4± 0.4	6.1± 0.3					
APC 3782	7.8± 0.5		6.0± 0.2		11.7± 0.5	12.6± 0.5	7.5± 0.3	12.0± 0.5		9.1± 0.4	4.5± 0.4					5.0± 0.3		12.0± 0.6	8.6± 0.4		7.4± 0.1	6.1± 0.8	7,4± 0.4	
APC 3804	5.0± 0.2		6.0± 0.2	17.3± 0.2	11.5± 0.4	5.8± 0.8	12.0± 0.4	11.9± 0.6		9.7± 0.5	6.0± 0.4					5.0± 0.4		11.0± 0.6	9.7± 0.3		9.0± 0.4	9.9± 0.5	6.6± 0.3	

(Continued)

TABLE 2 | Continued

Isolates ↓/Indicator →	*L. monocytogenes* L028	*L. monocytogenes* ATCC 33007	*L. monocytogenes* EDGe	*L. lactis* HP	*M. luteus* DSM 1790	*E. faecium* DPC 3675	*E. faecalis* ATCC 29200	*E. faecalis* DPC 5152	*E. faecalis* DSM 2570	*E. faecalis* VRE V583	*S. aureus* APC 3759	*S. aureus* DPC 5243	*S. aureus* Newman	*S. aureus* MRSA ST528	*S. aureus* MRSA ST530	*S. aureus* DPC 7673	*S. aureus* RF122	*St. agalactiae* ATCC 13813	*St. uberis* ATCC 5344	*C. tuberculostearicum* APC 3844	*C. avidum* APC 3846	*St. salivarius* APC 3843	*St. pyogenes* DPC 6992	*L. bulgaricus* LMG 6901
APC 3806	7.4± 0.2	1.5± 0.5		16.5± 0.7	10.3± 0.4	11.7± 0.3	8.6± 0.3	12.8± 0.2		9.2± 0.4	6.0± 0.2	9.1± 0.7				5.0± 0.2		10.9± 0.4	11.3± 0.4		10.3± 0.1	6.5± 0.8	5.9± 0.3	
APC 3810				5,6± 0.4							4.1± 0.2													7.9± 0.5
APC 3775				15.5± 0.2	7.0± 0.3	9.2± 0.3	5.5± 0.2	6.2± 0.2	7.7± 0.9	6.8± 0.4								5.8± 0.4	5.4± 0.3	11.1± 0.4		9.9± 0.4	6.1± 0.3	
S. aureus																								
APC 3774	3.6± 0.3			17.4± 0.3	14.3± 0.4	14.1± 0.5	6.5± 0.3	6.6± 0.2	8.9± 0.9	7.3± 0.4		10.3± 0.4						8.5± 0.3	6.3± 0.2	12.2± 0.5				
APC 3787	6.0± 0.3				7.9± 0.5	8.9± 0.4	6.7± 0.4	5.2± 0.3		6.0± 0.1								6.3± 0.3	6.3± 0.2					
APC 3887				20.0± 0.2	8.1± 0.3	7.6± 0.6	5.0± 0.3					11.5± 0.3												7.0± 0.3
APC 3809				9.7± 0.6	5,3± 0.6							8.7± 0.2						3.8± 0.3						7.4± 0.4
APC 3823				15.1± 0.2	9,1± 0.4							10.7± 0.2						2.7± 0.3						9.5± 0.3
APC 3813				9.6± 0.6	5.8± 0.3													5.2± 0.3						
APC 3822				3.9± 0.4	4.6± 0.5							5.3± 0.2						4.7± 0.5						
APC 3812				4,3± 0.4	4.8± 0.4													5.2± 0.4						3.1± 0.6
***S. hominis* APC 3824**						13.1± 0.5	7.8± 0.1			3.8± 0.6	4.7± 0.2													
***S. lugdunensis* APC 3758**											3.0± 0.2	3.0± 0.1	3.0± 0.2	3.1± 0.2	3.0± 0.2		2.9± 0.2						2.1± 0.2	
***P. proteogenes* APC 3760**											4.5± 0.3	4.0± 0.2	4.1± 0.3	3.5± 0.2	3.4± 0.4	2.9± 0.2	3.0± 0.2							

The numbers indicate the size of the inhibition zone with standard deviation. The zone size was measured as follows: diameter of zone – diameter of spot in millimeters. The experiment was performed in three independent replicates. None of the 29 potential bacteriocin producers inhibited C. kroppenstedtii APC 3845, B. cereus DPC 6087, B. subtilis NCTC 10073, E. coli MG1655 or E. coli O157.

TABLE 3 | Antimicrobial prediction by BAGEL3 and antiSMASH5 for the 80 bacterial isolates with distinct cross-immunity profile.

Donors	Strains	Bacteriocin		Delta-lysin	Siderophore	NRPS	CDPS	Phosphonate	Others
		BAGEL3	*antiSmash5*	*BAGEL3*	*antiSmash5*	*antiSmash5*	*antiSmash5*	*antiSMASH5*	*antiSMASH5*
H1	***S. aureus* APC 3809**	Class IId	–	2	Aureusimine	–	–	Terpene	
	***S. epidermidis* APC 3785**	Sactibiotic	–	–	Staphyloferrin	1	–	–	–
	***S. epidermidis* APC 3771; APC 3761; APC 3762; APC 3763; APC 3764; APC 3766; APC 3769; APC 3770**	–	–	1	Staphyloferrin	1	–	–	–
	***S. epidermidis* APC 3768; APC 3771; APC 3773**	–	–	–	Staphyloferrin	1	–	–	–
H2	***S. aureus* APC 3774**	Class IId		–	2	Aureusimine	–	–	Terpene
	***S. epidermidis* APC 3810**	Class IA; Class IId		1	Staphyloferrin	1	–	–	–
	***E. faecalis* APC 3825**	Class IB; Class IIb		–	–	–	–	–	–
	***S. epidermidis* APC 3775**	Class IA; Class IId; Sactibiotic	Class IA; Class IId	–	Staphyloferrin	1	–	–	–
H3	***E. faecium* APC 3827**	Class IIa; Class IIc		–	–	–	–	–	–
	***S. epidermidis* APC 3776; APC 3777**	–	–	1	Staphyloferrin	1	–	–	–
H4	***S. epidermidis* APC 3778**	–	Class IIc	–	Staphyloferrin	1	–	–	–
	***S. epidermidis* APC 3779**	–	Class IIb	–	Staphyloferrin	1	–	–	–
H5	***E. faecium* APC 3828; APC 3880**	Class IIa; Class IIc		–	–	–	–	–	–
	***S. epidermidis* APC 3780**	–		1	Staphyloferrin	1	–	–	–
	***S. aureus* APC 3821; APC 3881**	–		–	2	Aureusimine	–	–	Terpene
	***S. aureus* APC 3829**	Class IIc		–	2	Aureusimine	–	–	Terpene
	***S. epidermidis* APC 3882**	Sactibiotic	–	1	Staphyloferrin	1	–	–	–
H6	***S. aureus* APC 3822**	Class IIc		–	2	Aureusimine	–	–	Terpene
	***S. epidermidis* APC 3787; APC 3788; APC 3789; APC 3790; APC 3791**	–		–	Staphyloferrin	1	–	–	–
H7	***S. epidermidis* APC 3792; APC 3793**	–		1	Staphyloferrin	1	–	–	–
	S. hominis APC 3824	Class IB		–	1	–	–	1	-
	***S. epidermidis* APC 3794**	Sactibiotic	–	1	Staphyloferrin	1	–	–	–
H8	***S. epidermidis* APC 3781; APC 3795; APC 3798**	–		1	Staphyloferrin	1	–	–	–
	***S. epidermidis* APC 3796; APC 3797; APC 3883**	Sactibiotic	–	1	Staphyloferrin	1	–	–	–

(Continued)

TABLE 3 | Continued

Donors	Strains	Bacteriocin		Delta-lysin	Siderophore	NRPS	CDPS	Phosphonate	Others
		BAGEL3	*antiSmash5*	*BAGEL3*	*antiSmash5*	*antiSmash5*	*antiSmash5*	*antiSMASH5*	*antiSMASH5*
H9	***S. epidermidis* APC 3799; APC 3800; APC 3803**	–		1	Staphyloferrin	1	–	–	–
	***S. epidermidis* APC 3801; APC 3802**	–	Class IIb	–	Staphyloferrin	1	–	–	–
H10	***S. epidermidis* APC 3804; APC 3805; APC 3806**	Class IId; Class IIc		1	Staphyloferrin	1	1	–	–
	***S. epidermidis* APC 3782**	Sactibiotic; Class IId; Class IIc	Class IId; Class IIc	1	Staphyloferrin	1	1	–	–
H11	***S. epidermidis* APC 3783; APC 3784**	–		–	Staphyloferrin	1	–	–	–
	***S. aureus* APC 3814**	Class IIc		–	2	Aureusimine	–	–	Terpene
H12	***S. epidermidis* APC 3807**	–		1	Staphyloferrin	1	1	–	–
H13	***S. epidermidis* 3808**	Sactibiotic	–	1	Staphyloferrin	–	–	–	–
H14	***P. protegens* APC 3760**	Putidacin L1-like	2	–	–	6	1	–	Type III PKS; Type I PKS; betalactone; pyrrolnitrin; homoserine lactone cluster; arylpolyene
H15	***S. lugdunensis* APC 3758**	TOMM		–	1	3	1	–	Terpene
H16	***S. aureus* APC 3812; APC 3816; APC 3823;**	Class IId		–	2	Aureusimine	–	–	Terpene
H17	***S. aureus* APC 3813**	Class IIc	–	–	2	Aureusimine	–	–	Terpene
H18	***S. aureus* APC 3818; APC 3884**	Class IIc	–	–	2	Aureusimine	–	–	Terpene
H19	***S. aureus* APC 3885**	–		–	2	Aureusimine	–	–	Terpene
	***S. aureus* APC 3886; APC 3887**	Class IIc	–	–	2	Aureusimine	–	–	Terpene
H20	***S. aureus* APC 3819**	Class IIc	–	–	2	Aureusimine	–	–	Terpene
	***E. faecium* APC 3830; APC 3831; APC 3832; APC 3833; APC 3835; APC 3837**	Class IIa; Class IIc		–	–	–	–	–	–
H21	***S. aureus* APC 3820**	Class IIc; Class IId	–	1	2	Aureusimine	–	–	Terpene
H22	***S. aureus* APC 3815**	Class IIc	–	1	2	Aureusimine	–	–	Terpene
H23	***E. faecium* APC 3826**	Class IIa; Class IIc		–	–	–	–	–	–
H24	***E. faecium* APC 3836**	Class IIa; Class IIc		–	–	–	–	–	–
H25	***E. faecium* APC 3827**	Class IIa; Class IIc		–	–	–	–	–	–

The isolates are grouped per donor from whom the bacteria were isolated.

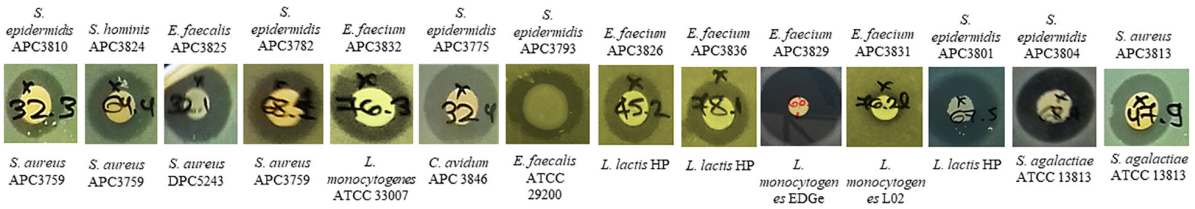

FIGURE 1 | Representative zones of inhibition from a selection of the 29 antimicrobial producers that demonstrated the strongest inhibition against *S. aureus* APC 3759 and *M. luteus* DSM 1790 against a selection of the 29 indicator strains.

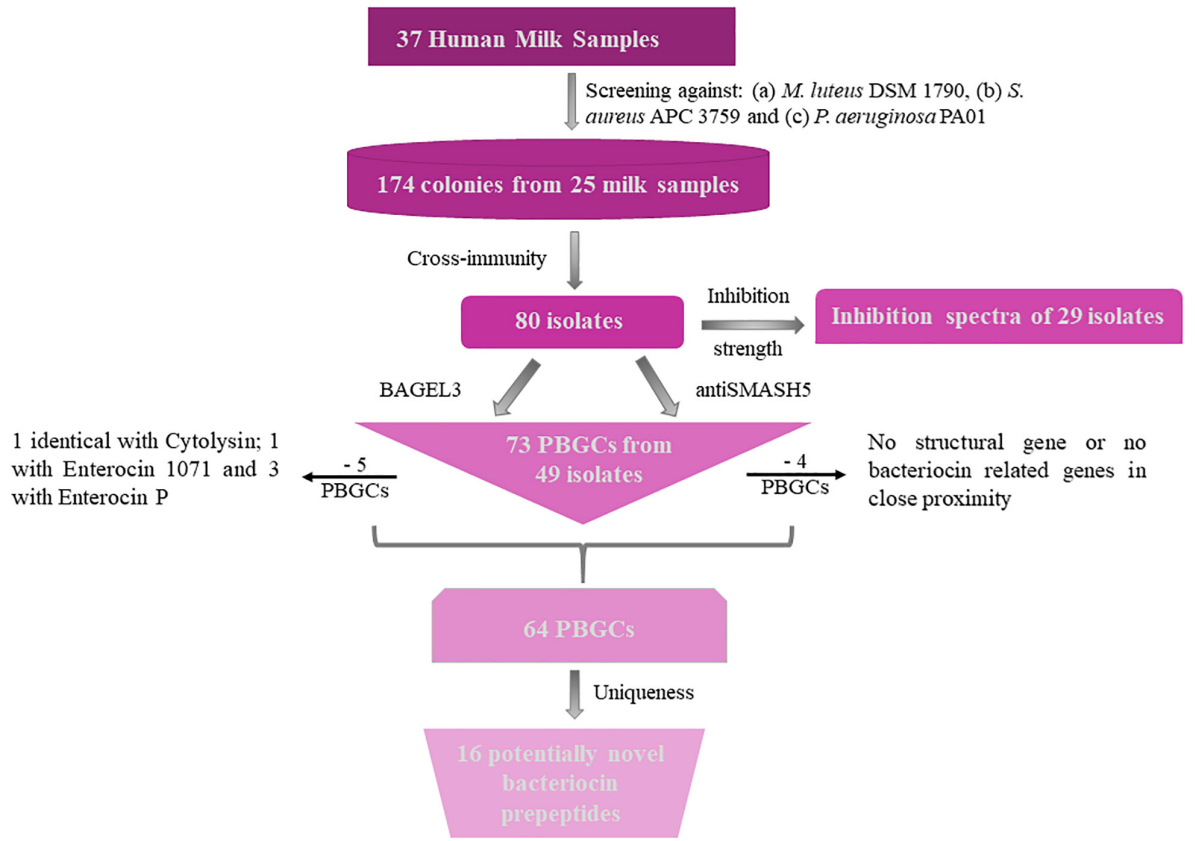

FIGURE 2 | Flow chart of bacteriocin screening performed for this study. PBGC stands for Potential Bacteriocin Gene Cluster.

ElxP), an ABC transporter (80.8% similarity with ElxT) and a third modification enzyme (78.6% similarity with ElxT).

Cytolysin (Uniprot accession number: Q52052 and GenBank accession number: P08136), a two-component class IB lantibiotic, was identified in *E. faecalis* APC 3825 (IB cluster type 1; **Figure 3B**). An additional class IB bacteriocin gene cluster, was found in *S. hominis* APC 3824, encoding a complete class IB lantibiotic (IB, cluster type 2). In *S. hominis* APC 3824, peptide α displayed 28.8% amino acid similarity with haloduracin α while peptide β displayed 33.3% amino acid similarity to haloduracin β (**Figure 3B**). The operon of APC 3824 contained several lantibiotic-related genes including two LanM enzymes (conserved domain PF0145), a putative peptidase (conserved domain PF00082) and two ABC transporters containing ATP-binding subunits (conserved domain PF00005). The operon also contained a two-component regulatory system comprised of a putative histidine kinase (conserved domain PF00512) and a putative transcriptional response regulator (conserved domains PF00072 and PF00486).

Sactibiotics

The sactibiotics are a subgroup of Class I bacteriocins that are characterized by intramolecular bridges between cysteine sulfur and α-carbon covalent bonds (Mathur et al., 2015). These modifications are performed by radical *S*-adenosylmethionine (SAM) proteins which catalyze the formation of these thioether bonds (Rea et al., 2010).

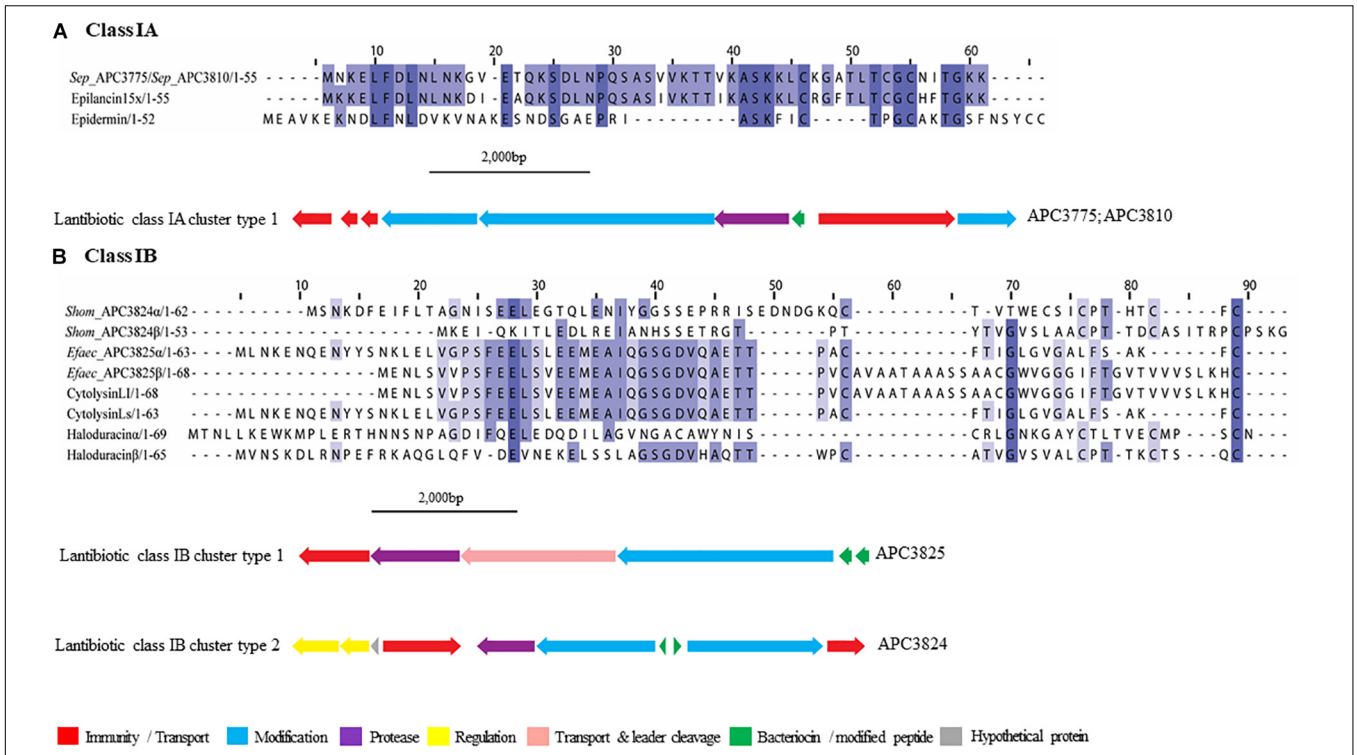

FIGURE 3 | Multiple Sequence Alignments (MSA) of lantibiotic prepeptides and biosynthetic gene clusters. **(A)** Class IA MSA and predicted biosynthetic gene cluster. *Sep* stands for *S. epidermidis*. The same prepeptide was identified in *S. epidermidis* APC 3775 and APC 3810. **(B)** Class IB MSA and predicted biosynthetic gene clusters. *Shom* and *Efaec* stand for *S. hominis* and *E. faecalis* respectively.

Four putative distinct sactibiotic peptides were predicted within eight *S. epidermidis* genomes (**Figure 4A**). However, when these predicted peptides were aligned with known sactibiotics, little homology was found (<20.6%).

Upstream of the gene encoding the putative bacteriocins of *S. epidermidis* APC 3785, APC 3796, APC 3797, and APC 3883 (Sactibiotics cluster type 1; **Figure 4B**), we detected a SAM protein (conserved domain PF04055) and an ABC transporter containing ATP-binding and permease subunits (conserved domain PF00005). The cluster also comprised a two-component regulatory system consisting of a response regulator and a histidine kinase (conserved domains PF00486, PF00072, PF00512, and PF02518, respectively). *S. epidermidis* APC 3782 had a different structural gene, even though the operon organization was similar to that of *S. epidermidis* APC 3785, APC 3796, APC 3797 and APC 3883. Downstream of the gene encoding the putative bacteriocin of *S. epidermidis* APC 3794 (Sactibiotics cluster type 2), we detected genes encoding a SAM protein (conserved domain PF04055), an ABC transporter comprised of ATP-binding (conserved domain PF00005) and permease subunits. The bacteriocin gene cluster also encoded a response regulator receiver domain, followed by a response regulator C-terminal domain and a histidine kinase. The genes encoding putative peptides of *S. epidermidis* APC 3775 (Sactibiotics cluster type 3; **Figure 4B**) and *S. epidermidis* APC 3882 (Sactibiotics cluster type 4; **Figure 4B**) were located downstream of the determinants for a histidine kinase (conserved domains PF00512; PF02518), a transcriptional response regulator (conserved domains PF00486; PF00072), an ABC transporter comprised of ATP-binding (conserved domain PF00005) and permease subunits and a SAM protein (conserved domain PF04055).

Class II Bacteriocins

Class II bacteriocins are defined by their unmodified nature (Eijsink et al., 2002) and their ability to permeabilize the membrane of target cells (Cotter et al., 2013). They are further divided based on the structure and activity of each class.

Class IIa bacteriocins

Four class IIa bacteriocins were detected by BAGEL3 in 11 *E. faecium* strains (**Figure 5A**) isolated from five different milk samples (**Table 3**). The prepeptide of *E. faecium* APC 3826 and APC 3828 displayed 94.4% similarity with Enterocin P (Uniprot accession number O30434; Cintas et al., 1997). The prepeptide identified in the genomes of *E. faecium* APC 3827, APC 3831, APC 3832, APC 3836, and APC 3837 was over 94.0% similar to Enterocin P while, *E. faecium* APC 3830, APC 3833, APC 3835, and APC 3880 had 100% identity to the mature peptide of Enterocin P, although the leader was different to Enterocin P by two amino acids (**Figure 5A**).

When the putative bacteriocin gene clusters were further assessed, four different gene clusters were obvious (**Figure 5B**).

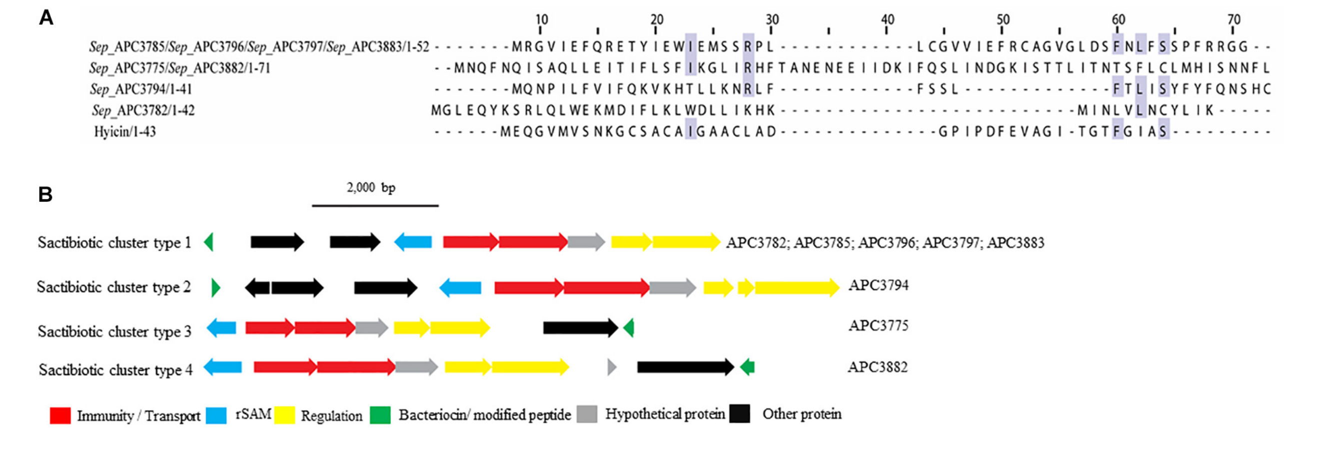

FIGURE 4 | Multiple Sequence Alignments (MSA) of sactibiotic prepeptides and biosynthetic gene clusters. **(A)** MSA of the identified sactibiotic prepeptides and the known sactibiotic hyicin. *Sep* stands for *S. epidermidis.* The same prepeptide was identified in *S. epidermidis* APC 3785, APC 3796, APC 3797, and APC 3883. The same applied for the prepeptide identified in *S. epidermidis* APC 3775 and APC 3882. **(B)** Biosynthetic gene clusters of identified sactibiotics.

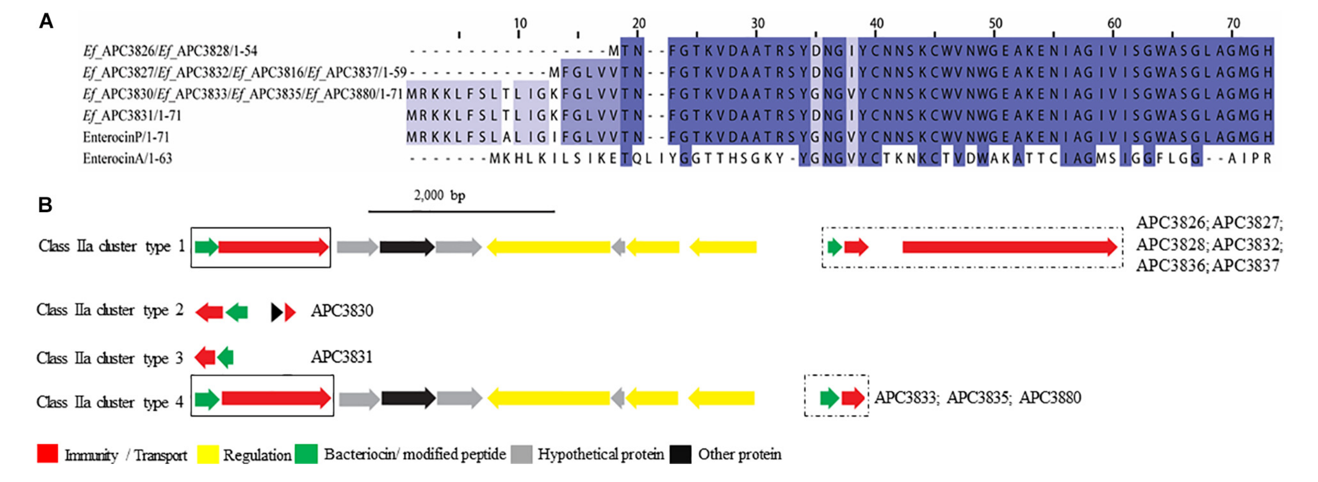

FIGURE 5 | Multiple Sequence Alignments (MSA) of class IIa bacteriocin prepeptides and biosynthetic gene clusters. **(A)** MSA of the identified class IIa prepeptides and known bacteriocins Enterocin P (Uniprot accession number O30434) and Enterocin A (Uniprot accession number C8C4N1). *Ef* stands for *E. faecium.* The same prepeptide was detected in *E. faecium* APC 3826 and APC 3828. The same applied for *E. faecium* APC 3827, APC 3832, APC 3836, and APC 3837. Moreover, an identical prepeptide was found in the genomes of *E. faecium* APC 3830, APC 3833, APC 3835, and APC 3880. **(B)** Biosynthetic gene clusters of identified class IIa bacteriocins. Class IIa-related proteins are surrounded by a solix box while class IIc-related proteins are encompassed in a dashed box.

E. faecium APC 3826, 3827, 3828, 3832, 3836, and 3837 (IIa cluster type 1) belonged to the same bacteriocin gene cluster which contained two genes including a gene encoding a putative bacteriocin (conserved domain PF01721). The cluster also consisted of a gene encoding an immunity protein (Uniprot accession number O30435; 98.9% identity to EntP immunity protein). *E. faecium* APC 3830 was the sole isolate encoding a class IIa cluster type 2 (**Figure 5B**) that comprised two genes encoding bacteriocin-related proteins namely, immunity proteins. One of them was located downstream of the prepeptide (98.9% similarity to EntP immunity protein) while the second one (100% identity to EntP immunity protein) was located upstream of the structural gene (conserved domain PF01721). The bacteriocin gene cluster of *E. faecium* APC 3831 (IIa cluster type 3; **Figure 5B**) consisted of two bacteriocin-related genes. Class IIa cluster type 3 comprised of an immunity protein (98.9% identity to immunity protein of EntP) located downstream of the structural gene (**Figure 5B**). *E. faecium* APC 3833, APC 3835, and APC 3880 encode the same gene cluster (IIa cluster type 4; **Figure 5B**) which is comparable to cluster type I apart from the absence of the gene encoding an ABC transporter.

Class IIb bacteriocins

Class IIb is comprised of two-peptide bacteriocins where the optimal antimicrobial activity requires the synergistic activity of both peptides (Nissen-Meyer et al., 2010). Two class IIb bacteriocin clusters were identified by BAGEL3 and antiSMASH5 (**Figures 6A,B**). BAGEL3 identified a bacteriocin gene cluster in *E. faecalis* APC 3825 where the prepeptide is 100% identical to Enterocin 1071 (Uniprot accession numbers: Q9L9U6 for

Enterocin 1071A and Q9L9U5 for Enterocin 1071B; Balla et al., 2000). A further class IIb operon was identified by antiSMASH5 in three *S. epidermidis* strains which were isolated from two milk samples (**Table 3**). The α prepeptide identified in *S. epidermidis* APC 3779, APC 3801, and APC 3802 was 36.4% similar to Lactococcin Gα (Uniprot accession number C5IHS6; Moll et al., 1996; **Figure 6A**) while the β prepeptide displayed 24.0% identity with Lactococccin Gβ (Uniprot accession number C5IHS7; **Figure 6A**; Moll et al., 1996; **Figure 6B**).

The bacteriocin gene cluster identified in *E. faecalis* APC 3825 displayed similar genetic organization to Enterocin 1071 (Balla and Dicks, 2005) with the putative immunity gene being 39.8% similar to the immunity protein of Lactococcin G and located downstream of the structural α gene (conserved domains PF08129 and PF10439). The cluster also contained genes encoding an ABC transporter responsible for export and cleavage of the bacteriocin (conserved domains PF00005 and PF03412) and an accessory protein, both located upstream of the second structural gene (conserved domains PF08129 and PF10439; **Figure 6C**). A second bacteriocin gene cluster was identified in three *S. epidermidis* isolates, namely APC 3779, APC 3801, and APC 3802. The identified bacteriocin gene cluster contained simple genetic organization with the gene encoding an ABC transporter (conserved domains PF00005 and PF03412) being located upstream of the α structural gene (**Figure 6C**).

Class IIc bacteriocins

Class IIc bacteriocins are known as circular bacteriocins because of the covalent linkage of the N- to C- termini. Apart from being highly hydrophobic, known members of class IIc bacteriocins display little homology to each other (Martin-Visscher et al., 2011). These bacteriocins act by targeting the cytoplasmic membrane leading to pore formation and eventual cell death (Perez et al., 2018).

Five potential class IIc bacteriocins (NCBI conserved domain TIGR03651) were detected (**Figure 7A**). More specifically, one potential class IIc bacteriocin was found in three *S. epidermidis* strains (APC 3782, APC 3804, and APC 3805) which were isolated from the same milk sample (**Table 3**) and displayed only 30.8% similarity to the circular bacteriocin Enterocin NKR-5-3B (Himeno et al., 2015; Uniprot accession number A0A0P0YL94). Moreover, a second putative class IIc bacteriocin was found in *S. epidermidis* APC 3778 with the prepeptide being 26.2% similar to Enterocin NKR-5-3B (**Figure 7A**). A third class IIc bacteriocin was detected in ten *S. aureus* strains (APC 3813, APC 3814, APC 3815, APC 3818, APC 3819, APC 3820, APC 3822, APC 3884, APC 3886, APC 3887) isolated from eight milk samples (**Table 3**) and the detected prepeptide was 30.1% similar to Enterocin NKR-5-3B (Uniprot accession number A0A0P0YL94). Furthermore, a fourth class IIc prepeptide was detected in *S. aureus* APC 3829 which exhibited 24.2% similarity to Enterocin NKR-5-3B (**Figure 7A**). Finally, a fifth class IIc prepeptide was found in 11 *E. faecium* strains (APC 3826, APC 3827, APC 3828, APC 3830, APC 3831, APC 3832, APC 3833, APC 3835, APC 3836, APC 3837, and APC 3880) isolated from six milk samples (**Table 3**) with the prepeptide sharing 95.4% similarity to Enterocin NKR-5-3B (Uniprot accession number A0A0P0YL94).

Five putative bacteriocin gene clusters for circular bacteriocins were identified (**Figure 7B**). Class IIc cluster type 1 is comprised of the three *S. epidermidis* strains (APC 3782, APC 3804, and APC 3805) and exhibits a simple genetic organization. The cluster was comprised of a gene encoding an ABC transporter containing an ATP-binding domain (conserved domain PF00005) located upstream of the putative bacteriocin (**Figure 7B**). *S. epidermidis* APC 3778 contained a bacteriocin gene cluster (Class IIc cluster type 2; **Figure 7B**) which consisted of a gene encoding an ABC transporter with a peptidase domain for cleaving the leader (conserved domains PF00005 and PF03412) located upstream of the putative bacteriocin. All ten *S. aureus* strains had the same organization in the bacteriocin gene cluster (IIc cluster type 3) which contained several bacteriocin-related genes including a transcriptional regulator and an ABC transporter containing an ATP-binding subunit. The bacteriocin gene cluster also consisted of genes encoding an ABC transporter composed of ATP-binding and permease subunits (conserved domain PF00005) located upstream of the putative structural gene (**Figure 7B**). *S. aureus* APC 3829 encoded a bacteriocin gene cluster (class IIc cluster type 4) which contained a transcriptional regulator and an ABC transporter (conserved domain PF00005) flanking the structural gene (**Figure 7B**). Within the 11 *E. faecium* strains, sharing identical structural genes, three subclasses were defined based on the organization of the gene clusters. All sub-clusters comprised of genes encoding an ABC transporter that contained ATP-binding and permease subunits (conserved domain PF00005). The sub-clusters were also composed of genes encoding a putative histidine kinase, a putative accessory protein regulator B gene and a response regulator transcription factor. The transcription factors are implicated in bacteriocin regulation, although it is not yet known to which of the two (class IIc or class IIa) bacteriocins they belong (class IIc cluster type 5a-5c; **Figure 7B**).

Class IId bacteriocins

Class IId bacteriocins are linear, single peptide bacteriocins that display no homology to class IIa bacteriocins (Cotter et al., 2013). One member of this class is Lactococcin 972, which is encoded as a 91-amino-acid prepeptide that includes a 25-amino-acid sec-dependent signal peptide and the final mature peptide (66 amino acids) (Martínez et al., 1999). Lactococcin 972 inhibits the growth of susceptible cells by interfering with septum formation (Martínez et al., 2000).

Two class IId prepeptides were identified in the study with the first being detected in six *S. epidermidis* strains identified from two human milk samples and displayed 21.1% similarity with Lactococcin 972 (Uniprot accession number: O86283; **Figure 8A**). The second was found in six *S. aureus* strains which were isolated from four human milk samples and was 36.3% similar to Lactococcin 972 (Uniprot accession number: O86283; **Figure 8A**).

Two bacteriocin class IId gene clusters were detected in this study with one being identical in all *S. epidermidis* (class IId cluster type 1) genomes while the other one was identical in all

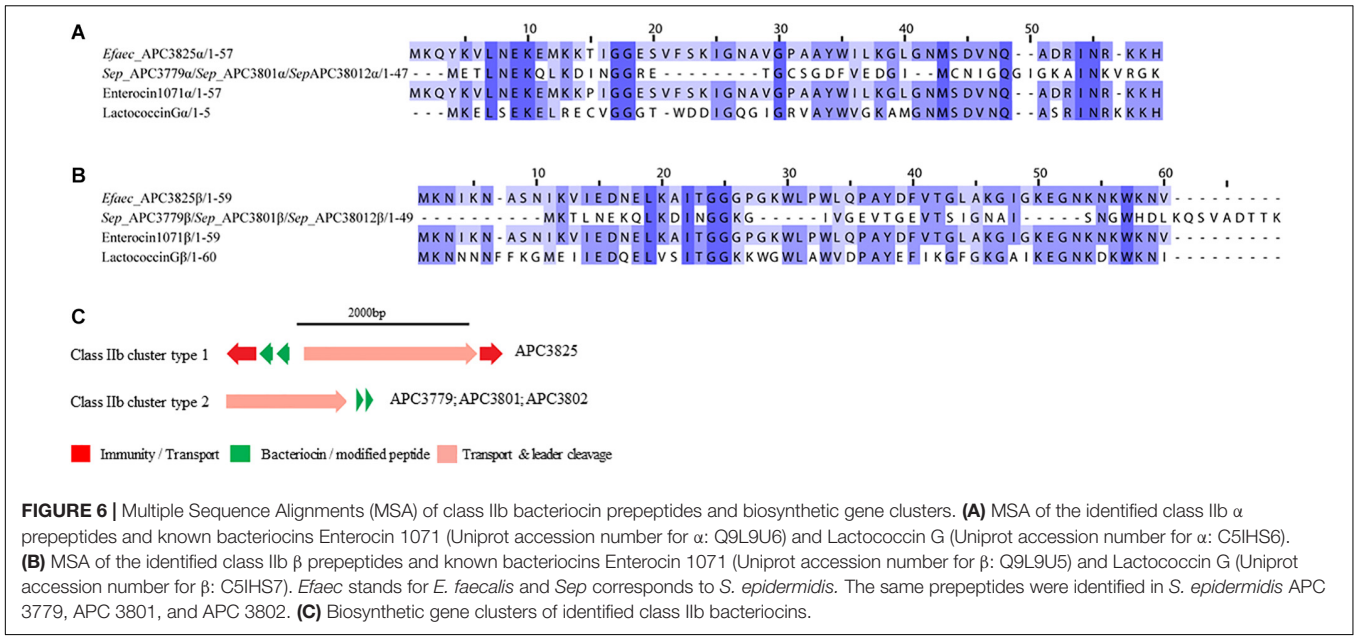

FIGURE 6 | Multiple Sequence Alignments (MSA) of class IIb bacteriocin prepeptides and biosynthetic gene clusters. **(A)** MSA of the identified class IIb α prepeptides and known bacteriocins Enterocin 1071 (Uniprot accession number for α: Q9L9U6) and Lactococcin G (Uniprot accession number for α: C5IHS6). **(B)** MSA of the identified class IIb β prepeptides and known bacteriocins Enterocin 1071 (Uniprot accession number for β: Q9L9U5) and Lactococcin G (Uniprot accession number for β: C5IHS7). *Efaec* stands for *E. faecalis* and *Sep* corresponds to *S. epidermidis*. The same prepeptides were identified in *S. epidermidis* APC 3779, APC 3801, and APC 3802. **(C)** Biosynthetic gene clusters of identified class IIb bacteriocins.

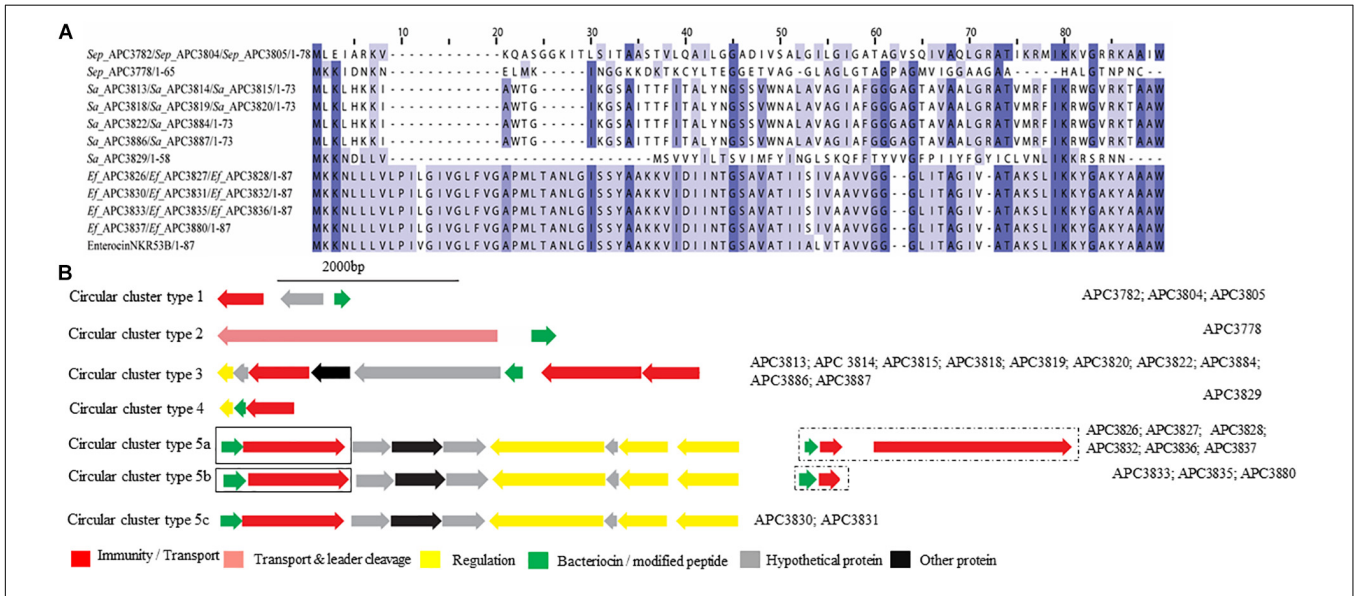

FIGURE 7 | Multiple Sequence Alignments (MSA) of class IIc bacteriocin prepeptides and biosynthetic gene clusters. **(A)** MSA of the identified class IIc prepeptides and known bacteriocin EnterocinNKR-5-3B (Uniprot accession number A0A0P0YL94). *Sep* corresponds to *S. epidermidis*, *Sa* stands for *S. aureus* and *Ef* for *E. faecium*. The same prepeptide was identified in *S. epidermidis* APC 3782, APC 3804, and APC 3805. The same prepeptide was detected in *S. aureus* APC 3813, APC 3814, APC 3815, APC 3818, APC 3819, APC 3820, APC 3822, APC 3884, APC 3886, and APC 3887. Also, identical prepeptide was found in the genomes of *E. faecium* APC 3826, APC 3827, APC 3828, APC 3830, APC 3831, APC 3832, APC 3833, APC 3835, APC 3836, APC 3837, and APC 3880. **(B)** Biosynthetic gene clusters of identified class IIc bacteriocins. Class IIc-related proteins are surrounded by a dashed box while class IIa-related proteins are encompassed in a solid box.

S. aureus genomes (class IId cluster type 2; **Figure 8B**). Class IId cluster type 1 displayed a simple genetic organization with genes encoding an ABC transporter containing a permease and an ATP-binding subunit (conserved domain PF00005), being located downstream of the structural gene (**Figure 8B**). Class IId cluster type 2 on the other hand, exhibited a different genetic organization and contained several bacteriocin-related genes including a putative immunity gene upstream of the structural gene and an ABC transporter containing a permease domain (conserved domain PF00005).

DISCUSSION

This study aimed to characterize bacteriocin producing strains isolated from healthy milk samples, combining both *in silico*

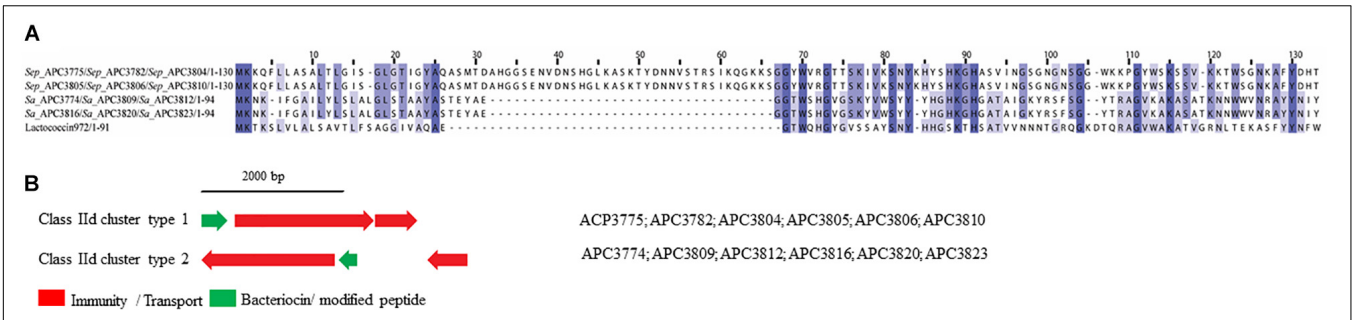

FIGURE 8 | Multiple Sequence Alignments (MSA) of class IId bacteriocin prepeptides and biosynthetic gene clusters. **(A)** MSA of the identified class IId prepeptides and known bacteriocin Lactococcin 972 (Uniprot accession number O86283). *Sep* corresponds to *S. epidermidis* and *Sa* stands for *S. aureus*. The same prepeptide was identified in *S. epidermidis* APC 3775, APC 3782, APC 3804, APC 3805, APC 3806, and APC 3810. The same prepeptides were detected in *S. aureus* APC 3774, APC 3809, APC 3812, APC 3813, APC 3816, APC 3820, and APC 3823. **(B)** Biosynthetic gene clusters of identified class IId bacteriocins.

and *in vitro* screening methods. This combinatorial approach enabled a more comprehensive estimation of bacteriocin production associated with human breast milk. Nevertheless, bacteriocin production can be a highly regulated process with strains requiring specific conditions and environments to induce production of these antimicrobials (Diep et al., 2000; Maldonado-Barragan et al., 2013). Therefore, the use of BAGEL3 and antiSMASH5 for bacteriocin screening facilitated the identification of bacteriocin operons in the 80 isolates with distinct immune profiles without the drawbacks and constraints of *in vitro* screening.

We screened strains isolated from the milk of 37 asymptomatic donors and found that 25 donors (67.6%) harbored strains with antimicrobial activity (**Table 3**) under the conditions tested. The isolated strains from the milk could have originated from the mother's skin, the infant's oral cavity, and/or the entero-mammary pathway (Angelopoulou et al., 2018), thus we cannot be certain about the source. During the initial screening, we observed activity against *S. aureus* APC 3759 and/or *M. luteus* DSM 1790. However, none of the strains exhibited activity against *P. aeruginosa* PA01 which is not unexpected, as bacteriocins produced by Gram-positive bacteria generally do not inhibit Gram-negative bacteria (Nikaido and Vaara, 1985; Nikaido, 2003). The majority of the bacterial species identified in this study encoding bacteriocin gene clusters are also known to encode virulence factors (Giormezis et al., 2015; Chessa et al., 2016; Madsen et al., 2017). Moreover, *S. aureus* and *S. epidermidis* are known as opportunistic pathogens in human mastitis (Angelopoulou et al., 2018). In addition, *Staphylococcus* and *Pseudomonas* belong to the healthy core milk microbiota (Boix-Amorós et al., 2016; Padilha et al., 2019). Among the isolated bacteria with high antimicrobial activity, it is notable the almost complete absence of members of the LAB group, with either high antimicrobial activity or encoding potential bacteriocins.

Cross-immunity screening resulted in the identification of 80 isolates with distinct profiles. Interestingly, strains *S. epidermidis* APC 3761, APC 3769, and APC 3772 came from the same donor (**Table 3**) yet they exhibited different cross-immunity profiles. However, these strains, also demonstrated immunity to the bacteriocin(s) produced by others of the same species, suggesting that these three strains might be distinct. In contrast, *S. epidermidis* APC 3765 and *S. epidermidis* APC 3790 demonstrated identical cross-immunity profiles even though they originated from different donors. This may be explained by the fact that different people harbor bacteria that produce the same bacteriocin(s). A similar situation was observed for *E. faecium* APC 3828, APC 3833, APC 3834, *Lactobacillus gasseri* APC 3841 and *C. kroppenstedtii* APC 3845, which exhibited identical immunity profiles though they originated from different donors and were produced by different species. We observed the same phenomena with other strains (**Supplementary Table S1**).

The combined use of BAGEL3 and antiSMASH5 in conjunction with the applied criteria led to the identification of 64 novel bacteriocin gene clusters. Among them, 16 (25%) novel bacteriocins were found while the remaining 48 bacteriocin gene clusters were identified in more than one isolate. The identified peptides belonged to all bacteriocin classes and included two lantibiotics, four sactibiotics, three class IIa, one class IIb, four circular (class IIc) and two class IId bacteriocins. This confirms that human milk is a rich source of bacteriocin producing strains. The identified bacteriocins targeted major human and bovine mastitis pathogens such as *S. aureus*, *C. tuberculostearicum* and *St. agalactiae* implying that breast milk microbiota could potentially play a beneficial role in the mammary health of lactating women by preventing breast infections and inflammation (Hunt et al., 2011). Some of the bacteriocin producing strains also potentially produce toxins. In contrast, bacteriocin producers have the potential to alter the intestinal ecology (Murphy et al., 2013), this may apply to the mammary gland of lactating women and could also influence the infant gastrointestinal tract (GIT) microbiota and the endogenous immune system, reinforcing the benefits of continued breastfeeding.

In the majority of the genomes (n = 66), antiSMASH5 identified secondary metabolites with potential antimicrobial activities, among others siderophores (Kohira et al., 2016), NRPSs including a lugdunin producer (a recently found thiazolidine-containing cyclic peptide antibiotic that prohibits colonization by *S. aureus*) (Zipperer et al., 2016), PKS (Zhang et al., 2014;

Li et al., 2018), terpenes (Gallucci et al., 2009; Zengin and Baysal, 2014), and pyrrolinitrin (el-Banna and Winkelmann, 1998). In 32 of the isolates, BAGEL3 also identified delta-lysins, which are members of the hemolytic polypeptide family toxins produced by staphylococci and known for their antimicrobial activity (Al-Mahrous et al., 2010). However, little is known about the regulation of the production of the aforementioned secondary metabolites in natural environments such as human milk.

Our study identified three lantibiotic gene clusters, one class IA and two class IB, from four isolates. Lantibiotics are small peptides that contain internal thioether bridges due to the interaction of dehydroalanine (Dha) or dehydrobutyrine (Dhb) with intrapeptide cysteines, resulting in the formation of (β-methyl)lanthionine residues (Lan/MeLan; McAuliffe et al., 2000). The formation of Lan/MeLan is catalyzed by LanB and LanC in class IA lantibiotics such as nisin with LanB catalyzing the dehydration of amino acids and LanC catalyzing thioether formation (Marsh et al., 2010). The biosynthesis of class IB lantibiotics is catalyzed by a single LanM enzyme with both dehydratase and cyclase activity. Class IA prepeptides have an FNLD conserved region at positions −15 and −20 and a proline at −2 from the cleavage site. These play an important role in peptide modifications (Lubelski et al., 2008). The LanA identified in *S. epidermidis* APC 3775 and APC 3810 possessed an FDLN motif with the proline at −2 similar to epilancin 15X (Ekkelenkamp et al., 2005).

Four sactibiotics were identified in our study with no similarities to previously characterized peptides. The *in silico* mining identified a histidine kinase and a response regulator, suggesting that the bacteriocins are subjected to a two-component regulatory system, previously reported in bovine non-*aureus* staphylococci (Carson et al., 2017).

Despite the fact that the majority of the identified bacteriocin gene clusters were class II, only ten prepeptides were unique. We identified three novel class IIa bacteriocins in 11 *E. faecium* isolates. The novel prepeptides contained a highly conserved consensus sequence in the N-terminus of YDNGI motif instead of the "pediocin box" YGNGV which is typical of the class (Drider et al., 2006). This is the first time that a different pediocin-box has been reported with the already known class IIa bacteriocins having a highly conserved pediocin box except where V can be occasionally replaced by L (Cui et al., 2012). *E. faecium* APC 3830, APC 3833, APC 3835, and APC 3880 have the potential to produce the same class IIa bacteriocin. The core peptide is 100% homologous to enterocin P though the signal peptide is somewhat different (two amino acid difference). The different leader could impact the optimal secretion of the bacteriocin and the maturation of the pre-bacteriocin by the ABC transporter as was demonstrated by Aucher et al. (2005). In that study, site-directed mutagenesis of the leader sequence of mesentericin Y105 revealed that the conserved hydrophobic amino acids and the C-terminal GG doublet of the leader are of critical importance for the secretion and maturation of the bacteriocin.

Four potential circular (class IIc) bacteriocins were identified with similarities to Enterocin NKR-5-3B, with the majority of the circular bacteriocins in staphylococci being detected in *S. aureus* according to the existing literature (Bastos et al., 2009). Here, we identified putative novel circular bacteriocins from *S. epidermidis, S. aureus,* and *E. faecium* which displayed the highest similarity to Enterocin NKR-5-3B. All of the detected putative prepeptides contained the conserved domain linked with the circularin A/uberolysin family (TIGR03651). To date, there are only 14 circular bacteriocins that have been characterized (Perez et al., 2018) and much of the biosynthetic mechanisms including the circularization process as well as the regulatory mechanisms for production remain largely unknown. This study provides an additional four novel members (an increase of ∼25%) that may help to further elucidate the biosynthesis of this intriguing class of bacteriocins.

Two class IId bacteriocins which are linear non-pediocin like bacteriocins were found in this study. The two class IId clusters exhibited some degree of similarity with each other and at the same time both of them contained the lactococcin 972 conserved domain. Usually bacteriocins similar to lactococcin display a narrow spectrum activity against *Lactococcus* mainly because of the manner in which they bind to receptors (Kjos et al., 2009). However, this was not the case here as the detected strains exhibited wider inhibition spectra and displayed activity against a wide variety of the tested indicators. For example, *S. aureus* APC 3774 was active against *L. monocytogenes, E. faecalis, S. aureus,* and *M. luteus* among others which could potentially suggest the production of additional antimicrobials.

We identified 16 novel biosynthetic clusters belonging to all bacteriocin sub-classes across 25 human milk samples. The latter suggests not only a high degree of diversity of bacteriocins in human milk but also that it can be regarded as a promising source of novel metabolites including bacteriocins with potential implications in host defense and immune modulatory effects. Moreover, this study highlights the importance of a targeted approach to discover new effective antimicrobials that could potentially be applied to maintain good health in humans. It is anticipated that over the next few years, the number of sequenced genomes will drastically increase due to the widespread use of Next-Generation Sequencing (NGS) and the lower cost of Whole Genome Sequencing (WGS) which is empowered by third generation sequencing technologies, such as PacBio (Rhoads and Au, 2015) and Oxford Nanopore (Lu et al., 2016). With this expected proliferation in genome sequence data, there is equally a need for phenotypic trait surveying of strains such as described here to gain a more comprehensive understanding of bacteriocin-mediated interactions among coexisting species in natural communities such as human milk. The latter suggests that an increasing experimental effort to gain a more comprehensive understanding of bacteriocin mediated interactions among coexisting bacterial species in natural communities is warranted.

DATA AVAILABILITY STATEMENT

The datasets generated for this study were submitted to GenBank under BioProject number PRJNA521309.

ETHICS STATEMENT

The studies involving human participants were reviewed and approved by the Cork Clinical Research Ethics Committee. The patients/participants provided their written informed consent to participate in this study.

AUTHOR CONTRIBUTIONS

AA performed the experiments and drafted the manuscript. AW advised on the screening and critically reviewed the manuscript. SS assembled the genomes and critically reviewed the manuscript. AS assembled the genomes of *P. protegens* APC 3760 and *S. lugdunensis* APC 3758, uploaded the genomes to NCBI, and critically reviewed the manuscript. PO'C, DF, LD, CS, and CH critically reviewed the manuscript. RR conceived the original idea and critically reviewed the manuscript.

FUNDING

This work was funded by APC Microbiome Ireland, a Centre for Science and Technology (CSET) funded by the Science Foundation Ireland (SFI), grant number SFI/12/RC/2273.

ACKNOWLEDGMENTS

The authors would like to thank the mothers involved in this study for the kind donation of their milk. Also, the authors would like to extend their most grateful thanks to Professor C. Anthony Ryan for securing ethical approval and Ms. Carol-Anne O'Shea, Ms. Grainne Meehan, and Ms. Clare Boyle for assisting with sample collection.

SUPPLEMENTARY MATERIAL

The Supplementary Material for this article can be found online at: https://www.frontiersin.org/articles/10.3389/fmicb.2020.00788/full#supplementary-material

TABLE S1 | Cross-immunity assays using overnight cultures from all the antimicrobial-producing strains tested against themselves and each other, with the list of antimicrobial-producing isolates down the left-hand side and the indicator strains across the top of the table. The dark green box represents inhibition of the indicator strain grown in TSB indicating that these strains might be different or sensitive to each other while light green box represents hazy zones. The yellow box represents inhibition of the indicator strain grown in MH indicating that these strains might be different or sensitive to each other while light yellow represents hazy zones. Dark blue box represents inhibition of the indicator strain grown in both conditions while light blue represents hazy zones. White boxes represent no inhibition, revealing target strains not being inhibited by the producing strain, indicating they are immune (related) to the bacteriocins produced by other producers.

REFERENCES

Abou-Dakn, M., Richardt, A., Schaefer-Graf, U., and Wöckel, A. (2010). Inflammatory breast diseases during lactation: milk stasis, puerperal mastitis, abscesses of the breast, and malignant tumors – current and evidence-based strategies for diagnosis and therapy. *Breast Care.* 5, 33–37. doi: 10.1159/000272223

Algburi, A., Zehm, S., Netrebov, V., Bren, A. B., Chistyakov, V., and Chikindas, M. L. (2017). Subtilosin prevents biofilm formation by Inhibiting bacterial quorum sensing. *Probiotics Antimicrob Proteins.* 9, 81–90. doi: 10.1007/s12602-016-9242-x

Al-Mahrous, M., Sandiford, S. K., Tagg, J. R., and Upton, M. (2010). Purification and characterization of a novel delta-lysin variant that inhibits *Staphylococcus aureus* and has limited hemolytic activity. *Peptides.* 31, 1661–1668. doi: 10.1016/j.peptides.2010.06.006

Altschul, S. F., Gish, W., Miller, W., Myers, E. W., and Lipman, D. J. (1990). Basic local alignment search tool. *J. Mol. Biol.* 215, 403–410. doi: 10.1016/S0022-2836(05)80360-2

Angelopoulou, A., Field, D., Ryan, C. A., Stanton, C., Hill, C., and Ross, R. P. (2018). The microbiology and treatment of human mastitis. *Med. Microbiol. Immunol.* 207, 83–94. doi: 10.1007/s00430-017-0532-z

Angelopoulou, A., Harris, H. M. B., Warda, A. K., O'Shea, C.-A., Ryan, C. A., Stanton, C., et al. (2020). Subclinical mastitis, a frequent but misidentified disease in lactating women. *Pediatrics* (in press).

Arnison, P. G., Bibb, M. J., Bierbaum, G., Bowers, A. A., Bugni, T. S., Bulaj, G., et al. (2013). Ribosomally synthesized and post-translationally modified peptide natural products: overview and recommendations for a universal nomenclature. *Nat. Prod. Rep.* 30, 108–160. doi: 10.1039/c2np20085f

Aucher, W., Lacombe, C., Hequet, A., Frere, J., and Berjeaud, J. M. (2005). Influence of amino acid substitutions in the leader peptide on maturation and secretion of mesentericin Y105 by *Leuconostoc mesenteroides*. *J. Bacteriol.* 187, 2218–2223. doi: 10.1128/JB.187.6.2218-2223.2005

Balla, E., Dicks, L. M., Du Toit, M., Van Der Merwe, M. J., and Holzapfel, W. H. (2000). Characterization and cloning of the genes encoding enterocin 1071A and enterocin 1071B, two antimicrobial peptides produced by *Enterococcus faecalis* BFE 1071. *Appl. Environ. Microbiol.* 66, 1298–1304. doi: 10.1128/aem.66.4.1298-1304.2000

Balla, E., and Dicks, L. M. T. (2005). Molecular analysis of the gene cluster involved in the production and secretion of enterocins 1071A and 1071B and of the genes responsible for the replication and transfer of plasmid pEF1071. *Int. J. Food. Microbiol.* 99, 33–45. doi: 10.1016/j.ijfoodmicro.2004.08.008

Bastos, M. C., Ceotto, H., Coelho, M. L., and Nascimento, J. S. (2009). Staphylococcal antimicrobial peptides: relevant properties and potential biotechnological applications. *Curr. Pharm. Biotechnol.* 10, 38–61. doi: 10.2174/138920109787048580

Biagi, E., Quercia, S., Aceti, A., Beghetti, I., Rampelli, S., Turroni, S., et al. (2017). The bacterial ecosystem of mother's milk and infant's mouth and gut. *Front. Microbiol.* 8:1214. doi: 10.3389/fmicb.2017.01214

Bierbaum, G., Götz, F., Peschel, A., Kupke, T., van de Kamp, M., and Sahl, H.-G. (1996). The biosynthesis of the lantibiotics epidermin, gallidermin. Pep5 and epilancin K7. *Antonie van Leeuwenhoek.* 69, 119–127. doi: 10.1007/BF00399417

Blin, K., Shaw, S., Steinke, K., Villebro, R., Ziemert, N., Lee, S. Y., et al. (2019). antiSMASH 5.0: updates to the secondary metabolite genome mining pipeline. *Nucleic Acids Res.* 47, W81–W87. doi: 10.1093/nar/gkz310

Boix-Amorós, A., Collado, M. C., and Mira, A. (2016). Relationship between milk microbiota, bacterial load, macronutrients, and human cells during lactation. *Front Microbiol.* 7:492. doi: 10.3389/fmicb.2016.00492

Bolger, A. M., Lohse, M., and Usadel, B. (2014). Trimmomatic: a flexible trimmer for Illumina sequence data. *Bioinformatics* 30, 2114–2120. doi: 10.1093/bioinformatics/btu170

Cabrera-Rubio, R., Mira, A., Isolauri, E., Laitinen, K., Salminen, S., and Collado, M. C. (2012). The human milk microbiome changes over lactation and is shaped by maternal weight and mode of delivery. *Am. J. Clin. Nutr.* 96, 544–551. doi: 10.1017/S2040174415001397

Carson, D. A., Barkema, H. W., Naushad, S., and De Buck, J. (2017). Bacteriocins of non-*aureus* staphylococci isolated from bovine milk. *Appl. Environ. Microbiol.* 83, e1015–e1017. doi: 10.1128/AEM.01015-17

Chessa, D., Ganau, G., Spiga, L., Bulla, A., Mazzarello, V., Campus, G. V., et al. (2016). *Staphylococcus aureus* and *Staphylococcus epidermidis* virulence strains as causative agents of persistent infections in breast implants. *Plos One* 11:e0146668. doi: 10.1371/journal.pone.0146668

Chikindas, M. L., Weeks, R., Drider, D., Chistyakov, V. A., and Dicks, L. M. (2018). Functions and emerging applications of bacteriocins. *Curr. Opin. Biotechnol.* 49, 23–28. doi: 10.1016/j.copbio.2017.07.011

Cintas, L. M., Casaus, P., Håvarstein, L. S., Hernández, P. E., and Nes, I. F. (1997). Biochemical and genetic characterization of enterocin P, a novel sec-dependent bacteriocin from *Enterococcus faecium* P13 with a broad antimicrobial spectrum. *Appl. Environ. Microbiol.* 63, 4321–4330. doi: 10.1128/aem.63.11.4321-4330.1997

Civardi, E., Garofoli, F., Tzialla, C., Paolillo, P., Bollani, L., and Stronati, M. (2013). Microorganisms in human milk: lights and shadows. *J. Matern. Fetal. Neonatal Med.* 26, 30–34. doi: 10.3109/14767058.2013.829693

Coburn, P. S., and Gilmore, M. S. (2003). The *Enterococcus faecalis* cytolysin: a novel toxin active against eukaryotic and prokaryotic cells. *Cell Microbiol.* 5, 661–669. doi: 10.1046/j.1462-5822.2003.00310.x

Collado, M. C., Delgado, S., Maldonado, A., and Rodríguez, J. M. (2009). Assessment of the bacterial diversity of breast milk of healthy women by quantitative real-time PCR. *Lett. Appl. Microbiol.* 48, 523–528. doi: 10.1111/j.1472-765X.2009.02567.x

Collins, F. W. J., O'Connor, P. M., O'Sullivan, O., Gómez-Sala, B., Rea, M. C., Hill, C., et al. (2017). Bacteriocin gene-trait matching across the complete *Lactobacillus* pan-genome. *Sci. Rep.* 7:3481. doi: 10.1038/s41598-017-03339-y

Cotter, P. D., Hill, C., and Ross, R. P. (2005). Bacteriocins: developing innate immunity for food. *Nat. Rev. Microbiol.* 3, 777–788. doi: 10.1038/nrmicro1273

Cotter, P. D., Ross, R. P., and Hill, C. (2013). Bacteriocins — a viable alternative to antibiotics? *Nat. Rev. Microbiol.* 11, 95–105. doi: 10.1038/nrmicro2937

Crispie, F., Twomey, D., Flynn, J., Hill, C., Ross, P., and Meaney, W. (2005). The lantibiotic lacticin 3147 produced in a milk-based medium improves the efficacy of a bismuth-based teat seal in cattle deliberately infected with *Staphylococcus aureus*. *J. Dairy Res.* 72, 159–167. doi: 10.1017/S0022029905000816

Cui, Y., Zhang, C., Wang, Y., Shi, J., Zhang, L., Ding, Z., et al. (2012). Class IIa bacteriocins: diversity and new developments. *Int. J. Mol. Sci.* 13, 16668–16707. doi: 10.3390/ijms131216668

Delgado, S., Garcia, P., Fernandez, L., Jimenez, E., Rodriguez-Banos, M., del Campo, R., et al. (2011). Characterization of *Staphylococcus aureus* strains involved in human and bovine mastitis. *FEMS Immunol. Med. Microbiol.* 62, 225–235. doi: 10.1111/j.1574-695X.2011.00806.x

Diep, D. B., Axelsson, L., Grefsli, C., and Nes, I. F. (2000). The synthesis of the bacteriocin sakacin A is a temperature-sensitive process regulated by a pheromone peptide through a three-component regulatory system. *Microbiology* 146, 2155–2160. doi: 10.1099/00221287-146-9-2155

Drider, D., Fimland, G., Héchard, Y., McMullen, L. M., and Prévost, H. (2006). The continuing story of class IIa bacteriocins. *Microbiol. Mol. Biol. Rev.* 70, 564–582. doi: 10.1128/MMBR.00016-05

Edgar, R. C. (2004). MUSCLE: multiple sequence alignment with high accuracy and high throughput. *Nucleic Acids Res.* 32, 1792–1797. doi: 10.1093/nar/gkh340

Egan, K., Field, D., Ross, R. P., Cotter, P. D., and Hill, C. (2018). In silico prediction and exploration of potential bacteriocin gene clusters within the bacterial genus *Geobacillus*. *Front. Microbiol.* 9:2116. doi: 10.3389/fmicb.2018.02116

Eijsink, V. G., Axelsson, L., Diep, D. B., Havarstein, L. S., Holo, H., and Nes, I. F. (2002). Production of class II bacteriocins by lactic acid bacteria; an example of biological warfare and communication. *Antonie Van Leeuwenhoek* 81, 639–654. doi: 10.1023/A:1020582211262

Ekkelenkamp, M. B., Hanssen, M., Danny Hsu, S. T., de Jong, A., Milatovic, D., and Verhoef, J. (2005). Isolation and structural characterization of epilancin 15X, a novel lantibiotic from a clinical strain of *Staphylococcus epidermidis*. *FEBS Lett.* 579, 1917–1922. doi: 10.1016/j.febslet.2005.01.083

el-Banna, N., and Winkelmann, G. (1998). Pyrrolnitrin from *Burkholderia cepacia*: antibiotic activity against fungi and novel activities against streptomycetes. *J. Appl. Microbiol* 85, 69–78. doi: 10.1046/j.1365-2672.1998.00473.x

Fernández, L., Delgado, S., Herrero, H., Maldonado, A., and Rodríguez, J. M. (2008). The bacteriocin nisin, an effective agent for the treatment of staphylococcal mastitis during lactation. *J. Hum. Lact.* 24, 311–316. doi: 10.1177/0890334408317435

Fernández, L., Langa, S., Martin, V., Maldonado, A., Jimenez, E., Martin, R., et al. (2013). The human milk microbiota: origin and potential roles in health and disease. *Pharmacol. Res.* 69, 1–10. doi: 10.1016/j.phrs.2012.09.001

Gallucci, M. N., Oliva, M., Casero, C., Dambolena, J., Luna, A., Zygadlo, J., et al. (2009). Antimicrobial combined action of terpenes against the food-borne microorganisms *Escherichia coli*, *Staphylococcus aureus* and *Bacillus cereus*. *Flavour Fragr. J.* 24, 348–354. doi: 10.1002/ffj.1948

Giormezis, N., Kolonitsiou, F., Makri, A., Vogiatzi, A., Christofidou, M., Anastassiou, E. D., et al. (2015). Virulence factors among *Staphylococcus lugdunensis* are associated with infection sites and clonal spread. *Eur. J. Clin. Microbiol. Infect Dis.* 34, 773–778. doi: 10.1007/s10096-014-2291-8

Heikkilä, M. P., and Saris, P. E. J. (2003). Inhibition of *Staphylococcus aureus* by the commensal bacteria of human milk. *J. Appl. Microbiol.* 95, 471–478. doi: 10.1046/j.1365-2672.2003.02002.x

Himeno, K., Rosengren, K. J., Inoue, T., Perez, R. H., Colgrave, M. L., Lee, H. S., et al. (2015). Identification, characterization, and three-dimensional structure of the novel circular bacteriocin, enterocin NKR-5-3B, from *Enterococcus faecium*. *Biochemistry* 54, 4863–4876. doi: 10.1021/acs.biochem.5b00196

Holmes, M. A., and Zadoks, R. N. (2011). Methicillin resistant *S. aureus* in human and bovine mastitis. *J. Mammary Gland. Biol. Neoplasia.* 16, 373–382. doi: 10.1007/s10911-011-9237-x

Hunt, K. M., Foster, J. A., Forney, L. J., Schütte, U. M. E., Beck, D. L., Abdo, Z., et al. (2011). Characterization of the diversity and temporal stability of bacterial communities in human milk. *PLoS One* 6:e21313. doi: 10.1371/journal.pone.0021313

Janek, D., Zipperer, A., Kulik, A., Krismer, B., and Peschel, A. (2016). High frequency and diversity of antimicrobial activities produced by nasal *Staphylococcus* strains against bacterial competitors. *PLoS Pathog.* 12:e1005812. doi: 10.1371/journal.ppat.1005812

Jiménez, E., Fernandez, L., Maldonado, A., Martin, R., Olivares, M., Xaus, J., et al. (2008). Oral administration of *Lactobacillus* strains isolated from breast milk as an alternative for the treatment of infectious mastitis during lactation. *Appl. Environ. Microbiol.* 74, 4650–4655. doi: 10.1128/AEM.02599-07

Kjos, M., Nes, I. F., and Diep, D. B. (2009). Class II one-peptide bacteriocins target a phylogenetically defined subgroup of mannose phosphotransferase systems on sensitive cells. *Microbiology* 155, 2949–2961. doi: 10.1099/mic.0.030015-0

Klostermann, K., Crispie, F., Flynn, J., Meaney, W. J., Ross, R. P., and Hill, C. (2009). Efficacy of a teat dip containing the bacteriocin lacticin 3147 to eliminate Gram-positive pathogens associated with bovine mastitis. *J. Dairy Res.* 77, 231–238. doi: 10.1017/S0022029909990239

Kohira, N., West, J., Ito, A., Ito-Horiyama, T., Nakamura, R., Sato, T., et al. (2016). *In vitro* antimicrobial activity of a siderophore cephalosporin, S-649266, against *enterobacteriaceae* clinical isolates, including carbapenem-resistant strains. *Antimicrob. Agents Chemother.* 60, 729–734. doi: 10.1128/AAC.01695-15

Kort, R., Caspers, M., van de Graaf, A., van Egmond, W., Keijser, B., and Roeselers, G. (2014). Shaping the oral microbiota through intimate kissing. *Microbiome* 2:41. doi: 10.1186/2049-2618-2-41

Kotelnikova, E. A., and Gelfand, M. S. (2002). Bacteriocin production by gram-positive bacteria and the mechanisms of transcriptional regulation. *Russ. J. Genet.* 38, 628–641. doi: 10.1023/A:1016035700012

Li, R., Fein, S. B., Chen, J., and Grummer-Strawn, L. M. (2008). Why mothers stop breastfeeding: mothers' self-reported reasons for stopping during the first year. *Pediatrics* 122, S69–S76. doi: 10.1542/peds.2008-1315i

Li, Y., Li, Y., Li, Q., Gao, J., Wang, J., Luo, Y., et al. (2018). Biosynthetic and antimicrobial potential of actinobacteria isolated from bulrush rhizospheres habitat in Zhalong Wetland. *China. Arch. Microbiol.* 200, 695–705. doi: 10.1007/s00203-018-1474-6

Lu, H., Giordano, F., and Ning, Z. (2016). Oxford nanopore MinION sequencing and genome assembly. *Genomics Proteomics Bioinformatics* 14, 265–279. doi: 10.1016/j.gpb.2016.05.004

Lubelski, J., Rink, R., Khusainov, R., Moll, G. N., and Kuipers, O. P. (2008). Biosynthesis, immunity, regulation, mode of action and engineering of the model lantibiotic nisin. *Cell Mol. Life. Sci.* 65, 455–476. doi: 10.1007/s00018-007-7171-2

Madsen, K. T., Skov, M. N., Gill, S., and Kemp, M. (2017). Virulence factors associated with *Enterococcus faecalis* infective endocarditis: a mini review. *Open Microbiol J.* 11, 1–11. doi: 10.2174/1874285801711010001

Maldonado-Barragan, A., Caballero-Guerrero, B., Lucena-Padros, H., and Ruiz-Barba, J. L. (2013). Induction of bacteriocin production by coculture is widespread among plantaricin-producing *Lactobacillus plantarum* strains with different regulatory operons. *Food Microbiol.* 33, 40–47. doi: 10.1016/j.fm.2012.08.009

Marsh, A. J., O'Sullivan, O., Ross, R. P., Cotter, P. D., and Hill, C. (2010). *In silico* analysis highlights the frequency and diversity of type 1 lantibiotic gene clusters in genome sequenced bacteria. *BMC Genomics* 11:679. doi: 10.1186/1471-2164-11-679

Martin, C. R., Ling, P.-R., and Blackburn, G. L. (2016). Review of infant feeding: key features of breast milk and infant formula. *Nutrients.* 8:279. doi: 10.3390/nu8050279

Martin, M. (2011). Cutadapt removes adapter sequences from high-throughput sequencing reads. *EMBnet J.* 17, 10–12. doi: 10.14806/ej.17.1.200

Martínez, B., Fernández, M., Suárez, E. J., and Rodríguez, A. (1999). Synthesis of lactococcin 972, a bacteriocin produced by *Lactococcus lactis* IPLA 972, depends on the expression of a plasmid-encoded bicistronic operon. *Microbiology* 145, 3155–3161. doi: 10.1099/00221287-145-11-3155

Martínez, B., Rodriguez, A., and Suárez, J. E. (2000). Lactococcin 972, a bacteriocin that inhibits septum formation in lactococci. *Microbiology* 146, 949–955. doi: 10.1099/00221287-146-4-949

Martin-Visscher, L. A., van Belkum, M. J., and Vederas, J. C. (2011). "Class IIc or circular bacteriocins," in *Prokaryotic Antimicrobial Peptides: From Genes to Applications*, eds D. Drider and S. Rebuffat (New York, NY: Springer), 213–236. doi: 10.1007/978-1-4419-7692-5_12

Mathur, H., Rea, M. C., Cotter, P. D., Hill, C., and Ross, R. P. (2015). The sactibiotic subclass of bacteriocins: an update. *Curr. Protein Pept. Sci.* 16, 549–558. doi: 10.2174/1389203716666150515124831

McAuliffe, O., Hill, C., and Ross, R. P. (2000). Each peptide of the two-component lantibiotic lacticin 3147 requires a separate modification enzyme for activity. *Microbiology* 146, 2147–2154. doi: 10.1099/00221287-146-9-2147

Mediano, P., Fernández, L., Jiménez, E., Arroyo, R., Espinosa-Martos, I., Rodríguez, J. M., et al. (2017). Microbial diversity in milk of women with mastitis: potential role of coagulase-negative staphylococci, viridans group streptococci, and corynebacteria. *J. Hum. Lact.* 33, 309–318. doi: 10.1177/0890334417692968

Moll, G., Ubbink-Kok, T., Hildeng-Hauge, H., Nissen-Meyer, J., Nes, I. F., Konings, W. N., et al. (1996). Lactococcin G is a potassium ion-conducting, two-component bacteriocin. *J. Bacteriol.* 178:600. doi: 10.1128/jb.178.3.600-605.1996

Murphy, E. F., Cotter, P. D., Hogan, A., O'Sullivan, O., Joyce, A., Fouhy, F., et al. (2013). Divergent metabolic outcomes arising from targeted manipulation of the gut microbiota in diet-induced obesity. *Gut.* 62, 220–226. doi: 10.1136/gutjnl-2011-300705

Nikaido, H. (2003). Molecular basis of bacterial outer membrane permeability revisited. *Microbiol. Mol. Biol. Rev.* 67, 593–656. doi: 10.1128/mmbr.67.4.593-656.2003

Nikaido, H., and Vaara, M. (1985). Molecular basis of bacterial outer membrane permeability. *Microbiol. Rev.* 49, 1–32. doi: 10.1128/mmbr.49.1.1-32.1985

Nissen-Meyer, J., Oppegård, C., Rogne, P., Haugen, H. S., and Kristiansen, P. E. (2010). Structure and mode-of-action of the two-peptide (class-IIb) bacteriocins. *Probiotics Antimicrob. Proteins.* 2, 52–60. doi: 10.1007/s12602-009-9021-z

Nurk, S., Meleshko, D., Korobeynikov, A., and Pevzner, P. A. (2017). metaSPAdes: a new versatile metagenomic assembler. *Genome Res.* 27, 824–834. doi: 10.1101/gr.213959

O'Sullivan, J. N., Rea, M. C., O'Connor, P. M., Hill, C., and Ross, R. P. (2019). Human skin microbiota is a rich source of bacteriocin-producing staphylococci that kill human pathogens. *FEMS Microbiol. Ecol.* 95:fiy241. doi: 10.1093/femsec/fiy241

Overbeek, R., Olson, R., Pusch, G. D., Olsen, G. J., Davis, J. J., Disz, T., et al. (2014). The SEED and the rapid annotation of microbial genomes using subsystems technology (RAST). *Nucleic Acids Res.* 42, D206–D214. doi: 10.1093/nar/gkt1226

Padilha, M., Danneskiold-Samsoe, N. B., Brejnrod, A., Hoffmann, C., Cabral, V. P., Iaucci, J. M., et al. (2019). The human milk microbiota is modulated by maternal diet. *Microorganisms* 7, 502. doi: 10.3390/microorganisms7110502

Paviour, S., Musaad, S., Roberts, S., Taylor, G., Taylor, S., Shore, K., et al. (2002). *Corynebacterium* species isolated from patients with mastitis. *Clin. Infect. Dis.* 35, 1434–1440. doi: 10.1086/344463

Perez, P. F., Doré, J., Leclerc, M., Levenez, F., Benyacoub, J., Serrant, P., et al. (2007). Bacterial imprinting of the neonatal immune system: lessons from maternal cells? *Pediatrics* 119:e724. doi: 10.1542/peds.2006-1649

Perez, R. H., Zendo, T., and Sonomoto, K. (2018). Circular and leaderless bacteriocins: biosynthesis, mode of action, applications, and prospects. *Front. Microbiol.* 9:2085. doi: 10.3389/fmicb.2018.02085

Rea, M. C., Sit, C. S., Clayton, E., Connor, P. M., Whittal, R. M., Zheng, J., et al. (2010). Thuricin CD, a posttranslationally modified bacteriocin with a narrow spectrum of activity against *Clostridium difficile*. *Proc. Natl. Acad. Sci. U.S.A.* 107, 9352–9357. doi: 10.1073/pnas.0913554107

Rhoads, A., and Au, K. F. (2015). PacBio sequencing and its applications. *Genom. Proteom. Bioin.* 13, 278–289. doi: 10.1016/j.gpb.2015.08.002

Ross, A. A., Doxey, A. C., and Neufeld, J. D. (2017). The skin microbiome of cohabiting couples. *mSystems* 2:e043-17. doi: 10.1128/mSystems.00043-17

Shah, M. M., Iihara, H., Noda, M., Song, S. X., Nhung, P. H., Ohkusu, K., et al. (2007). dnaJ gene sequence-based assay for species identification and phylogenetic grouping in the genus *Staphylococcus*. *Int. J. Syst. Evol. Microbiol.* 57, 25–30. doi: 10.1099/ijs.0.64205-0

van Heel, A. J., de Jong, A., Montalban-Lopez, M., Kok, J., and Kuipers, O. P. (2013). BAGEL3: Automated identification of genes encoding bacteriocins and (non-)bactericidal posttranslationally modified peptides. *Nucleic Acids Res.* 41, W448–W453. doi: 10.1093/nar/gkt391

Velásquez, J. E., Zhang, X., and van der Donk, W. A. (2011). Biosynthesis of the antimicrobial peptide epilancin 15X and its N-terminal lactate. *Chem. Biol.* 18, 857–867. doi: 10.1016/j.chembiol.2011.05.007

Waterhouse, A. M., Procter, J. B., Martin, D. M., Clamp, M., and Barton, G. J. (2009). Jalview Version 2-a multiple sequence alignment editor and analysis workbench. *Bioinformatics*25, 1189–1191. doi: 10.1093/bioinformatics/btp033

Wayah, S. B., and Philip, K. (2018). Pentocin MQ1: a novel, broad-spectrum, pore-forming bacteriocin from *Lactobacillus pentosus* CS2 with quorum sensing regulatory mechanism and biopreservative potential. *Front. Microbiol.* 9:564. doi: 10.3389/fmicb.2018.00564

WHO (2000). *Mastitis: Causes and Management*. Geneva: World Health Organization, 1–45.

Wong, S. C. Y., Poon, R. W. S., Chen, J. H. K., Tse, H., Lo, J. Y. C., Ng, T. K., et al. (2017). *Corynebacterium kroppenstedtii* is an emerging cause of mastitis especially in patients with psychiatric illness on antipsychotic medication. *Open Forum Infect. Dis.* 4:ofx096. doi: 10.1093/ofid/ofx096

Zengin, H., and Baysal, A. H. (2014). Antibacterial and antioxidant activity of essential oil terpenes against pathogenic and spoilage-forming bacteria and cell structure-activity relationships evaluated by SEM microscopy. *Molecules* 19, 17773–17798. doi: 10.3390/molecules191117773

Zhang, J., Du, L., Liu, F., Xu, F., Hu, B., Venturi, V., et al. (2014). Involvement of both PKS and NRPS in antibacterial activity in *Lysobacter enzymogenes* OH11. *FEMS Microbiol. Lett.* 355, 170–176. doi: 10.1111/1574-6968.12457

Zipperer, A., Konnerth, M. C., Laux, C., Berscheid, A., Janek, D., Weidenmaier, C., et al. (2016). Human commensals producing a novel antibiotic impair pathogen colonization. *Nature* 535, 511–516. doi: 10.1038/nature18634

Conflict of Interest: The authors declare that the research was conducted in the absence of any commercial or financial relationships that could be construed as a potential conflict of interest.

frontiers in Microbiology

REVIEW
published: 09 June 2020
doi: 10.3389/fmicb.2020.01183

A Structural View on the Maturation of Lanthipeptides

Marcel Lagedroste[1†], Jens Reiners[1,2†], C. Vivien Knospe[1], Sander H. J. Smits[1,2] and Lutz Schmitt[1*]*

[1] Institute of Biochemistry, Heinrich Heine University Düsseldorf, Düsseldorf, Germany, [2] Center for Structural Studies, Heinrich Heine University Düsseldorf, Düsseldorf, Germany

Lanthipeptides are ribosomally synthesized and posttranslationally modified peptides, which display diverse bioactivities (e.g., antifungal, antimicrobial, and antiviral). One characteristic of these lanthipeptides is the presence of thioether bonds, which are termed (methyl-) lanthionine rings. These modifications are installed by corresponding modification enzymes in a two-step modality. First, serine and threonine residues are dehydrated followed by a subsequent catalyzed cyclization reaction, in which the dehydrated serine and threonine residues are undergoing a Michael-type addition with cysteine residues. The dedicated enzymes are encoded by one or two genes and the classification of lanthipeptides is pending on this. The modification steps form the basis of distinguishing the different classes of lanthipeptides and furthermore reflect also important mechanistic differences. Here, we will summarize recent insights into the mechanisms and the structures of the participating enzymes, focusing on the two core modification steps – dehydration and cyclization.

Keywords: structural biology, biochemistry, lanthionine, enzymes, protein–protein interaction

OPEN ACCESS

Edited by:
Des Field,
University College Cork, Ireland

Reviewed by:
Manuel Montalban-Lopez,
University of Granada, Spain
Yuki Goto,
The University of Tokyo, Japan

****Correspondence:***
Sander H. J. Smits
Sander.Smits@hhu.de
Lutz Schmitt
lutz.schmitt@hhu.de

† These authors have contributed equally to this work

Specialty section:
This article was submitted to Antimicrobials, Resistance and Chemotherapy, a section of the journal Frontiers in Microbiology

Received: *30 March 2020*
Accepted: *08 May 2020*
Published: *09 June 2020*

Citation:
Lagedroste M, Reiners J, Knospe CV, Smits SHJ and Schmitt L (2020) A Structural View on the Maturation of Lanthipeptides. Front. Microbiol. 11:1183. doi: 10.3389/fmicb.2020.01183

INTRODUCTION

Ribosomally synthesized and posttranslationally modified peptides (RiPPs) are a large family of natural compounds of diverse biological functions (Arnison et al., 2013). Among the RiPPs, lanthipeptides form the largest sub-family (Skinnider et al., 2016), which is characterized by the presence of multiple lanthionine (Lan) or (methyl-) lanthionine rings ((Me)Lan)-, that restrict the conformational flexibility of the peptides and give rise to their high biological stability (Bierbaum et al., 1996). Common to lanthipeptides is the ribosomal biosynthesis of a precursor peptide that is composed of an N-terminal leader peptide (LP) and a C-terminal core peptide (CP), termed LanA (Oman and van der Donk, 2010; Arnison et al., 2013). While all posttranslational modifications (PTMs) are introduced only in the CP, the LP increases the efficiency of the PTMs to the lanthipeptide by its PTM machinery and keeps the peptide in an inactive state prior to translocation (van der Meer et al., 1994; Kuipers et al., 1993, 2004; Khusainov and Kuipers, 2012). The fully modified lanthipeptide is termed mLanA (Arnison et al., 2013). Subsequently, the LP is proteolytically removed either before or after secretion to the extracellular space via its cognate ABC transporter and the active lanthipeptide is released into the extracellular space (van der Meer et al., 1993, 1994; Nishie et al., 2011; Ortega et al., 2014). In general, all lanthipeptides share at least two common PTMs. The first one is the dehydration of serine and threonine residues, resulting in the formation of 2,3-didehydroalanine (Dha from serine) and 2,3-didehydrobutyrine (Dhb from threonine) (**Figure 1**; Gross and Morell, 1967, 1971; Gross et al., 1969). This reaction is catalyzed by

the dehydratase LanB or dehydratase domains depending on the classification of the lanthipeptide (see next section) (Gilmore et al., 1994; Gutowskieckel et al., 1994; Peschel et al., 1996; Karakas Sen et al., 1999). The second common PTM is the Michael-type addition of a cysteine side chain with the previously dehydrated amino acids yielding *meso*-lanthionine (from Dha) or (3-methyl-) lanthionine (from Dhb) (**Figure 1**) introduced by the cyclase LanC (Gross and Morell, 1967, 1971; Gross et al., 1969; Barber et al., 1988). Additionally to these two PTMs that are the foundation of lanthipeptides, a range of further modifications such as labionin (Lab) ring formation (**Figure 1**; Meindl et al., 2010; Iorio et al., 2014) or tailoring reactions such as halogenation of tryptophan residues, decarboxylation or acylation have been observed (Mortvedt et al., 1991; Kupke et al., 1992; Skaugen et al., 1994; van de Kamp et al., 1995; Heidrich et al., 1998; Ekkelenkamp et al., 2005; Castiglione et al., 2008; He et al., 2008; Velasquez et al., 2011; Huang and Yousef, 2015). However, these reactions are not further discussed in this review and the reader is referred to excellent reviews covering these aspects (Mortvedt et al., 1991; Kupke et al., 1992; Skaugen et al., 1994; van de Kamp et al., 1995; Heidrich et al., 1998; Ekkelenkamp et al., 2005; Castiglione et al., 2008; He et al., 2008; McIntosh et al., 2009; Meindl et al., 2010; Velasquez et al., 2011; Arnison et al., 2013; Dunbar and Mitchell, 2013; Iorio et al., 2014; Walsh, 2014; Huang and Yousef, 2015; Ortega and van der Donk, 2016; Repka et al., 2017).

In 2013, a new nomenclature was suggested that subdivides lanthipeptides based on their modification machinery in four families, termed class I–IV (**Figure 2**; Arnison et al., 2013) that are described in greater detail in the following sections. In this review, we will follow this new nomenclature. Furthermore, we will restrict ourselves to the two common maturation steps that occur in the cytosol of lanthipeptide producing strains.

LANTIBIOTICS – SPECIALIZED LANTHIPEPTIDES

The hallmark of lanthipeptides is the presence lanthionine or (methyl-) lanthionine rings. In cases that lanthipeptides possess antimicrobial activity they are called lantibiotics (Schnell et al., 1988; Arnison et al., 2013). However, other activities, such as antifungal, antiviral, morphogenetic, or antinociceptive have been described (Kodani et al., 2004, 2005; Ferir et al., 2013; Iorio et al., 2014; Mohr et al., 2015). The antimicrobial activity, which is mainly directed against Gram-positive bacteria where the target of most lantibiotics is the membrane and/or a specific receptor. A prominent example, nisin, a lantibiotic produced by *Lactococcus lactis*, targets the peptidoglycan precursor lipid II. Nisin contains five (Me)Lan rings, where the first two bind to the pyrophosphate moiety of lipid II and directly inhibit the cell wall synthesis. Additionally, nisin and lipid II molecules form pores in the cell membrane of the target cell in a stoichiometry of eight nisin and four lipid II molecules (Severina et al., 1998; Breukink et al., 1999; Wiedemann et al., 2001; Brumfitt et al., 2002; van Heusden et al., 2002; Hasper et al., 2004, 2006; Hsu et al., 2004; Chatterjee et al., 2005b; Breukink and de Kruijff, 2006; Lubelski et al., 2008; Bierbaum and Sahl, 2009; Schneider and Sahl, 2010; Islam et al., 2012). Despite its usage in the food industry for almost 50 years (Cotter et al., 2005) this dual mode of action explains why hardly any acquired resistances have been described in the literature.

THE FIRST MATURATION STEP – THE DEHYDRATION REACTION

The major discriminators among the four classes of lanthipeptides are the lanthipeptide modification enzymes. Here, four different routes corresponding to the four subfamilies (LanB, LanM, LanKC, and LanL) have evolved, which mainly differ in the mechanism of dehydrating serine and threonine residues (**Figure 2**).

Class I family dehydratases (LanB) contain the well-studied enzymes NisB or SpaB that dehydrate their substrates nisin (NisA) or subtilin (SpaA), respectively (Gross and Morell, 1967; Gross et al., 1969). NisB adopts a dimeric state in solution and interestingly interacts with the different maturation states of NisA and not only with its cognate substrate (unmodified NisA) in the low micromolar range (Mavaro et al., 2011). *In vivo* co-expression studies of NisB and the cyclase NisC without purification resulted in dehydration and cyclization of NisA indicating functional enzymes (Karakas Sen et al., 1999; Kluskens et al., 2005; Rink et al., 2005; Rink et al., 2007a). In 2013, Garg et al. (2013) demonstrated *in vitro* activity of purified NisB by using extracts of *Escherichia coli* and subsequently identified the cytosolic extract to be the key element for glutamylation of NisA. Finally, the addition of glutamyl-tRNA ($tRNA^{Glu}$), derived from glutamyl-tRNA synthetase, and glutamate to purified recombinant NisB restored the *in vitro* activity and consequently, polyglutamylated intermediates were identified by MS analysis (Ortega et al., 2015). This highlighted that the hydroxyl groups of serine and threonine in the CP of NisA were esterified with the alpha-carboxyl group of glutamate, where a cognate tRNA is the glutamyl-donor. Subsequently, the elimination of these activated residues resulted in the dehydrated residues Dha and Dhb. Of course, this reconstitution allowed a detailed study of the catalytic activity and the identification of essential amino acids of this LanB dehydratase (Garg et al., 2013; Bothwell et al., 2019). In 2015, the fruitful collaboration of the Wilfred van der Donk and Satish K. Nair groups also reported the crystal structure of NisB (**Figure 3A**). Similar to *in vitro* observations, NisB crystallized as a dimer (Ortega et al., 2015; Reiners et al., 2017). Importantly, NisB was co-expressed with NisA and parts of the LP including the FNLD box, which is pivotal for the interaction with NisB, were visible in the final electron density (shown in ball-and-stick representation in **Figure 3A**). In the crystal structure, the LP interacts with a twisted ß-strand resulting in an antiparallel, four-stranded ß-sheet. This resulted in a 2:2 stoichiometry of NisB:NisA, which is in contradiction to the *in vitro* data, which determined a 2:1 ratio of NisB:NisA using surface plasmon resonance (Mavaro et al., 2011). In 2019, a co-crystallization approach with a non-reactive substrate mimic also revealed a 2:2 stoichiometry of NisB-Val169Cys:NisA-Ser3Dap^{Glu}-Ser(-12)Cys

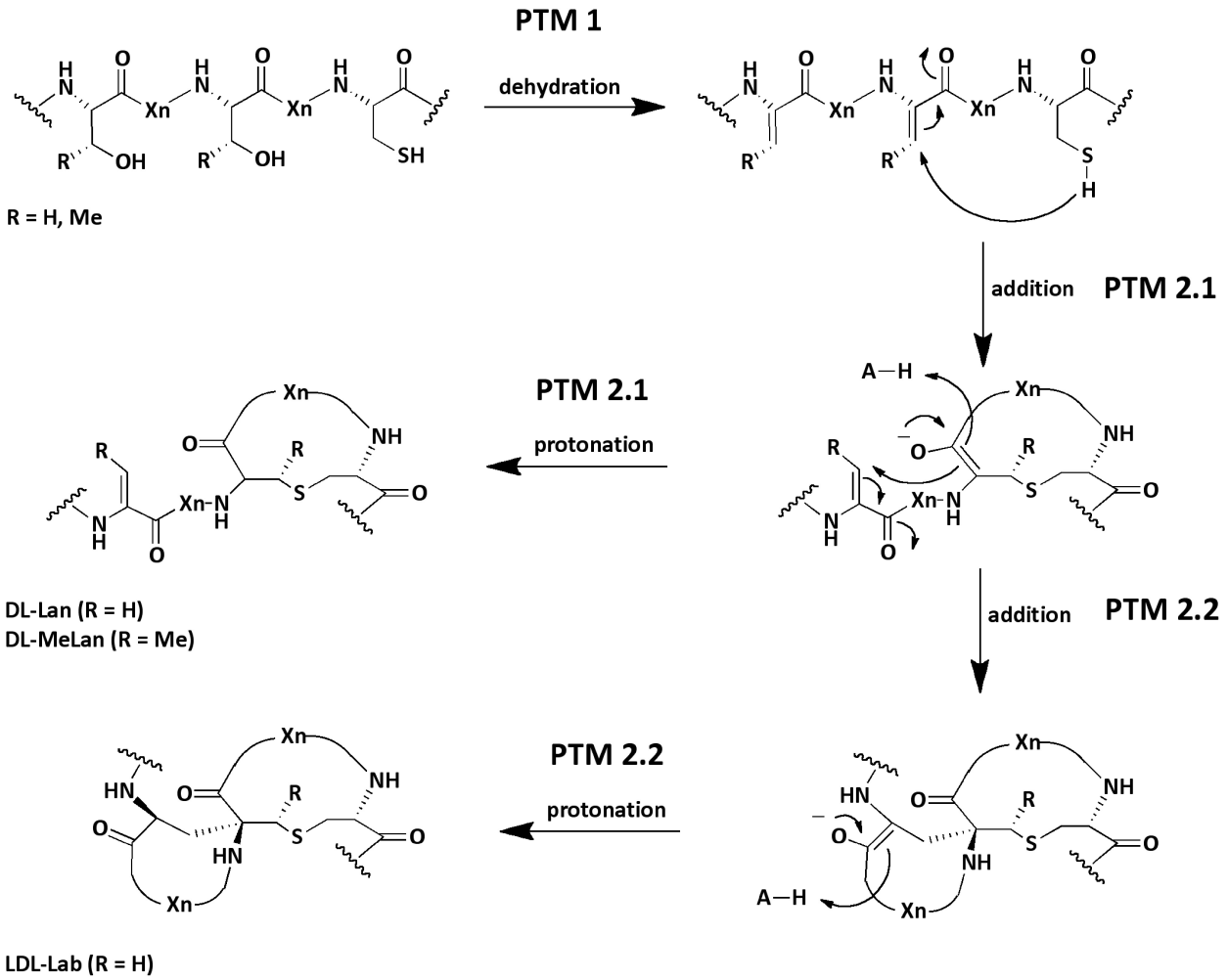

FIGURE 1 | Reaction and structure of common PTMs in lanthipeptides. During a first modification step (PTM 1) a dehydratase catalyzes the dehydration of serine and threonine residues (Dha, Dhb). In a second step (PTM 2.1) a cyclase catalyzes the Michael-type addition of a cysteine residue to a dehydrated amino acid. Within the active center an acid (H-A, e.g., His) protonates the enolate. Finally, the Lan or MeLan rings are formed. In some lanthipeptides an additional Michael-type addition reaction (PTM 2.2) is catalyzed by the cyclase yielding a Lab amino acid. In the scheme the stereochemistry of the chiral center in the final products are exemplary (e.g., DL-Lan; but LL-Lan is also possible). The acronym X_n stands for n-quantity amino acids. The scheme is modified and based on (Repka et al., 2017).

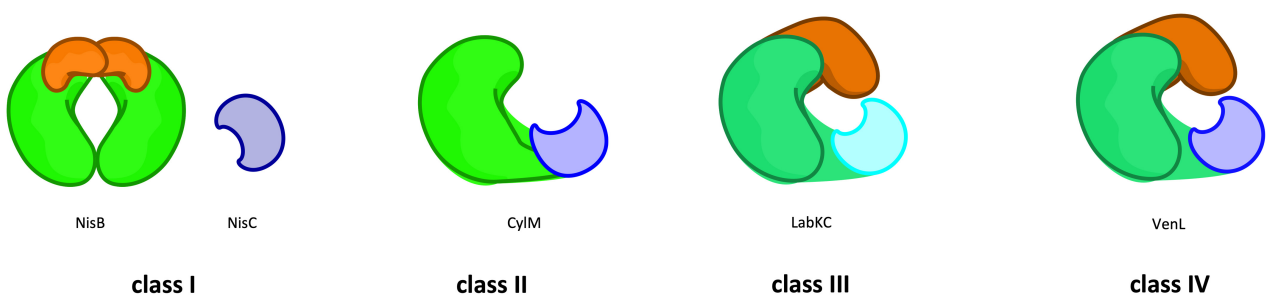

FIGURE 2 | Classes of lanthipeptides based on the modification machineries. The classification of lanthipeptides depends on their modification enzymes and their domain organization as well as those PTM mechanisms. In class I (e.g., NisB) the first PTM (dehydration) is catalyzed by a glutamylation/elimination-domain (green/orange). The dehydration in class II (e.g., CylM) take place in a kinase-domain (green). In class III (LabKC) and IV (VenL) this modification is catalyzed by a lyase/kinase-domain (dark green/dark orange). The second PTM (cyclization) is catalyzed by the zinc-dependent LanC enzyme (e.g., NisC; blue) or LanC-like domain (light blue), whereas in class III the LanC-like domain is independent from a zinc-ion (cyan). For further details see text.

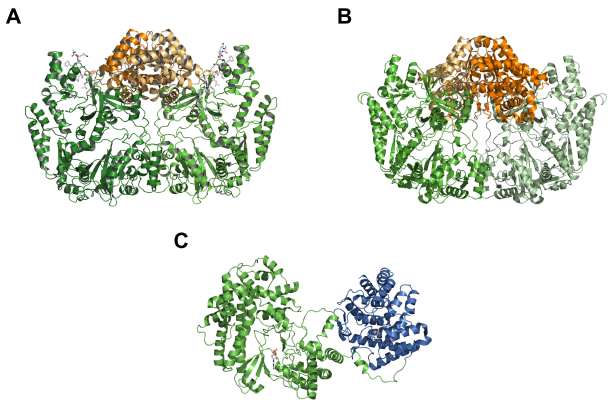

FIGURE 3 | Comparison of LanB and LanM crystal structures. **(A)** Crystal structure of dimeric NisB (PDB ID: 4WD; Ortega et al., 2015), representing the first example of a class I LanB dehydratase. The glutamylation domain is highlighted in green and light green, the elimination domain in orange and light orange. The part of the LP of NisA is shown in ball-and-stick representation. **(B)** Crystal structure of dimeric MibB (PBD ID: 5EHK; Ortega et al., 2016). Color-coding is as in panel **(A)**. **(C)** Crystal structure of CylM (PBD ID 5DZT; Dong et al., 2015), the first example of a LanM enzyme of class II lanthipeptides. The kinase-domain is shown in green and the cyclase-domain in blue. A bond AMP molecule within the kinase-domain is displayed as a ball-and-stick representation. Cartoons were generated using PyMol (www.pymol.org).

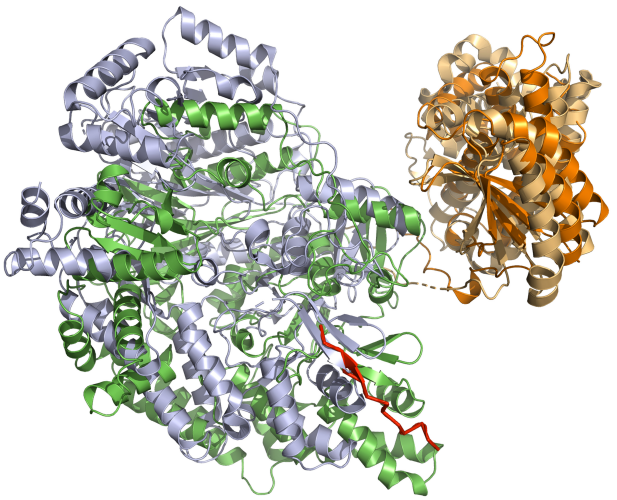

FIGURE 4 | Superimposition of NisB and MibB crystal structures. The superimposition is based on the elimination domain (residues 713–961 of NisB and 800–1048 for MibB with a RSMD of 3.6 Å over 618 Ca atoms). The glutamylation domain is shown in green (NisB) and gray (MibB), while the elimination domain is shown in light orange (NisB) and orange (MibB). For simplicity only monomers of NisB and MibB are shown. The bound LP of NisA in NisB is shown in red. Cartoons were generated using PyMol (www.pymol.org).

(Bothwell et al., 2019). Thus, the reason for this difference is still an open question.

NisB can be sub-divided into an N-terminal glutamylation domain (green and light green cartoons in **Figure 3A** of approximately 800 amino acid residues) and a C-terminal elimination domain (orange and light orange cartoons in **Figure 3A** of approximately 350 amino acid residues). This two-domain structural architecture was also found within MibB (**Figure 3B**), the class I LanB enzyme of NAI-107 (Ortega et al., 2016). Equally important, MibB like NisB requires $tRNA^{Glu}$ to catalyze the dehydration reaction. Three further examples of related LanB enzymes use so-called split LanB, where one protein is involved in aminoacylation and the other protein in the elimination of activated amino acid (aa) residues (Hudson et al., 2015; Mohr et al., 2015; Ozaki et al., 2016), also depend on the presence of $tRNA^{Glu}$ for dehydration. This clearly demonstrates that class I LanB enzymes use this rather unexpected mechanism to dehydrate serine and threonine residues in the CP of lanthipeptides.

In contrast to NisB (Ortega et al., 2015), MibB (Ortega et al., 2016) was crystallized in the absence of a substrate and displayed the same overall dimeric architecture composed of an approximately 800 amino acids large N-terminal glutamylation domain (green and light green in **Figure 3B**) and an approximately 350 amino acid large C-terminal elimination domain (orange and light orange in **Figure 3B**). The absence of the natural substrate allows the comparison with NisB to highlight structural changes that occur concomitant with substrate binding (**Figure 4**). As evident from the structural superimposition of both proteins using the C-terminal elimination domain as an anchor point, the glutamylation domain undergoes a translational and rotational motion resulting in a more compact shape of the LanB enzyme (**Figure 4**). This transition might be reminiscent of the conformational selection proposed for class II LanM enzymes. Here, the LanM enzyme is in equilibrium between an inactive and an active conformation. In the absence of substrate, more precise the LP, the equilibrium is shifted toward the inactive state, while binding of the LP shifts it toward the catalysis-competent state. This model is supported by experiments, in which the LP was added *in trans* or fused to the LanM enzyme (Levengood et al., 2007; Oman et al., 2012; Thibodeaux et al., 2015). In both cases, the isolated CP was modified although the fusion of the LP resulted in a more efficient system. Khusainov and Kuipers performed *in vivo* studies with separately expressed LP (NisA (1-23) and CP of nisin (NisA(24-57)-H_6), leaderless nisin (NisA(24-57)-H_6), and full-size nisin with a C-terminal extension and a His-tag (NisA(1-57)-H_6). These studies revealed partially modifications in spite of missing or in *trans* expressed LP, which led to the conclusion that the LP is not crucial for PTMs but increases the efficiency. However, only the fused LP led to complete modification (Khusainov and Kuipers, 2012). All in all, a mostly similar scenario could be suggested for class I LanB enzymes. In contrast, the LP of class III lanthipeptides seems to be crucial for PTMs (Müller et al., 2011; Wang and van der Donk, 2012).

Structural information is available for class II LanM enzymes (Siezen et al., 1996; Zhang et al., 2012) that encode the dehydration, elimination and cyclization domains on a single gene (**Figure 3C**). In clear contrast to LanB enzymes, these dehydratases require ATP and Mg^{2+} as cofactors as shown

experimentally for LctM in 2005 (Chatterjee et al., 2005a). The crystal structure of CylM (Dong et al., 2015) revealed the expected two-domain organization, an N-terminal dehydration domain (green in **Figure 3C**) and a C-terminal cyclization domain (blue in **Figure 3C**), which resemble the structure of NisC (Li et al., 2006), a class I LanC enzyme (see below). Not anticipated, the N-terminal domain displays structural similarities to eukaryotic lipid kinase domains bearing a novel, secondary structure topology. The activation loops of serine/threonine kinases including the P-loop are present as well as characteristic helices. Nevertheless, also a novel kinase activation domain is present, whose function was determined by mutational studies, explaining the dependence of LanM enzymes on ATP and Mg^{2+}. Here, in contrast to LanB enzymes (Garg et al., 2013), the dehydration relies on phosphorylation of serine and threonine residues of the substrate, the presence of phosphorylated instead of glutamylated intermediates and subsequent the elimination of inorganic phosphate (Chatterjee et al., 2005a). However, only AMP was observed in the structure and conclusions on the molecular mechanism of LanM function are not available at the moment.

The only recently discovered Class III (LanKC) and class IV (LanL) lanthipeptide modification enzymes, display a three-domain organization composed of a lyase, kinase and a C-terminal cyclase domain, which differs among the two classes (**Figure 2**; Goto et al., 2010; Meindl et al., 2010; Zhang et al., 2015). While the cyclase domain of LanL is apparently similar to the C-terminal domain of LanM enzymes or LanC and its activity also clearly relies on Zn^{2+}. On the contrary, the cyclase domain of LanKC is apparently not Zn^{2+}-dependent as it does not contain the highly conserved residues that are required for the coordination of this ion. Thus, two classes depending on the ability to coordinate Zn^{2+} or not were defined and the generic names LanKC (Class III) or LanL (class IV) were introduced (Kodani et al., 2004; Goto et al., 2010). Structural information is so far not available and insights into these lanthipeptide modification enzymes depend solely on genetic and functional data. Sequence analysis revealed similarities to serine/threonine kinases and effector proteins from Gram-negative and Gram-positive bacteria that catalyze the elimination of phosphorylated serine and threonine residues (phospholyases) in the N-terminal part of the protein (Young et al., 2003; Zhu et al., 2007; Chen et al., 2008). In contrast to class II LanM enzymes that are strictly ATP dependent, the kinase domains of LanKC and LanL have no real specificity for a phospho-donor. Depending on the enzyme under investigation, specificities for GTP/dGTP, ATP, ATP/GTP/CTP/TTP or any NTP/dNTP were discovered (Muller et al., 2010; Krawczyk et al., 2012b; Voller et al., 2012; Wang and van der Donk, 2012; Jungmann et al., 2016). However, based on the sequence similarities of the lyase and kinase domains, it can be assumed that the mechanisms of phosphorylation and elimination are shared between LanKC and LanL enzymes.

We have now a fairly detailed understanding of how the dehydration reactions are catalyzed in the different classes of lanthipeptides synthetases. Nevertheless, class I enzymes represent a special case as the dehydratase LanB and the cyclase LanC are separately expressed enzymes that can act on their own (Kluskens et al., 2005; Li et al., 2006; Li and van der Donk, 2007; Rink et al., 2007a; Garg et al., 2013). However, *in vivo* both enzymes are present. An elegant set of experiments using plasmid-based expression of the possible combinations of maturation enzymes demonstrated an astonishing inter-dependence between the dehydratase NisB and the cyclase NisC. Here, ring formation and dehydration acted in concert, which resulted in the protection of potential dehydration positions during ring formation (Karakas Sen et al., 1999; Koponen et al., 2002; Kluskens et al., 2005; Li et al., 2006; Li and van der Donk, 2007; Rink et al., 2007a,b; Lubelski et al., 2009; Oman and van der Donk, 2010; Plat et al., 2011, 2013; Khusainov and Kuipers, 2012; Khusainov et al., 2013; Garg et al., 2013; Ortega et al., 2015). This resulted in the proposal, that a strict N- to C-terminal directionality is operational in NisA maturation, suggesting that dehydration and ring formation is an intertwined process (Ortega et al., 2015). Consequently, such a directionality would also suggested a sort of channeling of the substrate that is bound to a LanB/LanC complex forcing the PTM reactions to start at the N-terminus and proceed all the way to the C-terminus before finalizing the maturation reactions. In 2014, Zhang et al. (2014) confirmed for NisB by mass-spectrometry (more precisely via HSEE analysis) an overall dehydration process from N- to- C- terminus, but a closer view revealed no strict directionality. In clear contrast, *in vitro* studies of the lanthipeptide NAI-107 (MibA, class I), suggest the absence of a N- to C-directionality, rather a C- to N-directionality, after dehydration of the N-terminus was observed (Ortega et al., 2016). The same C- to N-directionality was found for class III LanKC enzymes via single-mutation-studies (AciKC) and isotope labeling studies (LabKC) (Krawczyk et al., 2012a; Wang and van der Donk, 2012). Contrary to this, the synthetases of class II LctM and HalM2 revealed the opposite modification direction from N- to C-terminus (Lee et al., 2009). Surprisingly, the directionality of ProcM, also a class II synthetase, is distinct from the previous mentioned LacM enzymes. Zhang et al. (2012) investigated beside NisB also the dehydration directionality of ProcM, which revealed a generally C- to N-terminal direction of the dehydration process via mass-spectrometry. The difference regarding the directionality of the modification process within one class (i.e., ProcM and HalM2) may indicate that different binding modes are present. ProcM and HalM2 are not phylogenetically closely related, which could have led to distinct binding modes for the lanthipeptides (Zhang et al., 2012). This obviously raises the question whether a unique mechanism is operational and what the molecular ruler underlying these mechanisms actually is. Further structural studies of synthetases (LanM, LanKC, and LanL) with the lanthipeptide LanA or LP are undoubtly necessary to clear up the remaining questions before conclusions can be drawn. All in all, the directionality of the dehydration process is non-uniform among the class I dehydratases (LanBs) and class II synthetases. Consequential, the directionality can not be assumed based on the class of the lanthipeptide and each modification enzyme needs to be investigated.

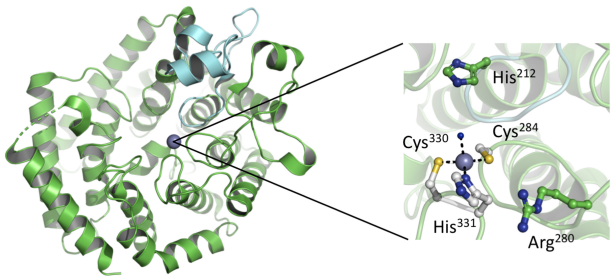

FIGURE 5 | Crystal structure of NisC. **(Left)** The overall crystal structure comprises an a,a toroidal fold (green) and a domain extension. This extension a SH2-like domain (cyan) is located close to the catalytic center. Within the active site a Zn^{2+} ion, shown as a gray sphere, is bound. **(Right)** Zoom-in into the active site of NisC. Residues important for the coordination of the Zn^{2+} ion (Cys284, His330, and Cys331) or function (His212 and Arg280) are shown in ball-and-stick representation. Cartoons were generated using PyMol (www.pymol.org).

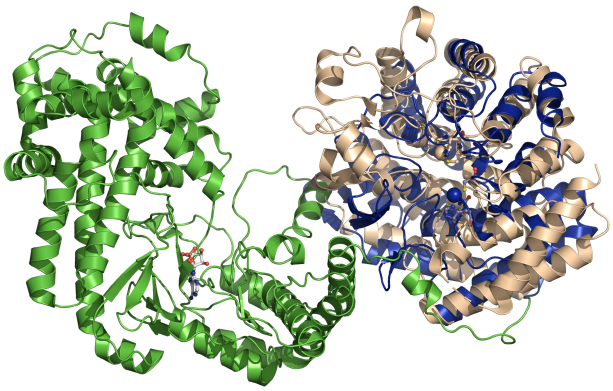

FIGURE 6 | Superimposition of NisC and CylM crystal structures. The superimposition is based on the cyclase domain of CylM (residues 641–992 of CylM). NisC is shown in blue and CylM in green (dehydratase domain) and light brown (cyclase domain). The bound AMP of CylM is shown in ball-and-stick representation. The two Zn^{2+} ions and the coordination amino acids are shown as blue sphere (NisC) and light brown sphere (CylM). The coordination amino acid residues are highlighted in ball-and-stick representation in blue (NisC) and light brown (CylM). Cartoons were generated using PyMol (www.pymol.org).

THE SECOND MATURATION STEP – THE CYCLIZATION REACTION

LanC enzymes and the cyclization domain of classes II–IV enzymes catalyze the nucleophilic attack of a thiolate (from Cys) to dehydrated amino acid (aa), where they facilitating the regio- and stereoselectivity to form thioether rings with the correct ring topology. Although, the lanthionine ring formation can occur spontaneously at basic pH values (pH > 7.5), however, leading to an erroneous stereochemistry of the Lan or (Me)Lan rings (Burrage et al., 2000; Okeley et al., 2000; Kuipers et al., 2004). Due to missing stereochemistry investigations of Lan and MeLan residues of lanthipeptides and the assumption that all Lan and (Me)Lan rings in lanthipeptides have the same "DL"-stereochemistry as previously shown for selected lantibiotics (Chatterjee et al., 2005b), the discovery that CylM can catalyze different stereochemistry within one single polypeptide was surprising. Furthermore, the studies of Tang and van der Donk (2013) revealed that the sequence of the lanthipeptide could be crucial for the stereoselectivity of ring formation.

The analysis of purified LanC enzymes (NisC and SpaC) revealed the presence of equal stoichiometric amounts of Zn^{2+} suggesting that the metal ion plays an essential role in deprotonating the thiol group of the cysteine residue, presumably by decreasing the pK_a value of the cysteine side chain (Okeley et al., 2003). Such a deprotonation or at least polarization accelerates the rate of Michael-type additions during the formation of the (Me)Lan rings. A detailed glimpse on the mechanism was possible, as the crystal structure of NisC was reported in 2006 (Li et al., 2006). The protein displays an a,a toroid consisting of six helices each, a SH2-like domain and one Zn^{2+} ion (**Figure 5**). The Zn^{2+} ion is coordinated by two highly conserved cysteine residues (Cys284 and Cys330) and one histidine residue (His331). Additionally, the tetragonal coordination sphere is complemented by a water molecule (inset of **Figure 5**). The presence of the SH2-like domain suggests that this domain interacts with dehydrated NisA, however there are no experimental evidence supporting this hypothesis and the functional role of this domain remains elusive. Based on the crystal structure of NisC, some residues conserved among LanC proteins were mutated (Li and van der Donk, 2007). There, the mutations of Cys284, Cys330, and His331 lead to inactive NisA. Interestingly, the ability to bind Zn^{2+} was preserved by mutating other active site residues (e.g., mutation H212N, H212F, and D141N) but no cyclization was detected. Thus, we slowly obtain a mechanistic picture of how NisC, but also LanC proteins in general, guide the formation of lanthionine rings. These insights will likely also hold for the cyclization domains of class II and class IV enzymes due to the structural conservation [**Figure 6** – comparison of CylM (LanM) and NisC (LanC)] or the conservation of residues identified to be essential for Zn^{2+} coordination or enzyme function. Noteworthy, an SH2-like domain (Mayer and Gupta, 1998; Li et al., 2006), which is found in NisC and might be involved in substrate binding, is not present in CylM. There, an additional subdomain is included in the cyclization domain, that seem to be important for substrate binding (Dong et al., 2015). Nevertheless, we still do not have structural information of the LanA–LanC complex and only this information will result in a final and complete picture. In contrast, the putative cyclization domain of class III enzymes (LanKC, i.e., AciKC) do not contain the conserved Zn^{2+} coordinating residues, which raises the question how cyclization takes place (Wang and van der Donk, 2012). Another important aspect of class III lanthipeptides is the presence of another type of cyclization, Lab or methyllabionin (MeLab; Meindl et al., 2010; Iorio et al., 2014). After the initial Michael-type addition of a cysteine residue and Dha, the system undergoes another Michael-type addition reaction with a second Dha residue, resulting in the formation of a methylene moiety based ring, a (Me)Lab ring.

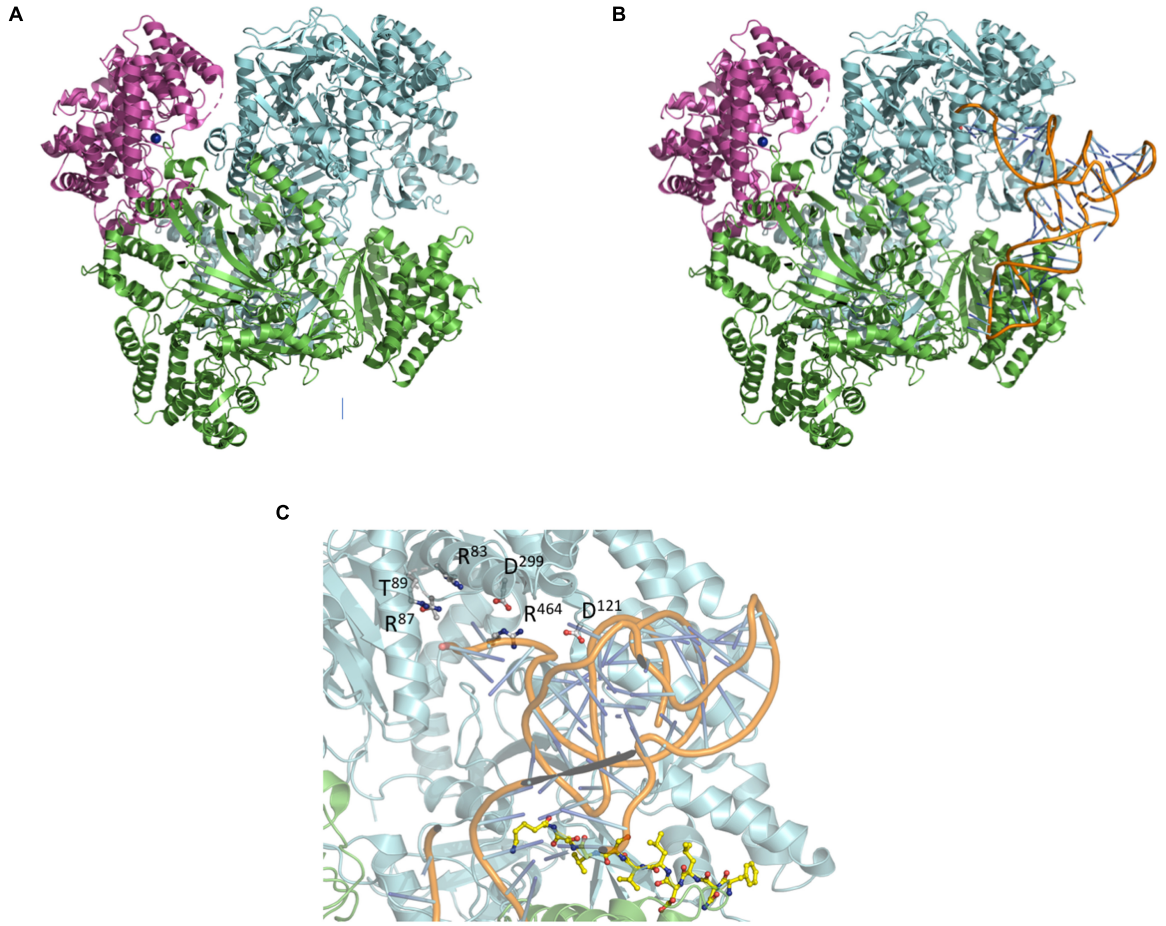

FIGURE 7 | Composition of the NisA maturation complex NisB and NisC and tRNA docking. **(A)** Crystal structures of NisC and NisB docked into the SAXS envelope (Reiners et al., 2017). **(B)** Docking of $tRNA^{Glu}$ into the NisA maturation complex composed of dimeric NisB (cartoon representation in green and cyan) and monomeric NisC (cartoon representation in magenta). The LP bound to NisB is shown in yellow ball-and-stick representation. **(C)** Zoom-in into the tip region of bound $tRNA^{Glu}$. Residues of NisB (Garg et al., 2013; Khusainov et al., 2013; Ortega et al., 2015), which resulted in abolished dehydration upon mutation (Arg87, Thr89, Asp121, Asp299, and Arg464), are highlighted in ball-and-stick representation. Cartoons were generated using PyMol (http://www.pymol.org).

However, one has to wait for structural insights into the LanKC family before further mechanistic conclusions can be drawn.

A CONCERTED ACTION DURING MATURATION

The individual domains of LanKC (class III) and LanL (class IV) enzymes are capable of catalyzing their individual reactions also in the absence of the other domains (Goto et al., 2011). This especially holds true for class I enzymes. However, early on, functional studies based on co-immunoprecipitation, yeast two hybrid approaches or mutational studies demonstrated that at least LanB and LanC act synergistically (Siegers et al., 1996; Kiesau et al., 1997; Lubelski et al., 2009). Moreover, a maturation complex consisting of not only NisB and NisC but also the ABC transporter NisT apparently exists during the modification of NisA (Siegers et al., 1996). Further support of a concerted action came from studies of subtilin, which suggested also the presence of such a complex composed of the dehydratase SpaB, the cyclase SpaC and the ABC transporter SpaT (Kiesau et al., 1997).

First insights into the assembly and architecture of a full class I lanthipeptide maturation complex was obtained for the lanthipeptide nisin. Reiners et al. (2017) used purified components to assemble the NisB/NisC/NisA maturation complex *in vitro*. Using size exclusion chromatography combined with multi-angle light scattering (SEC–MALS), they demonstrated that the complex was composed of a dimer of the dehydratase NisB, a monomer of the cyclase NisC and one molecule of the substrate, NisA resulting in a stoichiometry of 2:1:1 and a molecular weight of approximately 291 kDa. Importantly, the formation of the maturation complex was strictly dependent on the presence of the FNLD box within the LP as shown previously by *in vivo* and *in vitro* studies. Mutation of the four amino acids of the FNLD to AAAA completely prevented complex assembly (Khusainov et al., 2011, 2013; Mavaro et al., 2011; Plat et al., 2011, 2013; Abts et al., 2013).

From a mechanistic point of view, it was also important that a molecular signal was identified in this study that triggered disassembly of the maturation complex. Using a series of (Me)Lan ring mutants, e.g., Cys–Ala exchanges that prevented ring formation at the corresponding position, proved that the presence of the last, C-terminal (Me)Lan ring represented the 'disassembly signal'. This obviously goes nicely in hand with the *in vivo* situation, where a maturation complex should continue the PTM reaction and only release the fully modified product. In other words, the maturation complex is capable of reading out the stage of modifications and only the terminal modification state, the fully modified product is released, ready to be secreted by the cognate ABC transporter. Of course the exact molecular role of the ABC transporter within such a maturation complex is currently completely unknown and requires further investigations addressing its precise role.

Moving one step further, small-angle X-ray scattering (SAXS) was used to produce a low resolution envelope of the NisB/NisC/NisA complex allowing to determine the orientation of the individual high resolution crystal structures of NisB and NisC into the SAXS envelope (**Figure 7A**; Reiners et al., 2017). A comparison of apo-NisB and NisA-saturated NisB suggested the presence of a tunnel and therefore provided an idea for the actual substrate-binding site within the complex. This allowed therefore a first molecular glimpse on the molecular architecture of a maturation complex of a class I lanthipeptide (**Figure 7A**).

Following the protocol of Ortega et al. (2015) the crystal structure of $tRNA^{Glu}$ (extracted from pdb entry 1N78) was docked into the complex using the HDOCK server[1] employing standard settings (Yan et al., 2017). The proposed tertiary complex is shown in **Figure 7B**. Interestingly, the $tRNA^{Glu}$ binding sites are similar in the isolated NisB dimer and the maturation complex. Mapping residues, which result in impaired functionality, cluster around the potential $tRNA^{Glu}$-binding site (**Figure 7C**) suggesting that the model is of functional significance. Additional residues that were identified in mutational studies were also mapped on the proposed complex (Garg et al., 2013; Khusainov et al., 2013; Ortega et al., 2015). Noteworthy, the mutation of arginine and aspartate residues leading to a complete loss of dehydratase activity in NisB mapped in the close vicinity of the bound $tRNA^{Glu}$ (**Figure 7C**). Obviously, this *in silico* complex requires experimental verification. Nevertheless, it represents a starting point to design such experiments, which might help to understand the molecular mechanism by which the nisin maturation complex and eventually other maturation complexes of class I lanthipeptides operate.

[1] http://hdock.phys.hust.edu.cn

CONCLUSION AND OUTLOOK

Over the past years, we have seen tremendous advances in our understanding of lanthipeptides, especially class I lanthipeptides (lantibiotics) on the genetic, functional and structural level. Here, we have focused mainly on the mechanistic and structural insights of the modification process and the corresponding enzymes. The presented findings have answered many questions, but some questions are still open and even new questions arose. Considerably more work will need to be done to understand in detail the molecular coordination and timing of the maturation enzymes and their interplay with the exporter proteins. Only then, the fundamental question of why maturation intermediates of the substrates are not secreted can be answered. Even though literature exhibits great results using lanthipeptide modification enzymes (i.e., synthesis of an analog of angiotensin and an analog of the opioid dermorphin) without full knowledge regarding the mechanisms, a very detailed mechanistic understanding will facilitate higher efficiency regarding drug engineering and design (Luskens et al., 2008; Huo and van der Donk, 2016).

AUTHOR CONTRIBUTIONS

All authors wrote the manuscript.

FUNDING

The Center for Structural Studies is funded by the Deutsche Forschungsgemeinschaft DFG grant number 417919780. Research on Nisin was funded by the Deutsche Forschungsgemeinschaft DFG through grant Schm1279/13-1 to LS.

ACKNOWLEDGMENTS

We thank members of the Institute of Biochemistry for fruitfull discussions.

REFERENCES

Arnison, P. G., Bibb, M. J., Bierbaum, G., Bowers, A. A., Bugni, T. S., Bulaj, G., et al. (2013). Ribosomally synthesized and post-translationally modified peptide natural products: overview and recommendations for a universal nomenclature. *Nat. Prod. Rep* 30, 108–160. doi: 10.1039/c2np20085f

Skinnider, M. A., Johnston, C. W., Edgar, R. E., Dejong, C. A., Merwin, N. J., Rees, P. N., et al. (2016). Genomic charting of ribosomally synthesized natural product chemical space facilitates targeted mining. *Proc Natl Acad Sci U S A* 113, E6343–E6351.

Bierbaum, G., Szekat, C., Josten, M., Heidrich, C., Kempter, C., Jung, G., et al. (1996). Engineering of a novel thioether bridge and role of modified residues in the lantibiotic Pep5. *Appl Environ Microbiol* 62, 385–392.

Oman, T. J., and van der Donk, W. A. (2010). Follow the leader: the use of leader peptides to guide natural product biosynthesis. *Nat Chem Biol* 6, 9–18. doi: 10.1038/nchembio.286

Kuipers, O. P., Beerthuyzen, M. M., Siezen, R. J., and De Vos, W. M. (1993). Characterization of the nisin gene cluster nisABTCIPR of *Lactococcus lactis*. Requirement of expression of the nisA and nisI genes for development of immunity. *Eur. J. Biochem* 216, 281–291.

van der Meer, J. R., Rollema, H. S., Siezen, R. J., Beerthuyzen, M. M., Kuipers, O. P., and de Vos, W. M. (1994). Influence of amino acid substitutions in the nisin leader peptide on biosynthesis and secretion of nisin by *Lactococcus lactis*. *J. Biol. Chem* 269, 3555–3562.

Kuipers, A., de Boef, E., Rink, R., Fekken, S., Kluskens, L. D., Driessen, A. J., et al. (2004). NisT, the transporter of the lantibiotic nisin, can transport fully modified, dehydrated, and unmodified prenisin and fusions of the leader peptide with non-lantibiotic peptides. *J. Biol. Chem* 279, 22176–22182.

Khusainov, R., and Kuipers, O. P. (2012). When the leader gets loose: in vivo biosynthesis of a leaderless prenisin is stimulated by a trans-acting leader peptide. *Chembiochem* 13, 2433–2438. doi: 10.1002/cbic.201200437

Nishie, M., Sasaki, M., Nagao, J., Zendo, T., Nakayama, J., and Sonomoto, K. (2011). Lantibiotic transporter requires cooperative functioning of the peptidase domain and the ATP binding domain. *J Biol Chem* 286, 11163–11169. doi: 10.1074/jbc.M110.212704

Ortega, M. A., Velasquez, J. E., Garg, N., Zhang, Q., Joyce, R. E., Nair, S. K., et al. (2014). Substrate specificity of the lanthipeptide peptidase ElxP and the oxidoreductase ElxO. *ACS Chem. Biol.* 9, 1718–1725. doi: 10.1021/cb5002526

van der Meer, J. R., Polman, J., Beerthuyzen, M. M., Siezen, R. J., Kuipers, O. P., and De Vos, W. M. (1993). Characterization of the *Lactococcus lactis* nisin A operon genes nisP, encoding a subtilisin-like serine protease involved in precursor processing, and nisR, encoding a regulatory protein involved in nisin biosynthesis. *J Bacteriol* 175, 2578–2588.

Gross, E., and Morell, J. L. (1967). The presence of dehydroalanine in the antibiotic nisin and its relationship to activity. *J Am Chem Soc* 89, 2791–2792.

Gross, E., Morell, J. L., and Craig, L. C. (1969). Dehydroalanyllysine: identical COOH-terminal structures in the peptide antibiotics nisin and subtilin. *Proc Natl Acad Sci U S A* 62, 952–956.

Gross, E., and Morell, J. L. (1971). The structure of nisin. *J Am Chem Soc* 93, 4634–4635.

Karakas Sen, A., Narbad, A., Horn, N., Dodd, H. M., Parr, A. J., Colquhoun, I., et al. (1999). Post-translational modification of nisin. The involvement of NisB in the dehydration process. *Eur. J. Biochem.* 261, 524–532.

Gutowskieckel, Z., Klein, C., Siegers, K., Bohm, K., Hammelmann, M., and Entian, K. D. (1994). Growth Phase-Dependent Regulation and Membrane Localization of SpaB, a Protein Involved in Biosynthesis of the Lantibiotic Subtilin. *Applied and Environmental Microbiology* 60, 1–11.

Peschel, A., Ottenwalder, B., and Gotz, F. (1996). Inducible production and cellular location of the epidermin biosynthetic enzyme EpiB using an improved staphylococcal expression system. *Fems Microbiology Letters* 137, 279–284.

Gilmore, M. S., Segarra, R. A., Booth, M. C., Bogie, C. P., Hall, L. R., and Clewell, D. B. (1994). Genetic structure of the *Enterococcus faecalis* plasmid pAD1-encoded cytolytic toxin system and its relationship to lantibiotic determinants. *J Bacteriol* 176, 7335–7344.

Barber, M., Elliot, G. J., Bordoli, R. S., Green, B. N., and Bycroft, B. W. (1988). Confirmation of the structure of nisin and its major degradation product by FAB-MS and FAB-MS/MS. *Experientia* 44, 266–270.

Meindl, K., Schmiederer, T., Schneider, K., Reicke, A., Butz, D., Keller, S., et al. (2010). Labyrinthopeptins: a new class of carbacyclic lantibiotics. *Angew Chem Int Ed Engl* 49, 1151–1154.

Iorio, M., Sasso, O., Maffioli, I., Bertorelli, R., Monciardini, P., Sosio, M., et al. (2014). A glycosylated, labionin-containing lanthipeptide with marked antinociceptive activity. *ACS Chem Biol* 9, 398–404. doi: 10.1021/cb400692w

Mortvedt, C. I., Nissen-Meyer, J., Sletten, K., and Nes, I. F. (1991). Purification and amino acid sequence of lactocin S, a bacteriocin produced by *Lactobacillus sake* L45. *Appl Environ Microbiol* 57, 1829–1834.

Kupke, T., Stevanovic, S., Sahl, H. G., and Gotz, F. (1992). Purification and characterization of EpiD, a flavoprotein involved in the biosynthesis of the lantibiotic epidermin. *J Bacteriol* 174, 5354–5361.

Skaugen, M., Nissen-Meyer, J., Jung, G., Stevanovic, S., Sletten, K., Inger, C., et al. (1994). *In vivo* conversion of L-serine to D-alanine in a ribosomally synthesized polypeptide. *J Biol Chem* 269, 27183–27185.

van de Kamp, M., van den Hooven, H. W., Konings, R. N., Bierbaum, G., Sahl, H. G., Kuipers, O. P., et al. (1995). Elucidation of the primary structure of the lantibiotic epilancin K7 from *Staphylococcus epidermidis* K7. Cloning and characterisation of the epilancin-K7-encoding gene and NMR analysis of mature epilancin K7. *Eur J Biochem* 230, 587–600.

Heidrich, C., Pag, U., Josten, M., Metzger, J., Jack, R. W., Bierbaum, G., et al. (1998). Isolation, Characterization, and Heterologous Expression of the Novel Lantibiotic Epicidin 280 and Analysis of Its Biosynthetic Gene Cluster. *Appl Environ Microbiol* 64, 3140–3146.

Ekkelenkamp, M. B., Hanssen, M., Danny Hsu, S. T., de Jong, A., Milatovic, D., Verhoef, J., et al. (2005). Isolation and structural characterization of epilancin 15X, a novel lantibiotic from a clinical strain of *Staphylococcus epidermidis*. *FEBS Lett* 579, 1917–1922.

Castiglione, F., Lazzarini, A., Carrano, L., Corti, E., Ciciliato, I., Gastaldo, L., et al. (2008). Determining the structure and mode of action of microbisporicin, a potent lantibiotic active against multiresistant pathogens. *Chem Biol* 15, 22–31. doi: 10.1016/j.chembiol.2007.11.009

He, Z., Yuan, C., Zhang, L., and Yousef, A. E. (2008). N-terminal acetylation in paenibacillin, a novel lantibiotic. *FEBS Lett* 582, 2787–2792. doi: 10.1016/j.febslet.2008.07.008

Velasquez, J. E., Zhang, X., and van der Donk, W. A. (2011). Biosynthesis of the antimicrobial peptide epilancin 15X and its N-terminal lactate. *Chem Biol* 18, 857–867. doi: 10.1016/j.chembiol.2011.05.007

Huang, E., and Yousef, A. E. (2015). Biosynthesis of paenibacillin, a lantibiotic with N-terminal acetylation, by *Paenibacillus polymyxa*. *Microbiol Res* 181, 15–21. doi: 10.1016/j.micres.2015.08.001

McIntosh, J. A., Donia, M. S., and Schmidt, E. W. (2009). Ribosomal peptide natural products: bridging the ribosomal and nonribosomal worlds. *Nat Prod Rep* 26, 537–559.

Dunbar, K. L., and Mitchell, D. A. (2013). Revealing nature's synthetic potential through the study of ribosomal natural product biosynthesis. *ACS Chem Biol* 8, 473–487. doi: 10.1021/cb3005325

Walsh, C. T. (2014). Blurring the lines between ribosomal and nonribosomal peptide scaffolds. *ACS Chem Biol* 9, 1653–1661. doi: 10.1021/cb500 3587

Ortega, M. A., and van der Donk, W. A. (2016). New Insights into the Biosynthetic Logic of Ribosomally Synthesized and Post-translationally Modified Peptide Natural Products. *Cell Chem Biol* 23, 31–44. doi: 10.1016/j.chembiol.2015.11.012

Repka, L. M., Chekan, J. R., Nair, S. K., and van der Donk, W. A. (2017). Mechanistic Understanding of Lanthipeptide Biosynthetic Enzymes. *Chem Rev* 117, 5457–5520. doi: 10.1021/acs.chemrev.6b00591

Schnell, N., Entian, K. D., Schneider, U., Gotz, F., Zahner, H., Kellner, R., et al. (1988). Prepeptide sequence of epidermin, a ribosomally synthesized antibiotic with four sulphide-rings. *Nature* 333, 276–278.

Kodani, S., Hudson, M. E., Durrant, M. C., Buttner, M. J., Nodwell, J. R., and Willey, J. M. (2004). The SapB morphogen is a lantibiotic-like peptide derived from the product of the developmental gene ramS in *Streptomyces coelicolor*. *Proc Natl Acad Sci U S A* 101, 11448–11453.

Kodani, S., Lodato, M. A., Durrant, M. C., Picart, F., and Willey, J. M. (2005). SapT, a lanthionine-containing peptide involved in aerial hyphae formation in the streptomycetes. *Mol Microbiol* 58, 1368–1380.

Ferir, G., Petrova, I., Andrei, G., Huskens, D., Hoorelbeke, B., Snoeck, R., et al. (2013). The lantibiotic peptide labyrinthopeptin A1 demonstrates broad anti-HIV and anti-HSV activity with potential for microbicidal applications. *PLoS One* 8:e64010. doi: 10.1371/journal.pone.0064010

Mohr, K. I., Volz, C., Jansen, R., Wray, V., Hoffmann, J., Bernecker, S., et al. (2015). Pinensins: the first antifungal lantibiotics. *Angew Chem Int Ed Engl* 54, 11254–11258. doi: 10.1002/anie.201500927

Chatterjee, C., Paul, M., Xie, L., and van der Donk, W. A. (2005b). Biosynthesis and mode of action of lantibiotics. *Chem Rev* 105, 633–684.

Breukink, E., and de Kruijff, B. (2006). Lipid II as a target for antibiotics. *Nature Reviews Drug Discovery* 5, 321–332.

Lubelski, J., Rink, R., Khusainov, R., Moll, G. N., and Kuipers, O. P. (2008). Biosynthesis, immunity, regulation, mode of action and engineering of the model lantibiotic nisin. *Cell Mol Life Sci* 65, 455–476.

Bierbaum, G., and Sahl, H. G. (2009). Lantibiotics: mode of action, biosynthesis and bioengineering. *Curr Pharm Biotechnol* 10, 2–18.

Schneider, T., and Sahl, H. G. (2010). Lipid II and other bactoprenol-bound cell wall precursors as drug targets. *Curr Opin Investig Drugs* 11, 157–164.

Islam, M. R., Nagao, J., Zendo, T., and Sonomoto, K. (2012). Antimicrobial mechanism of lantibiotics. *Biochem Soc Trans* 40, 1528–1533. doi: 10.1042/BST20120190

Severina, E., Severin, A., and Tomasz, A. (1998). Antibacterial efficacy of nisin against multidrug-resistant Gram-positive pathogens. *J Antimicrob Chemother* 41, 341–347.

Breukink, E., Wiedemann, I., van Kraaij, C., Kuipers, O. P., Sahl, H. G., and de Kruijff, B. (1999). Use of the cell wall precursor lipid II by a pore-forming peptide antibiotic. *Science* 286, 2361–2364.

Wiedemann, I., Breukink, E., van Kraaij, C., Kuipers, O. P., Bierbaum, G., de Kruijff, B., et al. (2001). Specific binding of nisin to the peptidoglycan precursor lipid II combines pore formation and inhibition of cell wall biosynthesis for potent antibiotic activity. *J Biol Chem* 276, 1772–1779.

Brumfitt, W., Salton, M. R., and Hamilton-Miller, J. M. (2002). Nisin, alone and combined with peptidoglycan-modulating antibiotics: activity against methicillin-resistant *Staphylococcus aureus* and vancomycin-resistant enterococci. *J Antimicrob Chemother* 50, 731–734.

van Heusden, H. E., de Kruijff, B., and Breukink, E. (2002). Lipid II induces a transmembrane orientation of the pore-forming peptide lantibiotic nisin. *Biochemistry* 41, 12171–12178.

Hasper, H. E., de Kruijff, B., and Breukink, E. (2004). Assembly and stability of nisin-lipid II pores. *Biochemistry* 43, 11567–11575.

Hsu, S. T. D., Breukink, E., Tischenko, E., Lutters, M. A. G., de Kruijff, B., Kaptein, R., et al. (2004). The nisin-lipid II complex reveals a pyrophosphate cage that provides a blueprint for novel antibiotics. *Nature Structural & Molecular Biology* 11, 963–967.

Hasper, H. E., Kramer, N. E., Smith, J. L., Hillman, J. D., Zachariah, C., Kuipers, O. P., et al. (2006). An Alternative Bactericidal Mechanism of Action for Lantibiotic Peptides That Target Lipid II. *Science* 313, 1636–1637.

Cotter, P. D., Hill, C., and Ross, R. P. (2005). Bacteriocins: developing innate immunity for food. *Nat Rev Microbiol* 3, 777–788.

Mavaro, A., Abts, A., Bakkes, P. J., Moll, G. N., Driessen, A. J., Smits, S. H., et al. (2011). Substrate recognition and specificity of the NisB protein, the lantibiotic dehydratase involved in nisin biosynthesis. *J Biol Chem* 286, 30552–30560. doi: 10.1074/jbc.M111.263210

Rink, R., Kuipers, A., de Boef, E., Leenhouts, K. J., Driessen, A. J., Moll, G. N., et al. (2005). Lantibiotic structures as guidelines for the design of peptides that can be modified by lantibiotic enzymes. *Biochemistry* 44, 8873–8882.

Kluskens, L. D., Kuipers, A., Rink, R., de Boef, E., Fekken, S., Driessen, A. J., et al. (2005). Post-translational modification of therapeutic peptides by NisB, the dehydratase of the lantibiotic nisin. *Biochemistry* 44, 12827–12834.

Rink, R., Kluskens, L. D., Kuipers, A., Driessen, A. J., Kuipers, O. P., and Moll, G. N. (2007a). NisC, the cyclase of the lantibiotic nisin, can catalyze cyclization of designed nonlantibiotic peptides. *Biochemistry* 46, 13179–13189.

Garg, N., Salazar-Ocampo, L. M., and van der Donk, W. A. (2013). In vitro activity of the nisin dehydratase NisB. *Proc Natl Acad Sci U S A* 110, 7258–7263. doi: 10.1073/pnas.1222488110

Ortega, M. A., Hao, Y., Zhang, Q., Walker, M. C., van der Donk, W. A., and Nair, S. K. (2015). Structure and mechanism of the tRNA-dependent lantibiotic dehydratase NisB. *Nature* 517, 509–512. doi: 10.1038/nature13888

Bothwell, I. R., Cogan, D. P., Kim, T., Reinhardt, C. J., van der Donk, W. A., and Nair, S. K. (2019). Characterization of glutamyl-tRNA-dependent dehydratases using nonreactive substrate mimics. *PNAS* 116, 17245–17250. doi: 10.1073/pnas.1905240116

Reiners, J., Abts, A., Clemens, R., Smits, S. H., and Schmitt, L. (2017). Stoichiometry and structure of a lantibiotic maturation complex. *Sci Rep* 7, 42163. doi: 10.1038/srep42163

Ortega, M. A., Hao, Y., Walker, M. C., Donadio, S., Sosio, M., Nair, S. K., et al. (2016). Structure and tRNA Specificity of MibB, a Lantibiotic Dehydratase from Actinobacteria Involved in NAI-107 Biosynthesis. *Cell Chem Biol* 23, 370–380. doi: 10.1016/j.chembiol.2015.11.017

Ozaki, T., Kurokawa, Y., Hayashi, S., Oku, N., Asamizu, S., Igarashi, Y., et al. (2016). Insights into the Biosynthesis of Dehydroalanines in Goadsporin. *Chembiochem* 17, 218–223. doi: 10.1002/cbic.201500541

Hudson, G. A., Zhang, Z., Tietz, I., Mitchell, D. A., and van der Donk, W. A. (2015). In Vitro Biosynthesis of the Core Scaffold of the Thiopeptide Thiomuracin. *J. Am. Chem. Soc.* 137, 16012–16015. doi: 10.1021/jacs.5b10194

Thibodeaux, G. N., McClerren, A. L., Ma, Y., Gancayco, M. R., and van der Donk, W. A. (2015). Synergistic binding of the leader and core peptides by the lantibiotic synthetase HalM2. *ACS Chem Biol* 10, 970–977. doi: 10.1021/cb5009876

Levengood, M. R., Patton, G. C., and van der Donk, W. A. D. (2007). The leader peptide is not required for post-translational modification by lacticin 481 synthetase. *Journal of the American Chemical Society* 129, 10314.

Oman, T. J., Knerr, P. J., Bindman, N. A., Velasquez, J. E., and van der Donk, W. A. (2012). An engineered lantibiotic synthetase that does not require a leader peptide on its substrate. *J Am Chem Soc* 134, 6952–6955. doi: 10.1021/ja3017297

Müller, W. M., Ensle, P., Krawczyk, B., and Süssmuth, R. D. (2011). Leader Peptide-Directed Processing of Labyrinthopeptin A2 Precursor Peptide by the Modifying Enzyme LabKC. *Biochemistry* 50, 8362–8373. doi: 10.1021/bi200526q

Wang, H., and van der Donk, W. A. (2012). Biosynthesis of the class III lantipeptide catenulipeptin. *ACS Chem Biol* 7, 1529–1535.

Siezen, R. J., Kuipers, O. P., and de Vos, W. M. (1996). Comparison of lantibiotic gene clusters and encoded proteins. *Antonie Van Leeuwenhoek* 69, 171–184.

Zhang, Q., Yu, Y., Velasquez, J. E., and van der Donk, W. A. (2012). Evolution of lanthipeptide synthetases. *Proc Natl Acad Sci U S A* 109, 18361–18366. doi: 10.1073/pnas.1210393109

Chatterjee, C., Miller, L. M., Leung, Y. L., Xie, L., Yi, M., Kelleher, N. L., et al. (2005a). Lacticin 481 synthetase phosphorylates its substrate during lantibiotic production. *J Am Chem Soc* 127, 15332–15333.

Dong, S. H., Tang, W. X., Lukk, T., Yu, Y., Nair, S. K., and van der Donk, W. A. (2015). The enterococcal cytolysin synthetase has an unanticipated lipid kinase fold. *Elife* 4, e07607. doi: 10.7554/eLife.07607

Li, B., Yu, J. P., Brunzelle, J. S., Moll, G. N., van der Donk, W. A., and Nair, S. K. (2006). Structure and mechanism of the lantibiotic cyclase involved in nisin biosynthesis. *Science* 311, 1464–1467.

Goto, Y., Li, B., Claesen, J., Shi, Y., Bibb, M. J., and van der Donk, W. A. (2010). Discovery of unique lanthionine synthetases reveals new mechanistic and evolutionary insights. *PLoS Biol* 8:e1000339. doi: 10.1371/journal.pbio.1000339

Zhang, Q., Doroghazi, J. R., Zhao, X., Walker, M. C., and van der Donk, W. A. (2015). Expanded natural product diversity revealed by analysis of lanthipeptide-like gene clusters in actinobacteria. *Appl Environ Microbiol* 81, 4339–4350. doi: 10.1128/AEM.00635-15

Chen, L., Wang, H., Zhang, J., Gu, L., Huang, N., Zhou, J. M., et al. (2008). Structural basis for the catalytic mechanism of phosphothreonine lyase. *Nat Struct Mol Biol* 15, 101–102.

Young, T. A., Delagoutte, B., Endrizzi, J. A., Falick, A. M., and Alber, T. (2003). Structure of Mycobacterium tuberculosis PknB supports a universal activation mechanism for Ser/Thr protein kinases. *Nat Struct Biol* 10, 168–174.

Zhu, Y., Li, H., Long, C., Hu, L., Xu, H., Liu, L., et al. (2007). Structural insights into the enzymatic mechanism of the pathogenic MAPK phosphothreonine lyase. *Mol Cell* 28, 899–913.

Muller, W. M., Schmiederer, T., Ensle, P., and Sussmuth, R. D. (2010). In vitro biosynthesis of the prepeptide of type-III lantibiotic labyrinthopeptin A2 including formation of a C-C bond as a post-translational modification. *Angew Chem Int Ed Engl* 49, 2436–2440.

Krawczyk, B., Voller, G. H., Voller, J., Ensle, P., and Sussmuth, R. D. (2012b). Curvopeptin: a new lanthionine-containing class III lantibiotic and its co-substrate promiscuous synthetase. *Chembiochem* 13, 2065–2071. doi: 10.1002/cbic.201200417

Voller, G. H., Krawczyk, J. M., Pesic, A., Krawczyk, B., Nachtigall, J., and Sussmuth, R. D. (2012). Characterization of new class III lantibiotics–erythreapeptin, avermipeptin and griseopeptin from *Saccharopolyspora erythraea*, *Streptomyces avermitilis* and *Streptomyces griseus* demonstrates stepwise N-terminal leader processing. *Chembiochem* 13, 1174–1183. doi: 10.1002/cbic.201200118

Jungmann, N. A., van Herwerden, E. F., Hugelland, M., and Sussmuth, R. D. (2016). The Supersized Class III Lanthipeptide Stackepeptin Displays Motif Multiplication in the Core Peptide. *ACS Chem Biol* 11, 69–76. doi: 10.1021/acschembio.5b00651

Li, B., and van der Donk, W. A. (2007). Identification of essential catalytic residues of the cyclase NisC involved in the biosynthesis of nisin. *J Biol Chem* 282, 21169–21175.

Rink, R., Wierenga, J., Kuipers, A., Kluskens, L. D., Driessen, A. J. M., Kuipers, O. P., et al. (2007b). Dissection and modulation of the four distinct activities of nisin by mutagenesis of rings A and B and by C-terminal truncation. *Applied and Environmental Microbiology* 73, 5809–5816.

Lubelski, J., Khusainov, R., and Kuipers, O. P. (2009). Directionality and coordination of dehydration and ring formation during biosynthesis of the lantibiotic nisin. *J Biol Chem* 284, 25962–25972. doi: 10.1074/jbc.M109.026690

Plat, A., Kluskens, L. D., Kuipers, A., Rink, R., and Moll, G. N. (2011). Requirements of the engineered leader peptide of nisin for inducing modification, export, and cleavage. *Appl Environ Microbiol* 77, 604–611. doi: 10.1128/AEM.01503-10

Khusainov, R., Moll, G. N., and Kuipers, O. P. (2013). Identification of distinct nisin leader peptide regions that determine interactions with the modification enzymes NisB and NisC. *FEBS Open Bio* 3, 237–242. doi: 10.1016/j.fob.2013.05.001

Plat, A., Kuipers, A., Rink, R., and Moll, G. N. (2013). Mechanistic aspects of lanthipeptide leaders. *Curr Protein Pept Sci* 14, 85–96.

Koponen, O., Tolonen, M., Qiao, M., Wahlstrom, G., Helin, J., and Saris, P. E. (2002). NisB is required for the dehydration and NisC for the lanthionine formation in the post-translational modification of nisin. *Microbiology* 148(Pt 11), 3561–3568. doi: 10.1099/00221287-148-11-3561

Zhang, Q., Ortega, M., Shi, Y., Wang, H., Melby, J. O., Tang, W., et al. (2014). Structural investigation of ribosomally synthesized natural products by hypothetical structure enumeration and evaluation using tandem MS. *PNAS* 111, 12031–12036. doi: 10.1073/pnas.1406418111

Krawczyk, B., Ensle, P., Müller, W. M., and Süssmuth, R. D. (2012a). Deuterium Labeled Peprides Give Insights into the Directionality of Class III Lantibiotic synthetase LabKC. *J. Am. Chem. Soc.* 134, 9922–9925. doi: 10.1021/ja3040224

Lee, M. V., Ihnken, L. A., You, Y. O., McClerren, A. L., van, der Donk WA, and Kelleher, N. L. (2009). Distributive and Directional Behavior of Lantibiotic Synthetases Revealed by High-Resolution Tandem Mass Spectrometry. *J. Am. Chem. Soc.* 131, 12258–12264. doi: 10.1021/ja9033507

Burrage, S., Raynham, T., Williams, G., Essex, J. W., Allen, C., Cardno, M., et al. (2000). Biomimetic synthesis of lantibiotics. *Chem-Eur J* 6, 1455–1466.

Okeley, N. M., Zhu, Y. T., and van der Donk, W. A. (2000). Facile chemoselective synthesis of dehydroalanine-containing peptides. *Org Lett* 2, 3603–3606.

Tang, W., and van der Donk, W. A. (2013). The Sequence of the Enterococcal Cytolysin Imparts Unusual Lanthionine Stereochemistry. *Nat. Chem. Biol.* 9, 157–159. doi: 10.1038/nchembio.1162

Okeley, N. M., Paul, M., Stasser, J. P., Blackburn, N., and van der Donk, W. A. (2003). SpaC and NisC, the cyclases involved in subtilin and nisin biosynthesis, are zinc proteins. *Biochemistry* 42, 13613–13624.

Mayer, B. J., and Gupta, R. (1998). Functions of SH2 and SH3 domains. *Curr Top Microbiol Immunol* 228, 1–22.

Goto, Y., Okesli, A., and van der Donk, W. A. (2011). Mechanistic studies of Ser/Thr dehydration catalyzed by a member of the LanL lanthionine synthetase family. *Biochemistry* 50, 891–898. doi: 10.1021/bi101750r

Siegers, K., Heinzmann, S., and Entian, K. D. (1996). Biosynthesis of lantibiotic nisin. Posttranslational modification of its prepeptide occurs at a multimeric membrane-associated lanthionine synthetase complex. *J. Biol. Chem.* 271, 12294–12301.

Kiesau, P., Eikmanns, U., Gutowski-Eckel, Z., Weber, S., Hammelmann, M., and Entian, K. D. (1997). Evidence for a multimeric subtilin synthetase complex. *J Bacteriol* 179, 1475–1481.

Abts, A., Montalban-Lopez, M., Kuipers, O. P., Smits, S. H., and Schmitt, L. (2013). NisC binds the FxLx motif of the nisin leader peptide. *Biochemistry* 52, 5387–5395. doi: 10.1021/bi4008116

Khusainov, R., Heils, R., Lubelski, J., Moll, G. N., and Kuipers, O. P. (2011). Determining sites of interaction between prenisin and its modification enzymes NisB and NisC. *Mol Microbiol* 82, 706–718. doi: 10.1111/j.1365-2958.2011.07846.x

Yan, Y., Zhang, D., Zhou, P., Li, B., and Huang, S. Y. (2017). HDOCK: a web server for protein-protein and protein-DNA/RNA docking based on a hybrid strategy. *Nucleic Acids Res* 45, W365–W373. doi: 10.1093/nar/gkx407

Luskens, L. D., Nelemans, S. A., Rink, R., de Vries, L., Meter-Arkema, A., Wang, Y., et al. (2008). Angiotensin-(1-7) with Thioether Bridge: An Angiotensin-Converting Enzyme-resistant, Potent Angiotensin-(1-7) Analog. *JPET* 328, 849–855. doi: 10.1124/jpet.108.146431

Huo, L., and van der Donk, W. A. (2016). Discovery and Characterization of Bicereucin, an Unusual D-Amino Acid-Containing Mixed Two-Component Lantibiotic. *J. Am. Chem. Soc.* 138, 5254–5257. doi: 10.1021/jacs.6b02513

Conflict of Interest: The authors declare that the research was conducted in the absence of any commercial or financial relationships that could be construed as a potential conflict of interest.

frontiers in Microbiology

ORIGINAL RESEARCH
published: 14 July 2020
doi: 10.3389/fmicb.2020.01634

Heterologous Expression of the Class IIa Bacteriocins, Plantaricin 423 and Mundticin ST4SA, in *Escherichia coli* Using Green Fluorescent Protein as a Fusion Partner

Ross Rayne Vermeulen[1], *Anton Du Preez Van Staden*[1,2]* *and Leon Dicks*[1]*

[1] Department of Microbiology, Stellenbosch University, Stellenbosch, South Africa, [2] Department of Physiological Sciences, Stellenbosch University, Stellenbosch, South Africa

OPEN ACCESS

Edited by:
Des Field,
University College Cork, Ireland

Reviewed by:
Juan Borrero,
Complutense University of Madrid, Spain
Takeshi Zendo,
Kyushu University, Japan

***Correspondence:**
Anton Du Preez Van Staden
advstaden@outlook.com
Leon Dicks
LMTD@sun.ac.za

Specialty section:
This article was submitted to Antimicrobials, Resistance and Chemotherapy, a section of the journal Frontiers in Microbiology

Received: *17 February 2020*
Accepted: *23 June 2020*
Published: *14 July 2020*

Citation:
Vermeulen RR, Van Staden ADP and Dicks L (2020) Heterologous Expression of the Class IIa Bacteriocins, Plantaricin 423 and Mundticin ST4SA, in Escherichia coli Using Green Fluorescent Protein as a Fusion Partner. Front. Microbiol. 11:1634. doi: 10.3389/fmicb.2020.01634

The antilisterial class IIa bacteriocins, plantaricin 423 and mundticin ST4SA, have previously been purified from the cell-free supernatants of *Lactobacillus plantarum* 423 and *Enterococcus mundtii* ST4SA, respectively. Here, we present the fusions of mature plantaricin 423 and mundticin ST4SA to His-tagged green fluorescent protein (GFP) for respective heterologous expression in *Escherichia coli*. Fusion of plantaricin 423 and mundticin ST4SA to His-tagged GFP produced the fusion proteins GFP-PlaX and GFP-MunX, respectively. Both fusion proteins were autofluorescent, circumvented inclusion body formation and lowered the toxicity of class IIa bacteriocins during heterologous expression. Not only did GFP-class IIa fusion stabilize heterologous expression and boost yields, the fluorescent intensity of GFP-PlaX and GFP-MunX could be monitored quantitatively and qualitatively throughout expression and purification. This robust fluorometric property allowed rapid optimization of conditions for expression and bacteriocin liberation from GFP via the incorporated WELQut protease cleavage sequence. Incubation temperature and IPTG concentration had a significant effect on bacteriocin yield, and was optimal at 18°C and 0.1–0.2 mM, respectively. GFP-MunX was approximately produced at a yield of 153.30 mg/L culture which resulted in 12.4 mg/L active mundticin ST4SA after liberation and HPLC purification. While GFP-PlaX was produced at a yield of 121.29 mg/L culture, evidence suggests heterologous expression resulted in conformation isomers of WELQut liberated plantaricin 423.

Keywords: green fluorescent protein, plantaricin 423, mundticin ST4SA, heterologous expression, lactic acid bacteria, class IIa bacteriocins, fluorescent optimization, antilisterial activity

INTRODUCTION

Peptides are ubiquitous in physiological systems where they fulfill functions which are fundamental to life. Within human physiology alone, peptides function as hormones, neurotransmitters, growth factors, ion channel ligands or antimicrobials which makes them an attractive therapeutic resource (Otvos and Wade, 2014; Recio et al., 2017; Pfalzgraff et al., 2018; Kumar, 2019). In terms of

bioactivity, peptides generally show high selectivity, high efficacy and are normally well tolerated therapeutics due to their proteinaceous nature (Fosgerau and Hoffmann, 2015). However, peptides comprised of natural amino acids are not always ideal drug candidates due to their low oral bioavailability, poor stability and short plasma half-life (Otvos and Wade, 2014; Fosgerau and Hoffmann, 2015). Therefore, many challenges surround the use of antimicrobial peptides (AMP) as direct alternatives to classical antibiotic therapies. Fortunately, AMP producers are found throughout all kingdoms of life, which provides a wealth of chemical diversity and variable mechanisms of action over a wide range of environments (Brogden, 2005; Kumar et al., 2018). Using AMPs to combat resistance is more a task of elucidating peptides which provide a specific function within a specific environment and understanding the mechanisms which drive their activity. Therefore, any technique to improve the yield or spectrum of producible peptides is highly valuable, especially for uncharacterized AMPs identified through genome mining.

Bacteriocins are defined as AMPs that are ribosomally synthesized by bacteria and secreted into their environment to modulate the growth of other closely related bacterial species (Ennahar et al., 2000; Kotel'nikova and Gel'fand, 2002). Due to their proteinaceous nature, bacteriocins may not always be suitable antibiotic therapies, but have proven to be viable counterparts when microbial control is required in an environmental application. For example, fermented foods specifically produced by lactic acid bacteria (LAB), are examples of how bacteriocins can be used to help control unfavorable microbial contamination.

Species in the LAB phylum are Gram-positive, catalase negative, microaerophilic to anaerobic, asporogenous and low in GC content (Klein et al., 1998). Bacteriocin production is an important characteristic for LAB, which is evident in the wide range of bacteriocins produced from various classes and levels of complexity (Alvarez-Sieiro et al., 2016). The expression of multiple bacteriocin types or classes by a single LAB strain is common. This makes LAB metagenomes/genomes a fruitful mining ground for novel bacteriocins. Furthermore, LAB are native inhabitants of the gastrointestinal tract (GIT) and during GIT colonization bacteriocins produced by probiotic LAB undoubtedly play a role in shaping the local microbiome (Klein et al., 1998; Dicks and Botes, 2010; Brown, 2011; van Reenen and Dicks, 2011; Rupa and Mine, 2012).

Lactobacillus plantarum 423 and *Enterococcus mundtii* ST4SA are LAB which produce the class IIa bacteriocins plantaricin 423 and mundticin ST4SA, respectively (**Figure 1**). *Lactobacillus plantarum* 423 was isolated from sorghum beer and harbors the plantaricin 423 precursor peptide gene, *plaA*, on the pPLA4 plasmid (**Supplementary Table S1**). Plantaricin 423 inhibits a number of food-borne pathogens such as *Bacillus cereus*, *Clostridium sporogenes*, *E. faecalis*, *Listeria* spp. and *Staphylococcus* spp. (van Reenen et al., 1998; Maré et al., 2006). *Enterococcus mundtii* ST4SA was isolated from soybeans and harbors the mundticin ST4SA pre-bacteriocin gene *munST4SA* within the munST4 operon (**Supplementary Table S1**). Mundticin ST4SA is active against *E. faecalis*, *Streptococcus pneumoniae*, *Staphylococcus aureus*, and *L. monocytogenes* (Granger et al., 2008).

Class IIa, or pediocin-like bacteriocins, are heat stable with post-translational modifications limited to disulfide bond formation (Ennahar et al., 2000; Cui et al., 2012). These peptides have high anti-listeria activity and a conserved N-terminal YGNGV motif, or pediocin box (Eijsink et al., 2002; Kjos et al., 2011; Cui et al., 2012; Lohans and Vederas, 2012; Alvarez-Sieiro et al., 2016). Peptides in this subclass are normally 25 to 48 amino acids in length which results in peptide masses less than 10 kDa. These peptides have a broad range of antimicrobial activity, predominantly targeting related LAB species and different strains of *Staphylococcus* and *Listeria*. Operons encoding class IIa bacteriocins are found natively in producer genomes, as introduced transposable elements or associated to small and large plasmids. While operon locations and organizations vary, they must always encode for proteins or elements which ensure bacteriocin regulation, immunity, maturation and extracellular translocation (Drider et al., 2006; Cui et al., 2012).

The precursor peptides of class IIa bacteriocins are made up of three domains; a leader peptide, N-terminal pediocin box and pore-forming C-terminus (**Figure 1**). Each domain is responsible for a different step in achieving antimicrobial activity via membrane poration. Most leader peptides in class IIa have a characteristic double glycine cleavage signal, however, some have a sec translocase secretion signal sequence. The double-glycine-type leader fused to the N-terminus of the core peptide produces an inert precursor peptide and functions as a secretory signal which is recognized by the operon-encoded ABC transporter. Cleavage of the leader peptide during bacteriocin transmembrane translocation from the producer cell is mediated by the ABC transporter and produces a mature, unstructured, extracellular bacteriocin (Ennahar et al., 2000; Drider et al., 2006; Nissen-Meyer et al., 2009; Cui et al., 2012; Bédard et al., 2018). Only upon interaction with a target membrane does the N-terminal pediocin box form a cationic three-stranded anti-parallel β-sheet-like structure, stabilized by a conserved disulfide bond (Fregeau Gallagher et al., 1997; Wang et al., 1999; Uteng et al., 2003; Haugen et al., 2005; Nissen-Meyer et al., 2009; Oppegård et al., 2015). The N-terminus of the core peptide mediates bacteriocin binding to target cell walls via docking to an extracellular loop of the IIC protein (MptC) from the sugar transporter mannose phosphotransferase system (Man-PTS) (Ramnath et al., 2000; Gravesen et al., 2002; Kjos et al., 2010). While the N-terminus associates with the MptC, a flexible hinge allows the C-terminal hairpin-like domain to transverse and penetrate the hydrophobic core of the target cell membrane (**Figure 1**; Ennahar et al., 2000; Eijsink et al., 2002; Drider et al., 2006; Nissen-Meyer et al., 2009; Kjos et al., 2011; Cui et al., 2012). Accumulation of the class IIa bacteriocin within a target cell wall results in pore formation and leakage of essential metabolites, protons and charged ions which dissipates the target cell's transmembrane potential and pH gradient (Chikindas et al., 1993; Bennik et al., 1998; Montville and Chen, 1998). In addition, pediocin PA-1 was shown to cause the efflux of 2-α-aminoisobutyric acid a nonmetabolizable analog of alanine, and L-glutamate (Chikindas et al., 1993).

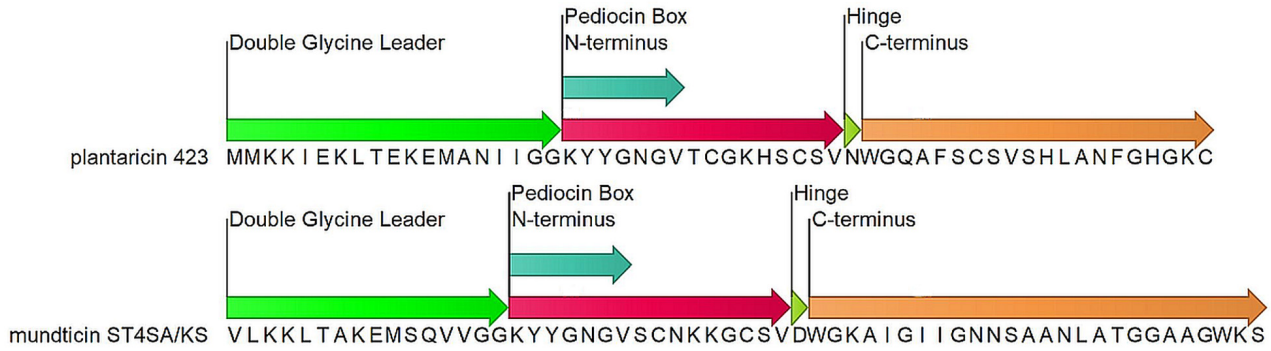

FIGURE 1 | Precursor bacteriocin amino acid sequences for Plantaricin 423 and mundticin ST4SA. Indicated domains: double glycine leader (green), N-terminus (red), conserved YGNGV motif or pediocin Box (light Blue), Flexible hinge (light green) and the pore forming C-terminus (orange).

Like many other class IIa bacteriocins, plantaricin 423 and mundticin ST4SA have previously been purified from the native producer's supernatant via an extensive purification process (van Reenen et al., 1998). For many bacteriocin classes like class IIa, peptides are usually chromatographically purified by taking advantage of their cationic and hydrophobic properties or smaller size (Lohans and Vederas, 2012). Not only is this process laborious with specific growth requirements, it can often result in poor or variable yields due to the inducible nature of bacteriocins, thus limiting their application (Carolissen-Mackay et al., 1997; Guyonnet et al., 2000; Lohans and Vederas, 2012). Furthermore, co-purification of active peptides is a possibility that can have a major downstream impact. Studies elucidating the mode of a bacteriocin's regulation are inherently complex but may be doomed to fail when bacteriocins are chromatographically co-purified with contaminants such as autoinducing peptides or pheromones produced by the wild type strain.

Advances in chemically synthesizing peptides, including bacteriocins, has become a readily available option and solves these types of purification problems. Chemical synthesis has undoubtedly increased the application of bacteriocins in many areas but has limitations and may not work for every peptide. This is especially applicable for peptides which have only been observed *in silico* meaning their correct tertiary structures remain elusive (Henninot et al., 2018). Therefore, it may be prudent to continue the development of robust heterologous bacteriocin expression systems for research and high scale production applications.

Many class IIa bacteriocins have been produced using heterologous expression systems in *Escherichia coli*. The main objective of these expression systems has been to improve the large-scale production and rapid purification of class IIa bacteriocins. Purification of N-terminal His-tagged pediocin PA-1 expressed in *E. coli* resulted in low concentrations of biologically active bacteriocin (Moon et al., 2005). The majority of heterologously expressed His-tagged pediocin PA-1 was found in the insoluble fraction, most likely due to the bacteriocin's solubility, size and the toxic effect on the *E. coli* host (Moon et al., 2005). The yields of heterologously expressed class IIa bacteriocins have been significantly improved when the mature peptide was fused to a larger, more soluble protein (Miller et al., 1998; Klocke et al., 2005; Moon et al., 2006; Beaulieu et al., 2007; Jasniewski et al., 2008; Liu et al., 2011). Although class IIa bacteriocins fused to thioredoxin are not secreted, this system produces the highest recorded yields ranging from 20 to 320 mg pure bacteriocin per liter of culture (Jasniewski et al., 2008; Liu et al., 2011). Thioredoxin is an 11.675 kDa highly soluble protein, which has a rigid solvent-accessible α-helix and can accumulate up to 40% of the total cellular protein in *E. coli* (LaVallie et al., 1993; Bell et al., 2013). Due to its size, solubility and cellular localization, thioredoxin aids in the expression and purification of class IIa bacteriocins by lowering toxicity and circumventing inclusion body packaging (LaVallie et al., 1993; Jasniewski et al., 2008; Liu et al., 2011; Bell et al., 2013; Kimple et al., 2013).

The Green Fluorescent Protein (GFP) gene, *mgfp5*, encodes a 26.908 kDa protein that forms a β-can cylindrical structure made up of 11 β-sheets surrounding a central axial-like α-helix producing fluorophore (Tsien, 1998; Zimmer, 2002). Posttranslational folding of GFP and chromophore formation is autocatalytic and does not require any cofactors except oxygen (Tsien, 1998; Zimmer, 2002). The folded protein is stable, soluble, non-toxic to *E. coli*, and has an excitation-emission autofluorescence at 488 and 509 nm, respectively. These characteristics make GFP applicable in molecular biology as a fluorescent cell marker, reporter gene or fusion tag (Tsien, 1998; Zimmer, 2002). The GFP gene *mgfp5* can be fused to class IIa bacteriocins in the same manner as the thioredoxin gene. Therefore, coupling sub-class IIa bacteriocins to GFP may provide many of the same benefits as thioredoxin but with the additional benefit of monitoring protein expression fluorometrically *in vivo* and in real time.

Presented here is the development of a fluorescent expression system to produce active plantaricin 423 and mundticin ST4SA using GFP as a fusion partner in *E. coli* BL21 (DE3). Furthermore, optimization approaches for expression, purification and cleavage using the fluorescent property of GFP is described.

RESULTS

GFP-Bacteriocin Fusion Constructs

In order to take advantage of GFP as a fusion partner, the genes encoding mature plantaricin 423 and mundticin ST4SA were fused to the C-terminus of His-tagged GFP in the pRSF-GFP-PlaX and pRSF-GFP-MunX plasmid constructs, respectively (**Supplementary Figures S5a,b**). The newly generated GFP-fusion proteins, GFP-PlaX and GFP-MunX were successfully expressed in *E. coli* while retaining the autofluorescent properties of GFP. Furthermore, the inclusion of the WELQut protease cleavage site (WELQ), between GFP and the respective bacteriocins, allowed for liberation of active bacteriocin (**Supplementary Figures S5a,b**). After initial success, we further optimized expression using GFP-MunX.

Optimization of GFP-MunX Expression in *E. coli* BL21

The fluorescent properties of GFP was used to evaluate the optimal expression conditions for increased yield production in terms of fluorescent output. This included different temperatures, expression times and IPTG concentrations, respectively.

Incubation Temperature Optimization for GFP-MunX Expression

Significantly higher fluorescent intensity was measured *in vivo* at 18 and 26°C compared to 37°C after 24 and 48 h of expression, respectively (**Figure 2A**). However, these *in vivo* measurements do not consider total wet cell weight and do not accurately represent total target protein expression at each temperature. For measurement of total target protein expression in terms of relative fluorescence units (RFUs), the formula in Eq. 1 was used (Raw data found in **Supplementary Table S2**).

$$\text{Total RFU} = \frac{\text{RFUs of Ni} - \text{NTA purified eluent}}{\text{wet cell weight used for purification}} \times \text{total cell weight} \quad (1)$$

Total RFU production for GFP-MunX is represented in **Figure 2B**, where significantly higher RFUs were produced at 18°C. This fluorescent intensity was correlated to the presence of antimicrobial activity after cleavage using SDS-PAGE analysis (**Supplementary Figure S2**).

Fluorometric Optimization of IPTG Induction

The effect of IPTG concentration on heterologous protein expression was monitored *in vivo* and in real time using the Tecan Spark M10^{TM} (Tecan Group Ltd., Austria) kinetic incubation program and humidity cassette (**Figure 3**). Fluorometric output of induced samples increased with time and were significantly affected by the IPTG concentration used for induction (**Figure 3A**). IPTG concentrations of 0.1 and 0.2 mM induced significantly higher fluorescence after 18 h incubation at 26°C compared to other IPTG concentrations (**Figure 3B**).

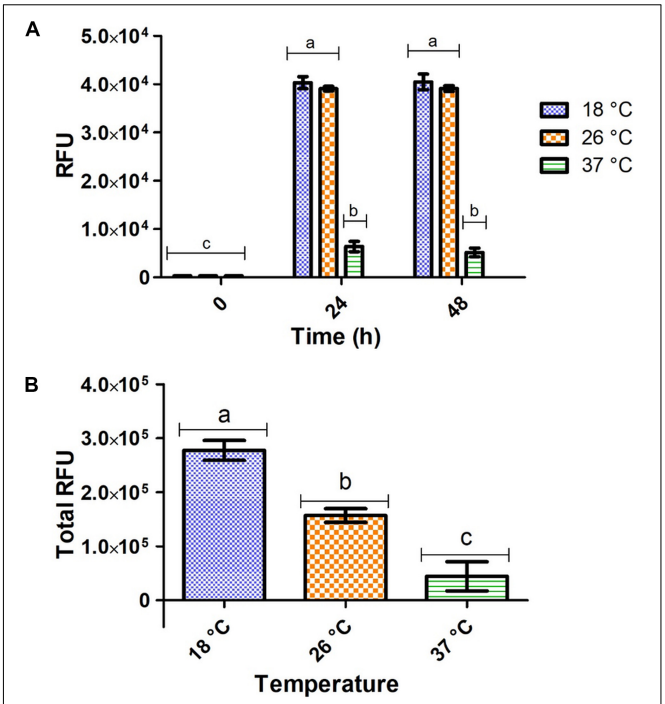

FIGURE 2 | Fluorometric intensity of *E. coli* pRSF-GFP-MunEx expressing GFP-MunEx at 18, 26, and 37°C. **(A)** *In vivo* fluorometric measurements after 0, 24, and 48 h. **(B)** The total relative amounts of GFP-MunEx calculated after protein extraction and Ni-NTA purification of the 48 h expression. Fluorometric intensity measured in Relative fluorescent units (RFU). Dissimilar letters on bars indicates means which are significantly different from one another according to Bonferroni post-test ($P < 0.05$).

Upscaled Production of GFP-PlaX and GFP-MunX With Yield Approximation

In order to determine the effect of larger scale expressions on the yield of our GFP-fusion system we performed experiments under, respectively, optimized conditions using the Minifors 5L fermenter.

The *E. coli* pRSF-GFP-PlaX and pRSF-GFP-MunX fermentations were incubated at 18°C after 0.1 mM IPTG induction for 48 h in a 3 L fermentation volume. After extraction, Ni-NTA purification and buffer exchange of the GFP-PlaX and GFP-MunX proteins, 39 mL of GFP-PlaX and 42 mL of GFP-MunX eluent was obtained. After lyophilization of 1 mL GFP-PlaX and GFP-MunX, 12.96 mg and 17.96 mg residual mass was measured, respectively. From SDS-PAGE analysis the purity of GFP-PlaX and GFP-MunX are approximately 72 and 61%, producing approximate concentrations of 9.33 and 10.95 mg/mL, respectively (**Supplementary Figure S3**). At these purities, the approximate yield of GFP-PlaX and GFP-MunX was 121.29 mg/L of culture and 153.30 mg/L of culture, respectively.

WELQut Cleavage Optimization

The WELQut cleavage reactions was optimized according to the stock concentrations of GFP-PlaX and GFP-MunX which were approximatly 9.33 mg/mL (12.96 mg/mL total protein)

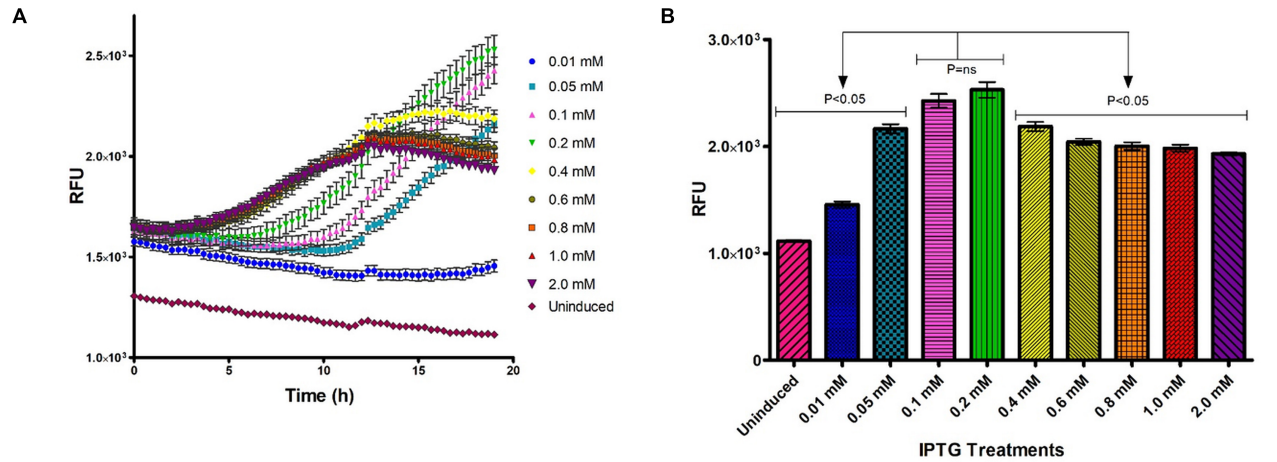

FIGURE 3 | Optimization of IPTG concentration for GFP-MunX expression at 26°C over time, fluorescent intensity was measured in relative fluorescent units (RFUs). **(A)** *In vivo* RFU measurements captured every 25 min, were $n = 3$ (biological triplicates measured in technical triplicate), each point represents the mean with SEM indicated by error bars. **(B)** Mean RFU output comparison for GFP-MunX expression after 19 h incubation over the indicated range of IPTG concentrations. Arrows indicate Tukey's multiple comparison test results identifying that 0.1 and 0.2 mM produce significantly higher RFU outputs from all other tests ($P < 0.05$).

and 10.95 mg/mL (17.96 mg/mL total protein), respectively. The GFP-PlaX and GFP-MunX cleavage reactions were incubated at 28°C and sampled at time intervals of 2, 4, 8, and 16 h for a range of sample to WELQut ratios (**Supplementary Figure S4**). From these results, the cleavage ratios which produced maximal antilisterial activity for GFP-PlaX and GFP-MunX cleavage after 16 h was confirmed at a WELQut to sample ratio of 1:10 and 1:25 (μL:μL), respectively (**Figure 4** and **Supplementary Table S5b**).

An important advantage of using GFP as a fusion partner is the ability to evaluate protease cleavage by visualizing migration patterns of fluorescent bands after electrophoretic separation. Determining optimal cleavage conditions in terms of activity of heterologously produced bacteriocin fusions is dependent on many variables. As such we confirmed the results for optimal cleavage by utilizing the maintained fluorescent properties of GFP after SDS-PAGE electrophoresis. Fluorescent bands were observed for GFP-PlaX, GFP-MunX, and GFP before and after cleavage, respectively (**Figures 5a–c**). These bands were then correlated to stained bands on the same SDS-PAGE gels (**Figures 5b–d**). An unexpected observation was the increase in size of GFP fluorescent bands of GFP-PlaX (band I) and GFP-MunX (band IV) after WELQut cleavage (band II and V, respectively). The fluorescent intensity of these larger bands (II and V) increases as increasing amounts of WELQut protease was added (columns 3 to 6 of **Figure 5**). This size increase of approximately 20 kDa might indicate the formation of a WELQut-GFP-bacteriocin complex forming upon WELQut liberation of plantaricin 423 and mundticin ST4SA, respectively.

The intensity of the uncleaved GFP-PlaX and GFP-MunX fluorescent bands decreases as the WELQut : sample ratio increases (**Figures 6a–c**). Complete cleavage could be observed for GFP-PlaX (lane 6, **Figure 5a**) and corresponds to the highest spot activity observed (**Figure 4A**). Complete cleavage was not achieved for GFP-MunX, with a slight fluorescent band observed at the location of uncleaved GFP-MunX (lane 6, **Figure 5c**). Interestingly, the maximal spotted activity of GFP-MunX was equal for ratios 1:25 and 1:10 (**Figure 4B**) despite apparent difference in cleavage efficiency observed in SDS-PAGE (lanes 5–6, **Figure 5c**).

Antimicrobial Activity Validation

While the respective bacteriocins were fused to GFP and produced a fluorescent complex, it was important to determine that antimicrobial activity was due to the liberated bacteriocin. The antimicrobial activity of plantaricin 423 and mundticin ST4SA post WELQut cleavage from GFP-PlaX and GFP-MunX proteins was investigated using SDS-PAGE under semi-native conditions (**Figure 6**). Using this method, the location of fluorescent GFP fusion proteins on the separated gel could be photographed and superimposed on the stained- and antilisterial gel overlay (**Figures 6a–c**). Antilisterial activity was observed as clear zones for the WELQut cleaved GFP-PlaX and GFP-MunX samples (**Figures 6a,b**). Antilisterial zones III and IV in **Figure 6b** correspond to the locations of mundticin ST4SA (4285 Da) and plantaricin 423 (3928 Da), respectively, indicating liberation of the core peptides from their respective GFP fusion partners. However, two additional zones of antilisterial activity (I and II in **Figure 6b**) were observed, which correspond to the approximate size and location of fluorescent GFP-MunX (31 874 Da) and GFP-PlaX (31 520 Da) (lane 5 and 6 of **Figure 6c**). From analysis of minimum inhibitory concentrations of cleaved GFP-MunX and –PlaX the BU/mL (bacteriocin units/mL) was determined to be 1600 and 83.33 BU/mL, respectively (**Supplementary Figures S5, S6**).

Peptide Yields and LC-MS

Mundticin ST4SA and plantaricin 423 were cleaved from one milliliter of His-tag purified GFP-MunX and GFP-PlaX, respectively, under optimal cleavage conditions. Cleavage reactions were purified using high performance liquid

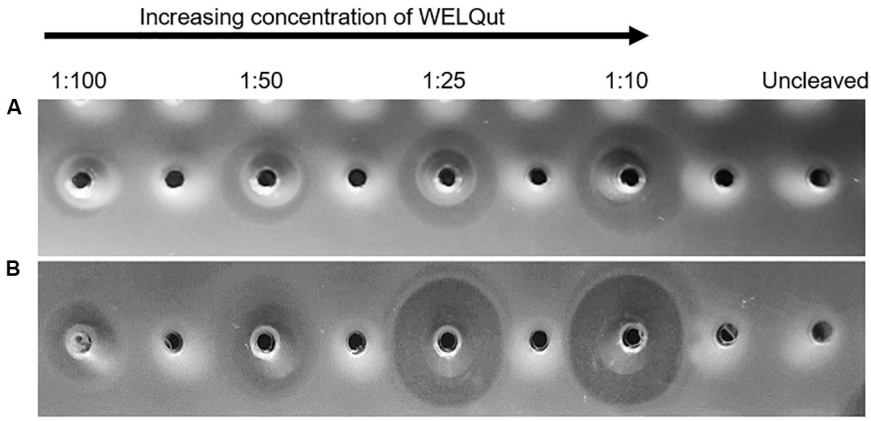

FIGURE 4 | Antimicrobial activity of plantaricin 423 and mundticin ST4SA at various WELQut : sample ratios. Antimicrobial activity of plantaricin 423 **(A)** and mundticin ST4SA **(B)** cleaved from Ni-NTA purified GFP-PlaX and GFP-MunX proteins, respectively. Cleavage assessed using the spot plate technique against *L. monocytogenes*. Cleavage ratios of WELQut : sample (μL:μL) indicated on top of panel. Cleavage was performed at 28°C for 16 h. Post cleavage, 100 μL of GFP-PlaX **(A)** and 10 μL GFP-MunX **(B)** was spotted from each cleavage reaction. Uncleaved GFP-PlaX **(A)** and GFP-MunX **(B)** did not show antilisterial activity.

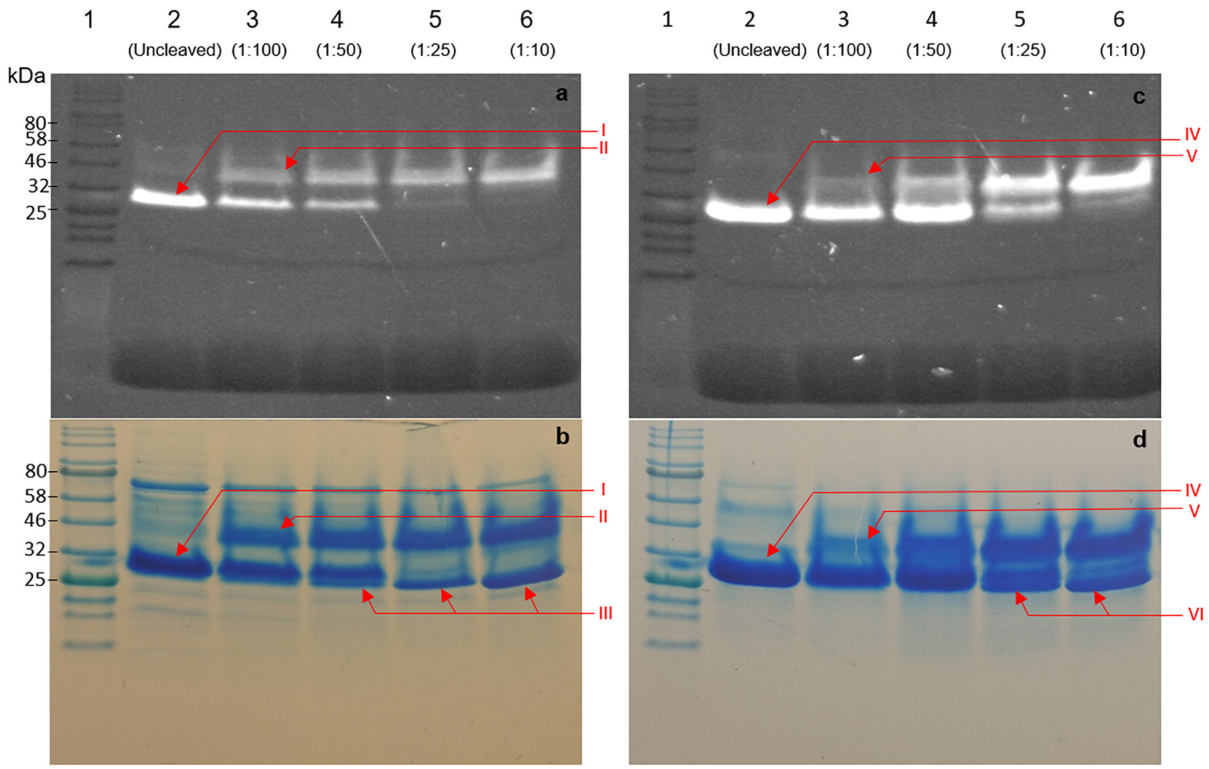

FIGURE 5 | SDS-PAGE analysis of WELQut cleaved GFP-PlaX **(a,b)** and GFP-MunX **(c,d)**. **(a,c)** represent unstained SDS-PAGE gels fluorometrically photographed. **(b,d)** represent stained gels of **(a,c)**. Lane: 1 – Ladder, 2 – uncleaved sample, 3 to 6 WELQut cleavage samples, sample ratios indicated. Band I – Uncleaved GFP-PlantEx, II – putative WELQut and GFP complex, III – WELQut, IV – Uncleaved GFP-MunX, V – putative WELQut and GFP complex, VI – WELQut.

chromatography (HPLC), single peaks were spot tested for antilisterial activity. Mundticin ST4SA activity was observed from a single peak while plantaricin 423 produced multiple active peaks with low levels of activity. The mundticin ST4SA fraction was lyophilized and the residual mass was weighed off. Optimal cleavage of GFP-MunX yielded 0.88 mg of active mundticin ST4SA, indicating that approximately 37.3 mg could be obtained from the 3 L fermentation corresponding to 12.4 mg/L mundticin ST4SA. The production yield of plantaricin 423 was not estimated due to multiple active peaks, showing weak activity, which is likely a result of different conformational isomers.

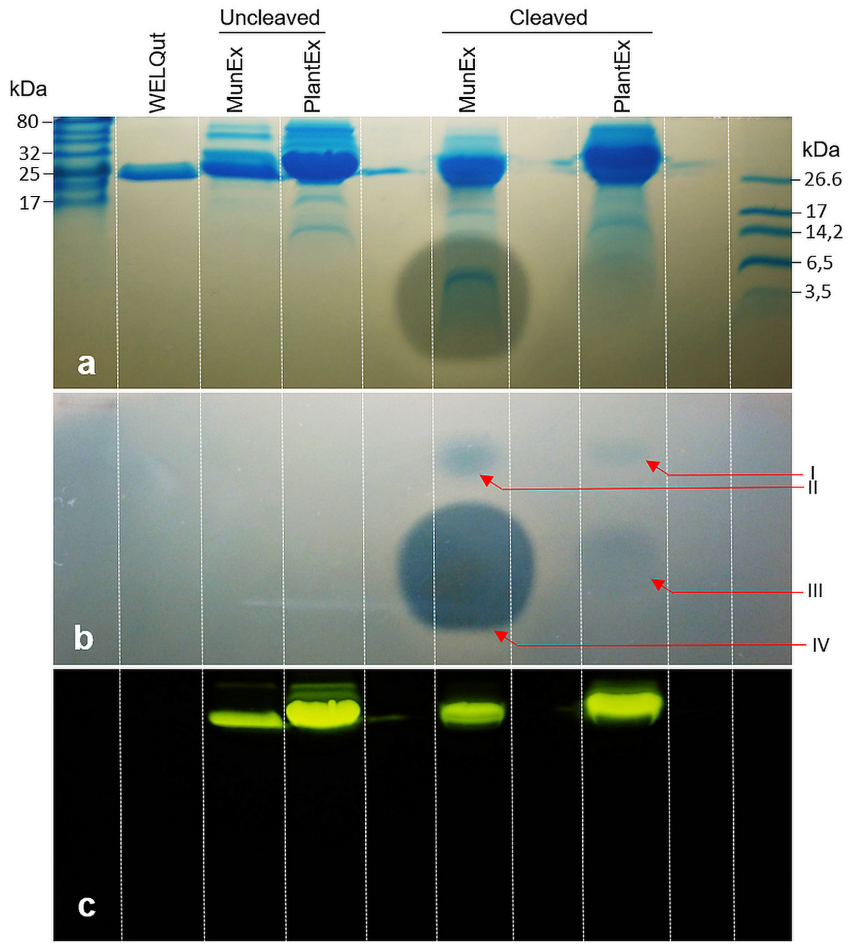

FIGURE 6 | Observed post cleavage antilisterial activity of liberated mundticin ST4SA and plantaricin 423 separated by SDS-PAGE. **(a)** Superimposition of duplicate SDS-PAGE separations which indicates the size of bands showing antilisterial activity. **(b)** Antilisterial SDS-PAGE overlay showing activity post WELQut cleavage at locations correlating to I – GFP-PlaX, II – GFP-MunX, III – mundticin ST4SA and IV – plantaricin 423. **(c)** Location of fluorescent bands in **(a)**.

Electrospray ionization-MS performed on HPLC-purified mundticin ST4SA confirmed the presence of a peptide with a mass corresponding to mature mundticin ST4SA (**Figure 7**). While an accurate mass of 4285.1355 Da was determined for mundticin ST4SA from the isotopic envelope of the $[M+5H]^{+5}$ species, the abundance of this charged species within the raw spectrum was low (**Figure 7**). However, the accurate mass measurement is in close agreement with the theoretical monoisotopic mass of 4285.0796 Da (equivalent to the formation of one disulfide bridge). Multiple attempts were made to determine the accurate mass of plantaricin 423, however, convincing data was not obtained.

DISCUSSION

Although expressing class IIa bacteriocins with a fusion partner redirects a portion of the metabolic flux away from bacteriocin synthesis, fusion increases overall yields by quenching the bacteriocin's toxicity to *E. coli* (Liu et al., 2011). Thioredoxin has been a popular fusion partner for the heterologous expression of many subclass IIa bacteriocins. In an attempt to increase the usefulness of a bacteriocin fusion partner, we evaluated GFP as a fluorescent fusion partner for the heterologous expression of plantaricin 423 and mundticin ST4SA. Plantaricin 423 and mundticin ST4SA were purified from the soluble fraction due to the increased size and solubility when fused to GFP, as seen with thioredoxin fusion to other subclass IIa bacteriocins (Beaulieu et al., 2007; Jasniewski et al., 2008; Liu et al., 2011). The stabilizing effects provided by thioredoxin fusion in *E. coli* for class IIa bacteriocin expression is also provided by GFP, without disrupting its autofluorescent property.

Maintained fluorescence provided the advantage of clear visualization of the target proteins, GFP-PlaX and GFP-MunX, throughout the expression, extraction, purification, and analysis processes which allowed for rapid optimization and trouble shooting. Fluorescent intensity could function as a proxy to guide optimizations because it correlated to the amount of GFP fusion protein.

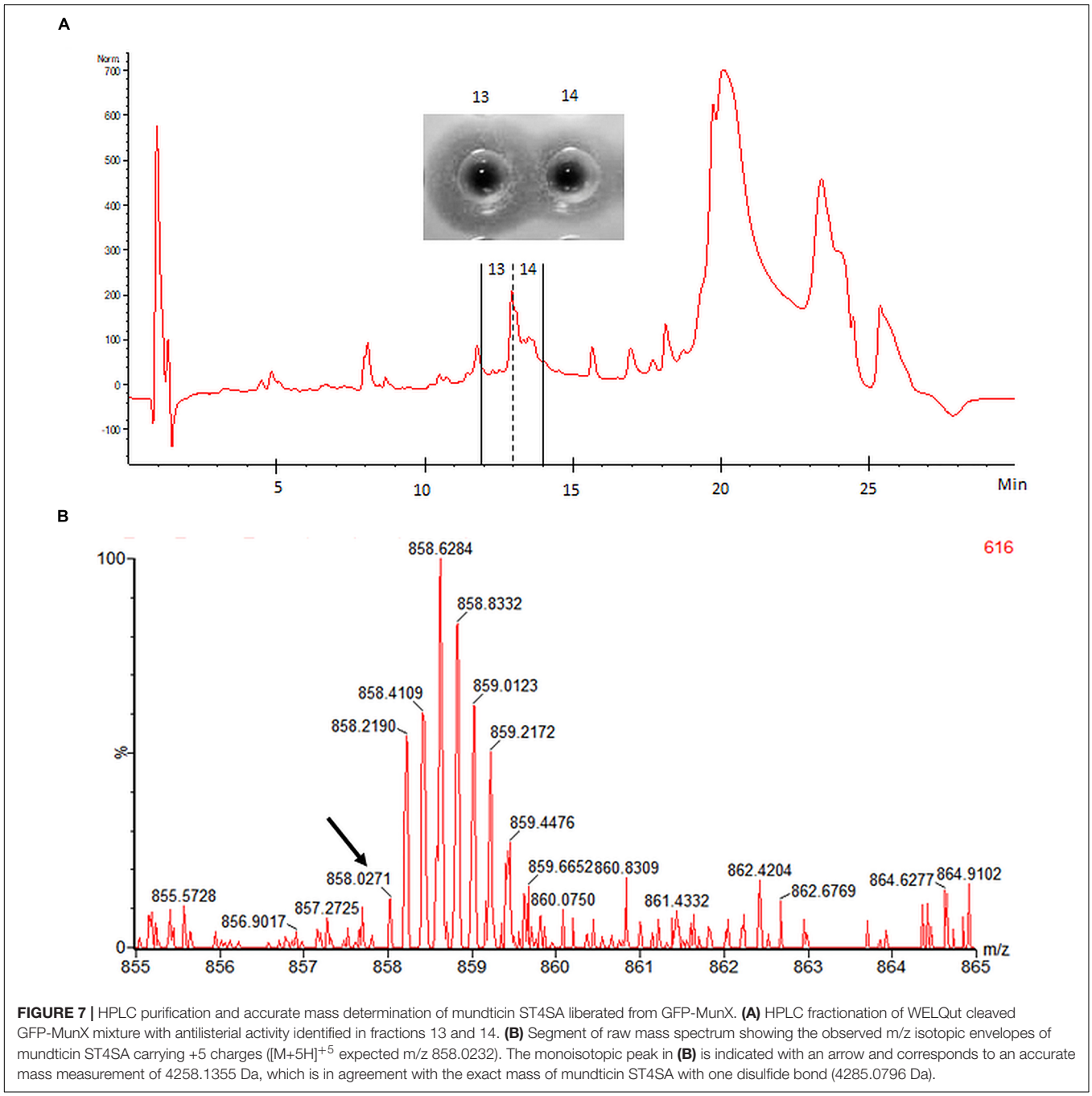

FIGURE 7 | HPLC purification and accurate mass determination of mundticin ST4SA liberated from GFP-MunX. **(A)** HPLC fractionation of WELQut cleaved GFP-MunX mixture with antilisterial activity identified in fractions 13 and 14. **(B)** Segment of raw mass spectrum showing the observed m/z isotopic envelopes of mundticin ST4SA carrying +5 charges ($[M+5H]^{+5}$ expected m/z 858.0232). The monoisotopic peak in **(B)** is indicated with an arrow and corresponds to an accurate mass measurement of 4258.1355 Da, which is in agreement with the exact mass of mundticin ST4SA with one disulfide bond (4285.0796 Da).

While previous studies have demonstrated that incubation temperature influences heterologous protein expression levels, to our knowledge, no study has considered this for the heterologous expression of class IIa bacteriocins (Sivashanmugam et al., 2009). Bacteriocins which have been expressed as fusion partners with thioredoxin include pediocin PA-1, carnobacteriocins BM1, and B2, divercin V41, enterocin P and piscicolin 124, with pediocin PA-1 also fused to mouse dihydrofolate reductase and enterocin A fused to cellulose-binding domain (Gibbs et al., 2004; Richard et al., 2004; Klocke et al., 2005; Cuozzo et al., 2006; Moon et al., 2006; Beaulieu et al., 2007; Jasniewski et al., 2008; Liu et al., 2011; Lohans and Vederas, 2012). These studies performed their expressions at 37°C or did not specify a temperature. While this study found that expression temperature significantly influenced the final GFP-bacteriocin yield in terms of RFU output. From this data it can be recommended that expression temperature is one of the first variables to be optimized for GFP-bacteriocin fusion expression. The ease of fluorometric optimization was also observed during IPTG treatments were real time *in vivo* results indicated that changes in IPTG concentrations significantly affected expression.

Evaluating what effect these variables will have on specific production rates would be a challenging and time-consuming task for non-fluorescent fusion partners. The GFP-bacteriocin fusion system boasts a great sense of confidence during heterologous expression of subclass IIa bacteriocins due to the high-quality data its convenient autofluorescent property provides. However, certain factors need to be taken into consideration. During expression temperature optimization, it was observed that the total wet cell weight must be taken into account when calculating total yield in terms of RFUs. *In vivo* measurements of GFP-MunX production indicate that there is no significant difference between the fermentations at 18 and 26°C. However, when the total RFUs produced were calculated after extraction and NI-NTA purification, nearly two times higher yields were obtained at 18°C as compared to 26°C. Without taking biomass into account, i*n vivo* fluorescent intensities can only be used to compare expression levels in real time as a means of coarse optimization. Therefore, *In vitro* (post purification) fluorescent intensities more accurately represent total target protein expression and are required for estimating yield.

Another major advantage of using GFP as a fusion partner is the ability to visualize fluorescence during SDS-PAGE analysis. Visualization indicated not only the location of the GFP fusion protein but also trends that occur during cleavage and liberation of the bacteriocin using WELQut protease. Therefore, loss of the GFP fusion protein at any stage of the extraction or purification process is immediately noticed. This robust fluorometric property of GFP can be attributed to the isolation of its fluorescent chromophore within the compact "β-can" cylindrical structure (Zimmer, 2002; Remington, 2011). The cylindrical structure provides resistance to sodium dodecyl sulfate (SDS), urea, beta-mercaptoethanol (BME) and dithiothreitol (DTT), however, its integrity is sensitive to pH and high temperature, hence the requirement for semi-native SDS-PAGE (Saeed and Ashraf, 2009; Krasowska et al., 2010).

The yields of most heterologously expressed subclass IIa bacteriocins, many of which are fused to thioredoxin, are rarely higher than tens of milligrams bacteriocin per liter of culture (Moon et al., 2006; Beaulieu et al., 2007; Liu et al., 2011; Lohans and Vederas, 2012). Under optimized conditions the GFP-PlaX and GFP-MunX fusion proteins were produced at approximately 121 mg/L of culture and 153 mg/L of culture, respectively. This would theoretically produce 15.08 and 20.56 mg/L mature plantaricin 423 and mundticin ST4SA assuming complete cleavage, respectively. After mature peptide cleavage, HPLC purification and lyophilization, 14.4 mg/L active mundticin ST4SA was recovered. Loss of sample during the purification process is expected and explains the difference between theoretical and observed mundticin ST4SA yields. Despite our promising yields, the highest yields for heterologous expression of class IIa bacteriocin were reported for carnobacteriocin B2 and BM1 fused to thioredoxin at 320 mg/L of culture (Jasniewski et al., 2008). Carnobacteriocin B2 and BM1 fusions were heterologously expressed in *E. coli* cultured in a fed-batch fermentation where pH, temperature and oxygen regulation were controlled. Jasniewski et al. (2008) reported that using a continuous supply of lactose for induction in the fed batch fermentation had a marked increase in heterologous expression. Future studies should consider expressing GFP as the fusion partner under such fed batch conditions at 18°C to assess whether GFP-subclass IIa fusion can improve on these yields. The yield of GFP-MunX and GFP-PlaX may also be improved by using alternative mechanisms of cell disruption such as alternative lysis buffers or mechanical methods.

A limiting factor observed in the current study was the liberation of active bacteriocin using WELQut protease. Cleavage at such an inefficient rate would be time consuming and costly, and therefore a major limiting factor for high scale production. An interesting observation was the apparent association of the WELQut protease with the respective fluorescent proteins post-cleavage causing an approximate 20 kDa size increase. Formation of a WELQut-GFP-bacteriocin complex is further supported by the presence of two unexpected zones of antilisterial activity observed post-cleavage at the location of fluorescent GFP-MunX and GFP-PlaX fusion protein bands. This WELQut-GFP-bacteriocin association might be indicative of a problematic cleavage as this phenomenon is unreported in the WELQut documentation or literature (Pustelny et al., 2014).

The WELQut protease is derived from the SpIB protease of *Staphylococcus aureu*s which is activated by proteolytic cleavage of an N-terminus signal peptide. Removal of the signal peptide allows subsequent formation of a characteristic hydrogen bond network (Pustelny et al., 2014). Pustelny et al. (2014) reports that signal peptide cleavage does not change the disposition of catalytic machinery nor does it perturb the hydrogen bond network in the vicinity of the catalytic site. The crucial elements within the active site are in place whether or not a signal peptide is attached, and does not depend on the signal peptide sequence (Pustelny et al., 2014). For this reason, Pustelny et al. (2014) postulates that interactions at the N-terminus affects the dynamics of SpIB as a whole which subsequently impacts substrate recognition and hydrolysis. Liberated plantaricin 423 and mundticin ST4SA may be interacting with SpIB at its N-terminus thus lowering its cleavage efficiency. Although, without fully understanding the mechanism of WELQut activation, hypothesizing how plantaricin 423 or mundticin ST4SA interfere with WELQut cleavage is difficult.

From the observations in the current study, and others, it is clear that the yields of heterologously expressed class IIa bacteriocins are not the biggest limiting factor for high scale production, but rather the liberation of the active core peptide. Fortunately, the maintained fluorescent property of GFP under semi-native SDS-PAGE conditions rapidly highlighted this bottleneck. The high yield of 320 mg/L obtained for carnobacteriocin B2 liberated from thioredoxin, was achieved using cyanogen bromide which unfortunately produces toxic samples that may limit downstream applications (Jasniewski et al., 2008). While studies like this one, which used a protease to liberate the subclass IIa bacteriocin from the fusion partner, are yet to achieve more than tens of milligrams pure bacteriocin per liter of culture (Moon et al., 2006; Beaulieu et al., 2007; Liu et al., 2011; Lohans and Vederas, 2012). This lower efficiency paired with the high cost of commercial proteases renders the approach unfeasible for high scale production. Using a bacteriocin's native

protease for fusion cleavage may lower costs and avoid any incompatibility issues as seen in this study with a potential increase in efficiency (Montalbán-López et al., 2018; Van Staden et al., 2019). In this regard the fluorescent property of GFP may prove a useful tool in identifying novel cleavage approaches or proteases effective at cleaving hydrophobic peptides containing disulfide bonds like subclass IIa bacteriocins.

Accurate mass determination for mundticin ST4SA and plantaricin 423 liberated from their GFP fusion partners was challenging. The determined accurate mass of 4285.1335 Da for mundticin ST4SA is in close agreement with the expected mass (4285.0796 Da) when one disulfide bond is formed. However, with the given concentration of mundticin ST4SA a relatively low abundance was observed during MS analysis.

Plantaricin 423 liberated from GFP-PlaX was not detected during MS analysis. Plantaricin 423 is similar to pediocin PA-1 as it has four cysteine residues which allows for the formation of two disulfide bonds. Different arrangements of the two bonds produce three conformational isomers of pediocin PA-1 with varying specific activities against *Listeria* (Oppegård et al., 2015; Bédard et al., 2018). This incorrect folding of pediocin PA-1 during heterologous expression is the result of an absent thioredoxin gene (Oppegård et al., 2015; Bédard et al., 2018). The thioredoxin gene, *papC*, is encoded by the native pediocin operon to guide correct disulfide bond formation for optimal specific activity and is also found in the *pla* operon (Mesa-Pereira et al., 2017). The low specific activity observed for liberated plantaricin 423 compared to mundticin ST4SA, in terms of RFUs, provides more evidence for the presence of conformational isomers.

Dividing the liberated mass of plantaricin 423 into different conformational isomers is exacerbating the difficulties experienced during LCMS analysis. These conformational isomers elute from the HPLC column in different fractions, which decreases the concentration of plantaricin 423 available for downstream analysis. Furthermore, activity was used to determine which fractions are submitted for MS, therefore fractions containing inactive plantaricin 423 were excluded altogether. This partitioning of the plantaricin 423 mass coupled with the potential for low abundance of charged species, may explain why plantaricin 423 was not detected during MS analysis. Modifications would need to be made to the current GFP-PlaX expression system to ensure correct disulfide bond formation before determining the production yield and accurate mass of plantaricin 423. In this regard, future studies should consider the co-expression of accessory proteins, such as the operon encoded thioredoxin proteins, to direct correct disulfide bond formation when conformational isomers are possible (Mesa-Pereira et al., 2017).

CONCLUSION

Fusion to GFP stabilized expression, simplified purification by reducing peptide hydrophobicity and assigned a fluorometric tag to the target protein. Not only does this autofluorescent property make handling the target peptide more intuitive but it provides a high degree of confidence and reproducibility during heterologous peptide expression and purification. Furthermore, because fluorescence correlates to the amount of target protein and specific activity, optimization of most steps is rapid and convenient which ultimately accelerates the rate of progress. Our goal here was to show that fluorescence produced by GFP can be used to optimize heterologous expression. Future studies should evaluate the relationship between specific activity and the fluorescent coefficient, and its usefulness or implications, and on what scale this occurs. With the development of inline fluorescent monitoring technologies, future studies should also identify if time, temperature and IPTG concentration have compounding effects to further boost yield. However, the yields for plantaricin 423 and mundticin ST4SA produced with this GFP-fusion system will benefit greatly by improving both cleavage efficiency and disulfide bond formation. Finally, novel subclass IIa bacteriocins can be easily identified by their conserved YGNGV motif and produced with a high degree of process certainty using the GFP-fusion approach described here. However, subclass IIa bacteriocins which contain more than two cysteine residues may need additional accessory genes and therefore modifications to the system presented here.

Purifying hydrophobic peptides for bioactivity characterization is a challenging task especially under the non-native conditions experienced during heterologous expression. However, the antilisterial activity of subclass IIa bacteriocins is easily assayed, which conveniently demonstrated here that GFP is an effective and readily optimizable peptide-fusion partner. The extent to which GFP can function as a fusion partner for heterologous expression of cationic, hydrophobic peptides with toxic effects to *E.* coli, should be further explored. Recently, it has been demonstrated that class I and class II lanthipeptides can still undergo posttranslational modification while fused to the C-terminal of GFP (Ongey et al., 2018; Si et al., 2018; Van Staden et al., 2019). These studies further promote fusion to GFP as an elegant approach to improve the heterologous expression of modified or unmodified cationic, hydrophobic peptides in *E. coli* while maintaining their bioactivity. Therefore, if GFP-fusion can provide more confidence during heterologous expression and purification of various antimicrobial peptides, GFP may become the fusion partner of choice for peptides with much broader bioactivities.

MATERIALS AND METHODS

Materials

Detailed information on materials and manufacture details are listed in the **Supplementary Material**.

Bacterial Strains and Culture Conditions

All bacterial strains used in this study can be found in **Supplementary Table S8**. The LAB, *Lactobacillus plantarum* 423 and *Enterococcus mundtii* ST4SA were cultured on De Man, Rogosa and Sharpe (MRS) media, at 37°C without agitation. Luria Bertani (LB) medium, supplemented with 1.2% agar for solid medium, was used to culture *Escherichia coli* BL21 (DE3) during molecular cloning protocols. *Listeria*

monocytogenes EGD-e was cultured on Brain Heart Infusion (BHI) media supplemented with 7.5 μg/mL Chloramphenicol. Terrific broth was used for the expression of heterologous proteins in recombinant *E. coli* BL21 (DE3) (Shi et al., 2011). For the selection and maintenance of pRSFDuet-1 (Novagen) derived plasmids, growth media were supplemented with 50 μg/mL kanamycin (Sigma).

Molecular Techniques

DNA analysis, manipulation, and plasmid cloning were performed according to Sambrook et al. (1989). Genomic DNA and plasmid DNA isolations from *L. plantarum* 423 and *E. mundtii* ST4SA were performed according to Moore et al. (Ausubel et al., 2003) and O'Sullivan and Klaenhammer (1993), respectively. Plasmid DNA extractions from *E. coli* were performed using the PureYield™ Plasmid Miniprep System according to the manufacturer's instructions.

T4 DNA ligase and restriction enzymes (RE) were used according to the manufacturer's instructions. Polymerase chain reaction (PCR) amplifications were performed using Q5 high-fidelity PCR DNA polymerase according to manufacturer's instructions in a GeneAmp PCR system 9700 (ABI, Foster City, CA, United States).

Oligonucleotides were designed using the CLC main workbench program (CLC bio, Aarhus, Denmark). DNA sequencing was performed by the Central Analytical Facilities (CAF) at the University of Stellenbosch, South Africa.

Agarose gel electrophoresis was used for the analysis and purification of RE digested DNA fragments in TBE buffer at 10 V/cm using the Ephortec™ 3000 V (Triad Scientific, Manasquan United States) power supply (Ausubel et al., 2003). Excised gel DNA fragments were purified using the Zymoclean™ gel DNA recovery kit.

GFP-Bacteriocin Fusion Plasmid Construction and Primer Design

The pRSFDuet-1 vector was used for the β–D–1-thiogalactopyranoside (IPTG) induction of the heterologously expressed His-tagged GFP-bacteriocin fusions in this study (Shi et al., 2011). The N-terminal of *mgfp5* (GFP) was fused to a hexahistidine tag in pRSFDuet-1 which was under the transcriptional control of the T7 promoter (**Supplementary Figure S7**). The double-glycine leader sequences from mundticin ST4SA and plantaricin 423 were excluded so that the core peptide's N-terminus was fused to the C-terminus of GFP. The WELQut protease recognition amino acid cleavage sequence was introduced between GFP and the respective core peptide sequences (**Supplementary Figure S5**). This site allowed for posttranslational cleavage and liberation of the core peptides using the WELQut protease.

The GFP_Bam_Fwd forward primer installed a *BamH*I site 5′ of *mgfp5* (GFP gene) for cloning into pRSFDuet-1 (**Supplementary Table S6**). The GFP_WELQ_Rev reverse primer extended the *mgfp5* sequence with an *Age*I restriction site followed by the DNA sequence encoding the WELQ amino acid sequence (recognition sequence for WELQut protease), followed by a *PstI* site (**Supplementary Figure S5**). The PlaX_Pst_Fwd/PlaX _Hind_Rev and MunX_Pst_Fwd/MunX_Hind_Rev primer sets annealed to the mature plantaricin 423 (*plaA*) and mundticin ST4SA (*munST4SA*) gene sequences, respectively, (**Supplementary Table S3**). These primer sets added 5′ *PstI* and 3′ *Hind*III restriction sites for cloning mature plantaricin 423 (*plaA*) or mundticin ST4SA (*munST4SA*) genes as GFP fusions in pRSFDuet-1, represented as the "core peptide" in **Supplementary Figure S5**. Detailed cloning procedure for the construction of pRSF-GFP-PlaX and pRSF-GFP-MunX may be found in the **Supplementary Material**.

Overexpression of GFP-Bacteriocin Fusion Proteins in *E. coli* BL21 (DE3)

Starter cultures of 30 mL LB broth containing 50 μg/mL kanamycin were inoculated with respective *E. coli* BL21 (DE3) transformants containing pRSF-GFP-PlaX or pRSF-GFP-MunX constructs. The starter cultures were incubated at 37°C for 12 h with constant agitation. Starter cultures were used as an inoculum for the expression of GFP-PlaX and GFP-MunX, respectively, (1% v/v). At an OD_{600} of 0.6–0.65, expression of the respective GFP fusion proteins was induced using 0.1 mM IPTG. Upscaled production in a 5 L fermenter (Minifors, Infors AG, CH – 4103 Bottmingen/Basel, Switzerland) is detailed in the **Supplementary Material**.

Ni-NTA Purification of GFP-MunX and GFP-PlaX Proteins

Induced cells were harvested by centrifugation at 8 000 *g* for 20 min at 4°C. The supernatant was discarded, and the cell pellet was resuspended in 15 mL/g wet weight SB buffer supplemented with 1 mg/mL lysozyme and incubated with agitation at 8°C for 45 min (Buffer compositions can be found in **Supplementary Table S7**). After incubation, the lysed cells were subjected to sonication (50% amplitude, 2 s pulse, 2 s pause, 6 min) using the Omni Ruptor 400 (Ultrasonic Homogenizer, Omni International). RNaseI and DNaseI were added to a final concentration of 10 and 5 μg/mL, respectively, and the lysate incubated at room temperature for 15 min. The cell lysate was then centrifuged for 90 min at 20 000 *g* at 4°C; the cell-free supernatant was collected. Imidazole was added to the cell-free supernatant to a final concentration of 10 mM.

The His-tagged GFP-bacteriocin fusion proteins, GFP-PlaX and GFP-MunX, were purified with immobilized metal affinity chromatography (IMAC) using the Ni-NTA superflow resin, according to the Qiagen expressionist handbook's instructions for batch purification. His-tagged proteins were purified using 25 mL of Qiagen Ni-NTA superflow resin in combination with a 26 mm diameter adjustable length flash column (Glasschem, Stellenbosch, South Africa). The Ni-NTA superflow resin was equilibrated in SB10 (SB buffer containing 10 mM imidazole) buffer and then added directly to the cell-free supernatant. The slurry was gently agitated for 2 h at 8°C using a shaker, after which the Ni-NTA superflow resin slurry was packed into the column. The ÄKTA purifier system (Amersham, Biosciences) was used for

IMAC purification according to the following program; 5 column volumes (CV) SB10 (2% B buffer where A is SB and B is SB500), washed with 10 CV of SB20 (4% B buffer), elution occurred in approximately 40 mL of SB500 (100% B buffer). Eluted proteins were detected at 254 and 280 nm, respectively. Eluted His-tagged proteins were desalted using size exclusion chromatography. The ÄKTA purifier system was used in conjunction with Sephadex G25 resin packed into column (16 × 65 mm, GE Healthcare) for exchanging the sample from SB500 to WELQut cut buffer.

Incubation Temperature Optimization for GFP-MunX Expression

Only the GFP-MunX fermentation was temperature optimized as cleaved GFP-MunX had a higher specific activity. The GFP-MunX expression temperature optimization was performed at 18, 26, and 37°C with three biological repeats of *E. coli* BL21 (DE3) harboring the pRSF-GFP-MunX plasmid. The three biological repeats of *E. coli* pRSF-GFP-MunX were used to inoculate three 400 mL flasks of terrific broth containing 50 μg/mL kanamycin. The cultures were grown at 37°C until induction using 0.1 mM IPTG at an $OD_{600\ nm}$ of 0.6–0.65. Each 400 mL culture was split into three 100 mL cultures that were incubated at 18, 26, and 37°C for 48 h, respectively.

To measure *in vivo* GFP-MunX expression, 1 mL samples from each flask were collected in triplicate at the time of induction; samples were collected again at 24 and 48 h and frozen at −80°C. After collection, samples were thawed, centrifuged and washed twice with potassium phosphate buffer (pH 7.4). The *in vivo* expression of GFP-MunX was fluorometrically measured in relative fluorescent units (RFUs) at 488 nm (excitation) and 509 nm (emission) using a Tecan Spark M10™ (Tecan Group Ltd., Austria).

After 48 h, the total GFP-MunX RFU production for each sample was calculated by harvesting the induced cells from 80 mL of culture (centrifugation 8000 × *g* for 20 min at 4°C). The mass of each cell pellet was then measured before resuspension in 15 mL/g wet weight SB buffer. The GFP-MunX in each sample was extracted and purified using IMAC as described previously. Briefly, 5 mL from each cell-free lysate was purified using 5 ml Ni–NTA Superflow cartridges. The RFUs of each Ni-NTA purified GFP-MunX sample was measured using the Tecan M10™ Spark (Tecan Group Ltd., Austria). The RFUs/g were then calculated for each sample by dividing the measured RFUs by the equivalent wet weight (g) of cells lysed for purification (i.e., grams of lysed cells in 5 mL). The total RFUs produced for each sample was calculated by multiplying the RFUs/g by the total wet weight of cells harvested in each sample.

Optimization of IPTG Concentration for Induction

Fluorometric intensity was used to optimize IPTG induction concentration for GFP-MunX expression using the Tecan Spark M10™'s (Tecan Group Ltd., Austria) kinetic incubation program and humidity cassette in a 96 well microtiter plate. Three biological repeats of *E. coli* BL21 (DE3) harboring the pRSF-GFP-MunX plasmid were inoculated into three 1 L Erlenmeyer flasks containing 200 mL filter sterilized terrific broth supplemented with 50 μg/mL kanamycin, and incubated at 37°C. Once an $OD_{600\ nm}$ of 0.55 was reached, each culture was chilled in an ice bath. Culture aliquots were then incubated with 0.01, 0.05, 0.1, 0.2, 0.4, 0.6, 0.8, 1, and 2 mM IPTG (final concentration) in triplicate in a 96 well microtiter plate. The microtiter plate was incubated within a humidity chamber by the Tecan Spark M10™ at 26°C for 20 h. Every 20 min the microtiter plate was shaken for 30 s, allowed to settle for 10 s, RFUs were then measured at 509 nm (emission) after excitation at 488 nm.

Concentration Estimation

One milliliter of Ni-NTA purified and buffer exchanged GFP-PlaX and GFP-MunX eluents were lyophilized and analytically weighed off in triplicate to estimate total protein mass. The purified GFP-PlaX and GFP-MunX samples were electrophoretically separated using tricine SDS-PAGE to estimate sample purity (Schägger and von Jagow, 1987). To avoid saturation during Coomassie staining the 10× dilutions of GFP-PlaX and GFP-MunX were used to estimate protein purity (**Supplementary Figure S3**). Gel analyzer 2010a[1] was used to determine the pixel density of each stained band in respective lanes and used to estimate sample purity (Lazer and GelAnalyzer, 2010). WELQut cleavage optimization.

Cleavage parameters were optimized using a modification of the method supplied by Thermo Fisher Scientific for the WELQut protease. The WELQut-to-sample ratios were set to 1:100, 1:50, 1:25, 1:5 (v/v) for 50 μL samples of GFP-PlaX and GFP-MunX, respectively, and diluted to a final volume of 250 μL in WELQut cut buffer (**Supplementary Table S7**). The corresponding units of WELQ to approximately 466.5 μg of GFP-PlaX was 2.5, 5, 10, and 50 U, respectively. The corresponding units of WELQ to approximately 547.5 μg of GFP-MunX was 2.5, 5, 10, and 50 U, respectively.

Antimicrobial Activity Assays

Antimicrobial activity of plantaricin 423 and mundticin ST4SA was assessed against *Listeria monocytogenes* EDG-e grown on Brain Heart Infusion media (BHI) containing 7.5 μg/mL chloramphenicol. The spot plate method was performed on solid medium (1% w/v agar) seeded with *Listeria monocytogenes* EDG-e. SDS-PAGE separations were assayed for activity by casting the polyacrylamide gel in an agar bilayer seeded with *Listeria monocytogenes* EDG-e. Before casting, the poly acrylamide gels were fixed for 20 min in a 25% isopropanol, 10% acetic acid fixing solution and then rinsed 3 × 15 min with sterile ultra-pure water.

The MIC of GFP-MunX and -PlaX against *L. monocytogenes* EDG-e was determined using a 96 well microtiter plate assay at various concentration of cleaved GFP-MunX and GFP-PlaX in technical and biological triplicate. An overnight culture of *L monocytogenes* EDG-e was used to inoculate BHI broth containing 7.5 μg/mL chloramphenicol at 1% v/v. GFP-MunX and GFP-PlaX was cleaved at the predetermined optimal

[1] http://www.gelanalyzer.com/

WELQut to sample ratios of 1:25 and 1:10, respectively. Serial dilutions of cleaved GFP-MunX and –PlaX stock concentrations were made (**Supplementary Figures S5, S6**). Due to the differences in GFP-MunX and -PlaX concentration and differences in mundticin ST4SA and plantaricin 423 specific activity, 10 μL of each GFP-MunX samples and 20 μLGFP-PlaX samples was added to 190 and 180 μL BHI broth containing *L. monocytogenes* EDG-e in a 96 well microtiter plate, respectively. Absorbance readings (595 nm) were recorded at times 0 and 18 h. Listerial inhibition was expressed as $I = 1 - (A_m/A_0)$, where A_m is the sample absorbance and A_0 the control (blank) absorbance at 595 nm (Cabo et al., 1999). One bacteriocin unit (BU) is defined here as the minimum amount of bacteriocin required to inhibit at least 50% of the indictor strain's growth in 200 μL culture volume (Cabo et al., 1999).

HPLC and LC-ESI-MS

For yield calculation of MunX, GFP-MunX was digested with WELQut protease as described elsewhere and injected onto a Discovery BIO Wide Pore C18 HPLC column (10 μm, 250 × 10 mm, Sigma-Aldrich). The sample was separated using a gradient of 10–90% Solvent B (Solvent B: 90% Acetonitrile/10% MilliQ, 0.1% TFA) over 12 min. Active peaks were collected and lyophilized in order to determine residual mass.

For ESI-MS analysis cleaved GFP-MunX was heated at 90°C for 10 min and cetrifuged (12000 × *g*, 10 min). The supernatant was subsequently injected onto a Hypersil Gold C18 HPLC column (5 μm, 4.6 × 100, Thermo Fisher Scientific). The sample was separated using a gradient of 10–50% Solvent B (Solvent B: Acetonitrile, 0.1% TFA) over 10 min. Peaks were collected and tested for activity as described elsewhere. Active peaks were concentrated using a SpeedyVac vacuum concentrator before ESI-MS analysis (CAF, Stellenbosch, South Africa).

Statistical Analysis

Statistical analysis was performed using Graph Prism Version 3.0 (Graph Pad Software, San Diego, CA). Data generated from the effect of incubation temperature, time and IPTG induction concentration on heterologous expression of GFP fusion constructs was represented as the mean with stand error of mean (SEM). Bonferroni post-tests was performed after a two-way ANOVA on *in vivo* incubation temperature optimization data to identify significant treatments over time. Tukey's Multiple Comparison Test was performed after a one-way ANOVA on the final time point data from IPTG optimization data only, to identify significant treatments. *P*-values < 0.05 were considered significant.

DATA AVAILABILITY STATEMENT

The datasets generated for this study are available on request to the corresponding author.

AUTHOR CONTRIBUTIONS

RV and AV conceptualized the study, performed the experiments, analyzed the data, and wrote the manuscript. LD was responsible for funding acquisition, aided in conceptualization of the study, and writing of the manuscript. AV and LD supervised RV. All authors contributed to the article and approved the submitted version.

FUNDING

RV received funding from the National Research Foundation of South Africa. AV received funding from Stellenbosch University.

ACKNOWLEDGMENTS

We thank Prof. Johan Rower and the Department of Biochemistry at Stellenbosch University for granting accesses to the Tecan Spark M10 as well as Prof. Marina Rautenbach (Biochemistry at the Stellenbosch University) and Miss Elzaan Booysen for assistance with HPLC troubleshooting and Mr. Jerard Gibbon for his vital insights and helpful suggestions. We also thank Dr. Michela Lizier for providing strains and plasmids.

SUPPLEMENTARY MATERIAL

The Supplementary Material for this article can be found online at: https://www.frontiersin.org/articles/10.3389/fmicb.2020.01634/full#supplementary-material

REFERENCES

Alvarez-Sieiro, P., Montalbán-López, M., Mu, D., and Kuipers, O. P. (2016). Bacteriocins of lactic acid bacteria: extending the family. *Appl. Microbiol. Biotechnol.* 100, 2939–2951. doi: 10.1007/s00253-016-7343-9

Ausubel, F. M., Brent, R., Kingston, R. E., Moore, D. D., Seidman, J. G., and Smith, J. A. (2003). *Current Protocols in Molecular Biology*, ed. K. Struhl (Hoboken, NJ: John Wiley & Sons, Inc.).

Beaulieu, L., Tolkatchev, D., Jette, J. F., Groleau, D., and Subirade, M. (2007). Production of active pediocin PA-1 in *Escherichia coli* using a thioredoxin gene fusion expression approach: cloning, expression, purification, and characterization. *Can. J. Microbiol.* 53, 1246–1258. doi: 10.1139/w07-089

Bédard, F., Hammami, R., Zirah, S., Rebuffat, S., Fliss, I., and Biron, E. (2018). Synthesis, antimicrobial activity and conformational analysis of the class IIa bacteriocin pediocin PA-1 and analogs thereof. *Sci. Rep.* 8:9029. doi: 10.1038/s41598-018-27225-3

Bell, M. R., Engleka, M. J., Malik, A., and Strickler, J. E. (2013). To fuse or not to fuse: what is your purpose? *Protein Sci.* 22, 1466–1477. doi: 10.1002/pro.2356

Bennik, M. H. J., Vanloo, B., Brasseur, R., Gorris, L. G. M., and Smid, E. J. (1998). A novel bacteriocin with a YGNGV motif from vegetable-associated *Enterococcus mundtii*: full characterization and interaction with target organisms. *Biochim. Biophys. Acta Biomembr.* 1373, 47–58. doi: 10.1016/S0005-2736(98)00086-8

Brogden, K. A. (2005). Antimicrobial peptides: pore formers or metabolic inhibitors in bacteria? *Nat. Rev. Microbiol.* 3, 238–250. doi: 10.1038/nrmicro1098

Brown, M. (2011). Modes of action of probiotics: recent developments. *J. Anim. Vet. Adv.* 10, 1895–1900. doi: 10.3923/javaa.2011.1895.1900

Cabo, M. L., Murado, M. A., Gonzalez, M. P., and Pastoriza, L. (1999). A method for bacteriocin quantification. *J. Appl. Microbiol.* 87, 907–914. doi: 10.1046/j.1365-2672.1999.00942.x

Carolissen-Mackay, V., Arendse, G., and Hastings, J. W. (1997). Purification of bacteriocins of lactic acid bacteria: problems and pointers. *Int. J. Food Microbiol.* 34, 1–16. doi: 10.1016/S0168-1605(96)01167-1

Chikindas, M. L., Garcia-Garcera, M. J., Driessen, A. J. M. M., Ledeboer, A. M., Nissen- Meyer, J., Nes, I. F., et al. (1993). Pediocin PA-1, a bacteriocin from *Pediococcus acidilactici* PAC1.0, forms hydrophilic pores in the cytoplasmic membrane of target cells. *Appl. Environ. Microbiol.* 59, 3577–3584. doi: 10.1128/aem.59.11.3577-3584.1993

Cui, Y., Zhang, C., Wang, Y., Shi, J., Zhang, L., Ding, Z., et al. (2012). Class IIa bacteriocins: diversity and new developments. *Int. J. Mol. Sci.* 13, 16668–16707. doi: 10.3390/ijms131216668

Cuozzo, S., Calvez, S., Prévost, H., and Drider, D. (2006). Improvement of enterocin P purification process. *Folia Microbiol.* 51, 401–405. doi: 10.1007/BF02931583

Dicks, L. M. T., and Botes, M. (2010). Probiotic lactic acid bacteria in the gastrointestinal tract: health benefits, safety and mode of action. *Benef. Microbes* 1, 11–29. doi: 10.3920/BM2009.0012

Drider, D., Fimland, G., Hechard, Y., McMullen, L. M., and Prevost, H. (2006). The continuing story of class iia bacteriocins. *Microbiol. Mol. Biol. Rev.* 70, 564–582. doi: 10.1128/MMBR.00016-05

Eijsink, V. G. H., Axelsson, L., Diep, D. B., Håvarstein, L. S., Holo, H., and Nes, I. F. (2002). Production of class II bacteriocins by lactic acid bacteria; an example of biological warfare and communication. *Antonie Van Leeuwenhoek* 81, 639–654. doi: 10.1023/A:1020582211262

Ennahar, S., Sashihara, T., Sonomoto, K., and Ishizaki, A. (2000). Class IIa bacteriocins: biosynthesis, structure and activity. *FEMS Microbiol. Rev.* 24, 85–106. doi: 10.1016/S0168-6445(99)00031-5

Fosgerau, K., and Hoffmann, T. (2015). Peptide therapeutics: current status and future directions. *Drug Discov. Today* 20, 122–128. doi: 10.1016/j.drudis.2014.10.003

Fregeau Gallagher, N. L., Sailer, M., Niemczura, W. P., Nakashima, T. T., Stiles, M. E., and Vederas, J. C. (1997). Three-dimensional structure of leucocin a in trifluoroethanol and dodecylphosphocholine micelles: spatial location of residues critical for biological activity in type IIa bacteriocins from lactic acid bacteria. *Biochemistry* 36, 15062–15072. doi: 10.1021/bi971263h

Gibbs, G. M., Davidson, B. E., and Hillier, A. J. (2004). Novel expression system for large-scale production and purification of recombinant class iia bacteriocins and its application to piscicolin 126. *Appl. Environ. Microbiol.* 70, 3292–3297. doi: 10.1128/AEM.70.6.3292-3297.2004

Granger, M., van Reenen, C. A. A., and Dicks, L. M. T. (2008). Effect of gastrointestinal conditions on the growth of *Enterococcus mundtii* ST4SA, and production of bacteriocin ST4SA recorded by real-time PCR. *Int. J. Food Microbiol.* 123, 277–280. doi: 10.1016/j.ijfoodmicro.2007.12.009

Gravesen, A., Ramnath, M., Rechinger, K. B., Andersen, N., Jänsch, L., Héchard, Y., et al. (2002). High-level resistance to class IIa bacteriocins is associated with one general mechanism in *Listeria monocytogenes*. *Microbiology* 148, 2361–2369. doi: 10.1099/00221287-148-8-2361

Guyonnet, D., Fremaux, C., Cenatiempo, Y., and Berjeaud, J. M. (2000). Method for rapid purification of class IIa bacteriocins and comparison of their activities. *Appl. Environ. Microbiol.* 66, 1744–1748. doi: 10.1128/AEM.66.4.1744-1748.2000.Updated

Haugen, H. S., Fimland, G., Nissen-Meyer, J., and Kristiansen, P. E. (2005). Three-dimensional structure in lipid micelles of the pediocin-like antimicrobial peptide curvacin A. *Biochemistry* 44, 16149–16157. doi: 10.1021/bi051215u

Henninot, A., Collins, J. C., and Nuss, J. M. (2018). The current state of peptide drug discovery: back to the future? *J. Med. Chem.* 61, 1382–1414. doi: 10.1021/acs.jmedchem.7b00318

Jasniewski, J., Cailliez-Grimal, C., Gelhaye, E., and Revol-Junelles, A. M. (2008). Optimization of the production and purification processes of carnobacteriocins Cbn BM1 and Cbn B2 from *Carnobacterium maltaromaticum* CP5 by heterologous expression in *Escherichia coli*. *J. Microbiol. Methods* 73, 41–48. doi: 10.1016/j.mimet.2008.01.008

Kimple, M. E., Brill, A. L., and Pasker, R. L. (2013). Overview of affinity tags for protein purification. *Curr. Protoc. Protein Sci.* 73, Unit 9.9. doi: 10.1002/0471140864.ps0909s73

Kjos, M., Borrero, J., Opsata, M., Birri, D. J., Holo, H., Cintas, L. M., et al. (2011). Target recognition, resistance, immunity and genome mining of class II bacteriocins from Gram-positive bacteria. *Microbiology* 157, 3256–3267. doi: 10.1099/mic.0.052571-0

Kjos, M., Salehian, Z., Nes, I. F., and Diep, D. B. (2010). An extracellular loop of the mannose phosphotransferase system component IIC is responsible for specific targeting by class IIa bacteriocins. *J. Bacteriol.* 192, 5906–5913. doi: 10.1128/JB.00777-10

Klein, G., Pack, A., Bonaparte, C., and Reuter, G. (1998). Taxonomy and physiology of probiotic lactic acid bacteria. *Int. J. Food Microbiol.* 41, 103–125. doi: 10.1016/S0168-1605(98)00049-X

Klocke, M., Mundt, K., Idler, F., Jung, S., and Backhausen, J. E. (2005). Heterologous expression of enterocin A, a bacteriocin from *Enterococcus faecium*, fused to a cellulose-binding domain in *Escherichia coli* results in a functional protein with inhibitory activity against *Listeria*. *Appl. Microbiol. Biotechnol.* 67, 532–538. doi: 10.1007/s00253-004-1838-5

Kotel'nikova, E. A., and Gel'fand, M. S. (2002). Production of bacteriocins by gram-positive bacteria and the mechanisms of transcriptional regulation. *Genetika* 38, 758–772. doi: 10.1023/A:1020522919555

Krasowska, J., Olasek, M., Bzowska, A., Clark, P. L., and Wielgus-Kutrowska, B. (2010). The comparison of aggregation and folding of enhanced green fluorescent protein (EGFP) by spectroscopic studies. *J. Spectrosc.* 24, 343–348. doi: 10.3233/spe-2010-0445

Kumar, M. S. (2019). Peptides and peptidomimetics as potential antiobesity agents: overview of current status. *Front. Nutr.* 6:11. doi: 10.3389/fnut.2019.00011

Kumar, P., Kizhakkedathu, J. N., and Straus, S. K. (2018). Antimicrobial peptides: diversity, mechanism of action and strategies to improve the activity and biocompatibility in vivo. *Biomolecules* 8:4. doi: 10.3390/biom8010004

LaVallie, E. R., DiBlasio, E. A., Kovacic, S., Grant, K. L., Schendel, P. F., and McCoy, J. M. (1993). A thioredoxin gene fusion expression system that circumvents inclusion body formation in the *E. coli* cytoplasm. *Nat. Biotechnol.* 11, 187–193. doi: 10.1038/nbt0293-187

Lazer, I., and GelAnalyzer, L. I. (2010). *Freeware 1D Gel Electrophoresis Image Analysis Software*. Available online at: http://www.gelanalyzer.com (accessed on 10 March 2011).

Liu, S., Han, Y., and Zhou, Z. (2011). Fusion expression of pedA gene to obtain biologically active pediocin PA-1 in *Escherichia coli*. *J. Zhejiang Univ. Sci. B* 12, 65–71. doi: 10.1631/jzus.B1000152

Lohans, C. T., and Vederas, J. C. (2012). Development of class iia bacteriocins as therapeutic agents. *Int. J. Microbiol.* 2012, 1–13. doi: 10.1155/2012/386410

Maré, L., Wolfaardt, G. M., and Dicks, L. M. T. (2006). Adhesion of *Lactobacillus plantarum* 423 and *Lactobacillus salivarius* 241 to the intestinal tract of piglets, as recorded with fluorescent in situ hybridization (FISH), and production of plantaricin 423 by cells colonized to the ileum. *J. Appl. Microbiol.* 100, 838–845. doi: 10.1111/j.1365-2672.2006.02835.x

Mesa-Pereira, B., O'Connor, P. M., Rea, M. C., Cotter, P. D., Hill, C., and Ross, R. P. (2017). Controlled functional expression of the bacteriocins pediocin PA-1 and bactofencin A in *Escherichia coli*. *Sci. Rep.* 7:3069. doi: 10.1038/s41598-017-02868-w

Miller, K. W., Schamber, R., Chen, Y., and Ray, B. (1998). Production of active chimeric pediocin AcH in *Escherichia coli* in the absence of processing and secretion genes from the *Pediococcus pap* operon. *Appl. Environ. Microbiol.* 64, 14–20. doi: 10.1128/aem.64.1.14-20.1998

Montalbán-López, M., Deng, J., van Heel, A. J., and Kuipers, O. P. (2018). Specificity and application of the lantibiotic protease NisP. *Front. Microbiol.* 9:160. doi: 10.3389/fmicb.2018.00160

Montville, T. J., and Chen, Y. (1998). Mechanistic action of pediocin and nisin: recent progress and unresolved questions. *Appl. Microbiol. Biotechnol.* 50, 511–519. doi: 10.1007/s002530051328

Moon, G. S., Pyun, Y. R., and Kim, W. J. (2005). Characterization of the pediocin operon of *Pediococcus acidilactici* K10 and expression of his-tagged recombinant pediocin PA-1 in *Escherichia coli*. *J. Microbiol. Biotechnol.* 15, 403–411.

Moon, G. S., Pyun, Y. R., and Kim, W. J. (2006). Expression and purification of a fusion-typed pediocin PA-1 in *Escherichia coli* and recovery of biologically

active pediocin PA-1. *Int. J. Food Microbiol.* 108, 136–140. doi: 10.1016/j.ijfoodmicro.2005.10.019

Nissen-Meyer, J., Rogne, P., Oppegard, C., Haugen, H., and Kristiansen, P. (2009). Structure-function relationships of the non-lanthionine-containing peptide (class II) bacteriocins produced by gram-positive bacteria. *Curr. Pharm. Biotechnol.* 10, 19–37. doi: 10.2174/138920109787048661

Ongey, E. L., Giessmann, R. T., Fons, M., Rappsilber, J., Adrian, L., and Neubauer, P. (2018). Heterologous biosynthesis, modifications and structural characterization of Ruminococcin-A, a lanthipeptide from the gut bacterium *Ruminococcus gnavus* E1, in *Escherichia coli*. *Front. Microbiol.* 9:1688. doi: 10.3389/fmicb.2018.01688

Oppegård, C., Fimland, G., Anonsen, J. H., and Nissen-Meyer, J. (2015). The pediocin PA-1 accessory protein ensures correct disulfide bond formation in the antimicrobial peptide pediocin PA-1. *Biochemistry* 54, 2967–2974. doi: 10.1021/acs.biochem.5b00164

O'Sullivan, D. J., and Klaenhammer, T. R. (1993). Rapid mini-prep isolation of high-quality plasmid DNA from *Lactococcus* and *Lactobacillus* spp. *Appl. Environ. Microbiol.* 59, 2730–2733. doi: 10.1128/aem.59.8.2730-2733.1993

Otvos, L., and Wade, J. D. (2014). Current challenges in peptide-based drug discovery. *Front. Chem.* 2:62. doi: 10.3389/fchem.2014.00062

Pfalzgraff, A., Brandenburg, K., and Weindl, G. (2018). Antimicrobial peptides and their therapeutic potential for bacterial skin infections and wounds. *Front. Pharmacol.* 9:281. doi: 10.3389/fphar.2018.00281

Pustelny, K., Zdzalik, M., Stach, N., Stec-Niemczyk, J., Cichon, P., Czarna, A., et al. (2014). Staphylococcal SplB serine protease utilizes a novel molecular mechanism of activation. *J. Biol. Chem.* 289, 15544–15553. doi: 10.1074/jbc.M113.507616

Ramnath, M., Beukes, M., Tamura, K., and Hastings, J. W. (2000). Absence of a putative mannose-specific phosphotransferase system enzyme IIAB component in a leucocin a-resistant strain of *Listeria monocytogenes*, as shown by two-dimensional sodium dodecyl sulfate-polyacrylamide gel electrophoresis. *Appl. Environ. Microbiol.* 66, 3098–3101. doi: 10.1128/AEM.66.7.3098-3101.2000

Recio, C., Maione, F., Iqbal, A. J., Mascolo, N., and De Feo, V. (2017). The potential therapeutic application of peptides and peptidomimetics in cardiovascular disease. *Front. Pharmacol.* 7:526. doi: 10.3389/fphar.2016.00526

Remington, S. J. (2011). Green fluorescent protein: a perspective. *Protein Sci.* 20, 1509–1519. doi: 10.1002/pro.684

Richard, C., Drider, D., Elmorjani, K., Prévost, H., and Marion, D. (2004). Heterologous expression and purification of active divercin V41, a class IIa bacteriocin encoded by a synthetic gene in *Escherichia coli* heterologous expression and purification of active divercin V41, a class IIa bacteriocin encoded by a synthetic gene. *Society* 186, 4276–4284. doi: 10.1128/JB.186.13.4276

Rupa, P., and Mine, Y. (2012). Recent advances in the role of probiotics in human inflammation and gut health. *J. Agric. Food Chem.* 60, 8249–8256. doi: 10.1021/jf301903t

Saeed, I. A., and Ashraf, S. S. (2009). Denaturation studies reveal significant differences between GFP and blue fluorescent protein. *Int. J. Biol. Macromol.* 45, 236–241. doi: 10.1016/j.ijbiomac.2009.05.010

Sambrook, J., Fritsch, E. F., and Maniatis, T. (1989). *Molecular Cloning: A Laboratory Manual. Mol. Cloning a Lab. Manual*. Available online at: https://www.cabdirect.org/cabdirect/abstract/19901616061 (accessed July 2, 2018).

Schägger, H., and von Jagow, G. (1987). Tricine-sodium dodecyl sulfate-polyacrylamide gel electrophoresis for the separation of proteins in the range from 1 to 100 kDa. *Anal. Biochem.* 166, 368–379. doi: 10.1016/0003-2697(87)90587-2

Shi, Y., Yang, X., Garg, N., and Van Der Donk, W. A. (2011). Production of lantipeptides in *Escherichia coli*. *J. Am. Chem. Soc.* 133, 2338–2341. doi: 10.1021/ja109044r

Si, T., Tian, Q., Min, Y., Zhang, L., Sweedler, J. V., van der Donk, W. A., et al. (2018). Rapid screening of lanthipeptide analogs via in-colony removal of leader peptides in *Escherichia coli*. *J. Am. Chem. Soc.* 140, 11884–11888. doi: 10.1021/jacs.8b05544

Sivashanmugam, A., Murray, V., Cui, C., Zhang, Y., Wang, J., and Li, Q. (2009). Practical protocols for production of very high yields of recombinant proteins using *Escherichia coli*. *Protein Sci.* 18, 936–948. doi: 10.1002/pro.102

Tsien, R. Y. (1998). The green fluorescent protein. *Annu. Rev. Biochem.* 67, 509–544. doi: 10.1146/annurev.biochem.67.1.509

Uteng, M., Hauge, H. H., Markwick, P. R. L., Fimland, G., Mantzilas, D., Nissen-Meyer, J., et al. (2003). Three-dimensional structure in lipid micelles of the pediocin-like antimicrobial peptide sakacin P and a sakacin P variant that is structurally stabilized by an inserted C-terminal disulfide bridge. *Biochemistry* 42, 11417–11426. doi: 10.1021/bi034572i

van Reenen, C. A., Dicks, L. M., and Chikindas, M. L. (1998). Isolation, purification and partial characterization of plantaricin 423, a bacteriocin produced by *Lactobacillus plantarum*. *J. Appl. Microbiol.* 84, 1131–1137. doi: 10.1046/j.1365-2672.1998.00451.x

van Reenen, C. A., and Dicks, L. M. T. (2011). Horizontal gene transfer amongst probiotic lactic acid bacteria and other intestinal microbiota: what are the possibilities? A review. *Arch. Microbiol.* 193, 157–168. doi: 10.1007/s00203-010-0668-3

Van Staden, A. D. P., Faure, L. M., Vermeulen, R. R., Dicks, L. M. T., and Smith, C. (2019). Functional expression of GFP-Fused Class I lanthipeptides in *Escherichia coli*. *ACS Synth. Biol.* 8, 2220–2227. doi: 10.1021/acssynbio.9b00167

Wang, Y., Henz, M. E., Fregeau Gallagher, N. L., Chai, S., Gibbs, A. C., Yan, L. Z., et al. (1999). Solution structure of carnobacteriocin B2 and implications for structure - Activity relationships among type IIa bacteriocins from lactic acid bacteria. *Biochemistry* 38, 15438–15447. doi: 10.1021/bi991351x

Zimmer, M. (2002). Green fluorescent protein (GFP): applications, structure, and related photophysical behavior. *Chem. Rev.* 102, 759–782. doi: 10.1021/cr010142r

Conflict of Interest: The authors declare that the research was conducted in the absence of any commercial or financial relationships that could be construed as a potential conflict of interest.

frontiers in Microbiology

ORIGINAL RESEARCH
published: 13 August 2020
doi: 10.3389/fmicb.2020.01805

Mutations Selected After Exposure to Bacteriocin Lcn972 Activate a Bce-Like Bacitracin Resistance Module in *Lactococcus lactis*

*Ana Belén Campelo[1], María Jesús López-González[1,2], Susana Escobedo[1,2], Thomas Janzen[3], Ana Rute Neves[3], Ana Rodríguez[1,2] and Beatriz Martínez[1,2]**

[1]DairySafe group, Department of Technology and Biotechnology of Dairy Products, Instituto de Productos Lácteos de Asturias (IPLA), Consejo Superior de Investigaciones Científicas (CSIC), Villaviciosa, Spain, [2]Instituto de Investigación Sanitaria del Principado de Asturias (ISPA), Oviedo, Spain, [3]Chr. Hansen A/S, Hørsholm, Denmark

OPEN ACCESS

Edited by:
Des Field,
University College Cork, Ireland

Reviewed by:
Dzung B. Diep,
Norwegian University of Life Sciences, Norway
Branko Jovčić,
University of Belgrade, Serbia

***Correspondence:**
Beatriz Martínez
bmf1@ipla.csic.es

Specialty section:
This article was submitted to Antimicrobials, Resistance and Chemotherapy, a section of the journal Frontiers in Microbiology

Received: *21 May 2020*
Accepted: *09 July 2020*
Published: *13 August 2020*

Citation:
Campelo AB, López-González MJ, Escobedo S, Janzen T, Neves AR, Rodríguez A and Martínez B (2020) Mutations Selected After Exposure to Bacteriocin Lcn972 Activate a Bce-Like Bacitracin Resistance Module in Lactococcus lactis. Front. Microbiol. 11:1805. doi: 10.3389/fmicb.2020.01805

Resistance against antimicrobial peptides (AMPs) is often mediated by detoxification modules that rely on sensing the AMP through a BceAB-like ATP-binding cassette (ABC) transporter that subsequently activates a cognate two-component system (TCS) to mount the cell response. Here, the *Lactococcus lactis* ABC transporter YsaDCB is shown to constitute, together with TCS-G, a detoxification module that protects *L. lactis* against bacitracin and the bacteriocin Lcn972, both AMPs that inhibit cell wall biosynthesis. Initially, increased expression of *ysaDCB* was detected by RT-qPCR in three *L. lactis* resistant to Lcn972, two of which were also resistant to bacitracin. These mutants shared, among others, single-point mutations in *ysaB* coding for the putative Bce-like permease. These results led us to investigate the function of YsaDCB ABC-transporter and study the impact of these mutations. Expression *in trans* of *ysaDCB* in *L. lactis* NZ9000, a strain that lacks a functional detoxification module, enhanced resistance to both AMPs, demonstrating its role as a resistance factor in *L. lactis*. When the three different *ysaB* alleles from the mutants were expressed, all of them outperformed the wild-type transporter in resistance against Lcn972 but not against bacitracin, suggesting a distinct mode of protection against each AMP. Moreover, P_{ysaD} promoter fusions, designed to measure the activation of the detoxification module, revealed that the *ysaB* mutations unlock transcriptional control by TCS-G, resulting in constitutive expression of the *ysaDCB* operon. Finally, deletion of *ysaD* was also performed to get an insight into the function of this gene. *ysaD* encodes a secreted peptide and is part of the *ysaDCB* operon. YsaD appears to modulate signal relay between the ABC transporter and TCS-G, based on the different response of the P_{ysaD} promoter fusions when it is not present. Altogether, the results underscore the unique features of this lactococcal detoxification module that warrant further research to advance in our overall understanding of these important resistance factors in bacteria.

Keywords: cell wall, bacteriocin, antimicrobial peptides, ABC transporter, resistance, *Lactococcus lactis*

INTRODUCTION

ATP-binding cassette (ABC) transporters are bacterial efflux pumps that mediate transport across the membrane at the expenses of the energy liberated by the hydrolysis of ATP (Du et al., 2018). They are constituted by a transmembrane domain (TMD) with a substrate-binding pocket and the nucleotide-binding domain (NBD) that alternate between two structural conformations, inward-open and outward-open, to translocate substrates. ABC transporters are functionally diverse and participate in bacterial virulence, quorum sensing, nutrient uptake, or export of toxic molecules. In particular, ABC transporters are regarded as the fastest-acting and very effective resistance mechanisms to many antimicrobials (Du et al., 2018). Moreover, their role as sensors and information processors in signal relay is being increasingly recognized (Piepenbreier et al., 2017).

In Firmicutes, some ABC transporters confer resistance to antimicrobial peptides (AMPs) including peptide antibiotics (e.g., bacitracin), host antimicrobial peptides (e.g., LL-37 and hBD3 defensins), and bacteriocins (e.g., nisin). Based on their domain architecture and phylogenetic relationships, five groups have been established (Gebhard, 2012). Two of them are required for the export of newly synthesized AMPs (SunT and NisT type) and three are involved in resistance (LanFEG, BceAB, and BcrAB type). BceAB-type transporters are characterized by the NBD protein BceA and the permease BceB with 10 transmembrane helices (TMH) and a large extracellular loop (EC_L) between TMH-VII and VIII. Many BceAB-type transporters are genetically and functionally linked to two component systems (TCS), involved in signal transduction and gene regulation. Actually, the Bce-type permeases and the histidine kinases of the cognate TCS have coevolved toward functional AMP detoxification modules (Dintner et al., 2011). Moreover, the histidine kinases of these TCSs are intramembrane-sensing kinases that completely rely on the ABC transporter to sense the AMP (Bernard et al., 2007). One of the best-characterized detoxification modules is BceRS-BceAB involved in resistance of *Bacillus subtilis* to bacitracin. The BceAB transporter actively participates in bacitracin resistance, likely by freeing its target from the antibiotic grip (Kobras et al., 2020), and interacts directly with the histidine kinase BceS to form a sensory complex that controls the expression of *bceAB* (Dintner et al., 2014). This detoxification module responds to a novel signaling mechanism, so-called flux sensing, whereby monitoring the activity of the individual ABC transporters is the cue to activating the cognate TCS and triggering the cell response (Fritz et al., 2015).

The role of BceAB-type transporters in sensing, together with their role in detoxification, has prompted their classification into three main functional groups proposed by Revilla-Guarinos et al. (2014): (i) those with a dual function involved in sensing and resistance (e.g., BceAB, ABC09 of *Lactobacillus casei*); (ii) sensing transporters that trigger the response but are unable to confer resistance on their own (e.g., VraFG that activates the GraXSR TCS in *Staphylococcus aureus*); and (iii) standalone detoxification pumps which are often regulated by a nongenetically linked TCS (e.g., VraDEH of *S. aureus*).

Additional or accessory components within the ABC/TCS resistance modules may also be present and are thought to be involved in fine tuning both signaling and transport activities. The cytosolic protein GraX from the TCS GraXRS of *S. aureus* has been shown to interact with the histidine kinase GraS, and it is required for GraR-gene activation (Falord et al., 2012). Likewise, *vraH*, located downstream in the *vraDEH* operon, encodes a small membrane protein, which is required for high-resistance to daptomycin and gallidermin (Popella et al., 2016). Other protecting mechanisms may also cluster with ABC/TCS detoxification modules. In *Streptococcus agalactiae*, the module NsrFP/NsrKR involved in nisin resistance is complemented with the nisin resistance protein Nsr, a nisin-degrading protease (Khosa et al., 2013; Reiners et al., 2017).

In a previous work, we have carried out adaptive evolution experiments with several *Lactococcus lactis* strains, which are used worldwide as starters in milk fermentation (López-González et al., 2018). These strains were grown under the selective pressure exerted by the bacteriocin Lcn972, a class IId bacteriocin that binds to lipid II and inhibits cell wall biosynthesis, triggering the cell envelope stress response in *Lactococcus* (Martínez et al., 2007, 2008). The preliminary insight into the genome of these mutants resistant to Lcn972 revealed that, among others, non-synonymous mutations often occurred in a putative Bce-like detoxification module, comprised by an ABC transporter (YsaDCB) and an adjacent TCS (TCS-G) (López-González et al., 2018). Precisely, three of these mutants shared mutations in *ysaB*, coding for a BceB-like permease and two of them were also resistant to bacitracin. These observations prompted us to hypothesize that the YsaDCB ABC transporter might be part of a Bce-like resistance module in *L. lactis*. Therefore, we set out to determine the role of YsaDCB in resistance to bacitracin and Lcn972 and to investigate the consequences of the *ysaB* mutations. The results show that *L. lactis* YsaDCB is involved in both sensing and resistance to AMPs and that those mutations in *ysaB* may impair either function. Moreover, YsaDCB is shown to protect against bacitracin and Lcn972 by a distinct mode of action. Finally, the secreted peptide YsaD is proposed to modulate signal transduction between the ABC transporter and the histidine kinase of TCS-G.

MATERIALS AND METHODS

Bacterial Strains and Growth Conditions

L. lactis strains used in this work and their main characteristics are listed in **Table 1**. The wild-type (WT) *L. lactis* L81 and L62 and their Lcn972R mutants L81-D1, L81-E2, and L62-G9 were grown at 30°C in M17 with lactose at 0.5% (LM17). For the plasmid-free laboratory strains *L. lactis* IL1403 and *L. lactis* NZ9000, glucose at 0.5% was used (GM17). Antibiotics chloramphenicol (Cm), erythromycin (Em), and tetracycline (Tet) were added at 5 μg/ml depending on the plasmid

TABLE 1 | Bacterial strains and plasmids used in this study.

Strain	Properties[a]	Reference
L. lactis* subsp. *lactis		
L81	WT strain, commercial starter culture	López-González et al. (2018)
L81-D1	Lcn972R from L81, *ysaB* mutation $F_{577}S$, $P_{605}T$	
L81-E2	Lcn972R from L81, *ysaB* mutation $F_{577}V$	
L62	WT strain, commercial starter culture	
L62-G9	Lcn972R from L62, *ysaB* mutation $I_{594}F$	
IL1403	Laboratory strain, plasmid free	Bolotin et al. (2001)
L. lactis* subsp. *cremoris		
NZ9000	Host for nisin-inducible gene expression; *ysaB* pseudogene	Kuipers et al. (1998)
Plasmid		
pUK200	Nisin-inducible expression vector. Cm^R	Wegmann et al. (1999)
pRCR	Promoter-probe vector, *mrfp* (mCherry). Cm^R	Mohedano et al. (2015)
pPTPL	Promoter-probe vector, *lacZ*. Tet^R	Burgess et al. (2004)
pILG	Based on pIL252. Em^R	Campelo et al. (2010)
pDCB_n	*ysaDCB* genes in pUK200, "n" stands for strain origin	This work
pCB_n	*ysaCB* genes in pUK200, "n" stands for strain origin	This work
pP_{ysaD}::*lacZ*	$ysaD_{IL}$ promoter fused to *lacZ* in pPTPL	This work
pRCR_P_{ysaD}::*mrfp*	$ysaD_{IL}$ promoter fused to *mrfp* in pRCR	This work
pIL_P_{ysaD}::*mrfp*	$ysaD_{IL}$ promoter fused to *mrfp* in pILG	This work

[a]*WT, wild-type; Cm, chloramphenicol; Tet, tetracycline; Em, erythromycin. L81-D1, L81-E2, and L62-G9 carry several mutations (López-González et al., 2018), but only those in ysaB are specified.*

(**Table 1**) and the same concentrations were used when two plasmids were present in the same lactococcal cell.

Antimicrobial Susceptibility Tests

Minimum inhibitory concentrations (MICs) were determined by the broth dilution method in microtiter plates as previously described (López-González et al., 2018). Two-fold dilutions of the antimicrobials to be tested (bacitracin, nisin, and vancomycin) were done in GM17 or LM17 broth depending on the lactococcal strain. Plates were inoculated with exponentially growing cells adjusted to an optical density at 600 nm (OD_{600}) of 0.05, and then further diluted 1/100. Susceptibility of the *L. lactis* NZ9000 clones carrying the expression plasmids pDCB_n and pCB_n (**Table 1**) was scored according to the inhibitory concentration able to inhibit growth by 50% (IC_{50}). IC_{50} was determined essentially as described by Reiners et al. (2017). IC_{50} plates were inoculated with overnight cultures adjusted to an OD_{600} of 0.1. For gene expression, 1 ng/ml of nisin was routinely added to both pre-cultures and IC_{50} determinations.

RNA Extraction and Analysis

Three independent cultures of *L. lactis* L81, *L. lactis* L62, and their Lcn972R mutants (**Table 1**) were grown on LM17 at 30°C until they reached an OD_{600} of 1.0, when RNAprotect Bacteria Reagent (Qiagen, Germany) was added. Total RNA was extracted using the Illustra RNAspin Mini Kit (GE Healthcare, UK) and treated with Turbo DNAse (Ambion) and SUPERase RNase Inhibitor (Ambion). RNA quality was checked by agarose gel electrophoresis, and its concentration was determined by absorbance at 260 nm in an Epoch microplate spectrophotometer (BioTek). One microgram of each RNA sample was used to generate cDNA with the iScript cDNA Synthesis Kit (Bio-Rad Laboratories, Hercules, CA).

RT-qPCR was performed in a 7500 Fast Real-Time PCR System (Applied Biosystems, Warrington, UK). Primers used for RT-qPCR are listed in **Supplementary Table 1** and were supplied by Macrogen (Korea). Amplification was carried out in 25 µl containing 2.5 µl of a 1:25 dilution of cDNA, 1× Power SYBR Green (Applied Biosystems), and each primer at a concentration of 0.2 µM. Each cDNA amplification was repeated in duplicate. After incubation at 95°C for 10 min, amplification proceeded with 40 cycles of 95°C for 15 s and 60°C for 1 min. Fold changes were calculated following the $2^{-\Delta\Delta Ct}$ method (Livak and Schmittgen, 2001), and the reference gene was the elongation factor Tu *tuf*.

PCR reactions to identify transcription units were performed in a MyCycler Thermal Cycler (Bio-Rad Laboratories). Primers are listed in **Supplementary Table 1**. PCR reactions were carried out in a final volume of 25 µl containing 1 µl of cDNA, 1× Taq DNA Polymerase Master Mix Red (Ampliqon, Denmark) and each primer at a concentration of 0.2 µM. PCR amplification conditions were as follows: 1 cycle at 95°C for 4 min followed by 30 cycles at 95°C for 30 s, 50°C for 30 s, and 72°C for 30 s and a final cycle at 72°C for 7 min. PCR controls were carried with either RNA or genomic DNA. PCR products were analyzed by 2% agarose gel electrophoresis.

pDCB and pCB Expression Plasmids

All the primers required for plasmid construction are listed in **Supplementary Table 1**. Restriction enzymes and T4 ligase were supplied by Eurofins Genomics (Germany) and Fisher Scientific (Spain), respectively, and used according to the manufacturer's instructions. Commercial kits were used for purification of chromosomal DNA (GenElute Bacterial Genomic DNA Kit, Sigma, Spain), plasmids (High Pure Plasmid Isolation Kit, Roche, Germany), and DNA fragments using Illustra GFX PCR DNA and Gel Band Purification Kit (GE Healthcare, UK). The expression plasmids were based on pUK200, placing the *ysaDCB* and *ysaCB* genes under the control of the inducible nisin promoter to yield the plasmids pDCB_n and pCB_n (**Table 1**), tagged after the source of the *ysa* genes as pDCB_IL (IL1403), pDCB_L81, pDCB_D1, pDCB_E2, pDCB_G9, pCB_IL, and pCB_L81. The genes were amplified by PCR with Pwo SuperYield polymerase (Roche, Spain) using as template genomic DNA from *L. lactis* strains IL1403, L81, D1, E2, and G9 and annealing T of 58°C. PCR products

were digested with RcaI and BamHI in the case of the pDCB_n plasmids and with NcoI and BamHI for the pCB_n plasmids. After digestion, the DNA fragments were ligated into pUK200 cut with NcoI and BamHI. The resulting plasmids were established into *L. lactis* NZ9000 by electroporation and checked by DNA sequencing (Macrogen, Spain) to confirm proper cloning.

P_{ysaD} Reporter Plasmids

The β-galactosidase reporter plasmid pP_{ysaD}::*lacZ* was based on pPTPL (**Table 1**). The promoter P_{ysaD} was amplified by PCR using Pwo SuperYield polymerase (Roche, Spain) and the primers described in **Supplementary Table 1**. As template, genomic DNA from *L. lactis* IL1403 was used since the upstream *ysaD* DNA sequence was identical in *L. lactis* IL1403, L81, and L62. The PCR product and the vector were digested by EcoRI and XbaI, ligated, and electroporated into *L. lactis* NZ9000. Two fluorescent reporter plasmids harboring the *mrfp* gene coding for mCherry were constructed (**Table 1**). pRCR_P_{ysaD}::*mrfp* was based on pRCR (**Table 1**). The PCR-amplified P_{ysaD} promoter was digested with XbaI only to leave the 5' end blunt and ligated into SmaI-XbaI-digested pRCR. *Escherichia coli* DH10B (Invitrogen) was used as an intermediate host for cloning. The plasmid was introduced into *L. lactis* strains IL1403 and NZ9000 and the lactose positive *L. lactis* L81, L81-D1, and L81-E2 by electroporation. The BglII-SacI DNA fragment encompassing the P_{ysaD}::*mrpf* fusion from pRCR_P_{ysaD}::*mrfp* was excised and cloned into pILG, digested with the same restriction enzymes to yield pIL_P_{ysaD}::*mrfp* (**Table 1**). This plasmid carries an erythromycin resistance marker, which made possible to maintain the reporter plasmid together with pDCB_n and pCB_n expression plasmids (Cm^R) in the same cell. Correct cloning was confirmed by DNA sequencing (Macrogen, Spain).

Activity of the P_{ysaD} Promoter With the Reporter Plasmid pP_{ysaD}::*lacZ*

Fresh overnight cultures of *L. lactis* NZ9000 clones carrying the different expression plasmids pDCB_n and pCB_n and the reporter plasmid pP_{ysaD}::*lacZ* were diluted to OD_{600} of 0.05 in GM17/Cm/Tet and nisin at 1 ng/ml to ensure expression of the *ysa* genes. When the clones reached an OD_{600} of 0.2–0.3 (approximately 3 h at 30°C), 2 ml samples were taken and bacitracin was added at 5 and 1 μg/ml and incubation proceeded for 30 min. Cultures without bacitracin were taken as baseline controls. Cells were collected by centrifugation, and the β-galactosidase reaction was carried out at 30°C for 10 min as described elsewhere (Martínez et al., 2007). β-Galactosidase activity assays were carried out, at least, with three independent cultures.

Activity of the P_{ysaD} Promoter With the Reporter Plasmid pIL_P_{ysaD}::*mrfp*

L. lactis NZ9000 pDCB_n and pCB_n and the reporter plasmid pIL_P_{ysaD}::*mrfp* were inoculated in GM17/Cm/Em and 1 ng/ml nisin and grown as described for pP_{ysaD}::*LacZ*. After induction with bacitracin (1 and 5 μg/ml) or Lcn972 (80, 40, and 20 AU/ml), cells (1 ml) were washed with saline phosphate buffer (PBS), pH 7.3, and collected in half of the initial volume. Cell suspensions were kept in the dark for 3 h for mCherry maturation (Garay-Novillo et al., 2019). Fluorescence (F) of 20-μl aliquots was quantified in a 7500 Fast Real-Time PCR System (Applied Biosystems, Warrington, UK) using the built-in presence/absence protocol for detecting ROX, a fluorophore with similar excitation (Ex. 580 nm) and emission (Em. 605 nm) wavelengths as mCherry (Ex. 587 nm, Em. 612 nm). After blank correction (PBS background), raw fluorescence data was normalized by dividing F by the OD_{600} of the cell suspensions (200 μl) measured in a Benchmark Plus microplate spectrophotometer (Bio-Rad).

Statistical Analysis

When indicated, differences were assessed by one-tailed *t*-test as implemented in Microsoft Excel 2010 (2010 Microsoft Corporation) and $p < 0.05$ was considered to be significant.

RESULTS

Resistance of Lcn972R *L. lactis* Mutants to AMPs Other Than Lcn972

In our previous work, three Lcn972 resistant mutants (Lcn972R) L81-D1, L81-E2, and L62-G9 (**Table 1**) were isolated after continuous exposure of the wild-type (WT) strains *L. lactis* subsp. *lactis* L81 and *L. lactis* subsp. *lactis* L62 to subinhibitory concentrations of the cell wall-active bacteriocin Lcn972. The preliminary phenotypic characterization already suggested that the two mutants L81-E2 and L62-G9 displayed cross-resistance to bacitracin, while L81-D1 was more susceptible than its parent *L. lactis* L81 (López-González et al., 2018). Standard MIC determinations confirmed that bacitracin MICs for L81-E2 and L62-G9 increased by 8- and 4-fold, respectively, whereas the MIC for *L. lactis* L81-D1 was reduced 2-fold (**Table 2**). MICs of other antimicrobials such as nisin and vancomycin also increased 2- or 4-fold for some Lcn972R mutants (**Table 2**) in line with our previous results (López-González et al., 2018).

TABLE 2 | Minimum inhibitory concentrations (MICs) of several antimicrobial peptides for *L. lactis* strains.

L. lactis	MIC			
	Lcn972 (AU/ml)[a]	Bacitracin (μg/ml)	Vancomycin (μg/ml)	Nisin (μg/ml)[b]
L81 (WT)	10	8	0.5	1
L81-D1	80	4	0.5	2
L81-E2	320	64	0.5	4
L62 (WT)	10	8	0.5	2
L62-G9	80	32	1	4
IL1403	40	0.125	0.5	ND
NZ9000	20	0.5	0.5	ND

[a]*Taken from López-González et al. (2018).*
[b]*ND, not determined.*

Presence of a BceAB-Like Detoxification Module in *L. lactis*

Three Lcn972R mutants L81-D1, L81-E2, and L62-G9 carried, among others, non-synonymous mutations in *ysaB*, a gene coding for the permease of a putative ABC transporter (López-González et al., 2018). Inspection of the genome of the WT strains L81 and L62 (European Nucleotide Archive under accession number ENA: PRJNA 492214) and the laboratory strain *L. lactis* subsp. *lactis* IL1403 (GenBank AE005176.1) revealed that *ysaB* is flanked by *ysaC* and genes encoding the TCS-G (**Figure 1A**). YsaC contains the ATP-binding domain and YsaB shares the features of BceB-like permeases with 10 transmembrane helices (TMHs) and an extracellular loop (233 aa), according to TMpred[1] and Psort[2] predictions. All the *ysaB* mutations detected in the Lcn972R strains mapped in the C-terminus. Three mutations ($F_{577}V$, $F_{577}S$, and $I_{594}F$) were found in the predicted inside loop between TMH VIII and IX. The additional mutation $P_{605}T$ detected in *L. lactis* L81-D1 was positioned within TMH IX. The genes encoding the TCS-G with the response regulator LlrG and the intramembrane histidine kinase KinG are located downstream of *ysaB* (**Figure 1A**). This genetic arrangement is similar to that found for other BceAB-like ABC transporters which are genetically linked to regulatory elements such as TCSs and involved in resistance to AMPs (Dintner et al., 2011).

Additional genes (*ysaD* and *ysaA*) were also identified (**Figure 1A**). Homology and conserved domain searches identified YsaD (119 aa) as a member of TIGR01655 (uncharacterized protein YxeA), a family of small uncharacterized secreted proteins which are found exclusively in Gram-positive bacteria. YsaA (354 aa) is predicted to be an integral membrane protein with nine TMHs. It contains a VanZ domain present in glycopeptide antibiotic resistance proteins (pfam04892), denoting a possible role in resistance to AMPs.

The module YsaDCB/TCS-G is present in 41 out of the 192 complete *L. lactis* genomes deposited at NCBI (as of June 2020) according to BLASTN[3] searches, and it seems highly conserved (over 80% identity at the nucleotide level) within the two *L. lactis* subspecies *cremoris* and *lactis*. It is worth mentioning that, in the laboratory workhorse strain *L. lactis* MG1363 and its derivative *L. lactis* NZ9000, the ABC transporter appears to be nonfunctional due to a stop codon at position 310 that created a truncated YsaB permease of 103 residues. Otherwise, its TCS-G is complete. A detailed comparison at the protein level and accession numbers is included in **Supplementary Table 2**.

The Putative Detoxification Module YsaDCB/TCS-G in *L. lactis* Is Transcribed in Two Polycistronic mRNAs

The genes of the putative Ysa-TCS-G module are transcribed in two polycistronic mRNAs as determined by RT-PCR using primers annealing within the gene ends (**Figure 1B**).

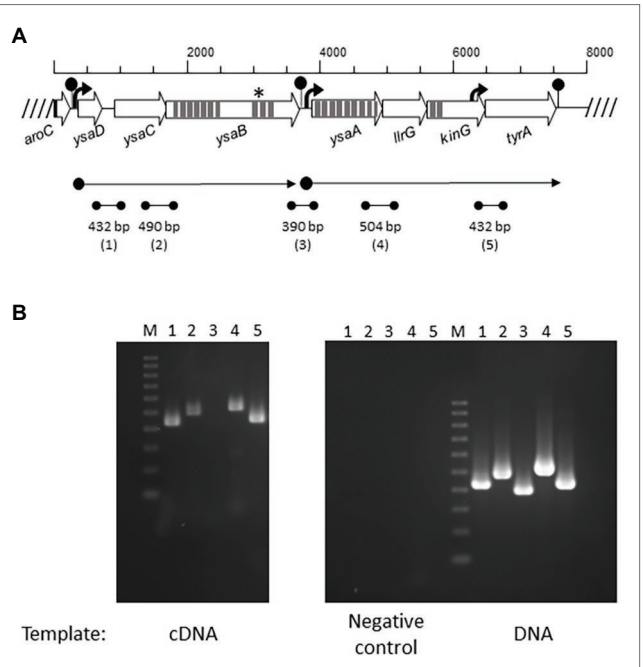

FIGURE 1 | Operon organization of the Ysa TCS-G module in *Lactococcus lactis*. **(A)** Overview of the *ysa* and flanking genes (open arrows). Promoters are depicted as black arrows and terminators as lollypops. Predicted transmembrane helices are shown as dark gray strips. Localization of *ysaB* mutations is marked with an asterisk (*). The two predicted mRNAs are displayed by dot-end arrows. Intergenic regions (1–5) amplified by RT-PCR are shown by dot-end lines. **(B)** RT-PCR amplified bands (1–5) using as template cDNA, RNA (negative control), and genomic DNA (positive control) from *L. lactis* L81.

Based on the amplification results, two mRNAs *ysaDCB* and *ysaA-llrG-kinG-tyrA* are synthesized. Consistent with this, two putative promoters could be identified upstream of *ysaD* (P*ysaD*) and *ysaA* (P*ysaA*), as well as three rho-independent terminators downstream of *aroC*, *ysaB*, and *tyrA* (**Figure 1B**). A positive PCR amplification of the intergenic region *kinG-tyrA* was detected, which could be due to the presence of a putative promoter at the 3' end of *kinG*, upstream of the forward primer used in RT-PCR (**Figure 1B**). The flanking genes *tyrA* and *aroC* coding for prephenate dehydrogenase and chorismate synthase, respectively, are involved in the biosynthesis of aromatic amino acids. Hence, it is unlikely that they participate in the transport and/or sensing functions of the YsaDCB/TCS-G module.

ysaDCB but Not TCS-G Genes Are Highly Expressed in Lcn972R *L. lactis* Mutants

Bearing in mind the role of BceAB-like transporters in resistance to AMPs, the expression levels of *ysaDCB*, *ysaA*, *llrG*, and *kinG* were determined in exponentially growing cultures of the *L. lactis* Lcn972R mutants by RT-qPCR. The expression of the TCS-G genes was not altered in any of the mutants. On the contrary, *ysaDCB* were upregulated in the Lcn972R mutants albeit to a different extent. Highest expression occurred in *L. lactis* L81-E2 (close to 20-fold), followed by *L. lactis*

[1]https://embnet.vital-it.ch/software/TMPRED_form.html
[2]https://www.psort.org/psortb/
[3]https://blast.ncbi.nlm.nih.gov/Blast.cgi

L62-G9 (up to 10-fold; **Figure 2**). In *L. lactis* L81-D1, which carries two *ysaB* mutations ($F_{577}S$ and $P_{605}T$) and is sensitive to bacitracin, the expression of *ysaDCB* was lower but still up to 5-fold compared to the WT *L. lactis* L81 (**Figure 2**). Closer inspection and resequencing of the PCR-amplified P_{ysaD} promoter in all these strains did not show any anomalies, which could explain the higher expression levels of the *ysaDCB* operon in the Lcn972R mutants.

Further confirmation of the increased expression of the *ysaDCB* genes in the Lcn972R *L. lactis* mutants was gathered by monitoring the functional expression of the fluorescent mCherry protein gene *mrfp* placed under the control of the P_{ysaD} promoter in the reporter plasmid pRCR_P_{ysaD}::*mrfp*. While hardly any fluorescence could be measured in both exponential and stationary phase cultures of *L. lactis* L81, fluorescence was 30-fold and 10-fold higher in *L. lactis* L81_E2 and *L. lactis* L81_D1 (**Supplementary Figure S1A**).

Of note, the expression levels of *ysaDCB* mirrored resistance to Lcn972 but not to bacitracin (**Table 2**). Despite their increased expression in *L. lactis* L81-D1, this mutant was more sensitive to bacitracin than the WT. Moreover, different susceptibility to bacitracin was also noticed within the laboratory strains *L. lactis* IL1403, with a complete YsaDCB transporter, and *L. lactis* NZ9000 that lacks a functional YsaB permease, being 4-fold more resistant to bacitracin than IL1403. These observations suggest that bacitracin resistance mechanisms other than YsaDCB are functional in *L. lactis*.

Mutated Versions of *ysaB* Provide Distinct Resistance Levels to Bacitracin and Lcn972

In order to confirm the suspected role of the YsaDCB transporter in bacitracin and Lcn972 resistance and assess the impact of the *ysaB* mutations, the WT and mutated *ysaB* genes were cloned under the inducible nisin promoter (plasmids pDCB_n) and expressed in the *L. lactis* NZ9000 background (*ysaB* deficient). In this way, the level of protection provided by the ABC transporter itself and its mutated versions could be assessed and compared within the same genetic background, independently of their own regulation and the other mutations present in the Lcn972R mutants. The transporter genes of *L. lactis* IL1403 were also cloned (pDCB_IL) because they have been previously linked to nisin resistance (Kramer et al., 2006). Dose-response curves showed that expression of the WT genes *ysaDCB* of *L. lactis* L81 and *L. lactis* IL1403 conferred a 5-fold increase in the bacitracin and Lcn972 concentration required to inhibit growth by 50% (IC_{50}), as compared to the control with the empty vector pUK200 (**Figure 3**). Hence, the role of YsaDCB in resistance of *L. lactis* to both AMPs was confirmed.

In the case of the mutated alleles of *ysaB*, represented by the *ysaDCB* operons from L81-D1, L81-E2, and L62-G9 (the WT *ysaDCB* from *L. lactis* L62 is identical to L81), contribution to resistance varied depending on the AMP (**Figure 3**). In line with the MICs reported in **Table 2**, the double *ysaB* mutant transporter pDCB_D1 failed to protect against bacitracin as judged by the low IC_{50} values, similar to those with the control *L. lactis* pUK200. On the contrary, the transporters in pDCB_E2

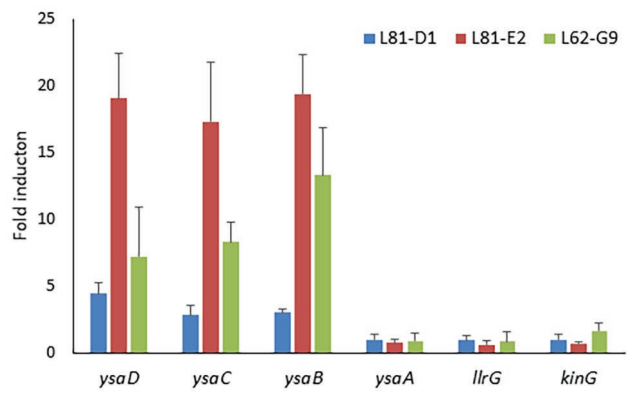

FIGURE 2 | Relative expression of Ysa and TCS-G genes in the *L. lactis* Lcn972R mutants determined by RT-qPCR. Relative gene expression was determined by the $2^{-\Delta\Delta Ct}$ method using the WT strains *L. lactis* L81 (for L81-D1 and L81-E2) and *L. lactis* L62 for L62-G9 as reference. Average of three biological replicates and SD (error bars) are shown.

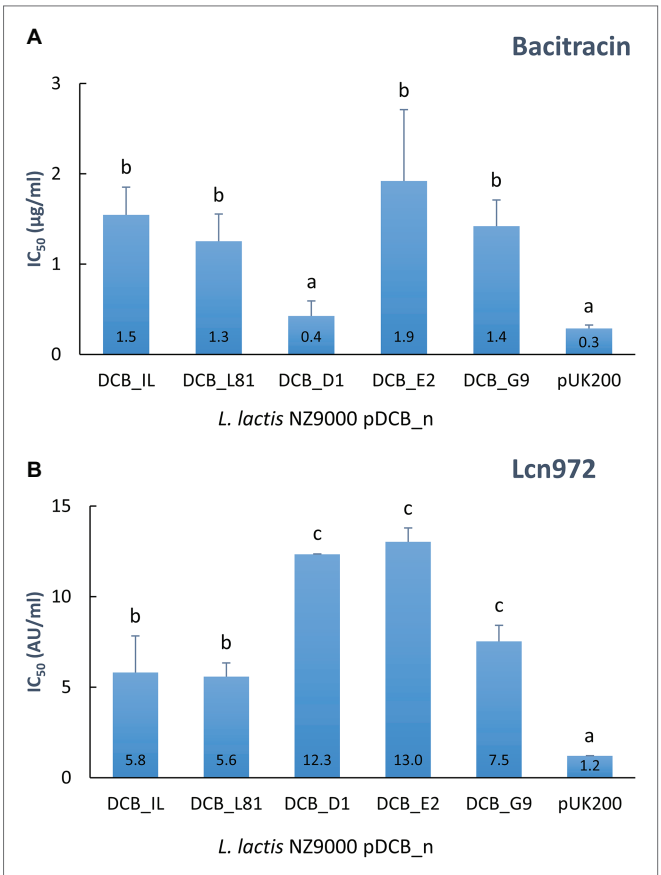

FIGURE 3 | Resistance to bacitracin **(A)** and Lcn972 **(B)** of *L. lactis* NZ9000 clones expressing the different versions of *ysaDCB* genes. Calculated IC_{50} values are displayed inside the bars. Average and SD from, at least, two independent IC_{50} determinations are shown. Values with different letters are significantly different ($p < 0.05$).

and pDCB_G9 provided similar levels of protection as the WT transporter. As for resistance to Lcn972, the scenario was different. Regardless of the *ysaB* allele, all the transporters boosted protection against Lcn972 over the WT genes ($p < 0.05$; **Figure 3** IC_{50}), with pDCB_G9 being less effective than pDCB_D1 and pDCB_E2 ($p < 0.05$). These results suggest that the mechanisms whereby YsaDCB protects *L. lactis* against bacitracin and Lcn972 might differ.

ysaB Mutations Trigger the P_{ysaD} Promoter in the Absence of Bacitracin

A mutagenesis study of the BceSR/BceAB resistance module has shown that single amino acid substitutions in the *B. subtilis* permease BceB may have different consequences in either signaling or resistance (Kallenberg et al., 2013). Moreover, the authors observed that those mutations that primarily affect the activity of the transporter tend to cluster in the C-terminal of the permease, which is the case with the *ysaB* mutations identified in the Lcn972R *L. lactis* mutants (see **Table 1**). Therefore, we next investigated if the mutations in *ysaB*, besides affecting resistance, could also alter onward signal transmission through the TCS-G and lead to induction of the *ysaDCB* operon upon detection of the stress. With this aim, bacitracin was chosen to measure P_{ysaD} promoter activity due to the different resistance levels provided by the *ysaB* alleles (see **Figure 3A**). We first confirmed that P_{ysaD} was silent (OFF-state) in *L. lactis* NZ9000 lacking *ysaB*, even in the presence of bacitracin. As shown in **Supplementary Figure S1B**, while mCherry fluorescence in *L. lactis* IL1403/pRCR_P_{ysaD}::*mrfp* increased proportionally to increasing bacitracin concentration, there was no response in *L. lactis* NZ9000/pRCR_P_{ysaD}::*mrfp*. Therefore, *L. lactis* NZ9000 was deemed as a suitable host to study the signaling ability of YsaDCB and the existence of any other mechanisms that could induce P_{ysaD} was ruled out.

To quantify the activity of the P_{ysaD} promoter in the *L. lactis* NZ9000 pDCB_n clones expressing the different *ysaB* alleles, the reporter plasmid pP_{ysaD}::*lacZ* was constructed in which a Tet resistance marker is present to help keeping both pDCB_n and reporter plasmids in *L. lactis* NZ9000. Although the β-galactosidase assay was not sensitive enough to detect activation of P_{ysaD} in the presence of pDCB_IL, the promoter was responsive to bacitracin when the *L. lactis* L81 *ysa* genes (pDCB_L81) were expressed (**Figure 4**). Hence, it was possible to compare signaling driven by the different *ysaB* alleles. Under non-inducing conditions, *L. lactis* NZ9000 expressing the mutated *ysaB* transporters exhibited a higher P_{ysaD} basal activity than that achieved with the WT transporter YsaDCB_L81 ($p < 0.05$). This basal activity was remarkably high in the presence of YsaDCB_E2 and YsaDCB_G9 transporters (**Figure 4**). Besides this apparent deregulation, the P_{ysaD} promoter was still induced by bacitracin, although the level of response was clearly diminished in relation to the WT transporter. In this latter case, β-galactosidase activity rose by 5-fold after the challenge with bacitracin at 5 μg/ml, whereas it only increased 1.2-fold in the presence of YsaDCB_D1 and 1.5-fold and in the presence of the other two mutated transporters.

The Secreted Peptide YsaD Seems to Modulate the Activity of the YsaDCB/TCS-G Module

The fact that *ysaD* forms an operon with *ysaCB* and that it is conserved within *L. lactis* raised the question whether this secreted peptide was somehow required for proper functioning of the YsaDCB/TCS-G module. Bearing in mind the dual role of the transporters in resistance and signal relay, we initially determined the IC_{50} values of bacitracin and Lcn972 for *L. lactis* NZ9000 expressing *ysaCB* from *L. lactis* IL1403 (pCB_IL) or from *L. lactis* L81 (pCB_L81) and compared to those expressing the whole cluster *ysaDCB* (**Table 3**). YsaD appears

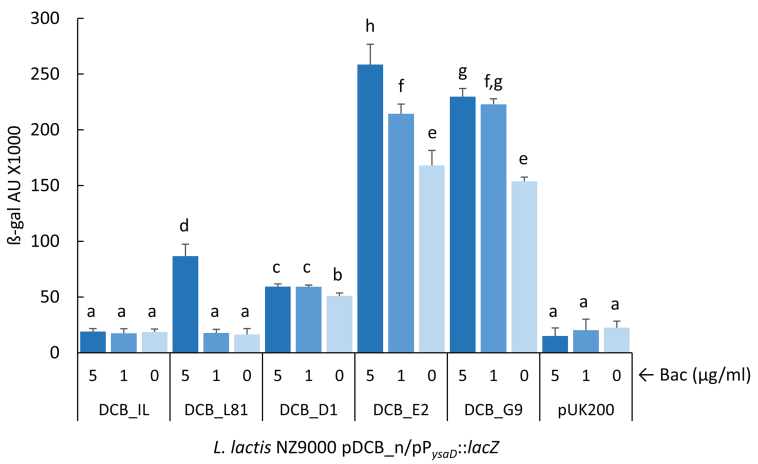

FIGURE 4 | Induction of P_{ysaD} by bacitracin. Exponentially growing *L. lactis* NZ9000 clones expressing the different versions of *ysaDCB* genes (pDCB_n) and carrying the reporter plasmid pP_{ysaD}::*lacZ* were challenged with varying concentrations of bacitracin (Bac) for 30 min. Average and SD from three independent experiments are shown. Values with different letters are significantly different ($p < 0.05$).

TABLE 3 | IC_{50} values[a] for *L. lactis* NZ9000 expressing *ysaCB*.

L. lactis NZ9000	Bacitracin (μg/ml)	Lcn972 (AU/ml)
pDCB_L81[b]	1.25 ± 0.30	5.58 ± 075
pCB_L81	2.41 ± 0.14*	6.63 ± 0.13
pDCB_IL[b]	1.55 ± 0.31	5.81 ± 2.02
pCB_IL	1.52 ± 0.23	4.45 ± 0.89
pUK200[b]	0.29 ± 0.01	1.21 ± 0.01

[a]*Average ± standard deviation of, at least, two independent biological replicates are shown.*
[b]*IC_{50} values are also shown in **Figure 3** but are included here for comparison.*
**p < 0.05, significant difference between pDCB_L81 vs. pCB_L81. For all clones, bacitracin and Lcn972 IC_{50} are increased in comparison with L. lactis NZ9000 with the empty vector pUK200.*

to be dispensable for resistance. All the clones were more resistant to bacitracin and Lcn972, compared to the control with the empty vector, and showed comparable bacitracin and Lcn972 IC_{50} values regardless the presence of *ysaD*. Only *L. lactis* NZ9000 pCB_L81 exhibited a 2-fold increase in the bacitracin IC_{50}, compared to pDCB_L81, suggesting a possible but marginal role of *ysaD* in resistance.

We also measured P_{ysaD} activity in the absence of *ysaD* to assess if YsaD could interfere with signal relay. Due to the low sensitivity of the *lacZ* reporter, unable to reveal induction of the P_{ysaD} promoter by the *L. lactis* IL1403 YsaDCB transporter, a more sensitive reporter plasmid pIL_P_{ysaD}::*mrfp*, based on the mCherry fluorescent protein, was used. This reporter was transferred to *L. lactis* NZ9000 pDCB_n and pCB_n clones. As shown in **Figure 5**, induction of P_{ysaD} by bacitracin in the presence of pDCB_IL could be demonstrated, albeit the response was roughly 10-fold lower than with pDCB_L81 (**Figure 5**). When the activity of P_{ysaD} was compared in the absence and presence of *ysaD* after the addition of bacitracin, the results were different depending on the transporter. The P_{ysaD} promoter was turned down in *L. lactis* NZ9000/pCB_L81, while it was strongly induced in *L. lactis* NZ9000/pCB_IL (**Figure 5**). This apparently incongruent behavior must rely on subtle differences within the L81 and IL1403 ABC transporters that could be important for the interaction with the *L. lactis* NZ9000 TCS-G (see section Discussion). Nonetheless, YsaD appears to modulate the activity of the YsaDCB/TCS-G module by altering signal relay. Finally, it is worth noting that attempts to show induction of P_{ysaD} by Lcn972 failed. All the reporter strains with either pDCB_n or pCB_n were exposed to Lcn972 at 80, 40, and 20 AU/ml, but fluorescence was never detected (data not shown).

DISCUSSION

The *L. lactis* YsaDCB ABC transporter is proposed to form a functional AMP detoxification module with the adjacent TCS-G, based on the genetic organization and the domain architecture of both the permease YsaB and the intramembrane-sensing histidine kinase KinG, two landmarks shared among AMP resistance modules in Firmicutes (Dintner et al., 2011; Gebhard, 2012). Accordingly, we have shown that increased expression of *ysaDCB* confers resistance against bacitracin and Lcn972 in *L. lactis* and that the module does not respond to bacitracin in the absence of a functional ABC transporter.

Previous studies have also linked this ABC transporter to nisin resistance in *L. lactis* (Kramer et al., 2006). Thereby, YsaDCB/TCS-G is able to provide resistance to cationic AMPs that differ in their mode of action. This is similar to other modules such as the staphylococcal GraXSR/VraFG and BraRS/BraDE reviewed by Kawada-Matsuo et al. (2011), whereas in *B. subtilis* the different Bce-like modules seem to be more specialized for bacitracin (BceSR/BceAB), nisin and other lipid II-binding lantibiotics (PsdRS/PsdAB) or cationic peptides such as the human defensin LL-37 (YxdJK/YxdLM-YxeA; Staron et al., 2011). The reason likely relies on the scope of the genes which are regulated by these resistance modules. Some modules only regulate the ABC transporter genes (e.g., BceSR/BceAB), while others (e.g., GraXSR/VraFG) include genes such as the *dlt* operon and *mprf* involved in D-alanylation of lipoteichoic acids and lysylination of phosphatidylglycerol, respectively, that

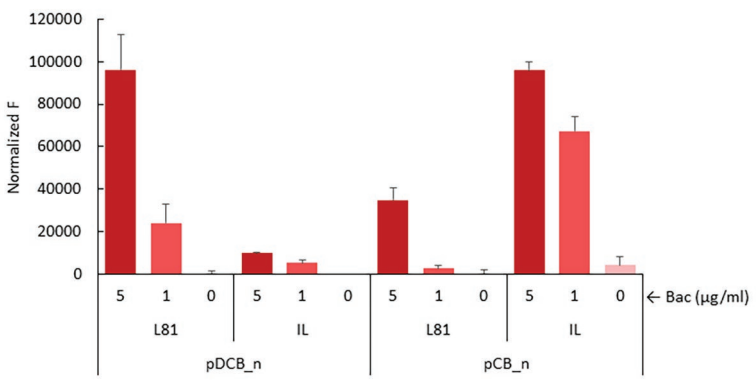

FIGURE 5 | Induction of P_{ysaD} in the presence of pDCB_n and pCB_n. Exponentially growing *L. lactis* NZ9000 clones expressing the full *ysaDCB* (DCB_n) operon or *ysaCB* (CB_n) lacking *ysaD* from *L. lactis* L81 (L81) or *L. lactis* IL1403 (IL) and the reporter plasmid pIL_P_{ysaD}::*mrfp* were challenged with bacitracin at 5 and 1 μg/ml for 30 min before mCherry fluorescence (F) was measured.

contribute to AMP resistance by decreasing the net negative charge of the bacterial surface. BraRS/BraDE and VirSR/VirAB also regulate the expression of other ABC transporters such as VraDEH in *S. aureus* and AnrAB in *Listeria monocytogenes*, respectively. These transporters likely function as a "hydrophobic vacuum cleaner," removing the AMPs out of their site of action (Collins et al., 2010; Hiron et al., 2011).

Our results have demonstrated that point mutations in *ysaB* activate the YsaDCB/TCS-G module. P_{ysaD} is active in the absence of bacitracin, when the mutated *ysaB* alleles are expressed in *L. lactis* NZ9000 and not in the case of the WT transporters. Gain-of-function mutations in the Bra(Nsa)SR/BraDE module have been mapped on *braS* or *braR* or on the TCS promoter in nisin-resistant *S. aureus* (Randall et al., 2018; Arii et al., 2019), but there are also examples in which mutations in the permease gene enhance resistance by inducing the expression of the ABC-transporter genes (Becker et al., 2009). In view of the current flux sensing model (Fritz et al., 2015), one possible explanation could be that the permease mutations reduce the activity of the YsaDCB transporter. This scenario would impose more pressure onto the system to increase the rate of *de novo* transporter synthesis and get more transporter molecules to relieve the stress. However, it is difficult to explain the constitutive expression in the absence of the AMP and the loss of responsiveness to AMP concentration, as observed with the mutated YsaDCB transporters. Moreover, since flux sensing relies on ATP hydrolysis, it would be clearly deleterious for the cells. Alternatively, the mutations in the YsaB permease could modify protein-protein interactions within the module, triggering activation of the histidine kinase, irrespectively of the activity of the YsaDCB transporter. Recently, it has been proposed that the ABC transporter BraDE, beyond its role in sensing and activation of BraSR regulon, also enables onward signal transduction through the histidine kinase BraS in some way, which is independent of ATP consumption (Randall et al., 2018). This role was proposed after observing that the nisin-resistant phenotype of a gain-of-function *braS* mutant lacking *braDE* could be complemented with an ATP-deficient *braDE* copy. In this scenario, it is conceivable that mutations in the permease could prompt activation of the TCS. However, further biochemical evidence is required to prove if this is the case of the *ysaB* mutations.

Increased expression of *ysaDCB*-D1 was not enough to confer resistance to bacitracin, whereas protection against Lcn972 was enhanced compared to the WT YsaDCB transporter. This takes us to speculate that YsaDCB may protect *L. lactis* by two different means. For bacitracin, it has been proposed that the *B. subtilis* BceAB transporter binds to the complex bacitracin-undecaprenyl pyrophosphate and releases the antibiotic from it, freeing the cell wall precursor to proceed with cell wall biosynthesis (Kobras et al., 2020). The double amino acid substitution $F_{577}S/P_{605}T$ in YsaB-D1 could make the ABC transporter less efficient for bacitracin release, and thus unable to protect against bacitracin. Kobras et al. (2020) also hypothesize that a similar target protection mechanism should also work for lipid II binding peptides such as mesarcidin and actagardine. However, YsaDCB-D1 is as effective as YsaDCB-E2 against Lcn972. Since YsaDCB-D1 is still competent to trigger activation of the module, we speculate that downstream activities (i.e., other functions regulated by the YsaDCB/TCS-G module) are responsible for resistance to Lcn972. In support of this hypothesis, motif-based searches, using the consensus binding sequence for BceR-like response regulators proposed by Dintner et al. (2011), detected a putative BceR-binding box in the promoter of the *dlt* genes in *L. lactis*. Moreover, D-alanylation of lipoteichoic acids is known to constitute an Lcn972 resistance factor (Roces et al., 2012).

The *L. lactis* BceAB-like transporter is equipped with an additional protein YsaD whose structural gene is co-transcribed with *ysaCB*. According to BlastP searches, YsaD belongs to the family TIGR01655 of small uncharacterized proteins with N-terminal signal sequences, conserved in Gram-positive organisms. These properties are shared with YxeA, in the *B. subtilis* module YxdJK/YxdLM-YxeA (Joseph et al., 2004), but its putative function has not been addressed so far. Our results suggest that these proteins may play an accessory role, modulating the activity of the transporter and/or governing signal transduction through protein-protein interactions within the module. Despite having an identical YsaD, removal of this protein had two opposite effects: a drop of signaling in the case of the transporter YsaDCB-L81 and boosting the otherwise poor ability of the *L. lactis* IL1403 transporter to activate *L. lactis* NZ9000 TCS-G (see **Figure 5**). Being aware that our experimental setup is not the best scenario to interrogate for fine tuning or regulatory feedback, simply because it relies on the formation of a heterologous ABC/TCS module, this discrepancy could be explained when specific YsaD-YsaB or YsaD-YsaB-KinG interactions regulate transport activity and that such interactions differ within these two transporters. Both YsaDCB-L81 and YsaDCB-IL are highly homologous with only one non-conservative amino acid substitution in the ATP-binding protein YsaC (E_{139} in L81 and K_{139} in IL1403), outside the conserved protein domains and unlikely to interfere with transport activity. The other one is in the YsaB permease (K_{621} in L81 and E_{621} in IL1403). This position is predicted to be located at the external linker between the last two TMHs IX and X. From our results and others (Kallenberg et al., 2013), it is known that single amino acid substitutions in the permease, namely, in the C-terminus, may severely alter signal transduction. Consistent with this, there is a 10-fold difference in the ability of the IL1403 and L81 transporters to trigger the P_{ysaD} promoter in response to bacitracin. ABC connectors or accessory proteins such as the cytosolic GraX and the small membrane protein VraH have already been described (Falord et al., 2012; Popella et al., 2016). Whether the same applies for a soluble and likely secreted peptide remains to be investigated. It is worth mentioning that in *L. lactis* there is an additional gene, *ysaA*, which is co-transcribed with the TCS-G gene and specifies for a transmembrane protein. YsaA, as yet unique to *L. lactis*, is likely to play a role in the transduction pathway too.

There was another result that will require further attention. Under the experimental conditions used in this work, we were unable to detect activation of P_{ysaD} by Lcn972, which is known

to bind to lipid II as many other Bce-like inducers. In a way, this was unexpected given that the gain-of-function mutations in *ysaB* were selected under the stress imposed by this bacteriocin (López-González et al., 2018). However, YsaDCB/TCS-G is likely regulating the *dlt* operon, which should protect against Lcn972 and, thereby, growth of gain-of-function mutants would be expedited. At this stage, it is difficult to propose a reasonable explanation for the lack of induction by Lcn972. We cannot disregard a host effect, i.e., that Lcn972 is unable to trigger the response in *L. lactis* NZ9000 but in other strain backgrounds, as recently observed with VirAB/VirRS in *L. monocytogenes* (Grubaugh et al., 2018; Jiang et al., 2019).

In conclusion, we have shown that YsaDCB/TCS-G participates in AMP resistance in *L. lactis* anticipating alternative mechanisms of resistance against different AMPs. Specific mutations which are easily selected under cell envelope stress have been shown to activate the module constitutively. Moreover, YsaDCB/TCS-G seems to be unique as to the intricate regulatory circuits due to the presence of additional proteins that modulate its activity, thereby warranting further research to understand these important resistance factors and their contribution to antimicrobial resistance. While for a nonpathogenic bacterium such as *L. lactis* antibiotic resistance may not be an issue of concern so far, this study opens new avenues for developing biotechnologically proficient strains able to withstand better the presence of bacteriocins or other cationic antimicrobials as lysozyme, currently in use as preservatives in food.

DATA AVAILABILITY STATEMENT

The original contributions presented in the study are included in the article/**Supplementary Material**, and further inquiries can be directed to the corresponding author.

AUTHOR CONTRIBUTIONS

AR and BM conceived and designed the study. AC, ML-G, SE, and BM performed the experiments. AN and TJ contributed with strains and materials. AR and BM wrote the draft manuscript. All authors participated in the interpretation of the results and read and approved the manuscript.

FUNDING

This work was funded by grants BIO2013-46266-R (Ministerio de Economía y Competitividad, Spain) and BIO2017-88147-R (AEI/FEDER, UE). Activities of the DairySafe group at IPLA-CSIC are also supported by IDI/2018/000119 (FEDER funds and program of Science, Technology and Innovation 2018-2020, Principado de Asturias, Spain).

ACKNOWLEDGMENTS

We would like to thank P. López and G. del Solar (CIB-CSIC, Spain) for sharing the plasmid pRCR and also the students Eric Schneider (NCSU, USA) and Celia Álvarez (University of Oviedo, Spain) for their help during their training. We acknowledge support of the publication fee by the CSIC Open Access Publication Support Initiative through its Unit of Information Resources for Research (URICI).

SUPPLEMENTARY MATERIAL

The Supplementary Material for this article can be found online at: https://www.frontiersin.org/articles/10.3389/fmicb.2020.01805/full#supplementary-material.

REFERENCES

Arii, K., Kawada-Matsuo, M., Oogai, Y., Noguchi, K., and Komatsuzawa, H. (2019). Single mutations in BraRS confer high resistance against nisin a in *Staphylococcus aureus*. *Microbiologyopen* 8:e791. doi: 10.1002/mbo3.791

Becker, P., Hakenbeck, R., and Henrich, B. (2009). An ABC transporter of *Streptococcus pneumoniae* involved in susceptibility to vancoresmycin and bacitracin. *Antimicrob. Agents Chemother.* 53, 2034–2041. doi: 10.1128/AAC.01485-08

Bernard, R., Guiseppi, A., Chippaux, M., Foglino, M., and Denizot, F. (2007). Resistance to bacitracin in *Bacillus subtilis*: unexpected requirement of the BceAB ABC transporter in the control of expression of its own structural genes. *J. Bacteriol.* 189, 8636–8642. doi: 10.1128/JB.01132-07

Bolotin, A., Wincker, P., Mauger, S., Jaillon, O., Malarme, K., Weissenbach, J., et al. (2001). The complete genome sequence of the lactic acid bacterium *Lactococcus lactis* ssp. *lactis* IL1403. *Genome Res.* 11, 731–753. doi: 10.1101/gr.GR-1697R

Burgess, C., O'Connell-Motherway, M., Sybesma, W., Hugenholtz, J., and van Sinderen, D. (2004). Riboflavin production in *Lactococcus lactis*: potential for in situ production of vitamin-enriched foods. *Appl. Environ. Microbiol.* 70, 5769–5777. doi: 10.1128/AEM.70.10.5769-5777.2004

Campelo, A. B., Rodriguez, A., and Martinez, B. (2010). Use of green fluorescent protein to monitor cell envelope stress in *Lactococcus lactis*. *Appl. Environ. Microbiol.* 76, 978–981. doi: 10.1128/AEM.02177-09

Collins, B., Curtis, N., Cotter, P. D., Hill, C., and Ross, R. P. (2010). The ABC transporter AnrAB contributes to the innate resistance of *Listeria monocytogenes* to nisin, bacitracin, and various beta-lactam antibiotics. *Antimicrob. Agents Chemother.* 54, 4416–4423. doi: 10.1128/AAC.00503-10

Dintner, S., Heermann, R., Fang, C., Jung, K., and Gebhard, S. (2014). A sensory complex consisting of an ATP-binding cassette transporter and a two-component regulatory system controls bacitracin resistance in *Bacillus subtilis*. *J. Biol. Chem.* 289, 27899–27910. doi: 10.1074/jbc.M114.596221

Dintner, S., Staron, A., Berchtold, E., Petri, T., Mascher, T., and Gebhard, S. (2011). Coevolution of ABC transporters and two-component regulatory systems as resistance modules against antimicrobial peptides in Firmicutes bacteria. *J. Bacteriol.* 193, 3851–3862. doi: 10.1128/JB.05175-11

Du, D., Wang-Kan, X., Neuberger, A., van Veen, H. W., Pos, K. M., Piddock, L. J. V., et al. (2018). Multidrug efflux pumps: structure, function and regulation. *Nat. Rev. Microbiol.* 16, 523–539. doi: 10.1038/s41579-018-0048-6

Falord, M., Karimova, G., Hiron, A., and Msadek, T. (2012). GraXSR proteins interact with the VraFG ABC transporter to form a five-component system required for cationic antimicrobial peptide sensing and resistance in *Staphylococcus aureus*. *Antimicrob. Agents Chemother.* 56, 1047–1058. doi: 10.1128/AAC.05054-11

Fritz, G., Dintner, S., Treichel, N. S., Radeck, J., Gerland, U., Mascher, T., et al. (2015). A new way of sensing: need-based activation of antibiotic resistance by a flux-sensing mechanism. *mBio* 6:e00975. doi: 10.1128/mBio.00975-15

Garay-Novillo, J. N., Garcia-Morena, D., Ruiz-Maso, J. A., Barra, J. L., and Del Solar, G. (2019). Combining modules for versatile and optimal labeling of lactic acid bacteria: two pMV158-family promiscuous replicons, a pneumococcal system for constitutive or inducible gene expression, and two fluorescent proteins. *Front. Microbiol.* 10:1431. doi: 10.3389/fmicb.2019.01431

Gebhard, S. (2012). ABC transporters of antimicrobial peptides in Firmicutes bacteria—phylogeny, function and regulation. *Mol. Microbiol.* 86, 1295–1317. doi: 10.1111/mmi.12078

Grubaugh, D., Regeimbal, J. M., Ghosh, P., Zhou, Y., Lauer, P., Dubensky, T. W. Jr., et al. (2018). The VirAB ABC transporter is required for VirR regulation of *Listeria monocytogenes* virulence and resistance to nisin. *Infect. Immun.* 86, e00901–e00917. doi: 10.1128/IAI.00901-17

Hiron, A., Falord, M., Valle, J., Debarbouille, M., and Msadek, T. (2011). Bacitracin and nisin resistance in *Staphylococcus aureus*: a novel pathway involving the BraS/BraR two-component system (SA2417/SA2418) and both the BraD/BraE and VraD/VraE ABC transporters. *Mol. Microbiol.* 81, 602–622. doi: 10.1111/j.1365-2958.2011.07735.x

Jiang, X., Geng, Y., Ren, S., Yu, T., Li, Y., Liu, G., et al. (2019). The VirAB-VirSR-AnrAB multicomponent system is involved in resistance of *Listeria monocytogenes* EGD-e to cephalosporins, bacitracin, nisin, benzalkonium chloride, and ethidium bromide. *Appl. Environ. Microbiol.* 85, e01470–e01519. doi: 10.1128/AEM.01470-19

Joseph, P., Guiseppi, A., Sorokin, A., and Denizot, F. (2004). Characterization of the *Bacillus subtilis* YxdJ response regulator as the inducer of expression for the cognate ABC transporter YxdLM. *Microbiology* 150, 2609–2617. doi: 10.1099/mic.0.27155-0

Kallenberg, F., Dintner, S., Schmitz, R., and Gebhard, S. (2013). Identification of regions important for resistance and signalling within the antimicrobial peptide transporter BceAB of *Bacillus subtilis*. *J. Bacteriol.* 195, 3287–3297. doi: 10.1128/JB.00419-13

Kawada-Matsuo, M., Yoshida, Y., Nakamura, N., and Komatsuzawa, H. (2011). Role of two-component systems in the resistance of *Staphylococcus aureus* to antibacterial agents. *Virulence* 2, 427–430. doi: 10.4161/viru.2.5.17711

Khosa, S., AlKhatib, Z., and Smits, S. H. (2013). NSR from *Streptococcus agalactiae* confers resistance against nisin and is encoded by a conserved nsr operon. *Biol. Chem.* 394, 1543–1549. doi: 10.1515/hsz-2013-0167

Kobras, C. M., Piepenbreier, H., Emenegger, J., Sim, A., Fritz, G., and Gebhard, S. (2020). BceAB-type antibiotic resistance transporters appear to act by target protection of cell wall synthesis. *Antimicrob. Agents Chemother.* 64, e02241–e02319. doi: 10.1128/AAC.02241-19

Kramer, N. E., van Hijum, S. A., Knol, J., Kok, J., and Kuipers, O. P. (2006). Transcriptome analysis reveals mechanisms by which *Lactococcus lactis* acquires nisin resistance. *Antimicrob. Agents Chemother.* 50, 1753–1761. doi: 10.1128/AAC.50.5.1753-1761.2006

Kuipers, O. P., de Ruyter, P. G. G. A., Kleerebezem, M., and de Vos, W. M. (1998). Quorum sensing-controlled gene expression in lactic acid bacteria. *J. Biotechnol.* 64, 15–21. doi: 10.1016/S0168-1656(98)00100-X

Livak, K. J., and Schmittgen, T. D. (2001). Analysis of relative gene expression data using real-time quantitative PCR and the $2^{-\Delta\Delta CT}$ method. *Methods* 25, 402–408. doi: 10.1006/meth.2001.1262

López-González, M. J., Escobedo, S., Rodríguez, A., Neves, A. R., Janzen, T., and Martínez, B. (2018). Adaptive evolution of industrial *Lactococcus lactis* under cell envelope stress provides phenotypic diversity. *Front. Microbiol.* 9:2654. doi: 10.3389/fmicb.2018.02654

Martínez, B., Böttiger, T., Schneider, T., Rodríguez, A., Sahl, H. G., and Wiedemann, I. (2008). Specific interaction of the unmodified bacteriocin Lactococcin 972 with the cell wall precursor lipid II. *Appl. Environ. Microbiol.* 74, 4666–4670. doi: 10.1128/AEM.00092-08

Martínez, B., Zomer, A. L., Rodríguez, A., Kok, J., and Kuipers, O. P. (2007). Cell envelope stress induced by the bacteriocin Lcn972 is sensed by the lactococcal two-component system CesSR. *Mol. Microbiol.* 64, 473–486. doi: 10.1111/j.1365-2958.2007.05668.x

Mohedano, M. L., García-Cayuela, T., Perez-Ramos, A., Gaiser, R. A., Requena, T., and López, P. (2015). Construction and validation of a mCherry protein vector for promoter analysis in *Lactobacillus acidophilus*. *J. Ind. Microbiol. Biotechnol.* 42, 247–253. doi: 10.1007/s10295-014-1567-4

Piepenbreier, H., Fritz, G., and Gebhard, S. (2017). Transporters as information processors in bacterial signalling pathways. *Mol. Microbiol.* 104, 1–15. doi: 10.1111/mmi.13633

Popella, P., Krauss, S., Ebner, P., Nega, M., Deibert, J., and Gotz, F. (2016). VraH is the third component of the *Staphylococcus aureus* VraDEH system involved in Gallidermin and Daptomycin resistance and pathogenicity. *Antimicrob. Agents Chemother.* 60, 2391–2401. doi: 10.1128/AAC.02865-15

Randall, C. P., Gupta, A., Utley-Drew, B., Lee, S. Y., Morrison-Williams, G., and O'Neill, A. J. (2018). Acquired nisin resistance in *Staphylococcus aureus* involves constitutive activation of an intrinsic peptide antibiotic detoxification module. *mSphere* 3, e00633–e00718. doi: 10.1128/mSphereDirect.00633-18

Reiners, J., Lagedroste, M., Ehlen, K., Leusch, S., Zaschke-Kriesche, J., and Smits, S. H. J. (2017). The N-terminal region of nisin is important for the BceAB-type ABC transporter NsrFP from *Streptococcus agalactiae* COH1. *Front. Microbiol.* 8:1643. doi: 10.3389/fmicb.2017.01643

Revilla-Guarinos, A., Gebhard, S., Mascher, T., and Zuniga, M. (2014). Defence against antimicrobial peptides: different strategies in Firmicutes. *Environ. Microbiol.* 16, 1225–1237. doi: 10.1111/1462-2920.12400

Roces, C., Courtin, P., Kulakauskas, S., Rodríguez, A., Chapot-Chartier, M. P., and Martínez, B. (2012). Isolation of *Lactococcus lactis* mutants simultaneously resistant to the cell wall-active bacteriocin Lcn972, lysozyme, nisin and bacteriophage c2. *Appl. Environ. Microbiol.* 78, 4157–4163. doi: 10.1128/AEM.00795-12

Staron, A., Finkeisen, D. E., and Mascher, T. (2011). Peptide antibiotic sensing and detoxification modules of *Bacillus subtilis*. *Antimicrob. Agents Chemother.* 55, 515–525. doi: 10.1128/AAC.00352-10

Wegmann, U., Klein, J. R., Drumm, I., Kuipers, O. P., and Henrich, B. (1999). Introduction of peptidase genes from *Lactobacillus delbrueckii* subsp. *lactis* into *Lactococcus lactis* and controlled expression. *Appl. Environ. Microbiol.* 65, 4729–4733. doi: 10.1128/AEM.65.11.4729-4733.1999

Conflict of Interest: AN and TJ are employees of Chr. Hansen A/S.

The remaining authors declare that the research was conducted in the absence of any commercial or financial relationships that could be construed as a potential conflict of interest.

frontiers in Microbiology

ORIGINAL RESEARCH
published: 11 September 2020
doi: 10.3389/fmicb.2020.576738

In silico Screening Unveil the Great Potential of Ruminal Bacteria Synthesizing Lasso Peptides

*Yasmin Neves Vieira Sabino[1], Katialaine Corrêa de Araújo[1], Fábia Giovana do Val de Assis[1], Sofia Magalhães Moreira[1], Thaynara da Silva Lopes[1], Tiago Antônio de Oliveira Mendes[2], Sharon Ann Huws[3] and Hilário C. Mantovani[1]**

[1] Departamento de Microbiologia, Universidade Federal de Viçosa, Viçosa, Brazil, [2] Departamento de Bioquímica e Biologia Molecular, Universidade Federal de Viçosa, Viçosa, Brazil, [3] Institute for Global Food Security, School of Biological Sciences, Medical Biology Centre, Queen's University Belfast, Belfast, United Kingdom

Studies of rumen microbial ecology suggest that the capacity to produce antimicrobial peptides could be a useful trait in species competing for ecological niches in the ruminal ecosystem. However, little is known about the synthesis of lasso peptides by ruminal microorganisms. Here we analyzed the distribution and diversity of lasso peptide gene clusters in 425 bacterial genomes from the rumen ecosystem. Genome mining was performed using antiSMASH 5, BAGEL4, and a database of well-known precursor sequences. The genomic context of the biosynthetic clusters was investigated to identify putative *lasA* genes and protein sequences from enzymes of the biosynthetic machinery were evaluated to identify conserved motifs. Metatranscriptome analysis evaluated the expression of the biosynthetic genes in the rumen microbiome. Several incomplete (n = 23) and complete (n = 11) putative lasso peptide clusters were detected in the genomes of ruminal bacteria. The complete gene clusters were exclusively found within the phylum *Firmicutes*, mainly (48%) in strains of the genus *Butyrivibrio*. The analysis of the genetic organization of complete putative lasso peptide clusters revealed the presence of co-occurring genes, including kinases (85%), transcriptional regulators (49%), and glycosyltransferases (36%). Moreover, a conserved pattern of cluster organization was detected between strains of the same genus/species. The maturation enzymes LasB, LasC, and LasD showed regions highly conserved, including the presence of a transglutaminase core in LasB, an asparagine synthetase domain in LasC, and an ABC-type transporter system in LasD. Phylogenetic trees of the essential biosynthetic proteins revealed that sequences split into monophyletic groups according to their shared single common ancestor. Metatranscriptome analyses indicated the expression of the lasso peptides biosynthetic genes within the active rumen microbiota. Overall, our *in silico* screening allowed the discovery of novel biosynthetic gene clusters in the genomes of ruminal bacteria and revealed several strains with the genetic potential to synthesize lasso peptides, suggesting that the ruminal microbiota represents a potential source of these promising peptides.

Keywords: precursor sequence, RiPPs, rumen, *Butyrivibrio*, antiSMASH 5, BAGEL4

OPEN ACCESS

Edited by:
Harsh Mathur,
Teagasc, Ireland

Reviewed by:
Piyush Baindara,
University of Missouri, United States
Takeshi Zendo,
Kyushu University, Japan
Nicholas Heng,
University of Otago, New Zealand

***Correspondence:**
Hilário C. Mantovani
hcm6@ufv.br

Specialty section:
This article was submitted to Antimicrobials, Resistance and Chemotherapy, a section of the journal Frontiers in Microbiology

Received: *26 June 2020*
Accepted: *17 August 2020*
Published: *11 September 2020*

Citation:
Sabino YNV, Araújo KC, Assis FGV, Moreira SM, Lopes TS, Mendes TAO, Huws SA and Mantovani HC (2020) In silico Screening Unveil the Great Potential of Ruminal Bacteria Synthesizing Lasso Peptides. Front. Microbiol. 11:576738. doi: 10.3389/fmicb.2020.576738

INTRODUCTION

Natural products have improved human quality of life and play a noteworthy role in drug discovery and development (Newman and Cragg, 2016). Among natural products, secondary metabolites stand out as scaffolds for the development of products for human medicine, animal health, crop protection, and numerous biotechnological applications (Bachmann et al., 2014). Traditional culture-based strategies for the screening of new molecules have been responsible for the discovery of many relevant enzymes and metabolites (Steele and Stowers, 1991; Winter et al., 2011). However, these approaches are largely driven by chance, making then costly, time-consuming, and often limited regarding the number of strains that can be used in large-scale screening endeavors (Tietz et al., 2017). The advent of microbial genomics and the increasing availability of computational tools to perform genome mining has evidenced the underexplored potential of some microbial species as alternative sources of new therapeutic agents (Winter et al., 2011). These tools and resources emerged as an alternative approach to identify novel biosynthetic gene clusters (BGCs) encoding putative bioactive metabolites and to assess the genetic potential of producer strains (Weber and Kim, 2016). Besides the discovery of new products, genome mining also contributes to understanding the connection between metabolites and the gene sequences that encode them, providing ecological insights about the role of individual microbial populations in the microbiome (Bachmann et al., 2014).

Secondary metabolites could play a diverse role in the environment by their wide range of biological activities. In this context, lasso peptides stand out as functionally diverse metabolites produced by several species of bacteria. Members of the lasso peptide family are reported to have antimicrobial (Salomon and Farías, 1992; Kuznedelov et al., 2011) and anti-viral activities (Frechet et al., 1994; Constantine et al., 1995). These molecules also can show receptor antagonism activities, such as the glucagon receptor antagonist BI-32169 (Potterat et al., 2004; Knappe et al., 2010) or act as enzyme inhibitors (Katahira et al., 1996; Yano et al., 1996). This functional diversity combined with their physicochemical properties makes lasso peptides attractive scaffolds for drug development (Knappe et al., 2011). Moreover, these molecules compose a class of ribosomally synthesized and post-translationally modified peptides (RiPPs), which are suitable for genome mining approaches due to the gene-encoded nature of their precursors (Maksimov and Link, 2014).

The lasso peptides typically contain 16–21 amino acid residues and are defined by their unusual topology, which resembles threaded lassos or slipknots. This peculiar structure is the result of cyclization, which is due to the amide bond between the amino group of an N-terminal Gly/Cys residue and the carboxyl group of a Glu/Asp residue at position 8 or 9 of the mature peptide (Bayro et al., 2003; Rosengren et al., 2003; Maksimov et al., 2012a). This post-translational modification is performed by a protease that shows homology to bacterial transglutaminases (LasB) and by a protein homologous to asparagine synthetase (LasC) (Duquesne et al., 2007a; Severinov et al., 2007). It is assumed that LasC is involved in the activation of the side-chain carboxyl group of the Glu/Asp residue at position 8 or 9, while LasB catalyzes the transfer of ammonia from glutamine to the activated side-chain carboxyl group. Following this, the cleavage of the precursor peptide releases an N-terminal Gly/Cys, and the cyclization takes place by a nucleophilic attack (Larsen et al., 1999; Makarova et al., 1999; Duquesne et al., 2007a; Yan et al., 2012). The gene D is also frequently found on the biosynthetic gene clusters of lasso peptides encoding an ABC transporter that is thought to play a role in immunity of producer cells against the antimicrobial activity of their lasso peptides (Solbiati et al., 1996, 1999; Bountra et al., 2017).

Studies based on genome mining have contributed to identifying new microbial species producing lasso peptides (Knappe et al., 2008; Maksimov et al., 2012b; Tietz et al., 2017). The ruminal ecosystem is composed of microbial communities that show high taxonomic and functional diversity (Morais and Mizrahi, 2019), and although it has been investigated as a source for novel enzymes and antimicrobials (Oyama et al., 2017; Neumann and Suen, 2018; Palevich et al., 2019), the rumen still represents an underexplored environment for the discovery of lasso peptides. Indeed, both culture-dependent and culture-independent approaches have revealed promising antimicrobial peptides from the rumen (Mantovani et al., 2002; Russell and Mantovani, 2002; Azevedo et al., 2015; Oyama et al., 2017, 2019). However, no systematic efforts have been made to investigate the potential of rumen bacteria to produce lasso peptides. The availability of hundreds of reference genomes from cultured ruminal bacteria through the Hungate1000 Project[1], offers an unprecedented opportunity to identify novel lasso peptides within the genomes of ruminal bacteria. The present study set out to perform an *in silico* screening of the genomes of the major bacterial species represented in the core ruminal microbiome in an attempt to identify biosynthetic gene clusters encoding putative lasso peptides. As such, this work aimed to *i*) characterize the distribution of BGCs potentially associated with the production of lasso peptides in the genomes of ruminal bacteria; *ii*) identify sequences of potential novel lasso peptide precursors, *iii*) evaluate the phylogenetic distribution and conservation of the biosynthetic genes/proteins predicted to encode lasso peptides, and *iv*) examine if these biosynthetic genes are expressed by the active rumen microbiota.

MATERIALS AND METHODS

Genomic Data Collection and Prediction of Lasso Peptides Within Rumen Bacterial Genomes

Genome files (.fasta) of 425 ruminal bacteria belonging to the Hungate1000 project (Seshadri et al., 2018) were downloaded from the NCBI (National Center for Biotechnology Information[2] and JGI (Joint Genome Institute[3]) websites (**Supplementary Table 1**).

[1]http://www.rmgnetwork.org/hungate1000.html
[2]http://www.ncbi.nlm.nih.gov/genome
[3]http://genome.jgi.doe.gov

To identify microcin producers, the amino acid sequences of McjA (AAD28494.1), McjB (AAD28495.1), McjC (AGC14226.1), and McjD (AGC14214.1), which are products of the *mcj*ABCD gene cluster, were downloaded from NCBI. A set of 68 lasso peptides previously described in the literature were also screened based on their core sequences (Zyubko et al., 2019) (**Supplementary Table 2**). Screening of these protein-coding genes in genomes of ruminal bacteria was performed by running BLASTx through the command line. The cut-off parameters used to consider positive hits were a minimum sequence identity of 30% and *E*-value $< 10^{-5}$. New putative biosynthetic gene clusters in the genomes of ruminal bacteria were predicted using the web-based genome mining tools of antiSMASH 5 (Blin et al., 2019) and BAGEL4 (van Heel et al., 2018).

The genes belonging to predicted clusters were generically named *lasA*, *lasB*, *lasC*, and *lasD*, corresponding to the following putative gene products: LasA, the lasso peptide precursor; LasB, the leader peptidase, LasC, the lasso cyclase and LasD, the ABC transporter (Arnison et al., 2013).

Distribution of BGCs Encoding Putative Lasso Peptides in the Genomes of Ruminal Bacteria

To verify the distribution of biosynthetic gene clusters encoding putative lasso peptides in the genomes of rumen bacteria, a phylogenetic tree was reconstructed using the 16S rRNA gene sequences from the rumen bacterial genomes analyzed in this study. The sequences were obtained from the Hungate1000 Project and aligned using RDP Release 11.5 aligner of the Ribosomal Database Project website (RDP[4]). The phylogenetic tree was reconstructed using the Approximately Maximum-Likelihood method by FastTree v2.1 (Price et al., 2010). The Interactive Tree of Life (iTOL) interface v4[5] (Letunic and Bork, 2019) was used to visualize and annotate the FastTree output file (.tree).

Genomic Context of the Lasso Peptide Biosynthetic Gene Clusters

When a putative biosynthetic gene cluster was predicted by BAGEL4 and/or antiSMASH 5 but the gene encoding the potential precursor peptide was not identified, the regions located upstream and downstream of the predicted biosynthetic genes were examined, covering a region varying from 4762 bp to 17083 bp in length. This analysis is based on the assumption that genes sharing similar occurrence patterns or located near each other within the genome are likely to be functionally related. For that, genomes were annotated using Prokka v1.12 (Seemann, 2014) (minimum contig size of 200 kb and *E*-value $< 10^{-6}$) through the Galaxy platform and manually inspected to identify sequences potentially encoding the lasso peptide precursor within the genomic context of the biosynthetic machinery minimally required for the production of lasso peptides. A manual analysis of the genes adjacent to the lasso peptide gene cluster was also performed to investigate the presence of co-occurring genes. When proteins were annotated as "hypothetical", BLAST analyses were performed in Uniprot to investigate the protein function using 30% of amino acid sequence similarity as the cut-off parameter.

Characterization of the Biosynthetic Proteins

Conservation Analysis of LasA, LasB, and LasC

Conserved motifs in putative lasso peptide precursors (LasA) and maturation enzymes (LasB, and LasC) were identified using the Batch Web CD-Search tool (Lu et al., 2020). Default parameters were used for the analysis and the results were filtered considering *E*-value $< 10^{-6}$. To analyze if the amino acid sequences of the biosynthetic precursors/proteins (LasA, LasB, and LasC) could be grouped according to the evolutionary history of the major species of bacteria from the rumen microbiome, phylogenetic trees were reconstructed based on the sequences of these proteins. The sequences were aligned using muscle 3.8.31. FastTree v2.1 was used to perform the tree reconstruction and iTOL was used to visualize and annotate the tree as described above. For LasA, the amino acid composition of conserved residues corresponding to the 44 amino acid residues located in the N-terminus of the protein was represented using WebLogo 2.8.2[6] and the default parameters.

Prediction of the LasA Core

Predictions of putative LasA core sequences followed patterns of the distribution of amino acid residues that have been extensively reported in the literature for precursor and mature lasso peptide sequences (Jia Pan et al., 2012; Maksimov et al., 2012a,b; Tietz et al., 2017). The core sequences of the putative lasso peptide precursors were inferred using BAGEL4, antiSMASH 5, and manual analyses of the genomic sequences flanking the putative gene clusters. The presence of glycine (G) at position 1 of the core peptide, followed by an aspartate (D) located at position 8 or 9 were used as criteria indicative of the N-terminal macrolactam ring matching the lasso peptides precursor pattern. The presence of threonine (T) in the leader peptide near the cleavage site was also taken into account, as well as the presence of conserved amino acids at particular positions in the precursor peptides, as indicated by the alignment of putative LasA sequences. All sequences predicted as a putative core of LasA were run through RiPPMiner[7] to confirm cross-links between post-translationally modified residues associated with the formation of a characteristic ring structure in lasso peptides (Agrawal et al., 2017).

Expression of Lasso Peptide Genes in Rumen Metatranscriptomes

The expression of the genes *lasA, lasB,* and *lasC* predicted in the genomes of ruminal bacteria were investigated using different metatranscriptome datasets from the rumen. Sequences

[4]https://rdp.cme.msu.edu/

[5]https://iTOL.embl.de/

[6]https://weblogo.berkeley.edu/logo.cgi

[7]http://www.nii.ac.in/~priyesh/lantipepDB/new_predictions/index.php#/~priyesh/lantipepDB/new_predictions/cyclizationPrediction.php

of fifteen metatranscriptomes were obtained from the sequence read archive (SRA) of NCBI[8] (Leinonen et al., 2011). These datasets included ruminal metatranscriptomes from dairy and beef cattle and sheep, as described in **Supplementary Table 3**.

To evaluate the expression of unique *lasA*, *lasB,* and *lasC* genes, sequences corresponding to these genes but showing more than 50% similarities in a distance matrix calculated using Clustal Omega (Sievers et al., 2011) were eliminated from the downstream analyses. Bowtie-build tool was then used to index the lasso peptide sequences and Bowtie2/2.2.8 (Langmead and Salzberg, 2012) was applied to align the genes and the metatranscriptome datasets. The alignment results were visualized through Tablet software 1.19.09.03 (Milne et al., 2012). The expression levels of *lasA*, *lasB,* and *lasC* were normalized calculating the number of reads per kilobase per million of mapped reads (RPKM) (Mortazavi et al., 2008).

RESULTS

Distribution of Predicted Biosynthetic Gene Clusters of Lasso Peptides in the Species of Ruminal Bacteria

In the current study, we performed data mining in 425 bacterial genomes representing the major species of bacteria from the rumen microbiome in an attempt to identify BGCs potentially associated with the production of lasso peptides. Computational tools were applied to search for sequences in the rumen bacterial genomes with similarities to genes that are known to be associated with the biosynthesis of lasso peptides. *Butyrivibrio proteoclasticus* P18 and *Lachnospiraceae bacterium* NK4A144 harbored a gene encoding a product matching the McjC protein previously characterized in the *mcjABCD* operon (30% as a sequence similarity cut-off and *E*-value $< 10^{-5}$), which is associated with the production of microcin J25. Moreover, mining the rumen bacterial genomes using the core regions of 68 lasso peptide precursors as query sequences revealed that *Actinomyces denticolens* PA and *Bacillus cereus* KPR-7A harbor sequences of core peptides highly similar (>70%) to Ssv-2083 and Paeninodim, respectively.

The BGCs predicted using BAGEL4 and antiSMASH 5 were divided into complete clusters, when containing all the genes considered to be essential (*lasA*, *lasB* and *lasC*) for the biosynthesis machinery required for lasso peptide production, and those which appear to be incomplete gene clusters, containing at least one (but not all) of the genes required for lasso peptide biosynthesis. The genome mining approaches revealed thirty-four ruminal bacterial genomes harboring incomplete or complete biosynthetic gene clusters potentially encoding putative lasso peptides (**Table 1**). The genomes with positive hits belonged mainly to the genera *Butyrivibrio*, of which 14 incomplete clusters and 3 complete clusters were identified out of 53 genomes analyzed. Members of the genus *Lachnospira* sp. ($n = 5$) harbored 3 incomplete and 2 complete biosynthetic gene clusters. Biosynthetic clusters containing all the essential genes for lasso peptide biosynthesis were also identified in the genomes of ruminal *Bacillus* sp. ($n = 3$), while other genera of ruminal bacteria, such as *Acetitomaculum*, *Actinomyces*, *Clostridium*, *Eubacterium*, and *Ruminococcus* presented clusters in lower abundance or the number of available genomes was too few to allow inferences about the abundance of putative lasso peptide gene clusters (**Supplementary Figure S1**).

The number of genes and biosynthetic clusters that were predicted in the ruminal bacterial genomes varied according to the computational tool used to screen for the lasso peptides (**Figure 1**). In total, BAGEL4 predicted putative lasso peptide biosynthetic gene clusters in 109 ruminal bacterial genomes. However, the majority of these genomes (75%) harbored only putative additional genes and genes with no predicted function. These additional genes were identified by BAGEL4 as encoding modification proteins such as GlyS, a glycosyltransferase; regulatory proteins such as LanK, a sensor histidine kinase, and LanR, a transcriptional regulator; immunity/transport proteins such as ABC transporter and transport/leader cleavage proteins as LanT. BAGEL4 also predicted putative coding regions showing similarity to the Ref90 clusters, including kinases and acetyltransferases, in addition to genes with no predicted function (**Figure 1**). The genes required for lasso peptide production were identified in 27 rumen bacterial genomes using BAGEL4, however, only incomplete gene clusters were detected using BAGEL4 as no *lasB* gene was identified within these genomes using this computational tool (**Table 1**). Predictions of BGCs using antiSMASH 5 indicated gene clusters likely to encode lasso peptides in 33 ruminal bacterial genomes with all harboring at least *lasA*, *lasB,* or *lasC*. In 27 (82%) of these genomes, the gene *lasD* was also detected. These *in silico* screening approaches combined identified complete lasso peptide gene clusters in 11 rumen bacterial genomes, of which three were harbored by members of the genera *Bacillus*, *Butyrivibrio* and *Lachnospira,* and two in strains of the genus *Ruminococcus* (**Table 1**). These results show a higher prevalence and diversity of lasso peptides gene clusters within the *Firmicutes* phylum, mainly among members of the *Lachnospiraceae* family (**Figure 1**).

Identification of Lasso Peptide Precursors in the Genomic Regions Surrounding the Biosynthetic Gene Clusters

BAGEL4 and/or antiSMASH 5 were effective to predict coding sequences homologous to the enzymes of the lasso peptide maturation pathway (LasB and LasC). However, the prediction of precursor sequences (LasA) was limited using these computational tools due to the inherent features of these peptides, such as their short length and sequence variability. We therefore investigated the genomic context of the gene clusters aiming to identify potential coding sequences containing the expected features of a lasso peptide precursor. This pattern-based search for novel lasso peptide precursors increased the number of rumen bacterial genomes harboring complete gene clusters to 33, including *Acetitomaculum ruminis* DSM 5522, *Eubacterium*

[8]https://www.ncbi.nlm.nih.gov/sra

TABLE 1 | Ruminal bacterial genomes harboring genes and gene clusters encoding putative lasso peptides predicted by BAGEL4 and antiSMASH 5.

Genomes[1]	BAGEL4				antiSMASH 5			
	lasA	***lasB***	***lasC***	***lasD***	***lasA***	***lasB***	***lasC***	***lasD***
Acetitomaculum ruminis DSM 5522	0	0	1	1	0	1	1	1
Actinomyces denticolens PA	1	0	1	1	0	0	0	0
***Bacillus cereus* KPR-7A**	0	0	0	0	1	1	1	1
***Bacillus licheniformis* VTM3R78**	0	0	1	1	1	1	1	1
***Bacillus* sp. MB2021**	0	0	1	1	1	1	1	1
***Butyrivibrio fibrisolvens* AB2020**	1	0	1	0	0	1	1	1
Butyrivibrio fibrisolvens AR40	0	0	1	0	0	1	1	0
***Butyrivibrio fibrisolvens* DSM 3071**	0	0	1	0	1	1	1	1
Butyrivibrio fibrisolvens MD2001	0	0	0	1	0	1	1	1
Butyrivibrio fibrisolvens WTE3004	0	0	1	0	0	1	1	1
Butyrivibrio fibrisolvens YRB2005	0	0	1	0	0	1	1	1
Butyrivibrio proteoclasticus B316	0	0	1	1	0	1	1	1
Butyrivibrio proteoclasticus FD2007	0	0	1	1	0	1	1	1
Butyrivibrio sp. FC2001	0	0	1	0	0	1	1	0
Butyrivibrio sp. INlla14	0	0	0	0	0	1	1	1
Butyrivibrio sp. MC2021	0	0	1	1	0	1	1	1
Butyrivibrio sp. NC3005	0	0	1	1	0	1	1	1
***Butyrivibrio* sp. VCD2006**	0	0	1	1	1	1	1	0
Butyrivibrio sp. XBB1001	0	0	1	1	0	1	1	1
Butyrivibrio sp. XPD2006	0	0	1	0	0	1	1	1
Butyrivibrio sp. YAB3001	0	0	1	1	0	1	1	1
Clostridium beijerinckii HUN142	0	0	1	0	0	1	1	1
Clostridium butyricum AGR2140	0	0	1	1	0	1	1	1
Eubacterium celullosolvens LD2006	0	0	0	0	0	1	1	0
***Lachnospira multipara* D15d**	0	0	1	1	1	1	1	1
Lachnospira multipara LB2003	0	0	1	1	0	1	1	1
***Lachnospira multipara* MC2003**	0	0	1	1	1	1	1	1
***Lachnospira multipara* ATCC 19207**	0	0	0	0	1	1	1	1
Lachnospira pectinoschiza M83	0	0	1	1	0	1	1	1
Lachnospiraceae bacterium KH1P17	0	0	0	0	0	1	1	0
Lachnospiraceae bacterium MA2020	0	0	1	1	0	1	1	1
Lachnospiraceae bacterium YSD2013	0	0	1	0	0	1	1	0
***Ruminococcus albus* 8**	0	0	0	0	1	1	1	1
***Ruminococcus flavefaciens* ATCC 19208**	1	0	0	1	1	1	1	1

[1] *Genomes in bold harbored all the essential biosynthetic genes (lasA, lasB, and lasC) required for lasso peptide production detected by using either BAGEL4 or antiSMASH 5. Number 1 represents the presence of a gene while "0" represents the absence of a gene.*

cellulosolvens LD2006, two species of *Clostridium*, two species of *Lachnospira*, three strains of *Lachnospiraceae bacterium* and 13 strains of *Butyrivibrio*.

The genomes of *Butyrivibrio* sp. NC3005, *Butyrivibrio* sp. YAB3001, *Lachnospira multipara* LB2003, *Lachnospira pectinoschiza* M83, and *Lachnospiraceae bacterium* YSD2013 showed more than one sequence with homology to the *lasA* gene and careful examination of all 33 rumen bacterial genomes also indicated distinct sequences in the putative biosynthetic clusters that were likely to encode a lasso peptide precursor in *Butyrivibrio* sp. AB2020. Additionally, different *lasA* sequences were predicted in the genome of *Ruminococcus flavefaciens* 19208 by BAGEL4 and antiSMASH 5. The putative LasA proteins predicted for all the rumen bacterial genomes harboring complete lasso peptides gene cluster are reported in **Supplementary Table 4**.

Expanding the genomic context analysis beyond the identification of *lasA* indicated that these biosynthetic clusters have a conserved pattern of genetic organization among groups of phylogenetically related organisms (**Figure 2**). Alignment of the lasso peptide gene clusters found in *Butyrivibrio fibrisolvens* indicated that these clusters contain additional genes such as nucleotidyltransferase, HPr kinase/phosphorylase, glycosyltransferase family 2 and EpsH, the sensor histidine kinase ResE and the transcriptional regulatory protein WalR. Other strains of *Butyrivibrio* sp. and *Butyrivibrio proteoclasticus* showed clusters containing the sensor protein kinase WalK, the transcriptional regulator SrrA, and the HPr kinase/phosphorylase, in addition to the essential biosynthetic genes. The lasso peptide gene cluster in strains of *Lachnospira* shared the serine kinase of the HPr protein and the sensor

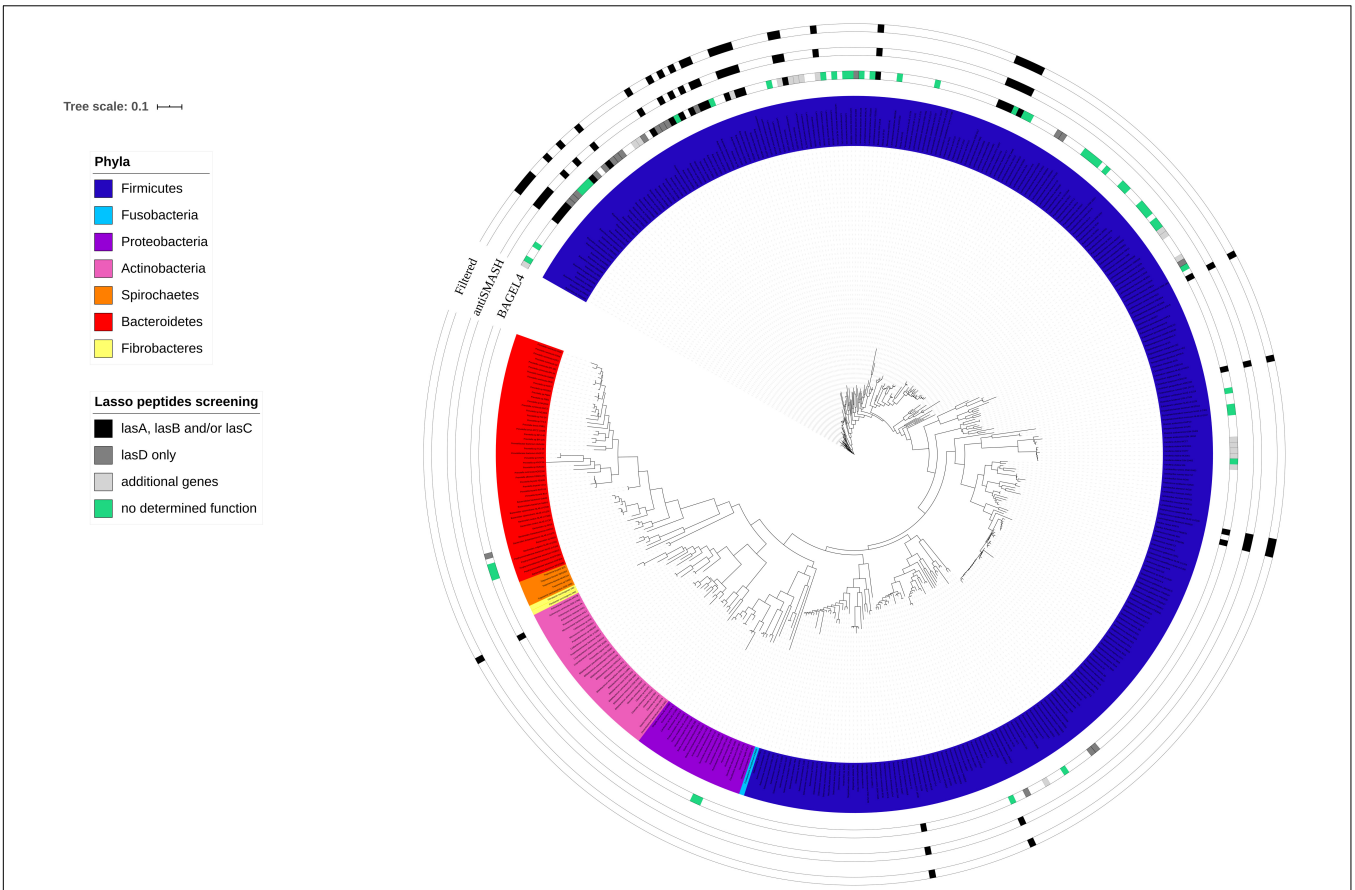

FIGURE 1 | Distribution of predicted genes and gene clusters encoding putative lasso peptides in ruminal bacterial genomes superimposed to the 16S rRNA phylogenetic tree. The colored innermost circle represents the bacterial phyla analyzed in this study. Squared boxes outside the phylogenetic tree show the lasso peptide genes within the ruminal bacterial genomes predicted by BAGEL4 and antiSMASH 5. Filtered genomes contain at least one of the essential biosynthetic genes (*lasA, lasB,* and *lasC*) required for lasso peptide production. The sequences of the 16S rRNA gene were obtained from the Hungate1000 database. The alignment was performed in RDP and the tree was reconstructed using FastTree 2.1 (Maximum Likelihood, 1000 replicates). Features shown in the figure were added using iTOL annotation.

histidine kinase WalK, besides the putative genes encoding LasA, LasB, LasC, and LasD proteins.

Among the species of ruminal bacteria, the HPr kinase/phosphorylase, coenzyme PQQ synthesis protein D (PqqD), and an uncharacterized nucleotidyltransferase were found in approximately 58%, 46% and 30% of the genomes analyzed in this study, respectively (**Supplementary Figure 2**). Moreover, different proteins showing similar functional annotations were found within the lasso peptide gene clusters among these bacterial genomes, including the sensory proteins ResE and WalK, serine kinases, transcriptional regulators (WalR and SrrA) and glycosyltransferases (EpsH) (**Supplementary Figure 2**).

Sequence Conservation Analysis of the Putative Lasso Peptide Proteins LasA, LasB, and LasC

Analysis of conserved elements in the lasso peptide biosynthesis machinery included LasA-like precursor peptides and proteins homologous to the lasso peptide maturation enzymes (LasB, LasC, and LasD). No conserved motifs were identified in the putative LasA amino acid sequences predicted in the genomes of ruminal bacteria analyzed in this study, indicating that these residues are hypervariable and therefore, subjected to neutral drift. However, genome mining enabled the identification of conserved motifs in homologs of the lasso peptide maturation enzymes LasB, LasC, and LasD, with variable frequency (**Table 2**). Two conserved motifs were identified in the LasB homologs, including a transglut_core3 motif of the transglutaminase-like superfamily, which is involved in the formation of lasso peptide amide crosslink and was found in 97% of the analyzed LasB proteins. Also, a MdlB motif of an ATPase and permease component of the ABC-type multidrug transport system was detected in the LasB homolog found in the genomes of *Ruminococcus albus* 8 and *Ruminococcus flavefaciens* ATCC 19208. In these genomes, the *lasB* gene appears to be fused with another gene encoding a transporter protein. The MdlB motif was also found in 87% of the LasD homologs predicted in the genomes of ruminal bacteria analyzed in this study, together

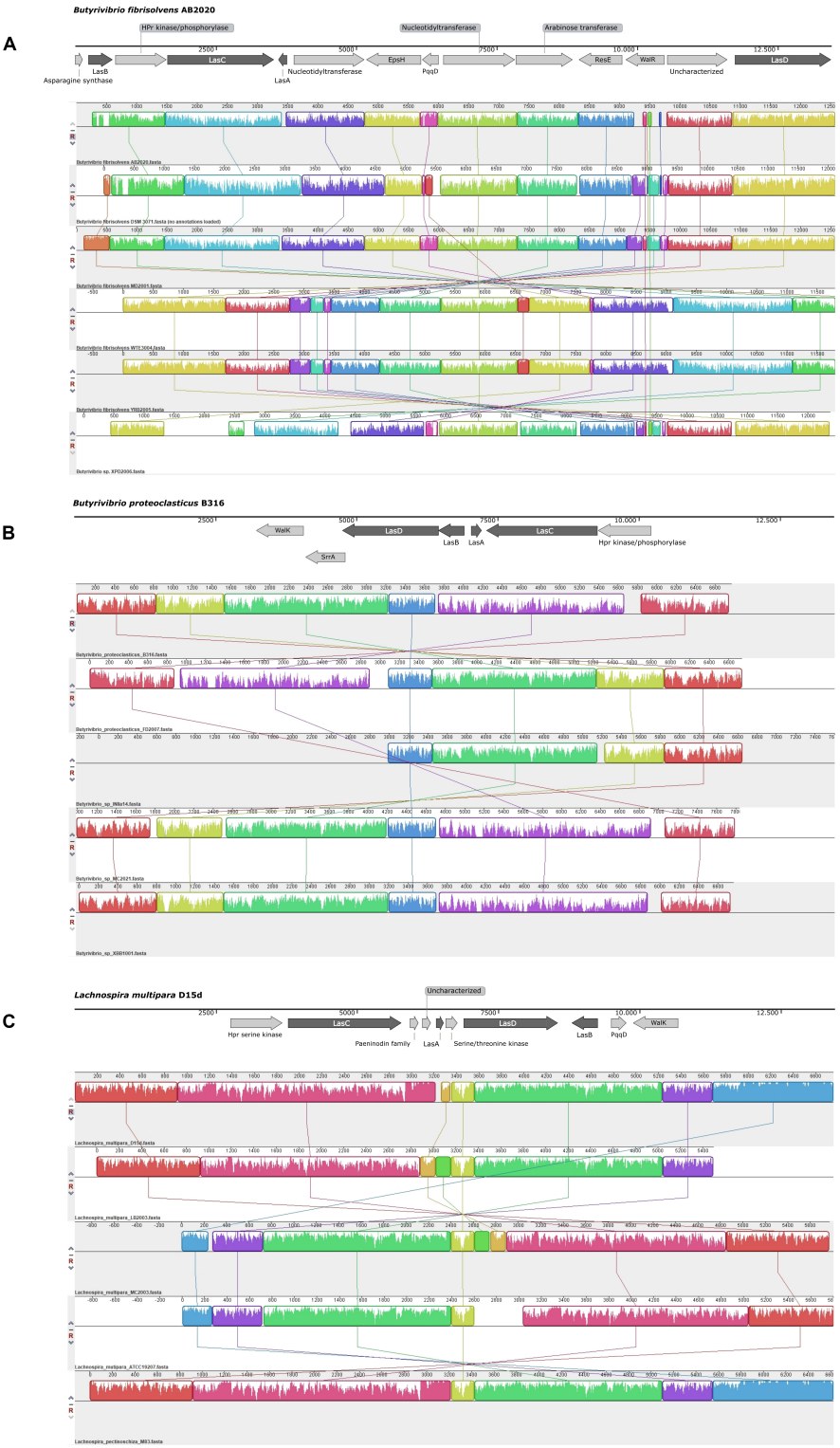

FIGURE 2 | Schematic representation of the putative lasso peptide gene clusters and their conserved genomic context in strains of *Butyrivibrio* [Panels **(A)** and **(B)**] and *Lachnospira* [Panel **(C)**]. Two groups of putative lasso peptide gene clusters are observed in *Butyrivibrio*: Panel **(A)** shows the larger biosynthetic cluster, identified in *Butyrivibrio fibrisolvens*, while Panel **(B)** shows the genetic organization of the conserved lasso peptide clusters in the genomes of *Butyrivibrio proteoclasticus* and unclassified *Butyrivibrio* strains. When the biosynthetic cluster was identified in the reverse DNA strand, the alignment blocks are shown in the opposite direction. The genomic regions containing the biosynthetic gene clusters were aligned using Mauve version 20150226 and the representation of the genomic context was generated using SnapGene 5.0.8.

TABLE 2 | Conserved motifs in lasso peptide maturation enzymes (LasB, LasC, and LasD) predicted in the genomes of ruminal bacteria.

Protein	Conserved motifs	Accession	Frequency	Coverage (%)
LasB	Transglut_core3	pfam13471	97%	45–100
	MdlB	COG1132	6%	100
LasC	AANH_like superfamily	cl00292	6%	100
	asn_synth_AEB superfamily	cl36928	74%	41–100
	Asn_Synthase_B_C	cd01991	18%	100
	AsnB	cd00712	6%	100
	AsnB superfamily	cl33852	6%	57–60
	Gn_AT_II superfamily	cl00319	15%	73–100
LasD	ABC_ATPase superfamily	cl25403	10%	98–100
	GlnQ	COG1126	3%	100
	HisM	COG0765	3%	100
	MdlB	COG1132	87%	89–100
	SunT superfamily	cl34455	3%	33
	UgpA	COG1175	3%	91

with five other domains of different ABC-type transporters occurring at much lower abundances. Six motifs were found in the LasC homologs, most of which belong to a conserved protein domain family (asn_synth_AEB superfamily) of the glutamine-hydrolyzing asparagine synthases.

Phylogenetic analysis of the predicted LasA precursor peptides grouped the sequences in three phylogroups each consisting of a different number of nodes (**Figure 3A**). The precursor peptides predicted in the genomes of most *Butyrivibrio* strains and all members of the genus *Lachnospira* analyzed in this study could be separated into three main distinct coherent clades. Sequences of lasso peptide precursors in the genomes of the genus *Ruminococcus* also generated a smaller and consistent clade within these phylogroups, while other sequences were spread throughout the phylogenetic tree. Although the overall amino acid sequence conservation was relatively low, residues located at positions 20–45 and 60–70 in the putative precursor peptides appeared with higher frequencies compared to other regions of the peptide (**Figure 3A**). As shown for the genomes of *Butyrivibrio* and *Lachnospira*, the 20–45 region contains a moderately to highly conserved glycine (G) residue spaced 8–9 positions away from an aspartate (D) residue, which are expected to form an isopeptide bond that installs the macrolactam into the N-terminus of the core peptide (**Figures 3B,C**). The glycine residue is also preceded at position 17 by a highly conserved threonine (T) residue that is often reported as an invariant residue present at the end of the leader peptides of lasso precursors (Knappe et al., 2009; Jia Pan et al., 2012; Hegemann et al., 2013a, 2014). Therefore, this pattern of conserved elements in the precursor sequences matches the chemical/structural properties that have been described for known lasso peptides, confirming their essential role in lasso peptide function and thereby ensuring the reliability of our outputs.

Phylogenetic analysis of the proteins predicted as homologous of the lasso peptide maturation enzymes demonstrated that amino acid sequences of the LasB and LasC proteins belonging to the genera *Butyrivibrio*, *Lachnospira*, and *Ruminococcus* split into distinct phylogroups within the genomes of ruminal bacteria (**Figures 4**, **5**). Also, sequences of the associated maturation enzymes appeared to be more conserved among the strains of *Butyrivibrio fibrisolvens* and *Lachnospira multipara*. The larger distancing of the LasB sequences observed in the clade containing members of the genus *Ruminococcus* is likely because these protein sequences are fused to a transporter protein.

Prediction of Putative Lasso Peptide Precursors in the Genomes of Ruminal Bacteria

Combining our sequence conservation analysis of the putative lasso peptide precursors (LasA) with the requirement of specific residues distributed at particular positions in the amino acid sequences of the mature lasso peptides allowed the identification of novel sequences that were likely to be precursor hits in the genomes of ruminal bacteria. In total, thirty-five LasA-like precursors were predicted in 29 genomes of ruminal bacteria investigated in the current study (**Table 3**). In *Butyrivibrio* sp. NC3005, *Butyrivibrio* sp. YAB3001, *Lachnospira multipara* LB2003, *Lachnospira pectinoschiza* M83, *Lachnospiraceae bacterium* YSD2013 and *Ruminococcus flavefaciens* ATCC 19208, at least two distinct LasA precursors were predicted in each genome. The predicted core peptide sequences indicated that the N-terminal isopeptide-bonded ring is likely to occur between a glycine residue (G) at position + 1 of the core and an aspartate residue (D) positioned 8–9 aa from the beginning of the core. Also, an invariant threonine residue (T) that has been indicated as a recognition element for the lasso peptide maturation enzymes was found at the end of the predicted leader peptide (position -3 from the start of the core). Our analysis also revealed that most of the identified LasA candidates present a highly conserved serine (S) residue in their C-terminal region. The length of the putative core peptide sequences varied from 21 to 42 amino acid residues, according to the sizes of their respective gene coding sequences (**Table 3**).

Expression Analysis of Putative Lasso Peptides Biosynthetic Genes in Ruminal Metatranscriptome Datasets

Expression of the putative lasso peptide precursors and associated maturation enzymes were generally low in the ruminal metatranscriptome datasets, varying from 0.01 to 4.26 reads per kilobase per million of mapped reads (RPKM). Nonetheles, the expression levels differed between the genes *lasA*, *lasB,* and *lasC* and the number of mapped reads also varied among the datasets of beef cattle, dairy cattle, and sheep examined in the current study. Overall, only reads corresponding to the genes *lasA, lasB,* and *lasC* of *Ruminococcus albus* 8 were represented simultaneously in at least two datasets under study (SRR873462 and SRR873454).

The gene *lasC* showed the highest number of reads mapping to a putative lasso peptide biosynthetic gene within the active ruminal microbial community, being detected in 13 out of the 15 datasets (**Figure 6C**). Only reads mapping to the *lasC* gene of *Lachnospira multipara* D15d, *Clostridium butyricum*

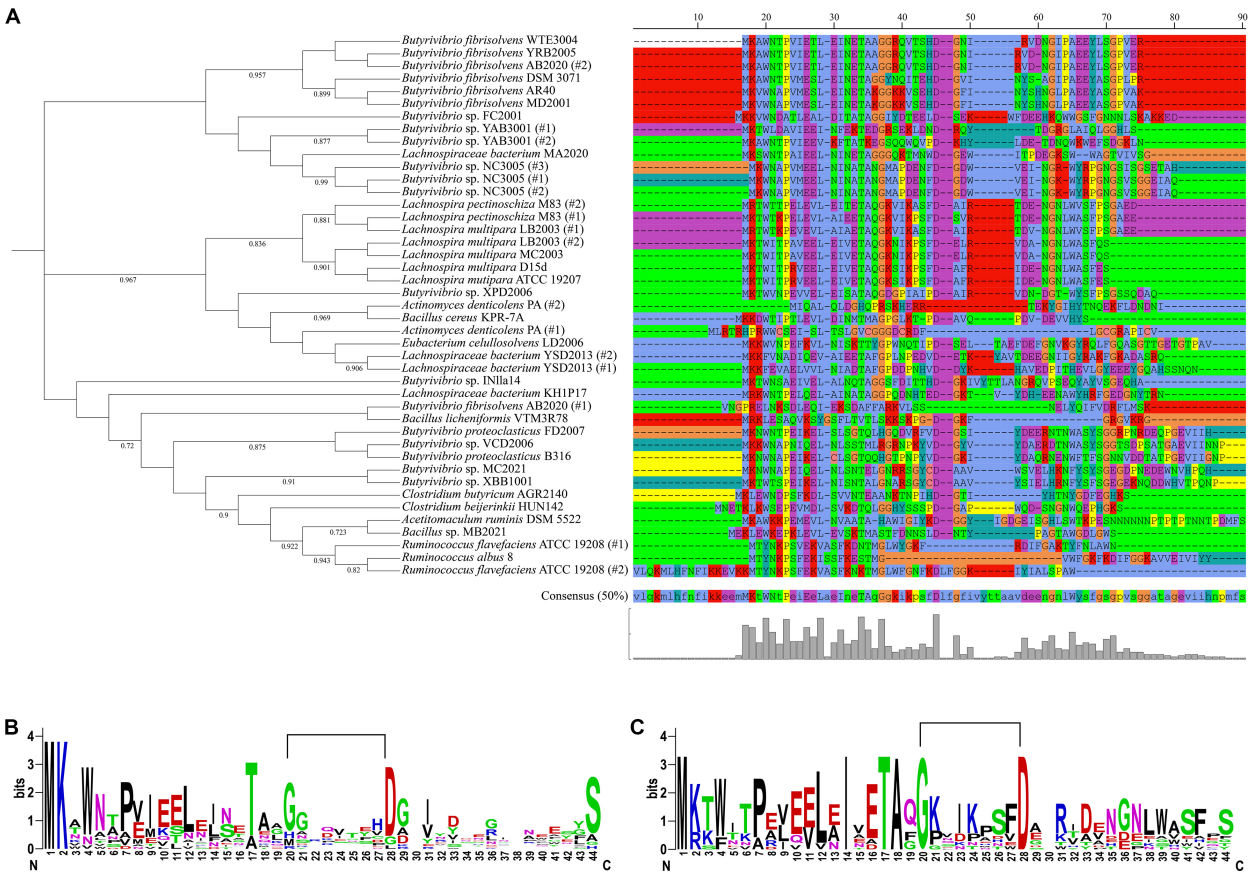

FIGURE 3 | Phylogenetic and sequence conservation analysis of LasA-like precursors predicted in the genomes of ruminal bacteria. **(A)** Phylogenetic tree of the LasA-like peptides showing the amino acid sequences of each putative lasso peptide precursor. Sequences were aligned using muscle 3.8.31 and the phylogenetic tree was reconstructed using FastTree 2.1 (Maximum Likelihood, 1000 replicates). Annotation was performed using iTOL. Only bootstrap values greater than 70% are shown at the nodal branches. **(B)** and **(C)** show web logos of the putative LasA amino acid sequences predicted in genomes of the genera *Butyrivibrio* (n = 20) and *Lachnospira* (n = 7), respectively. The lines connecting the conserved glycine (G) and aspartate (D) residues in the lasso peptides precursor indicate the predicted location of the characteristic N-terminal macrolactam ring of the mature peptide.

AGR2140, and *Ruminococcus albus* 8 were represented in the rumen of beef cattle, while for dairy cattle datasets, the mapped reads represented the *lasC* gene found in *Butyrivibrio proteoclasticus* B316, *Lachnospira multipara* D15d, and two species of *Clostridium*. The *lasC* gene also appears to be more broadly expressed in the ruminal metatranscriptomes of sheep, as reads of the genes that were found in eight bacterial genomes mapped to at least one out of the five datasets analyzed. Moreover, the expression of the *lasC* gene found in *Clostridium butyricum* ARG2140 and *Lachnospira multipara* D15d occurred across all the dataset groups (beef cattle, dairy cattle, and sheep) evaluated in the current study.

Reads mapping to the predicted *lasA* genes showed higher average RPKM values among the metatranscriptomes evaluated in the current study (**Figure 6A**). The highest RPKM value (4.26) was observed for reads mapping to the *lasA* sequences of *Butyrivibrio proteoclasticus* B316 in a beef cattle metatranscriptome. Only *lasA* reads from *Butyrivibrio* sp. XPD2006 and *Lachnospiraceae bacterium* YSD2013 (#1) were aligned to the dairy cattle metatranscriptomes. In the active ruminal microbial community of sheep, reads representing the *lasA* sequences of *Lachnospira multipara* D15d and *Ruminococcus albus* 8 mapped to two and three of the datasets under study, respectively.

Among the essential genes of the lasso peptide biosynthesis machinery, the genes corresponding to the maturation enzyme *lasB* were the least expressed across all the ruminal datasets examined in the current study. Only the reads corresponding to the *lasB* gene of *Bacillus* sp. MB2021 and *Ruminococcus albus* 8 could be mapped to a ruminal metatranscriptome, with the majority of the sequences aligned in the dairy cattle and sheep datasets (**Figure 6B**).

DISCUSSION

Lasso peptides represent a group of ribosomally synthesized and post-translationally modified peptides (RiPPs) with unique topology and diverse biological activities. The discovery of new lasso peptides may be hindered by the great sequence

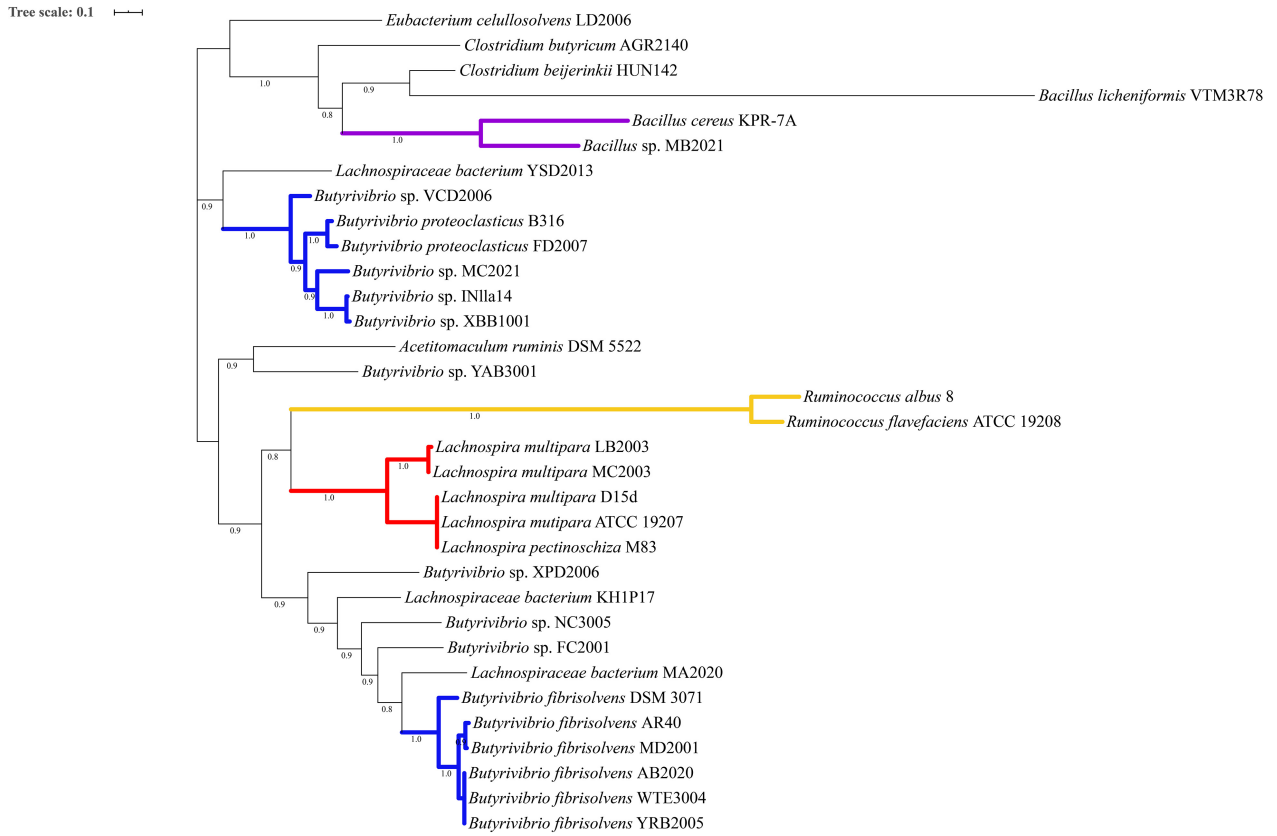

FIGURE 4 | Phylogenetic tree showing putative LasB proteins predicted in the genomes of ruminal bacteria. Colored clades represent members of particular genera or species sharing a single common ancestor. Protein sequences were predicted by antiSMASH 5 and aligned using muscle 3.8.31. The phylogenetic tree was reconstructed using FastTree 2.1 (Maximum Likelihood, 1000 replicates). Tree annotation was performed using iTOL. Only bootstrap values greater than 70% are shown at the nodal branches.

variation of these molecules. Previously, we applied genome mining approaches to explore the ruminal environment as a potential source of bacteriocins (Azevedo et al., 2015), and non-ribosomal peptides and polyketides (Moreira et al., 2020). Here, we performed an extensive *in silico* screen in publically available genomes of ruminal bacteria in an attempt to determine the prevalence and diversity of lasso peptides among major species of bacteria from the rumen. Additionally, we sought out to predict potentially novel lasso peptides in the genomes of different members of the rumen microbiome, thus guiding the future identification and characterization of these antimicrobial peptides in ruminal bacteria through *in vitro* studies.

The genetic screening using antiSMASH 5 and BAGEL4 revealed putative clusters for lasso peptides biosynthesis in 34 ruminal bacterial genomes, representing 8% of the total analyzed. From these, only 11 genomes presented clusters harboring all the essential genes of the biosynthesis machinery of lasso peptides, while in the other genomes the biosynthetic clusters were incomplete. However, after manually curating the genomic context of the incomplete gene clusters, thirty-three rumen bacterial genomes were found harboring complete lasso peptide clusters, confirming the limitations of using homology search tools to identify these biosynthetic genes through automated mining of complete and draft genomes. It should be emphasized, however, that both antiSMASH 5 and BAGEL4 are valuable tools for analyzing and identifying biosynthetic gene clusters in microbial genomes due to their intrinsic processivity, which allows fast screening of multiple datasets of genomic sequences. Nonetheless, computational tools may be limited by inherent constraints of their search algorithms, representativeness of the databases, and by singularities of the lasso peptide gene clusters, such as their small sizes and hypervariability of the precursor gene sequences (Tietz et al., 2017). Therefore, the examination of the genomic context flanking the essential genes may be a useful approach to refine pattern-based genome mining.

Lasso peptide production has been mainly associated with members of the phyla *Actinobacteria* and *Proteobacteria* and the best-studied molecules of this family are produced by representative species within these phyla (Weber et al., 1991; Salomon and Farías, 1992; Helynck et al., 1993; Potterat et al., 1994; Tsunakawa et al., 1995; Kimura et al., 1997; Knappe et al., 2008; Hegemann et al., 2013a). Moreover, genome-guided studies focused on natural product discovery often point to these bacterial phyla as promising sources of lasso peptides (Severinov et al., 2007; Hegemann et al., 2013b;

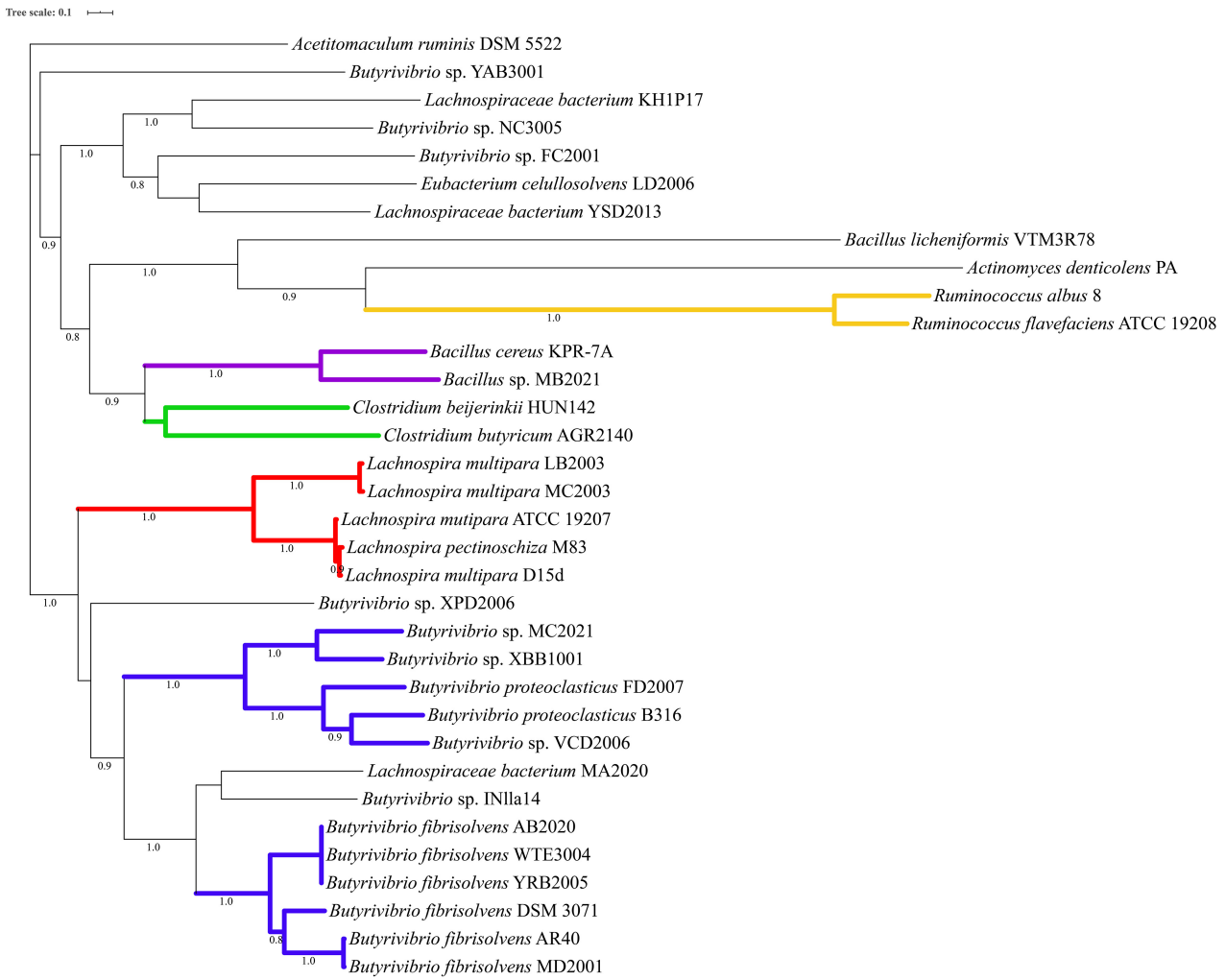

FIGURE 5 | Phylogenetic tree showing putative LasC proteins predicted in the genomes of ruminal bacteria. Colored clades represent members of particular genera or species sharing a single common ancestor. Protein sequences were predicted by antiSMASH 5 and aligned using muscle 3.8.31. The phylogenetic tree was reconstructed using FastTree 2.1 (Maximum Likelihood, 1000 replicates). Tree annotation was performed using iTOL. Only bootstrap values greater than 70% are shown at the nodal branches.

Maksimov and Link, 2014). However, our results indicate that genera of the phylum *Firmicutes* are probably the main producers of lasso peptides in the rumen environment, revealing these taxa as potential sources of new lasso peptides. These results are in agreement with a genome-guided exploration of the GenBank database, which highlighted the phyla *Firmicutes*, *Cyanobacteria*, *Euryarchaeota*, and *Bacteroidetes* as underexplored sources of lasso peptides (Tietz et al., 2017). The higher prevalence of lasso peptide gene clusters within the phylum *Firmicutes* reported in this study must take into account the abundance of sequenced genomes compared to other phyla of ruminal bacteria. Nonetheless, the presence of complete biosynthetic clusters observed in multiple strains of the phylum *Firmicutes* may increase the interest in exploring members of these taxa to accelerate the discovery of new bioactive molecules through *in silico* analyses and *in vitro* experimentation.

Analyses of the genomic context allowed the identification of additional co-occurring genes frequently found associated with the lasso peptide biosynthetic gene clusters, such as kinases, glycosyltransferases, and nucleotidyltransferases (Duquesne et al., 2007b; Tietz et al., 2017; Zyubko et al., 2019). These co-occurring genes provide additional evidence of the probable functionality of the gene clusters identified in the rumen bacterial genomes and their association with the essential biosynthesis genes appears to be characteristic among species of the phylum *Firmicutes* (Zhu et al., 2016c). Some of the additional genes flanking the biosynthetic clusters encode tailoring enzymes that introduce chemical modifications to the lasso peptides, including covalent modifications in their C-terminal region, such as phosphorylation (Zhu et al., 2016c), methylation (Gavrish et al., 2014) or acetylation (Zong et al., 2018). For example, HPr kinases found in *Paenibacillus dendritiformis* C454 are capable of modifying a C−terminal Ser in the lasso

TABLE 3 | Amino acid sequences of putative lasso peptide precursors predicted in the genomes of ruminal bacteria.

Genome	Predicted leader peptide	Predicted core peptide	Core lenght
Bacillus cereus KPR-7A	MKKDWTIPTLEVLDINM**T**MA	**G**PGLKTP**D**AVQPDVDEVVHY**S**	21
Butyrivibrio fibrisolvens AB2020	MKAWNTPVIETLEINE**T**AA	**G**GRQVTSH**D**GNIRVDNGIPAEEYL**S**GPVER	29
Butyrivibrio fibrisolvens AR40	MKVWNAPVMESLEINE**T**AK	**G**GKKVSEH**D**GFINYSHNGLPAEEYA**S**GPVAK	31
Butyrivibrio fibrisolvens DSM 3071	MKAWNTPVMESLEINE**T**AG	**G**YNQITEH**D**GVINYSAGIPAEEYA**S**GPLPR	30
Butyrivibrio fibrisolvens MD2001	MKVWNAPVMESLEINE**T**AK	**G**GKKVSEH**D**GFINYSHNGLPAEEYA**S**GPVAK	31
Butyrivibrio fibrisolvens WTE3004	MKAWNTPVIETLEINE**T**AA	**G**GRQVTSH**D**GNIRVDNGIPAEEYL**S**GPVER	30
Butyrivibrio fibrisolvens YRB2005	MKAWNTPVIETLEINE**T**AA	**G**GRQVTSH**D**GNIRVDNGIPAEEYL**S**GPVER	30
Butyrivibrio proteoclasticus B316	MKNWNAPEIKELCLSG**T**QQH	**G**TPNPYV**D**GKIYDAQRNENWFTF**S**GNNVDDTATPGEVIIGNP	42
Butyrivibrio proteoclasticus FD2007	MKNWNTPEIKELSLSG**T**QLH	**G**QDVRFV**D**GSIYDEERNTNWASY**S**GGRPNRDEQPGEVIIH	40
Butyrivibrio sp. FC2001	MKKVWNDATLEALDITA**T**AG	**G**IYDTEEL**D**SEKWFDEEHKQWWG**S**FGNNNLSKAKKED	37
Butyrivibrio sp. INlla14	MKTWNSAEIVELALNQ**T**AG	**G**SFDITTH**D**GKIVYTTLANGRQVP**S**EQYAYVSGEQHA	37
Butyrivibrio sp. MC2021	MKNWNAPEIQELNLSN**T**EL	**G**NRRSGYC**D**AAVWSVELHKNFYSY**S**GEGDPNEDEWNVHPQH	41
Butyrivibrio sp. NC3005 (#1, #2)	MKWNAPVMEELNINA**T**AN	**G**MAPDENF**D**GDWVEINGKWYRPGNG**S**VSGGEIAQ	34
Butyrivibrio sp. NC3005 (#3)	MKWNAPVMEELNINA**T**AN	**G**MAPDENF**D**GDWVEINGRWYRPGNG**S**ISGSETAH	34
Butyrivibrio sp. VCD2006	MKKWNAPNIQELNLSS**T**MLR	**G**RNPKYV**D**GYVYDAERDTNWASY**S**GGTSDPSATGAEVIINNP	42
Butyrivibrio sp. XBB1001	MKTWTSPEIKELNISN**T**AL	**G**NARSGYC**D**AAVYSIELHRNFYSF**S**GEGEKNQDDWHVTPQNP	42
Butyrivibrio sp. XPD2006	MKTWVNPEVVELEISA**T**AQ	**G**DGPIAIP**D**AIRVDNDGTWYSFPSG**SS**QDAQ	31
Butyrivibrio sp. YAB3001 (#1)	MKTWLDAVIEEINFEK**T**ED	**G**RSEKLDN**D**RQYTDGRGLAIQLGGHL**S**	27
Butyrivibrio sp. YAB3001 (#2)	MKAWNTPVIEEVKFTA**T**KE	**G**SQQWQVP**D**KHYLDETDNQWKWEF**S**DGKLN	30
Clostridium beijerinkii HUN142	MNETKLKWSEPEVMDLSVKD**T**QL	**G**GHYSSSP**D**GAPWQDSNGNWQEPHGK**S**	18
Eubacterium celullosolvens LD2006	MKKWVNPEFKVLNISK**T**TY	**G**PWNQTIP**D**SELTAEFDEFGNVKGYRQLFGQASGTTGETGTPAV	44
Lachnospira multipara D15d	MKTWITPRVEELEIVE**T**AQ	**G**KSIKPSF**D**AFRIDENGNLWASFE**S**	25
Lachnospira multipara LB2003 (#1)	MRTWTKPEVEVLAIAE**T**AQ	**G**KVIKASF**D**AIRTDVNGNLWVSFP**S**GAEE	28
Lachnospira multipara LB2003 (#2)	MKTWITPAVEELEIVE**T**AQ	**G**KNIKPSF**D**ELRVDANGNLWASFQ**S**	25
Lachnospira multipara MC2003	MKTWITPAVEELEIVE**T**AQ	**G**KNIKPSF**D**ELRVDANGNLWASFQ**S**	25
Lachnospira multipara ATCC 19207	MKTWITPRVEELEIVE**T**AQ	**G**KSIKPSF**D**AFRIDENGNLWASFE**S**	25
Lachnospira pectinoschiza M83 (#1)	MKTWTKPELEVLAIEE**T**AQ	**G**KVIKPSF**D**SVRTDENGNLWASFP**S**GAEE	29
Lachnospira pectinoschiza M83 (#2)	MRTWTTPELEVLEITE**T**AQ	**G**KVIKASF**D**AIRTDENGNLWVSFP**S**GAED	29
Lachnospiraceae bacterium KH1P17	MRKWNTPELQELAINA**T**AG	**G**PQDNHTE**D**GKTVYDHEENAWYHRFGEDGNYTRN	34
Lachnospiraceae bacterium MA2020	MKSWNTPAIEELNINE**T**AG	**G**GQKTMNW**D**GEWITPDEGK**S**WWAGTVIV**S**G	30
Lachnospiraceae bacterium YSD2013 (#1)	MKKFEVAELVVLNIAD**T**AF	**G**PDDPNHVD**D**YKHAVEDPITHEVLGYEEEYGQAH**SS**NQN	39
Lachnospiraceae bacterium YSD2013 (#2)	MKKFVNADIQEVAIEE**T**AF	**G**PLNPEDV**D**ETKYAVTDEEGNIIGYRAKFGKADA**S**RQ	37
Ruminococcus albus 8	MTYNKPSFEKISSFKES**T**M	**G**VWFGKFK**D**IFGGKAVVEIVIYY	23
Ruminococcus flavefaciens ATCC 19208 (#1)	MTYNKPSVEKVASFKDN**T**M	**G**LWYGKFR**D**IFGAKTYFNLAWN	22
Ruminococcus flavefaciens ATCC 19208 (#2)	MTYNKPSFEKVASFKNK**T**M	**G**LWFGNFK**D**LFGGKIYIAL**S**PAW	23

The precursor peptides are composed by the leader peptide + core peptide. Letters in bold represent conserved amino acid residues in the leader and core peptides involved in the maturation or post-translational modification of the lasso peptides. Numbers inside brackets were added when more than one LasA sequence were found in the same genome.

peptide precursor by adding one or more phosphate groups (Zhu et al., 2016b,c). In *Bacillus pseudomycoides* DSM 12442, producer of pseudomycoidin, the presence of the PsmN, a nucleotidyltransferase, was associated with the glycosylation of the C-terminal region (Zyubko et al., 2019). The advantages that these chemical modifications offer to the lasso peptides remains unclear, but they may affect peptide stability (Zyubko et al., 2019), regulate critical processes, such as signaling pathways (Zhu et al., 2016b) or influence the functioning of self-immunity systems in the producer cells (Zhu et al., 2016c; Zong et al., 2018).

A gene encoding a protein belonging to the PqqD enzyme superfamily frequently co-occurred with the lasso peptide biosynthesis genes in species of the genera *Butyrivibrio* and *Lachnospira*. It has been previously reported that the maturation enzyme B can be split between two separate open reading frames (proteins B1 and B2), and this genetic configuration seems a common feature in the lasso peptide gene clusters found in Gram-positive bacteria (Maksimov and Link, 2014; Cheung et al., 2016). Protein B1 is annotated as a homolog of the PqqD enzyme superfamily (Zhu et al., 2016a; Sumida et al., 2019), and acts as a RiPP recognition element that binds the leader peptide and delivers the precursor for processing, while protein B2 is homologous to the transglutaminases and is responsible for the processing of the precursor peptide.

The predicted products of the putative biosynthetic genes detected by antiSMASH 5 and BAGEL4 were subjected to motif analysis and results demonstrated that the LasB homologs found in the rumen bacterial genomes harbor conserved motifs of the transglutaminases family, while the predicted LasC homologs contain consensus motifs of the asparagine

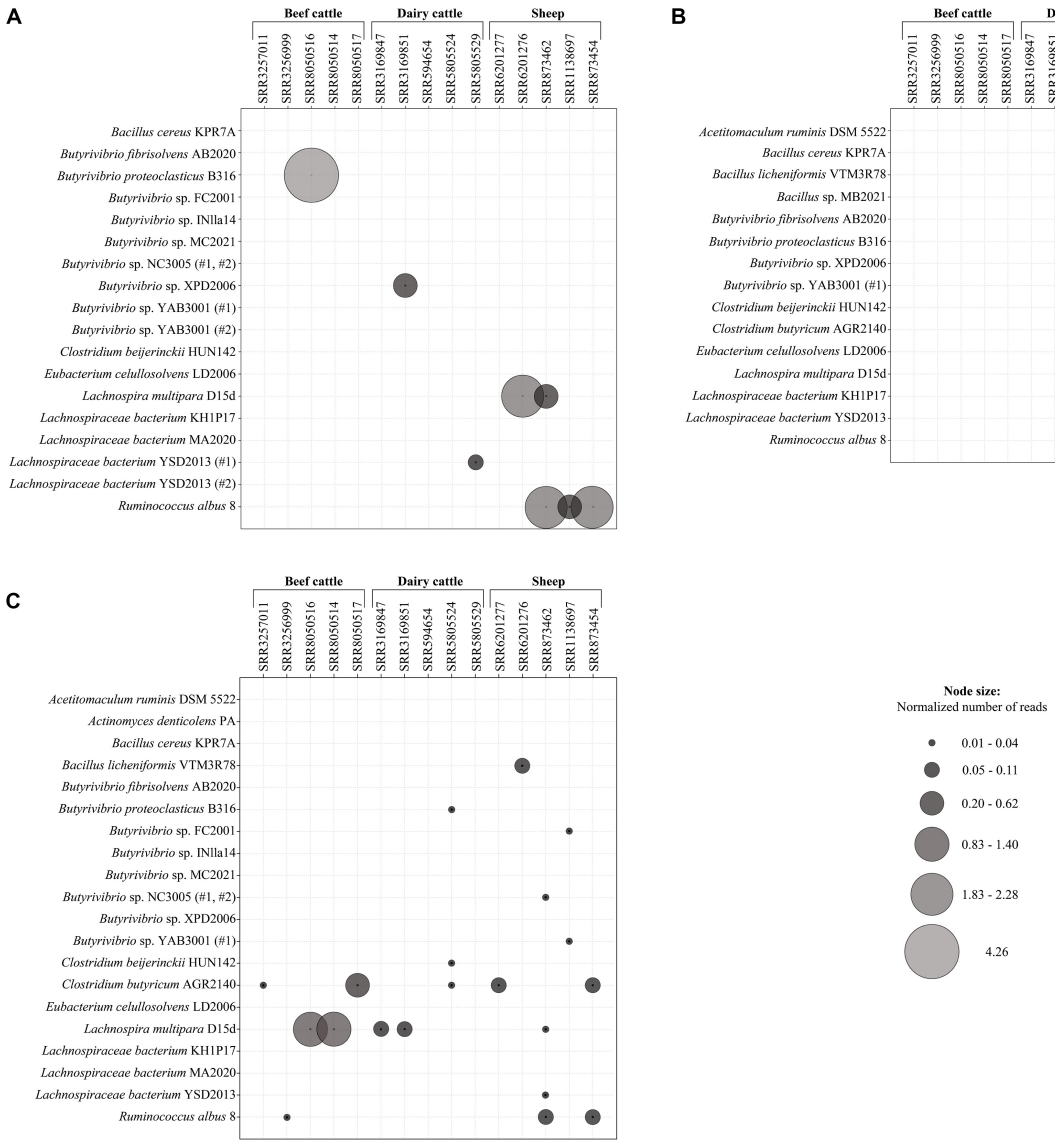

FIGURE 6 | Expression of putative *lasA* **(A)**, *lasB* **(B)**, and *lasC* **(C)** genes in different rumen metatranscriptomes. Node sizes represent the relative abundance of reads (expressed as RPKM) mapped to the corresponding bacterial genome in each dataset. The ruminal metatranscriptomes of dairy cattle, beef cattle, and sheep were obtained from the sequence read archive (SRA) in NCBI. The analyses were performed using Bowtie and the alignment was visualized in the software Tablet 1.19.09.03.

synthetase family. These analyses are in agreement with the genome mining data and provide evidence for the presence of conserved catalytic domains on the enzymes of the lasso peptide maturation pathway. The transglutaminases belong to a large family of cysteine proteases capable of catalyzing the formation of amide crosslinks (Makarova et al., 1999). These enzymes contain the Cys-His-Asp catalytic triad in their active site, which is conserved among the McjB and McjB-like proteins from various bacteria (Duquesne et al., 2007a). Evidence of this catalytic triad was also found on the LasB homologs predicted in the genomes of rumen bacteria investigated in the current study, being particularly conserved in species of *Butyrivibrio* (**Supplementary Figure 3**). In the species of *Ruminococcus*, the LasB homologs contained a fused ABC-transporter domain, a feature that has been previously described for other maturation enzymes of this group (Maksimov and Link, 2014; Tietz et al., 2017).

The phylogenetic analysis of the putative proteins encoded by the *lasA*, *lasB,* and *lasC* genes revealed monophyletic branches composed of strains of the same genera/species. Additionally, the genomic context analysis indicated that the lasso peptide clusters of phylogenetic-related bacteria show the same patterns of genetic organization and considerable conservation of the biosynthetic genes, suggesting that the lasso peptide biosynthetic genes can be inherited vertically, as proposed previously (Tietz et al., 2017).

Determination of putative *lasA* genes can be performed screening short ORFs flanking the biosynthetic genes and considering the requirement of specific amino acids at particular positions of the peptide precursor for the macrolactam ring formation (Knappe et al., 2008; Hegemann et al., 2013a). Besides, our pattern-based genome mining considered the high conservation of the amino acids involved in the amide bond and the genomic context conservation of the lasso peptide clusters. It has been demonstrated that despite the high sequence variation within the structural gene *lasA*, the amino acids that are involved in the formation of the macrolactam ring are conserved across different species of bacteria (Hegemann et al., 2013a; Zhu et al., 2016c). The presence of a conserved threonine residue near the cleavage site of the leader peptide may be required for the recognition and binding of the protease, which seems a crucial event for the effective processing of some lasso peptides precursors (Knappe et al., 2009; Jia Pan et al., 2012; Hegemann et al., 2013a, 2014). Phylogenetic analysis of the LasA sequences found in ruminal bacterial genomes confirmed the conservation of these nearly invariant amino acid residues providing further evidence that they may be related to the lasso peptide function even though some of the sequences were larger than expected. Moreover, phylogenetic analysis of known lasso peptides and the core peptide sequences described in the current study (**Supplementary Figure 4**) reinforces the novelty of the LasA-like sequences discovered in the genomes of ruminal bacteria, since the sequences diverged from a common ancestor when compared to the clades that grouped other lasso peptide families.

Some of the bacteria identified in the current study carrying a putative gene cluster for lasso peptide production are also potential producers of other antimicrobial compounds. For example, *Ruminococcus albus* 8 produces an antagonistic thermostable substance capable of inhibiting *Ruminococcus flavefaciens* (Odenyo et al., 1994). In addition, two gene clusters of sactipeptides and one cluster of a class III bacteriocin were found *in Ruminococcus albus* 8 (Azevedo et al., 2015). Bacteriocin gene clusters were also identified in the genomes of *Butyrivibrio fibrisolvens* MD2001, *Butyrivibrio proteoclasticus* B316, *Butyrivibrio proteoclasticus* FD2007, and *Lachnospira multipara* MC2003 (Azevedo et al., 2015), while genes associated with the biosynthesis of non-ribosomal peptides (NRP) and polyketides (PK) were reported in the genomes of *Bacillus cereus* KPR-7A and *Clostridium beijerinckii* HUN142 (Moreira et al., 2020). Altogether, the presence of gene clusters encoding for distinct classes of antimicrobial compounds in ruminal bacteria suggest the importance of these molecules in the rumen ecosystem and highlight their potential applications in controlling undesirable bacteria.

The genes considered essential to lasso peptide biosynthesis showed a low level of expression in the ruminal metatranscriptome datasets and were more expressed within the microbial community of the sheep rumen, which is in agreement with our previous observations indicating that non-ribosomal peptide synthetases (NRPS) and polyketide synthases (PKS) were also more abundant in the rumen microbiota of sheep (Moreira et al., 2020). Additionally, the reads corresponding to the genes found in *Butyrivibrio* sp., *Lachnospira* sp., and *Ruminococcus* sp. were most represented in the sheep metatranscriptomes, also confirming previous observations showing a higher prevalence of NRPS and PKS within members of these ruminal taxa (Moreira et al., 2020). Taken together, these results demonstrate the potential production of antimicrobial compounds by species of bacteria colonizing the rumen of sheep, which deserves further investigation.

The metatranscriptome analysis also revealed differences in the expression level of the essential lasso peptide biosynthetic genes (*lasA*, *lasB,* and *lasC*). Reads mapping simultaneously to all three essential genes was only observed for *Ruminococcus albus* 8 in two datasets from sheep, indicating that in these microbial communities complete biosynthesis machinery could be generated for lasso peptide production. Overall, reads mapping to the putative LasA precursors were more abundant than reads mapping to the maturation enzymes LasB and LasC. These differences may be due to regulation at transcriptional level controlling the gene expression, differences in RNA stability, or other mechanisms that are known to affect the biosynthesis of antimicrobial peptides and other natural products (Hindre et al., 2004; Trmcic et al., 2011).

The genome mining of lasso peptide biosynthetic clusters in genomes of ruminal bacteria confirmed that *in silico* screening is a fast, effective, and less expensive approach for discovery of these antimicrobial peptides. However, future research should further develop and confirm these initial findings through experiments designed to validate *in vitro* the production of lasso peptides by ruminal bacteria or heterologous expression of the predicted lasso peptides and to demonstrate their biological activity. Nonetheless, these computational analyses allow to narrow down substantially the genera/species potentially producing lasso peptides in the rumen ecosystem, thus guiding future culture-based efforts. Besides, the peptides predicted in the genomes of ruminal bacteria can serve as scaffolds to develop derivatives with improved antimicrobial activity, stability to proteases and lower cytotoxicity (Pan et al., 2010; Soudy et al., 2012), through chemical synthesis or heterologous expression without the need of culturing the producer organism. Overall, our results reveal that ruminal bacteria harbor the genetic arsenal necessary for the production of several not yet described lasso peptides. The discovery of new peptides from ruminal bacteria reinforces the potential of the rumen microbiome as an important source of secondary metabolites that require future characterization.

DATA AVAILABILITY STATEMENT

The datasets presented in this study can be found in online repositories. The names of the repository/repositories and accession number(s) can be found in the article/**Supplementary Material**.

AUTHOR CONTRIBUTIONS

HM, FA, SH, and TM conceived the project. YS, KA, TL, FA, TM, and SM performed the data analysis and interpretation of results under the supervision of HM. YS, KA, and HM wrote the manuscript. All authors read and approved the final manuscript.

FUNDING

This work has been supported by the Coordenação de Aperfeiçoamento de Pessoal de Nível Superior (CAPES; Brasília, Brazil, Proex PPGMBA/UFV, Grant Number 0001), Fundação de Amparo a Pesquisa do Estado de Minas Gerais (FAPEMIG; Belo Horizonte, Brazil), and the Conselho Nacional de Desenvolvimento Científico e Tecnológico (CNPq; Brasília, Brazil). We also thank the RCUK Newton Institutional Link Funding (172629373) and the INCT Ciência Animal.

SUPPLEMENTARY MATERIAL

The Supplementary Material for this article can be found online at: https://www.frontiersin.org/articles/10.3389/fmicb.2020.576738/full#supplementary-material

REFERENCES

Agrawal, P., Khater, S., Gupta, M., Sain, N., and Mohanty, D. (2017). RiPPMiner: a bioinformatics resource for deciphering chemical structures of RiPPs based on prediction of cleavage and cross-links. *Nucleic Acids Res.* 45, W80–W88. doi: 10.1093/nar/gkx408

Arnison, P. G., Bibb, M. J., Bierbaum, G., Bowers, A. A., Bugni, T. S., Bulaj, G., et al. (2013). Ribosomally synthesized and post-translationally modified peptide natural products: overview and recommendations for a universal nomenclature. *Nat. Prod. Rep.* 30, 108–160. doi: 10.1039/c2np20085f

Azevedo, A. C., Bento, C. B. P., Ruiz, J. C., Queiroz, M. V., and Mantovani, H. C. (2015). Distribution and genetic diversity of bacteriocin gene clusters in rumen microbial genomes. *Appl. Environ. Microbiol.* 81, 7290–7304. doi: 10.1128/AEM.01223-15

Bachmann, B. O., Van Lanen, S. G., and Baltz, R. H. (2014). Microbial genome mining for accelerated natural products discovery: is a renaissance in the making? *J. Ind. Microbiol. Biotechnol.* 41, 175–184. doi: 10.1007/s10295-013-1389-9

Bayro, M. J., Mukhopadhyay, J., Swapna, G. V. T., Huang, J. Y., Ma, L.-C., Sineva, E., et al. (2003). Structure of antibacterial peptide microcin J25: a 21-Residue lariat protoknot. *J. Am. Chem. Soc.* 125, 12382–12383. doi: 10.1021/ja036677e

Blin, K., Shaw, S., Steinke, K., Villebro, R., Ziemert, N., Lee, S. Y., et al. (2019). antiSMASH 5.0: updates to the secondary metabolite genome mining pipeline. *Nucleic Acids Res.* 47, W81–W87. doi: 10.1093/nar/gkz310

Bountra, K., Hagelueken, G., Choudhury, H. G., Corradi, V., El Omari, K., Wagner, A., et al. (2017). Structural basis for antibacterial peptide self-immunity by the bacterial ABC transporter McjD. *Embo J.* 36, 3062–3079. doi: 10.15252/embj.201797278

Cheung, W. L., Chen, M. Y., Maksimov, M. O., and Link, A. J. (2016). Lasso peptide biosynthetic protein larb1 binds both leader and core peptide regions of the precursor protein LarA. *ACS Cent. Sci.* 2, 702–709. doi: 10.1021/acscentsci.6b00184

Constantine, K. L., Friedrichs, M. S., Detlefsen, D., Nishio, M., Tsunakawa, M., Furumai, T., et al. (1995). High-resolution solution structure of siamycin II: novel amphipathic character of a 21-residue peptide that inhibits HIV fusion. *J. Biomol. NMR* 5, 271–286. doi: 10.1007/BF00211754

Duquesne, S., Destoumieux-Garzón, D., Zirah, S., Goulard, C., Peduzzi, J., and Rebuffat, S. (2007a). Two enzymes catalyze the maturation of a lasso peptide in *Escherichia coli*. *Chem. Biol.* 14, 793–803. doi: 10.1016/j.chembiol.2007.06.004

Duquesne, S., Petit, V., Peduzzi, J., and Rebuffat, S. (2007b). Structural and functional diversity of microcins, gene-encoded antibacterial peptides from enterobacteria. *J. Mol. Microbiol. Biotechnol.* 13, 200–209. doi: 10.1159/000104748

Frechet, D., Guitton, J. D., Herman, F., Faucher, D., Helynck, G., Monegier du Sorbier, B., et al. (1994). Solution structure of RP 71955, a new 21 amino acid tricyclic peptide active against HIV-1 virus. *Biochemistry* 33, 42–50. doi: 10.1021/bi00167a006

Gavrish, E., Sit, Clarissa, S., Cao, S., Kandror, O., Spoering, A., et al. (2014). Lassomycin, a ribosomally synthesized cyclic peptide, kills mycobacterium tuberculosis by targeting the ATP-Dependent Protease ClpC1P1P2. *Chem. Biol.* 21, 509–518. doi: 10.1016/j.chembiol.2014.01.014

Hegemann, J. D., Zimmermann, M., Xie, X., and Marahiel, M. A. (2013a). Caulosegnins I–III: a highly diverse group of lasso peptides derived from a single biosynthetic gene cluster. *J. Am. Chem. Soc.* 135, 210–222. doi: 10.1021/ja308173b

Hegemann, J. D., Zimmermann, M., Zhu, S., Klug, D., and Marahiel, M. A. (2013b). Lasso peptides from *proteobacteria*: genome mining employing heterologous expression and mass spectrometry. *Pep. Sci.* 100, 527–542. doi: 10.1002/bip.22326

Hegemann, J. D., Zimmermann, M., Zhu, S., Steuber, H., Harms, K., Xie, X., et al. (2014). Xanthomonins I–III: a new class of lasso peptides with a seven-residue macrolactam ring. *Angew. Chem. Int. Ed.* 53, 2230–2234. doi: 10.1002/anie.201309267

Helynck, G., Dubertret, C., Mayaux, J.-F., and Leboul, J. (1993). Isolation of RP 71955, a new anti-HIV-1 peptide secondary metabolite. *J. Antibiot.* 46, 1756–1757. doi: 10.7164/antibiotics.46.1756

Hindre, T., Le Pennec, J. P., Haras, D., and Dufour, A. (2004). Regulation of lantibiotic lacticin 481 production at the transcriptional level by acid pH. *FEMS Microbiol. Lett.* 231, 291–298. doi: 10.1016/S0378-1097(04)00010-2

Jia Pan, S., Rajniak, J., Maksimov, O. M., and James Link, A. (2012). The role of a conserved threonine residue in the leader peptide of lasso peptide precursors. *ChemComm.* 48, 1880–1882. doi: 10.1039/c2cc17211a

Katahira, R., Yamasaki, M., Matsuda, Y., and Yoshida, M. (1996). MS-271, A novel inhibitor of calmodulin-activated myosin light chain kinase from Streptomyces sp.—II. Solution structure of MS-271: characteristic features of the 'lasso' structure. *Bioorg. Med. Chem.* 4, 121–129. doi: 10.1016/0968-0896(95)00176-X

Kimura, K.-I., Kanou, F., Takahashi, H., Esumi, Y., Uramoto, M., and Yoshihama, M. (1997). Propeptin, a new inhibitor of prolyl endopeptidase produced by microbispora. I. Fermentation, isolation and biological properties. *J. Antibiot.* 50, 373–378. doi: 10.7164/antibiotics.50.373

Knappe, T. A., Linne, U., Robbel, L., and Marahiel, M. A. (2009). Insights into the biosynthesis and stability of the lasso peptide capistruin. *Chem. Biol.* 16, 1290–1298. doi: 10.1016/j.chembiol.2009.11.009

Knappe, T. A., Linne, U., Xie, X., and Marahiel, M. A. (2010). The glucagon receptor antagonist BI-32169 constitutes a new class of lasso peptides. *FEBS Lett.* 584, 785–789. doi: 10.1016/j.febslet.2009.12.046

Knappe, T. A., Linne, U., Zirah, S., Rebuffat, S., Xie, X., and Marahiel, M. A. (2008). Isolation and structural characterization of capistruin, a lasso peptide predicted from the genome sequence of *Burkholderia thailandensis* E264. *J. Am. Chem. Soc.* 130, 11446–11454. doi: 10.1021/ja802966g

Knappe, T. A., Manzenrieder, F., Mas-Moruno, C., Linne, U., Sasse, F., Kessler, H., et al. (2011). Introducing lasso peptides as molecular scaffolds for drug design: engineering of an integrin antagonist. *Angew. Chem. Int. Ed.* 50, 8714–8717. doi: 10.1002/anie.201102190

Kuznedelov, K., Semenova, E., Knappe, T. A., Mukhamedyarov, D., Srivastava, A., Chatterjee, S., et al. (2011). The antibacterial threaded-lasso peptide capistruin inhibits bacterial RNA polymerase. *J. Mol. Biol.* 412, 842–848. doi: 10.1016/j.jmb.2011.02.060

Langmead, B., and Salzberg, S. L. (2012). Fast gapped-read alignment with Bowtie 2. *Nat. Methods* 9, 357–359. doi: 10.1038/nmeth.1923

Larsen, T. M., Boehlein, S. K., Schuster, S. M., Richards, N. G. J., Thoden, J. B., Holden, H. M., et al. (1999). Three-dimensional structure of *Escherichia coli*

asparagine synthetase B: a short journey from substrate to product. *Biochemistry* 38, 16146–16157. doi: 10.1021/bi9915768

Leinonen, R., Sugawara, H., Shumway, M., and International Nucleotide Sequence Database (2011). The sequence read archive. *Nucleic Acids Res.* 39, D19–D21. doi: 10.1093/nar/gkq1019

Letunic, I., and Bork, P. (2019). Interactive tree of life (iTOL) v4: recent updates and new developments. *Nucleic Acids Res.* 47, W256–W259. doi: 10.1093/nar/gkz239

Lu, S., Wang, J., Chitsaz, F., Derbyshire, M. K., Geer, R. C., Gonzales, N. R., et al. (2020). CDD/SPARCLE: the conserved domain database in 2020. *Nucleic Acids Res.* 48, D265–D268. doi: 10.1093/nar/gkz991

Makarova, K. S., Aravind, L., and Koonin, E. V. (1999). A superfamily of archaeal, bacterial, and eukaryotic proteins homologous to animal transglutaminases. *Protein Sci.* 8, 1714–1719. doi: 10.1110/ps.8.8.1714

Maksimov, M. O., and Link, A. J. (2014). Prospecting genomes for lasso peptides. *J. Ind. Microbiol. Biotechnol.* 41, 333–344. doi: 10.1007/s10295-013-1357-4

Maksimov, M. O., Pan, S. J., and Link, A. J. (2012a). Lasso peptides: structure, function, biosynthesis, and engineering. *Nat. Prod. Rep.* 29, 996–1006. doi: 10.1039/c2np20070h

Maksimov, M. O., Pelczer, I., and Link, A. J. (2012b). Precursor-centric genome-mining approach for lasso peptide discovery. *Proc. Natl. Acad. Sci. U.S.A.* 109, 15223–15228. doi: 10.1073/pnas.1208978109

Mantovani, H. C., Hu, H., Worobo, R. W., and Russell, J. B. (2002). Bovicin HC5, a bacteriocin from *Streptococcus bovis* HC5. *Microbiology* 148(Pt 11), 3347–3352. doi: 10.1099/00221287-148-11-3347

Milne, I., Stephen, G., Bayer, M., Cock, P. J., Pritchard, L., Cardle, L., et al. (2012). Using Tablet for visual exploration of second-generation sequencing data. *Brief. Bioinform.* 14, 193–202. doi: 10.1093/bib/bbs012

Morais, S., and Mizrahi, I. (2019). The road not taken: the rumen microbiome, functional groups, and community states. *Trends Microbiol.* 27, 538–549. doi: 10.1016/j.tim.2018.12.011

Moreira, S. M., de Oliveira Mendes, T. A., Santanta, M. F., Huws, S. A., Creevey, C. J., and Mantovani, H. C. (2020). Genomic and gene expression evidence of nonribosomal peptide and polyketide production among ruminal bacteria: a potential role in niche colonization? *FEMS Microbiol. Ecol.* 96:fiz198. doi: 10.1093/femsec/fiz198

Mortazavi, A., Williams, B. A., McCue, K., Schaeffer, L., and Wold, B. (2008). Mapping and quantifying mammalian transcriptomes by RNA-Seq. *Nat. Methods* 5, 621–628. doi: 10.1038/nmeth.1226

Neumann, A. P., and Suen, G. (2018). The phylogenomic diversity of herbivore-associated fibrobacter spp. Is Correlated to Lignocellulose-Degrading Potential. *mSphere* 3:e00593-18. doi: 10.1128/mSphere.00593-18

Newman, D. J., and Cragg, G. M. (2016). Natural products as sources of new drugs from 1981 to 2014. *J. Nat. Prod.* 79, 629–661. doi: 10.1021/acs.jnatprod.5b01055

Odenyo, A. A., Mackie, R. I., Stahl, D. A., and White, B. A. (1994). The use of 16S rRNA-targeted oligonucleotide probes to study competition between ruminal fibrolytic bacteria: development of probes for Ruminococcus species and evidence for bacteriocin production. *Appl. Environ. Microb.* 60, 3688–3696. doi: 10.1128/aem.60.10.3688-3696.1994

Oyama, L. B., Girdwood, S. E., Cookson, A. R., Fernandez-Fuentes, N., Prive, F., Vallin, H. E., et al. (2017). The rumen microbiome: an underexplored resource for novel antimicrobial discovery. *NPJ Biofilms Microbiomes* 3, 1–9. doi: 10.1038/s41522-017-0042-1

Oyama, L. B., Olleik, H., Teixeira, A. C. N., Guidini, M. M., Pickup, J. A., Cookson, A. R., et al. (2019). In silico identification of novel peptides with antibacterial activity against multidrug resistant Staphylococcus aureus. *BioRxiv* Available online at: https://www.biorxiv.org/content/10.1101/577221v1 (accessed on 24 June 2020).

Palevich, N., Kelly, W. J., Leahy, S. C., Denman, S., Altermann, E., Rakonjac, J., et al. (2019). Comparative genomics of rumen Butyrivibrio spp. uncovers a continuum of polysaccharide-degrading capabilities. *Appl. Environ. Microbiol.* 86:e01993-19. doi: 10.1128/AEM.01993-19

Pan, S. J., Cheung, W. L., Fung, H. K., Floudas, C. A., and Link, A. J. (2010). Computational design of the lasso peptide antibiotic microcin J25. *Protein Eng. Des. Sel.* 24, 275–282. doi: 10.1093/protein/gzq108

Potterat, O., Stephan, H., Metzger, J. W., Gnau, V., Zähner, H., and Jung, G. (1994). Aborycin–A tricyclic 21-peptide antibiotic isolated from *Streptomyces griseoflavus*. *Justus Liebigs Ann. Chem.* 1994, 741–743. doi: 10.1002/jlac.199419940716

Potterat, O., Wagner, K., Gemmecker, G., Mack, J., Puder, C., Vettermann, R., et al. (2004). BI-32169, a bicyclic 19-peptide with strong glucagon receptor antagonist activity from Streptomyces sp. *J. Nat. Prod.* 67, 1528–1531. doi: 10.1021/np040093o

Price, M. N., Dehal, P. S., and Arkin, A. P. (2010). FastTree 2–approximately maximum-likelihood trees for large alignments. *PLoS One* 5:e9490. doi: 10.1371/journal.pone.0009490

Rosengren, K. J., Clark, R. J., Daly, N. L., Göransson, U., Jones, A., and Craik, D. J. (2003). Microcin J25 has a threaded sidechain-to-backbone ring structure and not a head-to-tail cyclized backbone. *J. Am. Chem. Soc.* 125, 12464–12474. doi: 10.1021/ja0367703

Russell, J. B., and Mantovani, H. C. (2002). The bacteriocins of ruminal bacteria and their potential as an alternative to antibiotics. *J. Mol. Microbiol. Biotechnol.* 4, 347–355.

Salomon, R. A., and Farías, R. N. (1992). Microcin 25, a novel antimicrobial peptide produced by *Escherichia coli*. *J. Bacteriol.* 174, 7428–7435. doi: 10.1128/jb.174.22.7428-7435.1992

Seemann, T. (2014). Prokka: rapid prokaryotic genome annotation. *Bioinformatics* 30, 2068–2069. doi: 10.1093/bioinformatics/btu153

Seshadri, R., Leahy, S. C., Attwood, G. T., Teh, K. H., Lambie, S. C., Cookson, A. L., et al. (2018). Cultivation and sequencing of rumen microbiome members from the Hungate1000 Collection. *Nat. Biotechnol.* 36, 359–367. doi: 10.1038/nbt.4110

Severinov, K., Semenova, E., Kazakov, A., Kazakov, T., and Gelfand, M. S. (2007). Low-molecular-weight post-translationally modified microcins. *Mol. Microbiol.* 65, 1380–1394. doi: 10.1111/j.1365-2958.2007.05874.x

Sievers, F., Wilm, A., Dineen, D., Gibson, T. J., Karplus, K., Li, W., et al. (2011). Fast, scalable generation of high-quality protein multiple sequence alignments using Clustal Omega. *Mol. Syst. Biol.* 7:539. doi: 10.1038/msb.2011.75

Solbiati, J. O., Ciaccio, M., Farías, R. N., González-Pastor, J. E., Moreno, F., and Salomón, R. A. (1999). Sequence analysis of the four plasmid genes required to produce the circular peptide antibiotic microcin J25. *J. Bacteriol.* 181, 2659–2662. doi: 10.1128/JB.181.8.2659-2662

Solbiati, J. O., Ciaccio, M., Farias, R. N., and Salomón, R. A. (1996). Genetic analysis of plasmid determinants for microcin J25 production and immunity. *J. Bacteriol.* 178, 3661–3663. doi: 10.1128/jb.178.12.3661-3663

Soudy, R., Wang, L., and Kaur, K. (2012). Synthetic peptides derived from the sequence of a lasso peptide microcin J25 show antibacterial activity. *Bioorg. Med. Chem.* 20, 1794–1800. doi: 10.1016/j.bmc.2011.12.061

Steele, D. B., and Stowers, M. D. (1991). Techniques for selection of industrially important microorganisms. *Annu. Rev. Microbiol.* 45, 89–106. doi: 10.1146/annurev.mi.45.100191.000513

Sumida, T., Dubiley, S., Wilcox, B., Severinov, K., and Tagami, S. (2019). Structural basis of leader peptide recognition in lasso peptide biosynthesis pathway. *ACS Chem. Biol.* 14, 1619–1627. doi: 10.1021/acschembio.9b00348

Tietz, J. I., Schwalen, C. J., Patel, P. S., Maxson, T., Blair, P. M., Tai, H.-C., et al. (2017). A new genome-mining tool redefines the lasso peptide biosynthetic landscape. *Nat. Chem. Biol.* 13, 470–478. doi: 10.1038/nchembio.2319

Trmcic, A., Monnet, C., Rogelj, I., and Bogovic Matijasic, B. (2011). Expression of nisin genes in cheese–a quantitative real-time polymerase chain reaction approach. *J. Dairy Sci.* 94, 77–85. doi: 10.3168/jds.2010-3677

Tsunakawa, M., Hu, S.-L., Hoshino, Y., Detlefson, D. J., Hill, S. E., Furumai, T., et al. (1995). Siamycins I and II, new anti-HIV peptides: I. Fermentation, isolation, biological activity and initial characterization. *J. Antibiot.* 48, 433–434. doi: 10.7164/antibiotics.48.433

van Heel, A. J., de Jong, A., Song, C., Viel, J. H., Kok, J., and Kuipers, O. P. (2018). BAGEL4: a user-friendly web server to thoroughly mine RiPPs and bacteriocins. *Nucleic Acids Res.* 46, W278–W281. doi: 10.1093/nar/gky383

Weber, T., and Kim, H. U. (2016). The secondary metabolite bioinformatics portal: computational tools to facilitate synthetic biology of secondary metabolite production. *Synth. Syst. Biotechnol.* 1, 69–79. doi: 10.1016/j.synbio.2015.12.002

Weber, W., Fischli, W., Hochuli, E., Kupfer, E., and Weibel, E. K. (1991). Anantin-a peptide antagonist of the atrial natriuretic factor (ANF). I. Producing organism, fermentation, isolation and biological activity. *J. Antibiot.* 44, 164–171. doi: 10.7164/antibiotics.44.164

Winter, J. M., Behnken, S., and Hertweck, C. (2011). Genomics-inspired discovery of natural products. *Curr. Opin. Chem. Biol.* 15, 22–31. doi: 10.1016/j.cbpa.2010.10.020

Yan, K.-P., Li, Y., Zirah, S., Goulard, C., Knappe, T. A., Marahiel, M. A., et al. (2012). Dissecting the maturation steps of the lasso peptide microcin J25 in vitro. *ChemBioChem* 13, 1046–1052. doi: 10.1002/cbic.201200016

Yano, K., Toki, S., Nakanishi, S., Ochiai, K., Ando, K., Yoshida, M., et al. (1996). MS-271, a novel inhibitor of calmodulin-activated myosin light chain kinase from Streptomyces sp.—I. isolation, structural determination and biological properties of MS-271. *Bioorg. Med. Chem.* 4, 115–120. doi: 10.1016/0968-0896(95)00175-1

Zhu, S., Fage, C. D., Hegemann, J. D., Mielcarek, A., Yan, D., Linne, U., et al. (2016a). The B1 protein guides the biosynthesis of a lasso peptide. *Sci. Rep.* 6:35604. doi: 10.1038/srep35604

Zhu, S., Fage, C. D., Hegemann, J. D., Yan, D., and Marahiel, M. A. (2016b). Dual substrate-controlled kinase activity leads to polyphosphorylated lasso peptides. *FEBS Lett.* 590, 3323–3334. doi: 10.1002/1873-3468.12386

Zhu, S., Hegemann, J. D., Fage, C. D., Zimmermann, M., Xie, X., Linne, U., et al. (2016c). Insights into the unique phosphorylation of the lasso peptide paeninodin. *J. Biol. Chem.* 291, 13662–13678. doi: 10.1074/jbc.M116.722108

Zong, C., Cheung-Lee, W. L., Elashal, H. E., Raj, M., and Link, A. J. (2018). Albusnodin: an acetylated lasso peptide from Streptomyces albus. *ChemComm.* 54, 1339–1342. doi: 10.1039/C7CC08620B

Zyubko, T., Serebryakova, M., Andreeva, J., Metelev, M., Lippens, G., Dubiley, S., et al. (2019). Efficient in vivo synthesis of lasso peptide pseudomycoidin proceeds in the absence of both the leader and the leader peptidase. *Chem. Sci.* 10, 9699–9707. doi: 10.1039/C9SC02370D

Conflict of Interest: The authors declare that the research was conducted in the absence of any commercial or financial relationships that could be construed as a potential conflict of interest.

frontiers in Microbiology

ORIGINAL RESEARCH
published: 16 September 2020
doi: 10.3389/fmicb.2020.571903

Kunkecin A, a New Nisin Variant Bacteriocin Produced by the Fructophilic Lactic Acid Bacterium, *Apilactobacillus kunkeei* FF30-6 Isolated From Honey Bees

Takeshi Zendo[1], Chihiro Ohashi[1], Shintaro Maeno[2], Xingguo Piao[1], Seppo Salminen[3], Kenji Sonomoto[1] and Akihito Endo[2]*

[1] Department of Bioscience and Biotechnology, Faculty of Agriculture, Graduate School, Kyushu University, Fukuoka, Japan, [2] Department of Food, Aroma and Cosmetic Chemistry, Faculty of Bioindustry, Tokyo University of Agriculture, Hokkaido, Japan, [3] Functional Foods Forum, University of Turku, Turku, Finland

OPEN ACCESS

Edited by:
Des Field,
University College Cork, Ireland

Reviewed by:
Auke J. van Heel,
University of Groningen, Netherlands
Maria Do Carmo De Freire Bastos,
Federal University of Rio de Janeiro, Brazil

***Correspondence:**
Takeshi Zendo
zendo@agr.kyushu-u.ac.jp

Specialty section:
This article was submitted to Antimicrobials, Resistance and Chemotherapy, a section of the journal Frontiers in Microbiology

Received: *12 June 2020*
Accepted: *12 August 2020*
Published: *16 September 2020*

Citation:
Zendo T, Ohashi C, Maeno S, Piao X, Salminen S, Sonomoto K and Endo A (2020) Kunkecin A, a New Nisin Variant Bacteriocin Produced by the Fructophilic Lactic Acid Bacterium, Apilactobacillus kunkeei FF30-6 Isolated From Honey Bees. Front. Microbiol. 11:571903. doi: 10.3389/fmicb.2020.571903

Apilactobacillus kunkeei FF30-6 isolated from healthy honey bees synthesizes the bacteriocin, which exhibits antimicrobial activity against *Melissococcus plutonius*. The bacteriocin, kunkecin A, was purified through three-step chromatography, and mass spectrometry revealed that its relative molecular mass was 4218.3. Edman degradation of purified kunkecin A showed only the N-terminal residue, isoleucine. Hence, alkaline alkylation made the subsequent amino acid residues accessible to Edman degradation, and 30 cycles were sequenced with 11 unidentified residues. Whole genome sequencing of *A. kunkeei* FF30-6, followed by Sanger sequencing, revealed that the genes encoding the proteins involved in lantibiotic biosynthesis were within the plasmid, pKUNFF30-6. Most of the identified proteins exhibited significant sequence similarities to the biosynthetic proteins of nisin A and its variants, such as subtilin. However, the kunkecin A gene cluster lacked the genes corresponding to *nisI*, *nisR*, and *nisK* of the nisin A biosynthetic gene cluster. A comparison of the gene products of *kukA* and *nisA* (kunkecin A and nisin A structural genes, respectively) suggested that they had similar post-translational modifications. Furthermore, the structure of kunkecin A was proposed based on a comparison of the observed and calculated relative molecular masses of kunkecin A. The structural analysis revealed that kunkecin A and nisin A had a similar mono-sulfide linkage pattern. Purified kunkecin A exhibited a narrow antibacterial spectrum, but high antibacterial activity against *M. plutonius*. Kunkecin A is the first bacteriocin to be characterized in fructophilic lactic acid bacteria and is the first nisin-type lantibiotic found in the family *Lactobacillaceae*.

Keywords: bacteriocins, lantibiotics, nisin, *Apilactobacillus kunkeei*, *Melissococcus plutonius*, fructophilic lactic acid bacteria

INTRODUCTION

Fructophilic lactic acid bacteria (FLAB) are only found in fructose-rich niches, such as flowers and fruits, and *Fructobacillus* spp. and *Apilactobacillus kunkeei*, formerly classified as *Lactobacillus kunkeei* (Zheng et al., 2020), are representatives of this group (Endo and Okada, 2008; Endo et al., 2012). Recent studies revealed that the genotypic and phenotypic characteristics of FLAB enable them to adapt to the fructose-rich niches (Endo et al., 2009, 2015, 2018). *A. kunkeei* was originally isolated from wine (Edwards et al., 1998) and was recently characterized as one of the major components of the gut microbiota in honey bee queens and larvae (Endo and Salminen, 2013; Vojvodic et al., 2013; Anderson et al., 2018). The species has been linked to the nectar and hive materials of honey bees (Anderson et al., 2013; Kwong and Moran, 2016). As *A. kunkeei* has a symbiotic relationship with the host insects, it has potential probiotic and paratransgenic applications to honey bees (Rangberg et al., 2015; Arredondo et al., 2018). A previous study reported that the culture supernatant from an *A. kunkeei* isolate exhibited anti-*Melissococcus plutonius* activity (Endo and Salminen, 2013), the causative agent of European foulbrood in honey bee larvae (Arai et al., 2012). Furthermore, this antibacterial activity was inhibited by a treatment with proteases (Endo and Salminen, 2013), which suggested the proteinaceous nature of this substance.

Bacteriocins are ribosomally synthesized antimicrobial peptides that exhibit bactericidal or bacteriostatic activity (Cotter et al., 2005b; Alvarez-Sieiro et al., 2016). Various bacterial species, including lactic acid bacteria (LAB), produce bacteriocins, whereas properties for bacteriocin production vary according to strains. The application of bacteriocins, particularly those derived from LAB, in food safety has been attracting increasing interest because most of them are active against several food spoilage bacteria and foodborne pathogens and are also easily degraded by gut proteases (Cleveland et al., 2001; Perez et al., 2014). Moreover, LAB bacteriocins have been evaluated as an alternative antibiotic agent for clinical applications (Heunis et al., 2013; Perez et al., 2014).

Nisin is the most-studied LAB bacteriocin. It is a class I bacteriocin that is also referred to as lantibiotics and is widely used as a safe food preservative (Delves-Broughton et al., 1996). Several natural variants of nisin are produced by strains belonging to *Lactococcus lactis*, such as nisin A (Gross and Morell, 1971), nisin Z (Mulders et al., 1991), nisin Q (Zendo et al., 2003; Fukao et al., 2008), and nisin F (de Kwaadsteniet et al., 2008), in addition to subtilin produced by strains of *Bacillus subtilis* (Banerjee and Hansen, 1988). Natural nisin variants produced by strains of other genera have recently been reported, such as nisin U (Wirawan et al., 2006), nisin H (O'Connor et al., 2015), nisin O (Hatziioanou et al., 2017), nisin J (O'Sullivan et al., 2020), and nisin P (Garcia-Gutierrez et al., 2020) by *Blautia* spp., *Staphylococcus* spp., and *Streptococcus* spp. All nisin variants share a basal structure consisting of five mono-sulfide bridges (lanthionine rings), and three dehydrated amino acid residues, which result from post-translational modifications but have some amino acid substitutions. The biosynthesis of nisin A requires eleven genes in three transcription units (Kuipers et al., 1995; de Ruyter et al., 1996). After the synthesis of NisA, the precursor of nisin A, NisB catalyzes the dehydration of Ser and Thr residues in NisA to dehydroalanine (Dha) and dehydrobutyrine (Dhb), respectively. NisC then catalyzes the cyclization of the dehydrated residues with five Cys residues to form lanthionine (Lan) and 3-methyllanthionine (MeLan), respectively. Modified NisA containing five mono-sulfide bridges and three dehydrated residues is secreted from the producer cell through NisT [an ATP-binding cassette (ABC) transporter]. The 23-amino-acid-long leader sequence of NisA is then cleaved by NisP (protease) outside the cell, and the 34-amino acid mature nisin A is released. The two-component regulatory system, NisK (histidine kinase)/NisR (response regulator) upregulates transcription units to enhance the synthesis of nisin A. Mature nisin A can also serve as an autoinducer. NisI (membrane protein) and NisFEG (ABC transporter) are two independent self-immunity systems that protect producer cells against the antimicrobial activity of nisin A. The other nisin variants are synthesized by a similar mechanism employing similar biosynthetic proteins (Yoneyama et al., 2008).

The honey bee isolate *A. kunkeei* FF30-6 produces an antibacterial peptide that exhibits anti-*M. plutonius* activity (Endo and Salminen, 2013). In the present study, we purified and characterized the structure and activity of a novel bacteriocin, which we named kunkecin A. The gene cluster encoding the proteins involved in bacteriocin biosynthesis was identified through a whole genome analysis of *A. kunkeei* FF30-6. The results of our analysis revealed that kunkecin A is a variant of nisin A, which had not yet been reported in the family *Lactobacillaceae*. Kunkecin A had a narrow antimicrobial spectrum but exhibited high antimicrobial activity against a few bacteria originating from honey bees, including *M. plutonius*.

RESULTS

Purification and Mass Determination of the Bacteriocin

The bacteriocin produced by *A. kunkeei* FF30-6 was purified from the culture supernatant using a three-step chromatography procedure. The active fraction containing the purified bacteriocin was obtained in the final step of reverse-phase high-performance liquid chromatography (HPLC). The active fraction was used to characterize the structure and assess its antibacterial activity. Electrospray ionization time-of-flight mass spectrometry (ESI-TOF MS) revealed that the relative molecular mass of the purified bacteriocin was 4218.3 (**Figure 1**). It was considered to be a novel bacteriocin and termed kunkecin A, because, to the best of our knowledge, its relative molecular mass has not been previously reported for any other bacteriocins in the literature or databases dedicated to bacteriocins such as Bactibase (Hammami et al., 2010) and BAGEL4 (Van Heel et al., 2018).

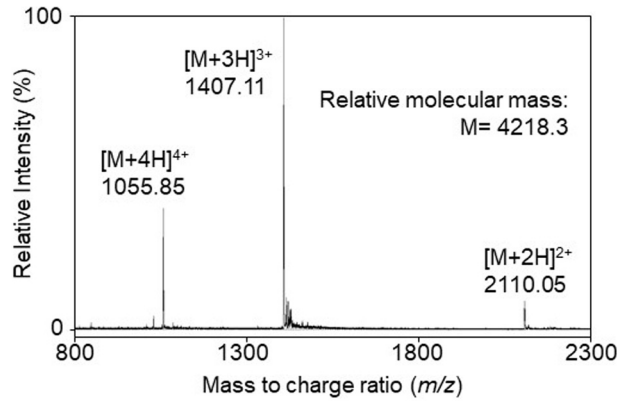

FIGURE 1 | The electrospray ionization time-of-flight (ESI-TOF) mass spectrum of the purified bacteriocin, kunkecin A, produced by *A. kunkeei* FF30-6. Multiple charged molecular ions were detected and are indicated.

Amino Acid Sequence Analysis of Kunkecin A

Edman degradation of purified kunkecin A detected only the N-terminal residue, isoleucine, but no other residues. This result suggested that there was a modified residue at the second position, such as a dehydrated amino acid residue, which inhibited Edman degradation. The purified peptide was further treated with alkaline 2-mercaptoethanol to enable the degradation reaction to access the modified residues in kunkecin A, following the methods described by Meyer et al. (1994). After 30 cycles of Edman degradation of the treated peptide, we obtained the following amino acid sequence: IXXYVLXXPG XIXGRLMGXN NKXKXXHXHS, where X indicates the cycle at which no amino acid was identified. This result strongly suggested that kunkecin A is a lantibiotic and that the second residue and subsequent X residues were post-translationally modified.

Identification of Kunkecin A Biosynthetic Genes in the Whole Genomic Sequence of *A. kunkeei* FF30-6

A previous study reported the draft genome sequence of *A. kunkeei* FF30-6 (NZ_BDDX00000000) with 25 contigs (Maeno et al., 2016). One of the contigs (contig no. 12) was suspected to be a putative plasmid sequence because it had a gene-encoding DNA replication initiator protein A. In the present study, we used Sanger sequencing to determine the possible plasmid structure. We obtained a circular plasmid, termed pKUNFF30-6, which consisted of 19,498 bp (**Supplementary Figure S1** and **Supplementary Table S1**). The complete plasmid sequence was analyzed using the DDBJ Fast Annotation and Submission Tool (DFAST, [1]) (Tanizawa et al., 2016), which revealed that eight bacteriocin-related genes were located on the plasmid (accession number, AP019008). The amino acid sequences of the gene products exhibited significant similarities to those of the proteins involved in the biosynthesis of nisin A (**Table 1**). This putative gene cluster consisting of eight consecutive genes (*orf10-17* of pKUNFF30-6) lacked the genes corresponding to *nisI*, *nisR*, and *nisK* in the nisin A biosynthetic cluster. Half of the genes in the cluster (*orf10-13*) were coded in the opposite direction to the other half, *orf14-17*. This is in contrast to nisin A biosynthetic genes, which were all coded in the same direction (**Figure 2**). Each gene in the kunkecin A biosynthetic gene cluster was named after the corresponding gene in the nisin A biosynthetic gene cluster (**Table 1** and **Figure 2**).

[1]https://dfast.nig.ac.jp/

Proposed Primary Structure of Kunkecin A

The precursor peptide of kunkecin A, KukA was similar to those of nisin A (NisA) and its natural variants (**Figure 3**). The cleavage site of the leader peptide of KukA was identified based on the alignment with NisA and the result of Edman degradation, as shown in **Figure 3**. The difference in the calculated (4327.0) and observed (4218.3) relative molecular masses of the KukA core peptide (**Figure 1**) indicated that six dehydrations occurred in the core peptide. Additionally, a comparative analysis of the structures of nisin A and kunkecin A revealed that modified residues were located at the position of X in the N-terminal sequence of kunkecin A obtained by Edman degradation. The positions of the modified residues were similar in nisin A, except for the 5th and 33rd residues, at which valine and histidine, respectively, were detected in kunkecin A both by Edman degradation and DNA sequence analysis. These modifications involved six dehydrations and concurred with the observed difference between the calculated and observed relative molecular masses of kunkecin A. Consequently, we proposed the structure of kunkecin A as shown in **Figure 4**. The structure of kunkecin A includes a dehydrobutyrine, lanthionine, and four 3-methyllanthionine residues with a similar ring pattern to that of nisin A. However, the C-terminal of kunkecin A was longer than that of nisin A.

TABLE 1 | Putative kunkecin A biosynthetic proteins encoded on genes identified in the plasmid, pKUNFF30-6, harbored by *A. kunkeei* FF30-6.

ORF No.*	Product name	Length (a.a.)	Putative function	Corresponding nisin A biosynthetic protein [identity (%)]
10	KukP	454	Leader peptidase	NisP (31%)
11	KukA	64	Kunkecin A precursor	NisA (54%)
12	KukC	437	Lantibiotic cyclase	NisC (25%)
13	KukT	577	Transporter	NisT (37%)
14	KukF	227	Self-immunity	NisF (48%)
15	KukE	241	Self-immunity	NisE (20%)
16	KukG	245	Self-immunity	NisG (22%)
17	KukB	996	Lantibiotic dehydratase	NisB (24%)

Gene numbers in the plasmid, pKUNFF30-6 (Supplementary Figure S1** and **Supplementary Table S1**).*

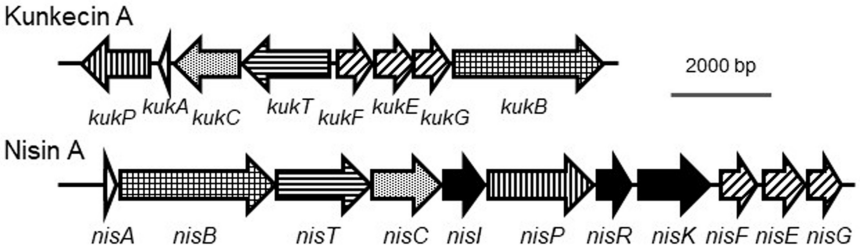

FIGURE 2 | Comparison of biosynthetic gene clusters of kunkecin A and nisin A. The putative kunkecin A biosynthetic genes are labeled with the same pattern as each corresponding gene in the nisin A biosynthetic cluster. No genes corresponding to *nisI*, *nisR*, or *nisK* (filled with black) were found in the kunkecin biosynthetic gene cluster.

```
                    Leader peptide                    Core peptide
            -25                          -1 | 1                          39
Kunkecin A  MSNFNDFNLGIK--KVHSGSKKGLEPR |ITSYVLCTPGCITGRLMGCNNKTKTCHCHSSNHFSFHAR
Subtilin    MSKFDDFDLDVV--KVSKQ-DSKITPQ |WKSESLCTPGCVTGALQTCFLQTLTCNCKISK-------
Nisin J     --MNNQFNLKSKSANVSGSKGNNLETR |ITSKSLCTPGCKTGALQTCFAKTATCHCSGHVHTK----
Nisin O1-2  MGKFDDFDLDVT--KTAA--QGGIEPK |YKSKSACTPGCPTGILMTCPLKTATCGCHITGK------
Nisin O3    MAKFDDFDLDVT--KTAA--QGGIEPK |YKSKSACTPGCPTGILMTCPLKTATCGCHITGK------
Nisin U     -MNNEDFNLDLI--KISKENNSGASPR |ITSKSLCTPGCKTGILMTCPLKTATCGCHFG--------
Nisin P     -MNNEDFNLDLV--TISKENNSGASPR |VTSKSLCTPGCKTGILMTCAIKTATCGCHFG--------
Nisin U2    -MSTKDFNLDLV--SVSKK-DSGASPR |VTSKSLCTPGCKTGILTGCPLKTATCGCHFG--------
Nisin H     -MSTNDFNLDLV--SVSKS-NAGASTR |FTSISMCTPGCKTGALMTCNYKTATCHCSIKVSK-----
Nisin Q     -MSTKDFNLDLV--SVSKT-DSGASTR |ITSISLCTPGCKTGVLMGCNLKTATCNCSVHVSK-----
Nisin F     -MSTKDFNLDLV--SVSKK-DSGASPR |ITSISLCTPGCKTGALMGCNMKTATCNCSVHVSK-----
Nisin A     -MSTKDFNLDLV--SVSKK-DSGASPR |ITSISLCTPGCKTGALMGCNMKTATCHCSIHVSK-----
Nisin Z     -MSTKDFNLDLV--SVSKK-DSGASPR |ITSISLCTPGCKTGALMGCNMKTATCNCSIHVSK-----
                .:*:*     .           : |.*   ***** ** *  *  :* ** *
```

FIGURE 3 | Amino acid sequence alignment of precursor peptides of kunkecin A and nisin variants. Each precursor was aligned using the Clustal Omega program. The dotted line indicates the cleavage site of the leader peptides. Asterisks indicate fully conserved positions. Colons and periods indicate positions conserved by amino acid residues with strong and weak similarity, respectively.

Antimicrobial Activity Spectrum of Kunkecin A

The antimicrobial activity of purified kunkecin A was evaluated against a panel of bacterial indicator strains as the minimum concentrations, causing clear inhibition zones by the spot-on-lawn assay. We also compared the antibacterial activity of purified kunkecin A with that of nisin A (**Table 2**). The antibacterial activity of kunkecin A was two-fold higher than that of nisin A against *M. plutonius*. Honey bee commensals show different sensitivities to the bacteriocins at the species level. *Lactobacillus apis*, *L. kullabergensis*, *Bombilactobacillus mellis*, and *Bifidobacterium asteroides* exhibited markedly higher tolerance (>four-fold) to kunkecin A than to nisin A, whereas others, including *Apilactobacillus apinorum*, *Bombilactobacillus mellifer*, and *Lactobacillus melliventiris*, showed the opposite reactions. The kunkecin A-producing strain, *A. kunkeei* FF30-6, and the nisin A-producer strain, *L. lactis* subsp. *lactis* NCDO 497, were highly tolerant to kunkecin A and nisin A. The tolerance to the kunkecin A and nisin A treatments may be attributed to self-immunity against their own and homologous bacteriocins. The American foulbrood-causing species, *Paenibacillus larvae* PL-1, was tolerant to kunkecin A or nisin A. The minimum concentrations for the inhibition of kunkecin A against some of the indicator strains, including a Gram-negative strain, *Escherichia coli*, were higher than the concentration at which self-immunity was observed.

The self-immunity was further examined by the deferred antagonism assay. Against *A. kunkeei* FF30-6, a very tiny inhibition zone with a clear edge was caused by *L. lactis* subsp. *lactis* NCDO 497, but no inhibition zone was formed by itself. On the other hand, against *L. lactis* subsp. *lactis* NCDO 497, no inhibition zones were formed by the both strains.

DISCUSSION

We previously reported that a culture supernatant of one of the *A. kunkeei* isolates, strain FF30-6, originated from honey bees inhibited the growth of the type strain of *M. plutonius* (Endo and Salminen, 2013). Since *A. kunkeei* is a promising candidate for

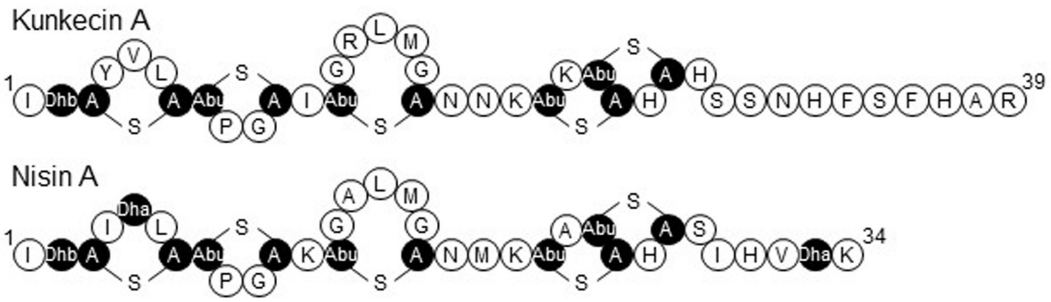

FIGURE 4 | The proposed primary structure of kunkecin A and the primary structure of nisin A. Unusual amino acids generated by post-translational modifications are indicated in black. Dha and Dhb indicate the dehydrated amino acids, dehydroalanine, and dehydrobutyrine, respectively. A-S-A and Abu-S-A indicate lanthionine and 3-methyllanthionine, respectively.

probiotic and paratransgenic in honey bees, it would be of interest to study its antagonistic activities in honey bee commensals.

The relative molecular mass of kunkecin A is unique among known bacteriocins and within the reported range for LAB bacteriocins and larger than those of most lantibiotics, including nisin A (Cotter et al., 2005a). However, further structural analyses on purified kunkecin A suggested that it shares amino acid sequences and positions of modified residues with nisin A and its variants. The conserved motif sequence (FNLD) of the leader peptide in nisin-group lantibiotics (Plat et al., 2011) was also detected in the kunkecin A leader peptide, except for the final 4th residue, which changed to glycine (**Figure 3**). The amino acid sequence of the N-terminal in kunkecin A begins with isoleucine and has a dehydrobutyrine at the second position, which is consistent with the results of Edman degradation. The comparative analysis of the observed and calculated relative molecular masses of kunkecin A revealed that the peptide underwent six dehydrations, including dehydrobutyrine at the second position. Furthermore, the comparison of kunkecin A and nisin A strongly suggested that kunkecin A contained totally five mono-sulfide linkages (one lanthionine and four 3-methyllanthionine), which are also found in nisin A. The amino acid sequences of the putative modification enzymes, KukB and KukC, also exhibited high similarities to those of the respective lantibiotic modification enzymes of nisin A and its variants. This result strongly indicated that the ring pattern of kunkecin A was similar to that of the nisin A-group lantibiotics.

In the putative kunkecin A biosynthetic gene cluster, eight genes on the plasmid pKUNFF30-6 encoded putative lantibiotic biosynthetic proteins and the kunkecin A precursor peptide. Putative kunkecin A biosynthetic proteins also exhibited significant sequence similarities to those involved in the biosynthesis of nisin A (**Table 1**). The function of these proteins was predicted to be similar to that of nisin A biosynthetic proteins. The kunkecin A precursor peptide, KukA, is dehydrated and cyclized by the lantibiotic modification enzymes, KukB and KukC, respectively. Modified KukA is secreted by the ABC transporter, KukT, and the leader peptide of KukA is cleaved by the cell-wall-anchored leader peptidase, KukP, outside the producer cell. The producer cell is protected by the self-immunity proteins, KukF, KukE, and KukG, which comprise another ABC transporter. In contrast to the nisin A biosynthetic gene cluster, the kunkecin A gene cluster lacks the genes corresponding to *nisI*, *nisR*, and *nisK*. NisI is responsible for self-immunity against nisin A (Kuipers et al., 1993), and NisR and NisK form a two-component regulatory system with nisin A as the autoinducer to regulate the biosynthesis of nisin A (Kuipers et al., 1995; de Ruyter et al., 1996). In the reported nisin-variant gene clusters, that of nisin H lacks the gene corresponding to *nisI* (O'Connor et al., 2015), while that of nisin J lacks the genes to *nisI*, *nisR*, and *nisK* (O'Sullivan et al., 2020).

NisI is a membrane-anchored lipoprotein that functions coordinately with the ABC transporter comprising NisF, NisE, and NisG for self-immunity in the producer cell (Stein et al., 2003). NisFEG or SpaFEG, the corresponding system to subtilin, alone is known to be sufficient to impart self-immunity against each cognate lantibiotic (Kuipers et al., 1993; Stein et al., 2003). This finding suggests that the KukFEG system was sufficient to protect producer cells against kunkecin A without the need for a protein corresponding to NisI or SpaI in nisin A or subtilin, respectively. The producer strain, *A. kunkeei* FF30-6 exhibited tolerance to both kunkecin A and nisin A (**Table 2**), while it was inhibited very weakly by nisin A-producing *L. lactis* NCDO 497 in the deferred antagonism assay. The less cross-immunity of *A. kunkeei* FF30-6 against the nisin A producer can be attributed to high production of nisin A and/or the lack of the NisI homologous protein. Although NisI and SpaI contributes less to total immunity than NisFEG and SpaFEG, respectively, previous studies reported that they protected producer cells from the pore formation activity of their respective cognate bacteriocins (Stein et al., 2005; AlKhatib et al., 2014). Additionally, SpaI has a very similar structure to NisI (Hacker et al., 2015) and interacts with the C-terminal of subtilin (Geiger et al., 2019). The lack of the NisI homologous protein in kunkecin A biosynthesis may be related to the C-terminal extension of kunkecin A and its resulting activity.

During nisin A biosynthesis, nisin A can activate the promoters located upstream of *nisA* and *nisF via* the two-component NisR/NisK regulatory system and trigger the synthesis of nisin A (Kuipers et al., 1995; de Ruyter et al., 1996). No regulatory genes were identified in the kunkecin A biosynthetic gene cluster. Additionally, gene organization in the

TABLE 2 | Antimicrobial spectra of kunkecin A and nisin A.

Indicator strains*	Minimum concentrations for inhibition (nM)	
	Kunkecin A	Nisin A
Bacillus subtilis JCM 1465^T	49	9
Kocuria rhizophila NBRC 12708	197	146
Enterococcus faecalis JCM 5803^T	1,578	73
Enterococcus faecium TUA 1344L	789	36
Listeria innocua ATCC 33090^T	197	18
Lapidilactobacillus dextrinicus JCM 5887^T	49	9
Latilactobacillus sakei subsp. *sakei* JCM 1157^T	25	9
Lactiplantibacillus plantarum subsp. *plantarum* JCM 1149^T	395	73
Leuconostoc mesenteroides subsp. *mesenteroides* JCM 6124^T	99	9
Lactococcus lactis subsp. *lactis* ATCC 19435^T	197	36
Lactococcus lactis subsp. *lactis* NCDO 497 (nisin A-producing LAB)	25,250	582
Escherichia coli JM109	12,625	291
Honey bee commensals		
Apilactobacillus kunkeei JCM 16173	197	146
Apilactobacillus kunkeei FMO-1	395	582
Apilactobacillus kunkeei FMO-15	197	582
Apilactobacillus apinorum JCM 30765^T	8	582
Lactobacillus helsingborgensis JCM 30766^T	197	291
Lactobacillus kimbladii JCM 30767^T	49	73
Lactobacillus melliventris JCM 30770^T	13	146
Lactobacillus apis SH3-5	789	146
Lactobacillus kullabergensis SH3-7	98	9
Bombilactobacillus mellifer JCM 30768^T	25	73
Bombilactobacillus mellis JCM 30769^T	789	73
Bifidobacterium asteroides SH3-1	49	9
Bifidobacterium coryneforme SH6-2	395	291
Bifidobacterium indicum SH4-4	3,156	1,164
Fructobacillus fructosus FMO-85	395	291
Apilactobacillus kunkeei FF30-6 (kunkecin A-producing LAB)	789	582
Honey bee pathogens		
Melissococcus plutonius ATCC 35311^T	13	25
Paenibacillus larvae PL-1	395	582

**The indicator strains were obtained from the following culture collections: JCM, Japan Collection of Microorganisms, Wako, Japan; NBRC, NITE Biological Resource Center, Chiba, Japan; ATCC, American Type Culture Collection, Manassas, VA; TUA, Tokyo University of Agriculture, Tokyo, Japan; NCDO, National Collection of Dairy Organisms, Reading, United Kingdom. JM109 was purchased from Takara Bio. The other indicator strains were from laboratory collections.*

kunkecin A gene cluster differed from that in the nisin A gene cluster. These two lines of evidence suggest that the regulation of kunkecin A synthesis differs from that of nisin A synthesis.

Kunkecin A exhibited higher antibacterial activity against *M. plutonius* than nisin A, even though these two lantibiotics share structural similarity. However, although they shared a mono-sulfide bridge pattern, kunkecin A lacked two dehydrated residues at positions five and 33 and possessed five extra amino acid residues in the C-terminal. These changes may be responsible for the differences observed in their antibacterial activities.

Melissococcus plutonius was one of the most sensitive strains to kunkecin A among the honey-bee-related microbes tested. Antibiotics generally kill pathogens and commensals, which may result in diarrhea and the development of drug-resistant bacterial strains in animals. The long-term antibiotic treatment of honey bee colonies in apiaries has led to the selection of genes that confer antibiotic-resistance to the gut microbiota of the honey bee (Tian et al., 2012). Consequently, the incidence of antibiotic-resistant foulbrood pathogens is high in countries, which use oxytetracycline in apiaries (Murray and Aronstein, 2006; Alippi et al., 2007; Murray et al., 2007; Tian et al., 2012). Furthermore, antibiotic treatments increase the mortality of honey bees (Raymann et al., 2017). The administration of a broad spectrum bacteriocin, such as nisin A, may also affect the gut microbiota in honey bees. The microbiota is crucial for the healthy development of honey bees (Zheng et al., 2017; Raymann et al., 2018). The population of commensal bacteria, such as *Bifidobacterium* is inversely associated with the population of *M. plutonius* in healthy honey bees. Further studies are needed to clarify whether kunkecin A is a useful tool for controlling pathogens in apiaries.

In the present study, we described a novel bacteriocin and lantibiotic, kunkecin A. This is the first bacteriocin reported from FLAB and is the first nisin-type lantibiotic found in the family *Lactobacillaceae*. A more detailed understanding of the regulatory mechanisms underlying kunkecin A biosynthesis may enhance the production of this novel lantibiotic for future applications.

MATERIALS AND METHODS

Strains and Culture Media

The bacteriocin-producing strain, *A. kunkeei* FF30-6 isolated from healthy honey bees (*Apis mellifera mellifera*) (Endo and Salminen, 2013) was cultured in fMRS medium, Lactobacilli MRS broth (MRS; BD Difco, Sparks, MD) supplemented with 2% (w/v) D-fructose (Nacalai Tesque, Kyoto, Japan). *Lapidilactobacillus dextrinicus* JCM 5887^T and *M. plutonius* ATCC 35311^T, used as general indicator strains for bacteriocin activity, were cultured in MRS medium at 30°C and KSBHI medium at 37°C, respectively. KSBHI medium was composed of Brain Heart Infusion (BHI) medium (Oxoid, Hampshire, United Kingdom) supplemented with 20.4 g/L of KH_2PO_4 and 10 g/L of soluble starch (Arai et al., 2012). The other bacterial strains that were used as indicator strains for the bacteriocin assay (**Table 2**) were cultured for 18 h under the optimal conditions recommended by the respective culture collections. All bacterial cultures were stored at −80°C with 15% glycerol and were propagated in the respective media at the recommended temperatures for 18 h before use.

Antibacterial Activity Assay

The antibacterial activity of bacteriocin was evaluated using the spot-on-lawn method (Ennahar et al., 2001), in which 10 μL of the bacteriocin preparation was spotted onto the bacterial lawn.

Regarding general indicator strains, Lactobacilli Agar AOAC (BD Difco) inoculated with an overnight culture of the indicator strain at a density of 10^7 CFU/mL was overlaid on an MRS agar plate [MRS supplemented with 1.2% (w/v) agar]. KSBHI medium and BHI medium supplemented with 5% (v/v) horse blood and 1.5% (w/v) agar were used for *M. plutonius* and *P. larvae*, respectively, instead of the double layer of Lactobacilli Agar AOAC and MRS agar. After an overnight incubation at the respective temperatures recommended for the indicator strain, the bacterial lawn was checked for inhibition zones. Regarding purified bacteriocins, two-fold serial dilutions of the solution containing a fixed concentration of a bacteriocin were assayed, and the minimum concentrations that resulted in a clear zone of inhibition on each indicator lawn were recorded as the intensity of the antibacterial activity. Each assay was performed in triplicate to confirm reproducibility.

To study a self-immunity against the own bacteriocins, the deferred-antagonism assay was further conducted by using the bacteriocin producers, *A. kunkeei* FF30-6 and *L. lactis* subsp. *lactis* NCDO 497 as indicator strains. The bacteriocin producing strains were stabbed into fMRS agar plate [fMRS supplemented with 1.5% (w/v) agar] and grown at 30°C for 8 h. Then, fMRS agar inoculated with an indicator strain was overlaid on the agar plate. After an overnight incubation, the bacterial lawn was examined for inhibition zones.

Purification of the Bacteriocin

The bacteriocin was purified using a three-step chromatography procedure that was previously described with minor modifications (Masuda et al., 2011). Purification was performed using four 250-mL cultures (total of 1 L) of *A. kunkeei* FF30-6 grown to the early stationary phase in fMRS medium at 30°C for 8 h with reciprocal shaking at 140 strokes/min. Cells were pelleted by centrifugation at 8000 *g* at 4°C for 20 min. Further, 20 g of activated Amberlite XAD-16 resin (Sigma-Aldrich, St. Louis, MO, United States) was added to the culture supernatant. The resin matrix was shaken slowly at 4°C for 4 h, and was then washed with 200 mL Milli-Q water, followed by 400 mL 50% (v/v) ethanol. The active fraction was eluted with 200 mL 70% (v/v) isopropanol containing 0.1% trifluoroacetic acid. The eluted active fraction was evaporated to 60 mL to remove isopropanol. The sample was then diluted with an equal volume of 50 mM sodium citrate buffer (pH 3.0, CB), and applied to an SP Sepharose Fast Flow cation-exchange chromatography column (internal diameter, 10 mm; length, 100 mm; GE Healthcare, Uppsala, Sweden) equilibrated with 50 mL CB. The column was washed with 50 mL CB and 100 mL of 0.3 M NaCl in CB. The active bacteriocin fraction was eluted with 40 mL of 0.6 M NaCl in CB. This active fraction was applied to a Capcell-Pak C18 MGII S5 column (internal diameter 4.6 mm; length 150 mm; Shiseido, Tokyo, Japan) in an LC-2000Plus HPLC system (JASCO, Tokyo, Japan). The active fractions were eluted at a flow rate of 1 mL/min with a linear gradient of 15–45% (v/v) of acetonitrile in the Milli-Q water-acetonitrile mobile phase containing 0.1% trifluoroacetic acid for 30 min. The main active fraction was further purified using reverse-phase HPLC under the same conditions. Purified active fractions were stored at −30°C. The antibacterial activities of the fractions obtained at each purification step were determined as described above using *L. dextrinicus* JCM 5887^T as an indicator strain. Nisin A was purified from a commercial nisin A preparation (Sigma) by using cation-exchange chromatography and reverse-phase HPLC, as described previously (Fujita et al., 2007). Regarding structural characterization, the purified fractions were concentrated using a SpeedVac concentrator (Savant, Farmingdale, NY, United States). To assess antibacterial activity, the solvent was completely removed by lyophilization, and the purified bacteriocin was dissolved in 10% (v/v) dimethyl sulfoxide (DMSO). Peptide concentrations were determined using a Pierce® BCA™ Protein Assay Kit (Takara Bio, Otsu, Japan).

Mass Spectrometry and Amino Acid Sequencing

The relative molecular masses of the purified fractions were analyzed by ESI-TOF MS using a JMS-T100LC mass spectrometer (JEOL, Tokyo, Japan). Amino acid sequences were determined based on Edman degradation using a PPSQ-31 protein sequencer (Shimadzu, Kyoto, Japan). In further analyses of the N-terminal sequences of peptides containing dehydrated residues and lanthionine, the purified peptide was treated with alkaline 2-mercaptoethanol, following the methods described by Meyer et al. (1994) and subjected to Edman degradation.

Identification of Bacteriocin-Related Genes

The draft genome sequence of *A. kunkeei* FF30-6 containing 25 contigs was obtained in the previous study with the accession number NZ_BDDX00000000 (Maeno et al., 2016). One of the contigs (contig no. 12), which exhibited plasmid-like genetic characteristics, was further sequenced using the following primers: FF306-c12-F (5′-AAAAGAATAGACAACCACCCA-3′) and FF306-c12-R (5′-CCTTTCTAAGAGGAATATGG-3′). The sequence of the plasmid termed pKUNFF30-6 was analyzed using DFAST[2] to detect bacteriocin-related genes. Potential genes were further analyzed using the BLAST program of the National Center for Biotechnology Information database[3]. The DNA and amino acid sequences obtained were analyzed using GENETYX-WIN software (GENETYX, Tokyo, Japan). The amino acid sequence alignment was analyzed using Clustal Omega[4].

DATA AVAILABILITY STATEMENT

The datasets presented in this study can be found in online repositories. The names of the repository/repositories and accession number(s) can be found below: https://www.ddbj.nig.ac.jp/, AP019008.

[2]https://dfast.nig.ac.jp/

[3]http://www.ncbi.nlm.nih.gov/BLAST/

[4]https://www.ebi.ac.uk/Tools/msa/clustalo/

AUTHOR CONTRIBUTIONS

TZ and AE designed the project, analyzed the data, and wrote the manuscript. CO, SM, and XP performed the experiments and analyzed the data. SS and KS supervised the project. All authors contributed to the article and approved the submitted version.

FUNDING

This work was partially supported by JSPS KAKENHI grant numbers JP24380051, JP26850054, and JP17H03797.

ACKNOWLEDGMENTS

We are grateful to Prof. M. Kimura and Asst. Prof. T. Nakashima of Kyushu University, Japan, for allowing us to access the automated protein sequencer. Computational analysis was performed on the NIG supercomputer at ROIS.

SUPPLEMENTARY MATERIAL

The Supplementary Material for this article can be found online at: https://www.frontiersin.org/articles/10.3389/fmicb.2020.571903/full#supplementary-material

REFERENCES

Alippi, A. M., López, A. C., Reynaldi, F. J., Grasso, D. H., and Aguilar, O. M. (2007). Evidence for plasmid-mediated tetracycline resistance in *Paenibacillus larvae*, the causal agent of American Foulbrood (AFB) disease in honeybees. *Vet. Microbiol.* 125, 290–303. doi: 10.1016/j.vetmic.2007.05.018

AlKhatib, Z., Lagedroste, M., Fey, I., Kleinschrodt, D., Abts, A., and Smits, S. H. J. (2014). Lantibiotic immunity: inhibition of nisin mediated pore formation by NisI. *PLoS One* 9:e102246. doi: 10.1371/journal.pone.0102246

Alvarez-Sieiro, P., Montalbán-López, M., Mu, D., and Kuipers, O. P. (2016). Bacteriocins of lactic acid bacteria: extending the family. *Appl. Microbiol. Biotechnol.* 100, 2939–2951. doi: 10.1007/s00253-016-7343-9

Anderson, K. E., Ricigliano, V. A., Mott, B. M., Copeland, D. C., Floyd, A. S., and Maes, P. (2018). The queen's gut refines with age: longevity phenotypes in a social insect model. *Microbiome* 6:108. doi: 10.1186/s40168-018-0489-1

Anderson, K. E., Sheehan, T. H., Mott, B. M., Maes, P., Snyder, L., Schwan, M. R., et al. (2013). Microbial ecology of the hive and pollination landscape: bacterial associates from floral nectar, the alimentary tract and stored food of honey bees (*Apis mellifera*). *PLoS One* 8:e83125. doi: 10.1371/journal.pone.0083125

Arai, R., Tominaga, K., Wu, M., Okura, M., Ito, K., Okamura, N., et al. (2012). Diversity of *Melissococcus plutonius* from honeybee larvae in Japan and experimental reproduction of European foulbrood with cultured atypical isolates. *PLoS One* 7:e33708. doi: 10.1371/journal.pone.0033708

Arredondo, D., Castelli, L., Porrini, M. P., Garrido, P. M., Eguaras, M. J., Zunino, P., et al. (2018). *Lactobacillus kunkeei* strains decreased the infection by honey bee pathogens *Paenibacillus larvae* and *Nosema ceranae*. *Benef. Microb.* 9, 279–290. doi: 10.3920/BM2017.0075

Banerjee, S., and Hansen, J. N. (1988). Structure and expression of a gene encoding the precursor of subtilin, a small protein antibiotic. *J. Biol. Chem.* 263, 9508–9514.

Cleveland, J., Montville, T. J., Nes, I. F., and Chikindas, M. L. (2001). *Bacteriocins*: safe, natural antimicrobials for food preservation. *Int. J. Food Microbiol.* 71, 1–20. doi: 10.1016/s0168-1605(01)00560-8

Cotter, P. D., Hill, C., and Ross, R. P. (2005a). Bacterial lantibiotics: strategies to improve therapeutic potential. *Curr. Protein Pept. Sci.* 6, 61–75. doi: 10.2174/1389203053027584

Cotter, P. D., Hill, C., and Ross, R. P. (2005b). Bacteriocins: developing innate immunity for food. *Nat. Rev. Microbiol.* 3, 777–788. doi: 10.1038/nrmicro1273

de Kwaadsteniet, M., ten Doeschate, K., and Dicks, L. M. T. (2008). Characterization of the Structural gene encoding nisin F, a new lantibiotic produced by a *Lactococcus lactis* subsp. *lactis* isolate from freshwater catfish (*Clarias gariepinus*). *Appl. Environ. Microbiol.* 74, 547–549. doi: 10.1128/AEM.01862-07

de Ruyter, P. G., Kuipers, O. P., Beerthuyzen, M. M., van Alen-Boerrigter, I., and de Vos, W. M. (1996). Functional analysis of promoters in the nisin gene cluster of *Lactococcus lactis*. *J. Bacteriol.* 178, 3434–3439. doi: 10.1128/jb.178.12.3434-3439.1996

Delves-Broughton, J., Blackburn, P., Evans, R. J., and Hugenholtz, J. (1996). Applications of the bacteriocin, nisin. *Antonie van Leeuwenhoek* 69, 193–202. doi: 10.1007/bf00399424

Edwards, C. G., Haag, K. M., Collins, M. D., and Hutson, R. A. (1998). *Lactobacillus kunkeei* sp. nov.: a spoilage organism associated with grape juice fermentations. *J. Appl. Microbiol.* 84, 698–702. doi: 10.1046/j.1365-2672.1998.00399.x

Endo, A., Futagawa-Endo, Y., and Dicks, L. M. T. (2009). Isolation and characterization of fructophilic lactic acid bacteria from fructose-rich niches. *Syst. Appl. Microbiol.* 32, 593–600. doi: 10.1016/J.SYAPM.2009.08.002

Endo, A., Irisawa, T., Futagawa-Endo, Y., Takano, K., du Toit, M., Okada, S., et al. (2012). Characterization and emended description of *Lactobacillus kunkeei* as a fructophilic lactic acid bacterium. *Int. J. Syst. Evol. Microbiol.* 62, 500–504. doi: 10.1099/ijs.0.031054-0

Endo, A., Maeno, S., Tanizawa, Y., Kneifel, W., Arita, M., Dicks, L., et al. (2018). Fructophilic lactic acid bacteria, a unique group of fructose-fermenting microbes. *Appl. Environ. Microbiol.* 84:e01290-18. doi: 10.1128/AEM.01290-18

Endo, A., and Okada, S. (2008). Reclassification of the genus *Leuconostoc* and proposals of *Fructobacillus fructosus* gen. nov., comb. nov., *Fructobacillus durionis* comb. nov., *Fructobacillus ficulneus* comb. nov. and *Fructobacillus pseudoficulneus* comb. nov. *Int. J. Syst. Evol. Microbiol.* 58, 2195–2205. doi: 10.1099/ijs.0.65609-0

Endo, A., and Salminen, S. (2013). Honeybees and beehives are rich sources for fructophilic lactic acid bacteria. *Syst. Appl. Microbiol.* 36, 444–448. doi: 10.1016/J.SYAPM.2013.06.002

Endo, A., Tanizawa, Y., Tanaka, N., Maeno, S., Kumar, H., Shiwa, Y., et al. (2015). Comparative genomics of *Fructobacillus* spp. and *Leuconostoc* spp. reveals niche-specific evolution of *Fructobacillus* spp. *BMC Genomics* 16:1117. doi: 10.1186/s12864-015-2339-x

Ennahar, S., Asou, Y., Zendo, T., Sonomoto, K., and Ishizaki, A. (2001). Biochemical and genetic evidence for production of enterocins A and B by *Enterococcus faecium* WHE 81. *Int. J. Food Microbiol.* 70, 291–301. doi: 10.1016/S0168-1605(01)00565-7

Fujita, K., Ichimasa, S., Zendo, T., Koga, S., Yoneyama, F., Nakayama, J., et al. (2007). Structural analysis and characterization of lacticin Q, a novel bacteriocin belonging to a new family of unmodified bacteriocins of gram-positive bacteria. *Appl. Environ. Microbiol.* 73, 2871–2877. doi: 10.1128/AEM.02286-06

Fukao, M., Obita, T., Yoneyama, F., Kohda, D., Zendo, T., Nakayama, J., et al. (2008). Complete covalent structure of nisin Q, new natural nisin variant, containing post-translationally modified amino acids. *Biosci. Biotechnol. Biochem.* 72, 1750–1755. doi: 10.1271/bbb.80066

Garcia-Gutierrez, E., O'Connor, P. M., Saalbach, G., Walsh, C. J., Hegarty, J. W., Guinane, C. M., et al. (2020). First evidence of production of the lantibiotic nisin P. *Sci. Rep.* 10:3738. doi: 10.1038/s41598-020-60623-0

Geiger, C., Korn, S. M., Häsler, M., Peetz, O., Martin, J., Kötter, P., et al. (2019). LanI-mediated lantibiotic immunity in *Bacillus subtilis*: functional analysis. *Appl. Environ. Microbiol.* 85:e00534-19. doi: 10.1128/AEM.00534-19

Gross, E., and Morell, J. L. (1971). The structure of nisin. *J. Am. Chem. Soc.* 93, 4634–4635.

Hacker, C., Christ, N. A., Duchardt-Ferner, E., Korn, S., Göbl, C., Berninger, L., et al. (2015). The solution structure of the lantibiotic immunity protein NisI and its interactions with nisin. *J. Biol. Chem.* 290, 28869–28886. doi: 10.1074/jbc.M115.679969

Hammami, R., Zouhir, A., Le Lay, C., Ben Hamida, J., and Fliss, I. (2010). BACTIBASE second release: a database and tool platform for bacteriocin characterization. *BMC Microbiol.* 10:22. doi: 10.1186/1471-2180-10-22

Hatziioanou, D., Gherghisan-Filip, C., Saalbach, G., Horn, N., Wegmann, U., Duncan, S. H., et al. (2017). Discovery of a novel lantibiotic nisin O from *Blautia obeum* A2-162, isolated from the human gastrointestinal tract. *Microbiology* 163, 1292–1305. doi: 10.1099/mic.0.000515

Heunis, T. D. J., Smith, C., and Dicks, L. M. T. (2013). Evaluation of a nisin-eluting nanofiber scaffold to treat *Staphylococcus aureus*-induced skin infections in mice. *Antimicrob. Agents Chemother.* 57, 3928–3935. doi: 10.1128/AAC.00622-13

Kuipers, O. P., Beerthuyzen, M. M., de Ruyter, P. G., Luesink, E. J., and de Vos, W. M. (1995). Autoregulation of nisin biosynthesis in *Lactococcus lactis* by signal transduction. *J. Biol. Chem.* 270, 27299–27304.

Kuipers, O. P., Beerthuyzen, M. M., Siezen, R. J., and de Vos, W. M. (1993). Characterization of the nisin gene cluster *nisABTCIPR* of *Lactococcus lactis* requirement of expression of the *nisA* and *nisI* genes for development of immunity. *Eur. J. Biochem.* 216, 281–291. doi: 10.1111/j.1432-1033.1993.tb18143.x

Kwong, W. K., and Moran, N. A. (2016). Gut microbial communities of social bees. *Nat. Rev. Microbiol.* 14, 374–384. doi: 10.1038/nrmicro.2016.43

Maeno, S., Tanizawa, Y., Kanesaki, Y., Kubota, E., Kumar, H., Dicks, L., et al. (2016). Genomic characterization of a fructophilic bee symbiont *Lactobacillus kunkeei* reveals its niche-specific adaptation. *Syst. Appl. Microbiol.* 39, 516–526. doi: 10.1016/J.SYAPM.2016.09.006

Masuda, Y., Ono, H., Kitagawa, H., Ito, H., Mu, F., Sawa, N., et al. (2011). Identification and characterization of leucocyclicin Q, a novel cyclic: bacteriocin produced by *Leuconostoc mesenteroides* TK41401. *Appl. Environ. Microbiol.* 77:e06348-11. doi: 10.1128/AEM.06348-11

Meyer, H. E., Heber, M., Eisermann, B., Korte, H., Metzger, J. W., and Jung, G. (1994). Sequence analysis of lantibiotics: chemical derivatization procedures allow a fast access to complete Edman degradation. *Anal. Biochem.* 223, 185–190. doi: 10.1006/ABIO.1994.1571

Mulders, J. W., Boerrigter, I. J., Rollema, H. S., Siezen, R. J., and de Vos, W. M. (1991). Identification and characterization of the lantibiotic nisin Z, a natural nisin variant. *Eur. J. Biochem.* 201, 581–584. doi: 10.1111/j.1432-1033.1991.tb16317.x

Murray, K. D., and Aronstein, K. A. (2006). Oxytetracycline-resistance in the honey bee pathogen *Paenibacillus larvae* is encoded on novel plasmid pMA67. *J. Apic. Res.* 45, 207–214. doi: 10.1080/00218839.2006.11101349

Murray, K. D., Aronstein, K. A., and de León, J. H. (2007). Analysis of pMA67, a predicted rolling-circle replicating, mobilizable, tetracycline-resistance plasmid from the honey bee pathogen, *Paenibacillus larvae*. *Plasmid* 58, 89–100. doi: 10.1016/j.plasmid.2007.02.001

O'Connor, P. M., O'Shea, E. F., Guinane, C. M., O'Sullivan, O., Cotter, P. D., Ross, R. P., et al. (2015). Nisin H is a new nisin variant produced by the gut-derived strain *Streptococcus hyointestinalis* DPC6484. *Appl. Environ. Microbiol.* 81, 3953–3960. doi: 10.1128/AEM.00212-15

O'Sullivan, J. N., O'Connor, P. M., Rea, M. C., O'Sullivan, O., Walsh, C. J., Healy, B., et al. (2020). Nisin J, a novel natural nisin variant, is produced by *Staphylococcus capitis* sourced from the human skin microbiota. *J. Bacteriol.* 202:e0639-19. doi: 10.1128/JB.00639-19

Perez, R. H., Zendo, T., and Sonomoto, K. (2014). Novel bacteriocins from lactic acid bacteria (LAB): various structures and applications. *Microb. Cell Fact* 13:S3. doi: 10.1186/1475-2859-13-S1-S3

Plat, A., Kluskens, L. D., Kuipers, A., Rink, R., and Moll, G. N. (2011). Requirements of the engineered leader peptide of nisin for inducing modification, export, and cleavage. *Appl. Environ. Microbiol.* 77, 604–611. doi: 10.1128/AEM.01503-10

Rangberg, A., Mathiesen, G., Amdam, G. V., and Diep, D. B. (2015). The paratransgenic potential of *Lactobacillus kunkeei* in the honey bee *Apis mellifera*. *Benef. Microb.* 6, 513–523. doi: 10.3920/BM2014.0115

Raymann, K., Bobay, L.-M., and Moran, N. A. (2018). Antibiotics reduce genetic diversity of core species in the honeybee gut microbiome. *Mol. Ecol.* 27, 2057–2066. doi: 10.1111/mec.14434

Raymann, K., Shaffer, Z., and Moran, N. A. (2017). Antibiotic exposure perturbs the gut microbiota and elevates mortality in honeybees. *PLoS Biol.* 15:e2001861. doi: 10.1371/journal.pbio.2001861

Stein, T., Heinzmann, S., Düsterhus, S., Borchert, S., and Entian, K.-D. (2005). Expression and functional analysis of the subtilin immunity genes *spaIFEG* in the subtilin-sensitive host *Bacillus subtilis* MO1099. *J. Bacteriol.* 187, 822–828. doi: 10.1128/JB.187.3.822-828.2005

Stein, T., Heinzmann, S., Solovieva, I., and Entian, K.-D. (2003). Function of *Lactococcus lactis* nisin immunity genes *nisI* and *nisFEG* after coordinated expression in the surrogate host *Bacillus subtilis*. *J. Biol. Chem.* 278, 89–94. doi: 10.1074/jbc.M207237200

Tanizawa, Y., Fujisawa, T., Kaminuma, E., Nakamura, Y., and Arita, M. (2016). DFAST and DAGA: web-based integrated genome annotation tools and resources. *Biosci. Microbiota Food Health* 35, 173–184. doi: 10.12938/bmfh.16-003

Tian, B., Fadhil, N. H., Powell, J. E., Kwong, W. K., and Moran, N. A. (2012). Long-term exposure to antibiotics has caused accumulation of resistance determinants in the gut microbiota of honeybees. *mBio* 3:e0377-12. doi: 10.1128/mBio.00377-12

Van Heel, A. J., De Jong, A., Song, C., Viel, J. H., Kok, J., and Kuipers, O. P. (2018). BAGEL4: a user-friendly web server to thoroughly mine RiPPs and bacteriocins. *Nucleic Acids Res.* 46, W278–W281. doi: 10.1093/nar/gky383

Vojvodic, S., Rehan, S. M., and Anderson, K. E. (2013). Microbial gut diversity of Africanized and European honey bee larval instars. *PLoS One* 8:e72106. doi: 10.1371/journal.pone.0072106

Wirawan, R. E., Klesse, N. A., Jack, R. W., and Tagg, J. R. (2006). Molecular and genetic characterization of a novel nisin variant produced by *Streptococcus uberis*. *Appl. Environ. Microbiol.* 72, 1148–1156. doi: 10.1128/AEM.72.2.1148-1156.2006

Yoneyama, F., Fukao, M., Zendo, T., Nakayama, J., and Sonomoto, K. (2008). Biosynthetic characterization and biochemical features of the third natural nisin variant, nisin Q, produced by *Lactococcus lactis* 61-14. *J. Appl. Microbiol.* 105, 1982–1990. doi: 10.1111/j.1365-2672.2008.03958.x

Zendo, T., Fukao, M., Ueda, K., Higuchi, T., Nakayama, J., and Sonomoto, K. (2003). Identification of the lantibiotic nisin Q, a new natural nisin variant produced by *Lactococcus lactis* 61-14 isolated from a river in Japan. *Biosci. Biotechnol. Biochem.* 67, 1616–1619. doi: 10.1271/bbb.67.1616

Zheng, H., Powell, J. E., Steele, M. I., Dietrich, C., and Moran, N. A. (2017). Honeybee gut microbiota promotes host weight gain via bacterial metabolism and hormonal signaling. *Proc. Natl. Acad. Sci. U.S.A.* 114, 4775–4780. doi: 10.1073/pnas.1701819114

Zheng, J., Wittouck, S., Salvetti, E., Franz, C. M. A. P., Harris, H. M. B., Mattarelli, P., et al. (2020). A taxonomic note on the genus *Lactobacillus*: description of 23 novel genera, emended description of the genus *Lactobacillus* Beijerinck 1901, and union of *Lactobacillaceae* and *Leuconostocaceae*. *Int. J. Syst. Evol. Microbiol.* 70, 2782–2858. doi: 10.1099/ijsem.0.004107

Conflict of Interest: The authors declare that the research was conducted in the absence of any commercial or financial relationships that could be construed as a potential conflict of interest.

frontiers in Microbiology

MINI REVIEW
published: 18 September 2020
doi: 10.3389/fmicb.2020.575981

Bacteriocins Targeting Gram-Negative Phytopathogenic Bacteria: Plantibiotics of the Future

William M. Rooney[1,2†], Ray Chai[2†], Joel J. Milner[1] and Daniel Walker[2*]*

[1] Plant Science Group, School of Life Sciences, Institute of Molecular, Cell and Systems Biology, University of Glasgow, Glasgow, United Kingdom, [2] College of Medical, Veterinary and Life Sciences, Institute of Infection, Immunity and Inflammation, University of Glasgow, Glasgow, United Kingdom

Gram-negative phytopathogenic bacteria are a significant threat to food crops. These microbial invaders are responsible for a plethora of plant diseases and can be responsible for devastating losses in crops such as tomatoes, peppers, potatoes, olives, and rice. Current disease management strategies to mitigate yield losses involve the application of chemicals which are often harmful to both human health and the environment. Bacteriocins are small proteinaceous antibiotics produced by bacteria to kill closely related bacteria and thereby establish dominance within a niche. They potentially represent a safer alternative to chemicals when used in the field. Bacteriocins typically show a high degree of selectivity toward their targets with no off-target effects. This review outlines the current state of research on bacteriocins active against Gram-negative phytopathogenic bacteria. Furthermore, we will examine the feasibility of weaponizing bacteriocins for use as a treatment for bacterial plant diseases.

Keywords: bacteriocins, Gram-negative bacteria, phytopathogenic bacteria, plant disease, plant disease management, food security, crops

OPEN ACCESS

Edited by:
Mathew Upton, University of Plymouth, United Kingdom

Reviewed by:
Natalia Soledad Rios Colombo, CONICET Centro de Referencia para Lactobacilos (CERELA), Argentina
Ping Li, Zhejiang Gongshang University, China

***Correspondence:**
Joel J. Milner
Joel.Milner@glasgow.ac.uk
Daniel Walker
Daniel.Walker@glasgow.ac.uk

[†] These authors share first authorship

Specialty section:
This article was submitted to Antimicrobials, Resistance and Chemotherapy, a section of the journal Frontiers in Microbiology

Received: *24 June 2020*
Accepted: *25 August 2020*
Published: *18 September 2020*

Citation:
Rooney WM, Chai R, Milner JJ and Walker D (2020) Bacteriocins Targeting Gram-Negative Phytopathogenic Bacteria: Plantibiotics of the Future. Front. Microbiol. 11:575981. doi: 10.3389/fmicb.2020.575981

INTRODUCTION

By 2050 the global population is predicted to surpass 9 billion requiring food production to increase by 70%, equivalent to 127×10^{15} kcal (Cole et al., 2018). Major food crops suffer from a lack of genetic diversity allowing pathogens and pests to rapidly spread throughout fields and devastate crops, causing yield losses of up to 32% (Oerke and Dehne, 2004).

Gram-negative bacterial phytopathogens are an important contributor to crop losses due to plant disease (Mansfield et al., 2012). For example, *Pseudomonas syringae* pv. *actinidiae*, the causal agent of the kiwifruit canker pandemic, triggered enormous damage to the New Zealand economy (Vanneste et al., 2013) depreciating the land value of orchards growing the popular kiwifruit variety Hort16A from 300,000 to 46,000 USD per hectare (Vanneste, 2017). Enterobacterial soft rot phytopathogens such as *Pectobacterium* and *Dickeya* spp. are collectively responsible for diseases in potato like black leg and tuber soft rot pre- and post-harvest (Pérombelon, 2002; Toth et al., 2011). These diseases are responsible for losses of €30 m per annum in the Netherlands alone (Pérombelon, 2002; Toth et al., 2011).

Abbreviations: CLB, Colicin-like bacteriocin; GM, genetically modified; IDR, intrinsically disordered region; LLB, lectin-like bacteriocin; LPS, lipopolysaccharide; MMBL, monocot-mannose binding lectin; PL1, putidacin L1; TBDT, TonB-dependent transporter.

Bacteriocins are proteinaceous antibiotics that are produced by both Gram-positive and Gram-negative bacteria (Cascales et al., 2007; Chavan and Riley, 2007). They target and kill related bacterial strains allowing producing strains to establish dominance within a niche (Chavan and Riley, 2007). Unlike conventional small molecule antibiotics, bacteriocins exhibit a narrow killing spectrum and cause minimal disruption to the commensal bacterial community (Chavan and Riley, 2007). A number of classification systems have been proposed to encompass the diversity of bacteriocins (Heng and Tagg, 2006; Chavan and Riley, 2007; Cotter et al., 2013). The classification of Chavan and Riley (2007) is based on size, splitting the bacteriocins into three groups; small peptide bacteriocins of <10 kDa, colicin-like bacteriocins (CLBs) which are multidomain proteins of 25–80 kDa and tailocins, which are large phage-like multimeric protein assemblies. This review focuses on the latter two of these groups as there is a dearth of information on small peptide bacteriocins active against phytopathogenic bacteria. In addition, in this review we cover an additional group, the lectin-like bacteriocins (LLBs), which although they fall within the size range of CBLs, are mechanistically distinct. We also provide examples of some orphan bacteriocins.

Bacteriocins have been identified in a number of important plant pathogenic bacterial genera including *Xanthomonas*, *Pseudomonas*, *Pectobacterium*, and *Agrobacterium* (Holtsmark et al., 2008; Grinter et al., 2012a). These include many important pathogens of crops such as rice, banana, potato, olives, peppers and tomatoes (Mansfield et al., 2012). In this review, we aim to outline the present landscape of research into bacteriocin plantibiotics (biological agents which selectively kill plant pathogenic bacteria) and discuss the practicalities of exploiting them to remedy plant disease.

COLICIN-LIKE BACTERIOCINS

CLBs are multi-domain proteins that possess a modular domain structure usually consisting of translocation, receptor binding and cytotoxic domains. The translocation domain typically incorporates, or consists of an intrinsically disordered region (IDR) at the extreme N-terminus of the protein, which is first to cross the outer membrane during uptake (Behrens et al., 2020). To target a specific bacterial species, CLBs often parasitize existing nutrient uptake pathways involving TonB dependent transporters (TBDTs). These TBDTs are frequently involved with the uptake of iron siderophores and other metal chelate complexes, such as vitamin B_{12}, from the environment (Michel-Briand and Baysse, 2002; Cascales et al., 2007). For most CLBs the IDR and translocation domains facilitate the import of bacteriocins across the outer membrane into the periplasmic space. Briefly, this is achieved by the IDR threading through the pore of an outer membrane transporter and interacting with components of the proton-motive force (PMF) responsive Ton or Tol complexes in the periplasm. Subsequently, the bacteriocin is actively pulled through the transporter in a PMF-dependent manner to cross the outer membrane (White et al., 2017). Methods of killing mediated by CLB cytotoxic domains include endonuclease activity (DNase, tRNase, and rRNase), depolarization of the inner-membrane, and inhibition of peptidoglycan synthesis (Michel-Briand and Baysse, 2002; Cascales et al., 2007).

In *Pectobacterium carotovorum*, three CLB nucleases termed carocins have been characterized. Two of the carocins, S1K (40 kDa) and carocin D (91 kDa) are DNases while the third, S2 (85 kDa) is a tRNAse (Chuang et al., 2007; Chan et al., 2009, 2011; Roh et al., 2010; Atanaskovic et al., 2020). In addition, two pectobacterial CLBs, pectocins M1 and M2 (both 29 kDa) have been characterized that possess cytotoxic domains homologous to that of colicin M and have been shown to similarly target lipid II (Grinter et al., 2012b). Cleavage of lipid II by colicin M-like bacteriocins results in inhibition of peptidoglycan biosynthesis and cell death (Harkness and Ölschläger, 1991). Interestingly, pectocin M1 and M2 lack an IDR at their N-termini and instead contain a single globular domain N-terminal to the cytotoxic domain that is homologous in both sequence and structure to plant ferredoxin (**Figure 1**; Grinter et al., 2012b, 2014). Like plant ferredoxin, these CLBs also contain a 2Fe-2S iron sulfur cluster and as subsequent research has shown, have evolved to parasitize an existing ferredoxin uptake system utilized by *Pectobacterium* spp. to acquire iron from its plant hosts. Uptake of ferredoxin is mediated by the TBDT FusA and the TonB-like protein FusB which work in concert to translocate ferredoxin into the periplasm (Grinter et al., 2016; Wojnowska and Walker, 2020). FusB acts both in removal of the plug from the lumen of FusA and directly binding to ferredoxin mediating its active translocation across the outer membrane via the lumen of FusA (Wojnowska and Walker, 2020). Within the periplasm, the processing protease FusC cleaves ferredoxin in two specific locations releasing its iron into the periplasm (Mosbahi et al., 2018). Competition assays with spinach ferredoxin and killing assays under iron limiting conditions show that ferredoxin-containing bacteriocins are translocated using the same pathway (Grinter et al., 2012b). Bioinformatic analysis has revealed another putative pectobacterial bacteriocin, pectocin P (35 kDa), that also contains a ferredoxin domain (Grinter et al., 2012b). However, the cytotoxic domain of pectocin P shares structural homology to lysozyme implying that uptake using the ferredoxin domain can be utilized as a general translocation pathway to deliver cytotoxic proteins into the periplasm. Lastly, two CLBs from *P. syringae* have been reported, syringacin M (30 kDa), which shares homology with colicin M, and a nuclease bacteriocin, S_{E9a} (64 kDa) related to pyocin S2 (Grinter et al., 2012c; Hockett et al., 2017). Unlike the colicin M-like pectocins M1 and M2, syringacin M does possess an N-terminal IDR and so likely has an uptake mechanism that is similar to the well-characterized colicins from *E. coli* (Grinter et al., 2012c).

Analysis of mutations in bacteria grown in the presence of bacteriocins suggest that resistance usually results from changes in the bacteriocin receptor (Cascales et al., 2007; Inglis et al., 2016). However, the development of resistance in the wild is still poorly understood and it may also depend on additional factors involving the receptor. For example, in iron limiting conditions, resistance to pyocin S2 is subject to negative selection as its receptor is required for the uptake of iron (Inglis et al.,

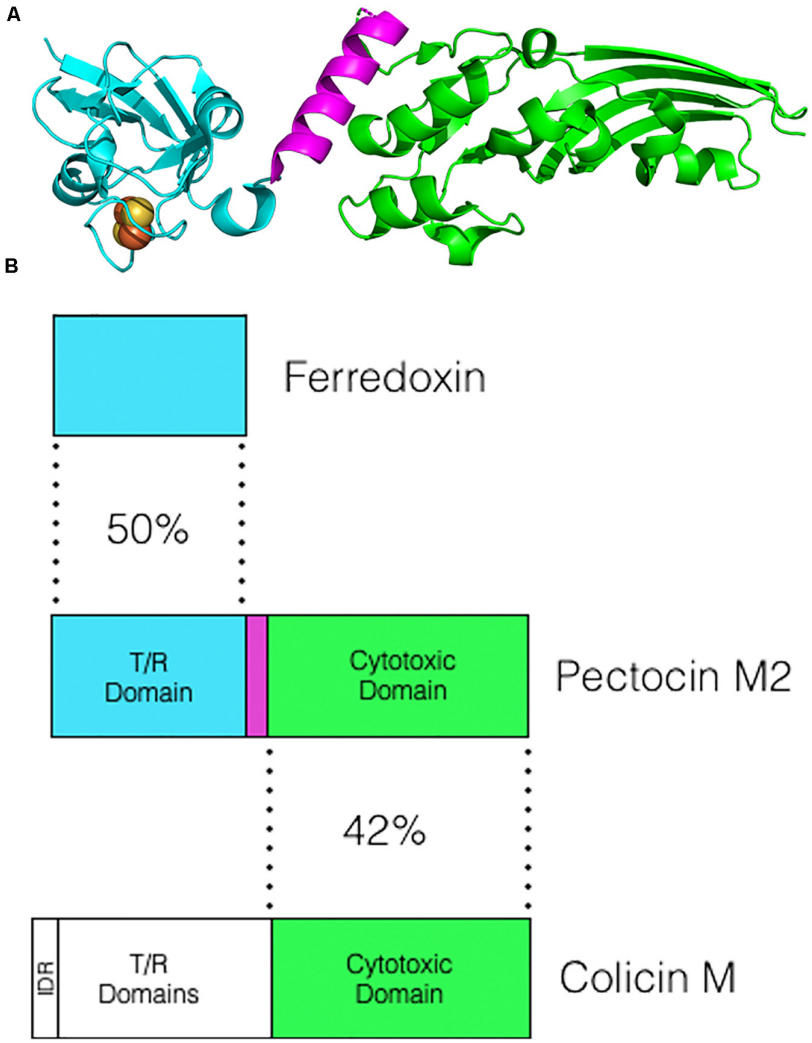

FIGURE 1 | Structure and homology of the ferredoxin containing pectocin M2. **(A)** The crystal structure of pectocin M2 (PDB:4N58). The ferredoxin domain is in cyan, the linker region in purple and the colicin M-like cytotoxic domain in green. The iron sulfur cluster located in the ferredoxin domain is represented as yellow and orange spheres. **(B)** The N-terminal domain of pectocin M2 (ZP_03825528) shares homology with spinach ferredoxin (1704156A). The C-terminal domain which is separated from the ferredoxin domain by a short helical linker shares homology with the lipid II-cleaving cytotoxic domain of colicin M (WP_000449474). Numbers shown are percentage identities calculated using the Needleman-Wunsch algorithm (Needle program) from EBI.

2016). As these receptors are typically involved in processes that are important for competition and cell survival, resistant strains tend to be less fit and show reduced pathogenicity in some environments.

LECTIN-LIKE BACTERIOCINS

LLBs are a distinct family of protein antibiotics found in *Pseudomonas*, *Burkholderia*, and *Xanthomonas* species (Ghequire et al., 2012a, 2013a). The hallmark of LLBs is the presence of monocot mannose-binding lectin (MMBLs) domains. MMBLs are expanded in both plants and animals and play a primitive defensive role against pests and pathogens (Ghequire et al., 2012b). LLBs possess at least 1 MMBL domain containing conserved QxDxNxVxYx sequences that constitute a carbohydrate-binding pocket. These MMBLs are instrumental in defining the selectivity of LLBs by enabling the docking onto D-rhamnose-containing lipopolysaccharide (LPS) on the cell surface (Ghequire et al., 2013b; McCaughey et al., 2014).

Our current understanding of LLBs arises predominantly from the study of pyocin L1 and putidacin L1 (PL1) isolated from *P. aeruginosa* and *P. putida*, respectively (Parret et al., 2003; McCaughey et al., 2014). PL1 (30 kDa) harbors 2 MMBL domains (**Figure 2A**) and phylogenetic analyses of the N- and C-terminal MMBL domains suggest distinct functions in LPS docking (Ghequire et al., 2013b). The N-terminal MMBL domains diverge substantially implying their importance in selectivity, whereas the C-terminal MMBL domains tightly cluster suggesting that their primary function are to bind to carbohydrates with high

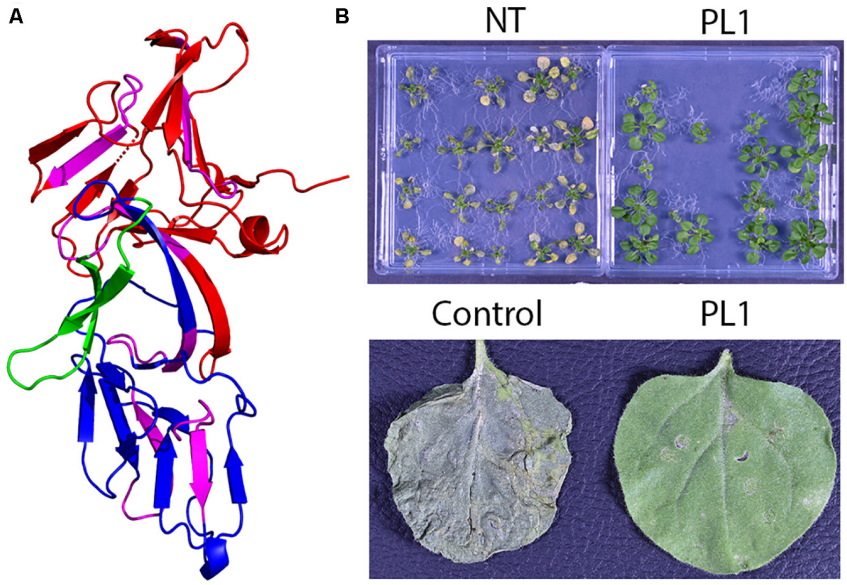

FIGURE 2 | LLBs can be provide robust disease resistance against *P. syringae*. **(A)** Structure of the LLB PL1 (PDB:4GC2). The N- and C-terminal MMBL domains are shown in red and blue, respectively, and C-terminal extension is shown in green. Within these domains the QxDxNxVxYx sugar binding motifs are shown in purple. The C-terminal extension is predicted to play a role in the cytotoxic action of PL1 by disrupting the function of BamA. **(B)** Non-transgenic (NT) vs. transgenic expression of PL1 in both Arabidopsis seedlings (upper panel) and *Nicotiniana benthamiana* leaves (lower panel) provides robust resistance against strains of *P. syringae* that are susceptible to PL1. These images were adapted from Rooney et al. (2019).

affinity (Ghequire et al., 2018b). Intriguingly, it was recently reported that LLBs containing 1 MMBL exhibit anti-microbial activity against Pseudomonads (Ghequire and De Mot, 2019). Although little is known about these bacteriocins isolated from soil- and plant-associated bacteria, their MMBLs share homology with the N-terminal MMBL domains of putidacin L1-type LLBs (Ghequire and De Mot, 2019).

Resistance to LLBs can arise from changes to LPS structure by susceptible bacteria (Ghequire et al., 2013b; McCaughey et al., 2014). However, LPS binding does not fully explain the selective nature of LLBs (Ghequire et al., 2013b). An exhaustive genetic study of resistant bacterial isolates identified novel changes in a surface-exposed extracellular loop of the outer membrane protein BamA (Ghequire et al., 2018a). BamA is a critical component of the β-barrel assembly machinery responsible for the chaperoning and insertion of β-barrel proteins into the outer membrane (Noinaj et al., 2017). Sequence alignments comparing PL1 sensitive and resistant strains identified the amino acid sequences of loop 6 of BamA as a genetic determinant of PL1 susceptibility. This was elegantly demonstrated when a "resistant" allele of BamA successfully rescued a PL1-sensitive strain from PL1-mediated killing *in vitro* (Ghequire et al., 2018a).

TAILOCINS

Tailocins are headless phage tail-like bacteriocins consisting of 8–14 individual components, including a sheath, core and baseplate (Ghequire et al., 2015b; Scholl, 2017). A producing cell releases 100s of particles and sometimes one particle is sufficient to eliminate a target cell (Scholl, 2017). Although tailocins from phytopathogenic bacteria share a high degree of similarity with contractile tail phages derived from *Myoviridae*, they have evolved independently, and represent an expansive group of protein complexes playing critical ecological roles like biofilm formation (Ghequire et al., 2015b; Turnbull et al., 2016). Tailocin-mediated killing occurs in two steps. Firstly, the tail fibers selectively bind to LPS of a target cell (Michel-Briand and Baysse, 2002). In turn, the sheath contracts and punctures the cell envelope, depolarizing the cell membrane and resulting in cell death (Scholl, 2017).

Tailocins are produced by a range of bacteria including *Pseudomonads* and *Pectobacterium* spp. (Nguyen et al., 2001; Hockett et al., 2015). Remarkably, tailocins from *P. syringae* have evolved independently of those of *P. aeruginosa* and do not share the same evolutionary ancestor (Ghequire and De Mot, 2015a; Hockett et al., 2015). This likely reflects the different environmental niches that *P. aeruginosa* and *P. syringae* occupy. Intriguingly, diversification and expansion of the tailocin family in *P. syringae* is driven by localized recombination of tailocin genes like those encoding the tail fibers (Baltrus et al., 2019).

Identification and genetic dissection of two distinct tailocins from *P. chlororaphis* has unmasked the robust competitive advantage tailocins provide in heterogeneous biofilms and the rhizosphere (Dorosky et al., 2017, 2018). Notably, *P. fluorescens* SF4c harbors a tailocin targeting *X. vesicatoria*, the causal agent of bacterial spot disease in tomatoes (Príncipe et al., 2018). In the case of *Pectobacterium* there are two highly similar tailocins, carotovoricin (Ctv)Er and CGE originating from *P. carotovorum IAM 1068* and *P. carotovorum* CGE234-M403,

respectively (Yamada et al., 2006). Indeed, both carotovoricins are identical apart from two 26 bp inverted repeats within and downstream of the tail fiber gene, which differentiates their killing spectrum (Nguyen et al., 2001). Notably, strains of *Pectobacterium* harboring CtvCGE are sold in Japan, under the name "Biokeeper" to manage bacterial soft rot infections in potatoes (Chuang et al., 1999).

Classically, tailocin tolerance arises from alterations in the LPS, enabling the targets to evade tailocin recognition (Scholl, 2017; Kandel et al., 2020). A recent study postulates that bacteria can persist in environments containing sub-lethal concentrations of tailocins (Kandel et al., 2020). Persistence is not a heritable genetic trait, and likely reflects heterogeneity of gene expression within a clonal population influenced by factors such as starvation and metabolic activity (Kandel et al., 2020). Persistence allows bacteria to bypass mutations which incur fitness costs providing the selective pressure is transient.

ORPHAN BACTERIOCINS AND PLANTIBIOTICS

Several bacteriocins from phytopathogens do not display homology with other well-characterized classes. For example, *X. campestris* pv. *glycines* 8ra produces a bacteriocin called glycinecin A (55 kDa), which is unusually encoded by two genes (Heu et al., 2001). Interestingly, although glycinecin A can be produced recombinantly in *E. coli*, active bacteriocin is only obtained when *glyA* and *glyB* are co-expressed in the same cell; active bacteriocin cannot be reconstituted by combining the two separately expressed polypeptides *in vitro* (Heu et al., 2001). There are two bacteriocins identified from *X. campestris* and *X. perforans*, glycinecin R, and BCN-A, containing Rhs repeats (pfam05593) which share homology with the toxin complex of the insect pathogen *Photorhabdus* (Roh et al., 2008; Marutani-Hert et al., 2020). The mode of action for these *Xanthomonas* bacteriocins are unknown.

The production of a very narrow spectrum bacteriocin-like substance agrocin 84 (1.4 kDa) by some non-pathogenic strains of *Agrobacterium tumefaciens* has been characterized and exploited to control crown gall diseases caused by pathogenic strains of *A. tumefaciens* (Kerr and Htay, 1974; Ellis et al., 1979). This small nucleotide antibiotic represses leucyl-tRNA synthetase activity (Tate et al., 1979; Kim et al., 2006). Remarkably, *A. tumefaciens* strains that successfully evolve resistance against agrocin 84 become non-pathogenic (Kerr, 1980). The success of agrocin 84 as a strategy to control crown gall disease resulted in the development of an agrocin 84-producing *A. tumefaciens* strain which was successfully trademarked and sold under the name Nogall by Bio-care Technology (Jones et al., 1988).

APPLICATIONS OF BACTERIOCINS AND FUTURE PERSPECTIVES

The control of bacterial phytopathogens in agriculture often relies on the application of chemicals containing copper or antibiotics, notably streptomycin. These often have detrimental impacts on human health and the environment and their long term success as a control measure can be limited by the development of resistance (Sundin and Bender, 1993; Damalas and Eleftherohorinos, 2011). For example, streptomycin treatment has been used extensively in orchards to mitigate diseases like fire blight and citrus greening. However, widespread applications of antibiotics in a field context has the potential to create reservoirs of resistance that can potentially transfer from plant pathogenic bacteria into bacterial pathogens of clinical importance (Norelli et al., 2003; McKenna, 2019).

A major driver of the success of the insecticidal protein *Bacillus thuringiensis* (Bt) toxin has been its high degree of target selectivity and its ease of expression *in planta*. Bacteriocins share similar characteristics. In both clinical and agricultural contexts this is highly advantageous as their use would be expected to cause minimal disruption to the microbiome. Like Bt toxins, bacteriocins can be expressed in plants or directly applied to crops. Nomad Biosciences have neatly illustrated the feasibility of expressing bacteriocins (LLBs and CLBs) in several plant species (Schulz et al., 2015; Paškevičius et al., 2017; Schneider et al., 2018). Furthermore, there is little evidence of bacteriocin toxicity in various animal models (Behrens et al., 2017). Bacteriocins are naturally produced by environmental bacteria, it is thought that they have limited toxicity toward humans, animals or benign environmental bacterial species and some bacteriocins are already classified as generally regarded as safe for use in food preservation (Schulz et al., 2015). As we have recently shown, bacteriocins can be expressed transgenically *in planta* to provide resistance against *P. syringae*. Expression of PL1 in two model plant species provided a strong resistance phenotype in plants challenged with several unrelated PL1-sensitive *P. syringae* field isolates (**Figure 2B**; Rooney et al., 2019) with bacterial titres in PL1 transgenic lines 1.5 log-units lower than in non-transgenic controls (Rooney et al., 2019).

Non-GM-based protocols for bacteriocin-based control measures include examples where non-pathogenic but bacteriocin producing strains of bacteria have been directly applied to crops, for example, Nogall and Biokeeper (Jones et al., 1988; Chuang et al., 1999). Alternatively, treatments using bacteriocins as a direct application to crops have shown promise in laboratory conditions against olive knot disease and bacterial spot disease of tomato (Lavermicocca et al., 2002; Príncipe et al., 2018). One potential issue in utilizing bacteriocins as a direct treatment is the requirement for large scale bacteriocin production. This maybe technically difficult for multi-component bacteriocins (e.g., tailocins) but should not be a problem for LLBs and CLBs where successful production *in planta* has already been demonstrated (Schulz et al., 2015; Paškevičius et al., 2017; Rooney et al., 2019).

The organization of bacteriocins into functional domains enables them to be readily engineered, providing a potential route for producing further variants by domain swapping to create new chimeric bacteriocins with altered target activities and modes of killing (Lukacik et al., 2012). Similarly, for CLBs appropriate domain swapping could yield chimeric bacteriocins for which there is no immunity protein-based resistance in the targeted

bacterial species (Akutsu et al., 1989). For tailocins, the exchange of tail fibers has already been shown to produce novel chimeras (Baltrus et al., 2019).

Despite the discovery and characterization of bacteriocins from phytopathogens, there is limited proof of a competitive advantage for the producing strain *in vivo*. Evidence suggests that soluble bacteriocins like CLBs function in the apoplastic space (endophytic fitness) whereas tailocins function in rhizosphere communities (epiphytic fitness) (Dorosky et al., 2018; Li et al., 2020). However, *in vitro* data suggests bacteriocins could work in concert in a conditionally redundant manner (Hockett et al., 2017).

Overall, bacteriocins represent an under-utilized resource of disease control. In the age of metagenomics, this can be easily remedied by the swift identification and characterization of new bacteriocins. This would allow bacteriocins to be rapidly deployed against current and emerging threats to important food crops.

AUTHOR CONTRIBUTIONS

WR, RC, JM, and DW contributed to the original manuscript and the editorial changes. All authors contributed to the article and approved the submitted version.

FUNDING

This work was funded by the BBSRC (Grant Refs: BB/T004207/1 and BB/L02022X/1).

REFERENCES

Akutsu, A., Masaki, H., and Ohta, T. (1989). Molecular structure and immunity specificity of colicin E6, an evolutionary intermediate between E-group colicins and cloacin DF13. *J. Bacteriol.* 171, 6430–6436. doi: 10.1128/jb.171.12.6430-6436.1989

Atanaskovic, I., Mosbahi, K., Sharp, C., Housden, N. G., Kaminska, R., Walker, D., et al. (2020). Targeted killing of *Pseudomonas aeruginosa* by Pyocin G occurs via the hemin transporter Hur. *J. Mol. Biol.* 432, 3869–3880. doi: 10.1016/j.jmb.2020.04.020

Baltrus, D. A., Clark, M., Smith, C., and Hockett, K. L. (2019). Localized recombination drives diversification of killing spectra for phage-derived syringacins. *ISME J.* 13, 237–249. doi: 10.1038/s41396-018-0261-3

Behrens, H. M., Lowe, E. D., Gault, J., Housden, N. G., Kaminska, R., Weber, T. M., et al. (2020). Pyocin S5 import into *Pseudomonas aeruginosa* reveals a generic mode of bacteriocin transport. *mBio* 11:e3230-19.

Behrens, H. M., Six, A., Walker, D., and Kleanthous, C. (2017). The therapeutic potential of bacteriocins as protein antibiotics. *Emerg. Top. Life Sci.* 1, 65–74. doi: 10.1042/etls20160016

Cascales, E., Buchanan, S. K., Duche, D., Kleanthous, C., Lloubes, R., Postle, K., et al. (2007). Colicin biology. *Microbiol. Mol. Biol. Rev.* 71, 158–229.

Chan, Y. C., Wu, H. P., and Chuang, D. Y. (2009). Extracellular secretion of Carocin S1 in *Pectobacterium carotovorum* subsp. *carotovorum* occurs via the type III secretion system integral to the bacterial flagellum. *BMC Microbiol.* 9:181. doi: 10.1186/1471-2180-9-181

Chan, Y. C., Wu, J. L., Wu, H. P., Tzeng, K. C., and Chuang, D. Y. (2011). Cloning, purification, and functional characterization of Carocin S2, a ribonuclease bacteriocin produced by *Pectobacterium carotovorum*. *BMC Microbiol.* 11:99. doi: 10.1186/1471-2180-11-99

Chavan, M. A., and Riley, M. A. (2007). *Molecular Evolution of Bacteriocins in Gram-Negative Bacteria. In*: *Bacteriocins Ecology and Evolution*. Berlin: Springer, 19–43.

Chuang, D. Y., Chien, Y. C., and Wu, H. P. (2007). Cloning and expression of the *Erwinia carotovora* subsp. *carotovora* gene encoding the low-molecular-weight bacteriocin carocin S1. *J. Bacteriol.* 189, 620–626. doi: 10.1128/jb.01090-06

Chuang, D. Y., Kyeremeh, A. G., Gunji, Y., Takahara, Y., Ehara, Y., and Kikumoto, T. (1999). Identification and cloning of an *Erwinia carotovora* subsp. *carotovora* bacteriocin regulator gene by insertional mutagenesis. *J. Bacteriol.* 181, 1953–1957. doi: 10.1128/jb.181.6.1953-1957.1999

Cole, M. B., Augustin, M. A., Robertson, M. J., and Manners, J. M. (2018). The science of food security. *NPJ Sci. Food* 2:14.

Cotter, P. D., Ross, R. P., and Hill, C. (2013). Bacteriocins-a viable alternative to antibiotics? *Nat. Rev. Microbiol.* 11, 95–105. doi: 10.1038/nrmicro2937

Damalas, C. A., and Eleftherohorinos, I. G. (2011). Pesticide exposure, safety issues, and risk assessment indicators. *Int. J. Environ. Res. Public Health* 8, 1402–1419. doi: 10.3390/ijerph8051402

Dorosky, R. J., Pierson, L. S., and Pierson, E. A. (2018). *Pseudomonas chlororaphis* produces multiple R-tailocin particles that broaden the killing spectrum and contribute to persistence in rhizosphere communities. *Appl. Environ. Microbiol.* 84:e01230-18. doi: 10.1128/AEM.01230-18

Dorosky, R. J., Yu, J. M., Pierson, L. S., and Pierson, E. A. (2017). *Pseudomonas chlororaphis* produces two distinct R-tailocins that contribute to bacterial competition in biofilms and on roots. *Appl. Environ. Microbiol.* 83:e00706-17. doi: 10.1128/AEM.00706-17

Ellis, J. G., Kerr, A., Van Montagu, M., and Schell, J. (1979). Agrobacterium: genetic studies on agrocin 84 production and the biological control of crown gall. *Physiol. Plant Pathol.* 15, 311–316. doi: 10.1016/0048-4059(79)90082-1

Ghequire, M. G. K., De Canck, E., Wattiau, P., Van Winge, I., Loris, R., Coenye, T., et al. (2013a). Antibacterial activity of a lectin-like *Burkholderia cenocepacia* protein. *MicrobiologyOpen* 2, 566–575. doi: 10.1002/mbo3.95

Ghequire, M. G. K., and De Mot, R. (2015a). The tailocin tale: peeling off phage tails. *Trends Microbiol.* 23, 587–590. doi: 10.1016/j.tim.2015.07.011

Ghequire, M. G. K., and De Mot, R. (2019). LlpB represents a second subclass of lectin-like bacteriocins. *Microbial Biotechnol.* 12, 567–573. doi: 10.1111/1751-7915.13373

Ghequire, M. G. K., Dillen, Y., Lambrichts, I., Proost, P., Wattiez, R., and De Mot, R. (2015b). Different ancestries of R tailocins in rhizospheric *Pseudomonas* isolates. *Genome Biol. Evol.* 7, 2810–2828. doi: 10.1093/gbe/evv184

Ghequire, M. G. K., Garcia-Pino, A., Lebbe, E. K. M., Spaepen, S., Loris, R., and de Mot, R. (2013b). Structural determinants for activity and specificity of the bacterial toxin LlpA. *PLoS Pathog.* 9:e1003199. doi: 10.1371/journal.ppat.1003199

Ghequire, M. G. K., Li, W., Proost, P., Loris, R., and De Mot, R. (2012b). Plant lectin-like antibacterial proteins from phytopathogens *Pseudomonas syringae* and *Xanthomonas citri*. *Environ. Microbiol. Rep.* 4, 373–380. doi: 10.1111/j.1758-2229.2012.00331.x

Ghequire, M. G. K., Loris, R., and De Mot, R. (2012a). MMBL proteins: from lectin to bacteriocin. *Biochem. Soc. Trans.* 40, 1553–1559. doi: 10.1042/bst20120170

Ghequire, M. G. K., Öztürk, B., and De Mot, R. (2018a). Lectin-like bacteriocins. *Front. Microbiol.* 9:2706. doi: 10.3389/fmicb.2018.02706

Ghequire, M. G. K., Swings, T., Michiels, J., Buchanan, S. K., and De Mot, R. (2018b). Hitting with a BAM: selective killing by lectin-like bacteriocins. *mBio* 9:e02138-17.)

Grinter, R., Josts, I., Mosbahi, K., Roszak, A. W., Cogdell, R. J., and Bonvin, A. M. J. J. (2016). Structure of the bacterial plant-ferredoxin receptor FusA. *Nat. Commun.* 7:133308. doi: 10.1038/ncomms13308

Grinter, R., Josts, I., Zeth, K., Roszak, A. W., Mccaughey, L. C., Cogdell, R. J., et al. (2014). Structure of the atypical bacteriocin pectocin M2 implies a novel mechanism of protein uptake. *Mol. Microbiol.* 93, 234–246. doi: 10.1111/mmi.12655

Grinter, R., Milner, J., and Walker, D. (2012a). Bacteriocins active against plant pathogenic bacteria. *Biochem. Soc. Trans.* 40, 1498–1502. doi: 10.1042/bst20120206

Grinter, R., Milner, J., and Walker, D. (2012b). Ferredoxin containing bacteriocins suggest a novel mechanism of iron uptake in *Pectobacterium* spp. *PLoS One* 7:e33033. doi: 10.1371/journal.pone.0033033

Grinter, R., Roszak, A. W., Cogdell, R. J., Milner, J. J., and Walker, D. (2012c). The crystal structure of the lipid II-degrading bacteriocin syringacin M suggests unexpected evolutionary relationships between colicin M-like bacteriocins. *J. Biol. Chem.* 287, 38876–38888. doi: 10.1074/jbc.m112.400150

Harkness, R. E., and Ölschläger, T. (1991). The biology of colicin M. *FEMS Microbiol. Lett.* 8, 27–41.

Heng, N. C. K., and Tagg, J. R. (2006). What's in a name? Class distinction for bacteriocins. *Nat. Rev. Microbiol.* 4:160. doi: 10.1038/nrmicro1273-c2

Heu, S., Oh, J., Kang, Y., Ryu, S., Cho, S. K., Cho, Y., et al. (2001). gly Gene cloning and expression and purification of glycinecin A, a bacteriocin produced by *Xanthomonas campestris* pv. *glycines* 8ra. *Appl. Environ. Microbiol.* 67, 4105–4110. doi: 10.1128/aem.67.9.4105-4110.2001

Hockett, K. L., Clark, M., Scott, S., and Baltrus, D. A. (2017). Conditionally redundant bacteriocin targeting by *Pseudomonas* syringae. *bioRxiv [Preprint]*. doi: 10.1101/167593

Hockett, K. L., Renner, T., and Baltrus, D. A. (2015). Independent co-option of a tailed bacteriophage into a killing complex in *Pseudomonas*. *mBio* 6:e00452-15. doi: 10.1128/mBio.00452-15

Holtsmark, I., Eijsink, V. G. H., and Brurberg, M. B. (2008). Bacteriocins from plant pathogenic bacteria. *FEMS Microbiol. Lett.* 280, 1–7. doi: 10.1111/j.1574-6968.2007.01010.x

Inglis, R. F., Scanlan, P., and Buckling, A. (2016). Iron availability shapes the evolution of bacteriocin resistance in *Pseudomonas aeruginosa*. *ISME J.* 10, 2060–2066. doi: 10.1038/ismej.2016.15

Jones, D. A., Ryder, M. H., Clare, B. G., Farrand, S. K., and Kerr, A. (1988). Construction of a Tra - deletion mutant of pAgK84 to safeguard the biological control of crown gall. *MGG Mol. Gen. Genet.* 212, 207–214. doi: 10.1007/bf00334686

Kandel, P. P., Baltrus, D. A., and Hockett, K. L. (2020). *Pseudomonas* can survive tailocin killing via persistence-like and heterogenous resistance mechanisms. *J. Bacteriol.* 202:e00142-20. doi: 10.1128/JB.00142-20

Kerr, A. (1980). Biological control of crown gall through production of Agrocin 84. *Plant Dis.* 64, 25–30.

Kerr, A., and Htay, K. (1974). Biological control of crown gall through bacteriocin production. *Physiol. Plant Pathol.* 4, 37–40. doi: 10.1016/0048-4059(74)90042-3

Kim, J. G., Byoung, K. P., Sung-Uk, K., Doil, C., Baek, H. N., Jae, S. M., et al. (2006). Bases of biocontrol: sequence predicts synthesis and mode of action of agrocin 84, the Trojan Horse antibiotic that controls crown gall. *Proc. Natl. Acad. Sci.* 103, 8846–8851. doi: 10.1073/pnas.0602965103

Lavermicocca, P., Lisa Lonigro, S., Valerio, F., Evidente, A., and Visconti, A. (2002). Reduction of olive knot disease by a bacteriocin from *Pseudomonas syringae* pv. *ciccaronei*. *Appl. Environ. Microbiol.* 68, 1403–1407. doi: 10.1128/aem.68.3.1403-1407.2002

Li, J. Z., Zhou, L. Y., Peng, Y. L., and Fan, J. (2020). *Pseudomonas* bacteriocin syringacin M released upon desiccation suppresses the growth of sensitive bacteria in plant necrotic lesions. *Microbial Biotechnol.* 13, 134–147. doi: 10.1111/1751-7915.13367

Lukacik, P., Barnard, T. J., Keller, P. W., Chaturvedi, K. S., Seddiki, N., Fairman, J. W., et al. (2012). Structural engineering of a phage lysin that targets Gram-negative pathogens. *Proc. Natl. Acad. Sci. U.S.A.* 109, 9857–9862. doi: 10.1073/pnas.1203472109

Mansfield, J., Genin, S., Magori, S., Citovsky, V., Sriariyanum, M., Ronald, P., et al. (2012). Top 10 plant pathogenic bacteria in molecular plant pathology. *Mol. Plant Pathol.* 13, 614–629. doi: 10.1111/j.1364-3703.2012.00804.x

Marutani-Hert, M., Hert, A. P., Tudor-Nelson, S. M., Preston, J. F., Minsavage, G. V., Stall, R. E., et al. (2020). Characterization of three novel genetic loci encoding bacteriocins associated with *Xanthomonas perforans*. *PLoS One* 15:e0233301. doi: 10.1371/journal.pone.0233301

McCaughey, L. C., Grinter, R., Josts, I., Roszak, A. W., Waløen, K. I., Cogdell, R. J., et al. (2014). Lectin-like bacteriocins from *Pseudomonas* spp. Utilise D-Rhamnose Containing Lipopolysaccharide as a Cellular Receptor. *PLoS Pathog.* 10:e1003898. doi: 10.1371/journal.ppat.1003898

McKenna, M. (2019). Antibiotics set to flood Florida's troubled orange orchards. *Nature* 567, 302–303. doi: 10.1038/d41586-019-00878-874

Michel-Briand, Y., and Baysse, C. (2002). The pyocins of *Pseudomonas aeruginosa*. *Biochimie* 26, 329–336.

Mosbahi, K., Wojnowska, M., Albalat, A., and Walker, D. (2018). Bacterial iron acquisition mediated by outer membrane translocation and cleavage of a host protein. *Proc. Natl. Acad. Sci. U.S.A.* 115, 6840–6845. doi: 10.1073/pnas.1800672115

Nguyen, H. A., Tomita, T., Hirota, M., Kaneko, J., Hayashi, T., and Kamio, Y. (2001). DNA inversion in the tail fiber gene alters the host range specificity of carotovoricin Er, a phage-tail-like bacteriocin of phytopathogenic *Erwinia carotovora* subsp. *carotovora Er*. *J. Bacteriol.* 183, 6274–6281. doi: 10.1128/jb.183.21.6274-6281.2001

Noinaj, N., Gumbart, J. C., and Buchanan, S. K. (2017). The β-barrel assembly machinery in motion. *Nat. Rev. Microbiol.* 15, 197–204. doi: 10.1038/nrmicro.2016.191

Norelli, J. L., Jones, A. L., and Aldwinckle, H. S. (2003). Fire blight management in the twenty-first century: using new technologies that enhance host resistance in apple. *Plant Dis.* 87, 756–765. doi: 10.1094/pdis.2003.87.7.756

Oerke, E. C., and Dehne, H. W. (2004). Safeguarding production—losses in major crops and the role of crop protection. *Crop Protect.* 23, 275–285. doi: 10.1016/j.cropro.2003.10.001

Parret, A. H. A., Schoofs, G., Proost, P., and De Mot, R. (2003). Plant lectin-like bacteriocin from a rhizosphere-colonizing *Pseudomonas* isolate. *J. Bacteriol.* 185, 897–908. doi: 10.1128/jb.185.3.897-908.2003

Paškevičius, Š, Starkevič, U., Misiūnas, A., Vitkauskienė, A., Gleba, Y., and Ražanskienė, A. (2017). Plant-expressed pyocins for control of *Pseudomonas aeruginosa*. *PLoS One* 12:e0185782. doi: 10.1371/journal.pone.0185782

Pérombelon, M. C. M. (2002). Potato diseases caused by soft rot erwinias: an overview of pathogenesis. *Plant Pathol.* 51, 1–12. doi: 10.1046/j.0032-0862.2001.short

Príncipe, A., Fernandez, M., Torasso, M., Godino, A., and Fischer, S. (2018). Effectiveness of tailocins produced by prin in controlling the bacterial-spot disease in tomatoes caused by *Xanthomonas vesicatoria*. *Microbiol. Res.* 213, 94–102. doi: 10.1016/j.micres.2018.05.010

Roh, E., Heu, S., and Moon, E. (2008). Genus-specific distribution and pathovar-specific variation of the glycinecin R gene homologs in Xanthomonas genomes. *J. Microbiol.* 46, 681–686. doi: 10.1007/s12275-008-0209-9

Roh, E., Park, T. H., Lee, S., Ryu, S., Oh, C. S., Rhee, S., et al. (2010). Characterization of a new bacteriocin, carocin D, from *Pectobacterium carotovorum* subsp. *carotovorum Pcc*21. *Appl. Environ. Microbiol.* 76, 7541–7549. doi: 10.1128/aem.03103-09

Rooney, W. M., Grinter, R. W., Correia, A., Parkhill, J., Walker, D. C., and Milner, J. J. (2019). Engineering bacteriocin-mediated resistance against the plant pathogen *Pseudomonas syringae*. *Plant Biotechnol. J.* 18, 1296–1306. doi: 10.1111/pbi.13294

Schneider, T., Hahn-Löbmann, S., Stephan, A., Schulz, S., Giritch, A., Naumann, M., et al. (2018). Plant-made *Salmonella* bacteriocins salmocins for control of *Salmonella* pathovars. *Sci. Rep.* 8:4078. doi: 10.1038/s41598-018-22465-9

Scholl, D. (2017). Phage tail–like bacteriocins. *Ann. Rev. Virol.* 4, 453–467. doi: 10.1146/annurev-virology-101416-041632

Schulz, S., Stephan, A., Hahn, S., Bortesi, L., Jarczowski, F., Bettmann, U., et al. (2015). Broad and efficient control of major foodborne pathogenic strains of *Escherichia coli* by mixtures of plant-produced colicins. *Proc. Natl. Acad. Sci. U.S.A.* 112, E5454–E5460.

Sundin, G. W., and Bender, C. L. (1993). Ecological and genetic analysis of copper and streptomycin resistance in *Pseudomonas syringae* pv. *syringae*. *Appl. Environ. Microbiol.* 59, 1018–1024. doi: 10.1128/aem.59.4.1018-1024.1993

Tate, M. E., Murphy, P. J., Roberts, W. P., and Kerr, A. (1979). Adenine N6-substituent of agrocin 84 determines its bacteriocin-like specificity [21]. *Nature* 280, 697–699. doi: 10.1038/280697a0

Toth, I. K., van der Wolf, J. M., Saddler, G., Lojkowska, E., Hélias, V., Pirhonen, M., et al. (2011). Dickeya species: an emerging problem for potato production in Europe. *Plant Pathol.* 60, 385–399. doi: 10.1111/j.1365-3059.2011.02427.x

Turnbull, L., Toyofuku, M., Hynen, A. L., Kurosawa, M., Pessi, G., Petty, N. K., et al. (2016). Explosive cell lysis as a mechanism for the biogenesis of bacterial membrane vesicles and biofilms. *Nat. Commun.* 7:11220. doi: 10.1038/ncomms11220

Vanneste, J. L. (2017). The scientific, economic, and social impacts of the New Zealand outbreak of bacterial canker of Kiwifruit (*Pseudomonas syringae* pv. *actinidiae*). *Ann. Rev. Phytopathol.* 55, 377–399. doi: 10.1146/annurev-phyto-080516-035530

Vanneste, J. L., Yu, J., Cornish, D. A., Tanner, D. J., Windner, R., Chapman, J. R., et al. (2013). Identification, virulence, and distribution of two biovars of *Pseudomonas syringae* pv. *actinidiae in New Zealand*. *Plant Dis.* 97, 708–719. doi: 10.1094/pdis-07-12-0700-re

White, P., Joshi, A., Rassam, P., Housden, N. G., Kaminska, R., Goult, J. D., et al. (2017). Exploitation of an iron transporter for bacterial protein antibiotic import. *Proc. Natl. Acad. Sci. U.S.A.* 114, 12051–12056. doi: 10.1073/pnas.1713741114

Wojnowska, M., and Walker, D. (2020). FusB energises import across the outer membrane through direct interaction with its ferredoxin substrate. *bioRxiv[Preprint]*. doi: 10.1101/749960

Yamada, K., Hirota, M., Niimi, Y., Nguyen, H. A., Takahara, Y., Kamio, Y., et al. (2006). Nucleotide sequences and organization of the genes for carotovoricin (Ctv) from *Erwinia carotovora* indicate that Ctv evolved from the same ancestor as *Salmonella* typhi prophage. *Biosci. Biotechnol. Biochem.* 70, 2236–2247. doi: 10.1271/bbb.60177

Conflict of Interest: The University of Glasgow has filed a patent on the transgenic expression of PL1 in plants with WR, JM, and DW listed as inventors (PCT/EP2018/057826).

The remaining author declares that the research was conducted in the absence of any commercial or financial relationships that could be construed as a potential conflict of interest.

frontiers in Microbiology

ORIGINAL RESEARCH
published: 20 October 2020
doi: 10.3389/fmicb.2020.573614

Insights in the Antimicrobial Potential of the Natural Nisin Variant Nisin H

Jens Reiners[1,2†], Marcel Lagedroste[1†], Julia Gottstein[1], Emmanuel T. Adeniyi[3], Rainer Kalscheuer[3], Gereon Poschmann[4], Kai Stühler[4,5], Sander H. J. Smits[1,2] and Lutz Schmitt[1*]*

[1] Institute of Biochemistry, Heinrich-Heine-University Düsseldorf, Düsseldorf, Germany, [2] Center for Structural Studies, Heinrich-Heine-University Düsseldorf, Düsseldorf, Germany, [3] Institute of Pharmaceutical Biology and Biotechnology, Heinrich-Heine-University Düsseldorf, Düsseldorf, Germany, [4] Institute for Molecular Medicine, Medical Faculty, Heinrich-Heine-University Düsseldorf, Düsseldorf, Germany, [5] Molecular Proteomics Laboratory, BMFZ, Heinrich-Heine-University-Düsseldorf, Düsseldorf, Germany

OPEN ACCESS

Edited by:
Des Field, University College Cork, Ireland

Reviewed by:
Oscar P. Kuipers, University of Groningen, Netherlands
Stefano Donadio, Naicons Srl, Italy

***Correspondence:**
Lutz Schmitt
lutz.schmitt@hhu.de
Sander H. J. Smits
sander.smits@hhu.de

[†] *These authors have contributed equally to this work*

Specialty section:
This article was submitted to Antimicrobials, Resistance and Chemotherapy, a section of the journal Frontiers in Microbiology

Received: *17 June 2020*
Accepted: *25 September 2020*
Published: *20 October 2020*

Citation:
Reiners J, Lagedroste M, Gottstein J, Adeniyi ET, Kalscheuer R, Poschmann G, Stühler K, Smits SHJ and Schmitt L (2020) Insights in the Antimicrobial Potential of the Natural Nisin Variant Nisin H. Front. Microbiol. 11:573614. doi: 10.3389/fmicb.2020.573614

Lantibiotics are a growing class of antimicrobial peptides, which possess antimicrobial activity against mainly Gram-positive bacteria including the highly resistant strains such as methicillin-resistant *Staphylococcus aureus* or vancomycin-resistant enterococci. In the last decades numerous lantibiotics were discovered in natural habitats or designed with bioengineering tools. In this study, we present an insight in the antimicrobial potential of the natural occurring lantibiotic nisin H from *Streptococcus hyointestinalis* as well as the variant nisin H F_1I. We determined the yield of the heterologously expressed peptide and quantified the cleavage efficiency employing the nisin protease NisP. Furthermore, we analyzed the effect on the modification via mass spectrometry analysis. With standardized growth inhibition assays we benchmarked the activity of pure nisin H and the variant nisin H F_1I, and their influence on the activity of the nisin immunity proteins NisI and NisFEG from *Lactococcus lactis* and the nisin resistance proteins *Sa*NSR and *Sa*NsrFP from *Streptococcus agalactiae* COH1. We further checked the antibacterial activity against clinical isolates of *Staphylococcus aureus*, *Enterococcus faecium* and *Enterococcus faecalis* via microdilution method. In summary, nisin H and the nisin H F_1I variant possessed better antimicrobial potency than the natural nisin A.

Keywords: lantibiotics, nisin, nisin H, MS analysis, antimicrobial activity

INTRODUCTION

Lantibiotics (lanthionine containing antibiotics) are a growing class of antimicrobial peptides (AMPs), which posses antimicrobial activity even against highly resistant strains such as methicillin-resistant *Staphylococcus aureus* (MRSA) or vancomycin-resistant *enterococci* (VRE) and some are already in pre-clinical trials (Mota-Meira et al., 2000; Jabes et al., 2011; Dawson and Scott, 2012; Crowther et al., 2013; Dischinger et al., 2014; Ongey et al., 2017; Brunati et al., 2018; Sandiford, 2019). Lantibiotics are peptides, containing 19–38 amino acids and are mainly produced by Gram-positive bacteria (Klaenhammer, 1993; Sahl and Bierbaum, 1998). In the last decades an increasing number of lantibiotic gene clusters were found by data-mining approaches using tools such as BAGEL4 (van Heel et al., 2018).

The best studied lantibiotic is nisin, which was first discovered in 1928 by Rogers and Whittier and belongs to the class I lantibiotics (Rogers, 1928; Rogers and Whittier, 1928; Arnison et al., 2013). It is used in the food industry since 1953 and obtained the status as generally recognized as safe (GRAS) in 1988 from the Food and Drug Administration (FDA) (Delves-Broughton et al., 1996). The class I lantibiotic nisin contains 34 amino acids and five (methyl)-lanthionine rings. These (methyl)-lanthionine rings require multiple posttranslational modifications (PTMs) which are introduced in the precursor peptide. First, the serine and threonine residues in the core peptide are dehydrated by a specific dehydratase NisB (lantibiotic class I LanB dehydratase) (Kaletta and Entian, 1989; Karakas Sen et al., 1999; Koponen et al., 2002; Ortega et al., 2015; Repka et al., 2017). The next step is a Michael-type condensation of dehydrated residues with the thiol group of a cysteine residue, thereby forming (methyl)-lanthionine rings, guided in a regio- and stereospecific manner by the cyclase NisC (class I lantibiotic cyclase) (Okeley et al., 2003; Li et al., 2006; Li and van der Donk, 2007; Repka et al., 2017). These characteristic (methyl)-lanthionine rings give lantibiotics high heat stability, resistance against proteolytic digestion and are responsible for the nanomolar antimicrobial activity (Gross and Morell, 1967; Rollema et al., 1995; Chan et al., 1996; Lu et al., 2010; Oppedijk et al., 2016).

The sequence of nisin A can be subdivided into three parts (see **Figure 1**). The N-terminal part with ring A, B, and C is responsible for binding to the cell wall precursor lipid II (Hsu et al., 2004). The hinge region is very flexible and allows reorientation of the C-terminal part to insert into the membrane (van Heusden et al., 2002; Hasper et al., 2004; Wiedemann et al., 2004; Medeiros-Silva et al., 2018), while changes in this region have a strong impact on the target antimicrobial activity (Zhou et al., 2015; Zaschke-Kriesche et al., 2019b). After penetrating the membrane, the C-terminal part with ring D and E forms a stable pore with a stoichiometry of eight nisin and four lipid II molecules, which subsequently leads to rapid cell death (Hasper et al., 2004; Wiedemann et al., 2004; Alkhatib et al., 2014a; Medeiros-Silva et al., 2018).

Unfortunately, some bacteria established resistance mechanism against lantibiotics. For instance lantibiotic producing strains express the immunity system LanI and LanFEG (Alkhatib et al., 2014a,b), which prevent a suicidal effect after the lantibiotic is secreted. In the case of nisin A from *Lactococcus lactis* these proteins are called NisI and NisFEG. But also non-lantibiotic producing strains showed resistance against lantibiotics like *Streptococcus agalactiae* COH1, which arises from the expression of the membrane-anchored peptidase *Sa*NSR and the ABC transporter *Sa*NsrFP (Khosa et al., 2013, 2016a,b; Reiners et al., 2017).

Several natural nisin variants have been discovered and up to now eight are known. First of all nisin A from *L. lactis* (Rogers and Whittier, 1928), nisin Z from *L. lactis* NIZO 221 86 (Mulders et al., 1991), nisin F from *L. lactis* F10 (de Kwaadsteniet et al., 2008), nisin Q from *L. lactis* 61-14 (Zendo et al., 2003), nisin O_1 to O_4 from *Blautia obeum* A2-162 (Hatziioanou et al., 2017), nisin U and U2 from *Streptococcus uberis* 42 and D536 (Wirawan et al., 2006), nisin P from *Streptococcus gallolyticus* subsp. *pasteurianus* (Zhang et al., 2012; Wu et al., 2014), nisin J from *Staphylococcus capitis* APC 2923 (O'Sullivan et al., 2020) and nisin H from *Streptococcus hyointestinalis* DPC 6484 (O'Connor et al., 2015).

In this study we focused on the natural nisin H variant (**Figure 1**). We used a standardized workflow for the characterization of lantibiotics, previous described in Lagedroste et al. (2019) to determine the impact on the expression, modification and antimicrobial properties of this nisin variant. We tested further the antimicrobial activity against some pathogen strains from *Staphylococcus aureus*, *Enterococcus faecium,* and *Enterococcus faecalis* using the microdilution method. As a reference we used the wild-type version of nisin A expressed using the same experimental setup. Furthermore, we exchanged the phenylalanine at position one (F_1) of nisin H to isoleucine, which is the natural amino acid of nisin A at this position (**Figure 1**). This position one was previously analyzed in nisin A and showed a major impact on different levels of the characterization (Lagedroste et al., 2019).

MATERIALS AND METHODS

Microorganisms and Culture Conditions

Cultures of *L. lactis* NZ9000 (Kuipers et al., 1997) containing the plasmids for immunity and resistance proteins were grown in M17 medium (Terzaghi and Sandine, 1975) at 30°C supplemented with 0.5% glucose [GM17 and the appropriate antibiotics descripted in Alkhatib et al. (2014a,b), Khosa et al. (2016b), Reiners et al. (2017), Lagedroste et al. (2019)]. For pre-nisin secretion, the *L. lactis* strain NZ9000 was grown in minimal medium (Jensen and Hammer, 1993) at 30°C supplemented with 0.5% glucose and the appropriate antibiotics. All bacteria used for minimum inhibitory concentration (MIC) determination of nisin variants [*Bacillus subtilis* 168; *S. aureus*: MSSA strain ATCC 29213, MRSA/VISA strain ATCC 700699; *E. faecium*: ATCC 35667, ATCC 700221 (vancomycin resistant); *E. faecalis*: ATCC 29212, ATCC 51299 (vancomycin resistant)] were cultivated in Mueller-Hinton broth (MHB) at 37°C and shaking at 150 rpm.

Cloning of Nisin H and the F_1I Variant

Nisin H was created as described in Reiners et al. (2017). The substitution of the phenylalanine at position one (F_1I) to an isoleucine was performed by site-directed mutagenesis. Here, we used the following primers (forward: 5′-GTGCATCACCACGCTTTACAAGTATTTCGC-3′; reverse: 5′-GCGAAATACTTGTAAAGCGTGGTGATGCAC-3′). After sequence analysis a competent *L. lactis* NZ9000 strain was transformed with the resulting plasmid via electroporation (Holo and Nes, 1989). The *L. lactis* NZ9000 strain already contain a vector (pil3-BTC) encoding for the modification and secretion proteins (Rink et al., 2005).

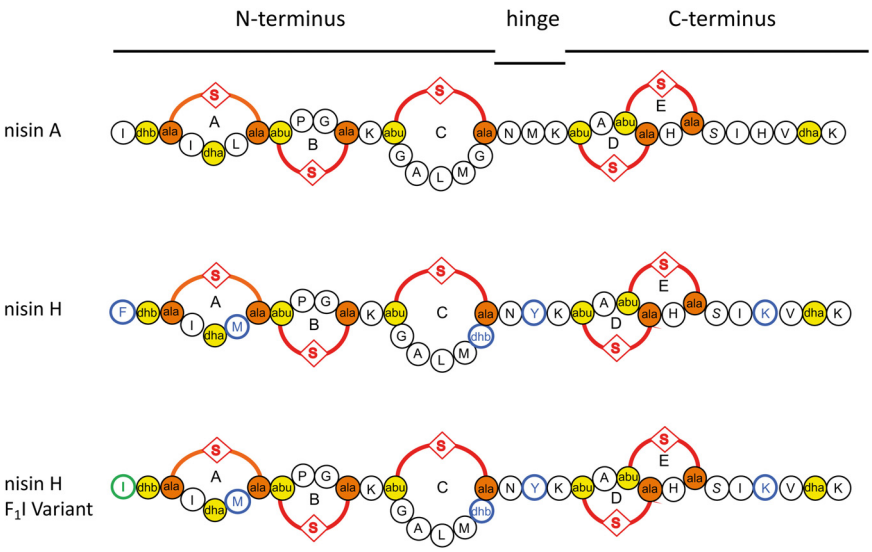

FIGURE 1 | Schematic overview of the used lantibiotics nisin A, nisin H, and the nisin H F_1I variant. Point mutations in nisin H and nisin H F_1I in comparison to nisin A are highlighted in blue. Dehydrated amino acids and cysteine residues involved in (methyl)-lanthionine ring formation (ring A, B, C, D, and E) are labeled in yellow and orange. The mutation of the nisin H F_1I variant is highlighted in green.

Expression, Purification and Activation of Pre-nisin Variants

The precursor of nisin H and its variant were expressed and purified as previously described (Abts et al., 2013; Alkhatib et al., 2014b; Lagedroste et al., 2017, 2019). Briefly, for pre-nisin secretion, the *L. lactis* strain NZ9000 was grown in minimal medium (Jensen and Hammer, 1993) supplemented with 0.5% glucose and 5 μg/ml of each erythromycin and chloramphenicol at 30°C. Cells were induced with 10 ng/ml nisin at an OD_{600} of 0.4 and further grown overnight at 30°C without shaking. After harvesting the cells, the 0.45 μm-filtered supernatant was loaded onto a HiTrap SP HP cation exchange chromatography column. After washing with 50 mM lactic acid, the buffer was changed to 50 mM Hepes pH 7 via gradient and the final elution was done with 50 mM Hepes pH 7, 500 mM NaCl buffer. Elution fractions were concentrated in a 3 kDa cutoff filter. With a soluble version of NisP, the activation of all variants was performed overnight at 8°C (Lagedroste et al., 2017). The yield and cleavage efficiency determination was done by RP-HPLC (Agilent Technologies 1260 Infinity II) with a LiChrospher WP 300 RP-18 end-capped column and an acetonitrile/water solvent system (Abts et al., 2013; Lagedroste et al., 2017, 2019).

MALDI-TOF Analysis: Dehydration and (Methyl)-Lanthionine Ring Analysis

With MALDI-TOF analysis we analyzed the modification state of nisin H and its variant. Dehydrations are directly visible in the spectra, due to the loss of mass (−18 Da). For the determination of the presence of (methyl)-lanthionine rings, we used the organic coupling agent CDAP (1-cyano-4 dimethylaminopyridinium tetrafluoroborate) that binds to free cysteine residues (Wu and Watson, 1998). The reaction of the coupling agent to free cysteine side chains would results in an increased mass in the spectra. The analysis was performed as previously descripted (Lagedroste et al., 2019). The samples were analyzed with MALDI-TOF (UltrafleXtreme, Bruker Daltonics, Bremen, Software: Compass 1.4) in positive mode.

Tandem Mass Spectrometric Analysis of Nisin H and Nisin H F_1I

Nisin H and the nisin H F_1I variant were purified using solid phase extraction (Oasis HLB, Waters) and finally resuspended in 0.1% trifluoroacetic acid. The samples were first subjected to liquid chromatography on a rapid separation liquid chromatography system (Ultimate 3000, Thermo Fisher Scientific) using an 1 h gradient and C18 columns as described (PMID 24646099) and further analyzed by a QExactive Plus mass spectrometer (Thermo Fisher Scientific) coupled via a nano-source electrospray interface. First, a precursor spectrum was acquired at a resolution of 140,000 (advanced gain control target 3E6, maximum ion time 50 ms, scan range 200–2000 m/z, profile data type). Subsequently, up to four 4–6-fold charged precursors were selected by the quadrupole (2 m/z isolation window), fragmented by higher-energy collisional dissociation (normalized collision energy 30) and recorded at a resolution of 35,000 (advanced gain control target 1E5, maximum ion time 50 ms, available scan range 200–2000 m/z, centroid data type).

Recorded spectra were analyzed by the MASCOT search engine (version 2.4.1, Matrix Science) and searches triggered by Proteome Discoverer (version 2.4.0.305, Thermo Fisher Scientific). A database was generated for the searches including 1000 randomly generated sequence entries each 34 amino acid long) and the sequences of nisin H and nisin H F_1I. Methionine oxidation and dehydration of serine and threonine residues were

considered as variable modifications and the precursor mass tolerance set to 10 ppm and the fragment mass tolerance set to 0.02 Da. For peptide validation, the Fixed Value PSM validator was used (1% false discovery rate) and the IMP-ptmRS node for site validation (PMID 22073976). No random sequences were found by the search.

Determination of the Antimicrobial Activity by Growth Inhibition Assay

The determination of the antimicrobial activity of the different nisin variants was tested using a growth inhibition assay. The used strains were described in Alkhatib et al. (2014a,b), Reiners et al. (2017), and Lagedroste et al. (2019).

Briefly, the *L. lactis* NZ9000 strains were grown in M17 medium (Terzaghi and Sandine, 1975) at 30°C supplemented with 0.5% glucose (GM17 and the appropriate antibiotics) overnight with 1 ng/ml nisin. In a 96-well plate, a serial dilution of the nisin variant was applied and incubated with the test strains at a final OD_{600} of 0.1 for 5 h at 30°C. Later on, the optical density was measured at 584 nm via 96-well plate reader BMG. The normalized optical density was plotted against the logarithm of the nisin concentration and the resulting inhibitory concentration (IC_{50}), represents the value where 50% of the cells died in the presence of the different nisin variants. By dividing the IC_{50} values of strains expressing the immunity or resistance proteins from the IC_{50} value of the sensitive strain we calculated the fold of immunity/resistance, which is an indicator for the recognition of nisin H or its variant by the immunity or resistance proteins.

Minimum Inhibitory Concentration Determination of Nisin Variants

Nisin variants were tested for antibacterial capabilities against *B. subtilis* and different strains from *S. aureus*, *E. faecium,* and *E. faecalis* using the microdilution method, according to the recommendations of Clinical and Laboratory Standards Institute (2012). Briefly, fresh cultures prepared from overnight cultures were incubated until exponential phase (OD ∼ 0.6) and seeded at 5×10^4 CFU/well in 96-well round-bottom microplates, in a total volume of 100 μL containing twofold serially diluted test peptides. Moxifloxacin was used as a positive control. Plates were incubated statically and aerobically for 24 h at 37°C. MICs were determined macroscopically by identifying the least concentration of peptides that resulted in complete inhibition of bacterial visual growth.

SYTOX Green Nucleic Acids Binding Assay

The cells of NZ9000Cm were grown overnight in GM17 supplemented with 5 mg/ml chloramphenicol. The overnight culture was diluted to an OD_{600} of 0.1 in fresh media and the cultures were grown until the OD_{600} reaches 0.3. The SYTOX green dye was added at a final concentration of 2.5 mM according to the manual of the manufacturer (Invitrogen). After reaching a stable baseline (∼200 s) we added 100 nM of the nisin variants. The fluorescence signal was measured at an excitation wavelength of 504 nm and emission wavelength of 523 nm, respectively (using a fluorolog Horiba III). After a stable baseline was reached, the nisin variant was added and the fluorescence was monitored over an additional time period. The measurement was performed at 30°C.

RESULTS

O'Connor et al. (2015) described a new natural nisin variant from *S. hyointestinalis* DPC 6484 and named it nisin H. In following, we compared nisin A and its natural variant nisin H, both heterologously produced in *L. lactis*, following the protocol of lantibiotic characterization (Lagedroste et al., 2019). We also included the nisin H F_1I variant.

The characterization starts with the expression, secretion and purification of the lantibiotic and its comparison to nisin A. The heterologously expressed and secreted nisin A and the variants nisin H and nisin H F_1I can be purified with high purity as observed on the Tricine-SDS-PAGE gel (**Figure 2A**). Nisin A was purified with a yield of 6.0 ± 0.3 mg/L of cell culture (Lagedroste et al., 2019), nisin H was expressed and purified with a yield of 5.3 ± 0.6 mg/L of cell culture, which is identical within experimental error. The nisin H F_1I variant displayed a slightly reduced yield of 4.9 ± 0.2 mg/L of cell culture (**Figure 2B** and **Table 1**).

An important step prior to the activity assay is the cleavage of the leader sequence form the pre-nisin variants, resulting in biologically active compounds. For the cleavage reaction, we used the peptidase NisP and monitored the cleavage efficiency via RP-HPLC (**Figures 2C–E**).

Intriguingly, the natural variant nisin H showed only a low cleavage efficiency of 15.6 ± 1.4%, compared to nisin A with 94.6 ± 2.0% (**Figure 2C** and **Table 1**). In comparison to nisin A, nisin H contains a phenylalanine at the first position (O'Connor et al., 2015), which apparently leads to a significant reduction in cleavage efficiency. The first residue of nisin A is an isoleucine, and as demonstrated before (Lagedroste et al., 2019), the introduction of aromatic residues at position one results in a clearly reduced cleavage efficiency. To counteract the lower cleavage efficiency of nisin H by NisP, we created a mutant of nisin H, in which the phenylalanine was substituted by isoleucine and termed it nisin H F_1I. For this variant, nisin H F_1I, the cleavage efficiency of the pre-lantibiotic was restored with an efficiency of 91.8 ± 0.8% (**Figure 2C** and **Table 1**), which corresponds to levels previously observed for nisin A. We monitored the cleavage via RP-HPLC, the pre-nisin elutes normally between 18 and 22 min (shown as blue dashed lines, **Figures 2D,E**). After cleavage by NisP, the leader peptide can be detected at 14.5 and 15.5 min in the chromatogram (shown as black lines, **Figures 2D,E**). For nisin H there was a high amount of uncleaved nisin H visible (eluting from 18 to 21 min) and only a small amount of cleaved product at 23–24 min (black lines, **Figure 2D**). For the nisin H F_1I variant, high amounts of leader peptide and cleaved product could be detected in the chromatogram, indicating high cleavage efficiency (black lines, **Figure 2E**). This efficiency was similar as observed for nisin A and in line with previous results that the position

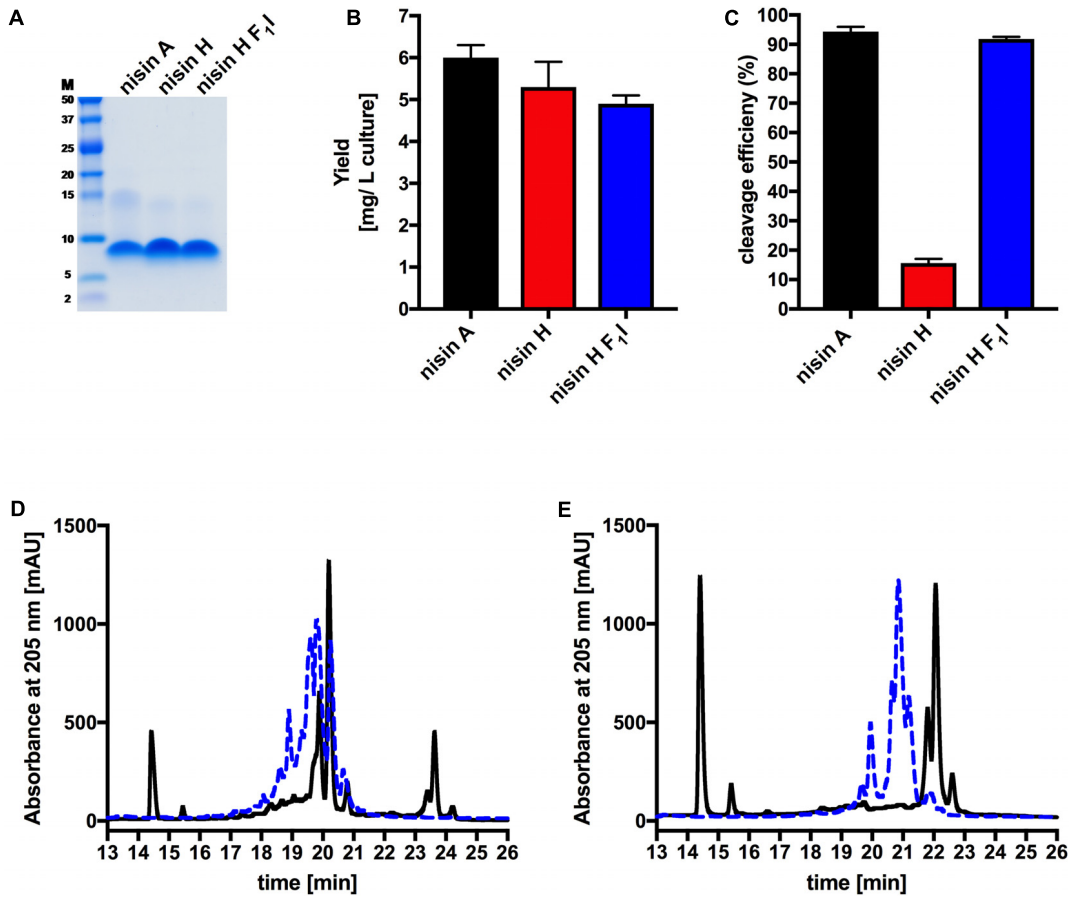

FIGURE 2 | Determination of purity, yield and cleavage efficiency of the pre-nisin variants. **(A)** Purity of the purified nisin A and the variants nisin H and nisin H F_1I (Marker: Precision Plus Protein Dual Xtra standards Bio-Rad). **(B)** Yields after purification of nisin A and their corresponding variants via cation-exchange chromatography. **(C)** Quantification of the cleavage efficiency of NisP. **(D)** Chromatogram of nisin H. **(E)** Chromatogram of the nisin H F_1I variant. The pre-nisin variants before NisP cleavage were shown by blue dashed lines and after NisP cleavage by black lines. Error bars represent the standard deviation of at least three biological replicates.

one is important for the cleavage reaction (Lagedroste et al., 2019). Thus, we assume, that the four other mutations naturally occurring in nisin H (compared to nisin A) do not interfere with cleavage, however the isoleucine at position one does.

The next step was to determine the modification state of the heterologous produced nisin H and its F_1I variant. As the natural variant nisin H contains ten possible residues in the core peptide that can be dehydrated, we were curious to determine if the modification machinery of nisin A was able to modify the peptide as efficiently (O'Connor et al., 2015). In the MALDI-TOF spectra, a dominant species of eightfold dehydrated residues was observed for nisin H, followed by a minor species containing nine- and sevenfold dehydrations. The possible 10-fold dehydrated species however was not observed (**Figure 3A** and **Table 1**). Furthermore no CDAP-coupling products were observed, which indicates that all cysteine residues are linked in (methyl)-lanthionine rings. We proved the functionality of the assay with unmodified pre-nisin A as demonstrated in Lagedroste et al. (2019). Thus, the modification enzymes were able to modify nisin H proving the promiscuity of the nisin modification machinery. Interestingly, the nisin H F_1I variant showed a dominant ninefold dehydrated species in comparison the nisin H wild-type (**Figure 3B** and **Table 1**) and also showed no CDAP-coupling products, indicating that all cysteine residues are closed to (methyl)-lanthionine rings. The difference in the dehydration pattern for the nisin H F_1I variant indicates a different accessibility of the serine and/or threonine residues in the core peptide for at least the dehydratase NisB. To validate which serine or threonine residues is dehydrated, we performed a tandem mass spectrometric

TABLE 1 | Determination of the yield, cleavage efficiency, dehydrations, and (methyl)-lanthionine ring formation for nisin A, nisin H, and nisin H F_1I.

Variant	Yield (mg/L culture)	Cleavage (%)	Dehydrations	Lanthionine rings
Nisin A	6.0 ± 0.3	94.6 ± 2.0	**8**, 7	5
Nisin H	5.3 ± 0.6	15.6 ± 1.4	9, **8**, 7	5
Nisin H F_1I	4.9 ± 0.2	91.8 ± 0.8	**9**, 8, 7, 6	5

Main species found in MALDI-TOF analysis are marked in bold.

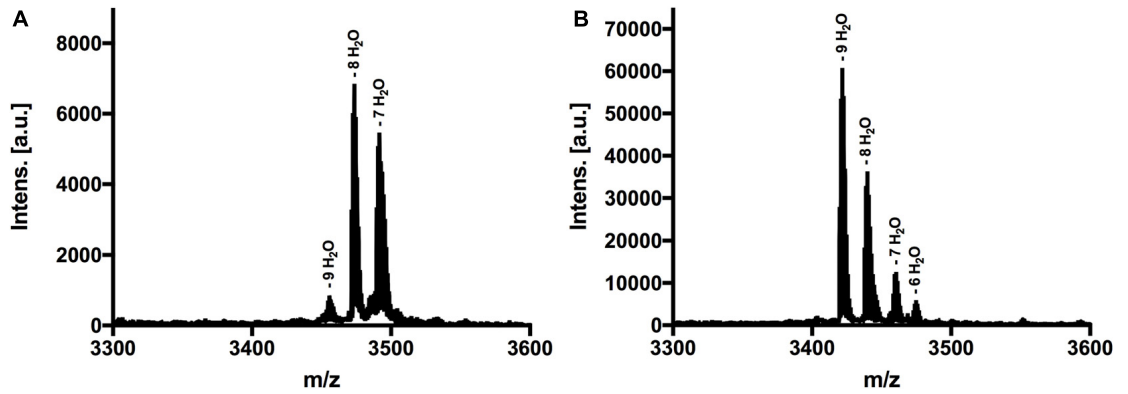

FIGURE 3 | MALDI-TOF analysis to determine dehydrations and (methyl)-lanthionine ring formations. **(A)** MS spectra of nisin H, threated with CDAP. Dominant species was eightfold dehydrated. **(B)** MS spectra of nisin H F_1I variant, threated with CDAP. Dominant species was ninefold dehydrated. Both variants showed no coupling products, indicating that all cysteine residues were involved in (methyl)-lanthionine rings.

analysis of nisin H and the F_1I variant. Here we found that the Thr_2 partially escape the dehydration in nisin H. Only in the small amount of the ninefold dehydrated species the Thr_2 is dehydrated, in all other species we found a mix in the dehydration pattern, where Thr_2 partially escape the dehydration. For example in the eightfold species we have a mix of dehydrated Thr_2 or Ser_{33}. In the nisin H F_1I variant the Thr_2 was in all species dehydrated, which suggests that, the phenylalanine at position one in nisin H is critical for the dehydratase NisB. Ser_{29} was never dehydrated in the found species.

Lantibiotics are very potent and possess an antimicrobial activity in the nanomolar range (Gross and Morell, 1967; Rollema et al., 1995; Chan et al., 1996; Lu et al., 2010; Oppedijk et al., 2016). To verify this potential for nisin H and the nisin H F_1I variant we used a standardized growth inhibition assay and first screened against the nisin sensitive *L. lactis* strain NZ9000Cm. Here, Cm stands for chloramphenicol resistance, which arises from the empty plasmid, which was transformed. In comparison to nisin A (IC_{50} value: 4.8 ± 0.7 nM), the heterologous expressed variant nisin H possessed a comparable IC_{50} value (5.3 ± 1.0 nM) (**Figure 4** and **Table 2**). Both values are in line with previously determined IC_{50} values for the strain NZ9000Cm (Reiners et al., 2017). The effect of the nisin H F_1I variant was more pronounced. For the NZ9000Cm sensitive strain we calculated an IC_{50} value of 14.2 ± 0.2 nM, approximately threefold lower than the wild-type nisin H (**Figure 4** and **Table 2**).

To test the effect of the nisin variants on the immunity proteins NisI (Alkhatib et al., 2014a) and NisFEG (Alkhatib et al., 2014b), as well as the resistance proteins *Sa*NSR (Khosa et al., 2016a) and *Sa*NsrFP (Reiners et al., 2017), we expressed each of them in a plasmid-based system in a *L. lactis* NZ9000 strain. We termed these strains NZ9000NisI, NZ9000NisFEG, NZ9000*Sa*NSR and NZ9000*Sa*NsrFP, respectively.

Nisin A displayed an IC_{50} value of 48.6 ± 6.3 nM against strain NZ9000NisI and 53.0 ± 4.5 nM against strain NZ9000NisFEG. For the resistance strains NZ9000*Sa*NSR and NZ9000*Sa*NsrFP nisin A displayed IC_{50} values of 73.0 ± 3.6 and 82.1 ± 3.1 nM, respectively (**Figure 4** and **Table 2**). By comparing theses values, we calculated the fold of immunity/resistance to 10.1 ± 2.0 for NZ9000NisI, 11.1 ± 1.9 for NZ9000NisFEG, 15.2 ± 2.5 for NZ9000*Sa*NSR and 17.1 ± 2.7 for NZ9000*Sa*NsrFP (**Table 2**). After the first screen against the sensitive strain NZ9000Cm, nisin H and its variant were used to screen against the strains expressing the immunity or resistance proteins.

Nisin H revealed an IC_{50} value of 43.2 ± 8.7 nM against the NZ9000NisI strain, similar to nisin A, and a fold of immunity of 8.1 ± 2.2. Against the NZ9000NisFEG strain we determined an IC_{50} value of 23.4 ± 3.3 nM for nisin H which displayed a fold of resistance of 4.4 ± 1.0. Against the NZ9000*Sa*NSR strain we obtained an IC_{50} value of 52.4 ± 9.9 nM, resulting in a fold of resistance of 9.8 ± 2.6. Nisin H showed an IC_{50} value of 86.4 ± 4.0 nM for the NZ9000*Sa*NsrFP strain, resulting in a fold of resistance of 16.2 ± 3.1 (**Figure 4** and **Table 2**). NZ9000*Sa*NsrFP showed the highest fold of resistance for nisin H [in-line with a previous report (Reiners et al., 2017)]. Intriguingly, strain NZ9000NisFEG showed a reduced immunity and consequently we propose that nisin H is not recognized as efficiently as nisin A. Even NZ9000*Sa*NSR had a reduced resistance. That could be due to the exchange of His_{31} against lysine in the C-terminal part of nisin H (**Figure 1**).

Surprisingly, all strains displayed a reducing resistance/immunity effect for the nisin H F_1I variant in comparison to nisin A and also, with exception of NZ9000FEG for nisin H. Against the NZ9000NisI strain we determined an IC_{50} value of 34.1 ± 0.3 nM for the nisin H F_1I variant, with a fold of resistance 2.4 ± 0.1, which is nearly threefold lower than for nisin A. We obtained an IC_{50} value of 32.1 ± 0.8 nM against the ABC transporter NZ9000NisFEG, with a fold of resistance 2.3 ± 0.1 (**Figure 4** and **Table 2**). Nisin H F_1I showed for the resistance strain NZ9000*Sa*NSR and NZ9000*Sa*NsrFP an IC_{50} value of 44.2 ± 1.3 and 50.2 ± 1.6 nM, respectively. The calculated folds of resistance were 3.1 ± 0.1 and 3.5 ± 0.1, respectively (**Figure 4** and **Table 2**) and both are fivefold less than the observed fold of resistances for nisin A.

Since a similar activity for nisin H and nisin A was observed it became obvious that both exhibit the same mode of action. In

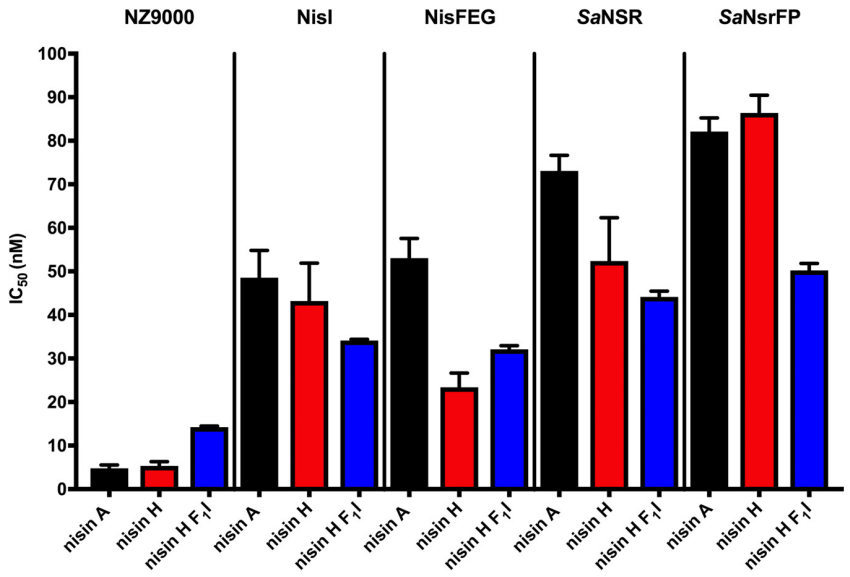

FIGURE 4 | Growth inhibition assays in the presence of nisin A and the nisin H varants. The lantibiotic nisin A (black bars), the heterologous expressed nisin H (red bars) and the position 1 variant of nisin H F_1I (blue bars) were used for growth inhibition (IC_{50}) with the strains NZ9000Cm, NZ9000NisI, NZ9000NisFEG, NZ9000*Sa*NSR, and NZ9000*Sa*NsrFP. Values represent the average of at least five biological independent measurements and the errors report the standard deviation of the mean (SDM).

TABLE 2 | IC_{50} values (nM) for nisin A, nisin H, and nisin H F_1I with the corresponding fold of resistance (FR) against the strains NZ9000Cm, NZ9000NisI, NZ9000NisFEG, NZ9000*Sa*NSR, and NZ9000*Sa*NsrFP.

Variant	NZ9000Cm	NZ9000NisI		NZ9000NisFEG		NZ9000*Sa*NSR		NZ9000*Sa*NsrFP	
		IC_{50}	FR	IC_{50}	FR	IC_{50}	FR	IC_{50}	FR
Nisin A	4.8 ± 0.7	48.6 ± 6.3	10.1 ± 2.0	53.0 ± 4.5	11.1 ± 1.9	73.0 ± 3.6	15.2 ± 2.5	82.1 ± 3.1	17.1 ± 2.7
Nisin H	5.3 ± 1.0	43.2 ± 8.7	8.1 ± 2.2	23.4 ± 3.3	4.4 ± 1.0	52.4 ± 9.9	9.8 ± 2.6	86.4 ± 4.1	16.2 ± 3.1
Nisin H F_1I	14.2 ± 0.2	34.1 ± 0.3	2.4 ± 0.1	32.1 ± 0.8	2.3 ± 0.1	44.2 ± 1.3	3.1 ± 0.1	50.2 ± 1.6	3.5 ± 0.1

the case of nisin A this combines growth inhibition with pore formation in the membrane with subsequent cell death. To test this we performed a SYTOX assay previously used for nisin A (Reiners et al., 2017). Here the SYTOX dye was added to *L. lactis* cells and displayed an increased fluorescence signal upon binding of DNA which is released from the cell upon pore formation (Roth et al., 1997). We use 100 nM of nisin A, nisin H and nisin H F_1I variant respectively and observed an almost instant fluorescence increase similar to the signal increase observed for nisin A (**Figure 5**). This shows that nisin H as well as its F_1I variant form pores in the membrane of *L. lactis* cell.

The nisin variants were further tested for antibacterial capabilities against *B. subtilis* and different pathogenic strains from *S. aureus*, *E. faecium,* and *E. faecalis* using the microdilution method, according to the recommendations of CLSI (2012). Here we found that nisin H and the F_1I variant performed almost identically or in most cases even better than the natural nisin A. Especially against the MSSA and MRSA strains, nisin H had significant lower MIC values of 0.19 and 0.78 μM, in comparison to 0.78 and 6.25 μM for nisin A, respectively (**Table 3**). Also, against *E. faecium* ATCC 35667, *B. subtilis* 168 as well as *E. faecium* ATCC 700221 (VRE), nisin H showed more potency with about two to eightfold lower MIC values than nisin A [0.39, 0.1, and 0.39 μM compared to 1.56, 0.78, and 0.78 μM for nisin A, respectively (**Table 3**)]. While the nisin H F_1I variant and nisin A had similar MIC values against both MSSA and MRSA strains, the nisin H F_1I variant only performed better than nisin A or nisin H against *E. faecalis* ATCC 51299 (VRE) with a MIC value of 0.78 μM compared to 1.56 μM for nisin A and nisin H. Against *E. faecium* ATCC 35667 and *B. subtilis* 168 nisin H F_1I was less efficient than nisin H, but still better than nisin A (**Table 3**).

DISCUSSION

We focused in this study on the natural variant nisin H and the nisin H F_1I mutant. Nisin H was discovered from the gut-derived strain *S. hyointestinalis* DPC6484 in 2015 by O'Connor et al. (2015). Here, we showed the heterologous expression of nisin H and the F_1I variant with the NICE-system in *L. lactis* (Eichenbaum et al., 1998; Mierau and Kleerebezem, 2005; Rink et al., 2005; Zhou et al., 2006; Lagedroste et al., 2019) and extended the characterization in terms of cleavage efficiency by the protease NisP and the antimicrobial activity against

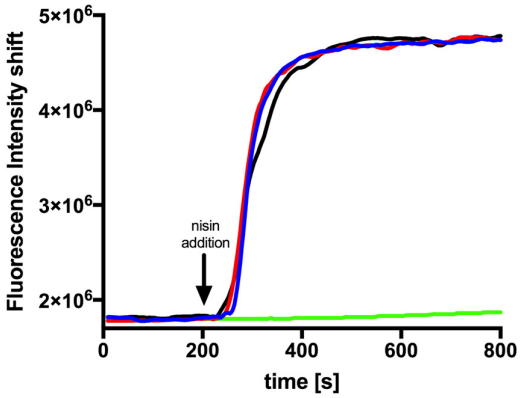

FIGURE 5 | Nisin mediated pore formation, visualized with the SYTOX green assay. The NZ9000Cm strain incubated with the SYTOX dye. After a stable baseline (~200 s), one of the nisin variants (100 nM) was added (indicated with an arrow). The fluorescence signal was measured using a fluorolog (Horiba III). The rapid increase in fluorescence indicates pore formation. The black line represents the addition of nisin A, the red line nisin H, and the blue line nisin H F_1I. As a control we added buffer shown as green line.

the immunity proteins NisFEG (Alkhatib et al., 2014b) and NisI (Alkhatib et al., 2014a), as well as the resistance proteins *Sa*NSR (Khosa et al., 2013; Khosa et al., 2016a,b) and *Sa*NsrFP (Khosa et al., 2016a; Reiners et al., 2017). We further tested for antibacterial capabilities against *B. subtilis* and different pathogenic strains from *S. aureus*, *E. faecium,* and *E. faecalis.*

Both lantibiotics, nisin H and the F_1I variant were purified in high amounts and purity with 5.3 ± 0.6 mg/L of cell culture for nisin H and 4.9 ± 0.2 mg/L of cell culture for nisin H F_1I variant, respectively (**Figure 2B** and **Table 1**). In comparison, the homologous expression of nisin H in *S. hyointestinalis* and nisin A in *L. lactis* NZ9700 results in a very low amount of 0.15 mg/L of cell culture and 0.50 mg/L of cell culture (O'Connor et al., 2015), respectively, which demonstrates the enormous potential of the NICE-system, for lantibiotic and even non-lantibiotic expression (Eichenbaum et al., 1998; Mierau and Kleerebezem, 2005; Rink et al., 2005; Zhou et al., 2006; Lagedroste et al., 2019).

An important step in the maturation of a lantibiotic is the cleavage of the leader peptide to become biological active. The cleavage efficiency of the natural substrate nisin A was determined with 94.6 ± 2.0%. For nisin H the cleaving efficiency was drastically reduced to 15.6 ± 1.4%. The first residue of nisin A is an isoleucine, while the corresponding residue in nisin H is phenylalanine and as demonstrated before (Lagedroste et al., 2019), aromatic residues prevent efficient cleavage likely by interfering with the S1′ binding pocket of NisP. With the nisin H F_1I variant, the cleavage efficiency was restored to 91.8 ± 0.8% (**Figures 1**, **2C** and **Table 1**). This indicated that the other point mutations naturally occurring in nisin H did not affect cleavage by NisP. With respect to other natural nisin variants, NisP cleavage could be a critical step. For example nisin O1 to O4 from *B. obeum* A2-162 (Hatziioanou et al., 2017) has a tyrosine or a threonine, respectively, at position one, which should also result in a low NisP cleavage efficiency. Natural variants such as nisin U (Wirawan et al., 2006), nisin J (O'Sullivan et al., 2019, 2020), nisin Q (Zendo et al., 2003), nisin Z (Mulders et al., 1991) and nisin F (de Kwaadsteniet et al., 2008) have an isoleucine and nisin U2 (Wirawan et al., 2006) and nisin P (Zhang et al., 2012; Wu et al., 2014) a valine at position one, which should result in high NisP cleavage efficiency.

Furthermore, we made a sequence alignment with Clustal Omega (Madeira et al., 2019) for the NshP (the natural protease for the nisin H cleavage) from *S. hyointestinalis* and NisP from *L. lactis* to see if there is any difference in the active site, which could be the reason for the reduced cleavage efficiency (**Figure 6A** and **Supplementary Figure 1**). Here the three important residues His_{306}, Asp_{259}, and Ser_{512} which build up the catalytic triad in NisP are conserved in NshP. We also calculated a homology model of NshP based on the known NisP structure (PDB code 4MZD) using Phyre2 (Kelley et al., 2015; **Figure 6B** and **Supplementary Figure 2**). Here, no significant differences are found within the overall fold as well as the active site which would explain the difference in the cleavage site. This is intriguing since the recognition site within the leader peptide differs between nisin A (sequence is ASPR) and nisin H (sequence is ASTR) (see **Supplementary Figure 3**). This suggests that the proteases NisP and NshP recognize their substrate by small difference in their active site.

Nevertheless, for an efficient cleavage, (methyl)-lanthionine rings have to be present. This even holds true in light of the presence of all (methyl)-lanthionine rings, which is generally assumed as the prerequisite for fast and efficient conversion of the pre-nisin to modified nisin (Plat et al., 2011;

TABLE 3 | MIC values for nisin A, nisin H, and nisin H F_1I against different pathogenic strains.

Organisms	Minimum inhibitory concentration (μM)		
	Nisin A	Nisin H	Nisin H F_1I
Staphylococcus aureus ATCC 29213 (MSSA)	0.78	0.19	0.78
Staphylococcus aureus ATCC 700699 (MRSA)	6.25	0.78	6.25
Enterococcus faecalis ATCC 29212	1.56	1.56	1.56
Enterococcus faecium ATCC 35667	1.56	0.39	0.78
Bacillus subtilis 168	0.78	0.1	0.39
Enterococcus faecalis ATCC 51299 (VRE)	1.56	1.56	0.78
Enterococcus faecium ATCC 700221 (VRE)	0.78	0.39	0.78

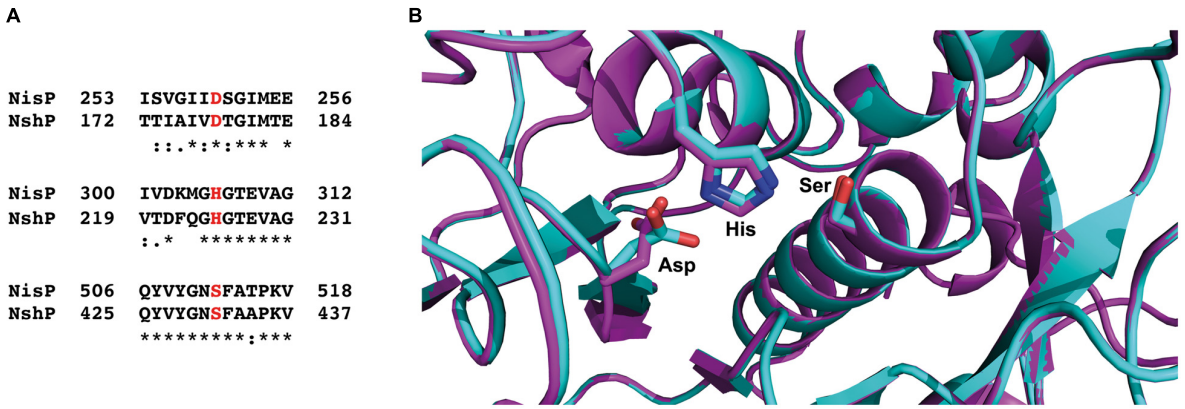

FIGURE 6 | Sequence alignment of NisP from *Lactococcus lactis* and NshP from *Streptococcus hyointestinalis*. **(A)** The important residues from the active site (Asp_{259}, His_{306}, and Ser_{512} for NisP and Asp_{178}, His_{225}, and Ser_{431} for NshP) are marked in red, shown together with the close neighborhood residues. The sequence alignment was done with Clustal Omega (Madeira et al., 2019). **(B)** Zoom-in into the active sites of NshP (magenta) and NisP (cyan). The important residues for the catalytic activity (Asp_{259}, His_{306}, and Ser_{512} for NisP and Asp_{178}, His_{225}, and Ser_{431} for NshP) are shown in stick representation. Figure was generated using Pymol (2015). For a full alignment and a corresponding homology model, please see **Supplementary Material**.

Lagedroste et al., 2017). To check the amount of dehydrations, necessary for (methyl)-lanthionine ring formation we applied MALDI-TOF analysis. The loss of water molecules within the peptide is directly visible in the reduced molecular weight, but not the (methyl)-lanthionine ring formation. Here we used 1-cyano-4 dimethylaminopyridinium tetrafluoroborate (CDAP) (Wu and Watson, 1998), which binds to free cysteine residues, indicating that these cysteines are not involved in a (methyl)-lanthionine ring. For both lantibiotics, nisin H and the nisin H F_1I variant no CDAP coupling products were found, indicating that no (methyl)-lanthionine ring is lacking (**Figure 3** and **Table 1**). Nisin H has 10 possible dehydration sites and is predicated to be ninefold dehydrated when expressed homologous (O'Connor et al., 2015). A minor species of nine dehydrations was found, but the dominant species was eightfold dehydrated. The dehydration pattern of the F_1I variant is changed in comparison to nisin H. Here we determined a dominant ninefold species (**Figure 3** and **Table 1**). This provides a hint, that position two of wild-type nisin H might not have been previously dehydrated, due to steric hindrance of the phenylalanine. To validate which serine or threonine residues is dehydrated, we perform a tandem mass spectrometric analysis of nisin H and the F_1I variant. Here we found that the Thr_2 partially escape the dehydration in nisin H. In the nisin H F_1I variant the Thr_2 was in all species dehydrated, which gives a hint that, the phenylalanine at position one in nisin H is critical for the dehydratase NisB. This is in line with previous data from the I_1F variant of nisin A, where the dominant species was sevenfold dehydrated and not eightfold as wild-type nisin A (Lagedroste et al., 2019). It has also been reported for the natural nisin Z (Mulders et al., 1991), that the I_1W mutation showed a partial inhibition of dehydration of the Thr_2 (Breukink et al., 1998), which could also be the case for nisin H with the aromatic phenylalanine at position one, resulting in eight dehydrations. A dehydration of position Ser_{29} normally goes in line with the lack of ring E (Lubelski et al., 2009), which drastically reduces the antimicrobial activity of nisin A against the sensitive NZ9000Cm strain (Alkhatib et al., 2014b; Khosa et al., 2016a; Reiners et al., 2017). Since the activity was high for nisin H and the F_1I variant, we expected that Ser_{29} was not dehydrated and tandem mass spectrometric analysis supported this.

Nisin H showed nearly the same activity as nisin A against the sensitive NZ9000Cm strain but the nisin H F_1I variant is roughly threefold less active. For the immunity protein NisI, it was revealed that nisin H has an identical activity like nisin A within experimental error. However, the nisin H F_1I variant exhibited a lower IC_{50} value of 34.1 ± 0.3 nM and due to the weaker wild-type activity more than a threefold lower fold of resistance (2.4 ± 0.1 compared to 8.1 ± 2.2) (**Figure 4** and **Table 2**). NisI recognizes the N-terminus of nisin (Wiedemann et al., 2001) and the lower IC_{50} could be due to the fact that Thr_2 is dehydrated in the nisin H F_1I variant in contrast to nisin H. An additional change is the leucine at position 6 against methionine in nisin H and the nisin H F_1I variant, which could be responsible for the better recognition by NisI.

The immunity protein NisFEG, in comparison to nisin A, showed a strong reduction in immunity in the presence of nisin H and the nisin H F_1I variant. NisFEG recognizes the C-terminus of nisin (Alkhatib et al., 2014b), which indicates that the point mutations of nisin H affect NisFEG. So, we suppose that nisin H and the nisin H F_1I variant are not recognized and subsequently transported out of the membrane like nisin A.

The resistance protein *Sa*NSR also recognizes the C-terminus of nisin (Khosa et al., 2016a), and cleaves nisin between the positions 28 and 29. Other studies showed that mutations in this area of the nisin molecule, e.g., $S_{29}P$ or $C_{28}P$ strongly reduce the efficiency of *Sa*NSR (Field et al., 2019; Zaschke-Kriesche et al., 2019a). We assume that the exchange of His_{31} against lysine in nisin H and the nisin H F_1I variant (**Figure 1**) has the same effect on *Sa*NSR thereby lowering the resistance efficiency to an IC_{50} value of 52.4 ± 2.6 nM for nisin H and 44.2 ± 1.3 nM for the nisin H F_1I variant, respectively (**Figure 4** and **Table 2**).

For the resistance protein *Sa*NsrFP, we observed an activity for nisin H identical to nisin A. *Sa*NsrFP recognizes the N-terminus of nisin (Reiners et al., 2017), which is affected due to the different dehydration pattern in wild-type nisin H in comparison to the nisin H F_1I variant. The nisin H F_1I variant showed a lower IC_{50} value of 50.2 ± 1.6 nM, compared to 86.4 ± 4.1 nM for nisin H. This effect is even more pronounced when comparing the fold of resistances of 16.2 ± 3.1 for nisin H to 3.5 ± 0.1 for the nisin H F_1I variant, respectively (**Figure 4** and **Table 2**).

This study demonstrated again that only a complete characterization of a lantibiotic reveals the full antimicrobial potential. Based on the IC_{50} value of the sensitive NZ9000Cm strain the F_1I variant might be classified as weakly antimicrobial active, but with respect to the immunity and resistance proteins, it becomes more interesting, due to its high activity even against the immunity proteins NisI and NisFEG from *L. lactis* and the nisin resistance proteins *Sa*NSR and *Sa*NsrFP from *S. agalactiae* COH1. Against the tested pathogenic bacteria, we found that nisin H and the nisin H F_1I variant performed almost identically or in the most cases even better than the natural nisin A. Nisin H displayed high antimicrobial potential against both methicillin-resistant and –susceptible the *S. aureus* strains, both vancomycin-resistant and -susceptible, *E. faecium* strains, as well as *B. subtilis.*

DATA AVAILABILITY STATEMENT

The raw data supporting the conclusions of this article will be made available by the authors, without undue reservation.

AUTHOR CONTRIBUTIONS

LS and SS conceived and directed this study. JR and ML conducted the expression, purification, MS-analysis, and the growth inhibition experiments. JG performed the SYTOX experiments. GP and KS performed the tandem mass spectrometric analysis. EA and RK performed the MIC experiments. JR, ML, SS, and LS wrote the manuscript. All authors read and approved the manuscript.

FUNDING

This work was supported by the Deutsche Forschungsgemeinschaft (DFG, grant Schm1279/13-1 to LS). The Center for Structural studies is funded by the DFG (Grant number 417919780 to SS). Project number 270650915 (Research Training Group GRK2158, TP2a to RK and TP4a to SS).

ACKNOWLEDGMENTS

We thank all members of the Institute of Biochemistry for fruitful discussions.

SUPPLEMENTARY MATERIAL

The Supplementary Material for this article can be found online at: https://www.frontiersin.org/articles/10.3389/fmicb.2020.573614/full#supplementary-material

REFERENCES

Abts, A., Montalban-Lopez, M., Kuipers, O. P., Smits, S. H., and Schmitt, L. (2013). NisC binds the FxLx motif of the nisin leader peptide. *Biochemistry* 52, 5387–5395. doi: 10.1021/bi4008116

Alkhatib, Z., Lagedroste, M., Fey, I., Kleinschrodt, D., Abts, A., and Smits, S. H. (2014a). Lantibiotic immunity: inhibition of nisin mediated pore formation by NisI. *PLoS One* 9:e102246. doi: 10.1371/journal.pone.0102246

Alkhatib, Z., Lagedroste, M., Zaschke, J., Wagner, M., Abts, A., Fey, I., et al. (2014b). The C-terminus of nisin is important for the ABC transporter NisFEG to confer immunity in *Lactococcus lactis*. *Microbiologyopen* 3, 752–763. doi: 10.1002/mbo3.205

Arnison, P. G., Bibb, M. J., Bierbaum, G., Bowers, A. A., Bugni, T. S., Bulaj, G., et al. (2013). Ribosomally synthesized and post-translationally modified peptide natural products: overview and recommendations for a universal nomenclature. *Nat. Prod. Rep.* 30, 108–160.

Breukink, E., Van Kraaij, C., Van Dalen, A., Demel, R. A., Siezen, R. J., De Kruijff, B., et al. (1998). The orientation of nisin in membranes. *Biochemistry* 37, 8153–8162. doi: 10.1021/bi972797l

Brunati, C., Thomsen, T. T., Gaspari, E., Maffioli, S., Sosio, M., Jabes, D., et al. (2018). Expanding the potential of NAI-107 for treating serious ESKAPE pathogens: synergistic combinations against Gram-negatives and bactericidal activity against non-dividing cells. *J. Antimicrob. Chemother.* 73, 414–424. doi: 10.1093/jac/dkx395

Chan, W. C., Leyland, M., Clark, J., Dodd, H. M., Lian, L. Y., Gasson, M. J., et al. (1996). Structure-activity relationships in the peptide antibiotic nisin: antibacterial activity of fragments of nisin. *FEBS Lett.* 390, 129–132. doi: 10.1016/0014-5793(96)00638-2

Clinical and Laboratory Standards Institute (2012). *Methods for Dilution Antimicrobial Susceptibility Tests for Bacteria that Grow Aerobically; Approved Standard*, 9th Edn. Wayne PA: Clinical and Laboratory Standards Institute.

Crowther, G. S., Baines, S. D., Todhunter, S. L., Freeman, J., Chilton, C. H., and Wilcox, M. H. (2013). Evaluation of NVB302 versus vancomycin activity in an in vitro human gut model of Clostridium difficile infection. *J. Antimicrob. Chemother.* 68, 168–176. doi: 10.1093/jac/dks359

Dawson, M. J., and Scott, R. W. (2012). New horizons for host defense peptides and lantibiotics. *Curr. Opin. Pharmacol.* 12, 545–550. doi: 10.1016/j.coph.2012.06.006

de Kwaadsteniet, M., Ten Doeschate, K., and Dicks, L. M. (2008). Characterization of the structural gene encoding nisin F, a new lantibiotic produced by a *Lactococcus lactis* subsp. lactis isolate from freshwater catfish (*Clarias gariepinus*). *Appl. Environ. Microbiol.* 74, 547–549. doi: 10.1128/aem.01862-07

Delves-Broughton, J., Blackburn, P., Evans, R. J., and Hugenholtz, J. (1996). Applications of the bacteriocin, nisin. *Antonie Van Leeuwenhoek* 69, 193–202. doi: 10.1007/bf00399424

Dischinger, J., Basi Chipalu, S., and Bierbaum, G. (2014). Lantibiotics: promising candidates for future applications in health care. *Int. J. Med. Microbiol.* 304, 51–62. doi: 10.1016/j.ijmm.2013.09.003

Eichenbaum, Z., Federle, M. J., Marra, D., De Vos, W. M., Kuipers, O. P., Kleerebezem, M., et al. (1998). Use of the lactococcal nisA promoter to regulate gene expression in gram-positive bacteria: comparison of induction level and promoter strength. *Appl. Environ. Microbiol.* 64, 2763–2769. doi: 10.1128/aem.64.8.2763-2769.1998

Field, D., Blake, T., Mathur, H., Pm, O. C., Cotter, P. D., Paul Ross, R., et al. (2019). Bioengineering nisin to overcome the nisin resistance protein. *Mol. Microbiol.* 111, 717–731.

Gross, E., and Morell, J. L. (1967). The presence of dehydroalanine in the antibiotic nisin and its relationship to activity. *J. Am. Chem. Soc.* 89, 2791–2792. doi: 10.1021/ja00987a084

Hasper, H. E., De Kruijff, B., and Breukink, E. (2004). Assembly and stability of nisin-lipid II pores. *Biochemistry* 43, 11567–11575. doi: 10.1021/bi049476b

Hatziioanou, D., Gherghisan-Filip, C., Saalbach, G., Horn, N., Wegmann, U., Duncan, S. H., et al. (2017). Discovery of a novel lantibiotic nisin O from Blautia obeum A2-162, isolated from the human gastrointestinal tract. *Microbiology* 163, 1292–1305. doi: 10.1099/mic.0.000515

Holo, H., and Nes, I. F. (1989). High-Frequency transformation, by electroporation, of *Lactococcus lactis* subsp. cremoris grown with glycine in osmotically stabilized media. *Appl. Environ. Microbiol.* 55, 3119–3123. doi: 10.1128/aem.55.12.3119-3123.1989

Hsu, S. T. D., Breukink, E., Tischenko, E., Lutters, M. A. G., De Kruijff, B., Kaptein, R., et al. (2004). The nisin-lipid II complex reveals a pyrophosphate cage that provides a blueprint for novel antibiotics. *Nat. Struct. Mol. Biol.* 11, 963–967. doi: 10.1038/nsmb830

Jabes, D., Brunati, C., Candiani, G., Riva, S., Romano, G., and Donadio, S. (2011). Efficacy of the new lantibiotic NAI-107 in experimental infections induced by multidrug-resistant Gram-positive pathogens. *Antimicrob. Agents Chemother.* 55, 1671–1676. doi: 10.1128/aac.01288-10

Jensen, P. R., and Hammer, K. (1993). Minimal requirements for exponential growth of *Lactococcus lactis*. *Appl. Environ. Microbiol.* 59, 4363–4366. doi: 10.1128/aem.59.12.4363-4366.1993

Kaletta, C., and Entian, K. D. (1989). Nisin, a peptide antibiotic: cloning and sequencing of the nisA gene and posttranslational processing of its peptide product. *J. Bacteriol.* 171, 1597–1601. doi: 10.1128/jb.171.3.1597-1601.1989

Karakas Sen, A., Narbad, A., Horn, N., Dodd, H. M., Parr, A. J., Colquhoun, I., et al. (1999). Post-translational modification of nisin. The involvement of NisB in the dehydration process. *Eur. J. Biochem.* 261, 524–532. doi: 10.1046/j.1432-1327.1999.00303.x

Kelley, L. A., Mezulis, S., Yates, C. M., Wass, M. N., and Sternberg, M. J. (2015). The Phyre2 web portal for protein modeling, prediction and analysis. *Nat. Protoc.* 10, 845–858. doi: 10.1038/nprot.2015.053

Khosa, S., Alkhatib, Z., and Smits, S. H. (2013). NSR from Streptococcus agalactiae confers resistance against nisin and is encoded by a conserved nsr operon. *Biol. Chem.* 394, 1543–1549. doi: 10.1515/hsz-2013-0167

Khosa, S., Frieg, B., Mulnaes, D., Kleinschrodt, D., Hoeppner, A., Gohlke, H., et al. (2016a). Structural basis of lantibiotic recognition by the nisin resistance protein from Streptococcus agalactiae. *Sci. Rep.* 6:18679.

Khosa, S., Lagedroste, M., and Smits, S. H. (2016b). Protein defense systems against the lantibiotic nisin: function of the immunity protein NisI and the resistance protein NSR. *Front. Microbiol.* 7:504. doi: 10.3389/fmicb.2016.00504

Klaenhammer, T. R. (1993). Genetics of bacteriocins produced by lactic acid bacteria. *FEMS Microbiol. Rev.* 12, 39–85. doi: 10.1016/0168-6445(93)90057-g

Koponen, O., Tolonen, M., Qiao, M., Wahlstrom, G., Helin, J., and Saris, P. E. J. (2002). NisB is required for the dehydration and NisC for the lanthionine formation in the post-translational modification of nisin. *Microbiology* 148, 3561–3568. doi: 10.1099/00221287-148-11-3561

Kuipers, O. P., De Ruyter, P. G., Kleerebezem, M., and De Vos, W. M. (1997). Controlled overproduction of proteins by lactic acid bacteria. *Trends Biotechnol.* 15, 135–140. doi: 10.1016/s0167-7799(97)01029-9

Lagedroste, M., Reiners, J., Smits, S. H. J., and Schmitt, L. (2019). Systematic characterization of position one variants within the lantibiotic nisin. *Sci. Rep.* 9:935.

Lagedroste, M., Smits, S. H. J., and Schmitt, L. (2017). Substrate specificity of the secreted nisin leader peptidase NisP. *Biochemistry* 56, 4005–4014. doi: 10.1021/acs.biochem.7b00524

Li, B., and van der Donk, W. A. (2007). Identification of essential catalytic residues of the cyclase NisC involved in the biosynthesis of nisin. *J. Biol. Chem.* 282, 21169–21175. doi: 10.1074/jbc.m701802200

Li, B., Yu, J. P., Brunzelle, J. S., Moll, G. N., Van Der Donk, W. A., and Nair, S. K. (2006). Structure and mechanism of the lantibiotic cyclase involved in nisin biosynthesis. *Science* 311, 1464–1467. doi: 10.1126/science.1121422

Lu, Y., Jiang, L., Chen, M., Huan, L., and Zhong, J. (2010). [Improving heat and pH stability of nisin by site-directed mutagenesis]. *Wei Sheng Wu Xue Bao* 50, 1481–1487.

Lubelski, J., Khusainov, R., and Kuipers, O. P. (2009). Directionality and coordination of dehydration and ring formation during biosynthesis of the lantibiotic nisin. *J. Biol. Chem.* 284, 25962–25972. doi: 10.1074/jbc.m109.026690

Madeira, F., Park, Y. M., Lee, J., Buso, N., Gur, T., Madhusoodanan, N., et al. (2019). The EMBL-EBI search and sequence analysis tools APIs in 2019. *Nucleic Acids Res.* 47, W636–W641.

Medeiros-Silva, J., Jekhmane, S., Paioni, A. L., Gawarecka, K., Baldus, M., Swiezewska, E., et al. (2018). High-resolution NMR studies of antibiotics in cellular membranes. *Nat. Commun.* 9:3963.

Mierau, I., and Kleerebezem, M. (2005). 10 years of the nisin-controlled gene expression system (NICE) in *Lactococcus lactis*. *Appl. Microbiol. Biotechnol.* 68, 705–717. doi: 10.1007/s00253-005-0107-6

Mota-Meira, M., Lapointe, G., Lacroix, C., and Lavoie, M. C. (2000). MICs of mutacin B-Ny266, nisin A, vancomycin, and oxacillin against bacterial pathogens. *Antimicrob. Agents Chemother.* 44, 24–29. doi: 10.1128/aac.44.1.24-29.2000

Mulders, J. W., Boerrigter, I. J., Rollema, H. S., Siezen, R. J., and De Vos, W. M. (1991). Identification and characterization of the lantibiotic nisin Z, a natural nisin variant. *Eur. J. Biochem.* 201, 581–584. doi: 10.1111/j.1432-1033.1991.tb16317.x

O'Sullivan, J. N., O'Connor, P. M., Rea, M. C., O'Sullivan, O., Walsh, C. J., Healy, B., et al. (2020). Nisin J, a novel natural nisin variant, is produced by *Staphylococcus capitis* Sourced from the human skin microbiota. *J. Bacteriol* 202. doi: 10.1128/JB.00639-19

O'Connor, P. M., O'Shea, E. F., Guinane, C. M., O'Sullivan, O., Cotter, P. D., Ross, R. P., et al. (2015). Nisin H is a new nisin variant produced by the gut-derived strain *Streptococcus hyointestinalis* DPC6484. *Appl. Environ. Microbiol.* 81, 3953–3960. doi: 10.1128/aem.00212-15

Okeley, N. M., Paul, M., Stasser, J. P., Blackburn, N., and Van Der Donk, W. A. (2003). SpaC and NisC, the cyclases involved in subtilin and nisin biosynthesis, are zinc proteins. *Biochemistry* 42, 13613–13624. doi: 10.1021/bi0354942

Ongey, E. L., Yassi, H., Pflugmacher, S., and Neubauer, P. (2017). Pharmacological and pharmacokinetic properties of lanthipeptides undergoing clinical studies. *Biotechnol. Lett.* 39, 473–482. doi: 10.1007/s10529-016-2279-9

Oppedijk, S. F., Martin, N. I., and Breukink, E. (2016). Hit 'em where it hurts: the growing and structurally diverse family of peptides that target lipid-II. *Biochim. Biophys. Acta* 1858, 947–957. doi: 10.1016/j.bbamem.2015.10.024

Ortega, M. A., Hao, Y., Zhang, Q., Walker, M. C., Van Der Donk, W. A., and Nair, S. K. (2015). Structure and mechanism of the tRNA-dependent lantibiotic dehydratase NisB. *Nature* 517, 509–512. doi: 10.1038/nature13888

O'Sullivan, J. N., Rea, M. C., O'Connor, P. M., Hill, C., and Ross, R. P. (2019). Human skin microbiota is a rich source of bacteriocin-producing staphylococci that kill human pathogens. *FEMS Microbiol. Ecol.* 95:fiy241.

Plat, A., Kluskens, L. D., Kuipers, A., Rink, R., and Moll, G. N. (2011). Requirements of the engineered leader peptide of nisin for inducing modification, export, and cleavage. *Appl. Environ. Microbiol.* 77, 604–611. doi: 10.1128/aem.01503-10

Pymol (2015). *The PyMOL Molecular Graphics System, Version 2.0*. New York, NY: Schrödinger.

Reiners, J., Lagedroste, M., Ehlen, K., Leusch, S., Zaschke-Kriesche, J., and Smits, S. H. J. (2017). The N-terminal region of nisin is important for the BceAB-Type ABC Transporter NsrFP from *Streptococcus agalactiae* COH1. *Front. Microbiol.* 8:1643. doi: 10.3389/fmicb.2017.01643

Repka, L. M., Chekan, J. R., Nair, S. K., and Van Der Donk, W. A. (2017). Mechanistic understanding of lanthipeptide biosynthetic enzymes. *Chem. Rev.* 117, 5457–5520. doi: 10.1021/acs.chemrev.6b00591

Rink, R., Kuipers, A., De Boef, E., Leenhouts, K. J., Driessen, A. J., Moll, G. N., et al. (2005). Lantibiotic structures as guidelines for the design of peptides that can be modified by lantibiotic enzymes. *Biochemistry* 44, 8873–8882. doi: 10.1021/bi050081h

Rogers, L. A. (1928). The inhibiting effect of streptococcus lactis on Lactobacillus Bulgaricus. *J. Bacteriol.* 16, 321–325. doi: 10.1128/jb.16.5.321-325.1928

Rogers, L. A., and Whittier, E. O. (1928). Limiting factors in the lactic fermentation. *J. Bacteriol.* 16, 211–229. doi: 10.1128/jb.16.4.211-229.1928

Rollema, H. S., Kuipers, O. P., Both, P., De Vos, W. M., and Siezen, R. J. (1995). Improvement of solubility and stability of the antimicrobial peptide nisin by

protein engineering. *Appl. Environ. Microbiol.* 61, 2873–2878. doi: 10.1128/aem.61.8.2873-2878.1995

Roth, B. L., Poot, M., Yue, S. T., and Millard, P. J. (1997). Bacterial viability and antibiotic susceptibility testing with SYTOX green nucleic acid stain. *Appl. Environ. Microbiol.* 63, 2421–2431. doi: 10.1128/aem.63.6.2421-2431.1997

Sahl, H. G., and Bierbaum, G. (1998). Lantibiotics: biosynthesis and biological activities of uniquely modified peptides from gram-positive bacteria. *Annu. Rev. Microbiol.* 52, 41–79. doi: 10.1146/annurev.micro.52.1.41

Sandiford, S. K. (2019). Current developments in lantibiotic discovery for treating Clostridium difficile infection. *Expert Opin. Drug. Discov.* 14, 71–79. doi: 10.1080/17460441.2019.1549032

Terzaghi, B. E., and Sandine, W. E. (1975). Improved medium for lactic Streptococci and Their Bacteriophages. *Appl. Microbiol.* 29, 807–813. doi: 10.1128/aem.29.6.807-813.1975

van Heel, A. J., De Jong, A., Song, C., Viel, J. H., Kok, J., and Kuipers, O. P. (2018). BAGEL4: a user-friendly web server to thoroughly mine RiPPs and bacteriocins. *Nucleic Acids Res.* 46, W278–W281.

van Heusden, H. E., De Kruijff, B., and Breukink, E. (2002). Lipid II induces a transmembrane orientation of the pore-forming peptide lantibiotic nisin. *Biochemistry* 41, 12171–12178. doi: 10.1021/bi026090x

Wiedemann, I., Benz, R., and Sahl, H. G. (2004). Lipid II-mediated pore formation by the peptide antibiotic nisin: a black lipid membrane study. *J. Bacteriol.* 186, 3259–3261. doi: 10.1128/jb.186.10.3259-3261.2004

Wiedemann, I., Breukink, E., Van Kraaij, C., Kuipers, O. P., Bierbaum, G., De Kruijff, B., et al. (2001). Specific binding of nisin to the peptidoglycan precursor lipid II combines pore formation and inhibition of cell wall biosynthesis for potent antibiotic activity. *J. Biol. Chem.* 276, 1772–1779. doi: 10.1074/jbc.m006770200

Wirawan, R. E., Klesse, N. A., Jack, R. W., and Tagg, J. R. (2006). Molecular and genetic characterization of a novel nisin variant produced by *Streptococcus uberis*. *Appl. Environ. Microbiol.* 72, 1148–1156. doi: 10.1128/aem.72.2.1148-1156.2006

Wu, J., and Watson, J. T. (1998). Optimization of the cleavage reaction for cyanylated cysteinyl proteins for efficient and simplified mass mapping. *Anal. Biochem.* 258, 268–276. doi: 10.1006/abio.1998.2596

Wu, Z., Wang, W., Tang, M., Shao, J., Dai, C., Zhang, W., et al. (2014). Comparative genomic analysis shows that *Streptococcus suis* meningitis isolate SC070731 contains a unique 105K genomic island. *Gene* 535, 156–164. doi: 10.1016/j.gene.2013.11.044

Zaschke-Kriesche, J., Behrmann, L. V., Reiners, J., Lagedroste, M., Groner, Y., Kalscheuer, R., et al. (2019a). Bypassing lantibiotic resistance by an effective nisin derivative. *Bioorg. Med. Chem.* 27, 3454–3462. doi: 10.1016/j.bmc.2019.06.031

Zaschke-Kriesche, J., Reiners, J., Lagedroste, M., and Smits, S. H. J. (2019b). Influence of nisin hinge-region variants on lantibiotic immunity and resistance proteins. *Bioorg. Med. Chem.* 27, 3947–3953. doi: 10.1016/j.bmc.2019.07.014

Zendo, T., Fukao, M., Ueda, K., Higuchi, T., Nakayama, J., and Sonomoto, K. (2003). Identification of the lantibiotic nisin Q, a new natural nisin variant produced by *Lactococcus lactis* 61-14 isolated from a river in Japan. *Biosci. Biotechnol. Biochem.* 67, 1616–1619. doi: 10.1271/bbb.67.1616

Zhang, Q., Yu, Y., Velasquez, J. E., and Van Der Donk, W. A. (2012). Evolution of lanthipeptide synthetases. *Proc. Natl. Acad. Sci. U.S.A.* 109, 18361–18366. doi: 10.1073/pnas.1210393109

Zhou, L., Van Heel, A. J., and Kuipers, O. P. (2015). The length of a lantibiotic hinge region has profound influence on antimicrobial activity and host specificity. *Front. Microbiol* 6:11. doi: 10.3389/fmicb.2015.00011

Zhou, X. X., Li, W. F., Ma, G. X., and Pan, Y. J. (2006). The nisin-controlled gene expression system: construction, application and improvements. *Biotechnol. Adv.* 24, 285–295. doi: 10.1016/j.biotechadv.2005.11.001

Conflict of Interest: The authors declare that the research was conducted in the absence of any commercial or financial relationships that could be construed as a potential conflict of interest.

frontiers in Microbiology

REVIEW
published: 05 November 2020
doi: 10.3389/fmicb.2020.590522

Combating Antimicrobial Resistance With New-To-Nature Lanthipeptides Created by Genetic Code Expansion

Hamid Reza Karbalaei-Heidari[1,2]* *and Nediljko Budisa*[2,3]*

[1] Department of Biology, Faculty of Sciences, Shiraz University, Shiraz, Iran, [2] Department of Chemistry, University of Manitoba, Winnipeg, MB, Canada, [3] Institute of Chemistry, Technical University of Berlin, Berlin, Germany

Due to the rapid emergence of multi-resistant bacterial strains in recent decades, the commercially available effective antibiotics are becoming increasingly limited. On the other hand, widespread antimicrobial peptides (AMPs) such as the lantibiotic nisin has been used worldwide for more than 40 years without the appearance of significant bacterial resistance. Lantibiotics are ribosomally synthesized antimicrobials generated by posttranslational modifications. Their biotechnological production is of particular interest to redesign natural scaffolds improving their pharmaceutical properties, which has great potential for therapeutic use in human medicine and other areas. However, conventional protein engineering methods are limited to 20 canonical amino acids prescribed by the genetic code. Therefore, the expansion of the genetic code as the most advanced approach in Synthetic Biology allows the addition of new amino acid building blocks (non-canonical amino acids, ncAAs) during protein translation. We now have solid proof-of-principle evidence that bioexpression with these novel building blocks enabled lantibiotics with chemical properties transcending those produced by natural evolution. The unique scaffolds with novel structural and functional properties are the result of this bioengineering. Here we will critically examine and evaluate the use of the expanded genetic code and its alternatives in lantibiotics research over the last 7 years. We anticipate that Synthetic Biology, using engineered lantibiotics and even more complex scaffolds will be a promising tool to address an urgent problem of antibiotic resistance, especially in a class of multi-drug resistant microbes known as superbugs.

Keywords: genetic code expansion, chemoselectivity, RiPPs, lantibiotics, non-canonical amino acids, nisin, superbugs, synthetic biology

OPEN ACCESS

Edited by:
Harsh Mathur,
Teagasc Food Research Center, Ireland

Reviewed by:
Sander H. J. Smits,
Heinrich Heine University, Germany
Manuel Montalban-Lopez,
University of Granada, Spain

***Correspondence:**
Hamid Reza Karbalaei-Heidari
karbalaei@shirazu.ac.ir;
hamid.karbalaeiheidari@umanitoba.ca
Nediljko Budisa
nediljko.budisa@umanitoba.ca;
nediljko.budisa@tu-berlin.de

Specialty section:
This article was submitted to Antimicrobials, Resistance and Chemotherapy, a section of the journal Frontiers in Microbiology

Received: *01 August 2020*
Accepted: *13 October 2020*
Published: *05 November 2020*

Citation:
Karbalaei-Heidari HR and Budisa N (2020) Combating Antimicrobial Resistance With New-To-Nature Lanthipeptides Created by Genetic Code Expansion. Front. Microbiol. 11:590522. doi: 10.3389/fmicb.2020.590522

ANTIMICROBIAL RESISTANCE AND SUPERBUGS

The use of antibiotics has enormously empowered modern medicine to save human lives and perform medical and surgical treatments under safe conditions (Aslam et al., 2018). In addition, treatment with antibiotics is one of the most important approaches to combat or prevent bacterial infections in animal populations and in the food industry. The widespread use of antibiotics began already during the Second World War, and Alexander Fleming himself was one of the first to recognize how improper use of these compounds could lead to antibiotic-resistant bacteria (Fleming, 1945). The habitats of our planet are saturated with various toxic substances, especially

those of anthropogenic origin, which has contributed significantly to the selection of resistant strains (Davies and Davies, 2010). Indeed, the excessive use of antibiotics in agriculture, in the environment, animals (food, pets, aquatic fauna) and human medicine, and their release into the environment through fertilizer/feces is the most plausible cause of antimicrobial resistance (AMR) (Manyi-Loh et al., 2018).

The emergence of pathogens causing enhanced morbidity and mortality due to modifications in various physiological and biochemical mechanisms has led to multi-resistant microbes known also as "superbugs" (Coast et al., 1996). For example, in different microbial strains, resistance has emerged at multiple levels of defense, starting from the entry level (through the limitation of drug permeability and the existence of efflux pumps) to the degradation of the antibiotics via their modification or hydrolysis. Next, lateral gene transfer, alteration of binding through target modification and escape of toxicity through bypass reactions and metabolic shunts were (among others) documented as mechanisms for the development of single or multiple resistances (Yelin and Kishony, 2018). To sum up, due to the rapid appearance of multi-drug resistant bacterial strains in last few decades, the use of commercially available antibiotics has become increasingly limited. A promising alternative could be the use of antimicrobial peptides (AMPs) with many variants already in clinical trials (**Table 1**). Many bioactive peptides produced from various microorganisms (e.g., actinobacteria, cyanobacteria, bacilli, fungi) have a potential to serve as drugs against numerous pathogens (Greber and Dawgul, 2017; Ongey et al., 2017; Koo and Seo, 2019).

ANTIMICROBIAL PEPTIDES

Antimicrobial peptides (AMPs) also known as host defence peptides are one of the most versatile natural products which represent alternatives to traditional antibiotics. In fact, AMPs are a special group of natural products that occur in almost every form of life, namely microorganisms, plants, and animals as an innate immune response (Ageitos et al., 2017). They can be used to treat various infections caused by pathogenic species with better efficacy, selectivity and specificity. Structurally, AMPs are versatile peptides with diverse lengths of almost always less than 80 amino acids in a linear or cyclic structure with a broad set of biotechnological applications, e.g., antibiotics, and inhibitors (Oliva et al., 2018).

Antimicrobial peptides can be classified on the basis of their parent organism, their biosynthetic production pathway (e.g., ribosomal or non-ribosomal origin), their activity spectrum, and their structural features (usually based on predominant secondary structure) or physicochemical properties (e.g., cationic/anionic, hydrophilic/hydrophobic etc.). They are structurally divided into five main classes, including (i) linear α-helical peptides, (ii) β–sheet-containing peptides, (iii) peptides with α- and β-structural elements, and (iv) extended or non-αβ secondary structure elements (e.g., polyproline helices) (Wang, 2015). Furthermore, they also occur in the form of (v) cyclic peptides and other topologically complex scaffolds, which are often ribosomally produced and post-translationally modified peptides (RiPPs) (Koehbach and Craik, 2019). Another classification system divides AMPs into natural, encrypted (Brand et al., 2012), and designed AMPs which are a product of specific genes or as part of larger proteins released after proteolysis, and the artificial ones developed by rational design techniques, respectively (Cardoso et al., 2016; Porto et al., 2017). **Figure 1** summarizes the various methods of AMPs classification in the current literature.

Three models (Carpet/Aggregation/Detergent-like model, Toroidal model, and Barrel-Stave model) have been proposed to explain the mechanism of action of AMPs for the ability to kill bacterial pathogens via membrane permeability (**Figure 2**). In all these models AMPs act in two sequential steps (Brogden, 2005). In the first step, electrostatic interactions are established between the positively charged amino acids in CAMPs with the negatively charged membrane surface, such as the pyrophosphate group of lipid-II in the cell membrane of microorganism or phosphatidylethanolamines in the outer leaflet of the target cell membrane. In the second step, the formation of pores within the membrane causes the bilayer to break open, which leads to extensive leakages and finally to cell death, particularly in Gram-positive bacteria. Detailed descriptions of detergent-like effects of amphipathic cationic AMPs and other models of membrane disruption by AMPs are described in great detail in the contemporary literature (see e.g., Zweytick et al., 2006). Achievable chemical diversity and variability in the production of peptides together with almost unlimited sequence space for matching their physicochemical properties and generating broad-spectrum antimicrobial activity make them a valid alternative to antibiotics in the effort to combat multi-drug resistant strains and save human lives in the face of future epidemic and other challenges (Ageitos et al., 2017). Nevertheless, several obstacles remain to be overcome in order to develop AMPs for medical use, such as toxicity, stability, and even bacterial resistance. Another obstacle is the lack of standard experimental procedures for quantifying AMP activity and we still do not have a clear picture of several AMP's mechanisms of action (Torres et al., 2019).

LANTHIPEPTIDES ARE RIBOSOMALLY PRODUCED AND POST-TRANSLATIONALLY MODIFIED PEPTIDES (RIPPS)

RiPPs are an important class of AMPs, ribosomally synthesized and post-translationally modified bio-active peptides in all three domains of life and show great structural diversity. They are subdivided into more than twenty well-known categories including lanthipeptides, linaridins, proteusins, linear azol(in)e-containing peptides (LAPs), cyanobactins, thiopeptides, bottromycins, microcins, lasso peptides, microviridins, sactipeptides, bacterial head-to-tail cyclized peptides, amatoxins and phallotoxins, cyclotides, orbitides, conopeptides, glycocins,

TABLE 1 | List of selected promising AMPs in preclinical or clinical trials.

	AMP type	Mechanism	Application	Trial phase	References
Mutacin 1140	Lantibiotic	Lipid-II binding	Bacterial infection	Pre-clinical	Kers et al., 2018
NVB333	Lantibiotic	Lipid II binding	Bronchoalveolar infection therapy	Pre-clinical	Boakes et al., 2016
NVB302	Lantibiotic	Lipid-II binding	*Clostridioides difficile* infections	Phase I	Boakes and Dawson, 2014
Duramycin	Lantibiotic	Binding to Phosphatidylethanolamine	Cystic fibrosis, Inhibit cell entry of viruses	Phase II	Huo et al., 2017
DPK-060	Kininogen-derived peptide	Membrane targeting	Atopic dermatitis	Phase II	Håkansson et al., 2019
OP−145	LL−37 derivative	Bacterial membrane dissolution	Chronic leg ulcers, Wound healing effect	Phase II	Ming and Huang, 2017
D2A21	Synthetic	Unknown	Burn wound infections	Phase III	Chalekson et al., 2002
SGX942 (Dusquetide)	Synthetic	Innate defense regulator	Oral Mucositis	Phase III	Kudrimoti et al., 2017
PXL01	Lactoferrin analog	Repressing secretion of cytokines	Post-surgical adhesions	Phase III	Nilsson et al., 2009
Omiganan (CLS001)	Indolicidin derivative	Affect the cytoplasmic membranes of bacteria	Catheter-related infections	Phase III	Feng et al., 2015
POL 7080 (RG7929)	Protegrin analog	Inhibiting LptD	Septicemia, lung and thigh models	Phase III	Srinivas et al., 2010

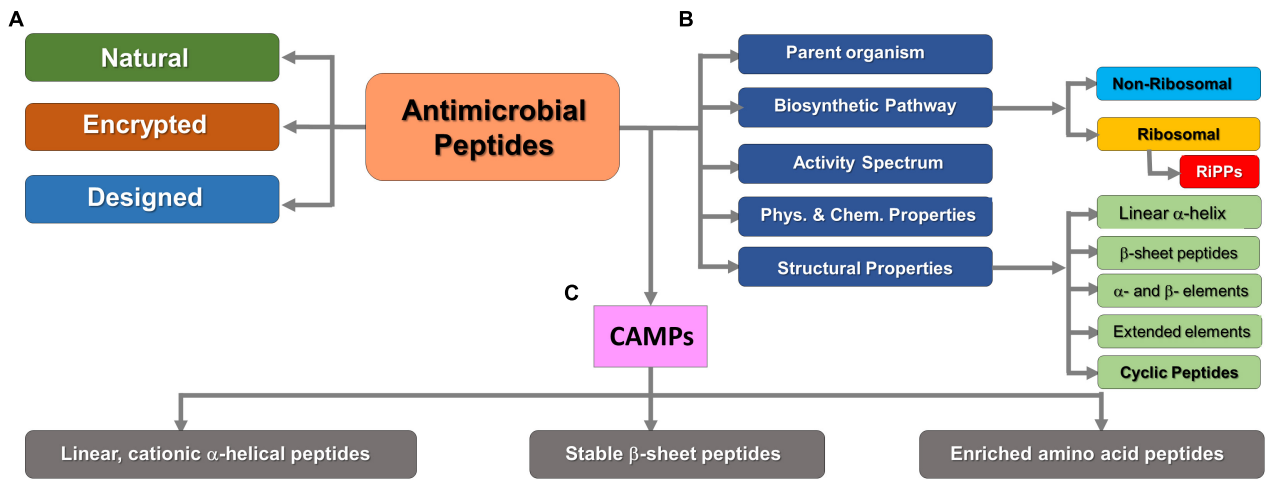

FIGURE 1 | Classification of AMPs on the basis of various criteria. **(A)** Based on gene encoding pattern (Data-mining strategy). **(B)** Significant cellular or thermodynamic criteria. **(C)** Subdivision of positively charged (cationic) AMPs. RiPPs are structurally diverse but exclusively synthesized by ribosomes. This figure was compiled from a variety of sources (Porto et al., 2017; Koehbach and Craik, 2019).

autoinducing peptides (AIPs), pyrroloquinoline quinone (PQQ), pantocin A and thyroid hormones, etc. (Arnison et al., 2013).

In this context, lanthipeptides are classified as one the largest group of RiPPs assigned in class I of bacterial-origin AMPs (bacteriocins). They are transformed into a mature active form by special post-translational modifications (PTMs) carried out by a battery of dedicated enzymes. Class I of bacteriocins include lantibiotics, linear azol(in)e-containing peptides (LAPs), thiopeptides, bottromycins, glycocins, lasso peptides, head-to-tail cyclized bacteriocins, sactibiotics, and lipolanthines (Acedo et al., 2018). Bacterial lanthipeptides exhibit outstanding properties such as conformational rigidity, increased metabolic and chemical stability as well as intense cell permeability that distinguish them from other heat-stable (class-II) and thermo-labile (class-III) bacteriocins (Alvarez-Sieiro et al., 2016). In addition to the four earlier types of lanthipeptides

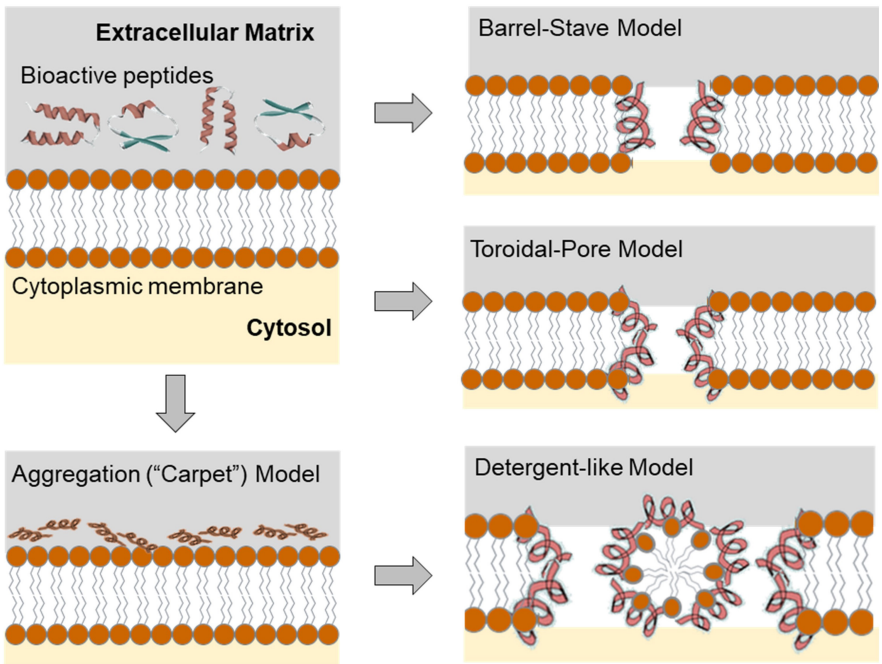

FIGURE 2 | Configuration of the target membrane environment leading to the initial electrostatic and hydrophobic interactions of the AMPs on the bacterial membrane. Initial molecular event of the effect of the AMPs leads to the different scenarios that can be described using transmembrane pore and non-pore models. The carpet model, without pores: AMPs aggregate on the bilayer surface resulting in detergent-like disintegration, whereby the membrane is fragmented into micelles. Conversely, in the "barrel stave" model, membrane pores are formed by interactions between the hydrophobic surface of the pore and the acyl chains of the lipid core of the bilayer. The "toroidal pore" model (wormhole) combines the effects described by both the barrel stave and the carpet model. For a more comprehensive overview see Sun et al. (2018). However, it should be noted that the different mechanisms of AMPs action presented here do not cover the entire range of ribosomally produced and post-translationally modified peptides (RiPPs, *vide infra*), since not all members of this group damage membranes or form pores, but have different targets and mechanisms of action.

classified based on the biosynthetic mechanisms involved in their structural maturation, the recently discovered modified peptides, including Cocaoidin and Lexapeptide, exhibited novel modification features such as different biosynthetic gene clusters and have been introduced as class V lanthipeptides (Ortiz-López et al., 2020; Xu et al., 2020).

In general, lantibiotics show an efficient ability to kill Gram-positive bacteria and are particularly important for those that exhibit drug resistance such as methicillin-resistant *Staphylococcus aureus* (MRSA), *Streptococcus pneumoniae* (MRSP), vancomycin intermediate *S. aureus* (VISA), vancomycin-resistant *enterococci* (VRE), *Clostridioides difficile*, etc. Instability and/or insolubility at physiological pH, susceptibility to proteolytic degradation, and a low level of their production are features that mainly limit the use of lantibiotics in the clinic. It should also be noted that the antimicrobial activity of lanthipeptides is well understood and characterized in some RiPPs such as nisin (achieved by lipid-II binding) (Kuipers et al., 1996). Later, the lipid-II binding activity of some lantibiotics was also demonstrated (Wiedemann et al., 2001; Breukink and de Kruijff, 2006), although in some of them the mechanisms of action have yet to be clarified. Nonetheless, low cytotoxicity of lantibiotics to human cells due to the absence of their main target lipid II or negative net charge in eukaryotic membranes (Lagedroste et al., 2019) along with a few examples of naturally occurring resistance (Draper et al., 2015; Khosa et al., 2016a,b; Clemens et al., 2018) make lantibiotics excellent lead compounds for development of new therapeutic options.

THE FEASIBILITY OF GENETIC ENGINEERING TO PRODUCE MORE POTENT LANTIBIOTICS

RiPPs Recombinant Expression for Classical Engineering—Nisin as an Example

A wide range of technologies are at our disposal for producing a peptide such as chemical synthesis, recombinant DNA technologies, and *in vitro* translation systems. The choice of a strategy for gene-encoded peptide production is largely determined by their size and chemical complexity. Peptides with sophisticated PTMs-generated structures such as RiPPs are preferably produced biosynthetically using host expression cells. Host cells with installed and functional PTM enzymes should be able to express RiPPs in an intact active form with distinctive architecture dominated by lanthionine bridges. In this context, the absence of a widely used large-scale production platform for

lantibiotics with consistent quality is one of the main drawbacks of their therapeutic application.

There are generally two options for recombinant expression of lantibiotics, homologous or heterologous expression systems. Homologous expression strategies have limited use in particular due to the difficulty of cultivating the original producers (Maffioli et al., 2015; Mohr et al., 2015) and/or the difficulty of lantibiotics expression induction under laboratory conditions (Wescombe et al., 2011; Garg et al., 2012). Conversely, heterologous biosynthesis with host cells such as *Lactococcus lactis*, *Bacillus subtilis*, *Bacillus cereus,* and *E. coli* are normally preferred and, in many cases, well established. So far, several genetically manipulatable *Streptomyces* strains, including *Streptomyces lividans* (Ahmed et al., 2020), *S. albus* (Myronovskyi et al., 2018), *S. coelicolor* M145 (Gomez-Escribano and Bibb, 2011), *S. venezuelae* ATCC 15439 (Kim et al., 2015), *S. avermitilis* (Komatsu et al., 2010) have been reported to synthesize natural products from genetically engineered biosynthetic gene clusters. However, *Escherichia coli* is still the most common and attractive option. A list of successful examples of recombinant expression of different RiPPs families in heterologous hosts such as *E. coli* and *Streptomyces* strains were recently compiled by Zhang and colleagues (Zhang et al., 2018). Heterologous production of lantibiotics is generally conducted as inactive form of the antimicrobial peptide (pre-lantibiotic) to prevent any detrimental effects on host cell growth and viability.

In addition, there is great interest to express lantibiotics in microbial host that should facilitate a straightforward and efficient engineering (Kuipers et al., 1996). Numerous conventional protein engineering approaches such as site-directed mutagenesis, directed evolution and various computational tools aid synthetic biologists and biochemists to selectively diversify the properties of expressed therapeutic peptides. These include manipulations of thermodynamic stability, increased bioavailability, reduced aggregation or enhanced specificity and proteolytic stability (Adhikari et al., 2019). In addition, the implementation of *in vitro* and *in vivo* approaches in combination with genome mining data and high-throughput screening strategies has opened up unprecedented opportunities to modify and even improve antimicrobial activity, manipulate the physicochemical properties and widening of the antibacterial spectrum in the production of lantibiotics (Field et al., 2015). Recently an attempt to design and biosynthesize a two-lipid II binding motifs-containing lantibiotic, called TL19, is the latest example showing 64-fold stronger activity against *Enterococcus faecium* than nisin (Zhao et al., 2020).

The potential of classical protein engineering in complex RiPPs is perhaps best illustrated by recombinant nisin, well known for its broad-spectrum antibacterial activity produced in certain strains of *L. lactis* (Lubelski et al., 2008). Nisin as the most widely used lantibiotic in the food industry over the past 50 years has undergone various methods of bioengineering with an aim to improving its function and/or physicochemical features (Shin et al., 2016). To expand the scope of its activity, several bioengineered variants of nisin have been generated by site-directed mutagenesis and by classical chemical modifications (Ross et al., 2012), including *in vitro* chemical synthesis (Knerr and van der Donk, 2012; Koopmans et al., 2015). For example, the use of the saturation mutagenesis approach has led to the production of nisin S29 derivatives with increased activity against a number of Gram-positive antibiotic-resistant pathogens. In addition, the increased antimicrobial activity was generated in comparison to the wild type nisin A when tested against Gram-negative food-borne pathogens (Field et al., 2012). Moreover, recombinant production of the nisin Z mutants N20K, M21K, N27K, H31K improved peptide solubility at alkaline pH (Rollema et al., 1995). Next, residue alterations at distinct locations enabled the improvement of antimicrobial activity (Islam et al., 2009; Healy et al., 2013; Geng and Smith, 2018), the enhancement of diffusion through complex polymers (Rouse et al., 2012), and widening effect on some Gram-negative bacteria (Field et al., 2012).

Studies on the effects of the hinge region (NMK) length between rings C and D on antimicrobial activity and host specificity of nisin was also performed (Zhou et al., 2015). Although most variants with shorter or larger hinge length are less active than the wild type, some variants (+2, +1, −1, −2) exhibited higher antimicrobial activity than the wild type nisin A in agar-well-diffusion assays against *L. lactis* MG1363, *Listeria monocytogenes*, *Enterococcus faecalis* VE14089, *Bacillus sporothermodurans* IC4, and *Bacillus cereus* 4153. In addition, an extended nisin A variant of the hinge region ($_{20}$NMKIV$_{24}$) has been introduced, bypassing the human pathogen's lantibiotic resistance while showing a slight decrease in antimicrobial activity (Zaschke-Kriesche et al., 2019). In this context, **Figure 3** represents different variants of nisin produced by classical protein engineering together with a graphical representation of the mechanism of action of this bioactive peptide.

However, the expression of lantibiotics in popular prokaryotic hosts like *E. coli* is challenging as these bacteria have no enzymes to perform suitable PTMs to convert pro-peptide into a mature bioactive peptide. Therefore, their recombinant expression has to be coupled with the co-expression of active PTM biosynthetic gene clusters either *in vitro* or *in vivo*. These strategies are not in the focus of our study and interested readers are directed to numerous studies and reviews dedicated to this topic (Zhang et al., 2018; Myronovskyi and Luzhetskyy, 2019). We are mainly concerned with the *in vivo* design strategies that focus to expand the functional scope of AMPs from ribosomal templates beyond the classical protein engineering approaches.

Beyond Classical Protein Engineering: Expanding the Scope of Protein Translation

It was argued that chemical and functional diversity delivered by PTMs in AMPs such as lantibiotics can be further supplemented or even expanded by the co-translational insertion of non-canonical amino acids (ncAAs) (Budisa, 2013). Indeed, a limited and conservative set of 20 canonical amino acids used by ribosomes to encode polypeptides in nature usually does not cover enough chemical space required to substantially expand

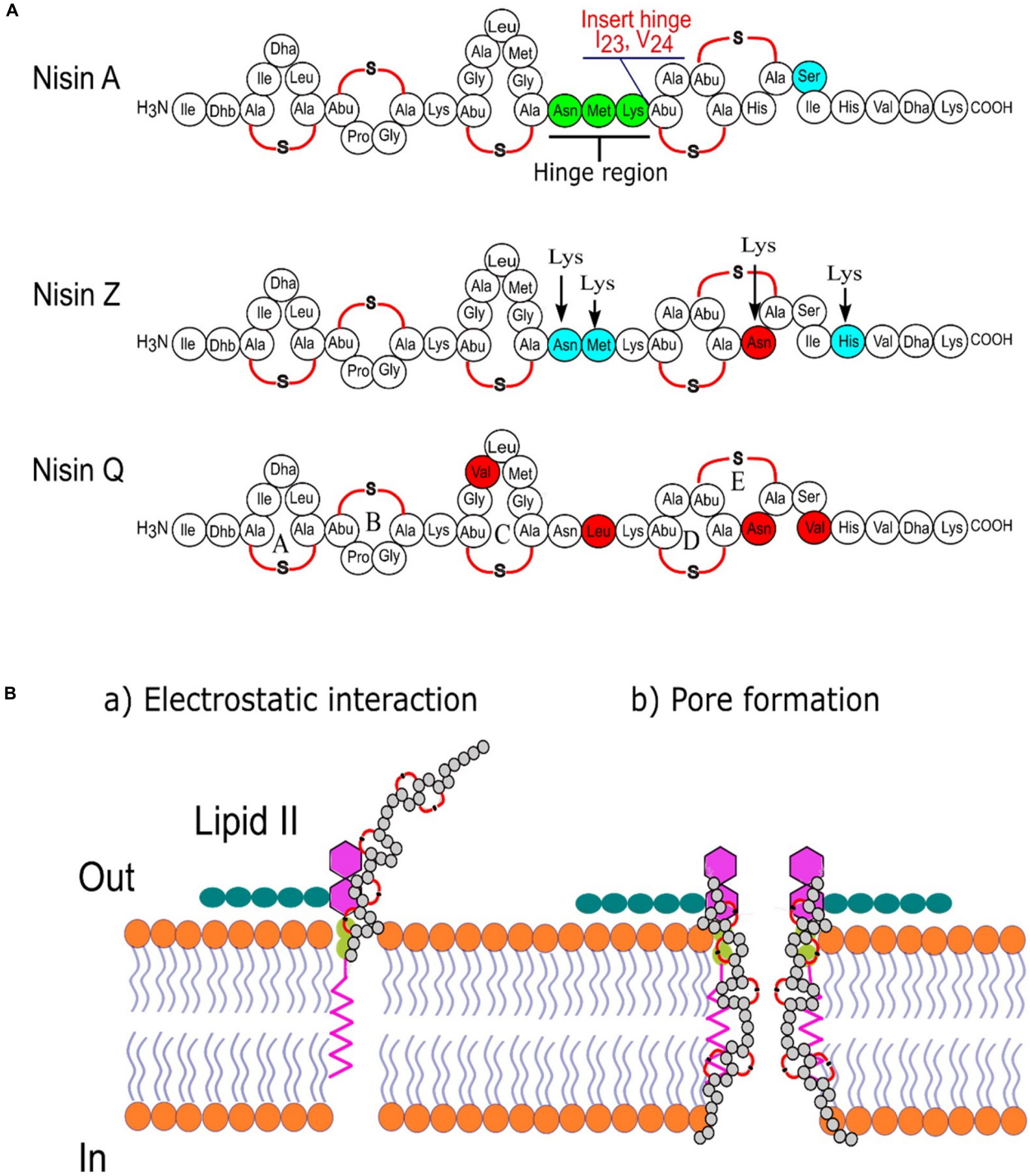

FIGURE 3 | Nisin is one of the best-studied ribosomally synthesized, pore-forming, cationic, antimicrobial peptides. **(A)** Sequence comparison of three nisin variants from *L. lactis* and marking the important regions of nisin targeted for bioengineering by classical molecular biology approaches (Chatterjee et al., 2005); **(B)** two-steps mode of action of nisin.

their functional and structural diversity. In nature, this is normally achieved by site-selective PTMs that create special non-canonical amino acid side chains such as dehydroalanine (Dha) and dehydrobutyrine (Dhb) in lantibiotics (**Figure 3**). To directly mimic these and similar PTMs, chemists used, e.g., rhodium-catalyzed arylations (Key and Miller, 2017), P450-catalyzed cyclopropanations (Gober et al., 2017), and photocatalytic activation (de Bruijn and Roelfes, 2018) in

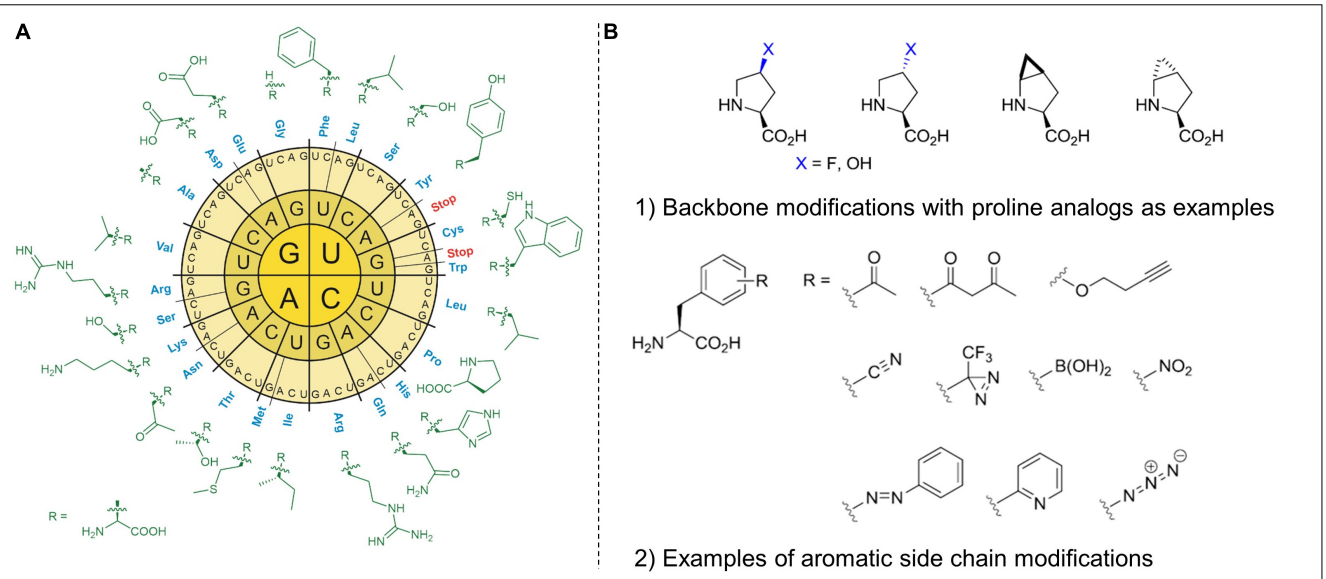

FIGURE 4 | The radial arrangement of the standard genetic code in RNA format **(A)** with the side chains of 20 canonical amino acids (cAA). The standard amino acid repertoire of the genetic code can be modified or expanded **(B)** by non-canonical amino acids (ncAAs). By reprogramming protein translation, the ncAAs can be incorporated into recombinant proteins using *in vivo* and *in vitro* methods. These insertions offer useful modifications that can be made to the protein main chain (backbone) and the amino acid side chains (aliphatic or aromatic). Modified backbones and side chains often have unique physicochemical properties with the potential to dramatically expand the chemical and functional space of ribosomally synthesized peptides and proteins.

thiopeptides, as well as metalloporphyrin-catalyzed alkylation of methionine in nisin (Maaskant and Roelfes, 2019) as attempts to obtaining novel AMPs with improved properties and/or activities. However, it is difficult to mimic PTM machinery chemically, whereas classical peptide synthetic protocols such as solid-phase peptide synthesis (SPPS) could not cover the chemical complexity of these natural products.

Therefore, the use of recombinant DNA technology that operates with heterologous expression of biosynthetic gene clusters and enriched with reprogrammed protein translation (**Figure 4**) can provide a reasonable solution to the above-mentioned problems (Hoesl and Budisa, 2012). It enables specific insertion of the biological, chemical, and physical properties delivered by ncAAs that can be accurately defined by the chemist at the bench. Cells equipped with various bioorthogonal chemistries have the potential to perform catalytic transformations that are not found in biology, including the creation of new metabolic and informational pathways (Devaraj, 2018). These modifications can also serve as redox sensors, spectroscopic markers (e.g., spin-labeling) or sensors of protein-ligand interactions. Metal-binding amino acids could lead to new structural, catalytic, or regulatory elements in proteins, while diazirines allow site-specific photo-crosslinking of the target protein to its substrate. Photoactive and photo-isomerizable ncAAs with novel photo-physical properties such as azobenzene side chains can be used to photo-regulate protein activity. Similarly, photocaged ncAAs can be activated by light to turn on enzymatic activity spatiotemporally (for review see Young and Schultz, 2010).

Directed evolution of aminoacyl-tRNA synthase (aaRS) plays a key role in the generation of such molecular tools. Desired ncAAs can be incorporated in a site-directed manner by reading in-frame stop codons, usually amber stop codons (UAG) with a suitable orthogonal pair (o-pair). Such a pair consists of an aaRS enzyme to activate the ncAA and its associated orthogonal tRNA (*vide infra*). However, the transition to recombinant production with such a possibility by using heterologous expression hosts is not trivial. For that reason, the residue-specific replacement of a particular amino acid at all positions in a protein sequence (known as selective pressure incorporation, *vide infra*) is a reasonable alternative as it does not require o-pairs (Budisa, 2004). Finally, the capacity of ncAAs incorporation should not interfere with the sequence of posttranslational modifications leading to the formation of lantibiotics and the restoration of their bioactivity.

With such systems in hands we would have very sophisticated tools to rationally engineer RiPPs scaffolds as now they can be redesigned by reprogrammed protein translation which utilize various ncAAs. This approach would have many advantages over the above discussed classical chemical or recombinant approaches as it enables: (i) genetic encoding of desired ncAAs and its sequence positioning; (ii) recombinant production under mild conditions at room temperature and atmospheric pressure; (iii) the targeted functionalization (e.g., various site-directed bioconjugations, light induced cross-linking, metal or cofactor binding, fluorophore or pharmacophore attachment, adhesiveness, etc.) (Cropp and Schultz, 2004). Crucial requirements to expand the scope of protein synthesis with ncAAs should be cellular uptake, their intracellular metabolic stability and translational activity (i.e., incorporation). Finally, it is necessary to reallocate (reassign)

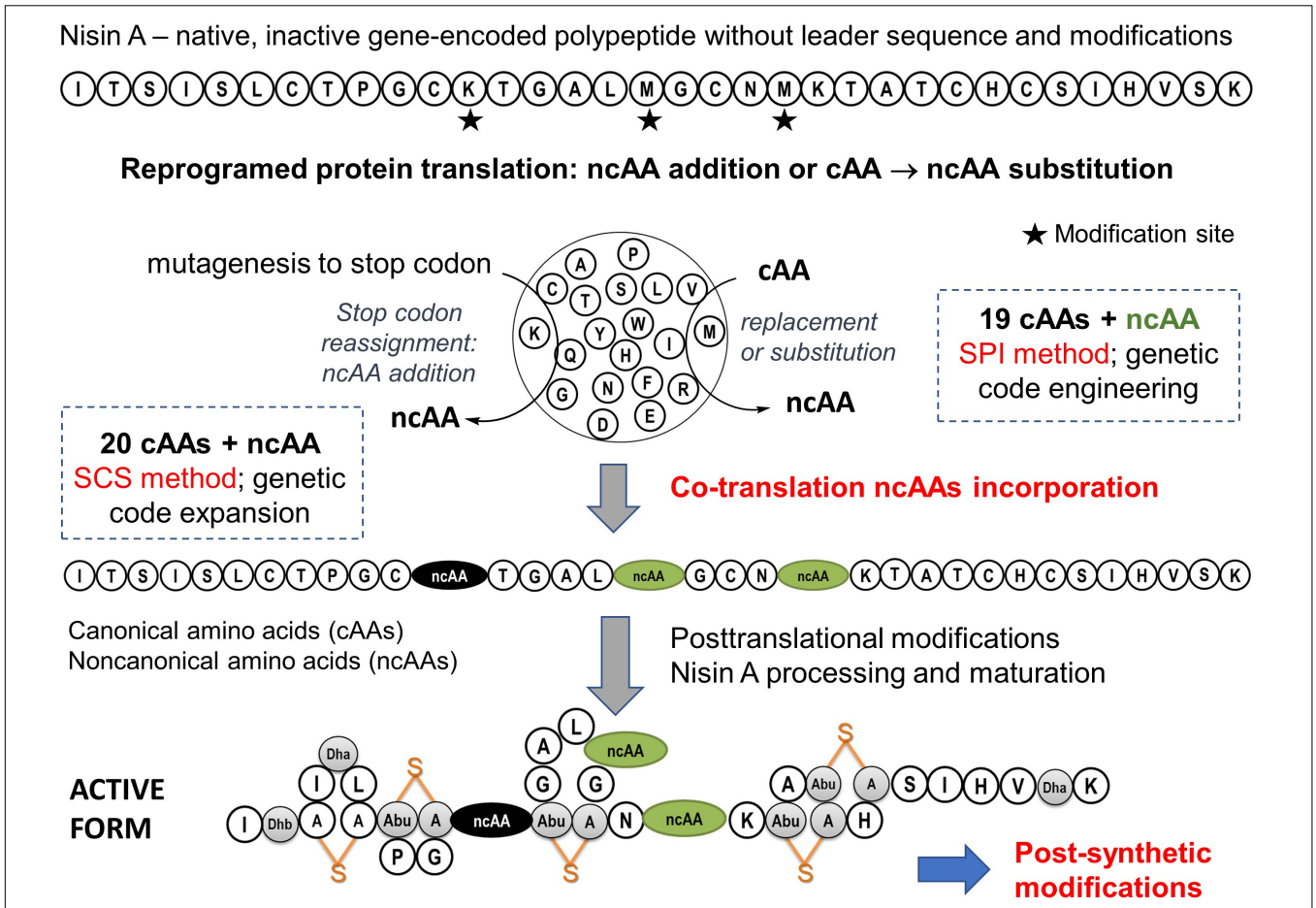

FIGURE 5 | Expansion of scope of the nisin A biosynthesis by ncAAs. The biosynthetic production of active nisin involves the expression of peptide precursors with 20 canonical amino acids as standard building blocks, followed by posttranslational modifications (PTMs). The active form of natural nisin is characterized by the presence of unusual posttranslationally introduced bridge structures known as lanthionines (depicted in orange). It is generally expected that the incorporation of ncAAs (i.e., co-translational modifications) along with post-synthetic modification options (e.g., click chemistry) will create additional functional and structural levels of RiPPs diversification. For example, new variants with improved properties such as stability, specificity, bioavailability, action spectrum and half-life could be created. This is particularly important in view of the fact that nisin is highly effective against a number of human clinical pathogens, including many multi-drug resistant strains (Piper et al., 2009). In recent years it has been clearly demonstrated that several variants of nisin increase activity or stability in different experimental setups (reviewed in Field et al., 2015).

coding triplets (codons) in the genetic code to insert ncAAs in target protein/peptide sequences.

RECOMBINANT LANTHIPEPTIDES PRODUCED BY INCORPORATING NON-CANONICAL AMINO ACIDS

Reprogrammed Protein Translation for Chemoselective Labeling of Lantibiotics

The bioexpression of lantibiotics is not fully comparable to the routine recombinant expression of soluble proteins because these polypeptides contain precursor (consisting of leader and core peptide) and recognition sequences. The core peptide is modified by post-translational modification (PTM) enzymes and upon proteolysis and export, transformed into a complex natural product. Unlike non-ribosomal natural products, native RiPPs cannot explore amino acids beyond the canonical 20 proteinogenic amino acids in the synthesis of precursor peptides, limiting their structural diversity at this level of ribosomal synthesis. On the other hand, from a biotechnological point of view, the great advantage of the ribosomal synthesis (coupled efficiently with PTMs) of bioactive compounds would be the possibility of achieving high chemical diversity at low genetic cost and to avoid supply of expensive precursors. The drawback that many unusual building blocks (found in non-ribosomal synthesis) are absent in RiPPs can be efficiently circumvented by genetic code expansion (GCE). The insertion of ncAAs (in different combinations of their numbers and chemistry) into growing peptide represents a novel level of chemical diversification of these sequences (**Figure 5**). Incorporated ncAAs can either directly interfere with PTMs or occupy sequence positions not affected by the PTM machineries. This provides

suitable bio-orthogonal reactive groups ('handles') amenable for various chemoselective ligand couplings. In addition, both site- and residue-specific incorporation techniques generally allow for fine chemical manipulations of the amino acid side chains, e.g., of Pro, Trp, Tyr, Met and to visualize them in spectroscopic recordings (Baumann et al., 2018).

Non-canonical amino acids equipped with specific chemical groups (azides, olefins, ketones and aldehydes, loaded and unloaded alkynes, halogens, oximes, hydrazones, boronic acid esters and acids, etc.) give polypeptide sequences a unique reactivity and chemoselectivity that allow easy and efficient bioconjugations to a variety of ligands (Agostini et al., 2017). The copper(I)-catalyzed Huisgen cycloaddition reaction between azides and alkynes (also known as "click chemistry") is widely used to functionalize labeled proteins since it takes place under physiological conditions allowing full retention of the protein structure (Kolb et al., 2001). For example, click chemistry proved to be efficient in producing nisin-peptoid hybrids for therapeutic use (Bolt et al., 2018). Further, *in vitro* metathesis reaction confirmed the capability of the variants for post-biosynthetic modifications such as conjugation reactions with ligands, labels, or tags using bio-orthogonal chemistry. Other alternatives include recently developed very efficient chemoselective methods; mainly copper-click, photoclick, and catalyzed oxime/hydrazone chemistries (Devaraj, 2018). This methodology could provide the RiPPs derivatives with an increase in chemical diversity such as enhanced proteolytic resistance, or increased bioavailability. Finally, bioexpression with various ncAAs combined with the possibilities for further chemical processing of RiPPs after maturation (i.e., semi-synthesis of mature products) makes the number of possible chemical combinations in antibiotic design virtually limitless.

To gain access to such a sophisticated chemistry in recombinant proteins, the incorporation of suitable ncAAs must be established in order to have possibilities for the site- or residue-specific functionalization of e.g., bioorthogonal alkyne- or azide-containing moieties. The simplest strategy for the *in vivo* insertion of ncAAs is based on the use of auxotrophic microbial systems and is known as selective pressure incorporation (SPI) (Minks et al., 2000). This methodology also exploits natural substrate tolerance ("substrate promiscuity") of protein translation machinery components toward ncAAs analogs. For example, with a Met-auxotrophic *E. coli* strain in Met-depleted medium, it was possible to express proteins in which methionine was replaced by different medium-supplemented Met analogs with a terminal azide or alkyne as a side chain (**Figure 6**). The incorporation protocol typically requires the addition of the ncAA analog in the growing medium, which is taken up by the cell machinery and used in protein translation (Budisa, 2004). Furthermore, the SPI is well known for higher translation yields without the need for extensive host engineering.

The SPI method essentially requires a genetically and metabolically stable auxotrophic expression host with ncAA recognized and activated by endogenous translation apparatus. Efficient and robust protein expression systems with controlled fermentation and expression conditions usually yield target proteins often similar to the wt-counterparts. This was demonstrated in 2012, when the first application of the SPI method for RiPPs was reported (Oldach et al., 2012). In particular, the residue-specific incorporation of various Trp, Met, and Pro analogs into the modular two-component lantibiotic lichenicidin proved to be fully attainable (**Figure 6**). In this system, the plasmid-encoded SPI-based expression of modular propeptides is coupled with the expression of the fosmid-encoded PTM machinery in the *E. coli* host cells. It has also been shown that lichenicidin with the Met analog homopropragylglycine (Hpg) can be post-synthetically functionalized by click chemistry using azidofluorescein as a ligand.

However, the fundamental disadvantage of the SPI method is that it allows residue-specific substitution of the canonical amino acid of interest by isosteric analogs, uncontrolled substitutions in the entire proteome, possibly endangering the heterologous PTM machinery and thus damaging the host expression cell. Furthermore, often in this approach the incorporation of ncAA is achieved in a statistical manner, which leads to a heterogeneity of the protein samples. This can be circumvented by using site-directed incorporation methods (**Figure 7**). However, if a site-directed ncAA incorporation is desired, the protein translation must be orthogonalized. A specific position in the protein to be labeled is mutated to the in-frame stop (usually amber) codon in the target gene. An essential part of this approach is therefore the introduction of in-frame stop codons (UAG) in target mRNAs decoded by the ribosome. In-frame stop codon suppression (i.e., readthrough) is achieved via a specially designed suppressor tRNA charged with ncAA (by a dedicated enzyme) and leads to the ncAA incorporation in a site-specific manner. This expands the amino acid repertoire of the genetic code and provides a basis for the technology known as stop-codon suppression (SCS) also as GCE. GCE generally requires the introduction of orthogonal aminoacyl-tRNA synthetase:tRNA pairs (o-pairs) into recombinant expression systems. Heterologous expression systems operating with orthogonal pairs are also known as orthogonal translation systems (OTS) in the literature. This research area is very well covered by a number of recent reviews (see, for example, Soye et al., 2015; Arranz-Gibert et al., 2018).

In orthogonal translation, usually a TAG (amber) stop codon is assigned to the ncAA and the orthogonal tRNA anticodon is mutated to CUA for position-specific incorporation. Orthogonal pairs of archaeal origin can be into eubacterial (such as *E. coli*) or eukaryotic hosts (such as *Saccharomyces cerevisiae*) and used to affect orthogonal translation (Wang et al., 2006). In particular, to engineer o-pairs, it is necessary to redesign an existing aaRS to activate the desired new ncAA substrate. Commonly used orthogonal pairs are based on *Methanocaldococcus jannaschii* tyrosyl-tRNA synthetase (*Mj*TyrRS) and *Methanosarcina mazei/barkeri* pyrrolysyl-tRNA synthetases (*Mm*PylRS or *Mb*PylRS). Compared to *E. coli* or eukaryotic hosts they show a distant phylogeny (due to their archaeal origin) that allows their implementation as o-pairs (i.e., they do not show cross-reactivity with the endogenous translational apparatus) (Budisa, 2006). Enzyme variants are generated by mutagenesis of the plasmid library and selected iterative positive/negative selection cycles (Bryson et al., 2017). This technology enables the incorporation of

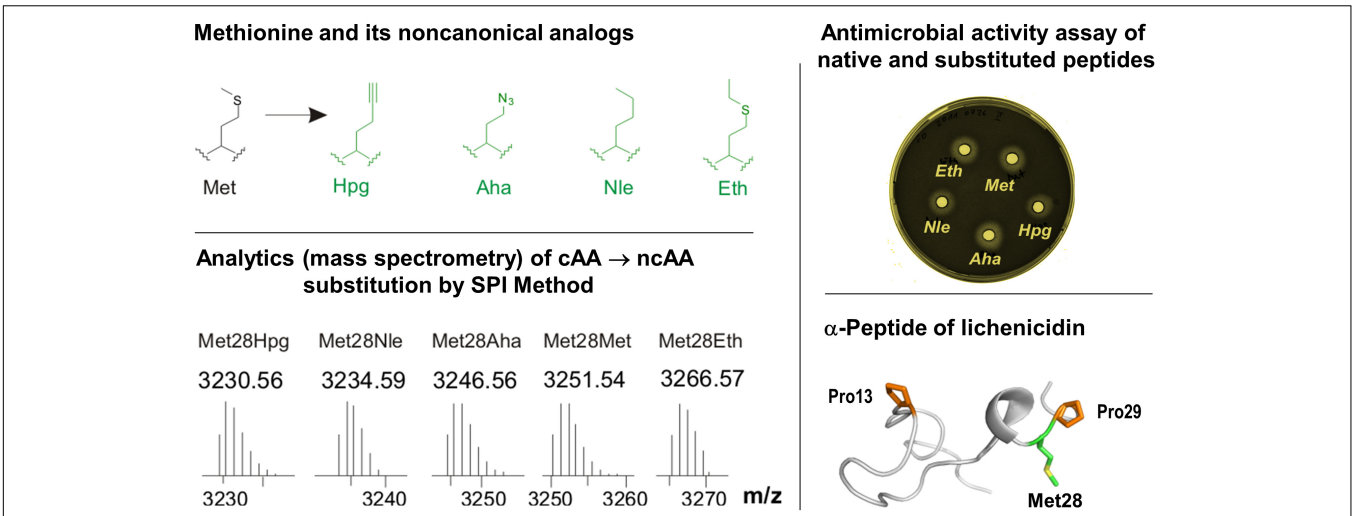

FIGURE 6 | Incorporation of Met analogs into the one subunit of the two-component lantibiotic lichenicidin using the SPI method. Top left: Structures of methionine and its analogs. Met, L-methionine; Aha, L-azidohomoalanine; Hpg, L-homopropargylglycine; Nle, L-norleucine and Eth, L-ethionine. These analogs were used to individually replace Met residues in the precursor peptide of lichenicidin (bottom right), which was also analytically confirmed (bottom left). The substituted α-peptide of lichenicidin underwent PTM-activity, whereby the linear precursor peptide was converted into a polycyclic form that exhibits antimicrobial activity when mixed with the β-peptide (top right). For more details see Oldach et al. (2012). Most recently, Kuipers and co-workers have demonstrated the use of click chemistry in the engineering of nisin by using SPI with the methionine analogs Hpg and Aha (Deng et al., 2020).

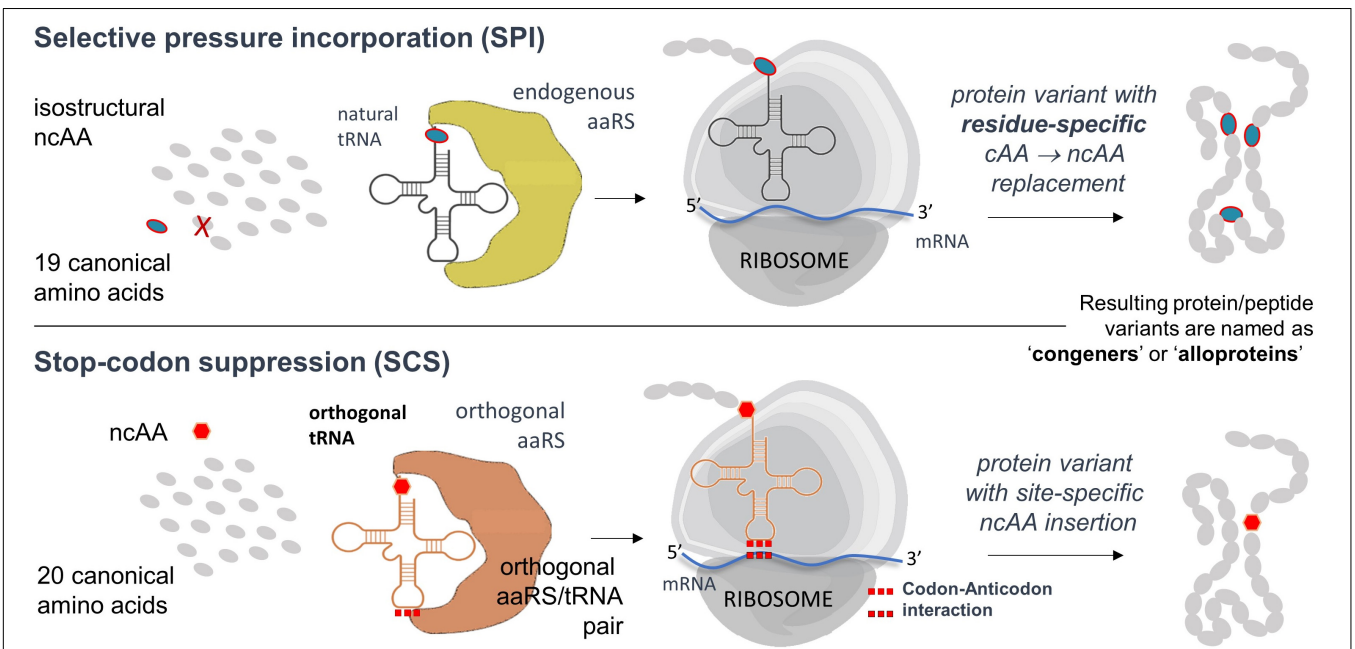

FIGURE 7 | Flow chart of the SPI and SCS methods. Both methods can be performed separately or combined in a single expression experiment (Hoesl and Budisa, 2011). Further details, advantages and disadvantages of both methods are described in the text.

ncAAs containing different chemical entities into protein, both at one position (site-directed) and at several positions (multi-site mode). Recently, we have developed a computer-aided approach (Baumann et al., 2019) to create highly diversified libraries of aminoacyl-tRNA synthetases (AARSs) and have demonstrated the engineering of orthogonal translations with up to 50-fold improved insertion efficiency. This was made possible by creating much larger libraries (with $> 10^9$ clones). In conventional directed evolution protocols, only about 10^7 clones are generated.

We and others have already applied and optimized orthogonal pairs for site-specific incorporation of fluorinated amino acids (Völler et al., 2015). Recently, we also have developed a novel and highly efficient orthogonal tyrosyl-tRNA synthetase from

Methanocaldococcus jannaschii (*Mj*TyrRS) for photo-activatable L-DOPA derivatives (Hauf et al., 2017). Similarly, we evolved a novel pyrrolysyl-tRNA synthetase from *Methanosarcina mazei* (*Mm*PylRS), which is able to incorporate S-allylcysteine (Sac) in response to amber stop codons (Exner et al., 2017). This *Mm*- or *Methanosarcina barkeri* PylRS (*Mb*PylRS) variants should be an ideal starting enzyme for the evolution of enzyme mutants with high specificity for smaller substrates. These and other advances in the field are recently summarized in a series of specific reviews (Arranz-Gibert et al., 2019; Budisa and Schneider, 2019) and highlights (Mayer, 2019; Yanagisawa et al., 2019).

Without a doubt, GCE will soon become a groundbreaking technology that will allow the catalysis of reactions that are not possible with canonical amino acids alone. More than 200 distinct ncAAs have been incorporated into various peptides and proteins so far (Vargas-Rodriguez et al., 2018). This technology has already yielded new-to-nature RiPPs and proteins in general with improved or novel physicochemical and biological properties which enabled the study of the structure-function relationship of proteins, imaging (Uttamapinant et al., 2015), probing (Chatterjee et al., 2013) and even the development of new therapeutics. Furthermore, it is possible to mask side chain functionalities of amino acids of interest by replacing them site-specifically with e.g., photo-caged ncAA. These masked substrates can then be non-invasively unmasked by UV light irradiation revealing critical functionalities (e.g., photo-caged residues which are substrates for *Mj*TyrRS and *Mm* or *Mb*PylRS-based orthogonal translation) (Drienovská and Roelfes, 2020). For the incorporation of ncAAs into RiPPs, various methods have been considered so far, ranging from *in vitro* synthesis reactions to residue and site-specific *in vivo* incorporation (Bartholomae et al., 2018). To maximize the yield and cost-effective production of lantibiotics, the biological synthesis of these compounds offers a viable alternative strategy with less downstream processing.

GCE as a Technology for New-To-Nature Lanthipeptides: Troubleshooting and Some Insider Tips

The deeper understanding of the molecular mechanisms behind the activities of AMPs, their selectivity and rational manipulation requires the application of novel technologies of peptide modifications. Incorporation of ncAAs is a particularly promising tool, which is able to deliver new chemical functions and specific probes into peptide structures. For example, Nagao et al. reported the first example of heterologous expression of the type II lantibiotic, nukacin ISK-1 in *E. coli* by co-expression of NukA and the modification enzyme NukM (Nagao et al., 2005). In the following years, this approach was increasingly replaced by the insertion of different ncAAs that mimic different PTMs, such as the photocrosslinker *p*-Benzoyl-L-Phe (pBpa) in protein and proteome chemistry due to the orthogonal translation rapid development using different vectors and expression systems in *E. coli* (Miyazaki et al., 2018). In general, the ncAA-insertion provides many advantageous properties when compared with PTMs, such as functional diversity, probing and controllable activity. In this context, **Table 2** represents a list of the new-to-nature RiPPs biosynthetically produced via GCE methodology.

We define lanthipeptides expressed recombinantly with ncAAs as "new-to-nature" because they are endowed with chemical functionalities that are normally a domain of classical organic chemistry. Most of such genetically encoded modifications introduced in proteins and peptides (*in vivo* and *in vitro*) take place on amino acid side chains and very seldom on protein backbones (like e.g., modified proline analogs; see **Figure 4**; Larregola et al., 2012). For example, D-amino acids, β-, or γ-amino acids, dipeptides and dipeptidomimetic analogs can be inserted into target polypeptide sequences by using engineered *in vitro* translation systems (Lee et al., 2019). Translation with backbone modification is difficult because ribosomes are being evolved to facilitate the polymerization of α-L-amino acids into polypeptides. Since the majority of the canonical amino acids can be considered to be derivatives of alanine (Kubyshkin and Budisa, 2019), the ncAA insertions (via SCS) or substitutions (via SPI) are mainly additions of new side-chain functionalities-a sort of useful co-translational addition to existing PTMs that should greatly expand the functional performance of modified peptides and proteins.

The engineering of orthogonal aminoacyl-tRNA synthetase/tRNA orthogonal pairs (o-pairs) for the site-specific incorporation of ncAAs is undoubtedly an important tool in protein and peptide design. However, it should be noted that orthogonalization of protein translation is usually associated with a significant decrease in system performance. Therefore, bio-expressions with orthogonal pairs require that the desired ncAA is available in large excess (Völler and Budisa, 2017). In addition, o-pairs based on both *Mj*TyrRS and *Mm*(*Mb*)PylRS scaffolds can have advantages and disadvantages in different environments. In bacterial host cells, *Mj*TyrRS often show a higher performance compared with PylRS-based systems (Rauch et al., 2016). In general, orthogonal translation with PylRS-derived o-pairs leads to lower yields of target protein, since this enzyme generally has a low catalytic efficiency (Baumann et al., 2016). While o-pairs based on *Mj*TyrRS allow a higher number of in-frame stop codons that can be suppressed, this is not the case with orthogonal translation based on PylRS (Zhao et al., 2018). Many strategies have been reported to alleviate these limitations, including the computational redesign of both enzymes as discussed elsewhere (Baumann et al., 2019).

The incorporation of ncAAs via SCS into proteins in general and RiPPs in particular is usually associated with reduced expression efficiency since the readthrough of stop codons is context-dependent. In particular, the insertion of in-frame stop codons in target sequences might generate so-called "context effects" with the competition with ribosomal release factors (RFs) for the readthrough (Plotkin and Kudla, 2011). Next, the insertion of a stop codon into a specific sequence is often associated with a high level of interference with natural mRNA folding (Gorochowski et al., 2015). This requires the optimization of mRNA sequences by applying a computer-aided design that should restore or even improve the strength of binding site interaction within the ribosome (Del Campo et al., 2015). For these reasons, "context effects"

TABLE 2 | List of the new-to-nature RiPPs produced by genetic code expansion technology reported so far.

	Type	Source/Host	New RiPPs	Activity*or Peptide yield (mg/L)	References
Prochlorisin A 3.2	Class II lantibiotic	*Prochlorococcus/ E. coli*	F26-pBpa	Equal	Shi et al., 2011
Capistruin	Lassopeptide	Actinobacteria/ *E. coli*	I4- Alk	0.110	Al Toma et al., 2015
			I4-Nbk	0.039	
			I4-BocK	0.110	
			I4-Ack	0.042	
			I4-Pck	0.041	
			A10- Alk	0.290	
			A10-Nbk	0.218	
			A10-BocK	0.435	
			A10-Ack	0.149	
			A10-Pck	0.143	
			G17-Alk	0.033	
			G17-Nbk	< LoQ	
			G17-BocK	0.013	
			G17-Ack	< LoQ	
			G17-Pck	< LoQ	
MccJ25	Lassopeptide	*E. coli/E. coli*	V6, I13- *m*Br-F	Less	Piscotta et al., 2015
			F10, F19- *m*Br-F	Equal	
			V6, I13- *m*NO_2-F	Less	
			F10, F19- *m*NO_2-F	Less	
			V6, I13- *m*Cl-F	Less	
			F10, F19- *m*Cl-F	Equal	
			V6, I13- *m*CF_3-F	Less	
			F10, F19- *m*CF_3-F	Less	
Thiocilin	Thiopeptide	*B. cereus/B. cereus*	T3, T4, V6, T8, T13-BocK	Decreased	Luo et al., 2016
			T3, T4, V6, T8, T13- AlocK	Decreased	
			T3, T4, V6, T8, T13- ProcK	Decreased	
Nisin A	Class I lantibiotic	*L. lactis/E. coli*	S3 -Fluoro-pAcF	2.00	Zambaldo et al., 2017
			T8- Fluoro-pAcF	1.50	
			T13- Fluoro-pAcF	3.00	
Cinnamycin	Class II Type B lantibiotic	*S. albus/S. albus*	R2-Alk	Decreased	Lopatniuk et al., 2017
			F10-Alk	Decreased	
Nisin A	Class I lantibiotic	*L. lactis/L. lactis* *L. lactis/E. coli*	I4-BocK	Equal	Bartholomae et al., 2018
			K12-BocK	Equal	
			I4-BocK		
			K12-BocK		
Lacticin 481	Class II lantibiotic	*L. lactis/E. coli*	W19-*o*-Cl-F, W19-*m*-Br-F, W19-*o*-NO_2-F, F21-*o*NO_2-F, F23-*o*-Cl-F	Increased	Kakkar et al., 2018
			W19, F21, F23- *o*Br-F W19, F21, F23- *o*NO_2-F W19, F21, F23- *m*Br-F W19, F21, F23- *m*CF_3-F	Decreased	

*ND, not determined. *Antimicrobial activity in comparison to wild-type; < LoQ = below the limit of quantification. L. lactis, Lactococcus lactis; S. albus, Streptomyces albus; pBpa, p-benzoyl-L-phenylalanine; Nbk, Nε-5-norbornene-2-yloxycarbonyl-L-lysine; Alk, Nε-AllocI-Lysine; Ack, Nε-2-azidoethyloxycarbonyl-L-lysine; Pck, Nε-2-propyn-1-yloxycarbonyl-L-lysine; Bock, Nε-Boc-L-lysine; mBr-F, meta-Bromo-phenylalanine; mNO2-F, meta-Nitro-phenylalanine; mCl-F, meta-Chloro-phenylalanine; mCF3-F, meta-trifluoromethyl-phenylalanine; AlocK, Ne-allyloxycarbonyl-L-lysine; ProcK, Ne-prop-2-ynyloxycarbonyl-L-lysine; pAcF, p-acetylphenylalanine.*

during the incorporation of ncAA in target sequences were investigated by randomly generating in-frame stop codons along the gene sequence with different proteins (summarized in Agostini et al., 2017).

The screening of an amber stop codon library with lantibiotic genes to study site-specific ncAAs incorporation efficiency could be of great importance to improve and enhance the biosynthesis of RiPPs with ncAAs. For example, we and others

recently established a reporter platform for SCS approach using three expression vectors capable of independent control of different groups of genes. Each sense codon in the core peptide region of NisA was replaced by TAG (amber) codon and screening of possibly suitable incorporation positions was assessed upon incorporation of various analogs (Bartholomae et al., 2018). Next, in addition to the feasibility of a position to incorporate ncAAs, the admissibility of target genes that can fold and modify is critical and must always be considered. This is best illustrated by the report of Shi et al. (2011), in which the orthogonal translation was performed with three different types of bioactive peptides, prochlorosins from class II lanthipeptides, two-component lantibiotic haloduracin and the class I lantibiotic, nisin.

As discussed above, the residue-specific replacement of a particular amino acid at all positions in a protein sequence with ncAA (i.e., SPI method) proved to be a reasonable alternative in some cases (Hoesl and Budisa, 2011). Moreover, incorporation of three different tryptophan analogs (5-fluoroTrp, 5-hydroxyTrp, and 5-methylTrp) into different positions of nisin (I1W, I4W, M17W, and V32W), which included the overexpression of tryptophanyl-tRNA synthetase (TrpRS) in *L. lactis* strain PA1002, showed a reasonable incorporation efficiency and suitable production yield (Zhou et al., 2016). However, in a comparative study between the efficiency of ncAA incorporation in orthogonal translation and by SPI method into the lasso peptide capistruin, the SCS approach showed higher efficiency (Al Toma et al., 2015).

Practical Expression, Purification, Monitoring Strategies, and Challenges With Novel Lanthipeptides

After induction and expression of the target gene, various conventional methods such as immobilized metal affinity chromatography (IMAC) and in rare cases, additional column chromatography were applied for the purification purposes. Due to the lack of a cell wall-anchored protease (NisP), and to avoid the requirement for immunity as well as to achieve higher production yield in *E. coli* (Montalbán-López et al., 2018), activation of the purified pre-lantibiotics is usually done by using native proteases or some commercial enzymes *in vitro*. To assess proper maturation of the lantibiotics, MS-analyses and bioactivity assays have been employed. In addition, RP-HPLC is one of the most convenient methods used for the measurement of the concentration before and after the activation by proteolytic cleavage of the leader peptide. Monitoring and quantification of the active lantibiotic by integrating the leader peptide peaks in RP-HPLC might be complicated due to alteration of running properties of the pre-lantibiotics and activated forms during the experiment and make it difficult to distinguish between similar peaks. This strategy has been used to determine the concentration of the activated lantibiotic during the production of genome-mining new lantibiotics as a hybrid containing the leader peptide of nisin (Lagedroste et al., 2019).

Another important issue is incomplete modification of target peptides such as lack of lanthionine ring formation or the defected dehydrations of Ser/Thr residues which lead to the disrupted recognition by the leader peptidases and severe decline of their antimicrobial activities. Although MS analysis of the cleavage products of pre-lantibiotics provides useful information about the dehydration reaction by the decrease of a water molecule mass (−18 Da), the technique cannot indicate the formation of methyl-lanthionine rings. In this regard, use of alkylation agents such as CDAP to bind the free cysteine thiol or peptide digestion approach using tandem MS-MS analysis to determine different patterns between wild type and mutant variants has recently been introduced (Kluskens et al., 2005). Verification of antimicrobial activity of recombinant lantibiotics can also be conducted by growth inhibition assay. Using lantibiotic-sensitive strains such as *L. lactis* strain NZ9000, *Listeria monocytogenes*, *Clostridioides difficile*, etc. have been reported in the literature (Field et al., 2010; Cebrián et al., 2019).

Several techniques have been developed for verification and quantification of nisin, such as turbidity assays (Berridge and Barrett, 1952), colorimetric assays (Wang et al., 2007) and agar diffusion bioassay (Mocquot and Lefebvre, 1956). Agar-based bioassay, as the most widely used method for quantifying nisin activity was implemented based on diffusion through agar gel seeded with nisin-sensitive indicator bacteria (Pongtharangkul and Demirci, 2004). The diameter of the inhibition zone generated by growth inhibition of indicator bacteria is correlated with the concentration of nisin. Factors such as nisin structure, concentration of agar, pH, existence of detergent, number of indicator cells and temperature can affect diffusion of nisin through agar. Several researchers have attempted to improve the accuracy, sensitivity, and reproducibility of conventional agar diffusion bioassays for nisin by optimizing several factors such as concentration of agar and buffering conditions, addition of a detergent like Tween 20, incubation time adjustment, and the temperature of pre-diffusion of the agar plates and even the size of wells on agar (Rogers and Montville, 1991; Wolf and Gibbons, 1996; Bonev et al., 2008; Lalpuria et al., 2013).

A modified form of agar diffusion bioassay was established upon activation of nisin by the membrane-associated protease enzyme (NisP). Antimicrobial activity of precursor lantibiotics and ncAA-modified variants synthesized by native producers or heterologously expressed by host cells could be determined using a sensitive indicator strain harboring appropriate genes for the maturation of the lantibiotic. For example, the nisin-sensitive indicator *L. lactis* NZ9000 pNZnisPT pIL253 showed reasonable applicability to assess functional and physicochemical properties of modified nisin variants like proline, tryptophan, and lysine incorporated analogs (Bartholomae et al., 2018). In addition, a bioactivity assay for two-component lantibiotics such as lichenicidin which requires the synergistic activity of two peptides was introduced which is called "deferred antagonist bioassay." Using agar well diffusion plates by mixing the cell-free supernatants of both separately producing strains in suitable proportions

against growth of the indicator strain and the measurement of inhibition radii after appropriate incubation at reasonable temperature aid us to easily screen a large library of lantibiotic mutants by avoiding time-consuming purification steps (Barbosa et al., 2019).

Most Recent Advances in Recombinant Lanthipeptides Production With an Expanded Genetic Code

Bindman et al. (2015) have demonstrated that co-translational backbone modification α-hydroxy acidic insertion works in RiPPs in response to in-frame amber codons (SCS method). They have shown the possibility of lantibiotic activation after co-translational incorporation of α-hydroxy acids into the precursor peptides in *E. coli*. The biosynthesis of lacticin 481 or nukacin ISK-1 analogs by incorporating Boc-HO-1, HO-Phe(3-Br)-OH or HO-Tyr(propargyl)-OH at the junction of the leader peptide to the core region of the lantibiotics (position + 1) was successful. This enabled an improved removal step of the leader peptide in a general manner without the need to screen for various proteases (Bindman et al., 2015). Efforts have also been reported to increase the chemical diversity of lasso peptides and even to determine the crystal structure of these complicated cyclic peptides in the presence of bromine atoms (Piscotta et al., 2015). Sixteen possible variants were expressed in *E. coli* at four positions (Val6, Ile3, Phe10, Phe19). Thereby, four meta-substituted Phe derivatives (*m*-ClPhe, *m*-BrPhe, *m*-NO_2Phe and *m*-CF_3Phe) were incorporated into MccJ25 using an engineered "polyspecific" *Mm*PylRS. The results showed that the yield of ncAA-substituted MccJ25 variants intensively depended on the position and the chemical nature of the substitutions.

The use of ncAAs with 1,3- or 1,2-aminothiol reactive groups to promote the cyclization of a downstream target peptide sequence via a C-terminal ligation/ring contraction mechanism has also been reported (Frost et al., 2015). It has been demonstrated to be useful for the formation of macrocyclic side-chain-to-tail peptides *in vitro* in a pH-controlled manner. This strategy controls the spontaneous cyclization of peptides of variable length and completely random sequences with a wide range of molecular arrangements, namely cyclic, lariat or C-terminal fused to a carrier protein in living bacterial cells. The co-expression of glutamyl-charged $tRNA^{Glu}$ in order to acylate specific Ser/Thr side chains with glutamate prior to the dehydration reaction was proposed by Zambaldo et al. (2017). The main intention was to overcome an incomplete dehydration phenomenon which occurs during incorporation of α-chloroacetamide-containing ncAA to nisin variants having altered macrocyclic topologies and antimicrobial activities. In an attempt to optimize biophysical properties of cinnamycin from *Streptococcus albus* for medical and industrial applications, three distinct pyrrolysine analogs were incorporated into two distinct positions of the antibiotic in Streptomycetes using the orthogonal pyrrolysyl-tRNA synthetase/$tRNA^{Pyl}$ pair from *Methanosarcina barkeri*. In spite of a low rate of incorporation, the data revealed that the type of ncAA and the position of incorporation are important to achieve suitable amounts of the new deoxycinnamycin derivatives (Lopatniuk et al., 2017). Last but not least, the stereochemical configuration of thioether bridges is an important issue, since recent studies indicate that it is the property of the sequence of the core peptide and not the modification enzyme that determines the stereochemical outcome of ring formation (Garg et al., 2016).

Although most of the reports regarding the site-specific incorporation of ncAAs in RiPPs have shown lower levels of antimicrobial activity of variants than the wild type, some rare reports presented slightly improved activity on analogs (**Table 2**). Notably, novel modified lantibiotic variants have encrypted potential to show appropriate activity against newly emerged pathogens.

CONCLUSION AND OUTLOOK

It has been estimated that 1.2 trillion USD are required to cover additional health expenditure per year expected by 2050 due to the rise of various AMRs (World Health Organization, 2020). The World Health Organization (WHO) has announced a global AMR response to coordinate this in collaboration with international partners. According to the WHO report on antimicrobial agents in clinical development stages in 2019, the majority of antibacterial agents are direct-acting small molecules (n = 108, 42.9%), followed by non-traditional approaches (n = 90, 35.7%), then AMPs (n = 27, 10.7%) as the main antibiotic agents (World Health Organization, 2019). It was also argued that the alarming rise in antibiotic resistance rates in the late 20th century is a clear indication that the golden age of antibiotics might be over (Wernicki, 2013). All these figures and projections urge us to reconsider current approaches and anticipate possible future paths to alternatives. In many cases, superbugs are characterized by increased multi-drug resistance, improved transmissibility and virulence, resulting in increased morbidity and mortality.

Multi-drug resistance in bacteria is a very complex problem, deeply rooted in the genetic and biochemical flexibility of bacteria, i.e., a highly pleiotropic phenomenon. Obviously, this problem cannot be solved only by simple solutions such as chemical modifications or variations of known lead substances. Therefore, we believe that the time is coming to use more extensively the most advanced methods of Synthetic Biology such as expanded genetic code to combat superbugs that have continuously evolved in most industrialized nations over the last 60 years. Here we attempted to summarize the efforts that have been made by the help of expanded genetic code to introduce new-to-nature lanthipeptides as promising alternatives to classical chemical agents. We have also tried to present new insights and progress in the field as well as the limitations and challenges which should be overcome in the future. We are firmly convinced that "radical" methods of genetic engineering (Davies and Church, 2019), such as the expansion of the genetic code, can

be a useful addition to the struggle against superbugs as a global threat to all of mankind.

In the present medical context and in the current environment of failing antibiotic protection, an obvious functional expansion is a fortification against post-surgery antibiotic infections, for example by coupling therapeutic proteins to antimicrobial modules. New approaches such as genetically encoded chemical conversion (GECCO) has also been recently introduced (Yang et al., 2019) to overcome limitations of translational machinery. This and other newly emerged approaches such as OTS optimization (Dulic et al., 2018), cell-free protein synthesis (Jin and Hong, 2018), genomically recorded strain development (Amiram et al., 2015), artificial codon box division (Iwane et al., 2016), and quadruplet codon and orthogonal ribosome (d'Aquino et al., 2018) are expected to open new avenues for exploiting chemistry in live systems to bioengineering of lanthipeptides. GCE as a research field has now reached the maturity to be efficiently implemented in the bioengineering of lanthipeptides to understand their structural complexity and the behavior of the entire biosynthesis machinery. This should provide a solid basis for expanding the chemical space of recombinant AMPs. The aim is not only improving their therapeutic properties to combat AMR but also to repurpose them functionally for, e.g., anticancer or antiviral activities. The application of co-translational incorporation of ncAAs by more than 200 different chemical entities available to us for rational manipulation of various scaffolds offers unprecedented opportunities to manage the supply of advanced peptide-based antimicrobials and other sophisticated drugs in the future.

AUTHOR CONTRIBUTIONS

HRK-H and NB planned and conceived. All authors read, critically revised, and approved the final manuscript.

FUNDING

This research was supported by SynCrop from the European Union's Horizon 2020 Research and Innovation Programme under the Marie Skłodowska-Curie grant agreement No 764591 and by Canada Research Chairs Program (Grant No. 950-231971).

ACKNOWLEDGMENTS

NB would like to thank Prof. Dr. Christian Thomsen, President of the Technical University of Berlin, for his continuous support. We acknowledge support by the Open Access Publication Fund of TU Berlin. We offer our sincere apologies to numerous authors of relevant works who were not included in this review; the omission was unintentional.

REFERENCES

Acedo, J. Z., Chiorean, S., Vederas, J. C., and Van Belkum, M. J. (2018). The expanding structural variety among bacteriocins from Gram-positive bacteria. *FEMS Microbiol. Rev.* 42, 805–828. doi: 10.1093/femsre/fuy033

Adhikari, S., Leissa, J. A., and Karlsson, A. J. (2019). Beyond function: engineering improved peptides for therapeutic applications. *AIChE J.* 66:e16776. doi: 10.1002/aic.16776

Ageitos, J. M., Sánchez-Pérez, A., Calo-Mata, P., and Villa, T. G. (2017). Antimicrobial peptides (AMPs): ancient compounds that represent novel weapons in the fight against bacteria. *Biochem. Pharmacol.* 133, 117–138. doi: 10.1016/j.bcp.2016.09.018

Agostini, F., Voller, J. S., Koksch, B., Acevedo-Rocha, C. G., Kubyshkin, V., and Budisa, N. (2017). Biocatalysis with unnatural amino acids: enzymology meets xenobiology. *Angew. Chem. Int. Ed.* 56, 9680–9703. doi: 10.1002/anie.201610129

Ahmed, Y., Rebets, Y., Estevez, M. R., Zapp, J., Myronovskyi, M., and Luzhetskyy, A. (2020). Engineering of *Streptomyces lividans* for heterologous expression of secondary metabolite gene clusters. *Microbial. Cell Fact.* 19:5. doi: 10.1186/s12934-020-1277-8

Al Toma, R. S., Kuthning, A., Exner, M. P., Denisiuk, A., Ziegler, J., Budisa, N., et al. (2015). Site-directed and global incorporation of orthogonal and isostructural noncanonical amino acids into the ribosomal lasso peptide capistruin. *ChemBioChem* 16, 503–509. doi: 10.1002/cbic.201402558

Alvarez-Sieiro, P., Montalbán-López, M., Mu, D., and Kuipers, O. P. (2016). Bacteriocins of lactic acid bacteria: extending the family. *Appl. Microbiol. Biotechnol.* 100, 2939–2951. doi: 10.1007/s00253-016-7343-9

Amiram, M., Haimovich, A. D., Fan, C., Wang, Y.-S., Aerni, H.-R., Ntai, I., et al. (2015). Evolution of translation machinery in recoded bacteria enables multi-site incorporation of nonstandard amino acids. *Nat. Biotechnol.* 33, 1272–1279. doi: 10.1038/nbt.3372

Arnison, P. G., Bibb, M. J., Bierbaum, G., Bowers, A. A., Bugni, T. S., Bulaj, G., et al. (2013). Ribosomally synthesized and post-translationally modified peptide natural products: overview and recommendations for a universal nomenclature. *Nat. Prod. Rep.* 30, 108–160. doi: 10.1039/c2np20085f

Arranz-Gibert, P., Patel, J. R., and Isaacs, F. J. (2019). The role of orthogonality in genetic code expansion. *Life* 9:58. doi: 10.3390/life9030058

Arranz-Gibert, P., Vanderschuren, K., and Isaacs, F. J. (2018). Next-generation genetic code expansion. *Curr. Opin. Chem. Biol.* 46, 203–211. doi: 10.1016/j.cbpa.2018.07.020

Aslam, B., Wang, W., Arshad, M. I., Khurshid, M., Muzammil, S., Rasool, M. H., et al. (2018). Antibiotic resistance: a rundown of a global crisis. *Infect. Drug Resist.* 11:1645. doi: 10.2147/IDR.S173867

Barbosa, J., Caetano, T., Mösker, E., Süssmuth, R., and Mendo, S. (2019). Lichenicidin rational site-directed mutagenesis library: a tool to generate bioengineered lantibiotics. *Biotechnol. Bioeng.* 116, 3053–3062. doi: 10.1002/bit.27130

Bartholomae, M., Baumann, T., Nickling, J. H., Peterhoff, D., Wagner, R., Budisa, N., et al. (2018). Expanding the genetic code of *Lactococcus lactis* and *Escherichia coli* to incorporate non-canonical amino acids for production of modified lantibiotics. *Front. Microbiol.* 9:657. doi: 10.3389/fmicb.2018.00657

Baumann, T., Exner, M., and Budisa, N. (2016). "Orthogonal protein translation using pyrrolysyl-tRNA synthetases for single-and multiple-noncanonical amino acid mutagenesis," in *Synthetic Biology–Metabolic Engineering*, eds H. Zhao, and A.-P. Zeng (Berlin: Springer), 1–19.

Baumann, T., Hauf, M., Richter, F., Albers, S., Möglich, A., Ignatova, Z., et al. (2019). Computational aminoacyl-tRNA synthetase library design for photocaged tyrosine. *Int. J. Mol. Sci.* 20:2343.

Baumann, T., Schmitt, F.-J., Pelzer, A., Spiering, V. J., Von Sass, G. J. F., Friedrich, T., et al. (2018). Engineering'golden'fluorescence by selective pressure incorporation of non-canonical amino acids and protein analysis by mass spectrometry and fluorescence. *J. Vis. Exp.* 134:e57017. doi: 10.3791/57017

Berridge, N., and Barrett, J. (1952). A rapid method for the turbidimetric assay of antibiotics. *Microbiology* 6, 14–20. doi: 10.1099/00221287-6-1-2-14

Bindman, N. A., Bobeica, S. C., Liu, W. R., and Van Der Donk, W. A. (2015). Facile removal of leader peptides from lanthipeptides by incorporation of a hydroxy acid. *J. Am. Chem. Soc.* 137, 6975–6978. doi: 10.1021/jacs.5b04681

Boakes, S., and Dawson, M. J. (2014). "Discovery and development of NVB302, a semisynthetic antibiotic for treatment of *Clostridium difficile* infection," in *Natural Products: Discourse, Diversity, and Design*, eds A. Osbourn, R. Goss, and G. T. Carter (Hoboken, NJ: John Wiley & Sons), 455–468. doi: 10.1002/9781118794623.ch24

Boakes, S., Weiss, W. J., Vinson, M., Wadman, S., and Dawson, M. J. (2016). Antibacterial activity of the novel semisynthetic lantibiotic NVB333 in vitro and in experimental infection models. *J. Antibiot.* 69, 850–857. doi: 10.1038/ja.2016.47

Bolt, H. L., Kleijn, L. H. J., Martin, N. I., and Cobb, S. L. (2018). Synthesis of antibacterial nisin-peptoid hybrids using click methodology. *Molecules* 23:1566. doi: 10.3390/molecules23071566

Bonev, B., Hooper, J., and Parisot, J. (2008). Principles of assessing bacterial susceptibility to antibiotics using the agar diffusion method. *J. Antimicrob. Chemother.* 61, 1295–1301. doi: 10.1093/jac/dkn090

Brand, G. D., Magalhães, M. T., Tinoco, M. L., Aragão, F. J., Nicoli, J., Kelly, S. M., et al. (2012). Probing protein sequences as sources for encrypted antimicrobial peptides. *PLoS One* 7:e45848. doi: 10.1371/journal.pone.0045848

Breukink, E., and de Kruijff, B. (2006). Lipid II as a target for antibiotics. *Nat. Rev. Drug Discov.* 5, 321–323. doi: 10.1038/nrd2004

Brogden, K. A. (2005). Antimicrobial peptides: pore formers or metabolic inhibitors in bacteria? *Nat. Rev. Microbiol.* 3, 238–250. doi: 10.1038/nrmicro1098

Bryson, D. I., Fan, C., Guo, L.-T., Miller, C., Söll, D., and Liu, D. R. (2017). Continuous directed evolution of aminoacyl-tRNA synthetases. *Nat. Chem. Biol.* 13, 1253–1260. doi: 10.1038/nchembio.2474

Budisa, N. (2004). Prolegomena to future experimental efforts on genetic code engineering by expanding its amino acid repertoire. *Angew Chem. Int. Ed.* 43, 6426–6463. doi: 10.1002/anie.200300646

Budisa, N. (2006). *Engineering the Genetic Code: Expanding the Amino Acid Repertoire for the Design of Novel Proteins*. Hoboken, NJ: John Wiley & Sons.

Budisa, N. (2013). Expanded genetic code for the engineering of ribosomally synthetized and post-translationally modified peptide natural products (RiPPs). *Curr. Opin. Biotechnol.* 24, 591–598. doi: 10.1016/j.copbio.2013.02.026

Budisa, N., and Schneider, T. (2019). Expanding the DOPA universe with genetically encoded, mussel-inspired bioadhesives for material sciences and medicine. *ChemBioChem* 20, 2163–2190. doi: 10.1002/cbic.201900030

Cardoso, M. H., Ribeiro, S. M., Nolasco, D. O., De La Fuente-Núñez, C., Felício, M. R., Gonçalves, S., et al. (2016). A polyalanine peptide derived from polar fish with anti-infectious activities. *Sci. Rep.* 6:21385. doi: 10.1038/srep21385

Cebrián, R., Macia-Valero, A., Jati, A. P., and Kuipers, O. P. (2019). Design and expression of specific hybrid lantibiotics active against pathogenic *Clostridium* spp. *Front. Microbiol.* 10:2154. doi: 10.3389/fmicb.2019.02154

Chalekson, C. P., Neumeister, M. W., and Jaynes, J. (2002). Improvement in burn wound infection and survival with antimicrobial peptide D2A21 (Demegel). *Plast. Reconstr. Surg.* 109, 1338–1343. doi: 10.1097/00006534-200204010-00020

Chatterjee, A., Guo, J., Lee, H. S., and Schultz, P. G. (2013). A genetically encoded fluorescent probe in mammalian cells. *J. Am. Chem. Soc.* 135, 12540–12543. doi: 10.1021/ja4059553

Chatterjee, C., Paul, M., Xie, L., and Van Der Donk, W. A. (2005). Biosynthesis and mode of action of lantibiotics. *Chem. Rev.* 105, 633–684.

Clemens, R., Zaschke-Kriesche, J., Khosa, S., and Smits, S. H. (2018). Insight into two ABC transporter families involved in lantibiotic resistance. *Front. Mol. Biosci.* 4:91. doi: 10.3389/fmolb.2017.00091

Coast, J., Smith, R. D., and Millar, M. R. (1996). Superbugs: should antimicrobial resistance be included as a cost in economic evaluation? *Health Econ.* 5, 217–226. doi: 10.1002/(sici)1099-1050(199605)5:3<217::aid-hec200<3.0.co;2-s

Cropp, T. A., and Schultz, P. G. (2004). An expanding genetic code. *Trends Genet.* 20, 625–630. doi: 10.1016/j.tig.2004.09.013

d'Aquino, A. E., Kim, D. S., and Jewett, M. C. (2018). Engineered Ribosomes for Basic Science and Synthetic Biology. *Annu. Rev. Chem. Biomol. Eng.* 9, 311–340. doi: 10.1146/annurev-chembioeng-060817-084129

Davies, J., and Davies, D. (2010). Resistance origins and evolution of antibiotic. *Microbiol. Mol. Biol. Rev.* 74, 417–433. doi: 10.1128/MMBR.00016-10

Davies, K., and Church, G. M. (2019). Radical technology meets radical application: an interview with George Church. *CRISPR J.* 2, 346–351. doi: 10.1089/crispr.2019.29074.gch

de Bruijn, A. D., and Roelfes, G. (2018). Chemical modification of dehydrated amino acids in natural antimicrobial peptides by photoredox catalysis. *Chem. Eur. J.* 24, 11314–11318. doi: 10.1002/chem.201803144

Del Campo, C., Bartholomäus, A., Fedyunin, I., and Ignatova, Z. (2015). Secondary structure across the bacterial transcriptome reveals versatile roles in mRNA regulation and function. *PLoS Genet.* 11:e1005613. doi: 10.1371/journal.pgen.1005613

Deng, J., Viel, J. H., Chen, J., and Kuipers, O. P. (2020). Synthesis and characterization of heterodimers and fluorescent nisin species by incorporation of methionine analogs and subsequent click chemistry. *ACS Synth. Biol.* 9, 2525–2536. doi: 10.1021/acssynbio.0c00308

Devaraj, N. K. (2018). The future of bioorthogonal chemistry. *ACS Cent. Sci.* 4, 952–959. doi: 10.1021/acscentsci.8b00251

Draper, L. A., Cotter, P. D., Hill, C., and Ross, R. P. (2015). Lantibiotic resistance. *Microbiol. Mol. Biol. Rev.* 79, 171–191. doi: 10.1128/mmbr.00051-14

Drienovská, I., and Roelfes, G. (2020). Expanding the enzyme universe with genetically encoded unnatural amino acids. *Nat. Catal.* 3, 1–10.

Dulic, M., Cvetesic, N., Zivkovic, I., Palencia, A., Cusack, S., Bertosa, B., et al. (2018). Kinetic origin of substrate specificity in post-transfer editing by leucyl-tRNA synthetase. *J. Mol. Biol.* 430, 1–16. doi: 10.1016/j.jmb.2017.10.024

Exner, M. P., Kuenzl, T., To, T. M., Ouyang, Z., Schwagerus, S., Hoesl, M. G., et al. (2017). Design of S-allylcysteine in situ production and incorporation based on a novel pyrrolysyl-tRNA synthetase variant. *ChemBioChem* 18, 85–90. doi: 10.1002/cbic.201600537

Feng, Q., Huang, Y., Chen, M., Li, G., and Chen, Y. (2015). Functional synergy of α-helical antimicrobial peptides and traditional antibiotics against Gram-negative and Gram-positive bacteria in vitro and in vivo. *Eur. J. Clin. Microbiol. Infect. Dis.* 34, 197–204. doi: 10.1007/s10096-014-2219-3

Field, D., Begley, M., O'connor, P. M., Daly, K. M., Hugenholtz, F., Cotter, P. D., et al. (2012). Bioengineered nisin a derivatives with enhanced activity against both Gram positive and Gram negative pathogens. *PLoS One* 7:e46884. doi: 10.1371/journal.pone.0046884

Field, D., Cotter, P. D., Hill, C., and Ross, R. P. (2015). Bioengineering lantibiotics for therapeutic success. *Front. Microbiol.* 6:1363. doi: 10.3389/fmicb.2015.01363

Field, D., Quigley, L., O'connor, P. M., Rea, M. C., Daly, K., Cotter, P. D., et al. (2010). Studies with bioengineered Nisin peptides highlight the broad-spectrum potency of Nisin V. *Microbial. Biotechnol.* 3, 473–486. doi: 10.1111/j.1751-7915.2010.00184.x

Fleming, A. (1945). *Penicillin - Nobel Lecture. Retrieved from NobelPrize.org. Nobel Media AB 2020.* Available online at: https://www.nobelprize.org/prizes/medicine/1945/fleming/lecture/

Frost, J. R., Jacob, N. T., Papa, L. J., Owens, A. E., and Fasan, R. (2015). Ribosomal synthesis of macrocyclic peptides in Vitro and in Vivo mediated by genetically encoded aminothiol unnatural amino acids. *ACS Chem. Biol.* 10, 1805–1816. doi: 10.1021/acschembio.5b00119

Garg, N., Goto, Y., Chen, T., and Van Der Donk, W. A. (2016). Characterization of the stereochemical configuration of lanthionines formed by the lanthipeptide synthetase GeoM. *Pept. Sci.* 106, 834–842. doi: 10.1002/bip.22876

Garg, N., Tang, W., Goto, Y., Nair, S. K., and Van Der Donk, W. A. (2012). Lantibiotics from *Geobacillus thermodenitrificans*. *Proc. Natl. Acad. Sci. U.S.A.* 109, 5241–5246. doi: 10.1073/pnas.1116815109

Geng, M., and Smith, L. (2018). Modifying the lantibiotic mutacin 1140 for increased yield, activity, and stability. *Appl. Environ. Microbiol.* 84, e830–e818. doi: 10.1128/AEM.00830-18

Gober, J. G., Ghodge, S. V., Bogart, J. W., Wever, W. J., Watkins, R. R., Brustad, E. M., et al. (2017). P450-mediated non-natural cyclopropanation of dehydroalanine-containing thiopeptides. *ACS Chem. Biol.* 12, 1726–1731. doi: 10.1021/acschembio.7b00358

Gomez-Escribano, J. P., and Bibb, M. J. (2011). Engineering *Streptomyces coelicolor* for heterologous expression of secondary metabolite gene clusters. *Microbial. Biotechnol.* 4, 207–215. doi: 10.1111/j.1751-7915.2010.00219.x

Gorochowski, T. E., Ignatova, Z., Bovenberg, R. A., and Roubos, J. A. (2015). Trade-offs between tRNA abundance and mRNA secondary structure support smoothing of translation elongation rate. *Nucleic Acids Res.* 43, 3022–3032. doi: 10.1093/nar/gkv199

Greber, K. E., and Dawgul, M. (2017). Antimicrobial peptides under clinical trials. *Curr. Top. Med. Chem.* 17, 620–628. doi: 10.2174/1568026616666160713143331

Håkansson, J., Ringstad, L., Umerska, A., Johansson, J., Andersson, T., Boge, L., et al. (2019). Characterization of the in vitro, ex vivo, and in vivo efficacy of the antimicrobial peptide DPK-060 used for topical treatment. *Front. Cell Infect. Microbiol.* 9:174. doi: 10.3389/fcimb.2019.00174

Hauf, M., Richter, F., Schneider, T., Faidt, T., Martins, B. M., Baumann, T., et al. (2017). Photoactivatable mussel-based underwater adhesive proteins by an expanded genetic code. *ChemBioChem* 18, 1819–1823. doi: 10.1002/cbic.201700327

Healy, B., Field, D., O'connor, P. M., Hill, C., Cotter, P. D., and Ross, R. P. (2013). Intensive mutagenesis of the nisin hinge leads to the rational design of enhanced derivatives. *PLoS One* 8:e79563. doi: 10.1371/journal.pone.0079563

Hoesl, M. G., and Budisa, N. (2011). Expanding and engineering the genetic code in a single expression experiment. *ChemBioChem* 12, 552–555. doi: 10.1002/cbic.201000586

Hoesl, M. G., and Budisa, N. (2012). Recent advances in genetic code engineering in *Escherichia coli*. *Curr. Opin. Biotechnol.* 23, 751–757.

Huo, L., Ökesli, A., Zhao, M., and Van Der Donk, W. A. (2017). Insights into the biosynthesis of duramycin. *Appl. Environ. Microbiol.* 83:e02698-16. doi: 10.1128/AEM.02698-16

Islam, M. R., Shioya, K., Nagao, J., Nishie, M., Jikuya, H., Zendo, T., et al. (2009). Evaluation of essential and variable residues of nukacin ISK-1 by NNK scanning. *Mol. Microbiol.* 72, 1438–1447. doi: 10.1111/j.1365-2958.2009.06733.x

Iwane, Y., Hitomi, A., Murakami, H., Katoh, T., Goto, Y., and Suga, H. (2016). Expanding the amino acid repertoire of ribosomal polypeptide synthesis via the artificial division of codon boxes. *Nat. Chem.* 8, 317–325. doi: 10.1038/nchem.2446

Jin, X., and Hong, S. H. (2018). Cell-free protein synthesis for producing 'difficult-to-express' proteins. *Biochem. Eng. J.* 138, 156–164. doi: 10.1016/j.bej.2018.07.013

Kakkar, N., Perez, J. G., Liu, W. R., Jewett, M. C., and Van Der Donk, W. A. (2018). Incorporation of nonproteinogenic amino acids in class I and II lantibiotics. *ACS Chem. Biol.* 13, 951–957. doi: 10.1021/acschembio.7b01024

Kers, J. A., Sharp, R. E., Defusco, A. W., Park, J. H., Xu, J., Pulse, M. E., et al. (2018). Mutacin 1140 lantibiotic variants are efficacious against *Clostridium difficile* infection. *Front. Microbiol.* 9:415. doi: 10.3389/fmicb.2018.00415

Key, H. M., and Miller, S. J. (2017). Site-and stereoselective chemical editing of thiostrepton by Rh-catalyzed conjugate arylation: new analogues and collateral enantioselective synthesis of amino acids. *J. Am. Chem. Soc.* 139, 15460–15466. doi: 10.1021/jacs.7b08775

Khosa, S., Frieg, B., Mulnaes, D., Kleinschrodt, D., Hoeppner, A., Gohlke, H., et al. (2016a). Structural basis of lantibiotic recognition by the nisin resistance protein from *Streptococcus agalactiae*. *Sci. Rep.* 6:18679. doi: 10.1038/srep18679

Khosa, S., Hoeppner, A., Gohlke, H., Schmitt, L., and Smits, S. H. (2016b). Structure of the response regulator NsrR from *Streptococcus agalactiae*, which is involved in lantibiotic resistance. *PLoS One* 11:e149903. doi: 10.1371/journal.pone.0149903

Kim, E. J., Yang, I., and Yoon, Y. J. (2015). Developing *Streptomyces venezuelae* as a cell factory for the production of small molecules used in drug discovery. *Arch. Pharm. Res.* 38, 1606–1616. doi: 10.1007/s12272-015-0638-z

Kluskens, L. D., Kuipers, A., Rink, R., De Boef, E., Fekken, S., Driessen, A. J., et al. (2005). Post-translational modification of therapeutic peptides by NisB, the dehydratase of the lantibiotic nisin. *Biochemistry* 44, 12827–12834. doi: 10.1021/bi050805p

Knerr, P. J., and van der Donk, W. A. (2012). Chemical synthesis and biological activity of analogues of the lantibiotic epilancin 15X. *J. Am. Chem. Soc.* 134, 7648–7651. doi: 10.1021/ja302435y

Koehbach, J., and Craik, D. J. (2019). The vast structural diversity of antimicrobial peptides. *Trends Pharmacol. Sci.* 40, 517–528. doi: 10.1016/j.tips.2019.04.012

Kolb, H. C., Finn, M. G., and Sharpless, K. B. (2001). Click chemistry: diverse chemical function from a few good reactions. *Angew. Chem.* 40, 2004–2021. doi: 10.1002/1521-3773(20010601)40:11<2004::aid-anie2004>3.3.co;2-x

Komatsu, M., Uchiyama, T., Omura, S., Cane, D. E., and Ikeda, H. (2010). Genome-minimized *Streptomyces* host for the heterologous expression of secondary metabolism. *Proc. Natl. Acad. Sci. U.S.A.* 107, 2646–2651. doi: 10.1073/pnas.0914833107

Koo, H. B., and Seo, J. (2019). Antimicrobial peptides under clinical investigation. *Pept. Sci.* 111:e24122. doi: 10.1002/pep2.24122

Koopmans, T., Wood, T. M., 't Hart, P., Kleijn, L. H., Hendrickx, A. P., Willems, R. J., et al. (2015). Semisynthetic lipopeptides derived from nisin display antibacterial activity and lipid II binding on par with that of the parent compound. *J. Am. Chem. Soc.* 137, 9382–9389. doi: 10.1021/jacs.5b04501

Kubyshkin, V., and Budisa, N. (2019). Anticipating alien cells with alternative genetic codes: away from the alanine world! *Curr. Opin. Biotechnol.* 60, 242–249. doi: 10.1016/j.copbio.2019.05.006

Kudrimoti, M., Curtis, A., Azawi, S., Worden, F., Katz, S., Adkins, D., et al. (2017). Dusquetide: reduction in oral mucositis associated with enduring ancillary benefits in tumor resolution and decreased mortality in head and neck cancer patients. *Biotechnol. Rep.* 15, 24–26. doi: 10.1016/j.btre.2017.05.002

Kuipers, O. P., Bierbaum, G., Ottenwälder, B., Dodd, H. M., Horn, N., Metzger, J., et al. (1996). Protein engineering of lantibiotics. *Antonie Van Leeuwenhoek* 69, 161–170. doi: 10.1007/BF00399421

Lagedroste, M., Reiners, J., Smits, S. H., and Schmitt, L. (2019). Systematic characterization of position one variants within the lantibiotic nisin. *Sci. Rep.* 9, 1–11. doi: 10.1038/s41598-018-37532-4

Lalpuria, M., Karwa, V., Anantheswaran, R. C., and Floros, J. D. (2013). Modified agar diffusion bioassay for better quantification of Nisaplin®. *J. Appl. Microbiol.* 114, 663–671. doi: 10.1111/jam.12078

Larregola, M., Moore, S., and Budisa, N. (2012). Congeneric bio-adhesive mussel foot proteins designed by modified prolines revealed a chiral bias in unnatural translation. *Biochem. Biophys. Res. Commun.* 421, 646–650. doi: 10.1016/j.bbrc.2012.04.031

Lee, J., Schwieter, K. E., Watkins, A. M., Yu, H., Schwarz, K. J., Lim, J., et al. (2019). Expanding the limits of the second genetic code with ribozymes. *Nat. Commun.* 10, 1–12. doi: 10.1038/s41467-019-12916-w

Lopatniuk, M., Myronovskyi, M., and Luzhetskyy, A. (2017). *Streptomyces albus*: a new cell factory for non-canonical amino acids incorporation into ribosomally synthesized natural products. *ACS Chem. Biol.* 12, 2362–2370. doi: 10.1021/acschembio.7b00359

Lubelski, J., Rink, R., Khusainov, R., Moll, G. N., and Kuipers, O. P. (2008). Biosynthesis, immunity, regulation, mode of action and engineering of the model lantibiotic nisin. *Cell Mol. Life Sci.* 65, 455–476. doi: 10.1007/s00018-007-7171-2

Luo, X., Zambaldo, C., Liu, T., Zhang, Y., Xuan, W., Wang, C., et al. (2016). Recombinant thiopeptides containing noncanonical amino acids. *Proc. Natl. Acad. Sci.* 113, 3615–3620. doi: 10.1073/pnas.1602733113

Maaskant, R. V., and Roelfes, G. (2019). Bioorthogonal metalloporphyrin-catalyzed selective methionine alkylation in the lanthipeptide nisin. *ChemBioChem* 20, 57–61. doi: 10.1002/cbic.201800493

Maffioli, S. I, Monciardini, P., Catacchio, B., Mazzetti, C., MüNch, D., Brunati, C., et al. (2015). Family of class I lantibiotics from actinomycetes and improvement of their antibacterial activities. *ACS Chem. Biol.* 10, 1034–1042. doi: 10.1021/cb500878h

Manyi-Loh, C., Mamphweli, S., Meyer, E., and Okoh, A. (2018). Antibiotic use in agriculture and its consequential resistance in environmental sources: potential public health implications. *Molecules* 23:795.

Mayer, C. (2019). Selection, addiction and catalysis: emerging trends for the incorporation of noncanonical amino acids into peptides and proteins in vivo. *ChemBioChem* 20, 1357–1364. doi: 10.1002/cbic.201800733

Ming, L., and Huang, J. A. (2017). The antibacterial effects of antimicrobial peptides OP-145 against clinically isolated multi-resistant strains. *Jpn. J. Infect. Dis.* 70, 601–603. doi: 10.7883/yoken.JJID.2017.090

Minks, C., Alefelder, S., Moroder, L., Huber, R., and Budisa, N. (2000). Towards new protein engineering: in vivo building and folding of protein shuttles for drug delivery and targeting by the selective pressure incorporation (SPI) method. *Tetrahedron* 56, 9431–9442. doi: 10.1016/S0040-4020(00)00827-9

Miyazaki, R., Myougo, N., Mori, H., and Akiyama, Y. (2018). A photo-cross-linking approach to monitor folding and assembly of newly synthesized proteins in a living cell. *J. Biol. Chem.* 293, 677–686. doi: 10.1074/jbc.M117.817270

Mocquot, G., and Lefebvre, E. (1956). A simple procedure to detect nisin in cheese. *J. Appl. Bacteriol.* 19, 322–323. doi: 10.1111/j.1365-2672.1956.tb00083.x

Mohr, K. I., Volz, C., Jansen, R., Wray, V., Hoffmann, J., Bernecker, S., et al. (2015). Pinensins: the first antifungal lantibiotics. *Angew. Chem. Int. Ed.* 54, 11254–11258. doi: 10.1002/anie.201500927

Montalbán-López, M., Deng, J., Van Heel, A. J., and Kuipers, O. P. (2018). Specificity and application of the lantibiotic protease NisP. *Front. Microbiol.* 9:160. doi: 10.3389/fmicb.2018.00160

Myronovskyi, M., and Luzhetskyy, A. (2019). Heterologous production of small molecules in the optimized *Streptomyces* hosts. *Nat. Prod. Rep.* 36, 1281–1294. doi: 10.1039/C9NP00023B

Myronovskyi, M., Rosenkränzer, B., Nadmid, S., Pujic, P., Normand, P., and Luzhetskyy, A. (2018). Generation of a cluster-free *Streptomyces albus* chassis strains for improved heterologous expression of secondary metabolite clusters. *Metab. Eng.* 49, 316–324. doi: 10.1016/j.ymben.2018.09.004

Nagao, J.-I., Harada, Y., Shioya, K., Aso, Y., Zendo, T., Nakayama, J., et al. (2005). Lanthionine introduction into nukacin ISK-1 prepeptide by co-expression with modification enzyme NukM in *Escherichia coli*. *Biochem. Biophys. Res. Commun.* 336, 507–513. doi: 10.1016/j.bbrc.2005.08.125

Nilsson, E., Björn, C., Sjöstrand, V., Lindgren, K., Münnich, M., Mattsby-Baltzer, I., et al. (2009). A novel polypeptide derived from human lactoferrin in sodium hyaluronate prevents postsurgical adhesion formation in the rat. *Ann. Surg.* 250, 1021–1028. doi: 10.1097/SLA.0b013e3181b246a7

Oldach, F., Al Toma, R., Kuthning, A., Caetano, T., Mendo, S., Budisa, N., et al. (2012). Congeneric lantibiotics from ribosomal in vivo peptide synthesis with noncanonical amino acids. *Angew. Chem. Int. Ed.* 51, 415–418. doi: 10.1002/anie.201106154

Oliva, R., Chino, M., Pane, K., Pistorio, V., De Santis, A., Pizzo, E., et al. (2018). Exploring the role of unnatural amino acids in antimicrobial peptides. *Sci. Rep.* 8:8888. doi: 10.1038/s41598-018-27231-5

Ongey, E. L., Yassi, H., Pflugmacher, S., and Neubauer, P. (2017). Pharmacological and pharmacokinetic properties of lanthipeptides undergoing clinical studies. *Biotechnol. Lett.* 39, 473–482. doi: 10.1007/s10529-016-2279-9

Ortiz-López, F. J., Carretero-Molina, D., Sánchez-Hidalgo, M., Martín, J., González, I., Román-Hurtado, F., et al. (2020). Cacaoidin, first member of the new lanthidin RiPP family. *Angew. Chem. Int. Ed.* 20:5187. doi: 10.1002/anie.202005187

Piper, C., Draper, L. A., Cotter, P. D., Ross, R. P., and Hill, C. (2009). A comparison of the activities of lacticin 3147 and nisin against drug-resistant *Staphylococcus aureus* and *Enterococcus* species. *J. Antimicrob. Chemother.* 64, 546–551. doi: 10.1093/jac/dkp221

Piscotta, F. J., Tharp, J. M., Liu, W. R., and Link, A. J. (2015). Expanding the chemical diversity of lasso peptide MccJ25 with genetically encoded noncanonical amino acids. *Chem. Commun.* 51, 409–412. doi: 10.1039/c4cc07778d

Plotkin, J. B., and Kudla, G. (2011). Synonymous but not the same: the causes and consequences of codon bias. *Nat. Rev. Genet.* 12, 32–42. doi: 10.1038/nrg2899

Pongtharangkul, T., and Demirci, A. (2004). Evaluation of agar diffusion bioassay for nisin quantification. *Appl. Microbiol. Biotechnol.* 65, 268–272. doi: 10.1007/s00253-004-1579-5

Porto, W. F., Pires, A. S., and Franco, O. L. (2017). Computational tools for exploring sequence databases as a resource for antimicrobial peptides. *Biotechnol. Adv.* 35, 337–349. doi: 10.1016/j.biotechadv.2017.02.001

Rauch, B. J., Porter, J. J., Mehl, R. A., and Perona, J. J. (2016). Improved incorporation of noncanonical amino acids by an engineered tRNATyr suppressor. *Biochemistry* 55, 618–628. doi: 10.1021/acs.biochem.5b01185

Rogers, A. M., and Montville, T. J. (1991). Improved agar diffusion assay for nisin quantification. *Food Biotechnol.* 5, 161–168. doi: 10.1080/08905439109549799

Rollema, H. S., Kuipers, O. P., Both, P., De Vos, W. M., and Siezen, R. J. (1995). Improvement of solubility and stability of the antimicrobial peptide nisin by protein engineering. *Appl. Environm. Microbiol.* 61, 2873–2878.

Ross, A. C., Mckinnie, S. M., and Vederas, J. C. (2012). The synthesis of active and stable diaminopimelate analogues of the lantibiotic peptide lactocin S. *J. Am. Chem. Soc.* 134, 2008–2011. doi: 10.1021/ja211088m

Rouse, S., Field, D., Daly, K. M., O'connor, P. M., Cotter, P. D., Hill, C., et al. (2012). Bioengineered nisin derivatives with enhanced activity in complex matrices. *Microbial. Biotechnol.* 5, 501–508.

Shi, Y., Yang, X., Garg, N., and Van Der Donk, W. A. (2011). Production of lantipeptides in *Escherichia coli*. *J. Am. Chem. Soc.* 133, 2338–2341. doi: 10.1021/ja109044r

Shin, J. M., Gwak, J. W., Kamarajan, P., Fenno, J. C., Rickard, A. H., and Kapila, Y. L. (2016). Biomedical applications of nisin. *J. Appl. Microbiol.* 120, 1449–1465. doi: 10.1111/jam.13033

Soye, B. J. D., Patel, J. R., Isaacs, F. J., and Jewett, M. C. (2015). Repurposing the translation apparatus for synthetic biology. *Curr. Opin. Chem. Biol.* 28, 83–90. doi: 10.1016/j.cbpa.2015.06.008

Srinivas, N., Jetter, P., Ueberbacher, B. J., Werneburg, M., Zerbe, K., Steinmann, J., et al. (2010). Peptidomimetic antibiotics target outer-membrane biogenesis in *Pseudomonas aeruginosa*. *Science* 327, 1010–1013. doi: 10.1126/science.1182749

Sun, E., Belanger, C. R., Haney, E. F., and Hancock, R. E. (2018). "Host defense (antimicrobial) peptides," in *Peptide Applications in Biomedicine, Biotechnology and Bioengineering*, ed. S. Koutsopoulos (Amsterdam: Elsevier), 253–285.

Torres, M. D., Sothiselvam, S., Lu, T. K., and De La Fuente-Nunez, C. (2019). Peptide design principles for antimicrobial applications. *J. Mol. Biol.* 431, 3547–3567. doi: 10.1016/j.jmb.2018.12.015

Uttamapinant, C., Howe, J. D., Lang, K., BeraìNek, V. C., Davis, L., Mahesh, M., et al. (2015). Genetic code expansion enables live-cell and super-resolution imaging of site-specifically labeled cellular proteins. *J. Am. Chem. Soc.* 137, 4602–4605. doi: 10.1021/ja512838z

Vargas-Rodriguez, O., Sevostyanova, A., Söll, D., and Crnkoviæ, A. (2018). Upgrading aminoacyl-tRNA synthetases for genetic code expansion. *Curr. Opin. Chem. Biol.* 46, 115–122. doi: 10.1016/j.cbpa.2018.07.014

Völler, J., Biava, H., Koksch, B., Hildebrandt, P., and Budisa, N. (2015). Orthogonal translation meets electron transfer: in vivo labeling of cytochrome c for probing local electric fields. *ChemBioChem* 16, 742–745. doi: 10.1002/cbic.201500022

Völler, J.-S., and Budisa, N. (2017). Coupling genetic code expansion and metabolic engineering for synthetic cells. *Curr. Opin. Biotechnol.* 48, 1–7. doi: 10.1016/j.copbio.2017.02.002

Wang, F., Cao, L. T., and Hu, S. H. (2007). A rapid and accurate 3-(4,5-dimethyl thiazol-2-yl)-2,5-diphenyl tetrazolium bromide colorimetric assay for quantification of bacteriocins with nisin as an example. *J. Zhejiang. Uni. Sci. B* 8, 549–554. doi: 10.1631/jzus.2007.B0549

Wang, G. (2015). "Improved methods for classification, prediction, and design of antimicrobial peptides," in *Computational Peptidology*, eds P. Zhou and J. Huang (New York, NY: Springer New York), 43–66.

Wang, L., Xie, J., and Schultz, P. G. (2006). Expanding the genetic code. *Annu. Rev. Biophys. Biomol. Struct.* 35, 225–249. doi: 10.1146/annurev.biophys.35.101105.121507

Wernicki, A. (2013). The End of the Golden Age of Antibiotics? *J. Vet. Sci. Anim. Husb.* 1:e103. doi: 10.15744/2348-9790.1.e103

Wescombe, P. A., Upton, M., Renault, P., Wirawan, R. E., Power, D., Burton, J. P., et al. (2011). Salivaricin 9, a new lantibiotic produced by *Streptococcus salivarius*. *Microbiology* 157, 1290–1299. doi: 10.1099/mic.0.044719-0

Wiedemann, I., Breukink, E., Van Kraaij, C., Kuipers, O. P., Bierbaum, G., De Kruijff, B., et al. (2001). Specific binding of nisin to the peptidoglycan precursor lipid II combines pore formation and inhibition of cell wall biosynthesis for potent antibiotic activity. *J. Biol. Chem.* 276, 1772–1779. doi: 10.1074/jbc.M006770200

Wolf, C., and Gibbons, W. (1996). Improved method for quantification of the bacteriocin nisin. *J. Appl. Bacteriol.* 80, 453–457. doi: 10.1111/j.1365-2672.1996.tb03242.x

World Health Organization (2019). *Antibacterial Agents in Preclinical Development: An Open Access Database*. Geneva: WHO.

World Health Organization (2020). *Global AMR Response*. Geneva: WHO.

Xu, M., Zhang, F., Cheng, Z., Bashiri, G., Wang, J., Hong, J., et al. (2020). Functional genome mining reveals a class V lanthipeptide containing a D-amino acid introduced by an F420H2-dependent reductase. *Angew. Chem. Int. Ed.* 20:8035. doi: 10.1002/anie.202008035

Yanagisawa, T., Kuratani, M., Seki, E., Hino, N., Sakamoto, K., and Yokoyama, S. (2019). Structural basis for genetic-code expansion with bulky lysine derivatives by an engineered pyrrolysyl-tRNA synthetase. *Cell Chem. Biol.* 26, 936-949. e913. doi: 10.1016/j.chembiol.2019.03.008

Yang, B., Wang, N., Schnier, P. D., Zheng, F., Zhu, H., Polizzi, N. F., et al. (2019). Genetically introducing biochemically reactive amino acids dehydroalanine and dehydrobutyrine in proteins. *J. Am. Chem. Soc.* 141, 7698–7703. doi: 10.1021/jacs.9b02611

Yelin, I., and Kishony, R. (2018). Antibiotic resistance. *Cell* 172, 1136-1136. e1131. doi: 10.1016/j.cell.2018.02.018

Young, T. S., and Schultz, P. G. (2010). Beyond the canonical 20 amino acids: expanding the genetic lexicon. *J. Biol. Chem.* 285, 11039–11044. doi: 10.1074/jbc.R109.091306

Zambaldo, C., Luo, X., Mehta, A. P., and Schultz, P. G. (2017). Recombinant macrocyclic lanthipeptides incorporating non-canonical amino acids. *J. Am. Chem. Soc.* 139, 11646–11649. doi: 10.1021/jacs.7b04159

Zaschke-Kriesche, J., Reiners, J., Lagedroste, M., and Smits, S. H. (2019). Influence of nisin hinge-region variants on lantibiotic immunity and resistance proteins. *Bioorg. Med. Chem.* 27, 3947–3953. doi: 10.1016/j.bmc.2019.07.014

Zhang, Y., Chen, M., Bruner, S. D., and Ding, Y. (2018). Heterologous production of microbial ribosomally synthesized and post-translationally modified peptides. *Front. Microbiol.* 9:1801. doi: 10.3389/fmicb.2018.01801

Zhao, D. L., Wang, D., Tian, X. Y., Cao, F., Li, Y. Q., and Zhang, C. S. (2018). Anti-Phytopathogenic and Cytotoxic Activities of Crude Extracts and Secondary Metabolites of Marine-Derived Fungi. *Mar. Drugs* 16:36. doi: 10.3390/md16010036

Zhao, X., Yin, Z., Breukink, E., Moll, G. N., and Kuipers, O. P. (2020). An engineered double lipid II binding motifs-containing lantibiotic displays potent and selective antimicrobial activity against *Enterococcus faecium*. *Antimicrob. Agents Chemother.* 64:e02050-19. doi: 10.1128/AAC.02050-19

Zhou, L., Shao, J., Li, Q., Van Heel, A. J., De Vries, M. P., Broos, J., et al. (2016). Incorporation of tryptophan analogues into the lantibiotic nisin. *Amino Acids* 48, 1309–1318. doi: 10.1007/s00726-016-2186-3

Zhou, L., Van Heel, A. J., and Kuipers, O. P. (2015). The length of a lantibiotic hinge region has profound influence on antimicrobial activity and host specificity. *Front. Microbiol.* 6:11. doi: 10.3389/fmicb.2015.00011

Zweytick, D., Pabst, G., Abuja, P. M., Jilek, A., Blondelle, S. E., Andrä, J., et al. (2006). Influence of N-acylation of a peptide derived from human lactoferricin on membrane selectivity. *Biochim. Biophys. Acta* 1758, 1426–1435. doi: 10.1016/j.bbamem.2006.07.001

Conflict of Interest: The authors declare that the research was conducted in the absence of any commercial or financial relationships that could be construed as a potential conflict of interest.

frontiers in Microbiology

REVIEW
published: 09 November 2020
doi: 10.3389/fmicb.2020.586433

Bacteriocins to Thwart Bacterial Resistance in Gram Negative Bacteria

Soufiane Telhig[1,2†], Laila Ben Said[1†], Séverine Zirah[2], Ismail Fliss[1] and Sylvie Rebuffat[2]*

[1] *Institute of Nutrition and Functional Foods, Université Laval, Québec, QC, Canada,* [2] *Laboratory Molecules of Communication and Adaptation of Microorganisms, Muséum National d'Histoire Naturelle, Centre National de la Recherche Scientifique, Paris, France*

An overuse of antibiotics both in human and animal health and as growth promoters in farming practices has increased the prevalence of antibiotic resistance in bacteria. Antibiotic resistant and multi-resistant bacteria are now considered a major and increasing threat by national health agencies, making the need for novel strategies to fight bugs and super bugs a first priority. In particular, Gram-negative bacteria are responsible for a high proportion of nosocomial infections attributable for a large part to *Enterobacteriaceae*, such as pathogenic *Escherichia coli*, *Klebsiella pneumoniae,* and *Pseudomonas aeruginosa*. To cope with their highly competitive environments, bacteria have evolved various adaptive strategies, among which the production of narrow spectrum antimicrobial peptides called bacteriocins and specifically microcins in Gram-negative bacteria. They are produced as precursor peptides that further undergo proteolytic cleavage and in many cases more or less complex posttranslational modifications, which contribute to improve their stability and efficiency. Many have a high stability in the gastrointestinal tract where they can target a single pathogen whilst only slightly perturbing the gut microbiota. Several microcins and antibiotics can bind to similar bacterial receptors and use similar pathways to cross the double-membrane of Gram-negative bacteria and reach their intracellular targets, which they also can share. Consequently, bacteria may use common mechanisms of resistance against microcins and antibiotics. This review describes both unmodified and modified microcins [lasso peptides, siderophore peptides, nucleotide peptides, linear azole(in)e-containing peptides], highlighting their potential as weapons to thwart bacterial resistance in Gram-negative pathogens and discusses the possibility of cross-resistance and co-resistance occurrence between antibiotics and microcins in Gram-negative bacteria.

Keywords: bacteriocins, microcins, antibiotics, resistance, Gram-negative bacteria, enterobacteria

OPEN ACCESS

Edited by:
Mathew Upton, University of Plymouth, United Kingdom

Reviewed by:
Daniel Walker, University of Glasgow, United Kingdom
David Šmajs, Masaryk University, Czechia

****Correspondence:***
Sylvie Rebuffat
sylvie.rebuffat@mnhn.fr

† These authors have contributed equally to this work

Specialty section:
This article was submitted to Antimicrobials, Resistance and Chemotherapy, a section of the journal Frontiers in Microbiology

Received: *23 July 2020*
Accepted: *16 October 2020*
Published: *09 November 2020*

Citation:
Telhig S, Ben Said L, Zirah S, Fliss I and Rebuffat S (2020) Bacteriocins to Thwart Bacterial Resistance in Gram Negative Bacteria. Front. Microbiol. 11:586433. doi: 10.3389/fmicb.2020.586433

INTRODUCTION

Since their discovery antibiotics have been routinely used in human medicine and in livestock production as therapeutic agents or growth promoters. Use of antibiotics for livestock greatly exceeds that of uses for humans, with approximately 70–80 percent of total consumption (Van Boeckel et al., 2017). Furthermore, the global use of antibiotics would rise by 67% by 2030 in

high-income countries and nearly double in Brazil, the Russian Federation, India, China and South Africa (Van Boeckel et al., 2015). According to the World Health Organization (World Health Organization [WHO], 2017) the overuse and misuse of antibiotics in human and animal, as well as the intrinsic capacity of antibiotics to induce broad spectrum killing (Wester et al., 2002) has led to the emergence of multidrug-resistant bacteria (MDR) that are rapidly increasing worldwide and have now become a serious public health problem. In 2016, the United Nations General Assembly recognized the use of antibiotics in the livestock sector as one of the primary causes of antimicrobial resistance (AMR) (Van Boeckel et al., 2017). Moreover, it has been shown that farm animal and human microbiota are reservoirs for AMR (Gibson et al., 2016; Pärnänen et al., 2018; Brown et al., 2019; Sun et al., 2020). Currently, AMR is already killing 700,000 people a year, and it is predicted to cause 10 million deaths per year by 2050 with a cumulative cost of US$ 100 trillion (de Kraker et al., 2016). According to the Centers for Disease Control and Prevention (CDC) AMR challenge, *Enterobacteriaceae*, including *Escherichia coli, Shigella*, *Salmonella,* and *Klebsiella* spp. amongst others, present a serious and/or urgent threat to world health. Indeed, as Gram-negative bacteria, *Enterobacteriaceae* are notorious for their capacity to resist antimicrobial therapy (Hawkey, 2015; Li et al., 2015; Zowawi et al., 2015). Furthermore, even though *Enterobacteriaceae* represent only a small percentage of the host microbiota and are not all pathogens, they are still responsible for important morbidity (Doi et al., 2017; MacVane, 2017), making them an important target for new drug development.

The AMR crisis is exacerbated by the fact that resistances are emerging and disseminating faster than the development of new drugs. Indeed, over the past three decades the number of developed and approved antibiotics has more than halved (Ventola, 2015), leading to an increasing demand for new antimicrobial agents or strategies. Genetically modified phages, antibacterial modified oligonucleotides, inhibitors of bacterial virulence and CRISPR-Cas9 strategy are also discussed for extrapolating them to the field of antimicrobial therapeutics (Dickey et al., 2017; Ghosh et al., 2019). Meanwhile, other promising strategies, such as probiotics, lysins and antimicrobial peptides are in various stages of development (Ghosh et al., 2019). Globally, although several alternatives exist in nature, the challenge still remains to demonstrate their efficacy and their use in human and animal.

Bacteriocins form a large family of antimicrobial peptides (AMP) produced by bacteria (Klaenhammer, 1988). Their biological characteristics and activities have been deeply described in a new web-accessible database named BACTIBASE, which is freely available at the http://bactibase.pfba-lab.org web-based platform. Bacteriocins can be either unmodified or posttranslationally modified peptides, the latter thus belonging to the large family of ribosomally synthesized and posttranslationally modified peptides (RiPPs) (Arnison et al., 2013; Montalbán-López et al., 2020). Known as inhibitors of pathogens *in vitro,* many bacteriocins have a high specific activity against clinical strains including antibiotic-resistant ones (Cotter et al., 2013). Their effectiveness as inhibitors of pathogenic and spoilage microorganisms has been largely explored (Davies et al., 1997; Deegan et al., 2006). It is thus widely believed that some could be usable for therapeutic purposes and as an alternative to conventional antibiotics (Snyder and Worobo, 2014; Egan et al., 2017).

Bacteriocins produced by enterobacteria are called microcins (Baquero and Moreno, 1984). They form a restricted and underexplored group of bacteriocins compared to the hundreds members of those from lactic acid bacteria, with only some twenty members identified so far, among which only around fifteen have been more deeply characterized (**Table 1** and **Supplementary Figure S1**). Microcins are less than 10 kDa modified or unmodified peptides (Rebuffat, 2012) having key ecological functions, and particularly a role in microbial competitions (Baquero et al., 2019; Li and Rebuffat, 2020). They have potent activity with minimum inhibitory concentrations (MIC) ranging in the nanomolar to micromolar range and narrow spectra of antimicrobial activity directed essentially against Gram-negative bacterial congeners (Rebuffat, 2012; Baquero et al., 2019). To exert their crucial roles in competition, microcins share a common strategy to penetrate into their bacterial targets. They piratize nutrient uptake pathways of phylogenetically close bacteria vying for the same resources. The iron import pathways is the most frequently attacked (Rebuffat, 2012). When inside bacteria, microcins interfere and perturb a variety of bacterial mechanisms, such as transcription (Adelman et al., 2004), translation (Metlitskaya et al., 2006), DNA structure (Vizán et al., 1991), mannose transport (Bieler et al., 2006), energy production (Trujillo et al., 2001; Zhao et al., 2015), or the cell envelope function (Destoumieux-Garzón et al., 2003; Gerard et al., 2005; Zhao et al., 2015). Due to their specific characteristics and complex mechanisms of action, microcins are viewed as a possible alternative to conventional antibiotics, helping with the immediate AMR problem (Cotter et al., 2013; Mills et al., 2017; Lu et al., 2019; Palmer et al., 2020). Because of their narrow spectrum of inhibition, they would potentially have less side effects than antibiotics, allowing preservation of the microbiota diversity and minimizing the risk of resistance dissemination.

However, since there is a finite number of entry points and potential targets within a bacterium, microcins and antibiotics can share similar bacterial receptors and pathways to reach their intracellular targets. Moreover, as for antibiotics, the application of specific microcins might be curtailed by the development of resistance (Cotter et al., 2013). Thus, bacteria might evolve common mechanisms of resistance against microcins and antibiotics. This review will highlight the potential of microcins as an alternative to antibiotics to fight against bacterial resistance in Gram-negative pathogens and discuss the possibilities of cross-resistance and co-resistance occurrence in Gram-negative bacteria.

CHARACTERISTICS OF MICROCINS

Bacteriocins that are produced by both Gram-positive and Gram-negative bacteria have been defined by James et al. (2013) as ribosomally synthesized peptides capable of mediating inhibitory effects against bacteria. In *Enterobacteriaceae* and

TABLE 1 | Structural characterization of microcins assembled into posttranslationally modified microcins (classes I and IIb) and unmodified microcins (class IIa) that contain or not disulfide bridges.

Class	Microcin	MM[a] (Da)	PTMs/disulfide bonds	Structure	Producing organism	References
Class I (modified)	McC	1177	Peptidyladenylate with the C-terminal Asp^{7} linked to AMP via a phosphoramidate linkage and bearing an aminopropyl on the phosphate	Nucleotide peptide	*E. coli*	Guijarro et al., 1995
	MccJ25	2107	Macrolactam ring between Gly^{1} and Glu^{8} threaded by the Tyr^{9}- Gly^{21} tail locked inside by Phe^{19} and Tyr^{20} side chains (lasso topology)	Lasso peptide	*E. coli*	Rosengren et al., 2003
	MccB17	3093	$Gly^{39}Ser^{40}Cys^{41}$ and $Gly^{54}Cys^{55}Ser^{56}$ motifs modified to oxazole-thiazole and thiazole-oxazole heterocycles	Linear azol(in)e-containing peptide (LAP)[b]	*E. coli*	Li et al., 1996
Class IIa (unmodified)	MccV	8734	1 disulfide bond (Cys^{76} – Cys^{87})	Unmodified peptide	*E. coli*	Fath et al., 1994
	MccL	8884	2 disulfide bonds (Cys^{29} – Cys^{33}; Cys^{78} – Cys^{89})	Unmodified peptide	*E. coli* LR05	Pons et al., 2004
	MccS[c]	9746	2 putative disulfide bonds (Cys^{57}, Cys^{90}, Cys^{109}, Cys^{118})	Unmodified peptide	*E. coli* G3/10	Zschüttig et al., 2012
	MccPDI[c]	9953	2 putative disulfide bonds (Cys^{57}, Cys^{90}, Cys^{109}, Cys^{118}) with Cys^{57}-Cys^{90} bond required for activity	Unmodified peptide	*E. coli* 25	Eberhart et al., 2012 Kaur et al., 2016
	MccN/24	7222	No disulfide bond (no Cys residue)	Unmodified peptide	Uropathogenic *E. coli*	
Class IIb	MccE492	7887[d] 8718[e]	Linear trimer of N-2,3-(dihydroxybenzoyl)-L-serine (DHBS) anchored at the C-terminal Ser^{84}	Siderophore peptide	*K. pneumoniae*	Thomas et al., 2004
	MccM	7284[d] 8115[e]	Linear trimer of N-2,3-(dihydroxybenzoyl)-L-serine (DHBS) anchored at the C-terminal Ser^{77}	Siderophore peptide	*E. coli* Nissle 1917	Vassiliadis et al., 2010
	MccH47	4865[d] 5696[e]	Linear trimer of *N*-2,3-(dihydroxybenzoyl)-L-serine (DHBS) anchored at the C-terminal Ser^{60}	Siderophore peptide	*E. coli* Nissle 1917	Vassiliadis et al., 2010

[a] *Average masses with the cysteines involved in disulfide bonds when relevant.*
[b] *Also termed thiazole-oxazole modified microcin (TOMM).*
[c] *Putative structure.*
[d] *Molecular mass without PTM.*
[e] *Molecular mass including the DHBS trimer PTM.*

more specifically in *E. coli,* microcins (for extensive reviews see Baquero and Moreno, 1984; Duquesne et al., 2007a; Baquero et al., 2019) have been shown to be produced along with colicins, which are large antibacterial proteins (Cascales et al., 2007). To distinguish them from colicins, the name "microcin" was coined since their first discovery (Asensio and Perez-Diaz, 1976), based on their smaller size of less than 10 kDa. Such as most bacteriocins, microcins are active against phylogenetically related bacteria including enteropathogenic *Klebsiella*, *Shigella*, *Salmonella* and *E. coli,* notorious for their capacity to develop antibiotic resistances, and considered serious and urgent threats by the CDC. These Gram-negative bacteriocins are ubiquitously distributed in Nature and their production is consistently observed in multiple genera. Those include *Escherichia*, *Salmonella*, *Shigella*, *Klebsiella*, *Enterobacter,* and *Citrobacter* (Gordon and O'Brien, 2006; Gordon et al., 2007; Budic et al., 2011; Drissi et al., 2015; Wang et al., 2016; Cheung-Lee et al., 2019). The development of DNA sequencing methods and the availability of an increasing number of genomes revealed that clusters of genes orthologous to microcin biosynthesis and self-immunity genes are widespread in bacteria. Indeed, analogs of historically described microcins produced by *Enterobacteriaceae,* essentially in the RiPP family, have been predicted and most often deeply characterized in other Gram-negative bacteria including human pathogens, *Helicobacter* (Bantysh et al., 2014), *Burkholderia* (Knappe et al., 2008), *Pseudomonas* (Metelev et al., 2013), *Klebsiella* (Metelev et al., 2017a,b; Travin et al., 2020), *Acinetobacter* (Metelev et al., 2017a), *Citrobacter* (Cheung-Lee et al., 2019), or in the symbiotic nitrogen-fixing bacterium *Rhizobium* (Travin et al., 2019) (**Supplementary Figure S1A**). They were even predicted in Gram-positive bacteria and cyanobacteria (Bantysh et al., 2014). This points that a sharp distinction between bacteriocins from Gram-positive and Gram-negative bacteria is artificial and that

the chemical diversity of microcin-like peptides is intended to expand rapidly.

The Two Classes of Microcins

Compared to the huge number of Gram-positive bacteriocins, microcins are distinguished by a high structural heterogeneity inside a restricted number of identified and well-characterized representatives. A widely accepted classification was proposed by Duquesne et al. (2007a) based on both the peptide size and degree of posttranslational modification (PTM). The known microcins are grouped in two classes, class I with molecular masses below 5 kDa and the presence of extensive PTM and class II with molecular masses between 5 and 10 kDa that can be modified or not (**Table 1**). A brief description of the microcins from the two classes is provided below to help following the next sections. For more detailed overview of the microcins, see two recent reviews (Baquero et al., 2019; Li and Rebuffat, 2020).

Class I assembles three plasmid-encoded microcins that have been well structurally characterized as RiPPs (**Supplementary Figure S1A**): microcin C (McC) a nucleotide peptide, microcin B17 (MccB17) a linear azol(in)e-containing peptide, and microcin J25 (MccJ25), a lasso peptide. McC is presently the only nucleotide member of the family. However, similar biosynthetic gene clusters are distributed within bacterial genomes (Bantysh et al., 2014), which suggests an unexplored diversity for such peptides. McC is produced by *E. coli* cells harboring the *mccABCDEF* gene cluster (**Figure 1**) under a *mccA*-encoded formylated heptapeptide precursor, which is further modified (Guijarro et al., 1995; Severinov and Nair, 2012) and processed into a structural mimic of aspartyl adenylate which is the toxic entity (Kazakov et al., 2008) (**Supplementary Figure S1A**). MccB17 is produced as a 69 amino acid precursor by *E. coli* strains bearing the *mcbABCDEFG* gene cluster (**Figure 1**). Mature MccB17 contains 43 amino acids that are structured into thiazole and oxazole heterocycles (4 thiazoles and 4 oxazoles rings either isolated or fused into oxazole/thiazole- and thiazole/oxazole-bis-heterocycles) by the PTM enzymes (Li et al., 1996; Ghilarov et al., 2019) (**Supplementary Figure S1A**). Such heterocycles are also found in hybrid non-ribosomal peptide-polyketide natural products such as the anti-tumor drug bleomycin, as well as in RiPPs such as cyanobactin (McIntosh and Schmidt, 2010) or streptolysin (Mitchell et al., 2009), forming the LAP [also termed thiazole/oxazole-modified microcin (TOMM)] peptide family (Melby et al., 2011). Microcin B-like bacteriocins produced by *Pseudomonas, Klebsiella* and *Rhizobium* have been reported (Metelev et al., 2013, 2017b; Travin et al., 2019). MccJ25 was isolated first from the *E. coli* strain AY25 isolated from an infant feces bearing the *mcjABCD* gene cluster (Salomón and Farias, 1992) (**Figure 1**). Its maturation from a 58 amino acid precursor into a 21 amino acid lasso peptide is ensured by two enzymes, McjB and McjC, encoded in the microcin gene cluster (Duquesne et al., 2007b; Yan et al., 2012). This unique lasso topology, which is characterized by threading of the C-terminal tail through a seven to nine lactam ring closed by an isopeptide bond, is locked in

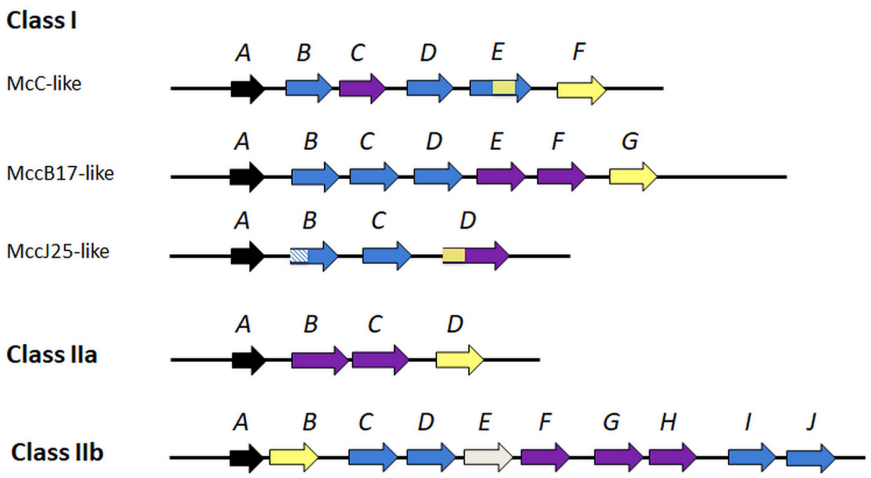

FIGURE 1 | A schematic representation of archetypical organization of microcin and microcin-like gene clusters. Arrows indicate individual microcin genes; arrows are not drown to scale and their direction does not necessarily indicate the direction of transcription that can change between homologous specific gene clusters. The A genes code for the precursors. Genes coding for microcin PTM enzymes and for export systems (efflux pumps, ABC exporters) that expel the microcins out of the producers are in blue and in violet, respectively. Genes whose products contribute to self-immunity of the producing strains (either immunity proteins or exporters/efflux pumps) are colored yellow. When genes code for proteins ensuring simultaneously two functions, they harbor the two corresponding colors. The gene coding for RRE, which ensures leader peptide recognition in MccJ25 and MccJ25-like peptides is shown as hatched motif. The functions of the different PTM enzymes are indicated as follows, taking McC, MccB17, MccJ25 and MccE492 as models. McC and analogs: *mccB* product ensures MccA adenylation, *mccD*- and *mccE*-encoded enzymes (MccD and MccE N-terminal domain) are required for phosphate modification with propylamine; MccB17 and analogs: *mcbBCD*-encoded three-component synthetase catalyzes dehydration and cyclization to form azolines, which are subsequently oxidized to azoles; MccJ25 and analogs: *mcjC* product acts as a lasso cyclase that closes the macrolactam ring through an isopeptide bond and *mcjB* product is a leader peptidase; MccE492 and siderophore peptides: *mceCDIJ* are required for PTM with *mceC* encoding a glycosyltransferase that ensures glycosylation of enterobactin and *mceD* an enterobactin esterase that cleaves the glycosylated enterobactin macrolactone ring into its linear derivatives. *mceIJ* are involved in attachment of the PTM to MccE492 C-terminus. The function of *mceE* gene (gray) is undefined.

place with the two bulky side chains of Phe and Tyr aromatic amino acids for MccJ25 (Rosengren et al., 2003) (**Supplementary Figure S1A**). It is responsible for the sturdiness of MccJ25 and is required for its antibacterial activity (Rebuffat et al., 2004; Wang and Zhang, 2018). Genome mining approaches have revealed a wide distribution of lasso peptides in Gram-positive and Gram-negative bacteria (Maksimov et al., 2012; Hegemann et al., 2013; Tietz et al., 2017; Cheung-Lee and Link, 2019). Many lasso peptides produced by proteobacteria do not show antibacterial activity (Hegemann et al., 2013). This questions their ecological role or can be due to difficulty to decipher the reasons for their narrow activity spectrum.

Class II microcins form a more homogeneous group than their class I cousins (**Table 1** and **Supplementary Figures S1B,C**), although they are subdivided into class IIa, encompassing MccL (Pons et al., 2004), MccN/24 (Kaur et al., 2016), MccPDI (Eberhart et al., 2012), MccS (Zschüttig et al., 2012) and MccV (Gratia, 1925), and class IIb (MccE492, MccH47, MccM, Vassiliadis et al., 2010). MccN was formely termed Mcc24 (O'Brien and Mahanty, 1994) and is termed MccN/24 in this review. What distinguishes class IIa from class IIb is the presence or not of a siderophore moiety derived from enterobactin anchored at the peptide C-terminal serine carboxylate (**Supplementary Figures S1B,C**). This catechol-type siderophore PTM sparked coining the name "siderophore microcins" to class IIb microcins (Rebuffat, 2012). Class II microcins result from a proteolytic processing of a precursor with a leader peptide extension, which occurs at a conserved double-glycine (or Gly-Ala) cleavage site, concomitantly with secretion. They have molecular masses between 5 and 10 kDa and exhibit high amino acid sequence similarities, even between class IIa and IIb (**Supplementary Figures S1B,C**). For examples, the class IIa unmodified MccV and MccN/24 possess high sequence similarities with the class IIb MccH47 and MccE492, respectively, although they do not carry a C-terminal PTM (O'Brien, 1996; Corsini et al., 2010). It was suggested that the conserved C-terminal sequence of these microcins can direct the presence or not of the siderophore PTM and that the C-terminal regions of MccV and MccH47 can be interchanged (Azpiroz and Laviña, 2007). It was further proposed that both class IIa and IIb microcins possess a modular structure (Azpiroz and Laviña, 2007; Morin et al., 2011).

Class IIa microcins have been characterized from *E. coli* strains from various origins. The MccN/24 producer is an uropathogenic *E. coli* (Kaur et al., 2016) and the MccL producer comes from poultry intestine (Sablé et al., 2003), while MccS is produced by a probiotic strain, *E. coli* G3/10 (Symbioflor2®; DSM17252) (Zschüttig et al., 2012). The producing strains are in some cases multi-microcin producers, such as *E. coli* LR05 that secretes MccB17, MccJ25 and the uncharacterized MccD93 in addition to MccL (Sablé et al., 2003). Their gene cluster organization includes the four basic genes only, one structural gene encoding the precursor peptide, two export genes and one immunity gene (Zschüttig et al., 2012) (**Figure 1**). If the five class IIa microcins are all devoid of PTMs, they are also all except MccN/24, stabilized by one (MccV) or two (MccL, MccPDI, MccS) disulfide bonds (Yang and Konisky, 1984; Sablé et al., 2003; Gerard et al., 2005; Morin et al., 2011; Zschüttig et al., 2012) (**Table 1** and **Supplementary Figure S1B**).

Contrasting with class IIa and class I, class IIb microcins (**Supplementary Figure S1C**) are chromosome-encoded (Poey et al., 2006). MccE492 is secreted by *Klebsiella pneumoniae* human fecal strain RYC492 (de Lorenzo, 1984) bearing the *mceABCDEFGHIJ* gene cluster (Destoumieux-Garzón et al., 2006; Vassiliadis et al., 2007; Nolan and Walsh, 2008) (**Figure 1**). It is the first siderophore microcin to be characterized (Thomas et al., 2004), although it was primarily described as an unmodified peptide (Wilkens et al., 1997). Actually, it was shown further to be secreted under both modified and less active unmodified forms, due to its PTM process (Vassiliadis et al., 2007). The MccE492 PTM was identified as a glucosylated linear trimer of *N*-(2,3 dihydroxybenzoyl)-L-serine (DHBS) linked to the C-terminal serine carboxylate (**Supplementary Figure S1C**). The functions of the enzymes involved in establishment of the MccE492 PTM, MceC, MceD, MceI/MceJ, were identified (Vassiliadis et al., 2007; Nolan and Walsh, 2008). MccH47, initially isolated from the human fecal *E. coli* strain H47 (Laviña et al., 1990) and MccM were both characterized as siderophore microcins produced by several *E. coli* strains, including the probiotic strain Nissle, 1917 (Mutaflor®) (Vassiliadis et al., 2010). MccH47 and MccM carry the same PTM as MccE492 (Vassiliadis et al., 2010). Siderophore microcins possess a modular structure, where the N-terminal region is responsible for their cytotoxicity and the C-terminal region, which carries the siderophore moiety, is involved in recognition and uptake. For an overview on siderophore microcins, see Massip and Oswald (2020).

Biosynthesis of Microcins

Microcin production takes place in the stationary phase (Baquero and Moreno, 1984) of bacterial growth, with the exceptions of MccE492 (de Lorenzo, 1984) and MccPDI (Eberhart et al., 2012). They are encoded by gene clusters, which exhibit a conserved organization, but contain a variable number of genes ranging from four to ten, according to the presence or not of PTMs on the mature microcin (**Figure 1**). These gene clusters are generally plasmid-borne, except the chromosomally encoded class IIb microcins. The general biosynthetic pathway of microcins (which also applies to other bacteriocins) starts with the ribosomal synthesis of a precursor peptide that is typically composed of two regions, an N-terminal leader part and a core region. The core peptide of modified microcins, which belong to the wide RiPP family, is the region where the PTMs take place (Montalbán-López et al., 2020). In some cases, such as the siderophore microcins, the modifications may result from the non-ribosomal pathway, making these microcins a rare bridge spanning ribosomal and non-ribosomal biosynthesis pathways (McIntosh et al., 2009). The leader is involved in binding to or activation of many of the PTM enzymes, but also maintains the maturing peptide inactive during the process (Arnison et al., 2013), thus contributing to the protection of producing cells as regard their own toxic microcin. For many modified microcins (MccJ25, McC), this binding involves a peptide binding domain (RiPP precursor peptide recognition element, RRE), also present in a wide proportion of RiPP PTM enzymes and

similar to a small protein involved in the biosynthesis of the RiPP pyrroloquinoline quinone (PQQ) (Burkhart et al., 2015; Sikandar and Koehnke, 2019). Recently, the crystal structure of the McbBCD synthetase ensuring the extensive modifications in MccB17 was solved, deciphering the organization and functioning of such a multimeric heterocyclase-dehydrogenase catalytic complex at the molecular level and affording the spatial relationships between the two distinct enzymatic activities and the leader peptide binding site (Ghilarov et al., 2019).

In all but a few cases, and irrespective of if the microcin is modified or not, maturation requires removal of the leader region to give the active bacteriocin (Drider and Rebuffat, 2011). This proteolytic cleavage is performed either before and independently of (class I), or concomitantly with (class II) export of the mature microcin (Beis and Rebuffat, 2019). It can be ensured either (i)- concomitantly with the PTM establishment by one of the dedicated enzymes (MccJ25 leader is cleaved off by the McjB leader peptidase encoded in the microcin gene cluster (Yan et al., 2012), or (ii)- by a protease from the producer, which is not encoded in the microcin gene cluster (MccB17 leader is cleaved off before export by the conserved proteins TldD/TldE which assemble as a heterodimeric metalloprotease to ensure this function) (Ghilarov et al., 2017), or (iii)- by a bifunctional ATP binding cassette (ABC) transporter of the peptidase-containing ATP-binding transporters (PCAT) family, which is encoded in the microcin gene cluster (cleavage of the class II microcin leader peptides is performed simultaneously with export of the maturated microcins by an ABC exporter endowed with an N-terminal protease extension) (Håvarstein et al., 1995; Massip and Oswald, 2020).

Self-Immunity of Microcin Producers

Microcin gene clusters vary in the number of genes contained and the presence of genes encoding PTM enzymes, and they all carry genes ensuring self-immunity (**Figure 1**). Each microcinogenic strain is protected against its arsenal of microcins and the self-immunity mechanisms differ from one microcin to another. For instance the self-immunity mechanism to McC is complex and relies on the products of three genes *mccC*, *mccE,* and *mccF* that ensure export of unprocessed microcin outside the cells (MccC pump) and modification of processed McC (MccE and MccF enzymes) (see section mechanisms of resistance) (Novikova et al., 2010; Agarwal et al., 2011, 2012). By contrast, the immunity mechanism to MccL depends on a single gene *mclI* that encodes an immunity protein (Sablé et al., 2003). Overall, self-immunity of the producers relies either on specific immunity proteins encoded in the gene clusters that bind to the toxic entities making them inefficient, or on efflux systems, mainly ABC transporters, which ensure export of the microcins to the external medium and simultaneously self-immunity of the producing bacteria. As examples, self-immunity to MccJ25 is provided exclusively by McjD, a highly specific ABC exporter which ensures simultaneously export of the microcin (Beis and Rebuffat, 2019), while full self-immunity to MccB17 requires both an immunity protein McbG and an ABC exporter McbEF (Collin and Maxwell, 2019).

MECHANISMS OF ACTION

Comparison of the mechanisms used by antibiotics and microcins to kill sensitive bacteria shows that they may share different bacterial receptors, translocators and final targets (**Table 2** and **Figure 2**). Thus, it is obvious that these two groups of antimicrobials may cross in several mechanisms of action. However, it is also expected that several mechanisms of action of microcins are very specific and are not involved in the inhibition activity of antibiotics. This characteristic is particularly relevant to address in terms of the risk of cross-resistance between microcins and antibiotics. These similarities and differences are highlighted below.

The Uptake Systems

The first obstacle to be overcome by an antimicrobial compound to reach its final target is the bacterial cell envelope (Collet et al., 2020). The extent of this barrier varies according to the target to be reached, the chemical structure of the antimicrobial compound and the bacterial species. For Gram-negative bacteria, antimicrobials have to pass first the outer membrane. Then, they can access the cytoplasmic membrane bilayer (inner membrane) and either insert inside or cross it for those antimicrobials having intracellular targets. Many antibiotics are hydrophilic compounds of low molecular mass and uptake across the outer membrane is ensured by passive diffusion using pores formed by specific β-barrel membrane proteins called porins. Porins are the most abundant proteins of the outer membrane in Gram-negative bacteria. They are classified as non-specific (general porins) and specific (selective porins), according to their threshold size and amino acids lining the aqueous channel (Choi and Lee, 2019). The transport varies according to the size, charge and hydrophilicity of the molecule. Recently, the dual function of the porin OmpF both as receptor and translocator for the pore-forming colicin N, has been elegantly demonstrated (Jansen et al., 2020). However, more hydrophobic or higher molecular mass compounds above the porin threshold require other strategies, among which hijacking receptors or transporters required for vital functions is a major one. Indeed, Gram-negative bacteriocins, colicins and microcins, widely parasitize such receptors to enter the periplasmic space, and particularly those involved in iron import. This receptor hijacking qualifies many microcins as "Trojan horse" compounds, as they mimic vital compounds that require being imported in cells, to penetrate sensitive bacteria (Duquesne et al., 2007a; Nolan and Walsh, 2008; Severinov and Nair, 2012).

Iron acquisition is an essential factor for microbial life. However, under aerobic conditions, free iron availability is limited by the very low solubility of ferric iron, and especially within a host, where iron is competed for by both the microbial community and the host (Wilson et al., 2016). To secure iron, bacteria have evolved to develop efficient Fe(III)-chelating agents (K_a ranging from 10^{23} to 10^{52}), termed siderophores, to scavenge iron from their surrounding environment and import it. A study by Lewis et al. (2010) showed that siderophores are sufficient for allowing the culture of bacteria previously unculturable in laboratory conditions. Siderophores are non-ribosomally synthesized (Crosa and Walsh, 2002) and are important for

TABLE 2 | Comparison of the mechanisms involved in the antibacterial activity and the bacterial resistance for well characterized microcins and for conventional antibiotics sharing common targets with microcins.

Antibiotic/Microcin	Mechanisms of action		Mechanisms of resistance	
	Function impaired/*Target*	**Uptake system (OM/IM)**	**Process/*Target***	**Mechanism**
Penicillins Cephalosporins Beta-lactams	– Bacterial cell wall disruption/*Peptidoglycan breaking*	– Porins; self-promoted pathway	– Inactivation/β-*lactam ring* – Mutations/*TonB Porins* – Efflux pumps overexpression	– β-lactam ring cleavage by β-lactamases – Decrease of uptake of the antibiotic due to modifications of TonB sequence – Decrease of uptake of the antibiotic – Pumping out of the antibiotic
Fosfomycin	– Bacterial cell wall/*Peptidoglycan biosynthesis: UDP-N-acetylglucosamine enolpyruvyl transferase, MurA* – Sugar transport into the cytoplasm	– GlpT, UhpT sugar transporters	– Mutations/*Mur A*	– Cys-Arg mutation in MurA active site – Mutations in GlpT, UhpT transporters
Polymixins Colistin/polymixin E	– Membrane permeabilization/*LPS binding leading to detergent effect* – Endotoxin neutralization	– Porins	– Enzymatic modification/*LPS* – Efflux pumps overexpression	– Modification of LPS by the MCR1 phosphoethanolamine transferase – Pumping out of the antibiotic
Rifamycins Rifampicin	– Protein synthesis- Transcription step/β *subunit of RNAP*	– Siderophore receptor FhuA – TonB system	Mutations./*RNAP* β *subunit*	– Mutations in *rpoB* gene
Streptolydigin	– Protein synthesis-Transcription step/*Inhibition of RNAP catalytic function by binding* β *and* β′ *subunits*	– Porins	– Mutations/*RNAP* β *and* β′ *subunits*	– Mutations in *rpoB* and *rpoC*
Albomycin	– Protein synthesis – Translation step/*Aminoacyl t-RNA synthetase*	– Siderophore receptor FhuA – TonB system	– Enzymatic modification/*Processed albomycin*	– Acetylation of processed albomycin by transacetylase RimL
Quinolones (nalidixic acid, ciprofloxacin, norfloxacin,. . .)	DNA replication/*Type II topoisomerases (DNA gyrase, topoisomerase IV*)		– Mutations – Protein interactions/*DNA gyrase, topoisomerase IV* – Enzymatic modification/*Piperazine ring* – Mutations/*Porins* – Efflux pumps overexpression	– Mutations in *gyrA, gyrB* or *parC, parE* (Ser^{83} in GyrA) – Protection of DNA gyrase and topoisomerase IV by the gyrase interacting protein qnr – Piperazine ring acetylation (AAC(6')-Ib-c) – Decrease of uptake of the antibiotic – Pumping out of the antibiotic
Chloramphenicol	– Protein synthesis/*Binding to 50S ribosome subunit inhibiting the formation of peptide bonds*	– Membrane transporter	– Enzymatic modification/*Chloramphenicol*	– Acetylation by chloramphenicol acetyltransferases CATs
Aminoglycosides	– Protein synthesis – Translation step/*Binding to 30S ribosome subunit*		– Enzymatic modification/*Aminoglycosides*	– Acetylation by acetyltransferases (AACs) – Phosphorylation by phosphotransferases (APHs) – Adenylation by nucleotidyltranferases (ANTs)
Tetracyclines	Protein synthesis -Translation step/*Binding to 30S ribosome subunit that blocks aminoacyl-tRNA binding to RNA-ribosome complex*	– Porins OmpF, OmpC	– Resistance genes acquisition – Enzymatic modification/*Tetracyclines* – Efflux pumps expression	– Acquisition of *tet,* or *otr* resistance genes leading to production of ribosomal production proteins Tet – Methylation by rRNA methylase – Pumping out of the antibiotic
MccJ25	– Protein synthesis-Transcription step/*Binding to* β′ *subunit of RNAP (secondary channel)*	– Siderophore receptor FhuA – TonB system – SbmA	– Mutations/*RNAP* β′ *subunit* – Efflux pumps expression	– Mutation in *rpoC* that encodes RNAP β′ subunit ($T^{931}I$) and additional mutations ($Q^{921}P$, $T^{934}M$, $H^{936}Y$) – Pumping out of the microcin by ABC exporters (McjB, YojI)/TolC

(Continued)

TABLE 2 | Continued

Antibiotic/Microcin	Mechanisms of action		Mechanisms of resistance	
	Function impaired/*Target*	**Uptake system (OM/IM)**	**Process/*Target***	**Mechanism**
MccB17	– DNA replication and topology maintenance/*Binding to DNA gyrase*	– Porin OmpF/ – SbmA	– Mutations/*GyrB, GyrA OmpF, OmpR SbmA* – Efflux pumps expression	– Mutations in GyrB and GyrA: GyrB ($W^{751}R$): full resistance; GyrB ($K^{447}E$), GyrA ($S^{83}W$): partial resistance – Mutations in *omp*F and *omp*R – Pumping out of the antibiotic by ABC exporter (McbEF)
McC	– Protein synthesis – Translation step/*Aspartyl-tRNA synthetase (Asp-RS)*	– Porin OmpF/YejABEF	– Inactivation of the antibiotic *Processed McC* – Efflux pumps expression	– Acetylation of processed McC by transacetylases [either encoded in McC gene cluster (MccE) or chromosome-encoded (RimL)] – Cleavage of the heptapeptide-nucleotide amide bond by carboxypeptidases [serine carboxypeptidase encoded in McC gene cluster (MccF)] – Cleavage of the phosphoramide bond in aspartamide adenosine by histidine triad hydrolases – Pumping out of the antibiotic by ABC exporter MccC
MccE492	– Inner membrane bilayer permeability/*Formation of channels* – Sugar transport/*Binding to inner membrane components of mannose phosphotransferase system permease (ManPTS)*	– Siderophore receptors FepA-, Cir-, Fiu-TonB system	– Mutations in uptake system at the inner membrane/*Catechol siderophore receptors* – Mutations in mannose uptake system/*ManXYZ*	– Mutations/deletions in FepA, Cir, Fiu, TonB – Deletion of inner membrane complex ManYZ
MccH47	– Energy production (ATP synthesis)/*Binding to F_0 subunits of ATP synthase*	– Siderophore receptors FepA Cir Fiu - TonB system	– Mutations in uptake system/*Catechol siderophore receptors*	– Mutations/deletions in FepA, Cir, Fiu
MccL	Membrane potential	– Siderophore receptor Cir -TonB system/SdaC	– Mutations in uptake systems/*Catechol siderophore receptor*	– Mutations in Cir, TonB
MccV	Inner membrane	– Siderophore receptor Cir -TonB system/ – SdaC	– Mutations in uptake systems/*Catechol siderophore receptor*, *SdaC*	– Mutations in Cir, TonB, SdaC
MccPDI	– Energy production/*ATP synthase* – Inner membrane permeability	– Porin OmpF	– Mutations/*Thiol-redox enzymes*, *OmpF*	– Mutations in *dsbA*, *dsbB* encoding thiol-redox enzymes making S-S bonds

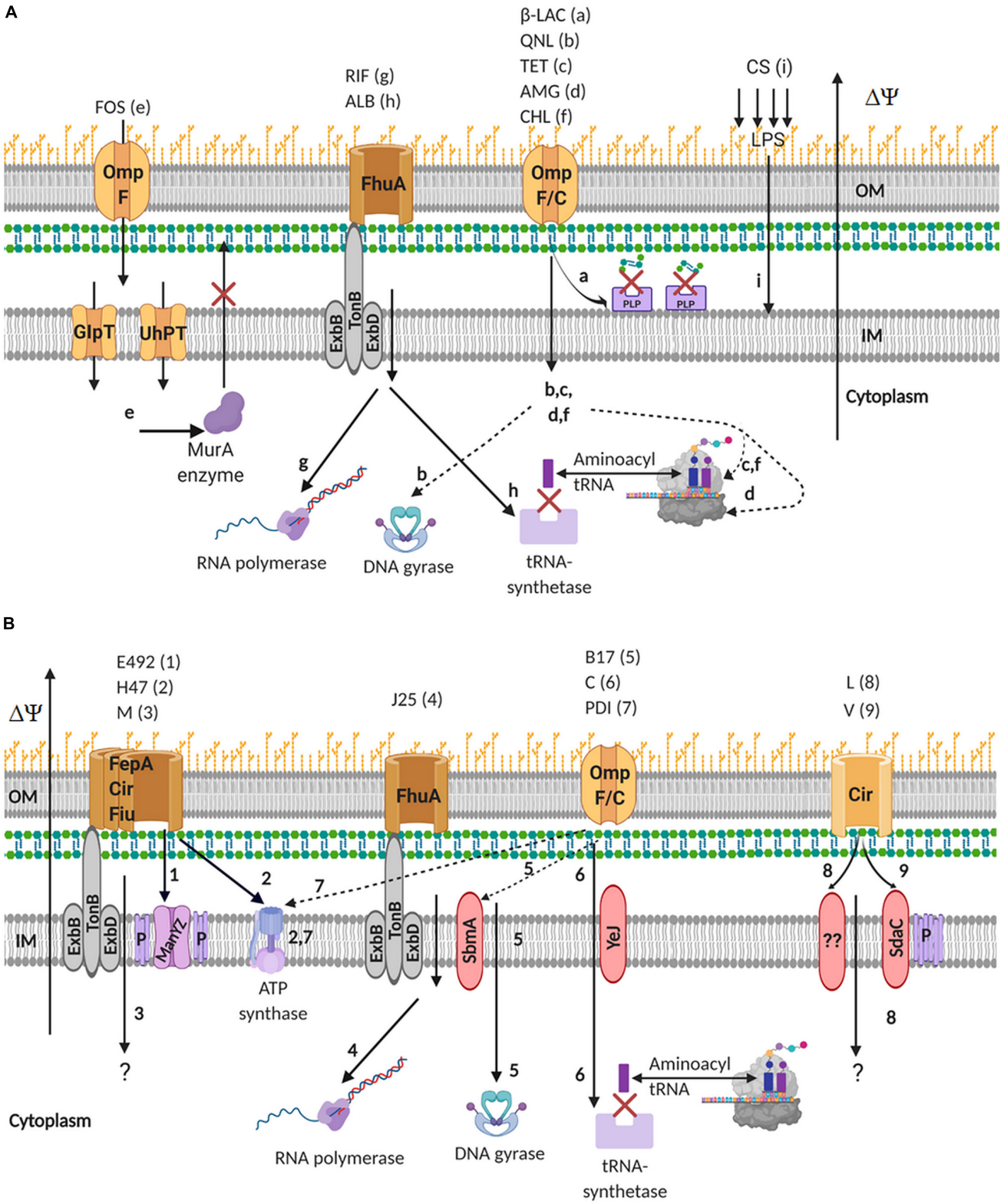

FIGURE 2 | Mechanisms of action of antibiotics **(A)** and microcins **(B)** against Gram-negative bacteria showing the membrane proteins involved in uptake into sensitive bacteria and the final targets. β-LAC, β-lactams; QNL, quinolones; TET, tetracycline; AMG, aminoglycosides; FOS, fosfomycin; CHL, chloramphenicol; CS, colistin; RIF, rifampicin; ALB, albomycin; P, pore; LPS, lipopolysaccharide. A letter and a number are assigned to each antibiotic and each microcin respectively, which are used in the scheme to identify the path they follow for their killing activity.

enteropathogen survival (Hantke, 2003). Concomitantly, iron availability has been observed to regulate MccE492 gene expression (Marcoleta et al., 2013). The resulting Fe(III)-siderophore complex is then internalized by the producing strains via high affinity siderophore receptors anchored at the outer membrane, which are specifically involved in this function, but also ensure other strategic roles in microbial communities (Kramer et al., 2019). Siderophore receptors consist of a 22-stranded antiparallel β-barrel with external loops serving as ligand binding sites and an N-terminal globular domain forming a plug that occludes the barrel (Krewulak and Vogel, 2008). They are specific to the different siderophore chemical types, such as FhuA for ferrichrome or Cir, Fiu, and FepA for catechol siderophores in enterobacteria. These receptors are coupled to the TonB-ExbB-ExbD three-component machinery anchored at the inner membrane (TonB system), which transfers the energy source from the proton motive force of the cytoplasmic membrane to the outer membrane (Krewulak and Vogel, 2008), thus permitting active transport.

All microcins, whatever they are of class I or II, use either the siderophore receptor or the porin path to reach their final target (**Figure 2B**). Siderophore microcins uptake requires the FepA-, Cir-, Fiu-TonB systems, with FepA having the most important role (Destoumieux-Garzón et al., 2006; Azpiroz and Laviña, 2007; Vassiliadis et al., 2010). Unmodified microcins use the Cir-TonB system (MccV, MccL) (Chehade and Braun, 1988; Morin et al., 2011), or the porin OmpF which screens incoming products in a non-specific manner (Sato et al., 2000; Kaeriyama et al., 2006) (MccPDI) (Zhao et al., 2015), while class I microcins either use FhuA (MccJ25) (Pugsley et al., 1986; Salomón and Farías, 1993; Mathavan et al., 2014), or OmpF (MccB17, MccC) (Laviña et al., 1986; Novikova et al., 2007) to reach the periplasmic space (**Figure 2B**). In the case of loss of function of the TonB system, MccE492, MccH47, and MccM retain antimicrobial activity, suggesting the involvement of another translocator, such as the TolA-TolQ-TolC system known to mediate the import of certain colicins (Lazdunski et al., 1998). Similar observations were made for MccL and MccV (Gerard et al., 2005; Morin et al., 2011), suggesting that the function of the ExbB protein could be replaced by its homolog TolQ in TonB-dependent microcin activity. However, although the presence of the siderophore PTM enhances its efficiency, the non-modified form of MccE492 (without the C-terminal siderophore) is also able to kill sensitive bacteria, but at a significantly lower level. On their side, antibiotics, which are essentially low molecular mass hydrophobic compounds, are most often transported inside target bacteria via porin or iron siderophore receptor pathways (**Table 2**).

Mechanisms of Action Common to Antibiotics and Microcins

Disruption of the Cytoplasmic Membrane

Permeabilization and/or disruption of the bacterial cytoplasmic membrane of Gram-negative bacteria is the main mechanism of action of the non-ribosomal peptide antibiotics polymyxins B and E (**Table 2** and **Figure 2A**), which share a high degree of structural similarity (Schindler and Teuber, 1975). Polymixin E (also called colistin) binds to the lipopolysaccharide (LPS) both in the bacterial outer membrane and in the cytoplasmic membrane and this interaction is essential for cytoplasmic membrane permeabilization, cell lysis and the bactericidal activity of this antibiotic (Sabnis et al., 2019). It should be noted that all polymyxins are inactive against Gram-positive bacteria, except few species such as *Streptococcus pyogenes* (Trimble et al., 2016).

Several class II microcins target the inner membrane, by perturbing either its integrity using different mechanisms of peptide membrane interaction, or the proteins which are embedded. This constitutes at least the primary part of their mechanism of action (**Table 2** and **Figure 2B**). Indeed, the final killing trajectory of MccE492 appears to stop at the inner membrane. MccE492 induces a rapid depolarization and permeabilization of *E. coli* cytoplasmic membrane, without provoking cell lysis (Lagos et al., 1993; Destoumieux-Garzón et al., 2006). It forms well-defined ion channels in planar phospholipid bilayers that are constituted of supramolecular peptide assemblies (Lagos et al., 1993; Destoumieux-Garzón et al., 2006). It also interacts with the mannose phosphotransferase system permease ManXYZ (Bieler et al., 2010), associating specifically with its inner membrane components ManYZ. Therefore, MccE492 both perturbs the inner membrane permeability and interferes with the transport of mannose to kill sensitive congeners. Besides, MccE492 is known to form amyloid fibrils (Bieler et al., 2005; Arranz et al., 2012; Aguilera et al., 2016) that play a role in modulating its antimicrobial activity. These aggregates have been observed more significantly with the unmodified form of MccE492, suggesting their formation is not only an additional mechanism of protection of the producer strain, but also may act as a toxin reservoir. MccV destabilizes the membrane potential (Yang and Konisky, 1984) and further interacts with an inner membrane transporter, the serine permease SdaC (Gerard et al., 2005), which is involved in serine transport and acts as a specific receptor for MccV. It can be suggested that a perturbation of serine transport in sensitive bacteria could result, or that SdaC could drive MccV to form channels in the inner membrane. MccE492 and MccV thus illustrate the combined use of two different mechanisms involving the inner membrane or its components to kill sensitive bacteria. MccL primary target is also the cytoplasmic membrane. It provokes disruption of membrane potential of *E. coli* cells, but without inducing permeabilization of the inner membrane (Morin et al., 2011). A potential inner membrane target for MccL has not been identified. Finally, it has to be mentioned that at higher concentrations than the MIC, MccJ25 induces perturbations of the cytoplasmic membrane permeability and disruption of the cytoplasmic membrane gradient in *Salmonella enterica* (Rintoul et al., 2001; Ben Said et al., 2020), and perturbation of the respiratory chain enzymes in *E. coli,* accompanied with stimulation of the production of reactive oxygen species (Bellomio et al., 2007).

Inhibition of Protein Biosynthesis

The bacterial 70S ribosome is composed of two ribonucleoprotein subunits forming the 30S and 50S subunits

(Yoneyama and Katsumata, 2006). Aminoglycosides (AGs), such as streptomycin or gentamicin, and tetracyclines bind to the 16S ribosomal RNA of the 30S subunit (Chopra and Roberts, 2001; Krause et al., 2016). AGs bind to the A-site of the ribosome, causing inhibition of translation of mRNA by codon misreading on delivery of the aminoacyl-tRNA (**Table 2** and **Figure 2A**). For their part, tetracyclines prevent incoming aminoacyl-tRNA from binding to the A site of the mRNA translation complex. As well, chloramphenicol inhibits protein synthesis by preventing the binding of t-RNAs to the A site of the ribosome (Kapoor et al., 2017). The bacterial ribosome is also the target for other antibiotic classes, such as the macrolides and ketolides or the streptogramins.

Contrasting with MccB17 and its *Pseudomonas* congeners which exert their antimicrobial activity by perturbing DNA topology setting up (see section below Inhibition of Nucleic Acid Biosynthesis), other MccB17-like bacteriocins perturb protein synthesis. Klebsazolicin from *K. pneumoniae,* which exhibits moderate antimicrobial activity against certain *E. coli*, *Klebsiella* and *Yersinia* strains (Metelev et al., 2013) targets the 70S ribosome and interferes with translation elongation. Moreover, it binds to the peptide exit tunnel, overlapping with the binding sites of macrolides or streptogramin-B. Similar to klebsazolicin, the MccB17-like phazolicin produced by *Rhizobium* sp., which exhibits narrow-spectrum antibacterial activity against some symbiotic bacteria of leguminous plants (Travin et al., 2019), also targets the 70S ribosome by obstructing the peptide exit tunnel, but through different binding mechanisms.

Albomycin, which consists of an antibiotic part linked to a siderophore moiety, inhibits aminoacyl t-RNA synthetases (aaRSs) that are essential for protein synthesis (Severinov and Nair, 2012) (**Table 2** and **Figure 2A**). Similar, McC targets the aspartyl-tRNA synthetase (Metlitskaya et al., 2006), making it a translation inhibitor (**Table 2** and **Figure 2B**). After having crossed the outer membrane thanks to the porin OmpF, McC requires the inner membrane ABC transporter YejABEF (Novikova et al., 2007) for its translocation within the cytoplasm. A comprehensive analysis by Vondenhoff et al. (2011) has shown that to mediate binding and translocation of substrates, the YejABEF transporter requires an N-terminal formyl-methionine and an arginine. These requirements are achieved with the formylated f-MRTGNAD heptapeptide part of the McC precursor. However, unlike other microcins, which are fully processed within the producing cells before export, further McC maturation is necessary within the target bacteria to attain its cytotoxic form. McC undergoes a double-step processing. First of which is the deformylation of the formylated heptapeptide precursor, essentially nullifying the detoxification process of its immunity protein *mccE*. This deformylation allows the second maturation step, which is ensured by broadly specific endoproteases PepA, PepB, and PepN, which remove the peptide moiety of the microcin. This last processing step releases the toxic entity, which is a non-hydrolyzable analog of aspartyl-adenylate (Asp-RS) that blocks aspartyl-tRNA synthetase and thus transcription (Kazakov et al., 2008). This subtle cheating mechanism nicely exemplifies the Trojan horse strategy used by microcins. Moreover, Ran et al. (2017) observed that when increasing the concentration until the mM level, McC was able to inhibit the activity of β-galactosidase, respiration chain dehydrogenases, and 6-phosphogluconate dehydrogenase without damaging the inner membrane, showing that McC develops a second mechanism of action that operates at higher concentrations.

Inhibition of Nucleic Acid Biosynthesis

Quinolone antibiotics (nalidixic acid, ciprofloxacin, . . .) inhibit DNA synthesis by targeting two essential type II topoisomerases, DNA gyrase and topoisomerase IV, and converting them into toxic enzymes that fragment the bacterial chromosome (**Table 2** and **Figure 2A**). These interactions result in erroneous unwinding of DNA, introduction of double strand breaks and cell death (Fabrega et al., 2009). Besides, rifampicin inhibits DNA-dependent RNA polymerase (RNAP) activity by forming a stable complex with the enzyme. It binds in a pocket of the RNAP β subunit, deep within the DNA/RNA channel, while away from the active site. The inhibitor directly blocks the path of the elongating RNA when the transcript becomes two to three nucleotides in length. It thus suppresses the initiation of RNA synthesis (Campbell et al., 2001).

The target of MccB17 is also a topoisomerase (**Table 2** and **Figure 2B**). MccB17 enters sensitive bacteria using the OmpF porin, diffuses through the periplasmic space and binds to the inner membrane transporter SbmA to be delivered into the cytoplasm (Laviña et al., 1986). It induces gyrase-dependent formation of a stable cleavage complex instead of the transient break that normally happens during the catalytic cycle. It causes covalent links between DNA gyrase and double stranded DNA, hence blocking DNA replication and maintenance. Similar to fluoroquinolones, MccB17 targets the cleavage of both DNA strands, which is a critical step in the DNA gyrase supercoiling cycle, but the MccB17-induced cleavage pattern is different from that of quinolones (for a review on MccB17 activity see Collin and Maxwell, 2019). The stringent role of the heterocycles in MccB17 activity has been evidenced (Roy et al., 1999). Introduction of an extra oxazole ring at position Ser^{52} in MccB17 results in 40% higher antibacterial activity than that of wild-type MccB17 (Roy et al., 1999). Bis-heterocycles play a particularly essential role, with the central MccB17 region that contains two thiazoles and a thiazole/oxazole forming the critical core for DNA cleavage (Collin and Maxwell, 2019). Moreover, the C-terminal part of MccB17 is crucial for both uptake by sensitive cells and DNA gyrase inhibition, while the N-terminal region is only moderately important for uptake (Shkundina et al., 2014). Interestingly, MccB17 congeners that belong to the LAP family of RiPPs do not share all similar mechanisms, targeting either DNA gyrase or the 70S ribosome. Indeed, MccB17-like compounds from *P. syringae* are active against *E. coli* and essentially *Pseudomonas* species including *P. aeruginosa*, through DNA gyrase inhibition (Metelev et al., 2013), while the other analogs do not (see section above "Inhibition of Protein Biosynthesis").

Such as rifampicin, the lasso peptide MccJ25 targets the RNAP (**Table 2** and **Figure 2B**). To reach its intracellular target, MccJ25 hijacks the ferrichrome receptor FhuA to cross the outer membrane (Mathavan et al., 2014) and is internalized

into the cytoplam by the inner membrane protein SbmA. Finally, MccJ25 binds to the RNAP secondary channel, which connects the enzyme surface with the RNAP catalytic center, and through which nucleotide triphosphate substrates (NTP) migrate to the catalytic center (Adelman et al., 2004; Mukhopadhyay et al., 2004), whereby inactivating transcription in a partial competitive manner. The loop is involved in recognition and uptake of MccJ25 by the iron-siderophore transporter FhuA, while the macrolactam ring and C-terminal tail are responsible for binding to the RNA polymerase target (Destoumieux-Garzón et al., 2005; Semenova et al., 2005). The crystal structure of MccJ25 bound to *E. coli* RNAP was determined and the residues critical for the interaction were identified (Braffman et al., 2019). MccJ25 binds deep within the secondary channel, such as to clash with NTP binding and explaining the partial competitive mechanism of inhibition with respect to NTPs previously proposed (Mukhopadhyay et al., 2004). Besides, it was shown that at higher concentrations, MccJ25 induces perturbations of the cytoplasmic membrane permeability and disruption of the cytoplasmic membrane gradient of *S. enterica* Newport (Rintoul et al., 2001). At much higher concentrations, it can also stimulate the production of reactive oxygen species (Bellomio et al., 2007). This shows once again the multiple mechanisms brought into play by a given microcin, which both explains their high efficiency and suggests lower risks of resistance acquisition. Several antibacterial lasso peptides, have been shown to also target RNAP through binding to the secondary channel, although their different antibacterial activity spectrum. This is the case for capistruin produced by *Burkholderia thailandensis* and active against *Burkholderia* and *Pseudomonas* species (Knappe et al., 2008; Kuznedelov et al., 2011; Braffman et al., 2019), ubonodin from *B. ubonensis* and active against pathogenic members of the *B. cepacia* complex (Cheung-Lee et al., 2020), citrocin from *Citrobacter* sp., active against *E. coli* and *Citrobacter* sp. (Cheung-Lee et al., 2019). By contrast, acinetodin and klebsidin from human-associated strains of *Acinetobacter* and *Klebsiella*, display no activity or low activity against *K. pneumoniae,* while they bind RNAP (Metelev et al., 2017b), showing that the spectrum of activity of lasso peptide microcins appears to be driven by the uptake in target bacteria rather than the intracellular target. This is in agreement with the spectrum of activity of MccJ25 against a collection of *Salmonella* strains, which is associated mainly with differences in the FhuA sequences (Ben Said et al., 2020).

Mechanisms of Action Specific to Microcins

MccH47 is bactericidal and targets the membrane bound F_0 proton channel subunits of ATP synthase (Trujillo et al., 2001; Rodriguez and Laviña, 2003; Palmer et al., 2020), causing an unregulated influx of protons. It uses FepA-, Cir-, Fiu-TonB dependent receptors to reach its inner membrane target (Patzer et al., 2003). The mechanism of action of the class IIa MccPDI is poorly identified. It was told to require close bacterial proximity to be cytotoxic, hence the name PDI (Proximity Dependent Inhibition) (Eberhart et al., 2012), since co-cultures of producing and sensitive strains separated by a semi-permeable film inhibit its activity. Why proximity is required for activity is unknown, but it could be only a consequence of a concentration-dependence effect (Lu et al., 2019). MccPDI that uses the porin OmpF to cross the outer membrane (Zhao et al., 2015; Lu et al., 2019) was shown (Zhao et al., 2015) to require a functional ATP synthase for exerting its cytotoxic activity, while (Lu et al., 2019) proposed it would induce membrane damage.

Mechanisms of Action Specific to Antibiotics

Inhibition of Cell Wall Formation

The cell envelope of Gram-negative bacteria consists of a phospholipid bilayer inner membrane that wraps the cytoplasm, and an asymetric outer membrane essentially composed of phospholipids at the inner leaflet and LPS at the outer leaflet, which protects the cell from the environment. In between is the periplasm that shelters a thin peptidoglycan layer (Collet et al., 2020). This double-membrane complex system and in particular the peptidoglycan, often called the cell wall, is a main target for antibiotics and antimicrobials. β-lactam antibiotics, which include in particular penicillins, cephalosporins and carbapenems, harbor the β-lactam ring in their structure that mimics the D-alanyl D-alanine terminal amino acid residues of the precursor subunits of the peptidoglycan layer, and so far interacts with penicillin binding proteins (PBPs). This induces a disruption of the peptidoglycan layer leading to the lysis of the bacterium (Kapoor et al., 2017). Besides, fosfomycin inhibits bacterial cell wall biosynthesis in an early stage; it integrates the cell and inactivates an essential enzyme in peptidoglycan synthesis (Dijkmans et al., 2017). β-lactams, mainly carpabenems and second, third and fourth generation of cephalosporins as well as fosfomycin have a broad spectrum antibacterial activity.

Inhibition of Folic Acid Metabolism

Trimethoprim and sulfonamides act at distinct steps in folic acid metabolism. Sulfonamides inhibit dihydropteroate synthase, which acts at an early step in folic acid biosynthesis in a competitive manner with higher affinity for the enzyme than the natural substrate, *p*-amino benzoic acid (PABA). For its part, trimethroprim inhibits dihydrofolate reductase, thus operating at a later stage of folic acid synthesis (Yoneyama and Katsumata, 2006).

MECHANISMS OF RESISTANCE AND POTENTIAL CROSS- AND CO-RESISTANCE BETWEEN ANTIBIOTICS AND MICROCINS

Various mechanisms of resistance to antibiotics and/or to microcins are reported including essentially modifications of the cellular target by mutations or protein interactions, changes in the structure of the antimicrobial molecule, perturbations of binding or penetration of the antibiotic into sensitive cells and specific cell wall modifications. Several mechanisms are specific, but bacteria may use common mechanisms of resistance against

microcins and antibiotics that could induce cross-resistance, which occurs when a single mechanism provides resistance to several antimicrobial molecules differing in their structures, simultaneously. In contrast, co-resistance occurs when two or more different resistance genes encoding several unrelated resistance mechanisms are located on the same genetic element (plasmid, transposon) (Chapman, 2003). In the following section, we describe different mechanisms of resistance and the possible occurrence of cross- and co-resistance between antibiotics and microcins (**Table 2** and **Figure 3**).

Prevention of Intracellular Accumulation of the Toxic Entity: Efflux Pumps and Decreased Uptake

On one side, outer membrane porins and inner membrane transporters, which are involved in the uptake of antibiotics and microcins into sensitive cells, and on the other side efflux pumps, which pump the toxic compounds out of the bacteria, both constitute a first line resistance strategy (Ghai and Ghai, 2018). Porins, which ensure passive uptake of substrates across the outer membrane (see section mechanisms of action above), serve as the first gate for many antibiotics and several class I and II microcins. Furthermore, efflux pumps can be specific for a single substrate or can confer resistance to multiple antimicrobials by facilitating their extrusion before they can reach their intended targets (Anes et al., 2015). In Gram-negative bacteria, overexpression of efflux pumps is one of the mechanisms of resistance to β-lactams (Amaral et al., 2014) and to quinolones encoded by *qep*A and *oqx*AB genes (Fabrega et al., 2009). Likewise, reduced porin levels, which induce decrease of antibiotic concentration inside sensitive cells, is another mechanism of resistance to β-lactams in Gram-negative bacteria (Pfeifer et al., 2010), including *K. pneumoniae* (Jacoby et al., 2004) and *P. aeruginosa* (Li et al., 1994). Besides, mutations and deletions of genes encoding porins induce resistance to antibiotics. Indeed, *ompF* mutant was resistant to several β-lactam antibiotics in some Gram-negative pathogens, including *E. coli* and the deletion of OmpA resulted in increased susceptibility to several antibiotics including β-lactams in *A. baumannii* (Smani et al., 2014).

For microcins, the *E. coli* ABC exporter of unknown function YojI, mediates resistance to MccJ25 by pumping the microcin out of the cells with the help of TolC, maintaining its concentration below the toxic concentration (Delgado et al., 2005). YojI is located at the inner membrane and is coupled to the TolC protein at the outer membrane which ensures the last

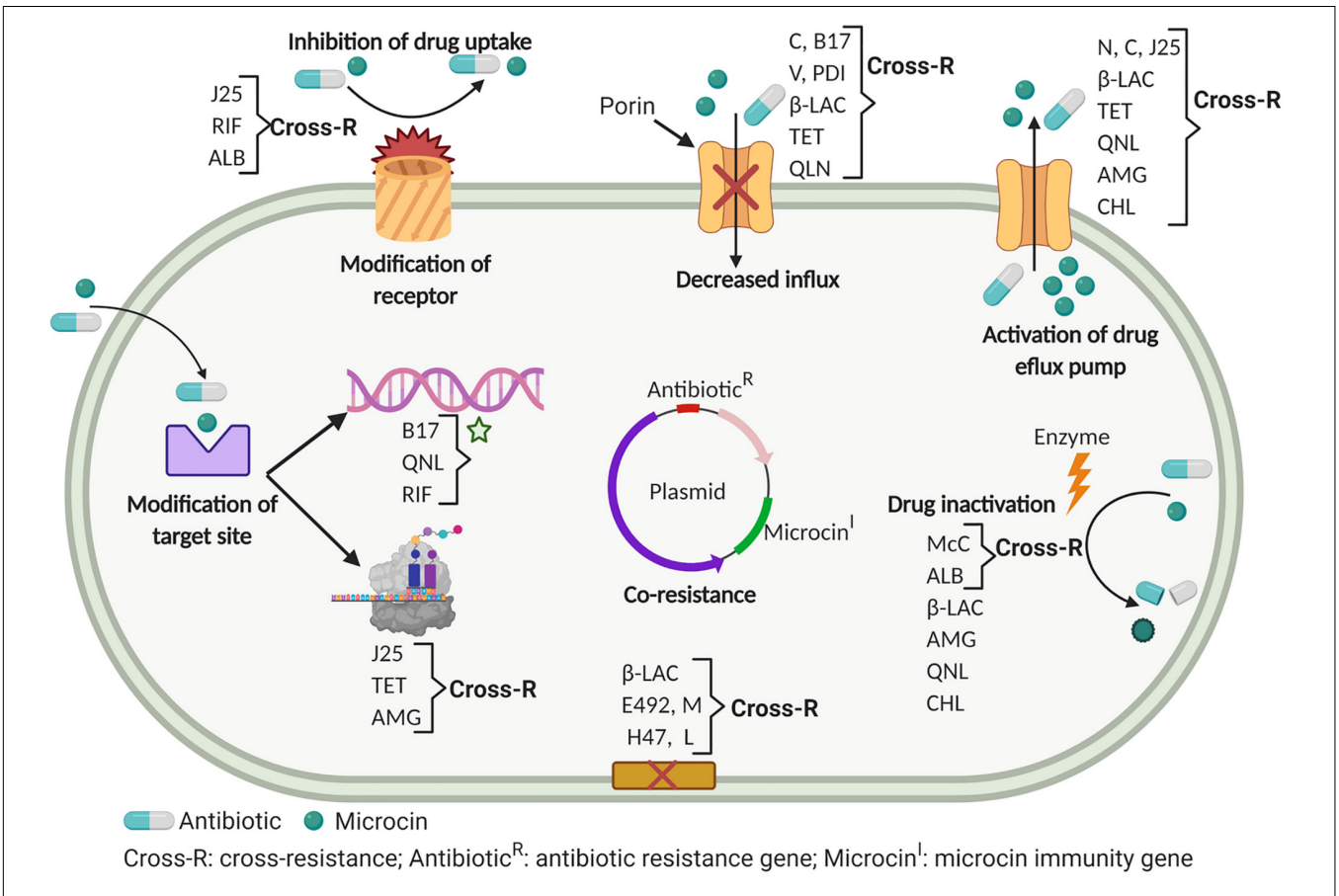

FIGURE 3 | Mechanisms of cross-resistance and co-resistance of antibiotics and microcins in Gram-negative bacteria. β-LAC, β-lactams; QNL, quinolones; TET, tetracycline; AMG, aminoglycosides; FOS, fosfomycin; CHL, chloramphenicol; CS, colistin; RIF, rifampicin; ALB, albomycin.

export step, similar to the MccJ25 gene cluster-encoded ABC exporter McjD, which warrants both microcin export and self-immunity for the producing cells (Bountra et al., 2017; Beis and Rebuffat, 2019). Similarly, McC is expelled from producing cells through a major facilitator superfamily (MFS) efflux pump (Severinov and Nair, 2012). Thus, the activation of several efflux pumps simultaneously could induce a co-resistance to antibiotics and microcins.

The iron-siderophore receptor FhuA is not only required for iron import, but it is also a target for bacteriocins (colicin M, MccJ25) and antibiotics (albomycin, rifamycin). Indeed, FhuA external loops L3, L4, L7, L8, and L11 are involved in the sensitivity to colicin M and the antibiotics albomycin and rifamycin. So far, a further mutation, insertion or deletion in the sequence encoding these loops may induce a cross-resistance between colicin M and these two antibiotics (Wang et al., 2018). Concomitantly, MccJ25 was also shown to require a primary interaction with the FhuA external loops L5, L7, L8 and L11 for its recognition and further internalization via this receptor (Destoumieux-Garzón et al., 2005). The level of sensitivity to MccJ25 also varies depending on the acquisition of specific FhuA, with a maximal sensitivity obtained with *E. coli* FhuA, while several *Salmonella* serovars are resistant due to a lack of efficiency of their FhuA receptor for MccJ25 uptake (Vincent et al., 2004; Ben Said et al., 2020). Similarly, various mutations in FhuA, especially in the cork domain, were reported to reduce the uptake and consequently the sensitivity to albomycin (Endriss et al., 2003). It could thus be hypothesized too that cross-resistance can occur between MccJ25 and albomycin. Besides, membrane permeabilization induced by a synthetic cationic peptide $(KFF)_3K$ was shown to induce the sensitivity of MccJ25 resistant clinical isolates, thus making the microcin entry independent of FhuA and SbmA proteins (Pomares et al., 2010), and thus confirming that microcin uptake is the first source of resistance to MccJ25. Therefore, both uptake decrease of the toxic entity and pumping it out of the sensitive cells are efficient mechanisms to confer resistance to MccJ25.

Resistance to siderophore microcins which carry a catechol siderophore PTM is also primarily induced by uptake impairment (Thomas et al., 2004; Massip and Oswald, 2020). As seen before, MccE492, MccM and MccH47 are recognized and internalized in sensitive bacteria via the TonB-dependent FepA, Fiu and Cir iron-catecholate receptors. According to Thomas et al. (2004), a *fepA*, *fiu* double mutation, the triple *cir*, *fiu*, *fepA* mutation and the *tonB* mutation induce complete resistance to MccE492, MccM, and MccH47, while deletion of *exbB* and *exbD* does not affect the sensitivity to all three siderophore microcins (Vassiliadis et al., 2010). Although it does not carry a siderophore PTM, MccL requires the TonB dependent catecholate receptor Cir for uptake. Mutations/deletions in Cir and TonB, or suppression of the proton motive force, which is required for the TonB function, afford MccL resistance in *E. coli* and *Salmonella,* while the proteins involved in serine or sugar transport are not involved (Morin et al., 2011). On the other hand, a mutation in the energy transducer TonB was shown to reduce uptake and confer resistance to ceftazidime. Moreover, ceftazidime-resistant TonB mutants were shown to be cross-resistant to fluoroquinolones and lactivicin, a siderophore-conjugated non-β-lactam antibiotic (Calvopina et al., 2020). Thus, a high probability exists for a possible cross-resistance between these antibiotics and microcins.

Resistance to MccN/24 is afforded by mutations in genes encoding the outer membrane porin OmpF (Jeanteur et al., 1994), or the inner membrane transporter SdaC involved in serine uptake and used for MccV activity (Gerard et al., 2005). Resistance to MccPDI also involves OmpF and more precisely the $K^{47}G^{48}N^{49}$ amino acid motif found in the predicted outer loop L1 of the porin (Zhao et al., 2015; Lu et al., 2019). In addition, mutations in DsbA and DsbB proteins, presumably involved in the formation of disulfide bonds in OmpF, induce resistance to MccPDI (Zhao et al., 2015). Mutations in *ompF* and *ompR* genes encoding OmpF induce a reduced sensitivity to MccB17. Moreover, a mutation in the *sbm*A gene encoding the inner membrane transporter SbmA, which translocates MccB17 from the inner membrane to the cytoplasm, induces high resistance to MccB17 (Laviña et al., 1986).

As regard the efflux systems involved in resistance to microcins, resistance to MccN/24 is controlled by the multiple antibiotic resistance (*mar*) operon (Carlson et al., 2001), which modulates efflux pump and porin expression via two encoded transcription factors, MarR and MarA (Sharma et al., 2017). MarA plays an important role in antibiotic resistance by activating the expression of the *acrAB-tolC* encoded efflux pump (Zhang et al., 2008) and also regulates biofilm formation (Kettles et al., 2019). Resistance to MccN/24 in *Salmonella* cells appears concomitantly with a multiple antibiotic resistance phenotype to ciprofloxacin, tetracycline, chloramphenicol and rifampicin (Carlson et al., 2001). So far, cross-resistance between MccN/24 and antibiotics raised above is quite possible.

Additional mechanisms involve specific cell wall modifications. Those include surexpression of capsule polysaccharides that can increase resistance to various antimicrobials including both antibiotics, in particular polymixins, and antimicrobial peptides (Campos et al., 2004). Interestingly, capsule polysaccharides are not involved in MccJ25 resistance of the YojI deficient strain (Delgado et al., 2005). Alterations of the LPS resulting in truncated LPS structures promote, among other pleiotropic effects, resistance to antimicrobial peptides and hydrophobic antibiotics (Pagnout et al., 2019).

Changes in Target Sites

To allow DNA supercoiling, bacteria use two type II topoisomerases, DNA gyrase and topoisomerase IV, which are both the targets of quinolones. They form a ternary cleavage complex gyrase/DNA/quinolone, thus blocking DNA replication. Mutations in genes encoding DNA gyrase (*gyrA*, *gyrB*) and topoisomerase IV (*parC*, *parE*) lead to quinolone resistance. Besides, a plasmid-mediated protection of DNA gyrase and topoisomerase IV from the action of quinolones is ensured in a non-specific manner by the gyrase interacting protein Qnr. Qnr is a 218 amino acid pentapeptide repeat protein (PRP) encoded by *qnr* genes, which blocks the action of quinolones on the DNA gyrase and topoisomerase IV in a lesser

extent (Fabrega et al., 2009; Jacoby et al., 2015). Indeed, one of these mutations is the well-known GyrB $W^{751}R$ mutation which induces resistance to quinolones and is also linked to resistance to MccB17 (Vizán et al., 1991). GyrB Trp^{751} is strongly implicated in the interaction of DNA gyrase with MccB17 (Heddle et al., 2001) and *gyrB* point mutation changing Trp^{751} for Arg leads to a protein variant resistant to MccB17 (del Castillo et al., 2001). Additionally, partial resistance to MccB17 is provided by mutations at position 83 in GyrA or 447 in GyrB (Jacoby et al., 2015). Consequently, cross-resistance to MccB17 and quinolones could occur. Otherwise, it is well known that immunity genes are responsible for protecting the producing bacteria from their own bacteriocin. Indeed, three genes *mcbE, mcbF,* and *mcbG* are involved in cell protection from endogenous and exogenous MccB17. Interestingly strains harboring these genes are shown to be highly resistant to fluoroquinolones (Tran and Jacoby, 2002). These mechanisms seem to be responsible for co-resistance to MccB17 and quinolones.

Mutation of the gene *rpo*B encoding the β′ subunit of RNAP (see section mechanisms of action above) induces resistance to rifampicin (Campbell et al., 2001; Goldstein, 2014). Likewise, alterations in the 30S or 50S subunit of the ribosome lead to resistance to antibiotics that act on these proteins, mainly tetracycline, chloramphenicol, streptolydigin and aminoglycosides (Kapoor et al., 2017). Similarly, first studies performed to understand the mechanism of action of MccJ25 have shown that a point mutation causing a substitution of Thr^{931} for Ile in the conserved segment of the *rpo*C gene coding for the largest RNAP subunit β′ conferred resistance to MccJ25, suggesting a mechanism involving occlusion of the RNAP secondary channel (Delgado et al., 2001; Yuzenkova et al., 2002). It was shown further from the crystal structure of the MccJ25-RNAP complex that MccJ25 binds within the RNAP secondary channel and interferes with the traffic of NTPs to the catalytic center (Braffman et al., 2019). Furthermore, additional *rpoC* mutations affecting amino acids in the conserved segments G, G′ and F and exposed into the RNAP secondary channel, also led to MccJ25 resistance *in vivo* and *in vitro*. While MccJ25 acts on the β′ subunit, and rifampicin on the β subunit, streptolydigin acts on both subunits. So far, a cross-resistance between MccJ25 and the above cited antibiotics mainly streptolydigin and rifampicin appears to be highly expected (Yang and Price, 1995; Temiakov et al., 2005).

For other antibiotics and microcins, no specific cross-resistance appears to be predictable. Chromosomally mediated colistin resistance occurs mainly via the addition of cationic moieties onto the negatively charged lipid A, while the plasmid mediated colistin resistance (MCR) is acquired via a plasmid-borne copy of an *mcr* gene. MCR-1 is the most prevalent MCR enzyme reported for the first time in 2015 followed by nine homologs described to date (Carroll et al., 2019). MCR-1-mediated colistin resistance confers protection against this last resort antibiotic via the presence of modified LPS within the cytoplasmic membrane, rather than the outer membrane (Sabnis et al., 2019). More precisely, the phosphoethanolamine transferase activity of MCR-1 adds a cationic phosphoethanolamine moiety to the anionic lipid domain A of LPS, which results in a net negative charge decrease and thus a lower affinity for the polymyxins.

Fosfomycin inhibits the bacterial cell wall synthesis at the early initiating step of the peptidoglycan synthesis. More specifically, it inhibits UDP-*N*-acetylglucosamine enolpyruvyl transferase (or MurA), the enzyme involved in transfer of the enolpyruvyl part of phosphoenolpyruvate to the 3′-hydroxyl group of UDP-*N*-acetylglucosamine, which is the first step in the biosynthesis pathway of peptidoglycan. Mutations in the *murA* gene confer resistance to fosfomycin due to the replacement of cysteine with aspartate in the active site of MurA, which prevents fosfomycin binding (Falagas et al., 2019). Moreover, resistance to fosfomycin can occur from chromosomal mutations in the structural genes that encode the GlpT and UhpT membrane transporters. GlpT and UhpT transport glycerol-3-phosphate and glycerol-6-phosphate sugars in bacteria, respectively and are used by fosfomycin to facilitate its entry in bacteria. These mutations block fosfomycin cell penetration (Falagas et al., 2019).

On the microcin side, the F_1F_0-ATP synthase has been shown to be the target of MccH47 (Rodriguez and Laviña, 2003) and MccPDI (Zhao et al., 2015). *E. coli* ATP synthase consists of a membrane-bound F_0 sector, which ensures proton translocation, connected to a cytoplasmic F_1 sector. They form a complex made up of eight different subunits, which are encoded by the *atp* operon, *atpIBEFHAGDC*. Three subunits form the F_0 proton channel and five subunits the catalytic F_1 domain. Mutations on genes *atpB*, *atpE*, *atpF* encoding the three subunits F_0a, F_0c, F_0b respectively, which constitute the F_0 proton channel, result in resistance to MccH47 (Rodriguez and Laviña, 2003). Furthermore, deletion of genes encoding subunits in the F_1 and F_0 domains of ATP synthase (*atpA* and *atpF* encoding $F_1\alpha$ and F_0b subunits, or *atpE* and *atpH* encoding F_0c and $F_1\delta$ subunits), result in a loss of susceptibility to MccPDI simultaneously to the loss of ATP synthase function (Zhao et al., 2015). None of these mechanisms appears to be shared between antibiotics and microcins.

Inactivation of the Toxic Entity

Several Gram-negative bacteria produce different enzymes that are able to modify antibiotics and thus induce resistance, such as the very well-known β-lactamases, which disrupt the specific structure of β-lactams (Sawa et al., 2020). β-lactamases are classified into four classes including group 1 (class C) cephalosporinases, group 2 (classes A and D) broad-spectrum, inhibitor-resistant, and extended-spectrum β-lactamases as well as serine carbapenemases, and group 3 (class B) metallo-β-lactamases (Bush and Jacoby, 2010). Other enzymes including aminoglycosides modifying enzymes, such as phosphotransferases (APHs), nucleotidyltranferases (ANTs) and acetyltransferases (AACs), which phosphorylate, adenylate and acetylate these compounds, respectively could also be involved in development of resistance (Ramirez and Tolmasky, 2010).

Acetylation is a widespread and efficient mechanism of resistance against different antibiotics. Modification of the piperazine ring of the fluoroquinolones is induced by an acetylase AAC(6′)-Ib-cr, which provides one of the mechanisms of resistance of bacteria to quinolones (Fabrega et al., 2009).

Chloramphenicol is also inactivated by acetylation which is performed by chloramphenicol acetyltransferases (CATs) (Smale, 2010). Acetylation is also a major mechanism of resistance to McC, then suggesting a high risk of cross-resistance between chloramphenicol and McC. Before its ultimate processing by non-specific aminopeptidases, which happens in sensitive cells to release the toxic non-hydrolyzable analog of aspartyl-adenylate, McC is exported outside the producer by the MccC pump and uptaken by sensitive cells using the porin OmpF and the inner membrane transporter YejABEF (see section Mechanisms of action). However, although most of produced McC is efficiently exported, intracellular processing also occurs inside the producing cells that ineluctably leads to the accumulation of the toxic entity that cannot be exported by the MccC pump and results in self-poisoning. Therefore, *E. coli mcc* gene clusters include genes (*mccE* and *mccF*) that encode proteins ensuring the self-immunity of the producer. The MccE acetyltransferase acetylates the α-amino group of processed McC, making it unable to bind to AspRS (Agarwal et al., 2011). So far, MccE makes *E. coli* simultaneously resistant to albomycin and McC (Novikova et al., 2010). MccE belongs to the general control non-repressible 5-related *N*-acetyltransferases (GNAT) superfamily, and shows high similarity with chromosomally encoded acetyltransferases RimI, RimJ, and RimL, which acetylate the N-termini of ribosomal proteins S18, S5, and L12 (Salah Ud-Din et al., 2016). Indeed, *E. coli* RimL induces resistance to McC by acetylating the amino group of the processed McC aspartate by the same mechanism as MccE (Kazakov et al., 2014). Similarly, when overproduced, RimL makes cells resistant to albomycin by acetylating processed albomycin, which contains a pyrimidine nucleotide instead of adenosine. Subsequently, a potential cross-resistance between McC and albomycin is quite possible (Kazakov et al., 2014). The MccF serine protease hydrolyses the carboxamide bond between the C-terminal aspartamide and AMP of both intact and processed McC, thus inactivating the aspartyl-adenylate (Agarwal et al., 2012). Moreover, McC inactivation is also ensured by phosphoramidases belonging to the histidine-triad (HIT) superfamily hydrolases that can either be encoded in certain *mcc*-like biosynthetic clusters or by genes located elsewhere in bacterial genomes (Yagmurov et al., 2020). Resistance to McC-like compounds produced by *S. enterica*, *Nocardiopsis kunsanensis*, *P. fluorescens* or *Hyalangium minutum* is conferred by hydrolysis of the phosphoramide bond in the toxic aspartamide-adenylate (Yagmurov et al., 2020).Therefore, it appears that resistance to McC and McC-like microcins by toxin inactivation can occur via both enzymes encoded in the microcin biosynthesis clusters and more generalist and non-specific enzymes sharing structural similarities.

Finally, impairment of the final three-dimensional structure of the antibacterial peptide, such as by preventing the formation of disulfide bridges, could be a last mechanism resulting in resistance to microcins. This has been poorly explored until now, but is however illustrated by MccPDI for which mutations in *dsbA*, *dsbB* genes induce resistance to MccPDI (Zhao et al., 2015). Genes *dsbA*, *dsbB* encode DsbA and DsbB thiol-redox enzymes that usually catalyze disulfide bond formation for proteins that are transported into the periplasm, and which would be possibly involved in formation of the disulfide bond that stabilizes this microcin.

INHIBITORY EFFECT OF MICROCINS AGAINST ANTIBIOTIC RESISTANT GRAM-NEGATIVE BACTERIA

The spectrum of inhibitory activity of microcins includes a wide number of bacteria which are phylogenetically related to the producing strain including *Salmonella, Shigella* and *E. coli*. The inhibition activity of the different microcins against non-multidrug-resistant strains has been reported in the literature. However, the potency of these microcins specifically against MDR bacteria has not been systematically described and only few studies have addressed this special issue.

MccJ25 was shown to exhibit a high antimicrobial activity against MDR *Salmonella* and *E. coli* (Martin-Gómez et al., 2019; Yu et al., 2019). The antimicrobial activity of MccJ25 was also extensively studied against a collection of MDR strains of *S. enterica* spp. *enterica* (Ben Said et al., 2020). Interestingly, this study has shown that *Salmonella* strains exhibit various sensitivity profiles to MccJ25 and that MIC values vary from 0.06 to 400 μg/mL (0.028–189 nM), independently of the resistance profiles to antibiotics or the serovars. Other studies have shown that MccJ25 displays a great inhibitory potential against *Salmonella* and *E. coli* (Sablé et al., 2000; Delgado et al., 2001; Rintoul et al., 2001; Soudy et al., 2012). MccPDI is known to inhibit foodborne pathogenic enterohemorrhagic *E. coli* serotypes O157:H7 and O26 (Eberhart et al., 2012) as well as *Shigella* strains and *E. coli* isolates that are MDR strains (Lu et al., 2019). Likewise, MccH47 has demonstrated a potent effect against *Enterobacteriaceae* MDR strains including *Salmonella* and *E. coli* carbapenemase, extended spectrum β-lactamase and metallo-β-lactamase producers. MccH47 has MIC values less than 75 μg/mL (13 μM) for all tested strains (Palmer et al., 2020).

The remaining microcins revealed similar narrow spectra of activity against non-MDR *Enterobacteriaceae,* mainly *Salmonella* and *E. coli.* Indeed, MccE492 was shown to have inhibitory activity *in vitro* against a wide range of *Enterobacteriaceae* including *Klebsiella*, *Enterobacter*, *E. coli* and *Salmonella* while MccM was shown to inhibit *Salmonella* and *E. coli* (Vassiliadis et al., 2010). MccN/24 is active against *E. coli* and *S. enterica* Typhimurium, but not against *L. monocytogenes* or *Campylobacter jejuni* (Wooley et al., 1999). It was also reported by Kaur et al. (2016) that MccN/24 exhibits a potent activity against *Salmonella* strains. Furthermore, MccV is active against some pathogenic *E. coli* with MIC values ranging from 7.7×10^{-3} to 13.25 μg/mL (0.89–1517.94 nM) (Boubezari et al., 2018). MccS is lethal to virulent enterohemorrhagic and enteropathogenic *E. coli* through inhibiting the adherence of EPEC *E. coli* to intestinal epithelial cells in an *in vitro* adherence assay (Zschüttig et al., 2012). MccL exhibits a strong antibacterial activity against *Enterobacteriaceae*, including the *S. enterica* serovars Typhimurium and Enteritidis (Morin et al., 2011).

Only a few studies have systematically assessed the efficiency of microcins (and, more generally, of bacteriocins), for the

inhibition of MDR bacteria, and/or the microcin/bacteriocin and antibiotic cross-resistance (Ben Said et al., 2020; Kuznetsova et al., 2020). Although the activities reported so far are encouraging, more systematic studies on the inhibitory potential of microcins against MDR strains remain necessary to confirm the potential of microcins as alternatives to antibiotics against MDR and are thus of high research priority. Future directions of research should relate to both qualitative and quantitative *in vitro* characterization of the inhibitory activity of different microcins against a large panel of clinical isolates of MDR pathogenic bacteria of medical and veterinary interest, coming from well characterized reference collections. The development of resistance of these strains against the various microcins deserves being invertigated as well as studying the possible synergistic effects between microcins and certain antibiotics or biocides, as already started with Gram-positive bacteriocins (Mathur et al., 2017). Indeed, the identification of compounds with synergistic or additive effects could represent an effective strategy to limit the development of bacteria resistant to both microcins and antibiotics. Such an approach, and more widely combination treatment therapeutic strategies, could be facilitated by the development of optimized methods to quantify synergy effects more rapidly and efficiently (Fatsis-Kavalopoulos et al., 2020).

MICROCINS AND THE IMMUNE SYSTEM

Inflammation is one of the key processes allowing the immune system being alerted of risks for the host, such as pathogen attacks. But its dysregulation results in chronic inflammation and subsequent diseases, pointing that inflammation results in both beneficial and adverse effects. In general, interactions of bacteriocins or microcins with the immune system have not been investigated deeply, which hampers evaluating previsible risks and benefits for all characterized microcins. MccE492 was reported to induce apoptosis against human cell lines without inducing an inflammatory response (Hetz et al., 2002; Lagos et al., 2009). But most of all, two microcins, MccB17 and especially MccJ25, have been chiefly studied in this regard.

A pionneer study showed that polyclonal antibodies were raised in rabbits against mature MccB17, indicating that it could induce immune reaction once introduced in host body (Yorgey et al., 1993). In an in-depth study on the effects of oxazole compounds on intestinal inflammation (Iyer et al., 2018) have shown that, similar to environmental or synthetic ones, short-size oxazole compounds derived from MccB17 degradation were able to induce inflammation in mouse intestinal epithelial cells, while full-length MccB17 was not (Iyer et al., 2018; Collin and Maxwell, 2019). This effect was attributed to a cascade response where oxazole compounds activate IDO1, the rate-limiting enzyme in tryptophan catabolism, and in turn tryptophan-derived metabolites activate the aryl hydrocarbon receptor Ahr, which limits CD1d-restricted production of the anti-inflammatory cytokine IL-10 and results in natural killer T-cell mediated intestinal inflammation (Iyer et al., 2018). It was pointed that this oxazole-induced intestinal inflammation is independent of the antimicrobial activity of the compounds. Moreover, it was proposed that the CD1d-dependent immunomodulatory effect is limited by the size of the compounds, explaining the absence of effect of native MccB17, although its content in oxazole rings.

An *in vitro* study showed that MccJ25 protects IPEC-J2 cells against enterotoxigenic *E. coli* (ETEC) without raising cytotoxicity and alleviates the inflammatory responses through modulation of the levels of pro-inflammatory cytokines, interleukins 6 (IL-6), IL-8 and tumor necrosis factor-α (TNF-α) (Yu et al., 2018a). An anti-inflammatory effect of MccJ25 associated with killing of the pathogen was shown in an ETEC-infected mouse model (Ding et al., 2020; Yu et al., 2020). Similar to gentamicin treated mice, the levels of pro-inflammatory cytokines were significantly decreased in jejunum, ileum and colon tissues of mice administered MccJ25, compared to the control group, while the anti-inflammatory IL-10 level increased. Inhibition of ETEC-induced expression of inflammatory cytokines in the jejunum was proposed to be due to down-regulation by MccJ25 of the NF-κB and mitogen-activated protein kinase (MAPK) pathways (Ding et al., 2020). Moreover, absence of immunomodulatory effect and toxicity of MccJ25 was observed at the therapeutic dose (9 mg/kg), much higher doses only (18 mg/kg) being able to cause a low toxicity (Yu et al., 2018b). Furthermore, MccJ25 also decreases the serum concentration levels of the pro-inflammatory cytokines IL-6, IL-1β, and TNF-α, together with an increase in anti-inflammatory IL-10 in weaned pigs (Wang et al., 2020) and in broiler chicken (Yu et al., 2017) fed with MccJ25-supplemented diet. Taken together, these *in vivo* studies conducted in different animal models indicate that MccJ25 diet supplementation can lower inflammation together with affording protection against pathogens, providing interesting perspectives in inflammatory intestinal diseases. Therefore, it appears that none of the studied microcins appears to induce adverse inflammation imbalance and have a detrimental effect on the host.

POTENTIAL APPLICATIONS OF MICROCINS AND FUTURE PROSPECT

Microcins exhibit a number of advantages for potential applications, among which their absence of toxicity to eukaryotic cells and their chemical stability. Indeed, the three-dimensional structures or PTMs of most microcins increases their stability to harsh conditions, such as those that are encountered in the gut (Naimi et al., 2020). This favors their delivery to the gut without the help of specific formulations, if not for avoiding immunity response. However, unfortunately, the spectrum of inhibitory activity of the different microcins has not been deeply investigated, hampering significant development in veterinary or human medical domains. The antimicrobial activity of most microcins (MccB17, McC and a few others) was determined in order to decipher their mechanism of action and the most tested bacterium was *E. coli* (Heddle et al., 2001; Metlitskaya et al., 2006; Severinov and Nair, 2012). Thus, while for a few microcins the spectrum of inhibition is well known, for the remaining this information is still missing. A more systematic study involving a significant number of clinical and veterinary

pathogens, including MDR strains, remains necessary to establish the exact spectrum of inhibition of each microcin.

An important characteristic making microcins good candidates as alternatives to antibiotics is that they are prominent actors of competitions in microbiota and particularly in the gut microbiota, which is the most studied. Microcins play a significant role in niche competition (for a review see Li and Rebuffat, 2020), essentially in interference competition, which involves the secretion of harmful molecules such as the microcins, for direct attack of competitors. But also in a lesser extent, they are involved in the indirect process of exploitative competition, as exemplified by siderophore microcins which are able to capture iron and thus deplete the surroundings of this essential element. Thereby, the siderophore microcins MccH47 and MccM, both produced by the probiotic *E. coli* strain Nissle 1917, have been shown to mediate competition among *Enterobacteriaceae* in mouse model and to impair the growth of the pathogen *S. enterica* serovar Typhimurium in the inflamed gut, where iron is scarce, without perturbing significantly the microbiota equilibrium (Sassone-Corsi et al., 2016). Thanks to their natural role in their niche, which involves both high potency and narrow spectrum of activity, the molecules from microbiota, such as the microcins in the gut microbiota (Donia and Fischbach, 2015; Garcia-Gutierrez et al., 2019), or other bacteriocins in the rumen (Oyama et al., 2017), are thus of high potential. However, exploration of the capacity of microorganisms belonging to various microbiota still remains underdeveloped so far. Its development in combination with genome mining approaches and innovative computational technologies should allow finding novel microcins, and possibly novel mechanisms of action.

To explore the potential applications of microcins in animal and human health, *in vivo* studies have been conducted, although they are still few and only concern a few microcins, essentially MccJ25. For instance, a significant decrease of *S.* Typhimurium was recorded in chicken, using an *E. coli* transformant strain producing MccN/24, although continuous administration of the transformant was needed to ensure colonization within the *in vivo* model (Wooley et al., 1999). MccJ25 has been shown to decrease *S. enterica* counts in the liver and spleen in mice (Lopez et al., 2007) and in the gastrointestinal tract of turkeys (Forkus et al., 2017), and to relieve diarrhea and systematic inflammation in weaned pigs (Yu et al., 2017). Furthermore, MccJ25 was shown to improve performance, fecal microbiota composition and systematic inflammation of broilers (Wang et al., 2020). Further studies are needed however to validate the potential of microcins as therapeutic agents in human or veterinary medicine.

Finally, developing safe probiotics engineered to produce potent microcins is a complementary and efficient approach. It relies on previous studies of commercially available probiotics, *E. coli* Nissle 1917 (Mutaflor®) and *E. coli* G3/10 (Symbioflor2®), producers of microcins MccH47 and MccM (Sassone-Corsi et al., 2016; Massip and Oswald, 2020) and MccS (Zschüttig et al., 2012), respectively, which were shown to act in bacterial competition and kill pathogens in inflamed gut (Sassone-Corsi et al., 2016), or suppress adherence of enteropathogenic *E. coli* (Zschüttig et al., 2012). Thus, *S. enterica* carriage was significantly reduced in turkey gastrointestinal tract using *E. coli* Nissle engineered to produce MccJ25 (Forkus et al., 2017). Furthermore, *E. coli* Nissle was engineered to produce MccH47 in response to tetrathionate, which is produced in gut inflammation conditions and is favorable to *Salmonella* growth (Palmer et al., 2018). In this system, MccH47 was produced in response to the tetrathionate environmental signal serving as an inducing molecule, and inhibited the pathogen *S.* Typhimurium, both in static inhibition assays and in ecological competition experiments.

CONCLUSION

As it can be seen through this review, microcins offer an attractive track for designing novel antimicrobial strategies and envisage alternatives to conventional antibiotics, despite the potential risks of resistance, cross-resistance and co-resistance that have been pointed. The microcin attractivity relies first on their two-step mechanisms of action. The first step ensures uptake of the microcin and involves most often a Trojan horse strategy. It is exemplarily illustrated by MccC, for which the last processing step of the uptaken harmless nucleotide peptide is ensured in the targeted bacteria by common proteases. It is also exemplified by siderophore microcins (MccE492, MccM, MccH47) or the lasso microcin MccJ25 that mimic the natural ligands of siderophore receptors to hijack them. The second step implies either membrane perturbations or inhibition of critical enzymes, and therefore vital functions in bacteria. Indeed, in certain cases such strategies are shared by antibiotics, which can result in cross-resistance, as pointed in this review. These two steps can also constitute a drawback toward resistance development as inhibiting one of them could potentially confer resistance to microcin. However, a few microcins, such as McC and MccJ25, bring into play a second and independent mechanism that intervenes at higher concentrations. Such a secondary mechanism has not been brought to light for other microcins, but it must be said that it has not been thoroughly investigated. Such a succession of different mechanisms limits the emergence of bacterial resistance, as the energetic costs induced by setting up distinct resistance mechanisms simultaneously is hard to assume by the bacteria.

Other characteristics, which have been underlined in the review, support their interesting potential: (i) a potent activity in the GI tract, (ii) a narrow spectrum of activity, which makes them active against pathogens while preserving host microbiota, (iii) an important role in microbial competitions, which makes them actors in maintaining microbiota equilibrium, (iv) an efficient activity *in vivo* in different animal models. Developing strategies based on Nature-derived mechanisms and molecules that are able to minimize both niche perturbations and resistance thus appears as a promising direction in the light of recent analysis of the frequency and mechanisms of resistance of antimicrobial peptides and antibiotics (Kintses et al., 2019). Finally, as the production costs of antimicrobial peptides and in particular of RiPPs remain high, a possible strategy to use microcins and simultaneously increase their potency could be to associate them to conventional antibiotics. This would take

full advantage of the lower costs of production of antibiotics, of an increased potency when synergistic effects are obtained, and of the possibility of combining distinct mechanisms of action. Therefore, relying on the current knowledge on the topology of microcins and their targets, the microcin biosynthesis pathways, and their mechanisms of action and of resistance, directions of research involving a more dynamic exploration of diverse microbiota associated with the development of microcin bioengineering would presumably accelerate the diversification of anti-AMR strategies.

AUTHOR CONTRIBUTIONS

All authors listed have made a substantial, direct and intellectual contribution to the work, approved the final manuscript for publication. ST and LBS drafted the manuscript and contributed equally to its preparation. SR, IF, and SZ revised the manuscript. LBS and SR wrote the final version of the manuscript. ST, LBS, and SZ designed and prepared the figures.

FUNDING

We acknowledge financial support received for this work from the International Development research Center (IDRC 109048-001), the National Science and Engineering Research Council of Canada (grant number 06593-2018; NSERC-METABIOLAC industrial research chair grant number IRCPJ 499946-15) and the National Museum of Natural History (MNHN).

SUPPLEMENTARY MATERIAL

The Supplementary Material for this article can be found online at: https://www.frontiersin.org/articles/10.3389/fmicb.2020.586433/full#supplementary-material

REFERENCES

Adelman, K., Yuzenkova, J., La Porta, A., Zenkin, N., Lee, J., Lis, J. T., et al. (2004). Molecular mechanism of transcription inhibition by peptide antibiotic Microcin J25. *Mol. Cell.* 14, 753–762. doi: 10.1016/j.molcel.2004.05.017

Agarwal, V., Metlitskaya, A., Severinov, K., and Nair, S. K. (2011). Structural basis for microcin C7 inactivation by the MccE acetyltransferase. *J. Biol. Chem.* 286, 21295–21303. doi: 10.1074/jbc.M111.226282

Agarwal, V., Tikhonov, A., Metlitskaya, A., Severinov, K., and Nair, S. K. (2012). Structure and function of a serine carboxypeptidase adapted for degradation of the protein synthesis antibiotic microcin C7. *Proc. Natl. Acad. Sci. U.S.A.* 109, 4425–4430. doi: 10.1073/pnas.1114224109

Aguilera, P., Marcoleta, A., Lobos-Ruiz, P., Arranz, R., Valpuesta, J. M., Monasterio, O., et al. (2016). Identification of key amino acid residues modulating intracellular and in vitro microcin E492 amyloid formation. *Front. Microbiol.* 7:35. doi: 10.3389/fmicb.2016.00035

Amaral, L., Martins, A., Spengler, G., and Molnar, J. (2014). Efflux pumps of Gram-negative bacteria, what they do, how they do it, with what and how to deal with them. *Front. Pharmacol.* 4:168. doi: 10.3389/fphar.2013.00168

Anes, J., McCusker, M. P., Fanning, S., and Martins, M. (2015). The ins and outs of RND efflux pumps in *Escherichia coli*. *Front. Microbiol.* 6:587. doi: 10.3389/fmicb.2015.00587

Arnison, P. G., Bibb, M. J., Bierbaum, G., Bowers, A. A., Bugni, T. S., Bulaj, G., et al. (2013). Ribosomally synthesized and post-translationally modified peptide natural products, overview and recommendations for a universal nomenclature. *Nat. Prod. Rep.* 30, 108–160. doi: 10.1039/c2np20085f

Arranz, R., Mercado, G., Martin-Benito, J., Giraldo, R., Monasterio, O., Lagos, R., et al. (2012). Structural characterization of microcin E492 amyloid formation, Identification of the precursors. *J. Struct. Biol.* 178, 54–60. doi: 10.1016/j.jsb.2012.02.015

Asensio, C., and Perez-Diaz, J. C. (1976). A new family of low molecular weight antibiotics from enterobacteria. *Biochem. Biophys. Res. Commun.* 69, 7–14. doi: 10.1016/s0006-291x(76)80264-1

Azpiroz, M. F., and Laviña, M. (2007). Modular structure of microcin H47 and colicin V. *Antimicrob. Agents Chemother.* 51, 2412–2419. doi: 10.1128/AAC.01606-06

Bantysh, O., Serebryakova, M., Makarova, K. S., Dubiley, S., Datsenko, K. A., and Severinov, K. (2014). Enzymatic synthesis of bioinformatically predicted microcin C-like compounds encoded by diverse bacteria. *mBio* 5:e01059-14. doi: 10.1128/mBio.01059-14

Baquero, F., Lanza, V. F., Baquero, M. R., Del Campo, R., and Bravo-Vazquez, D. A. (2019). Microcins in *Enterobacteriaceae*, Peptide antimicrobials in the eco-active intestinal chemosphere. *Front. Microbiol.* 10:2261. doi: 10.3389/fmicb.2019.02261

Baquero, F., and Moreno, F. (1984). The microcins. *FEMS Microbiol. Lett.* 23, 117–124. doi: 10.1007/978-3-642-76974-0_12

Beis, K., and Rebuffat, S. (2019). Multifaceted ABC transporters associated to microcin and bacteriocin export. *Res. Microbiol.* 170, 399–406. doi: 10.1016/j.resmic.2019.07.002

Bellomio, A., Vincent, P. A., de Arcuri, B. F., Farias, R. N., and Morero, R. D. (2007). Microcin J25 has dual and independent mechanisms of action in *Escherichia coli*, RNA polymerase inhibition and increased superoxide production. *J. Bacteriol.* 189, 4180–4186. doi: 10.1128/jb.00206-07

Ben Said, L., Emond-Rheault, J. G., Soltani, S., Telhig, S., Zirah, S., Rebuffat, S., et al. (2020). Phenomic and genomic approaches to studying the inhibition of multiresistant *Salmonella enterica* by microcin J25. *Environ. Microbiol.* 22, 2907–2920. doi: 10.1111/1462-2920.15045

Bieler, S., Estrada, L., Lagos, R., Baeza, M., Castilla, J., and Soto, C. (2005). Amyloid formation modulates the biological activity of a bacterial protein. *J. Biol. Chem.* 280, 26880–26885. doi: 10.1074/jbc.M502031200

Bieler, S., Silva, F., and Belin, D. (2010). The polypeptide core of microcin E492 stably associates with the mannose permease and interferes with mannose metabolism. *Res. Microbiol.* 161, 706–710. doi: 10.1016/j.resmic.2010.07.003

Bieler, S., Silva, F., Soto, C., and Belin, D. (2006). Bactericidal activity of both secreted and nonsecreted microcin E492 requires the mannose permease. *J. Bacteriol.* 188, 7049–7061. doi: 10.1128/jb.00688-06

Boubezari, M. T., Idoui, T., Hammami, R., Fernandez, B., Gomaa, A., and Fliss, I. (2018). Bacteriocinogenic properties of *Escherichia coli* P2C isolated from pig gastrointestinal tract, purification and characterization of microcin V. *Arch. Microbiol.* 200, 771–782. doi: 10.1007/s00203-018-1482-6

Bountra, K., Hagelueken, G., Choudhury, H. G., Corradi, V., El Omari, K., Wagner, A., et al. (2017). Structural basis for antibacterial peptide self-immunity by the bacterial ABC transporter McjD. *Embo. J.* 36, 3062–3079. doi: 10.15252/embj.201797278

Braffman, N. R., Piscotta, F. J., Hauver, J., Campbell, E. A., Link, A. J., and Darst, S. A. (2019). Structural mechanism of transcription inhibition by lasso peptides microcin J25 and capistruin. *Proc. Natl. Acad. Sci. U.S.A.* 116, 1273–1278. doi: 10.1073/pnas.1817352116

Brown, E. E. F., Cooper, A., Carrillo, C., and Blais, B. (2019). Selection of multidrug-resistant bacteria in medicated animal feeds. *Front. Microbiol.* 10:456. doi: 10.3389/fmicb.2019.00456

Budic, M., Rijavec, M., Petkovsek, Z., and Zgur-Bertok, D. (2011). *Escherichia coli* bacteriocins, antimicrobial efficacy and prevalence among isolates from patients with bacteraemia. *PLoS One* 6:e28769. doi: 10.1371/journal.pone.0028769

Burkhart, B. J., Hudson, G. A., Dunbar, K. L., and Mitchell, D. A. (2015). A prevalent peptide-binding domain guides ribosomal natural product biosynthesis. *Nat. Chem. Biol.* 11, 564–570. doi: 10.1038/nchembio.1856

Bush, K., and Jacoby, G. A. (2010). Updated functional classification of beta-lactamases. *Antimicrob. Agents Chemother.* 54, 969–976. doi: 10.1128/aac.01009-09

Calvopina, K., Dulyayangkul, P., Heesom, K. J., and Avison, M. B. (2020). TonB-dependent uptake of beta-lactam antibiotics in the opportunistic human pathogen *Stenotrophomonas maltophilia*. *Mol. Microbiol.* 113, 492–503. doi: 10.1111/mmi.14434

Campbell, E. A., Korzheva, N., Mustaev, A., Murakami, K., Nair, S., Goldfarb, A., et al. (2001). Structural mechanism for rifampicin inhibition of bacterial RNA polymerase. *Cell* 104, 901–912. doi: 10.1016/s0092-8674(01)00286-0

Campos, M. A., Vargas, M. A., Regueiro, V., Llompart, C. M., Albertí, S., and Bengoechea, J. A. (2004). Capsule polysaccharide mediates bacterial resistance to antimicrobial peptides. *Infect. Immun.* 72, 7107–7114. doi: 10.1128/IAI.72.12.7107-7114.2004

Carlson, S. A., Frana, T. S., and Griffith, R. W. (2001). Antibiotic resistance in *Salmonella enterica* serovar Typhimurium exposed to microcin-producing *Escherichia coli*. *Appl. Environ. Microbiol.* 67, 3763–3766. doi: 10.1128/aem.67.8.3763-3766.2001

Carroll, L. M., Gaballa, A., Guldimann, C., Sullivan, G., Henderson, L. O., and Wiedmann, M. (2019). Identification of novel mobilized colistin resistance gene mcr-9 in a multidrug-resistant, colistin-susceptible *Salmonella enterica* serotype Typhimurium isolate. *mBio* 10:e0853-19. doi: 10.1128/mBio.00853-19

Cascales, E., Buchanan, S. K., Duché, D., Kleanthous, C., Lloubès, R., Postle, K., et al. (2007). Colicin biology. *Microbiol. Mol. Biol. Rev.* 71, 158–229. doi: 10.1128/mmbr.00036-06

Chapman, J. S. (2003). Disinfectant resistance mechanisms, cross-resistance, and co-resistance. *Int. Biodeterior. Biodegrad.* 51, 271–276. doi: 10.1016/S0964-8305(03)00044-1

Chehade, H., and Braun, V. (1988). Iron-regulated synthesis and uptake of colicin V. *FEMS Microbiol. Lett.* 52, 177–181. doi: 10.111/j.1574-6968.1988.tb02591.x

Cheung-Lee, W. L., and Link, A. J. (2019). Genome mining for lasso peptides, past, present, and future. *J. Ind. Microbiol. Biot.* 46, 1371–1379. doi: 10.1007/s10295-019-02197-z

Cheung-Lee, W. L., Parry, M. E., Cartagena, A. J., Darst, S. A., and Link, A. J. (2019). Discovery and structure of the antimicrobial lasso peptide citrocin. *J. Biol. Chem.* 294, 6822–6830. doi: 10.1074/jbc.RA118.006494

Cheung-Lee, W. L., Parry, M. E., Zong, C., Cartagena, A. J., Darst, S. A., Connell, N. D., et al. (2020). Discovery of ubonodin, an antimicrobial lasso peptide active against members of the *Burkholderia cepacia* complex. *Chembiochem.* 21, 1335–1340. doi: 10.1002/cbic.201900707

Choi, U., and Lee, C. R. (2019). Distinct roles of outer membrane porins in antibiotic resistance and membrane integrity in *Escherichia coli*. *Front. Microbiol.* 10:953. doi: 10.3389/fmicb.2019.00953

Chopra, I., and Roberts, M. (2001). Tetracycline antibiotics, mode of action, applications, molecular biology, and epidemiology of bacterial resistance. *Microbiol. Mol. Biol. Rev.* 65, 232–260. doi: 10.1128/mmbr.65.2.232-260.2001

Collet, J.-F., Cho, S.-H., Iorga, B. I., and Goemans, C. V. (2020). How the assembly and protection of the bacterial cell envelope depend on cysteine residues. *J. Biol. Chem.* 295, 11984–11994. doi: 10.1074/jbc.REV120.011201

Collin, F., and Maxwell, A. (2019). The microbial toxin Microcin B17, prospects for the development of new antibacterial agents. *J. Mol. Biol.* 431, 3400–3426. doi: 10.1016/j.jmb.2019.05.050

Corsini, G., Karahanian, E., Tello, M., Fernandez, K., Rivero, D., Saavedra, J. M., et al. (2010). Purification and characterization of the antimicrobial peptide microcin N. *FEMS Microbiol. Lett.* 312, 119–125. doi: 10.1111/j.1574-6968.2010.02106.x

Cotter, P. D., Ross, R. P., and Hill, C. (2013). Bacteriocins - a viable alternative to antibiotics? *Nat. Rev. Microbiol.* 11, 95–105. doi: 10.1038/nrmicro2937

Crosa, J. H., and Walsh, C. T. (2002). Genetics and assembly line enzymology of siderophore biosynthesis in bacteria. *Microbiol. Mol. Biol. Rev.* 66, 223–249. doi: 10.1128/mmbr.66.2.223-249.2002

Davies, E. A., Bevis, H. E., and Delves-Broughton, J. (1997). The use of the bacteriocin, nisin, as a preservative in ricotta-type cheeses to control the food-borne pathogen *Listeria monocytogenes*. *Lett. Appl. Microbiol.* 24, 343–346. doi: 10.1046/j.1472-765x.1997.00145.x

de Kraker, M. E., Stewardson, A. J., and Harbarth, S. (2016). Will 10 million people die a year due to antimicrobial resistance by 2050? *PLoS Med.* 13:e1002184. doi: 10.1371/journal.pmed.1002184

de Lorenzo, V. (1984). Isolation and characterization of microcin E 492 from *Klebsiella pneumoniae*. *Arch. Microbiol.* 139, 72–75. doi: 10.1007/BF00692715

Deegan, L. H., Cotter, P. D., Hill, C., and Ross, P. (2006). Bacteriocins, biological tools for bio-preservation and shelf-life extension. *Int. Dairy J.* 16, 1058–1071. doi: 10.1016/j.idairyj.2005.10.026

del Castillo, F. J., del Castillo, I., and Moreno, F. (2001). Construction and characterization of mutations at codon 751 of the *Escherichia coli* gyrB gene that confer resistance to the antimicrobial peptide microcin B17 and alter the activity of DNA gyrase. *J. Bacteriol.* 183, 2137–2140. doi: 10.1128/jb.183.6.2137-2140.2001

Delgado, M. A., Rintoul, M. R., Farias, R. N., and Salomón, R. A. (2001). *Escherichia coli* RNA polymerase is the target of the cyclopeptide antibiotic microcin J25. *J. Bacteriol.* 183, 4543–4550. doi: 10.1128/jb.183.15.4543-4550.2001

Delgado, M. A., Vincent, P. A., Farias, R. N., and Salomón, R. A. (2005). YojI of *Escherichia coli* functions as a microcin J25 efflux pump. *J. Bacteriol.* 187, 3465–3470. doi: 10.1128/jb.187.10.3465-3470.2005

Destoumieux-Garzón, D., Duquesne, S., Peduzzi, J., Goulard, C., Desmadril, M., Letellier, L., et al. (2005). The iron-siderophore transporter FhuA is the receptor for the antimicrobial peptide microcin J25, role of the microcin Val11-Pro16 beta-hairpin region in the recognition mechanism. *Biochem. J.* 389, 869–876. doi: 10.1042/bj20042107

Destoumieux-Garzón, D., Peduzzi, J., Thomas, X., Djediat, C., and Rebuffat, S. (2006). Parasitism of iron-siderophore receptors of *Escherichia coli* by the siderophore-peptide microcin E492m and its unmodified counterpart. *Biometals* 19, 181–191. doi: 10.1007/s10534-005-4452-9

Destoumieux-Garzón, D., Thomas, X., Santamaria, M., Goulard, C., Barthélémy, M., Boscher, B., et al. (2003). Microcin E492 antibacterial activity, evidence for a TonB-dependent inner membrane permeabilization on *Escherichia coli*. *Mol. Microbiol.* 49, 1031–1041. doi: 10.1046/j.1365-2958.2003.03610.x

Dickey, S. W., Cheung, G. Y. C., and Otto, M. (2017). Different drugs for bad bugs, antivirulence strategies in the age of antibiotic resistance. *Nat. Rev. Drug Discov.* 16, 457–471. doi: 10.1038/nrd.2017.23

Dijkmans, A. C., Zacarias, N. V. O., Burggraaf, J., Mouton, J. W., Wilms, E. B., van Nieuwkoop, C., et al. (2017). Fosfomycin, pharmacological, clinical and future perspectives. *Antibiotics* 6:24. doi: 10.3390/antibiotics6040024

Ding, X., Yu, H., and Qiao, S. (2020). Lasso peptide microcin J25 effectively enhances gut barrier function and modulates inflammatory response in an enterotoxigenic *Escherichia coli*-challenged mouse model. *Int. J. Mol. Sci.* 21:E6500. doi: 10.3390/ijms21186500

Doi, Y., Bonomo, R. A., Hooper, D. C., Kaye, K. S., Johnson, J. R., Clancy, C. J., et al. (2017). Gram-negative bacterial infections, research priorities, accomplishments, and future directions of the antibacterial resistance leadership group. *Clin. Infect. Dis.* 64, S30–S35. doi: 10.1093/cid/ciw829

Donia, M. S., and Fischbach, M. A. (2015). Human Microbiota. Small molecules from the human microbiota. *Science* 349:1254766. doi: 10.1126/science.1254766

Drider, D., and Rebuffat, S. (2011). *Antimicrobial Peptides, From Genes to Applications*. New York, NY: Springer-Verlag New York.

Drissi, F., Buffet, S., Raoult, D., and Merhej, V. (2015). Common occurrence of antibacterial agents in human intestinal microbiota. *Front. Microbiol.* 6:441. doi: 10.3389/fmicb.2015.00441

Duquesne, S., Destoumieux-Garzón, D., Peduzzi, J., and Rebuffat, S. (2007a). Microcins, gene-encoded antibacterial peptides from enterobacteria. *Nat. Prod. Rep.* 24, 708–734. doi: 10.1039/b516237h

Duquesne, S., Destoumieux-Garzón, D., Zirah, S., Goulard, C., Peduzzi, J., and Rebuffat, S. (2007b). Two enzymes catalyze the maturation of a lasso peptide in *Escherichia coli*. *Chem. Biol.* 14, 793–803. doi: 10.1016/j.chembiol.2007.06.004

Eberhart, L. J., Deringer, J. R., Brayton, K. A., Sawant, A. A., Besser, T. E., and Call, D. R. (2012). Characterization of a novel microcin that kills enterohemorrhagic *Escherichia coli* O157, H7 and O26. *Appl. Environ. Microbiol.* 78, 6592–6599. doi: 10.1128/AEM.01067-12

Egan, K., Ross, R. P., and Hill, C. (2017). Bacteriocins, antibiotics in the age of the microbiome. *Emerging Top Life Sci.* 1, 55–63. doi: 10.1042/ETLS20160015

Endriss, F., Braun, M., Killmann, H., and Braun, V. (2003). Mutant analysis of the *Escherichia coli* FhuA protein reveals sites of FhuA activity. *J. Bacteriol.* 185, 4683–4692. doi: 10.1128/jb.185.16.4683-4692.2003

Fabrega, A., Madurga, S., Giralt, E., and Vila, J. (2009). Mechanism of action of and resistance to quinolones. *Microb. Biotechnol.* 2, 40–61. doi: 10.1111/j.1751-7915.2008.00063.x

Falagas, M. E., Athanasaki, F., Voulgaris, G. L., Triarides, N. A., and Vardakas, K. Z. (2019). resistance to fosfomycin, mechanisms, frequency and clinical consequences. *Int. J. Antimicrob. Agents* 53, 22–28. doi: 10.1016/j.ijantimicag.2018.09.013

Fath, M. J., Zhang, L. H., Rush, J., and Kolter, R. (1994). Purification and characterization of colicin V from *Escherichia coli* culture supernatants. *Biochemistry* 33, 6911–6917. doi: 10.1021/bi00188a021

Fatsis-Kavalopoulos, N., Roemhild, R., Tang, P.-C., Kreuger, J., and Andersson, D. I. (2020). CombiANT, antibiotic interaction testing made easy. *PLoS Biol.* 18:e3000856. doi: 10.1371/journal.pbio.3000856

Forkus, B., Ritter, S., Vlysidis, M., Geldart, K., and Kaznessis, Y. N. (2017). Antimicrobial probiotics reduce *Salmonella enterica* in turkey gastrointestinal tracts. *Sci. Rep.* 7:40695. doi: 10.1038/srep40695

Garcia-Gutierrez, E., Mayer, M. J., Cotter, P. D., and Narbad, A. (2019). Gut microbiota as a source of novel antimicrobials. *Gut Microb.* 10, 1–21. doi: 10.1080/19490976.2018.1455790

Gerard, F., Pradel, N., and Wu, L. F. (2005). Bactericidal activity of colicin V is mediated by an inner membrane protein, SdaC, of *Escherichia coli*. *J. Bacteriol.* 187, 1945–1950. doi: 10.1128/jb.187.6.1945-1950.2005

Ghai, I., and Ghai, S. (2018). Understanding antibiotic resistance via outer membrane permeability. *Infect. Drug Resist.* 11, 523–530. doi: 10.2147/IDR.S156995

Ghilarov, D., Serebryakova, M., Stevenson, C. E. M., Hearnshaw, S. J., Volkov, D. S., Maxwell, A., et al. (2017). The origins of specificity in the microcin-processing protease TldD/E. *Structure* 25, 1549–1561.e5. doi: 10.1016/j.str.2017.08.006

Ghilarov, D., Stevenson, C. E. M., Travin, D. Y., Piskunova, J., Serebryakova, M., Maxwell, A., et al. (2019). Architecture of microcin B17 synthetase. An octameric protein complex converting a ribosomally synthesized peptide into a DNA gyrase poison. *Mol. Cell.* 73, 749–762.e5. doi: 10.1016/j.molcel.2018.11.032

Ghosh, C., Sarkar, P., Issa, R., and Haldar, J. (2019). Alternatives to conventional antibiotics in the era of antimicrobial resistance. *Trends Microbiol.* 27, 323–338. doi: 10.1016/j.tim.2018.12.010

Gibson, M. K., Wang, B., Ahmadi, S., Burnham, C. A., Tarr, P. I., Warner, B. B., et al. (2016). Developmental dynamics of the preterm infant gut microbiota and antibiotic resistome. *Nat. Microbiol.* 1:16024. doi: 10.1038/nmicrobiol.2016.24

Goldstein, B. P. (2014). Resistance to rifampicin, a review. *J. Antibiot.* 67, 625–630. doi: 10.1038/ja.2014.107

Gordon, D. M., and O'Brien, C. L. (2006). Bacteriocin diversity and the frequency of multiple bacteriocin production in *Escherichia coli*. *Microbiology* 152, 3239–3244. doi: 10.1099/mic.0.28690-0

Gordon, D. M., Oliver, E., and Littlefield-Wyer, J. (2007). "The diversity of bacteriocins in Gram-negative bacteria," in *Bacteriocins, Ecology and Evolution*, eds M. A. Riley and M. A. Chavan (Berlin: Springer).

Gratia, A. (1925). Sur un remarquable exemple d'antagonisme entre deux souches de colibacille. *C. R. Soc. Biol.* 93, 1041–1042.

Guijarro, J. I., González-Pastor, J. E., Baleux, F., San Millán, J. L., Castilla, M. A., Rico, M., et al. (1995). Chemical structure and translation inhibition studies of the antibiotic microcin C7. *J. Biol. Chem.* 270, 23520–23532. doi: 10.1074/jbc.270.40.23520

Hantke, K. (2003). Is the bacterial ferrous iron transporter FeoB a living fossil? *Trends Microbiol.* 11, 192–195. doi: 10.1016/s0966-842x(03)00100-8

Håvarstein, L. S., Diep, D. B., and Nes, I. F. (1995). A family of bacteriocin ABC transporters carry out proteolytic processing of their substrates concomitant with export. *Mol. Microbiol.* 16, 229–240. doi: 10.1111/j.1365-2958.1995.tb02295.x

Hawkey, P. M. (2015). Multidrug-resistant Gram-negative bacteria, a product of globalization. *J. Hosp. Infect.* 89, 241–247. doi: 10.1016/j.jhin.2015.01.008

Heddle, J. G., Blance, S. J., Zamble, D. B., Hollfelder, F., Miller, D. A., Wentzell, L. M., et al. (2001). The antibiotic microcin B17 is a DNA gyrase poison, characterisation of the mode of inhibition. *J. Mol. Biol.* 307, 1223–1234. doi: 10.1006/jmbi.2001.4562

Hegemann, J. D., Zimmermann, M., Zhu, S., Klug, D., and Marahiel, M. A. (2013). Lasso peptides from *proteobacteria*. Genome mining employing heterologous expression and mass spectrometry. *Biopolymers* 100, 527–542. doi: 10.1002/bip.22326

Hetz, C., Bono, M. R., Barros, L. F., and Lagos, R. (2002). Microcin E492, a channel-forming bacteriocin from *Klebsiella pneumoniae*, induces apoptosis in some human cell lines. *Proc. Natl. Acad. Sci. U.S.A.* 99, 2696–2701. doi: 10.1073/pnas.052709699

Iyer, S. S., Gensollen, T., Gandhi, A., Oh, S. F., Neves, J. F., Collin, F., et al. (2018). Dietary and microbial oxazoles induce intestinal inflammation by modulating aryl hydrocarbon receptor responses. *Cell* 173, 1123–1134.e11. doi: 10.1016/j.cell.2018.04.037

Jacoby, G. A., Corcoran, M. A., and Hooper, D. C. (2015). Protective effect of Qnr on agents other than quinolones that target DNA gyrase. *Antimicrob. Agents Chemother.* 59, 6689–6695. doi: 10.1128/aac.01292-15

Jacoby, G. A., Mills, D. M., and Chow, N. (2004). Role of beta-lactamases and porins in resistance to ertapenem and other beta-lactams in *Klebsiella pneumoniae*. *Antimicrob. Agents Chemother.* 48, 3203–3206. doi: 10.1128/aac.48.8.3203-3206.2004

James, R., Lazdunski, C., and Pattus, F. (2013). *Bacteriocins, Microcins and Lantibiotics*. Berlin: Springer.

Jansen, K. B., Inns, P. G., Housden, N. G., Hopper, J. T. S., Kaminska, R., Lee, S., et al. (2020). Bifurcated binding of the OmpF receptor underpins import of the bacteriocin colicin N into *Escherichia coli*. *J. Biol. Chem.* 295, 9147–9156. doi: 10.1074/jbc.RA120.013508

Jeanteur, D., Schirmer, T., Fourel, D., Simonet, V., Rummel, G., Widmer, C., et al. (1994). Structural and functional alterations of a colicin-resistant mutant of OmpF porin from *Escherichia coli*. *Proc. Natl. Acad. Sci. U.S.A.* 91, 10675–10679. doi: 10.1073/pnas.91.22.10675

Kaeriyama, M., Machida, K., Kitakaze, A., Wang, H., Lao, Q., Fukamachi, T., et al. (2006). OmpC and OmpF are required for growth under hyperosmotic stress above pH 8 in *Escherichia coli*. *Lett. Appl. Microbiol.* 42, 195–201. doi: 10.1111/j.1472-765X.2006.01845.x

Kapoor, G., Saigal, S., and Elongavan, A. (2017). Action and resistance mechanisms of antibiotics, A guide for clinicians. *J. Anaesthesiol. Clin. Pharmacol.* 33, 300–305. doi: 10.4103/joacp.JOACP_349_15

Kaur, K., Tarassova, O., Dangeti, R. V., Azmi, S., Wishart, D., McMullen, L., et al. (2016). Characterization of a highly potent antimicrobial peptide microcin N from uropathogenic *Escherichia coli*. *FEMS Microbiol. Lett.* 363:fnw095. doi: 10.1093/femsle/fnw095

Kazakov, T., Kuznedelov, K., Semenova, E., Mukhamedyarov, D., Datsenko, K. A., Metlitskaya, A., et al. (2014). The RimL transacetylase provides resistance to translation inhibitor microcin C. *J. Bacteriol* 196, 3377–3385. doi: 10.1128/jb.01584-14

Kazakov, T., Vondenhoff, G. H., Datsenko, K. A., Novikova, M., Metlitskaya, A., Wanner, B. L., et al. (2008). *Escherichia coli* peptidase A, B, or N can process translation inhibitor microcin C. *J. Bacteriol.* 190, 2607–2610. doi: 10.1128/jb.01956-07

Kettles, R. A., Tschowri, N., Lyons, K. J., Sharma, P., Hengge, R., Webber, M. A., et al. (2019). The *Escherichia coli* MarA protein regulates the ycgZ-ymgABC operon to inhibit biofilm formation. *Mol. Microbiol.* 112, 1609–1625. doi: 10.1111/mmi.14386

Kintses, B., Méhi, O., Ari, E., Számel, M., Györkei, A., Jangir, P. K., et al. (2019). Phylogenetic barriers to horizontal transfer of antimicrobial peptide resistance genes in the human gut microbiota. *Nat. Microbiol.* 4, 447–458. doi: 10.1038/s41564-018-0313-5

Klaenhammer, T. R. (1988). Bacteriocins of lactic acid bacteria. *Biochimie* 70, 337–349. doi: 10.1016/0300-9084(88)90206-4

Knappe, T. A., Linne, U., Zirah, S., Rebuffat, S., Xie, X., and Marahiel, M. A. (2008). Isolation and structural characterization of capistruin, a lasso peptide predicted from the genome sequence of *Burkholderia thailandensis* E264. *J. Am. Chem. Soc.* 130, 11446–11454. doi: 10.1021/ja802966g

Kramer, J., Özkaya, Ö, and Kümmerli, R. (2019). Bacterial siderophores in community and host interactions. *Nat. Rev. Microbiol.* 18, 152–163. doi: 10.1038/s41579-019-0284-4

Krause, K. M., Serio, A. W., Kane, T. R., and Connolly, L. E. (2016). Aminoglycosides. An overview. *Cold Spring Harb. Perspect. Med.* 6:a027029. doi: 10.1101/cshperspect.a027029

Krewulak, K. D., and Vogel, H. J. (2008). Structural biology of bacterial iron uptake. *Biochim. Biophys. Acta* 1778, 1781–1804. doi: 10.1016/j.bbamem.2007.07.026

Kuznedelov, K., Semenova, E., Knappe, T. A., Mukhamedyarov, D., Srivastava, A., Chatterjee, S., et al. (2011). The antibacterial threaded-lasso peptide capistruin inhibits bacterial RNA polymerase. *J. Mol. Biol.* 412, 842–848. doi: 10.1016/j.jmb.2011.02.060

Kuznetsova, M. V., Gizatullina, J. S., Nesterova, L. Y., and Starčič Erjavec, M. (2020). *Escherichia coli* isolated from cases of colibacillosis in Russian poultry farms (Perm Krai), Sensitivity to antibiotics and bacteriocins. *Microorganisms* 8:741. doi: 10.3390/microorganisms8050741

Lagos, R., Tello, M., Mercado, G., Garcia, V., and Monasterio, O. (2009). Antibacterial and antitumorigenic properties of microcin E492, a pore-forming bacteriocin. *Curr. Pharm. Biotechnol.* 10, 74–85. doi: 10.2174/138920109787048643

Lagos, R., Wilkens, M., Vergara, C., Cecchi, X., and Monasterio, O. (1993). Microcin E492 forms ion channels in phospholipid bilayer membrane. *FEBS Lett.* 321, 145–148. doi: 10.1016/0014-5793(93)80096-d

Laviña, M., Gaggero, C., and Moreno, F. (1990). Microcin H47, a chromosome-encoded microcin antibiotic of *Escherichia coli*. *J. Bacteriol.* 172, 6585–6588. doi: 10.1128/jb.172.11.6585-6588.1990

Laviña, M., Pugsley, A. P., and Moreno, F. (1986). Identification, mapping, cloning and characterization of a gene (sbmA) required for microcin B17 action on *Escherichia coli* K12. *J. Gen. Microbiol.* 132, 1685–1693. doi: 10.1099/00221287-132-6-1685

Lazdunski, C. J., Bouveret, E., Rigal, A., Journet, L., Lloubès, R., and Bénédetti, H. (1998). Colicin import into *Escherichia coli* cells. *J. Bacteriol.* 180, 4993–5002. doi: 10.1128/JB.180.19.4993-5002.1998

Lewis, K., Epstein, S., D'Onofrio, A., and Ling, L. L. (2010). Uncultured microorganisms as a source of secondary metabolites. *J. Antibiot.* 63, 468–476. doi: 10.1038/ja.2010.87

Li, X. Z., Ma, D., Livermore, D. M., and Nikaido, H. (1994). Role of efflux pump(s) in intrinsic resistance of *Pseudomonas aeruginosa*, active efflux as a contributing factor to beta-lactam resistance. *Antimicrob. Agents Chemother.* 38, 1742–1752. doi: 10.1128/aac.38.8.1742

Li, X. Z., Plesiat, P., and Nikaido, H. (2015). The challenge of efflux-mediated antibiotic resistance in Gram-negative bacteria. *Clin. Microbiol. Rev.* 28, 337–418. doi: 10.1128/cmr.00117-14

Li, Y., and Rebuffat, S. (2020). The manifold roles of microbial ribosomal peptide-based natural products in physiology and ecology. *J. Biol. Chem.* 295, 34–54. doi: 10.1074/jbc.REV119.006545

Li, Y.-M., Milne, J. C., Madison, L. L., Kolter, R., and Walsh, C. T. (1996). From peptide precursors to oxazole and thiazole-containing peptide antibiotics, microcin B17 synthase. *Science* 274, 1188–1193. doi: 10.1126/science.274.5290.1188

Lopez, F. E., Vincent, P. A., Zenoff, A. M., Salomón, R. A., and Farias, R. N. (2007). Efficacy of microcin J25 in biomatrices and in a mouse model of *Salmonella* infection. *J. Antimic. Chem.* 59, 676–680. doi: 10.1093/jac/dkm009

Lu, S. Y., Graça, T., Avillan, J. J., Zhao, Z., and Call, D. R. (2019). Microcin PDI inhibits antibiotic-resistant strains of *Escherichia coli* and *Shigella* through a mechanism of membrane disruption and protection by homotrimer self-immunity. *Appl. Environ. Microbiol.* 85:e0371-19. doi: 10.1128/aem.00371-19

MacVane, S. H. (2017). Antimicrobial resistance in the intensive care unit, A focus on Gram-negative bacterial infections. *J. Intensive Care Med.* 32, 25–37. doi: 10.1177/0885066615619895

Maksimov, M. O., Pelczer, I., and Link, A. J. (2012). Precursor-centric genome-mining approach for lasso peptide discovery. *Proc. Natl. Acad. Sci. U.S.A.* 109, 15223–15228. doi: 10.1073/pnas.1208978109

Marcoleta, A., Marin, M., Mercado, G., Valpuesta, J. M., Monasterio, O., and Lagos, R. (2013). Microcin E492 amyloid formation is retarded by posttranslational modification. *J. Bacteriol.* 195, 3995–4004. doi: 10.1128/jb.00564-13

Martin-Gómez, H., Jorba, M., Albericio, F., Viñas, M., and Tulla-Puche, J. (2019). Chemical Modification of microcin J25 reveals new insights on the stereospecific requirements for antimicrobial activity. *Int. J. Mol. Sci.* 20:5152. doi: 10.3390/ijms20205152

Massip, C., and Oswald, E. (2020). Siderophore-microcins in *Escherichia coli*, determinants of digestive colonization, the first step toward virulence. *Front. Cell Infect. Microbiol.* 10:381. doi: 10.3389/fcimb.2020.00381

Mathavan, I., Zirah, S., Mehmood, S., Choudhury, H. G., Goulard, C., Li, Y., et al. (2014). Structural basis for hijacking siderophore receptors by antimicrobial lasso peptides. *Nat. Chem. Biol.* 10, 340–342. doi: 10.1038/nchembio.1499

Mathur, H., Field, D., Rea, M. C., Cotter, P. D., Hill, C., and Ross, R. P. (2017). Bacteriocin-antimicrobial synergy, a medical and food perspective. *Front. Microbiol.* 8:1205. doi: 10.3389/fmicb.2017.01205

McIntosh, J. A., Donia, M. S., and Schmidt, E. W. (2009). Ribosomal peptide natural products, bridging the ribosomal and nonribosomal worlds. *Nat. Prod. Rep.* 26, 537–559. doi: 10.1039/b714132g

McIntosh, J. A., and Schmidt, E. W. (2010). Marine molecular machines, heterocyclization in cyanobactin biosynthesis. *Chembiochem* 11, 1413–1421. doi: 10.1002/cbic.201000196

Melby, J. O., Nard, N. J., and Mitchell, D. A. (2011). Thiazole/oxazole-modified microcins, complex natural products from ribosomal templates. *Curr. Opin. Chem. Biol.* 15, 369–378. doi: 10.1016/j.cbpa.2011.02.027

Metelev, M., Arseniev, A., Bushin, L. B., Kuznedelov, K., Artamonova, T. O., Kondratenko, R., et al. (2017a). Acinetodin and klebsidin, RNA polymerase targeting lasso peptides produced by human isolates of *Acinetobacter gyllenbergii* and *Klebsiella pneumoniae*. *ACS Chem. Biol.* 12, 814–824. doi: 10.1021/acschembio.6b01154

Metelev, M., Osterman, I. A., Ghilarov, D., Khabibullina, N. F., Yakimov, A., Shabalin, K., et al. (2017b). Klebsazolicin inhibits 70S ribosome by obstructing the peptide exit tunnel. *Nat. Chem. Biol.* 13, 1129–1136. doi: 10.1038/nchembio.2462

Metelev, M., Serebryakova, M., Ghilarov, D., Zhao, Y., and Severinov, K. (2013). Structure of microcin B-like compounds produced by *Pseudomonas syringae* and species specificity of their antibacterial action. *J. Bacteriol.* 195, 4129–4137. doi: 10.1128/jb.00665-13

Metlitskaya, A., Kazakov, T., Kommer, A., Pavlova, O., Praetorius-Ibba, M., Ibba, M., et al. (2006). Aspartyl-tRNA synthetase is the target of peptide nucleotide antibiotic microcin C. *J. Biol. Chem.* 281, 18033–18042. doi: 10.1074/jbc.M513174200

Mills, S., Ross, R. P., and Hill, C. (2017). Bacteriocins and bacteriophage; a narrow-minded approach to food and gut microbiology. *FEMS Microbiol. Rev.* 41, S129–S153. doi: 10.1093/femsre/fux022

Mitchell, D. A., Lee, S. W., Pence, M. A., Markley, A. L., Limm, J. D., Nizet, V., et al. (2009). Structural and functional dissection of the heterocyclic peptide cytotoxin streptolysin S. *J. Biol. Chem.* 284, 13004–13012. doi: 10.1074/jbc.M900802200

Montalbán-López, M., Scott, T. A., Ramesh, S. I., Rahman, R., van Heel, A. J., Viel, J. H., et al. (2020). New developments in RiPP discovery, enzymology and engineering. *Nat. Prod. Rep.* doi: 10.1039/d0np00027b [Epub ahead of print].

Morin, N., Lanneluc, I., Connil, N., Cottenceau, M., Pons, A. M., and Sablé, S. (2011). Mechanism of bactericidal activity of microcin L in *Escherichia coli* and *Salmonella enterica*. *Antimicrob. Agents Chemother.* 55, 997–1007. doi: 10.1128/aac.01217-10

Mukhopadhyay, J., Sineva, E., Knight, J., Levy, R. M., and Ebright, R. H. (2004). Antibacterial peptide microcin J25 inhibits transcription by binding within and obstructing the RNA polymerase secondary channel. *Mol. Cell.* 14, 739–751. doi: 10.1016/j.molcel.2004.06.010

Naimi, S., Zirah, S., Taher, M. B., Theolier, J. E., Fernandez, B., Rebuffat, S. F., et al. (2020). Microcin J25 exhibits inhibitory activity against *Salmonella* Newport in continuous fermentation model mimicking swine colonic conditions. *Front. Microbiol.* 11:988. doi: 10.3389/fmicb.2020.00988

Nolan, E. M., and Walsh, C. T. (2008). Investigations of the MceIJ-catalyzed posttranslational modification of the microcin E492 C-terminus, linkage of ribosomal and nonribosomal peptides to form "trojan horse" antibiotics. *Biochemistry* 47, 9289–9299. doi: 10.1021/bi800826j

Novikova, M., Kazakov, T., Vondenhoff, G. H., Semenova, E., Rozenski, J., Metlytskaya, A., et al. (2010). MccE provides resistance to protein synthesis inhibitor microcin C by acetylating the processed form of the antibiotic. *J. Biol. Chem.* 285, 12662–12669. doi: 10.1074/jbc.M109.080192

Novikova, M., Metlitskaya, A., Datsenko, K., Kazakov, T., Kazakov, A., Wanner, B., et al. (2007). The *Escherichia coli* Yej transporter is required for the uptake of translation inhibitor microcin C. *J. Bacteriol.* 189, 8361–8365. doi: 10.1128/jb.01028-07

O'Brien, G. J. (1996). *Molecular Analysis of Microcin 24, Genetics, Secretion and Mode of Action of a Novel Microcin*. Ph. D thesis, University of Canterbury, Christchurch.

O'Brien, G. J., and Mahanty, H. K. (1994). Colicin 24, a new plasmid-borne colicin from a uropathogenic strain of *Escherichia coli*. *Plasmid* 31, 288–296. doi: 10.1006/plas.1994.1030

Oyama, L. B., Girdwood, S. E., Cookson, A. R., Fernandez-Fuentes, N., Privé, F., Vallin, H. E., et al. (2017). The rumen microbiome, an underexplored resource for novel antimicrobial discovery. *NPJ Biofilms Microb.* 3:33. doi: 10.1038/s41522-017-0042-1

Pagnout, C., Sohm, B., Razafitianamaharavo, A., Caillet, C., Offroy, M., Leduc, M., et al. (2019). Pleiotropic effects of *rfa*-gene mutations on *Escherichia coli* envelope properties. *Sci. Rep.* 9:9696. doi: 10.1038/s41598-019-46100-3

Palmer, J. D., Mortzfeld, B. M., Piattelli, E., Silby, M. W., McCormick, B. A., and Bucci, V. (2020). Microcin H47, A Class IIb microcin with potent activity against multidrug resistant *Enterobacteriaceae*. *ACS Infect. Dis.* 6, 672–679. doi: 10.1021/acsinfecdis.9b00302

Palmer, J. D., Piattelli, E., McCormick, B. A., Silby, M. W., Brigham, C. J., and Bucci, V. (2018). Engineered probiotic for the inhibition of *Salmonella* via tetrathionate-induced production of microcin H47. *ACS Infect. Dis.* 4, 39–45. doi: 10.1021/acsinfecdis.7b00114

Pärnänen, K., Karkman, A., Hultman, J., Lyra, C., Bengtsson-Palme, J., Larsson, D. G. J., et al. (2018). Maternal gut and breast milk microbiota affect infant gut antibiotic resistome and mobile genetic elements. *Nat. Commun.* 9:3891. doi: 10.1038/s41467-018-06393-w

Patzer, S. I., Baquero, M. R., Bravo, D., Moreno, F., and Hantke, K. (2003). The colicin G, H and X determinants encode microcins M and H47, which might utilize the catecholate siderophore receptors FepA, Cir, Fiu and IroN. *Microbiology* 149, 2557–2570. doi: 10.1099/mic.0.26396-0

Pfeifer, Y., Cullik, A., and Witte, W. (2010). Resistance to cephalosporins and carbapenems in Gram-negative bacterial pathogens. *Int. J. Med. Microbiol.* 300, 371–379. doi: 10.1016/j.ijmm.2010.04.005

Poey, M. E., Azpiroz, M. F., and Laviña, M. (2006). Comparative analysis of chromosome-encoded microcins. *Antimicrob. Agents Chemother.* 50, 1411–1418. doi: 10.1128/aac.50.4.1411-1418.2006

Pomares, M. F., Delgado, M. A., Corbalan, N. S., Farias, R. N., and Vincent, P. A. (2010). Sensitization of microcin J25-resistant strains by a membrane-permeabilizing peptide. *Appl. Environ. Microbiol.* 76, 6837–6842. doi: 10.1128/aem.00307-10

Pons, A. M., Delalande, F., Duarte, M., Benoit, S., Lanneluc, I., Sablé, S., et al. (2004). Genetic analysis and complete primary structure of microcin L. *Antimicrob. Agents Chemother.* 48, 505–513. doi: 10.1128/aac.48.2.505-513.2004

Pugsley, A. P., Moreno, F., and De Lorenzo, V. (1986). Microcin-E492-insensitive mutants of *Escherichia coli* K12. *J. Gen. Microbiol.* 132, 3253–3259. doi: 10.1099/00221287-132-12-3253

Ramirez, M. S., and Tolmasky, M. E. (2010). Aminoglycoside modifying enzymes. *Drug Resist. Updat.* 13, 151–171. doi: 10.1016/j.drup.2010.08.003

Ran, R., Zeng, H., Zhao, D., Liu, R., and Xu, X. (2017). The novel property of heptapeptide of microcin C7 in affecting the cell growth of *Escherichia coli*. *Molecules* 22:432. doi: 10.3390/molecules22030432

Rebuffat, S. (2012). Microcins in action, amazing defence strategies of *Enterobacteria*. *Biochem. Soc. Trans.* 40, 1456–1462. doi: 10.1042/bst20120183

Rebuffat, S., Blond, A., Destoumieux-Garzón, D., Goulard, C., and Peduzzi, J. (2004). Microcin J25, from the macrocyclic to the lasso structure, implications for biosynthetic, evolutionary and biotechnological perspectives. *Curr. Protein Pept. Sci.* 5, 383–391. doi: 10.2174/1389203043379611

Rintoul, M. R., de Arcuri, B. F., Salomón, R. A., Farias, R. N., and Morero, R. D. (2001). The antibacterial action of microcin J25, evidence for disruption of cytoplasmic membrane energization in *Salmonella* Newport. *FEMS Microbiol. Lett.* 204, 265–270. doi: 10.1111/j.1574-6968.2001.tb10895.x

Rodriguez, E., and Laviña, M. (2003). The proton channel is the minimal structure of ATP synthase necessary and sufficient for microcin H47 antibiotic action. *Antimicrob. Agents Chemother.* 47, 181–187. doi: 10.1128/aac.47.1.181-187.2003

Rosengren, K. J., Clark, R. J., Daly, N. L., Göransson, U., Jones, A., and Craik, D. J. (2003). Microcin J25 has a threaded sidechain-to-backbone ring structure and not a head-to-tail cyclized backbone. *J. Am. Chem. Soc.* 125, 12464–12474. doi: 10.1021/ja0367703

Roy, R. S., Kelleher, N. L., Milne, J. C., and Walsh, C. T. (1999). In vivo processing and antibiotic activity of microcin B17 analogs with varying ring content and altered bisheterocyclic sites. *Chem. Biol.* 6, 305–318. doi: 10.1016/s1074-5521(99)80076-3

Sablé, S., Duarte, M., Bravo, D., Lanneluc, I., Pons, A. M., Cottenceau, G., et al. (2003). Wild-type *Escherichia coli* producing microcins B17, D93, J25, and L; cloning of genes for microcin L production and immunity. *Can. J. Microbiol.* 49, 357–361. doi: 10.1139/w03-047

Sablé, S., Pons, A. M., Gendron-Gaillard, S., and Cottenceau, G. (2000). Antibacterial activity evaluation of microcin J25 against diarrheagenic *Escherichia coli*. *Appl. Environ. Microbiol.* 66, 4595–4597. doi: 10.1128/aem.66.10.4595-4597.2000

Sabnis, A., Klöckner, A., Becce, M., Evans, L. E., Furniss, R. C. D., Mavridou, D. A. I., et al. (2019). Colistin kills bacteria by targeting lipopolysaccharide in the cytoplasmic membrane. *bioRxiv* [Preprint], doi: 10.1101/479618

Salah Ud-Din, A. I., Tikhomirova, A., and Roujeinikova, A. (2016). Structure and functional diversity of GCN5-related N-acetyltransferases (GNAT). *Int. J. Mol. Sci.* 17:1018. doi: 10.3390/ijms17071018

Salomón, R. A., and Farias, R. N. (1992). Microcin 25, a novel antimicrobial peptide produced by *Escherichia coli*. *J. Bacteriol.* 174, 7428–7435. doi: 10.1128/jb.174.22.7428-7435.1992

Salomón, R. A., and Farías, R. N. (1993). The FhuA protein is involved in microcin 25 uptake. *J. Bacteriol.* 175, 7741–7742. doi: 10.1128/jb.175.23.7741-7742.1993

Sassone-Corsi, M., Nuccio, S. P., Liu, H., Hernandez, D., Vu, C. T., Takahashi, A. A., et al. (2016). Microcins mediate competition among *Enterobacteriaceae* in the inflamed gut. *Nature* 540, 280–283. doi: 10.1038/nature20557

Sato, M., Machida, K., Arikado, E., Saito, H., Kakegawa, T., and Kobayashi, H. (2000). Expression of outer membrane proteins in *Escherichia coli* growing at acid pH. *Appl. Environ. Microbiol.* 66, 943–947. doi: 10.1128/aem.66.3.943-947.2000

Sawa, T., Kooguchi, K., and Moriyama, K. (2020). Molecular diversity of extended-spectrum beta-lactamases and carbapenemases, and antimicrobial resistance. *J. Intens. Care* 8:13. doi: 10.1186/s40560-020-0429-6

Schindler, P. R., and Teuber, M. (1975). Action of polymyxin B on bacterial membranes, morphological changes in the cytoplasm and in the outer membrane of *Salmonella typhimurium* and *Escherichia coli* B. *Antimicrob. Agents Chemother.* 8, 95–104. doi: 10.1128/aac.8.1.95

Semenova, E., Yuzenkova, Y., Peduzzi, J., Rebuffat, S., and Severinov, K. (2005). Structure-activity analysis of microcinJ25, distinct parts of the threaded lasso molecule are responsible for interaction with bacterial RNA polymerase. *J. Bacteriol.* 187, 3859–3863. doi: 10.1128/jb.187.11.3859-3863.2005

Severinov, K., and Nair, S. K. (2012). Microcin C, biosynthesis and mechanisms of bacterial resistance. *Future Microbiol.* 7, 281–289. doi: 10.2217/fmb.11.148

Sharma, P., Haycocks, J. R. J., Middlemiss, A. D., Kettles, R. A., Sellars, L. E., Ricci, V., et al. (2017). The multiple antibiotic resistance operon of enteric bacteria controls DNA repair and outer membrane integrity. *Nat. Commun.* 8:1444. doi: 10.1038/s41467-017-01405-7

Shkundina, I., Serebryakova, M., and Severinov, K. (2014). The C-terminal part of microcin B is crucial for DNA gyrase inhibition and antibiotic uptake by sensitive cells. *J. Bacteriol.* 196, 1759–1767. doi: 10.1128/jb.00015-14

Sikandar, A., and Koehnke, J. (2019). The role of protein-protein interactions in the biosynthesis of ribosomally synthesized and post-translationally modified peptides. *Nat. Prod. Rep.* 36, 1576–1588. doi: 10.1039/c8np00064f

Smale, S. T. (2010). Chloramphenicol acetyltransferase assay. *Cold Spring Harb. Protoc.* 2010:pdb.prot5422. doi: 10.1101/pdb.prot5422

Smani, Y., Fàbrega, A., Roca, I., ánchez-Encinales, V. S., Vila, J., and Pachón, J. (2014). Role of OmpA in the multidrug resistance phenotype of *Acinetobacter baumannii*. *Antimicrob. Agents Chemother.* 58, 1806–1808. doi: 10.1128/aac.02101-13

Snyder, A. B., and Worobo, R. W. (2014). Chemical and genetic characterization of bacteriocins, antimicrobial peptides for food safety. *J. Sci. Food Agric.* 94, 28–44. doi: 10.1002/jsfa.6293

Soudy, R., Wang, L., and Kaur, K. (2012). Synthetic peptides derived from the sequence of a lasso peptide microcin J25 show antibacterial activity. *Bioorg. Med. Chem.* 20, 1794–1800. doi: 10.1016/j.bmc.2011.12.061

Sun, J., Liao, X. P., D'Souza, A. W., Boolchandani, M., Li, S. H., Cheng, K., et al. (2020). Environmental remodeling of human gut microbiota and antibiotic resistome in livestock farms. *Nat. Commun.* 11:1427. doi: 10.1038/s41467-020-15222-y

Temiakov, D., Zenkin, N., Vassylyeva, M. N., Perederina, A., Tahirov, T. H., Kashkina, E., et al. (2005). Structural basis of transcription inhibition by antibiotic streptolydigin. *Mol. Cell.* 19, 655–666. doi: 10.1016/j.molcel.2005.07.020

Thomas, X., Destoumieux-Garzón, D., Peduzzi, J., Afonso, C., Blond, A., Birlirakis, N., et al. (2004). Siderophore peptide, a new type of post-translationally modified antibacterial peptide with potent activity. *J. Biol. Chem.* 279, 28233–28242. doi: 10.1074/jbc.M400228200

Tietz, J. I., Schwalen, C. J., Patel, P. S., Maxson, T., Blair, P. M., Tai, H.-C., et al. (2017). A new genome-mining tool redefines the lasso peptide biosynthetic landscape. *Nat. Chem. Biol.* 13, 470–478. doi: 10.1038/nchembio.2319

Tran, J. H., and Jacoby, G. A. (2002). Mechanism of plasmid-mediated quinolone resistance. *Proc. Natl. Acad. Sci. U.S.A.* 99, 5638–5642. doi: 10.1073/pnas.082092899

Travin, D. Y., Bikmetov, D., and Severinov, K. (2020). Translation-targeting RiPPs and where to find them. *Front. Genet.* 11:226. doi: 10.3389/fgene.2020.00226

Travin, D. Y., Watson, Z. L., Metelev, M., Ward, F. R. I, Osterman, A. I, Khven, M., et al. (2019). Structure of ribosome-bound azole-modified peptide phazolicin rationalizes its species-specific mode of bacterial translation inhibition. *Nat. Commun.* 10:4563. doi: 10.1038/s41467-019-12589-5

Trimble, M. J., Mlynarcik, P., Kolar, M., and Hancock, R. E. (2016). Polymyxin, Alternative mechanisms of action and resistance. *Cold Spring Harb. Perspect. Med.* 6:a025288. doi: 10.1101/cshperspect.a025288

Trujillo, M., Rodriguez, E., and Laviña, M. (2001). ATP synthase is necessary for microcin H47 antibiotic action. *Antimicrob. Agents Chemother.* 45, 3128–3131. doi: 10.1128/aac.45.11.3128-3131.2001

Van Boeckel, T. P., Brower, C., Gilbert, M., Grenfell, B. T., Levin, S. A., Robinson, T. P., et al. (2015). Global trends in antimicrobial use in food animals. *Proc. Natl. Acad. Sci. U.S.A.* 112, 5649–5654. doi: 10.1073/pnas.1503141112

Van Boeckel, T. P., Glennon, E. E., Chen, D., Gilbert, M., Robinson, T. P., Grenfell, B. T., et al. (2017). Reducing antimicrobial use in food animals. *Science* 357, 1350–1352. doi: 10.1126/science.aao1495

Vassiliadis, G., Destoumieux-Garzón, D., Lombard, C., Rebuffat, S., and Peduzzi, J. (2010). Isolation and characterization of two members of the siderophore-microcin family, microcins M and H47. *Antimicrob. Agents Chemother.* 54, 288–297. doi: 10.1128/aac.00744-09

Vassiliadis, G., Peduzzi, J., Zirah, S., Thomas, X., Rebuffat, S., and Destoumieux-Garzón, D. (2007). Insight into siderophore-carrying peptide biosynthesis, enterobactin is a precursor for microcin E492 posttranslational modification. *Antimicrob. Agents Chemother.* 51, 3546–3553. doi: 10.1128/aac.00261-07

Ventola, C. L. (2015). The antibiotic resistance crisis, part 1, causes and threats. *P&T* 40, 277–283.

Vincent, P. A., Delgado, M. A., Farias, R. N., and Salomón, R. A. (2004). Inhibition of *Salmonella enterica* serovars by microcin J25. *FEMS Microbiol. Lett.* 236, 103–107. doi: 10.1016/j.femsle.2004.05.027

Vizán, J. L., Hernández-Chico, C., del Castillo, I., and Moreno, F. (1991). The peptide antibiotic microcin B17 induces double-strand cleavage of DNA mediated by *E. coli* DNA gyrase. *EMBO J.* 10, 467–476. doi: 10.1002/j.1460-2075.1991.tb07969.x

Vondenhoff, G. H., Dubiley, S., Severinov, K., Lescrinier, E., Rozenski, J., and Van Aerschot, A. (2011). Extended targeting potential and improved synthesis of microcin C analogs as antibacterials. *Bioorg. Med. Chem.* 19, 5462–5467. doi: 10.1016/j.bmc.2011.07.052

Wang, G., Li, X., and Wang, Z. (2016). APD3, the antimicrobial peptide database as a tool for research and education. *Nucleic Acids Res.* 44, D1087–D1093. doi: 10.1093/nar/gkv1278

Wang, G., Song, Q., Huang, S., Wang, Y., Cai, S., Yu, H., et al. (2020). Effect of antimicrobial peptide microcin J25 on growth performance, immune regulation, and intestinal microbiota in broiler chickens challenged with *Escherichia coli* and *Salmonella*. *Animals* 10:345. doi: 10.3390/ani10020345

Wang, X. W., and Zhang, W. B. (2018). Chemical topology and complexity of protein architectures. *Trends Biochem. Sci.* 43, 806–817. doi: 10.1016/j.tibs.2018.07.001

Wang, Y., Chen, X., Hu, Y., Zhu, G., White, A. P., and Koster, W. (2018). Evolution and sequence diversity of FhuA in *Salmonella* and *Escherichia*. *Infect. Immun.* 86:e00573-18. doi: 10.1128/iai.00573-18

Wester, C. W., Durairaj, L., Evans, A. T., Schwartz, D. N., Husain, S., and Martinez, E. (2002). Antibiotic resistance, a survey of physician perceptions. *Arch. Intern. Med.* 162, 2210–2216. doi: 10.1001/archinte.162.19.2210

Wilkens, M., Villanueva, J. E., Cofré, J., Chnaiderman, J., and Lagos, R. (1997). Cloning and expression in *Escherichia coli* of genetic determinants for production of and immunity to microcin E492 from *Klebsiella pneumoniae*. *J. Bacteriol.* 179, 4789–4794. doi: 10.1128/jb.179.15.4789-4794.1997

Wilson, B. R., Bogdan, A. R., Miyazawa, M., Hashimoto, K., and Tsuji, Y. (2016). Siderophores in iron metabolism, from mechanism to therapy potential. *Trends Mol. Med.* 22, 1077–1090. doi: 10.1016/j.molmed.2016.10.005

Wooley, R. E., Gibbs, P. S., and Shotts, E. B. Jr. (1999). Inhibition of *Salmonella* Typhimurium in the chicken intestinal tract by a transformed avirulent avian *Escherichia coli*. *Avian Dis.* 43, 245–250. doi: 10.2307/1592614

World Health Organization [WHO] (2017). *Antibiotic Resistance Fact Sheet*. Geneva: WHO.

Yagmurov, E., Tsibulskaya, D., Livenskyi, A., Serebryakova, M., Wolf, Y. I., Borukhov, S., et al. (2020). Histidine-triad hydrolases provide resistance to peptide-nucleotide antibiotics. *mBio* 11:e0497-20. doi: 10.1128/mBio.00497-20

Yan, K. P., Li, Y., Zirah, S., Goulard, C., Knappe, T. A., Marahiel, M. A., et al. (2012). Dissecting the maturation steps of the lasso peptide microcin J25 in vitro. *Chembiochem* 13, 1046–1052. doi: 10.1002/cbic.201200016

Yang, C. C., and Konisky, J. (1984). Colicin V-treated *Escherichia coli* does not generate membrane potential. *J. Bacteriol.* 158, 757–759. doi: 10.1128/JB.158.2.757-759.1984

Yang, X., and Price, C. W. (1995). Streptolydigin resistance can be conferred by alterations to either the beta or beta' subunits of *Bacillus subtilis* RNA polymerase. *J. Biol. Chem.* 270, 23930–23933. doi: 10.1074/jbc.270.41.23930

Yoneyama, H., and Katsumata, R. (2006). Antibiotic resistance in bacteria and its future for novel antibiotic development. *Biosci. Biotechnol. Biochem.* 70, 1060–1075. doi: 10.1271/bbb.70.1060

Yorgey, P., Davagnino, J., and Kolter, R. (1993). The maturation pathway of microcin B17, a peptide inhibitor of DNA gyrase. *Mol. Microbiol.* 9, 897–905. doi: 10.1111/j.1365-2958.1993.tb01747.x

Yu, H., Ding, X., Shang, L., Zeng, X., Liu, H., Li, N., et al. (2018a). Protective ability of biogenic antimicrobial peptide microcin J25 against enterotoxigenic *Escherichia coli*-induced intestinal epithelial dysfunction and inflammatory responses IPEC-J2 cells. *Front. Cell Infect. Microbiol.* 8:242. doi: 10.3389/fcimb.2018.00242

Yu, H., Shang, L., Zeng, X., Li, N., Liu, H., Cai, S., et al. (2018b). Risks related to high-dosage recombinant antimicrobial peptide microcin J25 in mice model, intestinal microbiota, intestinal barrier function, and immune regulation. *J. Agric. Food Chem.* 66, 11301–11310. doi: 10.1021/acs.jafc.8b03405

Yu, H., Li, N., Zeng, X., Liu, L., Wang, Y., Wang, G., et al. (2019). A comprehensive antimicrobial activity evaluation of the recombinant microcin J25 against the foodborne pathogens *Salmonella* and *E. coli* O157:H7 by using a matrix of conditions. *Front. Microbiol.* 10:1954. doi: 10.3389/fmicb.2019.01954

Yu, H., Wang, Y., Zeng, X., Cai, S., Wang, G., Liu, L., et al. (2020). Therapeutic administration of the recombinant antimicrobial peptide microcin J25 effectively enhances host defenses against gut inflammation and epithelial barrier injury induced by enterotoxigenic *Escherichia coli* infection. *FASEB J.* 34, 1018–1037. doi: 10.1096/fj.201901717R

Yu, H. T., Ding, X. L., Li, N., Zhang, X. Y., Zeng, X. F., Wang, S., et al. (2017). Dietary supplemented antimicrobial peptide microcin J25 improves the growth performance, apparent total tract digestibility, fecal microbiota, and intestinal barrier function of weaned pigs. *J. Anim. Sci.* 95, 5064–5076. doi: 10.2527/jas2017.1494

Yuzenkova, J., Delgado, M., Nechaev, S., Savalia, D., Epshtein, V., Artsimovitch, I., et al. (2002). Mutations of bacterial RNA polymerase leading to resistance to microcin J25. *J. Biol. Chem.* 277, 50867–50875. doi: 10.1074/jbc.M209425200

Zhang, A., Rosner, J. L., and Martin, R. G. (2008). Transcriptional activation by MarA, SoxS and Rob of two tolC promoters using one binding site, a complex promoter configuration for tolC in *Escherichia coli*. *Mol. Microbiol.* 69, 1450–1455. doi: 10.1111/j.1365-2958.2008.06371.x

Zhao, Z., Eberhart, L. J., Orfe, L. H., Lu, S. Y., Besser, T. E., and Call, D. R. (2015). Genome-wide screening identifies six genes that are associated with susceptibility to *Escherichia coli* microcin PDI. *Appl. Environ. Microbiol.* 81, 6953–6963. doi: 10.1128/aem.01704-15

Zowawi, H. M., Harris, P. N., Roberts, M. J., Tambyah, P. A., Schembri, M. A., Pezzani, M. D., et al. (2015). The emerging threat of multidrug-resistant Gram-negative bacteria in urology. *Nat. Rev. Urol.* 12, 570–584. doi: 10.1038/nrurol.2015.199

Zschüttig, A., Zimmermann, K., Blom, J., Goesmann, A., Pöhlmann, C., and Gunzer, F. (2012). Identification and characterization of microcin S, a new antibacterial peptide produced by probiotic *Escherichia coli* G3/10. *PLoS One* 7:e033351. doi: 10.1371/journal.pone.0033351

Conflict of Interest: The authors declare that the research was conducted in the absence of any commercial or financial relationships that could be construed as a potential conflict of interest.

frontiers in Microbiology

ORIGINAL RESEARCH
published: 12 November 2020
doi: 10.3389/fmicb.2020.589666

Synthetic Peptide Libraries Designed From a Minimal Alpha-Helical Domain of AS-48-Bacteriocin Homologs Exhibit Potent Antibacterial Activity

*Jessica N. Ross[1†], Francisco R. Fields[1], Veronica R. Kalwajtys[1], Alejandro J. Gonzalez[1], Samantha O'Connor[3], Angela Zhang[1], Thomas E. Moran[1], Daniel E. Hammers[1,2], Katelyn E. Carothers[1,2] and Shaun W. Lee[1,2]**

[1] Department of Biological Sciences, University of Notre Dame, Notre Dame, IN, United States, [2] Eck Institute for Global Health, University of Notre Dame, Notre Dame, IN, United States, [3] Department of Chemistry and Biochemistry, University of Notre Dame, Notre Dame, IN, United States

OPEN ACCESS

Edited by:
Des Field,
University College Cork, Ireland

Reviewed by:
Natalia Soledad Rios Colombo,
CONICET Centro de Referencia para Lactobacilos (CERELA), Argentina
Raul Raya,
CONICET Centro de Referencia para Lactobacilos (CERELA), Argentina
Jiro Nakayama,
Kyushu University, Japan

***Correspondence:**
Shaun W. Lee
lee.310@nd.edu;
Shaun.W.Lee.310@nd.edu

[†]These authors share first authorship

Specialty section:
This article was submitted to Antimicrobials, Resistance and Chemotherapy, a section of the journal Frontiers in Microbiology

Received: 31 July 2020
Accepted: 08 October 2020
Published: 12 November 2020

Citation:
Ross JN, Fields FR, Kalwajtys VR, Gonzalez AJ, O'Connor S, Zhang A, Moran TE, Hammers DE, Carothers KE and Lee SW (2020) Synthetic Peptide Libraries Designed From a Minimal Alpha-Helical Domain of AS-48-Bacteriocin Homologs Exhibit Potent Antibacterial Activity. Front. Microbiol. 11:589666. doi: 10.3389/fmicb.2020.589666

The circularized bacteriocin enterocin AS-48 produced by *Enterococcus* sp. exhibits antibacterial activity through membrane disruption. The membrane-penetrating activity of enterocin AS-48 has been attributed to a specific alpha-helical region on the circular peptide. Truncated, linearized forms containing these domains have been shown to preserve limited bactericidal activity. We utilized the amino acid sequence of the active helical domain of enterocin AS-48 to perform a homology-based search of similar sequences in other bacterial genomes. We identified similar domains in three previously uncharacterized AS-48-like bacteriocin genes in *Clostridium sordellii*, *Paenibacillus larvae*, and *Bacillus xiamenensis*. Enterocin AS-48 and homologs from these bacterial species were used as scaffolds for the design of a minimal peptide library based on the active helical domain of each bacteriocin sequence. 95 synthetic peptide variants of each scaffold peptide, designated *Syn-enterocin*, *Syn-sordellicin*, *Syn-larvacin*, and *Syn-xiamensin*, were designed and synthesized from each scaffold sequence based on defined biophysical parameters. A total of 384 total peptides were assessed for antibacterial activity against Gram-negative and Gram-positive bacteria. Minimal Inhibitory Concentrations (MICs) as low as 15.6 nM could be observed for the most potent peptide candidate tested, with no significant cytotoxicity to eukaryotic cells. Our work demonstrates for the first time a general workflow of using minimal domains of natural bacteriocin sequences as scaffolds to design and rapidly synthesize a library of bacteriocin-based antimicrobial peptide variants for evaluation.

Keywords: bacteriocin, antimicrobial peptide, enterocin, synthetic peptide, antibiotics

INTRODUCTION

New chemical and biological scaffolds for the design of antibiotic compounds have become a highly prioritized area of research, especially as novel pandemics and secondary bacterial infections become a wider global concern (Rosenberg and Goldblum, 2006). Antimicrobial peptides (AMPs) represent a broad source of chemical and functional discovery for the development of novel

antibiotics (Boman, 2003). Although AMPs are highly diverse, and span the range from prokaryotes to lower and higher eukaryotes, many AMPs have conserved structural features, with common amphiphilic and alpha helical domains (Jenssen et al., 2006; Fjell et al., 2012; Uggerhøj et al., 2015; Haney et al., 2017). A common mechanism by which AMPs exert direct antimicrobial activity involves the accumulation of the peptide on the bacterial cell surface, with subsequent membrane disruption, leading to cell death (Nakajima, 2003; Brogden, 2005; Lv et al., 2014; Ong et al., 2014; Mahlapuu et al., 2016). Strategies to improve the activity of natural AMPs have focused on biophysical approaches to increase both the targeting affinity for anionic bacterial membranes and to improve their ability to penetrate lipid membrane domains, as well as altering properties including heat stability, solubility, and protease resistance for more effective therapeutic use (Fjell et al., 2012; Field et al., 2015a; Mikut et al., 2016; Torres et al., 2019).

The AMPs of bacteria, known broadly as bacteriocins, are a group of genetically encoded and ribosomally produced peptides that exist in operons containing the genes necessary for its assembly and export (Alvarez-Sieiro et al., 2016). Although bacteriocins are highly diverse in structure and function, the most fundamental division of bacteriocins, based on structure, is into class I (modified) and class II (unmodified) types (Cotter et al., 2013; Alvarez-Sieiro et al., 2016). In both cases, bacteriocins are believed to undergo the cleavage of a leader sequence from the core peptide domain. In addition to leader sequence cleavage, class I peptides are subject to additional post-translational modifications, including heterocyclization, glycosylation, and head-to-tail circularization (Arnison et al., 2013; Cotter et al., 2013; Alvarez-Sieiro et al., 2016). The class I bacteriocin nisin, which has been widely approved for use as a food preservative, is currently being researched for increased activity against infectious bacteria (Field et al., 2015a,c, 2019). Nisin is distinguished by post-translational installation of dehydroalanine and a thioether polycyclic lanthionine bridge (Field et al., 2015b; Murinda et al., 2003). Thiopeptides, a type of class I bacteriocin containing thiazole rings, have been used for the development of antibiotic lead compounds for the treatment of *Clostridium difficile* infections. Using a naturally occurring thiopeptide as a scaffold, the compound LFF57 was designed by using traditional medicinal chemistry and structure activity relationship approaches and is now in clinical trials (Lamarche et al., 2012; Mullane et al., 2015). Despite these significant advances, however, bacteriocins are still highly underrepresented as template sources for the design of linear AMPs.

Enterocin AS-48 is a circular, largely unmodified bacteriocin (Class I or Class II) produced by *Enterococcus* sp. and has been most commonly studied as a possible food preservative (Gálvez et al., 1989; González et al., 2000; Gómez et al., 2012; Caballero Gómez et al., 2013; Burgos et al., 2015). This bacteriocin is first produced as a prepropeptide consisting of a leader sequence and a propeptide. Subsequent proteolytic cleavage of the leader sequence results in a propeptide that undergoes head to tail macrocyclization to produce the active product (Sánchez-Hidalgo et al., 2011). Mature AS-48 consists of five alpha helices, with cationic residues clustered within helices four and five. These residues have been hypothesized as critical for the antimicrobial activity of AS-48 (Jiménez et al., 2005; Montalbán-López et al., 2011; Sánchez-Hidalgo et al., 2011). However, peptide variants consisting of portions of this region obtained by limited proteolysis or chemical synthesis were not found to retain full antibacterial activity (Montalbán-López et al., 2008, 2011; Sánchez-Hidalgo et al., 2011).

Our previous studies have demonstrated that active regions of bacteriocins such as AS-48 can be minimized and utilized as scaffolds to design novel, bacteriocin-based minimal peptides (Fields et al., 2018). Using rational design criteria based on a set of biophysical parameters, minimal domain bacteriocin library variants can be designed and tested for improved antibacterial activity. Several key biophysical parameters have been shown to improve the activity of the library peptide candidates (Uggerhøj et al., 2015; Fields et al., 2018). The substitution of basic residues in the minimal peptide increases the affinity of the peptide for the bacterial membrane (Fjell et al., 2012). Increased incorporation of hydrophobic residues at specific locations can also improve the ability of the minimal peptide to penetrate the lipid membrane domain (Uggerhøj et al., 2015). Further, since AMPs are typically amphipathic, key amino acid substitutions to increase the amphipathic nature of the minimal peptide candidate can also improve the ability of the peptide to target, bind to, and disrupt the bacterial membrane (Ong et al., 2014; Wang et al., 2017). In a general heuristic for library design, these amino acid substitutions can be systematically incorporated and evaluated in assays to gain additional insights into a general strategy for improved antimicrobial peptide design.

In this study, we sought to develop a systematic library-based synthetic strategy for the design and testing of linear reductive AMPs from gene sequences of full-length AS-48 bacteriocins. We utilized the known AS-48 sequence from *Enterococcus* sp. as well as three previously unidentified AS-48-like bacteriocin genes present in *Clostridium sordellii*, *Paenibacillus larvae*, and *Bacillus xiamenensis* as scaffolds for the design of a minimal peptide library based on the active helical domain of each bacteriocin sequence. Our efforts present a systematic approach to identifying and verifying portions of AS-48 bacteriocins as scaffolds for the design of synthetic AMPs and their subsequent optimization for charge and hydrophobicity using a library-based approach.

MATERIALS AND METHODS

Peptide Design

The sequence of the cationic, alpha helical regions four and five from enterocin AS-48 was subjected to protein BLAST to identify homologous regions in other bacterial species. This peptide domain was confirmed to be highly conserved in *C. sordellii*, *P. larvae*, and *B. xiamenensis*, confirming the identified peptides as AS-48-like bacteriocins (**Supplementary Table S1**). The libraries were rationally designed to increase antimicrobial activity of the four peptide scaffolds using three approaches. (1) Single amino acids, within the helical wheel, were

flipped in a step-wise fashion to slowly increase the amphipathic nature of the peptide (Fjell et al., 2012). (2) A single, basic amino acid substitution was made, switching a short-chained amino acid for lysine, hypothesized to increase affinity of the peptides to an anionic bacterial membrane (Morita et al., 2013; Jin et al., 2016). (3) Aliphatic and non-polar short-chained amino acids were replaced with tryptophan, theorized to increase the ability of the peptides to penetrate bacterial membranes (Fimland et al., 2002; Nguyen et al., 2010). The libraries were subsequently named for their parent peptide scaffold as syn(synthetic)-enterocin, syn-sordellicin, syn-larvacin, and syn-xiamencin. Each library was composed of 96 peptides, including 95 variants in addition to the parent peptide.

Peptide Synthesis

All 384 peptide sequences, which contained 25 amino acids each, were commercially synthesized by GenScript (Piscataway, NJ, United States). Synthesis was confirmed to be >95% pure and was verified by HPLC and mass spectrometry prior to use (GenScript). All peptides were dissolved in 10% DMSO to final stock concentrations of 1.28 mM. For circular dichroism (CD) spectroscopy, peptides were dissolved in nanopure water to minimize background noise.

Computational Structure Modeling

Three-dimensional peptide models were predicted using the PEPFOLD online server and visualized using PyMOL (Maupetit et al., 2009). Helical wheel predictions, to illustrate changes in amphipathicity, were made via EMBOSS: pepwheel predictive software (Schiffer and Edmundson, 1967).

Peptide Screening and MIC Determination

Peptides were screened against *Escherichia coli* (BL21), *Streptococcus pyogenes* (M1T1 5448, hereby referred to as M1), *Pseudomonas aeruginosa* (PAO1), and *Staphylococcus aureus* (USA300). Overnight bacterial cultures were grown in optimal media for each species: Luria-Bertani (LB) broth for *E. coli*, *P. aeruginosa*, and *S. aureus*, and Todd-Hewitt (TH) broth for *S. pyogenes*. Cultures were pelleted and re-suspended in Mueller-Hinton (MH) broth for peptide screens or minimal inhibitory concentration (MIC) assays, with 1×10^6 CFU/mL bacteria added per well (Wiegand et al., 2008). MICs for each parent peptide were identified against each bacterial strain as previously described (Fields et al., 2018). Members of each peptide library were screened against each bacterial strain at half of the MIC of the corresponding parent peptide to identify library members with increased antimicrobial activity relative to the parent peptide. Libraries whose parent peptides exhibited MICs >128 μM against a particular bacterial strain were not screened against that strain. Following each screen, peptides that exhibited antimicrobial activity were subjected to full MIC assays, as previously described (Fields et al., 2018). Minimal bactericidal concentrations (MBCs) were determined following the respective MIC assays by plating aliquots from wells corresponding to each peptide concentration from the 96-well plate used for the MIC on species-appropriate agar. Plates were incubated at 37°C overnight, and MBCs were identified as the lowest concentrations of peptide at which no colonies were obtained. A Synergy H1 Microplate Reader (BioTek, Winooski, VT, United States) was used to determine the MICs and identify peptides with greater antimicrobial activity than the corresponding parent peptide by measuring OD 600 of the bacterial cultures in 96-well microtiter plates.

Peptide Cytotoxicity and Hemolysis Assays

To assess cytotoxicity of optimized peptides in mammalian cells, an immortalized human keratinocyte cell line (HaCaT) was used. Cells were grown to 80% confluency in 24-well culture dishes and washed with PBS (Thermo Fisher). Each peptide was diluted in fresh Dulbecco's Modified Eagle Medium (DMEM), supplemented with 10% fetal bovine serum (FBS), to desired concentrations corresponding to MIC experiments and incubated with cells for 16 h in triplicate at 37°C, 5% CO_2. After incubation, the cells were washed with sterile PBS, followed by a covered incubation with 4 μM ethidium homodimer (Molecular Probes) for 30 min at room temperature. Fluorescence was measured using the Synergy H1 Microplate Reader set to 528 nm excitation, 617 nm emission, and a cutoff value of 590 nm. Saponin (0.1% wt/vol, Sigma) was added to each well followed by a covered incubation for 20 min at room temperature, followed by another measurement on the Synergy H1 Microplate Reader using the same settings to normalize readings to the number of cells per well and determine the percent cytotoxicity. Peptides were characterized as cytotoxic at a particular concentration if incubation with that concentration of peptide resulted in more than 20% cell death after 16 h, which corresponded to the percent cytotoxicity in HaCaTs treated with the vehicle control under the same conditions.

To determine if peptide variants were hemolytic, fresh defibrinated whole sheep blood (Hardy Diagnostics) was washed three times in cold PBS, and washed blood was diluted 1:25 in PBS. Treatments were applied at a 1:10 ratio of sample:blood, where the sample was either 10% Triton, PBS, or a specific peptide concentration corresponding to concentrations used in the MIC assays. Treatments were incubated with the blood for 1 h at 37°C. Following incubation, samples were centrifuged at $0.4 \times g$ for 10 min at 4°C, and the absorbance of the supernatants at 450 nm was measured on the Synergy H1 Microplate Reader to measure the release of hemoglobin. Percent hemolysis was quantified by normalizing to the negative and positive controls.

Circular Dichroism Spectroscopy

Using a Jasco CD Spectrometer, peptide variants were scanned from 190 to 250 nm at 20 nm/min in a 2 mm cuvette. Peptides were diluted to a final concentration of 25 μM and suspended in either nanopure water, 9 mM SDS (Sigma-Aldrich), or 50% trifluoroethanol (TFE) (Sigma-Aldrich). Scans were run in triplicate and averaged. Blanks using the solvents were quantified to subtract from the peptide scans.

Fluorescence Microscopy and Fluorescence-Activated Cell Sorting

To observe bacterial cell death in the presence of peptide in real time, fluorescence microscopy was employed using GFP-expressing *E. coli* strain BL21. MIC assays were conducted against BL21-GFP to determine the peptide concentration used for microscopy experiments. The peptide was suspended in PBS and added to diluted bacterial cells. GFP-expressing *E. coli* in the presence of peptide were imaged on the Eclipse Ti-E inverted microscope (Nikon) using GFP and DIC channels for 8 h at 37°C, with images taken every 10 min (Fields et al., 2020). Syn-xiamencin-2, a peptide with no detectable antimicrobial activity below 128 μM was also evaluated as a negative peptide candidate control.

For determination of bacterial cell death via membrane disruption, bacterial cells were subjected to propidium iodide (PI) uptake and quantified using fluorescence-activated cell sorting (FACS). *E. coli* strain BL21 were first diluted to a OD 600 of 1.0. Cells were washed three times in 0.85% NaCl (saline) solution and resuspended in either 1.5 mL of either saline, 70% isopropyl alcohol, or peptide diluted to either 2, 4, 8, 16 or 32 μM in saline for 1 h at ambient temperature. Following incubation, cells were pelleted and resuspended in 1 mL of saline with 1.5 μL/mL propidium iodide and incubated in the dark for 15 min. The samples were washed again with saline three times and run through a Beckman Coulter FC500 flow cytometer. The FL3 detector, using the propidium iodine PE-Alexa Fluor 610 emission filter, was used to sort the cells. 1×10^4 events were collected for each sample run.

RESULTS

Peptide Library Design

Previous studies demonstrated that the antimicrobial activity of full-length enterocin AS-48 can largely be attributed to cationic helices four and five (Montalbán-López et al., 2008). Since linearized forms containing this region have been shown to be active and capable of optimization, we hypothesized that homologous regions in similar enterocin AS-48-like natural sequences could also serve as a scaffold for peptide sequence optimization. We utilized the truncated 25 amino acid sequence from the active domain of enterocin AS-48 to bioinformatically search for other AS-48 like homologs having high conservation in this active domain, as was previously done to identify safencin AS-48 (Fields et al., 2018, 2020). Three additional species were identified with highly conserved AS-48-like domain regions, namely, *C. sordellii*, *P. larvae*, and *B. xiamenensis* (**Supplementary Table S1**). Each 25 amino acid sequence of the AS-48 domain was designated as the parent peptide (Peptide No. 1 in series) and used as a scaffold to build a series of library peptide variants with systematic amino acid substitutions to improve the activity of the original peptide. To increase affinity of the peptide variants to the anionic bacterial membrane, lysine was incorporated into the peptide, being substituted for a short-chained amino acid. In order to potentially increase penetration of the bacterial membrane, aliphatic and non-polar short-chained amino acids were substituted with the inclusion of the aromatic amino acid tryptophan, along with increasing the amphipathic nature of the peptides by flipping specific amino acids within the helical wheel. All changes were made in a step-wise fashion to build the peptide libraries. The four libraries, syn(synthetic)-enterocin, syn-sordellicin, syn-larvacin, and syn-xiamencin, were synthesized to 95% purity (GenScript).

Screening and MIC Determination

Each parent peptide was first tested for MIC values against *E. coli* (BL21), *S. pyogenes* (M1), *P. aeruginosa* (PAO1), and *S. aureus* (USA300). All 95 peptide variants in each library were screened at one-half the MIC value of the parent peptide. Peptide variants within each library screen were determined to be a positive hit if inhibition was confirmed during screening. Further, if a peptide variant outperformed its parent scaffold against all screened bacterial species, the peptide was characterized as an optimized peptide variant and MIC assays were subsequently performed using these peptides. All parent peptide scaffolds were found to have a MIC above 128 μM against *S. aureus* USA300. Additionally, the parent peptide syn-larvacin-1 and syn-xiamencin-1 had MIC above 128 μM against PAO1.

Syn-sordellicin Library

Syn-sordellicin-1 was determined to have a MIC of 8 μM against BL21, 8 μM against M1 and 16 μM against PAO1, thus this library was screened against BL21 at 4 μM, M1 at 4 μM, and PAO1 at 8 μM. Fourteen of the 95 screened peptides in this library were determined to be significantly antimicrobial against all three screened bacterial species (**Figure 1A**). Notably, syn-sordellicin-64, -80, and -96 exhibited MICs as low as 250 nM against BL21. Syn-sordellicin-11 and -16 were determined to have MIC against M1 at 500 and 250 nM, respectively. Against PAO1, syn-sordellicin-43 exhibited an MIC of 2 μM, which was the lowest MIC observed across all optimized peptide variants. Additionally, nine of the fourteen optimized peptide variants exhibited MIC below 128 μM against USA300; the best peptide variant against USA300 being syn-sordellicin-64 with a MIC and MBC of 8 μM (**Table 1A**).

Syn-larvacin Library

Syn-larvacin-1 was determined to have a MIC of 32 μM against BL21 and 8 μM against M1, therefore the peptide variants were screened at 16 and 4 μM, respectively. Fourteen of the 95 screened peptides outperformed its parent scaffold peptide against all four screened bacterial species (**Figure 1B**). Of these, five peptide variants exhibited MICs below 500 nM against BL21; syn-larvacin-27 and -39 exhibited MIC and MBC as low as 15.6 nM. Against M1, syn-larvacin-27, -69, -71, and -72 were confirmed to have MICs of 125 nM. As shown in **Table 1B**, the optimized peptides against USA300 showed a large range of activity, with MICs between 250 nM and 64 μM. Notably, syn-larvacin-71 had an MIC of 250 nM against USA300. Against PAO1, the fourteen syn-larvacin optimized peptides had MIC values between 16 and 64 μM.

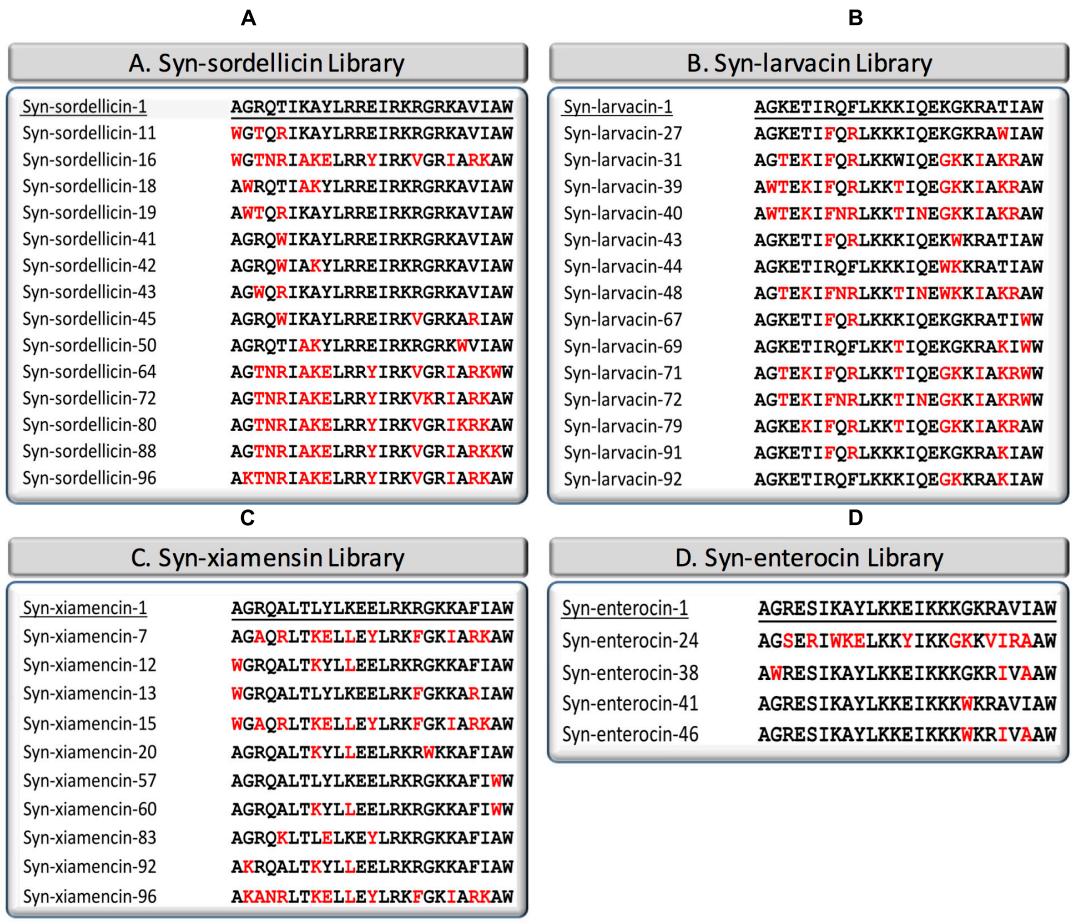

FIGURE 1 | Amino acid sequence alignment of optimized variants from four AS-48 domain derived scaffold libraries. Syn-sordellicin library **(A)**, syn-larvacin library **(B)**, syn-xiamencin library **(C)**, and syn-enterocin **(D)** library indicate amino acid changes of optimized peptide variants, as compared to the parent scaffold, in red.

Syn-xiamencin Library

Syn-xiamencin-1 was determined to have a MIC of 32 μM against BL21 and 16 μM to M1, therefore the peptide variants of this library were screened at 16 μM against BL21 and 8 μM against M1. Ten optimized peptide variants were established (**Figure 1C**). The syn-xiamencin library was most effective against M1, establishing MICs to be as low as 250 and 500 nM for syn-xiamencin-13 and-7, respectively. Against BL21, many optimized peptide variants exhibited MICs and MBCs as low as 1 and 2 μM, including syn-enterocin-15, -20, and -96. Half of the optimized peptide variants against USA300 exhibited MICs below 128 μM, while eight of the ten exhibited MICs below 128 μM to PAO1. Between both bacterial species, successful peptide variants had MICs between 8 and 128 μM (**Table 1C**).

Syn-enterocin Library

Syn-enterocin-1 was determined to have a MIC of 32 μM against BL21, 32 μM against M1, and 128 μM against PAO1, therefore all peptide variants were screened at 16 μM against BL21, 16 μM against M1 and 64 μM against PAO1. After screening, syn-enterocin-24, -38, -41, and -46 were confirmed to be optimized peptides for further studies (**Figure 1D**). These four peptide variants were then analyzed to confirm their individual MIC and MBC against the screened species, BL21, M1, and PAO1, along with assessing further activity against USA300 (**Table 1D**). It was determined that syn-enterocin-24 and -46 had MICs of 64 and 32 μM, respectively, against USA300, with MBC values above 128 μM.

Cytotoxicity and Hemolytic Activity of Optimized Peptide Variants

Based on our previous screening and MIC determination, 42 optimized peptide variants with low MIC values against our panel of bacterial pathogens were selected for cytotoxicity assays against human keratinocytes (HaCaTs). HaCaT cytotoxicity was assessed by membrane permeabilization using ethidium homodimer assays. Four optimized peptide variants, all within the syn-sordellicin library, were found to be significantly cytotoxic (>30% cytotoxicity). Our most cytotoxic peptide was syn-sordellicin-64, exhibiting significant cytotoxicity in a dose-dependent manner, at 32 μM and above. Syn-sordellicin-19, -72, and -88 were also found to be cytotoxic at concentrations

TABLE 1 | Antimicrobial activity of AS-48 domain derived peptide libraries. Broth microdilutions of optimized peptide variants within the syn-sordellicin **(A)**, syn-larvacin **(B)**, syn-xiamencin **(C)**, and syn-enterocin **(D)** libraries were used to determine antimicrobial activity against isolates of *E. coli*, *S. pyogenes*, *S. aureus*, and *P. aeruginosa*. MIC and MBC were established after 16 h incubation. Assays were done in triplicate and growth inhibition was determined by measuring the optical density at 600 nm.

	***E. coli* (BL21)**		***S. pyogenes* (M1)**		***S. aureus* (USA300)**		***P. aeruginosa* (PAO1)**	
Peptide Variant	**MIC**	**MBC**	**MIC**	**MBC**	**MIC**	**MBC**	**MIC**	**MBC**
A.								
Syn-sordellicin-1	8 μM	8 μM	8 μM	8 μM	>128 μM	>128 μM	16 μM	16 μM
Syn-sordellicin-11	2 μM	2 μM	0.5 μM	0.5 μM	>128 μM	>128 μM	8 μM	8 μM
Syn-sordellicin-16	1 μM	1 μM	0.25 μM	0.5 μM	16 μM	32 μM	8 μM	8 μM
Syn-sordellicin-18	1 μM	1 μM	4 μM	4 μM	32 μM	32 μM	4 μM	8 μM
Syn-sordellicin-19	2 μM	2 μM	2 μM	2 μM	>128 μM	>128 μM	8 μM	16 μM
Syn-sordellicin-41	2 μM	2 μM	2 μM	4 μM	>128 μM	>128 μM	16 μM	16 μM
Syn-sordellicin-42	2 μM	2 μM	4 μM	4 μM	>128 μM	>128 μM	16 μM	16 μM
Syn-sordellicin-43	1 μM	1 μM	2 μM	4 μM	32 μM	32 μM	2 μM	4 μM
Syn-sordellicin-45	1 μM	1 μM	2 μM	2 μM	32 μM	32 μM	16 μM	32 μM
Syn-sordellicin-50	1 μM	1 μM	2 μM	2 μM	>128 μM	>128 μM	8 μM	16 μM
Syn-sordellicin-64	0.25 μM	0.5 μM	1 μM	1 μM	8 μM	8 μM	8 μM	8 μM
Syn-sordellicin-72	0.5 μM	0.5 μM	1 μM	1 μM	16 μM	16 μM	16 μM	16 μM
Syn-sordellicin-80	0.25 μM	0.5 μM	2 μM	2 μM	64 μM	64 μM	16 μM	16 μM
Syn-sordellicin-88	1 μM	1 μM	1 μM	1 μM	64 μM	64 μM	16 μM	16 μM
Syn-sordellicin-96	0.25 μM	0.25 μM	0.5 μM	0.5 μM	32 μM	32 μM	8 μM	16 μM
B.								
Syn-larvacin-1	32 μM	>128 μM	8 μM	64 μM	>128 μM	>128 μM	>128 μM	>128 μM
Syn-larvacin-27	<0.0156 μM	<0.0156 μM	0.125 μM	0.5 μM	8 μM	8 μM	32 μM	64 μM
Syn-larvacin-31	1 μM	1 μM	0.25 μM	0.25 μM	8 μM	8 μM	64 μM	128 μM
Syn-larvacin-39	<0.0156 μM	<0.0156 μM	2 μM	4 μM	1 μM	4 μM	16 μM	64 μM
Syn-larvacin-40	2 μM	2 μM	0.25 μM	4 μM	4 μM	4 μM	16 μM	16 μM
Syn-larvacin-43	1 μM	1 μM	4 μM	4 μM	4 μM	4 μM	16 μM	16 μM
Syn-larvacin-44	0.5 μM	1 μM	0.5 μM	0.5 μM	32 μM	32 μM	16 μM	32 μM
Syn-larvacin-48	4 μM	4 μM	8 μM	8 μM	8 μM	8 μM	16 μM	32 μM
Syn-larvacin-67	4 μM	4 μM	0.25 μM	0.25 μM	64 μM	64 μM	16 μM	32 μM
Syn-larvacin-69	2 μM	16 μM	0.125 μM	0.5 μM	16 μM	16 μM	32 μM	32 μM
Syn-larvacin-71	0.25 μM	0.25 μM	0.125 μM	0.125 μM	<0.25 μM	<0.25 μM	16 μM	32 μM
Syn-larvacin-72	0.25 μM	0.25 μM	0.125 μM	2 μM	>128 μM	>128 μM	32 μM	64 μM
Syn-larvacin-79	16 μM	32 μM	>128 μM	>128 μM	4 μM	8 μM	64 μM	>128 μM
Syn-larvacin-91	1 μM	2 μM	0.5 μM	0.5 μM	2 μM	2 μM	32 μM	64 μM
Syn-larvacin-92	2 μM	2 μM	1 μM	1 μM	2 μM	8 μM	64 μM	128 μM
C.								
Syn-xiamencin-1	32 μM	32 μM	16 μM	16 μM	>128 μM	>128 μM	>128 μM	>128 μM
Syn-xiamencin-7	4 μM	4 μM	0.5 μM	0.5 μM	>128 μM	>128 μM	64 μM	128 μM
Syn-xiamencin-12	16 μM	16 μM	2 μM	2 μM	>128 μM	>128 μM	64 μM	64 μM
Syn-xiamencin-13	16 μM	32 μM	0.25 μM	0.25 μM	>128 μM	>128 μM	>128 μM	>128 μM
Syn-xiamencin-15	2 μM	2 μM	1 μM	1 μM	64 μM	128 μM	>128 μM	>128 μM
Syn-xiamencin-20	1 μM	1 μM	2 μM	2 μM	32 μM	32 μM	64 μM	64 μM
Syn-xiamencin-57	16 μM	16 μM	4 μM	8 μM	16 μM	32 μM	>128 μM	>128 μM
Syn-xiamencin-60	4 μM	8 μM	2 μM	4 μM	>128 μM	>128 μM	>128 μM	>128 μM
Syn-xiamencin-83	16 μM	32 μM	4 μM	4 μM	>128 μM	>128 μM	128 μM	>128 μM
Syn-xiamencin-92	4 μM	8 μM	4 μM	8 μM	8 μM	8 μM	16 μM	16 μM
Syn-xiamencin-96	2 μM	2 μM	4 μM	4 μM	8 μM	8 μM	16 μM	16 μM
D.								
Syn-enterocin-1	32 μM	32 μM	32 μM	32 μM	>128 μM	>128 μM	>128 μM	>128 μM
Syn-enterocin-24	2 μM	2 μM	16 μM	16 μM	64 μM	>128 μM	8 μM	16 μM
Syn-enterocin-38	4 μM	8 μM	16 μM	16 μM	>128 μM	>128 μM	32 μM	32 μM
Syn-enterocin-41	4 μM	4 μM	16 μM	16 μM	>128 μM	>128 μM	16 μM	16 μM
Syn-enterocin-46	2 μM	4 μM	8 μM	8 μM	32 μM	>128 μM	8 μM	16 μM

of 64 μM and above (**Supplementary Figure S1**). Due to their cytotoxicity, these four peptide variants were removed from further characteristic studies. All other optimized peptide variants, along with their parent peptide scaffold, were not cytotoxic at their established MIC concentrations. Across all peptide libraries, 29 of the optimized peptide variants exhibited minimal hemolytic activity (**Supplementary Table S2**). Of these, 17 showed hemolytic activity above 32 μM. Syn-sordellicin-64, in line with cytotoxicity data, exhibited hemolysis down to 250 nM. Syn-sordellicin-64 was found to be broadly antibacterial, including having the lowest MIC value against USA300 compared to the other syn-sordellicin peptides tested, giving reason to the cytotoxicity and hemolytic activity observed. Only peptide variants which showed no hemolytic activity below their MIC values were retained as potential antimicrobial candidates. These data suggest that our library approach to designing minimal peptides using AS-48 like bacteriocin domains results in very low eukaryotic toxicity overall, consistent with the natural forms of AS-48.

Selection of Broad-Spectrum and Narrow-Spectrum Candidates

We next categorized our optimized peptides into broad- and narrow-spectrum candidates based on their established MIC values, cytotoxicity and hemolytic activity (**Figure 2**). Optimized peptide variants were characterized as broad-spectrum candidates based on low MICs against a majority of the panel of bacterial pathogens tested. Based on these criteria, peptides were ranked and the top four, syn-sordellicin-43, syn-larvacin-40, syn-larvacin-43, and syn-xiamencin-96, were chosen as our broad-spectrum candidates to study further. Four peptides which exhibited narrow-spectrum bioactivity were selected as candidates. All narrow-spectrum peptide candidates had an established MIC below 250 nM to at least one of our tested bacterial species. Syn-sordellicin-96 and syn-larvacin-71 were found to have an MIC and MBC of 250 nM for BL21, while Syn-larvacin-27 and -39 had MIC and MBC below 15.6 nm. Against M1, syn-larvacin-27 and -71 had MICs of 125 nm. Syn-larvacin-71 also had the lowest MIC established against USA300 at 250 nM. The lowest MIC seen for PAO1 was syn-sordellicin-43 at 2 uM, a peptide chosen for broad-spectrum activity.

Secondary Structure and Mode of Action Analysis of Optimized Peptide Variants

Secondary structures of each optimized peptide candidate were first analyzed using the prediction software PEPFOLD and visualized on PyMOL (**Figure 3**). All eight peptide candidates were shown to have alpha helical structures of various lengths. Visualization showed all analyzed peptide variants as amphipathic, having large hydrophobic and cationic regions on opposing sides of the helical structures. Helical wheel predictions using EMBOSS also showed a strong preference for amphipathicity (**Figure 3**). To validate our computational data, CD spectroscopy was done to observe the peptide structural behavior in controlled microenvironments. Using 9 mM SDS and 50% TFE to mimic the bacterial membrane environments, local minima were observed at 209 nm and 222 nm and a maximum peak at 192 nm in all four peptide variants, indicating the presence of an alpha-helical structure. In nanopure water, random coiling conformation is suggested by the observed dip around 195 nm (**Figure 4**). These data suggest that the peptides adopt an amphipathic alpha-helical structure with cationic regions, following the common theme for previously characterized AMPs (Wang et al., 2017; Fields et al., 2018).

To assess bacterial membrane disruption as a potential mode of action for peptide candidates, we utilized live imaging of GFP-expressing *E. coli* BL21 and observed loss of membrane integrity in real-time over 8 h after incubation with peptides. As observed through live-imaging, GFP-expressing bacteria treated with Syn-xiamencin-2 showed increased fluorescence over the 8 h, indicating no GFP leakage (**Figure 5A**). However, GFP-expressing bacteria exhibited GFP leakage when treated with all tested optimized peptides, as shown by a decrease in fluorescence over the course of the 8 h (**Figures 5B–E**). GFP leakage in the presence of the optimized peptides suggests membrane disruption as the mode of action. In order to further examine if membrane disruption is the cause of bacterial cell death, permeabilization of the bacterial membrane by peptide candidates was assessed through a propidium iodide (PI) stain. If the bacterial membrane was disrupted, PI is able to enter cells and emit a fluorescent signal upon intercalation with DNA. Thus, fluorescence emitting cells are used as a proxy indicating cell death via membrane disruption. FACS analysis was used to sort PI positive cells in the presence of peptide candidates. Data collected showed an increase in PI positive cells, in a dose-dependent manner when incubated with syn-larvacin 27 and syn-larvacin 43 for 1 h, while syn-xiamencin-2 had no increase in PI positive cells, as compared to saline solution (**Figure 6**).

DISCUSSION

In this study, we demonstrate that the active helical domain of enterocin AS-48 and related homologs can be leveraged as basic scaffolds to build a substantial library of small, chemically synthesized AMPs that can be evaluated for activity. These peptide variants are designed using systematic biophysical parameters in order to obtain a large dataset. Larger datasets may give insight to how traits, such as hydrophobicity and amphipathicity, improve the activity and specificity of the bacteriocin variant from the original sequence. Importantly, we establish a general workflow that combines bioinformatic searches to discover novel bacteriocins to serve as initial peptide library scaffolds and biophysically guided rational design of synthetic AMP libraries.

Our results identify a large number of peptide variants possessing more potent bioactivity than their parent scaffold. Although in general terms, minimal domains of full-length bacteriocins are likely to display diminished antibacterial activity, our results provide evidence that the antimicrobial activity of truncated peptide candidates can be restored and even further improved using systematic amino acid substitution. Overall, our data support long-standing, general trends regarding AMP

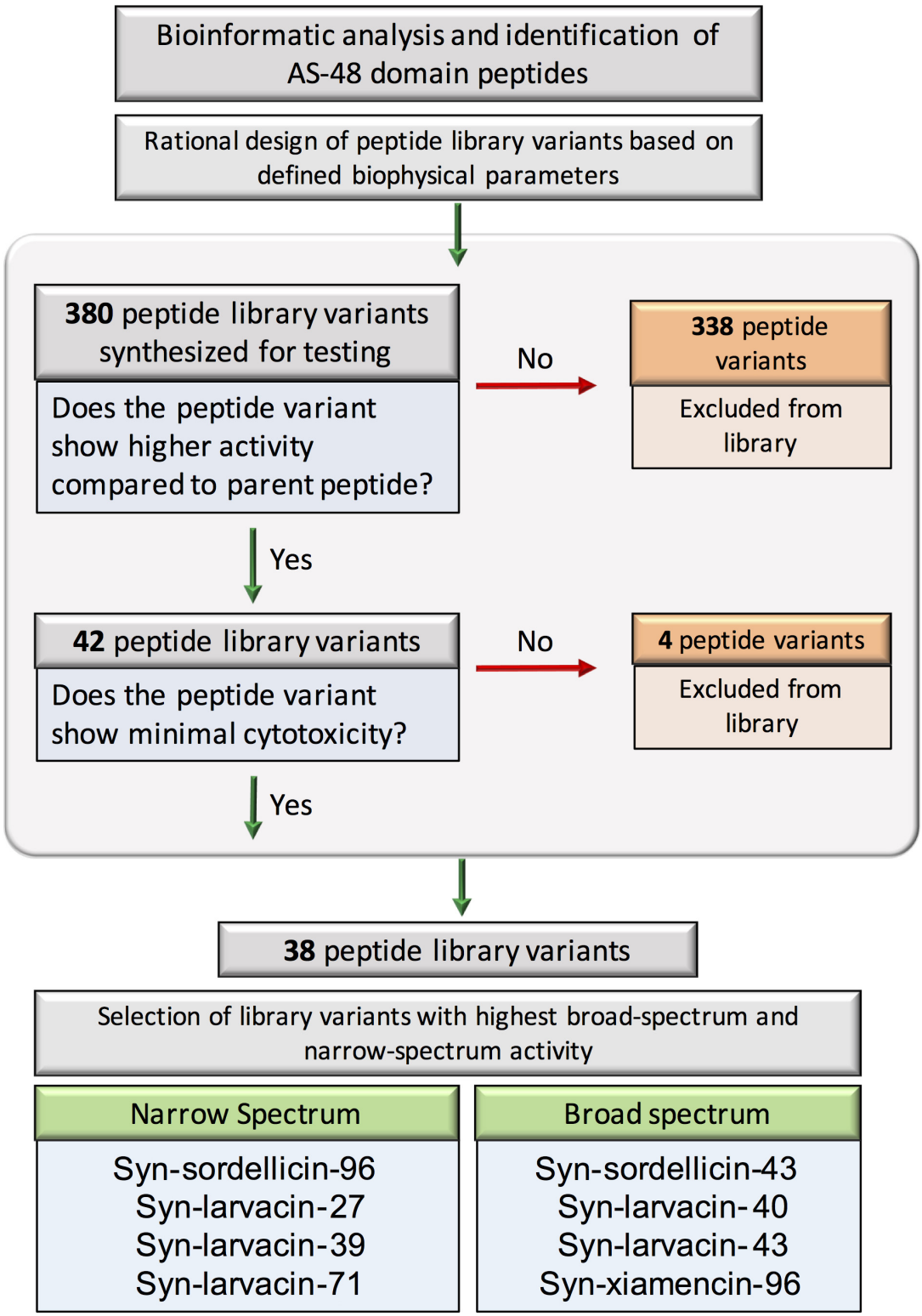

FIGURE 2 | Flowchart showing the general strategy and summary for the design and evaluation of AS-48 domain- based minimal peptide libraries. Bioinformatic analysis and identification of AS-48 domain homologs resulted in 380 total peptide variants initially synthesized for testing. Peptides were excluded if they were outperformed by their parent scaffold in any of the species tested. Additional peptides with significant eukaryotic toxicity were also excluded. Eight peptides were identified to have the highest bactericidal activity either across all four tested species or the highest significant activity against single tested species; these were deemed the representative broad- and narrow-spectrum peptides, respectively and subject to further analysis.

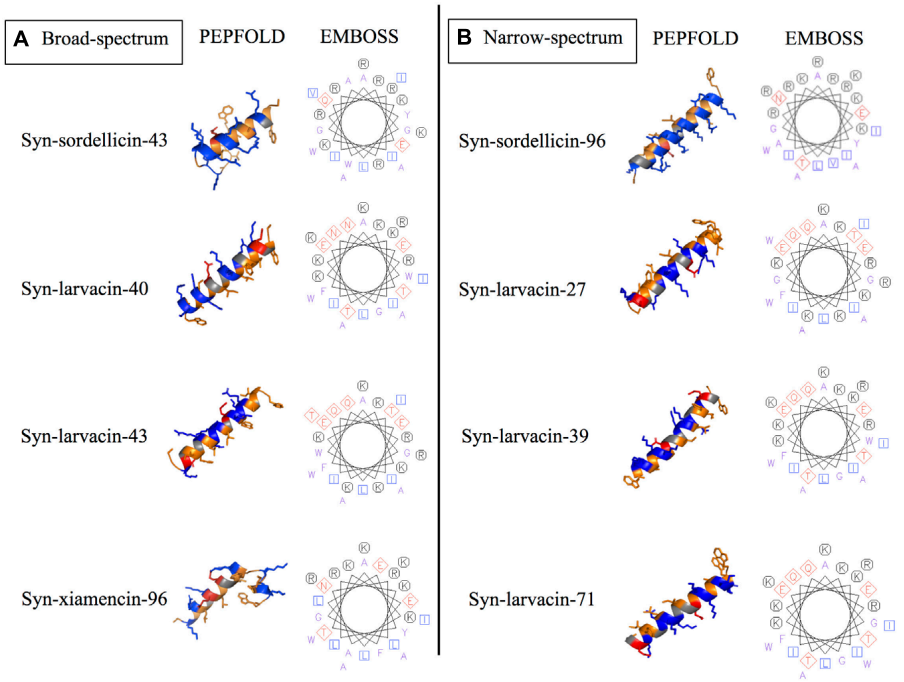

FIGURE 3 | Structural prediction tools display residue substitutions of candidate peptide variants *in silico*. PEPFOLD was used for the prediction of the secondary structure of optimized peptide variants, while EMBOSS software pepwheel was used to visualize the location of residues looking down the helical axis. PyMOL was used to show hydrophobic (orange), cationic (blue), and anionic (red). These secondary structure and helical wheel projections show the chosen representatives for optimized peptide variants that showed broad-spectrum **(A)** and narrow-spectrum activities **(B)**.

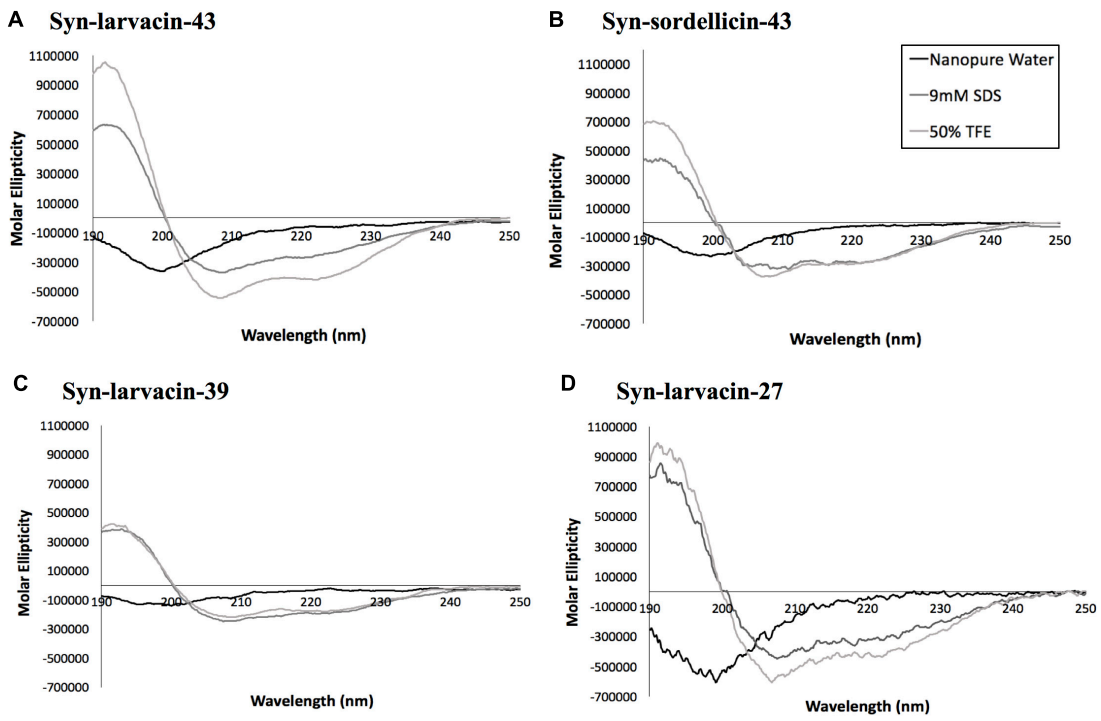

FIGURE 4 | Assessment of secondary structures of candidate peptides by circular dichroism analysis. Broad-spectrum peptides, syn-larvacin-43 **(A)** and syn-sordellicin-43 **(B)**, and narrow-spectrum peptides, syn-larvacin-39 **(C)** and syn-larvacin-27 **(D)** were diluted to 25 μM in either nanopure water, 9 mM SDS or 50% TFE to observe folding behavior in these solvent systems. Spectral scans were collected in triplicate and averaged.

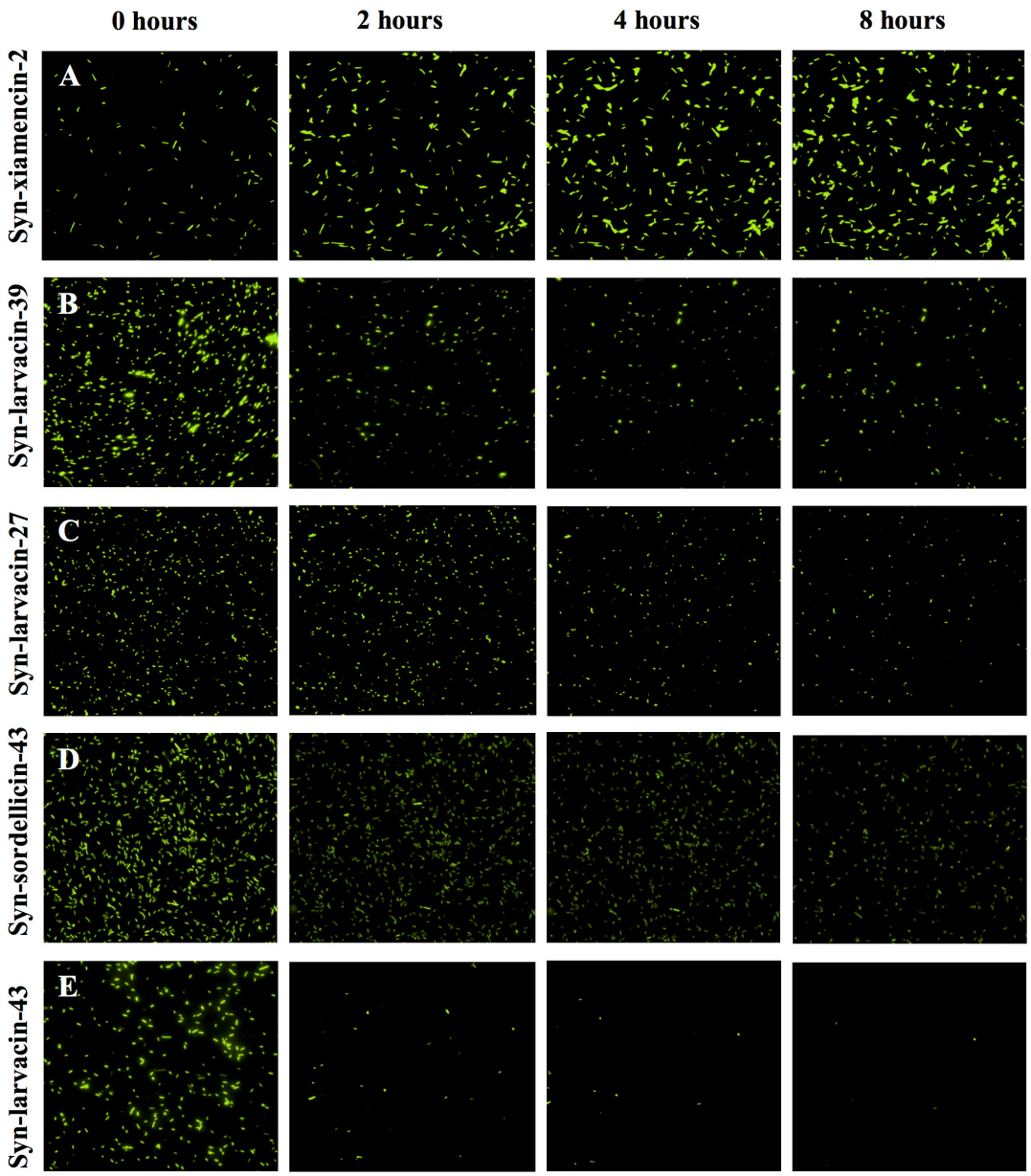

FIGURE 5 | Live-imaging GFP-expressing *E. coli* incubated with optimized peptides. Cells were treated with 16 μM of each peptide variant and fluorescence was captured every 10 min for 8 h. 0, 2, 4, and 8 h time points show the change in fluorescence over time. Syn-xiamencin-2 **(A)** was used as a negative control, as it has no bactericidal activity against *E. coli*. Syn-larvacin-39 **(B)**, syn-larvacin-27 **(C)**, syn-sordellicin-43 **(D)**, and syn-larvacin-43 **(E)** each showed significant decrease in fluorescence over the 8 h, indicating GFP leakage.

design. Namely, MICs can be decreased with amino acid substitutions that increase overall amphipathicity of the peptide. The replacement of short-chained amino acids, alanine and glycine, with a positively charged lysine, was also shown to increase potency of peptide variants. This is likely due to the ability to increase the cationic character of the peptide in key locations that served to increase the overall affinity of the peptide for the anionic bacterial membrane.

Another strategy we employed to increase the antimicrobial activity of the peptide variants was to replace aliphatic and non-polar short-chained amino acids with tryptophan, which increases the affinity of peptides to the interfacial regions of the bacterial membrane, aiding in peptide insertion. In some cases, substitution of glycine, a helix-breaking amino acid, for another amino acid, extends the helical nature of the peptide, which correlates to an overall increased helical propensity (Ong et al., 2014). This may be the cause of the observed increase in antimicrobial activity of some of our peptide variants. For example, replacement of glycine with either lysine or tryptophan, in the 2nd amino acid position on the

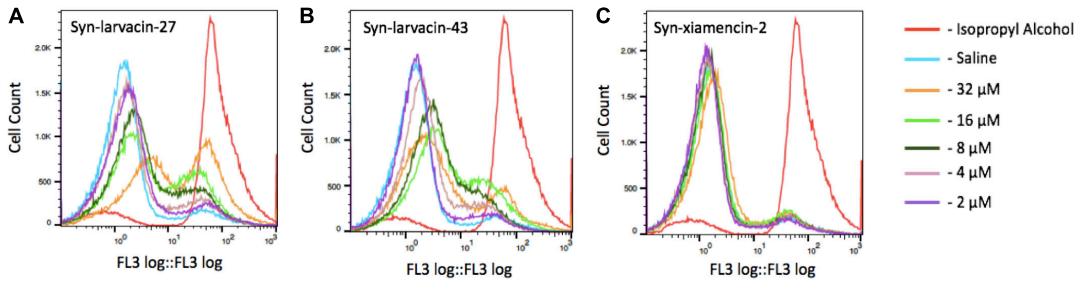

FIGURE 6 | Fluorescence-activated cell sorting of propidium iodide stained *E. coli* cells. Bacterial cells were incubated for 1 h in the presence of isopropyl alcohol, saline or peptide variant. Isopropyl alcohol was used as a positive control, resulting in a large peak within the PI florescence range, indicated a large amount of cell death. While cells treated with syn-larvacin-27 **(A)** and syn-larvacin-43 **(B)** show higher cell counts of PI-stained cells in a dose-dependent manner. Treatment with syn-xiamencin-2 **(C)** was observed to have no significant difference with negative control cells treated with saline.

N-terminus end was seen to improve antimicrobial activity as shown by syn-sordellicin-18, -16, -96, syn-larvacin-39, -40, syn-xiamencin-92, -96, and syn-enterocin-38. The location of the tryptophan substitution also correlated with lower MICs, with trends being observed within the peptide library groups. The syn-larvacin library showed increased antimicrobial activity with the substitution of a tryptophan in the 24th amino acid position, near the C-terminus. This was demonstrated in the cluster of improved antimicrobial activities observed between syn-larvacin-67 through syn-larvacin-72, which all contained tryptophan at the key amino acid position. In the syn-sordellicin and syn-xiamencin libraries, the substitution of tryptophan for the first N-terminal alanine contributed to five of our library candidates showing improved MICs.

A key method for increasing the amphipathic nature of peptide variants, hypothesized to increase peptide penetration into the hydrophobic core of the bacterial membrane, was to flip amino acids within the helical wheel (Wang et al., 2017). Many patterns emerge when further analyzing successful changes in amphipathicity of our optimized peptides. 18 of the 42 peptide variants that had flipped the positively charged amino acid in the 3rd position and the 5th position threonine, serine or alanine showed decreased MIC values. More specifically, our syn-sordellicin library successfully increased bioactivity of eight peptide variants through flipping of the 7th position lysine and 8th position alanine, six peptide variants through flipping the 9th position tyrosine and 13th position glutamic acid, and seven peptide variants through flipping the 16th position arginine and 21st position valine. Similar patterns were observed in the syn-larvacin library, with 11 peptide variants exhibiting increased antimicrobial activity from flipping the 7th position arginine and 9th position phenylalanine. Nine of these peptides were improved by flipping the 17th position lysine and 18th position glycine or tryptophan post substitution, and finally seven peptides showed increased bioactivity as a result of flipping the 19th position arginine and 23rd position isoleucine. These trends emerge in the other libraries as well, indicating the importance of changes in amphipathic nature of peptide scaffolds to increase antibacterial activity.

Despite the large number of library peptide candidates evaluated in this study, we observed remarkably low eukaryotic cytotoxicity rates from most of these peptides, consistent with the low overall observed eukaryotic toxicity inherent in full-length natural AS-48 bacteriocins. This demonstrates that despite the strong alpha-helical nature of the peptide variants, they do not exhibit significant membrane penetrating activity against eukaryotic cells. Significant host cell cytotoxicity was largely limited to four of the fifteen peptides in the syn-sordellicin library, with all other library variants showing appreciably no cytotoxicity to the HaCaT cell lines used in our assays. These data demonstrate that our minimal peptide libraries retain specificity to bacterial membranes, even with amino acid substitutions that improve activity against bacteria.

CONCLUSION

In conclusion, our work demonstrates a general strategy of using minimal domains of natural bacteriocin sequences as scaffolds to design a substantial library of bacteriocin-based variants for evaluation. Given the general limitations in natural product isolation and purification, especially with regard to bacteriocins (Katz and Baltz, 2016), our approach allows for the use of chemical peptide synthesis to generate a large number of bacteriocin-based peptide variants for assessment. Further, the large number of bacteriocin variants that can be tested validate the biophysical approach to improve the activity of the peptide from which the natural product is based. Importantly, we show that genomics tools to discover related sequences of a known bacteriocin can be utilized as scaffolds to construct library variants that show improved activity over the original sequence. Future studies will be needed to determine the efficacy, stability, and toxicity of these peptide candidates *in vivo* and to evaluate their potential for use in clinical, agricultural and industrial settings.

DATA AVAILABILITY STATEMENT

All datasets presented in this study are included in the article/ **Supplementary Material**.

AUTHOR CONTRIBUTIONS

JR, FF, and SL conceived of study and designed all experiments. VK, AG, SO'C, AZ, TM, DH, and KC assisted with experiments. JR and SL wrote the manuscript. KC, SL, JR, DH, and TM edited and assisted with the manuscript preparation including figure design. All authors contributed to the article and approved the submitted version.

FUNDING

This work was supported by a National Institutes of Health (NIH) Innovator Grant (DP2OD008468-01) awarded to SL.

ACKNOWLEDGMENTS

We would like to acknowledge Dr. Giselle Jacobson at the Biophysics Core Facility and Dr. Charles Tessier at the IUSM-South Bend Imaging and Flow Cytometry Core Facility for assistance with CD Spectroscopy and FACS studies, respectively. We would also like to thank Dr. Joshua Shrout at the University of Notre Dame for gifting the PAO1 strain.

SUPPLEMENTARY MATERIAL

The Supplementary Material for this article can be found online at: https://www.frontiersin.org/articles/10.3389/fmicb.2020.589666/full#supplementary-material

Supplementary Figure S1 | Cytotoxic activity of four optimized peptides from the syn-sordellicin library. Peptide dilutions were added to HaCaT cell lines and incubated for 16 h. Cytotoxicity is classified as cell death occurring in >20% of cells.

Supplementary Table S1 | BLASTp search of the alpha-helical domain of the AS-48 sequence from *E. faecalis* identified three species with homologous regions. The sequences are compared by showing fully conserved residues with (*). Residues which have similar biochemical properties are indicated by (:). When residues have opposing charges, they are shown with (.). Blank space shows no conservation of residues.

Supplementary Table S2 | Hemolysis was evaluated using sheep erythrocytes. Incubation with each peptide was performed for 1 h and read at 450 nm. Percent hemolysis above 10% of positive control (Triton X-100) was characterized as significantly hemolytic in our evaluation.

REFERENCES

Alvarez-Sieiro, P., Montalbán-López, M., Mu, D., and Kuipers, O. P. (2016). Bacteriocins of lactic acid bacteria: extending the family. *Appl. Microbiol. Biotechnol.* 100, 2939–2951. doi: 10.1007/s00253-016-7343-9

Arnison, P. G., Bibb, M. J., Bierbaum, G., Bowers, A. A., Bugni, T. S., Bulaj, G., et al. (2013). Ribosomally synthesized and post-translationally modified peptide natural products: overview and recommendations for a universal nomenclature. *Nat. Product Rep.* 30, 108–160.

Boman, H. G. (2003). Antibacterial peptides: basic facts and emerging concepts. *J. Intern. Med.* 254, 197–215. doi: 10.1046/j.1365-2796.2003.01228.x

Brogden, K. A. (2005). Antimicrobial peptides: pore formers or metabolic inhibitors in bacteria? *Nat. Rev. Microbiol.* 3, 238–250. doi: 10.1038/nrmicro1098

Burgos, M. J., Aguayo, M. C., Pulido, R. P., Gálvez, A., and López, R. L. (2015). Inactivation of *Staphylococcus aureus* in oat and soya drinks by enterocin AS-48 in combination with other antimicrobials. *J. Food Sci.* 80, 2030–2034.

Caballero Gómez, N., Abriouel, H., Grande, M. J., Pérez Pulido, R., and Gálvez, A. (2013). Combined treatments of enterocin AS-48 with biocides to improve the inactivation of methicillin-sensitive and methicillin-resistant *Staphylococcus aureus* planktonic and sessile cells. *Int. J. Food Microbiol.* 163, 96–100. doi: 10.1016/j.ijfoodmicro.2013.02.018

Cotter, P. D., Ross, R. P., and Hill, C. (2013). Bacteriocins-a viable alternative to antibiotics? *Nat. Rev. Microbiol.* 11, 95–105. doi: 10.1038/nrmicro2937

Field, D., Blake, T., Mathur, H., O' Connor, P. M., Cotter, P. D., Ross, R. P., et al. (2019). Bioengineering nisin to overcome the nisin resistance protein. *Mol. Microbiol.* 111, 717–731.

Field, D., Cotter, P. D., Hill, C., and Ross, R. P. (2015a). Bioengineering lantibiotics for therapeutic success. *Front. Microbiol.* 6:1363. doi: 10.3389/fmicb.2015.01363

Field, D., Cotter, P. D., Ross, R. P., and Hill, C. (2015b). Bioengineering of the model lantibiotic nisin. *Bioengineered* 5979, 37–41.

Field, D., Gaudin, N., Lyons, F., O'Connor, P. M., Cotter, P. D., Hill, C., et al. (2015c). A bioengineered nisin derivative to control biofilms of *Staphylococcus pseudintermedius* edited by *P. sumby*. *PLoS One* 10:e0119684. doi: 10.1371/journal.pone.0119684

Fields, F. R., Carothers, K. E., Balsara, R. D., Ploplis, V. A., Castellino, F. J., and Lee, S. W. (2018). Rational design of Syn-safencin, a novel linear antimicrobial peptide derived from the circular bacteriocin safencin AS-48. *J. Antibiot.* 71, 592–600. doi: 10.1038/s41429-018-0032-4

Fields, F. R., Manzo, G., Hind, C. K., Janardhanan, J., Foik, I. P., Silva, P. D. C., et al. (2020). Synthetic antimicrobial peptide tuning permits membrane disruption and interpeptide synergy. *ACS Pharmacol. Transl. Sci.* 3, 418–424. doi: 10.1021/acsptsci.0c00001

Fimland, G., Eijsink, V. G. H., and Nissen-Meyer, J. (2002). Mutational analysis of the role of tryptophan residues in an antimicrobial peptide. *Biochemistry* 41, 9508–9515. doi: 10.1021/bi025856q

Fjell, C. D., Hiss, J. A., Hancock, R. E. W., and Schneider, G. (2012). Designing antimicrobial peptides: form follows function. *Nat. Rev. Drug Discov.* 11, 37–51. doi: 10.1038/nrd3591

Gálvez, A., Maqueda, M., Martínez-Bueno, M., and Valdivia, E. (1989). Bactericidal and bacteriolytic action of peptide antibiotic AS-48 against gram-positive and gram-negative bacteria and other organisms. *Res. Microbiol.* 140, 57–68. doi: 10.1016/0923-2508(89)90060-0

Gómez, N. C., Abriouel, H., Grande, J., Pulido, R. P., and Gálvez, A. (2012). Effect of enterocin AS-48 in combination with biocides on planktonic and sessile *Listeria monocytogenes*. *Food Microbiol.* 30, 51–58. doi: 10.1016/j.fm.2011.12.013

González, C., Langdon, G. M., Bruix, M., Gálvez, A., Valdivia, E., Maqueda, M., et al. (2000). Bacteriocin AS-48, a microbial cyclic polypeptide structurally and functionally related to mammalian NK-lysin. *Proc. Natl. Acad. Sci. U.S.A.* 97, 11221–11226. doi: 10.1073/pnas.210301097

Haney, E. F., Mansour, S. C., and Hancock, R. E. W. (2017). Antimicrobial peptides: an introduction. *Methods Mol. Biol.* 1548, 3–22. doi: 10.1007/978-1-4939-6737-7_1

Jenssen, H., Hamill, P., and Hancock, R. E. W. (2006). Peptide antimicrobial agents. *Clin. Microbiol. Rev.* 19, 491–511.

Jiménez, M. A., Barrachi-Saccilotto, A. C., Valdivia, E., Maqueda, M., and Rico, M. (2005). Design, NMR characterization and activity of a 21-residue peptide fragment of bacteriocin AS-48 containing its putative membrane interacting region. *J. Peptide Sci.* 11, 29–36. doi: 10.1002/psc.589

Jin, L., Bai, X., Luan, N., Yao, H., Zhang, Z., Liu, W., et al. (2016). A designed tryptophan- and lysine/arginine-rich antimicrobial peptide with therapeutic potential for clinical antibiotic-resistant *Candida albicans* vaginitis. *J. Med. Chem.* 59, 1791–1799. doi: 10.1021/acs.jmedchem.5b01264

Katz, L., and Baltz, R. H. (2016). Natural product discovery: past, present, and future. *J. Ind. Microbiol. Biotechnol.* 43, 155–176. doi: 10.1007/s10295-015-1723-5

Lamarche, M. J., Leeds, J. A., Amaral, A., Brewer, J. T., Bushell, S. M., Deng, G., et al. (2012). Discovery of LFF571: an investigational agent for clostridium difficile infection. *J. Med. Chem.* 55, 2376–2387. doi: 10.1021/jm201685h

Lv, Y., Wang, J., Gao, H., Wang, Z., Dong, N., Ma, Q., et al. (2014). Antimicrobial properties and membrane-active mechanism of a potential α-helical antimicrobial derived from cathelicidin PMAP-36 edited by R. H. Khan. *PLoS One* 9:e86364. doi: 10.1371/journal.pone.0086364

Mahlapuu, M., Håkansson, J., Ringstad, L., and Björn, C. (2016). Antimicrobial peptides: an emerging category of therapeutic agents. *Front. Cell. Infect. Microbiol.* 6:194. doi: 10.3389/fcimb.2016.00194

Maupetit, J., Derreumaux, P., and Tuffery, P. (2009). PEP-FOLD: an online resource for de novo peptide structure prediction. *Nucleic Acids Res.* 37(Suppl. 2), 498–503.

Mikut, R., Ruden, S., Reischl, M., Breitling, F., Volkmer, R., and Hilpert, K. (2016). Improving short antimicrobial peptides despite elusive rules for activity. *Biochim. Biophys. Acta Biomembr.* 1858, 1024–1033. doi: 10.1016/j.bbamem.2015.12.013

Montalbán-López, M., Martínez-Bueno, M., Valdivia, E., and Maqueda, M. (2011). Expression of linear permutated variants from circular enterocin AS-48. *Biochimie* 93, 549–555. doi: 10.1016/j.biochi.2010.11.011

Montalbán-López, M., Spolaore, B., Pinato, O., Martínez-Bueno, M., Valdivia, E., Maqueda, M., et al. (2008). Characterization of linear forms of the circular enterocin AS-48 obtained by limited proteolysis. *FEBS Lett.* 582, 3237–3242. doi: 10.1016/j.febslet.2008.08.018

Morita, S., Tagai, C., Shiraishi, T., Miyaji, K., and Iwamuro, S. (2013). Differential mode of antimicrobial actions of arginine-rich and lysine-rich histones against gram-positive *Staphylococcus aureus*. *Peptides* 48, 75–82. doi: 10.1016/j.peptides.2013.07.025

Mullane, K., Lee, C., Bressler, A., Buitrago, M., Weiss, K., Dabovic, K., et al. (2015). Multicenter, randomized clinical trial to compare the safety and efficacy of LFF571 and vancomycin for clostridium difficile infections. *Antimicrob. Agents Chemother.* 59, 1435–1440. doi: 10.1128/aac.04251-14

Murinda, S. E., Rashid, K. A., and Roberts, R. F. (2003). In vitro assessment of the cytotoxicity of nisin, pediocin, and selected colicins on simian virus 40–transfected human colon and vero monkey kidney cells with trypan blue staining viability assays. *J. Food Protect.* 66, 847–853. doi: 10.4315/0362-028x-66.5.847

Nakajima, Y. (2003). "Mode of action and resistance mechanisms of antimicrobial macrolides," in *Macrolide Antibiotics: Chemistry, Biology, and Practice*, Second Edn, ed. S. Ômura (Cambridge, MA: Academic Press), 453–499. doi: 10.1016/b978-012526451-8/50011-4

Nguyen, L. T., Chau, J. K., Perry, N. A., de Boer, L., Zaat, S. A. J., and Vogel, H. J. (2010). Serum stabilities of short tryptophan- and arginine-rich antimicrobial peptide analogs. *PLoS One* 5:e12684. doi: 10.1371/journal.pone.0012684

Ong, Z. Y., Wiradharma, N., and Yang, Y. Y. (2014). Strategies employed in the design and optimization of synthetic antimicrobial peptide amphiphiles with enhanced therapeutic potentials. *Adv. Drug Deliv. Rev.* 78, 28–45. doi: 10.1016/j.addr.2014.10.013

Rosenberg, M., and Goldblum, A. (2006). Computational protein design: a novel path to future protein drugs. *Curr. Pharm. Des.* 12, 3973–3997. doi: 10.2174/138161206778743655

Sánchez-Hidalgo, M., Montalbán-López, M., Cebrián, R., Valdivia, E., Martínez-Bueno, M., and Maqueda, M. (2011). AS-48 bacteriocin: close to perfection. *Cell. Mol. Life Sci.* 68, 2845–2857. doi: 10.1007/s00018-011-0724-4

Schiffer, M., and Edmundson, A. B. (1967). Use of helical wheels to represent the structures of proteins and to identify segments with helical potential. *Biophys. J.* 7, 121–135. doi: 10.1016/s0006-3495(67)86579-2

Torres, M. D. T., Sothiselvam, S., Lu, T. K., and de la Fuente-Nunez, C. (2019). Peptide design principles for antimicrobial applications. *J. Mol. Biol.* 431, 3547–3567. doi: 10.1016/j.jmb.2018.12.015

Uggerhøj, L. E., Poulsen, T. J., Munk, J. K., Fredborg, M., Sondergaard, T. E., Frimodt-Moller, N., et al. (2015). Rational design of alpha-helical antimicrobial peptides: Do's and Don'ts. *ChemBioChem* 16, 242–253. doi: 10.1002/cbic.201402581

Wang, C. K., Shih, L. Y., and Chang, K. Y. (2017). Large-scale analysis of antimicrobial activities in relation to amphipathicity and charge reveals novel characterization of antimicrobial peptides. *Molecules* 22:2037. doi: 10.3390/molecules22112037

Wiegand, I., Hilpert, K., and Hancock, R. E. W. (2008). Agar and broth dilution methods to determine the minimal inhibitory concentration (MIC) of antimicrobial substances. *Nat. Protoc.* 3, 163–175. doi: 10.1038/nprot.2007.521

Conflict of Interest: The authors declare that the research was conducted in the absence of any commercial or financial relationships that could be construed as a potential conflict of interest.

frontiers in Microbiology

ORIGINAL RESEARCH
published: 20 November 2020
doi: 10.3389/fmicb.2020.575334

Conjugation of Synthetic Polyproline Moietes to Lipid II Binding Fragments of Nisin Yields Active and Stable Antimicrobials

*Jingjing Deng[1], Jakob H. Viel[1], Vladimir Kubyshkin[2,3], Nediljko Budisa[2,3] and Oscar P. Kuipers[1]**

[1] Department of Molecular Genetics, University of Groningen, Groningen, Netherlands, [2] Institute of Chemistry, Technical University of Berlin, Berlin, Germany, [3] Department of Chemistry, University of Manitoba, Winnipeg, MB, Canada

Coupling functional moieties to lantibiotics offers exciting opportunities to produce novel derivatives with desirable properties enabling new functions and applications. Here, five different synthetic hydrophobic polyproline peptides were conjugated to either nisin AB (the first two rings of nisin) or nisin ABC (the first three rings of nisin) by using click chemistry. The antimicrobial activity of nisin ABC + O6K3 against *Enterococcus faecium* decreased 8-fold compared to full-length nisin, but its activity was 16-fold better than nisin ABC, suggesting that modifying nisin ABC is a promising strategy to generate semi-synthetic nisin hybrids. In addition, the resulting nisin hybrids are not prone to degradation at the C-terminus, which has been observed for nisin as it can be degraded by nisinase or other proteolytic enzymes. This methodology allows for getting more insight into the possibility of creating semi-synthetic nisin hybrids that maintain antimicrobial activity, in particular when synthetic and non-proteinaceous moieties are used. The success of this approach in creating viable nisin hybrids encourages further exploring the use of different modules, e.g., glycans, lipids, active peptide moieties, and other antimicrobial moieties.

Keywords: click chemistry, RiPPs, lantibiotics, nisin, polyproline peptides

OPEN ACCESS

Edited by:
Paul David Cotter, Teagasc Food Research Centre, Ireland

Reviewed by:
Ratchaneewan Aunpad, Thammasat University, Thailand
Hilario C. Mantovani, Universidade Federal de Viçosa, Brazil

***Correspondence:**
Oscar P. Kuipers
o.p.kuipers@rug.nl

Specialty section:
This article was submitted to Antimicrobials, Resistance and Chemotherapy, a section of the journal Frontiers in Microbiology

Received: *23 June 2020*
Accepted: *30 October 2020*
Published: *20 November 2020*

Citation:
Deng J, Viel JH, Kubyshkin V, Budisa N and Kuipers OP (2020) Conjugation of Synthetic Polyproline Moietes to Lipid II Binding Fragments of Nisin Yields Active and Stable Antimicrobials. Front. Microbiol. 11:575334. doi: 10.3389/fmicb.2020.575334

INTRODUCTION

Nisin is the first discovered and the best studied lantibiotic and it is produced by *Lactococcus lactis* (Rogers, 1928). In addition to its natural presence in fermented foods, nisin has been applied as a food preservative for many decades, because of its excellent activity against food spoilage (Hansen and Sandine, 1994; Gharsallaoui et al., 2016). Beyond its role in food safety and preservation, nisin has potential therapeutic applications. It is for instance effective against many Gram-positive antibiotic-resistant organisms, such as methicillin-resistant *Staphylococcus aureus* (MRSA) and vancomycin-resistant *Enterococcus* (VRE) (Shin et al., 2016). The exceptional activity of nisin is derived from a unique structure, containing one lanthionine and four methyllanthionine rings, which has a dual mode of action. The first two rings (AB) form a lipid II recognition site. By binding to the peptidoglycan precursor lipid II, nisin inhibits cell wall biosynthesis. The last two rings (DE), which are connected to rings ABC through a hinge region, constitute a membrane insertion domain. After rings AB dock to lipid II (Brötz et al., 1998), rings DE and the tail can insert into the bacterial membrane

to create pores, where nisin forms pores (Lubelski et al., 2008). Nisin's dual mode of action increases its antimicrobial activity, and decreases the chance of resistance development in target organisms. These features make nisin an attractive candidate for development into an antibiotic alternative. Unfortunately, nisin is readily degraded in the gut, which precludes oral delivery. Also, the administering of nisin by injection, especially at its full-length, is limited by the instability of its dehydro-residues. If possible, these problems should be addressed to broaden the scope of nisin application in the therapeutic setting. A promising strategy to achieve this has been provided by the chemical coupling of specific (protease resistant) moieties to nisin, and semi-synthetic fragments of nisin. This approach allows for the synthesis of novel derivatives with useful properties like increased stability, alleviating some of nisin's characteristics that are problematic in its potential role as an antibiotic alternative.

The coupling of peptides to compatible moieties can be achieved through the widely used click chemistry method (Ahmad Fuaad et al., 2013). "Copper (I)-catalyzed azide-alkyne cycloaddition (CuAAC)" is the most common reaction representing the click chemistry. It is a region selective copper (I) catalytic cycloaddition reaction between an azide and an alkyne leading to the formation of a triazole. The molecules connected to the respective reagents are effectively "clicked" together (Kolb et al., 2001). Due to its reliability, specificity, biocompatibility, easiness to perform, and mild reaction conditions, click chemistry is being used increasingly in diverse areas, such as bioconjugation, drug design and polymer science (Thirumurugan et al., 2013; McKay and Finn, 2014; Jiang et al., 2019). The success of click chemistry in the field of peptide modification can be attributed to the resulting triazole ring which resembles an amide bond, and which increases the stability of the resulting molecule. This is achieved at least in part by increasing the molecule's resistance to proteases, as the triazole aligns with the biological targets through hydrogen bonding and dipole interactions (Ahmad Fuaad et al., 2013). Peptide coupling through click chemistry has been the subject of several studies toward the development of target-specific bacterial probes and expanding application possibilities of this method (Arnusch, 2008; Yoganathan et al., 2011; Oldach et al., 2012; Slootweg et al., 2013a, 2014; Koopmans et al., 2015; Bolt et al., 2018). A prominent example of applying click chemistry to enhance lantibiotics, is that of coupling nisin AB to lipid moieties (Koopmans et al., 2015). The resulting hybrid molecules exhibited increased stability, as well as potent antimicrobial activity against drug-susceptible and -resistant strains of Gram-positive bacteria. In other studies, the lipid II-binding motif (rings AB) of nisin has been conjugated with various functional molecules (Arnusch, 2008; Koopmans et al., 2015; Bolt et al., 2018).

Here, a range of experiments was designed for the synthesis of nisin hybrids by coupling specific synthetic polyproline peptides, some of which containing cationic residues, to either nisin AB or nisin ABC. These polyproline peptides (**Figure 1**) were designed based on a polyproline structural skeleton using a proline analog [(*2S,3aS,7aS*)-octahydroindole-2-carboxylic acid, Oic] to display a linear and hydrophobic structure affine to a lipid membrane (Kubyshkin and Budisa, 2018; Kubyshkin et al., 2019). The selected properties of these nisin hybrids should aid in the membrane translocation of their C-terminal region and, as the molecular weight of the clicked polyproline moieties ranges between 0.5 and 1.5 kDa, the resulting molecules remain well under nisin in size. Hypothetically, the lipid-II targeting nisin AB would guide the conjugate to the bacterial membrane, where the hydrophobic tail would flip into the membrane core, tightly anchoring the conjugate. The newly synthesized nisin hybrids were compared to nisin with regard to their antimicrobial activity, and susceptibility to proteolytic degradation.

MATERIALS AND METHODS

Bacterial Strains and Plasmids

Indicator strains and plasmids used in this work are given in **Table 1**.

Preparation of Nisin AB-Azide

Nisin AB was purified in accordance with protocols reported previously (Slootweg et al., 2013b). Briefly, nisin (180 mg) was dissolved in 150 mL Tris buffer (5 mmol Tris acetate, 5 mmol $CaCl_2$, 25 mmol sodium acetate, pH 7.0) and the solution was cooled on ice for 15 min. Then trypsin (15 mg) was added and warmed up to room temperature for 15 min. The reaction was performed at 30°C for 16 h and an extra 15 mg trypsin was added. After 24 h incubation, another 15 mg trypsin was added and the reaction was performed for another 24 h. The reaction mixture was acidified with hydrochloric acid (1 M) to pH 4.0 followed by adding 3 mL acetonitrile and concentrated *in vacuo*. The pure nisin AB was purified from the mixture by RP-HPLC with the water-acetonitrile gradient mobile phase containing trifluoroacetic acid (0.1%) and lyophilized to obtain a white powder (20 mg). Nisin AB (10 mg, 8.6 μmol) was dissolved in *N,N*-dimethylformamide (DMF) (100 μl) and azidopropylamine (44 μl, 43.2 mg, 432 μmol), *N,N*-diisopropylethylamine (DIPEA, 6 μl, 34.8 μmol), and (benzotriazol-1-yloxy)-tris-(dimethylamino) phosphonium hexafluorophosphate (BOP, 7.6 mg, 17.2 μmol) or (benzotriazol-1-yl-oxy)-tris-(pyrrolidino)phosphonium hexafluorophosphate (PyBOP, 9 mg, 17.2 μmol) were added. The reaction was vortexed for 20 min and subsequently quenched with 5 mL buffer (water : acetonitrile, 95:5 vol+ 0.1% trifluoroacetic acid). The reaction mixture was purified by RP-HPLC with the water-acetonitrile gradient mobile phase containing trifluoroacetic acid (0.1%) and pure nisin AB-azide was lyophilized to obtain a white powder (8 mg).

Preparation of Nisin ABC-Azide

α-chymotrypsin was used to digest nisin to generate nisin ABC. Nisin (180 mg) was dissolved in 150 mL Tris buffer (25 mmol Tris acetate, pH7.5) and the solution was cooled on ice for 15 min. Then α-chymotrypsin (15 mg) was added and warmed up to room temperature for 15 min.

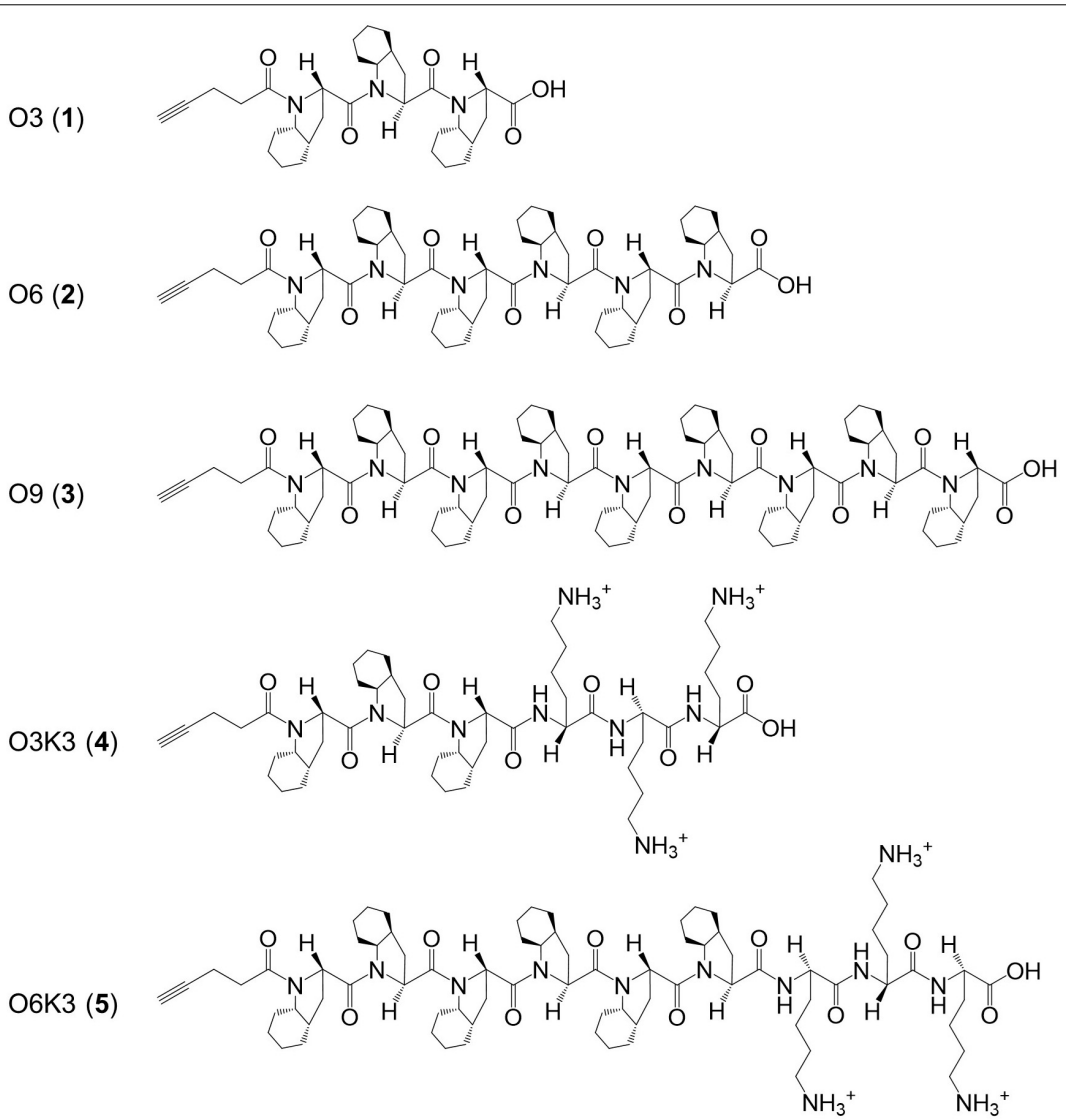

FIGURE 1 | Structure of the hydrophobic polyproline peptides O3, O6, O9, O3K3, and O6K3 for putative membrane anchoring. The peptides were constructed with a hydrophobic proline analog (*2S,3aS,7aS*)-octahydroindole-2-carboxylic acid (Oic, designated as O) and lysine residues (Lys, K).

TABLE 1 | Strains and plasmids used in this work.

Indicator strains	**Characteristics**	**References**
Micrococcus flavus		Lab collection
Lactococcus lactis NZ9000		Lab collection
Staphylococcus aureus MW2	Methicillin resistant (MRSA)	The University Medical Center Groningen, The Netherlands
Enterococcus faecium LMG 16003	Avaparicin and vancomycin resistant (VRE)	Laboratory of Microbiology, Gent, Belgium
Listeria monocytogenes LMG 10470		Montalbán-López et al., 2018
Plamids	**Characteristics**	**References**
pEmpty	pNZ8048, pSH71 origin of replication, P_{nisA} promoter and empty multiple cloning site, chloramphenicol resistance	Kuipers et al., 1998
pNSR	pNZ-SV-SaNSR, pSH71 origin of replication, expression of nsr under the control of P_{nisA} promoter, chloramphenicol resistance	Khosa et al., 2013, 2016

The enzymatic digestion was performed same as described for nisin AB. Nisin ABC was purified from the mixture by RP-HPLC with the water-acetonitrile gradient mobile phase containing trifluoroacetic acid (0.1%) and then lyophilized to obtain a white powder (20 mg). Nisin ABC (10 mg, 6.5 μmol) was dissolved in DMF (50 μl). The azide-coupling reaction was performed same as described for nisin AB.

Preparation of the Hydrophobic Polyproline Peptides

The polyproline-containing peptides were prepared using a manual Fmoc-based solid-phase peptide synthesis scheme as described (Kubyshkin and Budisa, 2018). The sequences were grown on 2-clorotrityl resins pre-loaded with either Fmoc-Oic-OH or Fmoc-Lys (Boc)-OH (Fmoc = fluorenylmethyloxycarbonyl, Boc = tert-butyloxycarbonyl). The resin loading was estimated at 0.7–0.8 mmol/g. The synthesis was performed in DMF using 2.5 equiv. of the Fmoc-amino acid pre-activated with the mixture of 2.5 equiv. 2-(1H-benzotriazole-1-yl)-1,1,3,3-tetramethylaminium tetrafluoroborate (TBTU) and 2.5 equiv.1-hydroxybenzotriazole (HOBt) mixture under addition of 5 equiv. DIPEA. The N-terminal pentynyl moiety was installed under coupling with pentynoic acid under same activation conditions. The Fmoc group was removed by treatment with 22 vol% piperidine in DMF. The final peptides were cleaved off the resin by treatment with hexafluoroisopropanol : dichloromethane (1:3, vol: vol) mixture. The peptides were additionally purified on short silica gel columns using dichloromethane-methanol gradient elution. Pentynyl-(Oic)9-OH (O9) peptide was additionally purified by precipitation from methanol. The Boc-group was removed from the lysine side-chains by treatment with 4 M hydrogen chloride in dioxane. The identity and purity of the final peptides were confirmed by mass-spectra (ESI-Orbitrap) and ^{1}H-NMR spectra (CD_3OD, 700 MHz). The peptides were obtained in 10–50 mg quantities.

Click Chemistry

A stock solution of $CuSO_4$ (10 mg, 100 mM), sodium ascorbate (200 mg, 1 M) 2-(4-((bis((1-(tert-butyl)-1H-1,2,3-triazol-4-yl)methyl)amino)methyl)-1H-1,2,3-triazol-1-yl)-acetic acid (BTTAA, 25 mg, 50 mM), and tris((1-hydroxy-propyl-1H-1,2,3-triazol-4-yl)methyl)amine (THPTA, 25 mg, 250 mM) in deionized water and a stock solution of O3 (1 mg, 36 mM), O6 (1.8 mg, 36 mM), O9 (2.6 mg, 36 mM), O3K3 (1.9 mg, 36 mM) and O6K3 (2.7 mg, 36 mM) in DMF (50 μl) were prepared, aliquoted and stored at −20°C for further use. Firstly, nisin AB-azide (25 μg, 0.02 μmol) or nisin ABC-azide (40 μg, 0.02 μmol) were dissolved in 100 mM phosphate buffer (pH7.0, final reaction volume: 200 μl). Then, the appropriate O3, O6, O9, O3K3, or O6K3 (5 μl, 0.18 μmol) and $CuSO_4$ (4 μl, 0.4 μmol) : THPTA (8 μl, 2 μmol) or BTTAA (40 μl, 2 μmol)-premix were added followed by the addition of sodium ascorbate (20 μl, 20 μmol). The reaction was performed at 37°C for 1 h and purified directly by RP-HPLC with the water-acetonitrile gradient mobile phase containing trifluoroacetic acid (0.1%). The pure product-containing fractions were lyophilized to obtain nisin hybrids **6–15** as white fluffy powders (**Figure 2**). The reaction was further scaled up in ratio to obtain more products.

Agar Well Diffusion Assay

Agar well diffusion assay against *Micrococcus flavus* was performed as described previously (van Heel et al., 2013). 0.15 nmol of each sample was added to each well. The agar plate was incubated at 30°C overnight, after which the zone of inhibition was measured.

Determination of the Minimal Inhibitory Concentration (MIC)

All samples were resuspended in 0.05% aqueous acetic acid solution and the peptide amount was quantified by HPLC according to Schmitt et al. (Schmitt et al., 2019). The indicator strains MW2-MRSA, *Enterococcus faecium, Listeria monocytogenes*, *and Lactococcus lactis* were first streaked on GM17 plate and cultured overnight. The peptide samples were diluted with 0.05% acetic acid to a concentration of 40–320 μM (depending on the estimated activity of the peptide and the strain tested). The MIC value test was performed according to Wiegand et al. (2008).

RESULTS

Production of Nisin AB-Azide and Nisin ABC-Azide

Nisin was digested using trypsin and chymotrypsin, respectively, to generate nisin AB and nisin ABC fragments (**Figure 2**). The desired truncated nisin molecules were purified from the digestion mixture with yields in the milligram range, in accordance with protocols reported previously (Slootweg et al., 2013b). After purification, an azide linker was added to the C-terminus of the acquired nisin fragments. Since the truncated variants with the azide linker were needed in relatively large quantities for the generation of the semi-synthetic analogs, the previously reported peptide coupling procedure was optimized for this study. Initially, addition of the azide linker was done by coupling azidopropylamine to nisin AB in the presence of BOP as the coupling reagent. HPLC analysis of the reactions performed under these conditions showed substantial amounts of substrate remained unreacted, resulting in a reaction efficiency of only 7.4% (**Supplementary Figure 1**). Prolonging the reaction time to 1 h did not increase the conversion. However, by substituting the coupling reagent BOP for PyBOP, the reaction efficiency could be increased to 89% (**Supplementary Figure 1**). For reactions of this nature, PyBOP was shown to be a better coupling reagent than to BOP. Using the optimized conditions from the above experiment, azidopropylamine was coupled to nisin AB and

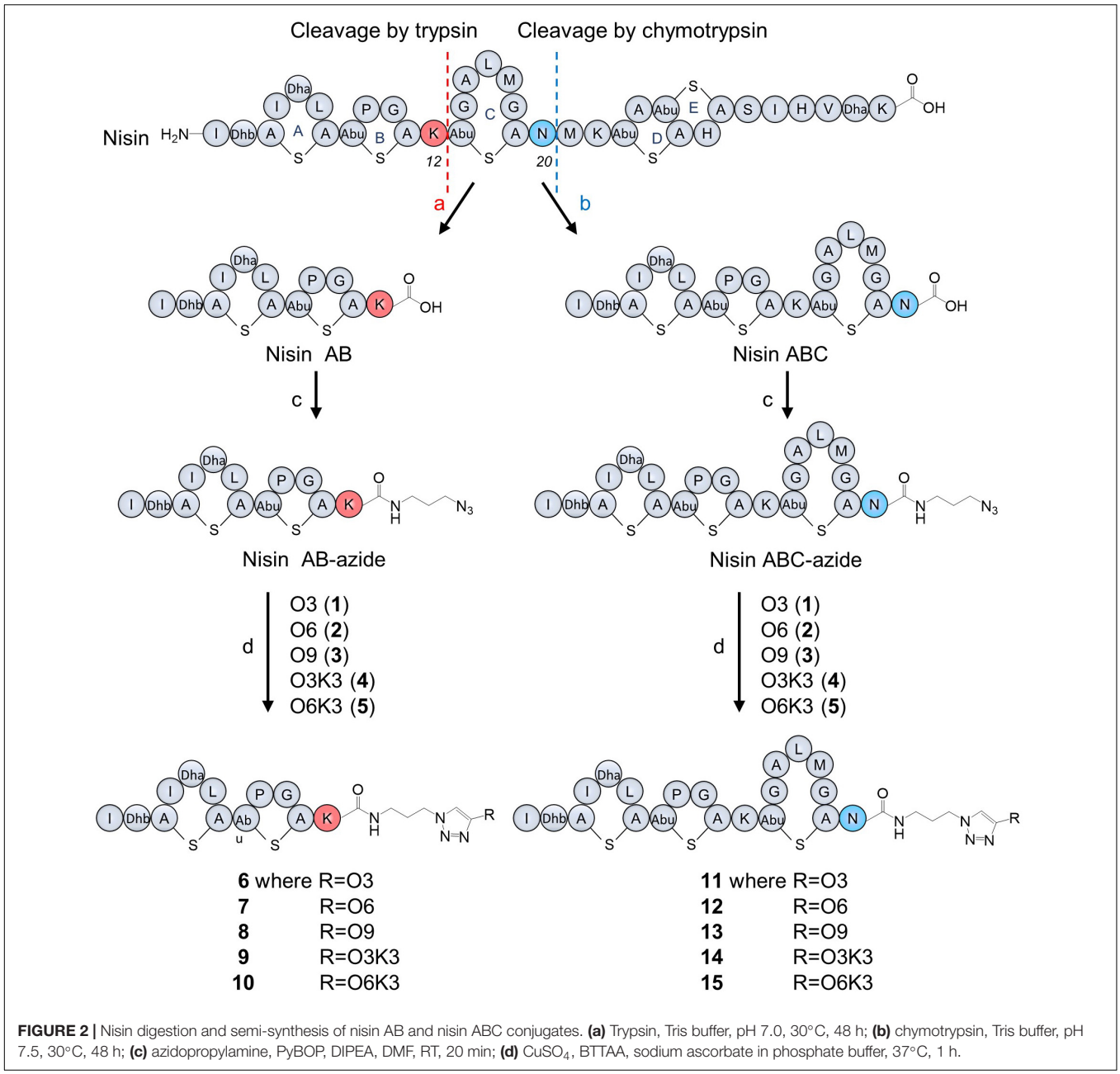

FIGURE 2 | Nisin digestion and semi-synthesis of nisin AB and nisin ABC conjugates. **(a)** Trypsin, Tris buffer, pH 7.0, 30°C, 48 h; **(b)** chymotrypsin, Tris buffer, pH 7.5, 30°C, 48 h; **(c)** azidopropylamine, PyBOP, DIPEA, DMF, RT, 20 min; **(d)** $CuSO_4$, BTTAA, sodium ascorbate in phosphate buffer, 37°C, 1 h.

nisin ABC in a reaction containing PyBOP/DIPEA to give nisin AB-azide and nisin ABC-azide in 89 and 87% yield, respectively, which was purified by HPLC and characterized by MALDI-TOF. The resulting nisin AB-azide and nisin ABC-azide contain convenient handles for ligation to alkynes via CuAAC.

Production of Nisin AB and Nisin ABC Conjugates

Five hydrophobic polyproline peptides (**1**–**5**) were coupled to nisin AB-azide and nisin ABC-azide (**Figure 2**). The first click reaction was attempted with O3 (**1**) and nisin AB-azide in the presence of THPTA as copper (I)-stabilizing ligand. Analysis by HPLC showed that a good amount of product was formed under these reaction conditions. Increasing the reaction temperature to 50°C and extending the reaction time to 2 h led to degradation rather than increased conversion. The conversion could however be increased by using BTTAA as substitute for THPTA as copper (I)-stabilizing ligand improved the conversion. The best results were obtained using 9 equiv. O3, 20 equiv. $CuSO_4$, 100 equiv. BTTAA and 1,000 equiv. sodium ascorbate, reacted at 37°C for 1 h. Under these optimized conditions, the click reaction of nisin AB-azide and nisin ABC-azide with the five hydrophobic polyproline peptides (**1**–**5**) were carried out successfully to give semi-synthetic nisin

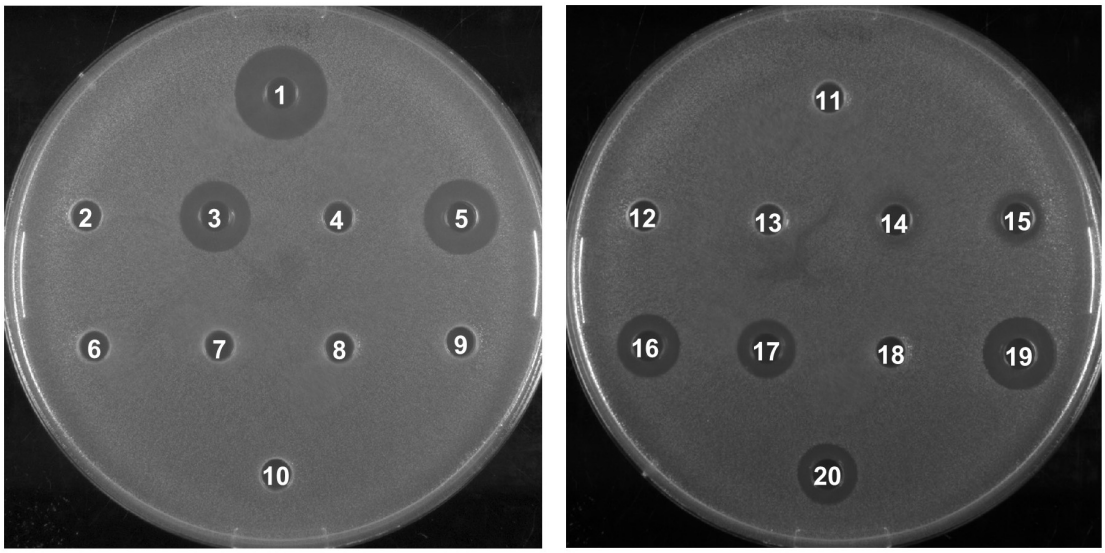

FIGURE 3 | Antimicrobial activity of semi-synthetic nisin hybrids against *M. flavus* by agar well diffusion assay. 1: Nisin; 2: Nisin AB; 3: Nisin ABC; 4: Nisin AB-azide; 5: Nisin ABC-azide; 6: O3; 7: O6; 8: O9; 9: O3K3; 10: O6K3; 11: Nisin AB + O3; 12: Nisin AB + O6; 13: Nisin AB + O9; 14: Nisin AB + O3K3; 15: Nisin AB + O6K3; 16: Nisin ABC + O3; 17: Nisin ABC + O6; 18: Nisin ABC + O9; 19: Nisin ABC + O3K3; 20: Nisin ABC + O6K3.

TABLE 2 | MIC value (μM) of nisin AB and nisin ABC conjugates.

Peptides	MW2-MRSA	*E. faecium*	*L. monocytogenes*	*L. lactis* NZ9000 (pEmpty)	*L. lactis* NZ9000 (pNSR)
Nisin	5.0	0.31	2.5	0.16	2.5
O3	>320	>320	>320	>320	ND
O6	>320	>320	>320	>320	ND
O9	>320	>320	>320	>320	ND
O3K3	>160	>160	>160	>160	ND
O6K3	>80	>80	>80	>80	ND
Nisin AB	>320	160	>320	>40	ND
Nisin AB + O3	ND	ND	ND	>40	ND
Nisin AB + O6	ND	ND	ND	20	ND
Nisin AB + O9	ND	ND	ND	5.0	ND
Nisin AB + O3K3	ND	ND	ND	>40	ND
Nisin AB + O6K3	ND	ND	ND	10	ND
Nisin ABC	40	40	40	5.0	ND
Nisin ABC + O3	>80	20	>80	5.0	ND
Nisin ABC + O6	80	5	20	5.0	5.0
Nisin ABC + O9	>80	10	40	5.0	ND
Nisin ABC + O3K3	80	40	80	2.5	ND
Nisin ABC + O6K3	80	2.5	10	2.5	2.5

In red: MIC values that are improved in comparison to one of nisinAB or nisin ABC. In blue: the effect of the nisinase presence is depicted. ND: not determined.

hybrids **6–15** in 42–54% yields. The resulting semi-synthetic nisin hybrids **6–15** were further characterized by MALDI-TOF.

Antimicrobial Activity of Nisin AB and Nisin ABC Conjugates

To investigate the biological activity of the nisin hybrids, an agar well diffusion assay and a growth inhibition assay were performed. *M. flavus* was used as the indicator strain for the agar well diffusion assay, and 0.15 nmol of each sample was added to each well (**Figure 3**). The results showed that nisin AB and five hydrophobic polyproline moieties (**1–5**) are not active alone and nisin has the highest activity. Of the nisin AB conjugates, nisin AB + O6K3 is the only active one. Notably, with the exception of nisin ABC + O9, all four nisin ABC conjugates showed activity. Most notably the activity of nisin ABC + O3K3 is considerably higher than that of nisin ABC. Antimicrobial activity of all compounds was tested by growth inhibition assays against two clinically relevant Gram-positive

pathogens, i.e., methicillin resistant *S. aureus* and vancomycin resistant *E. faecium*, as well as *L. monocytogenes*, and *L. lactis*. Their minimal inhibitory concentration (MIC) was determined using an established broth microdilution assay (**Table 2**), using nisin as a positive control. Nisin AB was devoid of activity at the highest concentration tested except against *E. faecium*. Since of the nisin AB conjugates only nisin AB + O6K3 showed activity in the agar well diffusion assay, they were only tested against *L. lactis*. In this growth inhibition assay, nisin AB + O9 showed the best activity among the five nisin AB conjugates. Nisin ABC conjugates displayed a retained or even increased activity against *E. faecium* and *L. lactis* compared to nisin ABC alone, whereas activity against MW2-MRSA diminished. The antimicrobial activity of nisin ABC + O6K3 against *E. faecium*, *L. monocytogenes*, and *L. lactis* decreased only 8-, 4-, and 12-fold compared to full nisin, respectively. Strikingly, its antimicrobial activity against *E. faecium*, *L. monocytogenes*, and *L. lactis* increased 16-, 4-, and 2-fold compared to nisin ABC, respectively, and increased all twice compared to nisin ABC + O6, respectively. Compared to nisin ABC, nisin ABC + O6K3 displayed improved activity against *E. faecium*, *L. monocytogenes*, and *L. lactis* but decreased activity against MW2-MRSA while nisin ABC + O9 showed enhanced activity against *E. faecium* although activity against other strains was retained or even reduced. An additional test was performed to assess if the resistance to proteolytic degradation of the semi-synthetic nisin hybrids had improved compared to the parent compound. Nisin, nisin ABC + O6K3, and nisin ABC + O6 were exposed to the nisin resistance protein (NSR), a peptidase that cleaves the linear C-terminus of nisin. For this experiment, an activity test was performed against the NSR producing strain *L. lactis* NZ9000 (pNSR). In this test, NSR conferred its producing strain over 16-fold resistance toward nisin in MIC, caused by the proteolytic cleavage at the C-terminal tail of nisin. The hybrids Nisin ABC + O6K3 and nisin ABC + O6 bypassed this nisin resistance mechanism, having identical MICs against NZ9000 regardless of it producing NSR.

DISCUSSION

In this research, an efficient and direct method for the preparation of nisin hybrids was developed. Nisin AB and nisin ABC fragments were obtained by enzymatic digestion of nisin and these fragments were subsequently C-terminally functionalized with azidopropylamine. Five hydrophobic polyproline peptides (without and with cationic residues) were synthesized and coupled to nisin AB-azide and nisin ABC-azide by using click chemistry. Ten newly synthesized nisin hybrids were obtained and their antimicrobial activities were tested. The agar diffusion assay showed that the activity of nisin ABC conjugates are much better than nisin AB conjugates. These results are in line with previous studies that showed that variants lacking ring C, or where ring C is not closed, lack antimicrobial activity (Chan et al., 1996). It is noteworthy that while nisin AB is inactive having a lysine at the C-terminus, it gains higher activity through conjugation with O6K3 than with the more hydrophobic O6. The growth inhibition experiments showed that the activity of nisin ABC + O6K3 are better than nisin ABC + O6 and nisin ABC + O9, again indicating that addition of lysines (positive charge) at the C-terminal region can improve the activity. The antimicrobial activity of nisin ABC + O6K3 against *E. faecium* was 8-fold less active than full-length nisin. However, the activity was 16-fold better than nisin ABC, suggesting that modifying nisin ABC is a promising strategy to generate semi-synthetic nisin hybrids. It is notable that the inhibition activities of the semi-synthetic hybrids did not fully correlate when comparing solid media tests and broth MIC tests. However, this effect has been described for many nisin mutants, e.g., nisin A and nisin Z (de Vos et al., 1993). These compounds have an identical MIC, but a single amino acid difference leads to different halo sizes on diffusion assays, which is likely caused by altered diffusion properties. The five polyproline moieties that were tested in this study have varying hydrophobicities. Therefore, the lack of correlation between both essay results are likely caused by their distinct diffusion characteristics. In addition to their increased activity, these variants are not prone to degradation at the C-terminus by NSR, as was observed for nisin. Although the full proteolytic resistance of the conjugates was not tested, polyproline chains commonly have resistance against proteolysis in general, and convey this property to the nisin hybrids, providing a proof of concept. Notably, the method described in this study can be applied to conjugate other compatible (synthetic and non-proteinaceous) moieties that can provide the desired resistance to specific proteases. Nisin AB-azide and nisin ABC-azide can be readily generated with yields in the milligram range according to our optimized protocol. Future studies may focus on coupling peptides, especially anti-Gram-negative peptides, with nisin ABC-azide. Overall, this study highlights how lantibiotic fragments can be used as lead structures to create novel variants with altered properties (e.g., stability, activity, and specificity) via chemical coupling.

DATA AVAILABILITY STATEMENT

All datasets generated for this study are included in the article/**Supplementary Material**, further inquiries can be directed to the corresponding author.

AUTHOR CONTRIBUTIONS

JD and OK planned, conceived, and analyzed the experiments. VK designed the polyproline moieties. JD, JV, and VK performed the experiments. JD, VK, NB, and OK drafted the manuscript and contributed to the data interpretation. All authors read, critically revised, and approved the final manuscript.

FUNDING

JD was supported by the Chinese Scholarship Council (CSC). JV was supported by the Netherlands Organization for Scientific

Research (NWO, ALWOP. 214). VK was supported by the DFG-funded research group 1805.

ACKNOWLEDGMENTS

We thank Manuel Montalban-Lopez (Department of Microbiology, Faculty of Sciences, University of Granada, Spain) for helpful discussions and thank Sander H. J. Smits for the pNSR construct (Institute of Biochemistry, Heinrich Heine University).

SUPPLEMENTARY MATERIAL

The Supplementary Material for this article can be found online at: https://www.frontiersin.org/articles/10.3389/fmicb.2020.575334/full#supplementary-material

REFERENCES

Ahmad Fuaad, A. A. H., Azmi, F., Skwarczynski, M., and Toth, I. (2013). Peptide conjugation via CuAAC 'click' chemistry. *Molecules* 18, 13148–13174. doi: 10.3390/molecules181113148

Arnusch, C. J. (2008). The vancomycin-nisin (1-12) hybrid restores activity against vancomycin resistant enterococci. *Biochemistry* 47, 12661–12663. doi: 10.1021/bi801597b

Bolt, H. L., Kleijn, L. H. J., Martin, N. I., and Cobb, S. L. (2018). Synthesis of antibacterial nisin (-) peptoid hybrids using click methodology. *Molecules* 23:1566. doi: 10.3390/molecules23071566

Brötz, H., Josten, M., Wiedemann, I., Schneider, U., Götz, F., Bierbaum, G., et al. (1998). Role of lipid-bound peptidoglycan precursors in the formation of pores by nisin, epidermin and other lantibiotics. *Mol. Microbiol.* 30, 317–327. doi: 10.1046/j.1365-2958.1998.01065.x

Chan, W. C., Leyland, M., Clark, J., Dodd, H. M., Lian, L.-Y., Gasson, M. J., et al. (1996). Structure-activity relationships in the peptide antibiotic nisin antibacterial activity of fragments of nisin. *FEBS Lett.* 390, 129–132. doi: 10.1016/0014-5793(96)00638-2

de Vos, W. M., Mulders, J. W., Siezen, R. J., Hugenholtz, J., and Kuipers, O. P. (1993). Properties of nisin Z and distribution of its gene, nisZ, in *Lactococcus lactis*. *Appl. Environ. Microbiol.* 59, 213–218. doi: 10.1128/AEM.59.1.213-218

Gharsallaoui, A., Oulahal, N., Joly, C., and Degraeve, P. (2016). Nisin as a food preservative: part 1: physicochemical properties, antimicrobial activity, and main uses. *Crit. Rev. Food Sci. Nutr.* 56, 1262–1274. doi: 10.1080/10408398.2013.763765

Hansen, J. N., and Sandine, W. E. (1994). Nisin as a model food preservative. *Crit. Rev. Food Sci. Nutr.* 34, 69–93. doi: 10.1080/10408399409527650

Jiang, X., Hao, X., Jing, L., Wu, G., Kang, D., Liu, X., et al. (2019). Recent applications of click chemistry in drug discovery. *Expert Opin. Drug Discov.* 14, 779–789. doi: 10.1080/17460441.2019.1614910

Khosa, S., AlKhatib, Z., and Smits, S. H. (2013). NSR from *Streptococcus agalactiae* confers resistance against nisin and is encoded by a conserved nsr operon. *Biol. Chem.* 394, 1543–1549. doi: 10.1515/hsz-2013-0167

Khosa, S., Frieg, B., Mulnaes, D., Kleinschrodt, D., Hoeppner, A., Gohlke, H., et al. (2016). Structural basis of lantibiotic recognition by the nisin resistance protein from *Streptococcus agalactiae*. *Sci. Rep.* 6:18679. doi: 10.1038/srep18679

Kolb, H. C., Finn, M. G., and Sharpless, K. B. (2001). Click chemistry: diverse chemical function from a few good reactions. *Angew. Chem. Int. Ed.* 40, 2004–2021. doi: 10.1002/1521-3773(20010601)40:11<2004::AID-ANIE2004>3.0.CO;2-5

Koopmans, T., Wood, T. M., Hart, P. T., Kleijn, L. H. J., Hendrickx, A. P. A., Willems, R. J. L., et al. (2015). Semisynthetic lipopeptides derived from nisin display antibacterial activity and lipid II binding on par with that of the parent compound. *J. Am. Chem. Soc.* 137, 9382–9389. doi: 10.1021/jacs.5b04501

Kubyshkin, V., and Budisa, N. (2018). Exploring hydrophobicity limits of polyproline helix with oligomeric octahydroindole-2-carboxylic acid. *J. Pept. Sci.* 24:e3076. doi: 10.1002/psc.3076

Kubyshkin, V., Grage, S. L., Ulrich, A. S., and Budisa, N. (2019). Bilayer thickness determines the alignment of model polyproline helices in lipid membranes. *Phys. Chem. Chem. Phys.* 21:22396. doi: 10.1039/c9cp02996f

Kuipers, O. P., de Ruyter, P. G. G. A., Kleerebezem, M., and de Vos, W. M. (1998). Quorum sensing-controlled gene expression in lactic acid bacteria. *J. Biotechnol.* 64, 15–21. doi: 10.1016/S0168-1656(98)00100-X

Lubelski, J., Rink, R., Khusainov, R., Moll, G. N., and Kuipers, O. P. (2008). Biosynthesis, immunity, regulation, mode of action and engineering of the model lantibiotic nisin. *Cell. Mol. Life Sci.* 65, 455–476. doi: 10.1007/s00018-007-7171-2

McKay, C. S., and Finn, M. G. (2014). Click chemistry in complex mixtures: bioorthogonal bioconjugation. *Chem. Biol.* 21, 1075–1101. doi: 10.1016/j.chembiol.2014.09.002

Montalbán-López, M., Deng, J., van Heel, A. J., and Kuipers, O. P. (2018). Specificity and application of the lantibiotic protease NisP. *Front. Microbiol.* 9:160. doi: 10.3389/fmicb.2018.00160

Oldach, F., Al Toma, R., Kuthning, A., Caetano, T., Mendo, S., Budisa, N., et al. (2012). Congeneric lantibiotics from ribosomal *in vivo* peptide synthesis with noncanonical amino acids. *Angew. Chem. Int. Ed.* 51, 415–418. doi: 10.1002/anie.201106154

Rogers, L. A. (1928). The inhibiting effect of *Streptococcus Lactios* on *Lactobacillus Bulgaricus*. *J. Bacteriol.* 16, 321–325.

Schmitt, S., Montalbán-López, M., Peterhoff, D., Deng, J., Wagner, R., Held, M., et al. (2019). Analysis of modular bioengineered antimicrobial lanthipeptides at nanoliter scale. *Nat. Chem. Biol.* 15, 437–443. doi: 10.1038/s41589-019-0250-5

Shin, J. M., Gwak, J. W., Kamarajan, P., Fenno, J. C., Rickard, A. H., and Kapila, Y. L. (2016). Biomedical applications of nisin. *J.Appl. Microbiol.* 120, 1449–1465. doi: 10.1111/jam.13033

Slootweg, J. C., Peters, N., van Ufford, H. L. C. Q., Breukink, E., Liskamp, R. M. J., and Rijkers, D. T. S. (2014). Semi-synthesis of biologically active nisin hybrids composed of the native lanthionine ABC-fragment and a cross-stapled synthetic DE-fragment. *Bioorg. Med. Chem.* 22, 5345–5353. doi: 10.1016/j.bmc.2014.07.046

Slootweg, J. C., van der Wal, S., van Ufford, H. C. Q., Breukink, E., Liskamp, R. M. J., and Rijkers, D. T. S. (2013a). Synthesis, antimicrobial activity, and membrane permeabilizing properties of C-terminally modified nisin conjugates accessed by CuAAC. *Bioconj. Chem.* 24, 2058–2066. doi: 10.1021/bc400401k

Slootweg, J. C., Liskamp, R. M. J., and Rijkers, D. T. S. (2013b). Scalable purification of the lantibiotic nisin and isolation of chemical/enzymatic cleavage fragments suitable for semi-synthesis. *J. Pept. Sci.* 19, 692–699. doi: 10.1002/psc.2551

Thirumurugan, P., Matosiuk, D., and Jozwiak, K. (2013). Click chemistry for drug development and diverse chemical-biology applications. *Chem. Rev.* 113, 4905–4979. doi: 10.1021/cr200409f

van Heel, A. J., Mu, D., Montalbán-López, M., Hendriks, D., and Kuipers, O. P. (2013). Designing and producing modified, new-to-nature peptides

with antimicrobial activity by use of a combination of various lantibiotic modification enzymes. *ACS Synth. Biol.* 2, 397–404. doi: 10.1021/sb3001084

Wiegand, I., Hilpert, K., and Hancock, R. E. W. (2008). Agar and broth dilution methods to determine the minimal inhibitory concentration (MIC) of antimicrobial substances. *Nat. Protoc.* 3, 163–175. doi: 10.1038/nprot.2007.521

Yoganathan, S., Sit, C. S., and Vederas, J. C. (2011). Chemical synthesis and biological evaluation of galliderminsiderophore conjugates. *Org. Biomol. Chem.* 9, 2133–2141. doi: 10.1039/c0ob00846j

Conflict of Interest: The authors declare that the research was conducted in the absence of any commercial or financial relationships that could be construed as a potential conflict of interest.

Advantages of publishing in Frontiers

OPEN ACCESS
Articles are free to read for greatest visibility and readership

FAST PUBLICATION
Around 90 days from submission to decision

HIGH QUALITY PEER-REVIEW
Rigorous, collaborative, and constructive peer-review

TRANSPARENT PEER-REVIEW
Editors and reviewers acknowledged by name on published articles

Frontiers
Avenue du Tribunal-Fédéral 34
1005 Lausanne | Switzerland

Visit us: www.frontiersin.org
Contact us: frontiersin.org/about/contact

REPRODUCIBILITY OF RESEARCH
Support open data and methods to enhance research reproducibility

DIGITAL PUBLISHING
Articles designed for optimal readership across devices

FOLLOW US
@frontiersin

IMPACT METRICS
Advanced article metrics track visibility across digital media

EXTENSIVE PROMOTION
Marketing and promotion of impactful research

LOOP RESEARCH NETWORK
Our network increases your article's readership